R-08-08

Description of surface hydrology and near-surface hydrogeology at Forsmark

Site descriptive modelling

SDM-Site Forsmark

Per-Olof Johansson
Artesia Grundvattenkonsult AB

December 2008

Svensk Kärnbränslehantering AB
Swedish Nuclear Fuel
and Waste Management Co
Box 250, SE-101 24 Stockholm
Tel +46 8 459 84 00

ISSN 1402-3091
SKB Rapport R-08-08

Description of surface hydrology and near-surface hydrogeology at Forsmark

Site descriptive modelling

SDM-Site Forsmark

Per-Olof Johansson
Artesia Grundvattenkonsult AB

December 2008

Preface

The Swedish Nuclear Fuel and Waste Management Company (SKB) has conducted site investigations at two different locations, the Forsmark and Laxemar-Simpevarp areas, with the objective of siting a repository for spent nuclear fuel.

The present report constitutes a summary and synthesis of the work on surface hydrology and near-surface hydrogeology of the site investigation at Forsmark. The site investigation was conducted during 2002–2007 and included extensive field work, data sampling, laboratory analyses and tests, and data analyses and modelling. In the text, references are given to numerous reports on these investigations and analyses.

Selection of material from these reports and data as well as additional interpretations and integration based on supplied material is the responsibility of the author of the present report.

Important contributions to the present report have been delivered by:

Johan Öhman, Golder Associates AB, who carried out most of the work on presentation of times series data.

Kent Werner, EmpTec, who prepared the updating of the slug-test analysis presented in Section 3.4.1.

Björn Holgersson, SWECO, who conducted most of the re-calculations of point water heads to environmental water heads presented under *Point water heads and environmental water heads* in Section 3.4.2 and in Appendix 2

Fredrik Marelius and Petter Stenström, WSP Sverige AB, who were responsible for the work on *General characteristics of brooks* in Section 3.3.3 and *Costal basins* in Section 3.3.5, respectively.

Mats Tröjbom, Mopelikan, who carried out the principal component and independent component analyses, and the partial least squares modelling presented under *Sea boundary* in Section 3.5.1. He also conducted the additional principal component analyses in Section 3.5.4 *Hydrochemical data för interpretation of the flow systems* not presented in /Tröjbom et al. 2007/.

John Juston, Juston Konsult AB, who was responsible for the modelling presented in Section 4.2 *Catchment-based simulation of surface discharge and groundwater depths*.

Emma Bosson, SKB, and Lars-Göran Gustafsson and Mona Sassner, DHI, who carried out the MIKE-SHE modelling which is summarised in Section 4.3. They also provided valuable feedback from the quantitative modelling to the concepeptual modelling.

Sven Follin, SF Geologic, and Sten Berglund, SKB, with whom fruitful discussions have taken place on the interpretation of data and the conceptual model. Sven Follin has also contributed with valuable information of the bedrock hydrogeology and Sten Berglund has reviewed the report.

Summary

The Swedish Nuclear Fuel and Waste Management Company (SKB) has conducted site investigations at two different locations, the Forsmark and Laxemar-Simpevarp areas, with the objective of siting a geological repository for spent nuclear fuel. This report describes the modelling of the surface hydrology and near-surface hydrogeology that was performed for the final site descriptive model of Forsmark produced in the site investigation stage, SDM-Site Forsmark.

The Forsmark area is situated on the eastern coast of Sweden, c. 120 km north of Stockholm. The site investigation area is characterized by a low relief with a small-scale topography. The study area is almost entirely below 20 metres above sea level. Forest is the dominating land cover. The main lakes, Lake Fiskarfjärden, Lake Bolundsfjärden, Lake Eckarfjärden and Lake Gällsboträsket, all have sizes of less than one km^2 and are quite shallow. No major water courses flow through the central parts of the site investigation area. Wetlands are frequent and cover more than 25% of some sub-catchments. Till is the dominating Quaternary deposit (QD), covering c. 75% of the terrestrial area. Bedrock outcrops are frequent, but constitute only c. 5% of the area. The QD's are shallow, usually less than 5 m deep.The greatest depth to bedrock recorded in a drilling is 16 m. In the wetlands the organic deposits can rest directly on till, or be underlain by sand and clay above the till.

The annual precipitation during the site investigation was quite close to the longterm average of 559 mm estimated by SMHI (the Swedish Meteorological and Hydrological Institute). For the four-year period of June 2003–May 2007, the mean annual precipitation recorded in the local measurements was 563 mm. The mean annual calculated potential evapotranspiration for the same period was 526 mm. A longterm overall water balance of the area may be estimated based on 30-year precipitation data from SMHI-stations surrounding the site investigation area and the reletively short-term site specific meterorological and hydrological monitoring data, as follows: precipitation = 560 mm/year, actual evapotranspiration = 400–410 mm/year, and runoff = 150–160 mm/year.

Granitic rocks are dominating the bedrock of the area. The bedrock hydrogeology reveals a significant hydraulic anisotropy within the tectonic lens, which covers the central part of the site investigation area. The upper c. 150 m of bedrock contains high-transmissive horizontal fractures/sheet joints. Below the uppermost c. 150 m of the bedrock, the high-transmissive horizontal fractures/sheet joints vanish and the conductive fracture frequency becomes very low and the fractures fairly low-transmissive. In some of the 1,000 m deep cored boreholes there are almost no flowing fractures observed below c. 150 m depth.

The close correlation between the topography of the ground surface and the groundwater level in the QD implies that surface water and groundwater divides for the QD's can be assumed to coincide. Regarding groundwater levels in the upper bedrock there is no strong coupling to the topography of the ground surface. This is most evident in the tectonic lens where the upper c. 150 m of the bedrock is known to have frequent horizontal and sub-horizonal highly transmissive fractures. However, westward increasing groundwater levels in the bedrock outside the tectonic lens indicate that the water divides of the flow systems involving the near-surface bedrock follow the surface water divide towards River Forsmarksån. This means that the topography can be used for delineation of the inland boundary also for these systems.

From the conclusion that groundwater divides for the shallow groundwater systems limited to QD (till), where the major part of the water flow takes place, coincide with the surface water divides, follows that such systems only may have lateral boundaries to the sea in the "rest catchments" adjacent to the sea with no surface discharge in water courses. For the flow systems involving also the near-surface bedrock, the situation is different due to the highly transmissive horizontal and sub-horizontal fracture zones extending below the sea. The vertical contact

between these zones and the sea, directly via outcropping or indirectly via vertical fractures, will determine the boundary conditions of these systems. The superficial horizontal sheet joints have a tendency to follow the topography of the bedrock surface implying that direct hydraulic contact with the sea via outcropping is considered to be less common.

During events of very high sea water levels, sea water flows into several of the lakes (Norra Bassängen, Puttan, Bolundsfjärden, Lillfjärden and Fiskarfjärden). In connection with these events, the sea obviously has an impact on both surface water and groundwater flow systems in these lakes and their surroundings.

With few exceptions, the infiltration capacity of the soils in the area exceeds the rainfall and snowmelt intensities. The groundwater levels in many monitoring wells in QD were within one metre below the ground all the year, and the groundwater level was on average less than 0.7 m below ground during 50% of the time. Also in what can be considered as typical recharge areas, the average groundwater level was as shallow as 1.2 m below ground. The annual variation of the groundwater level is mostly less than one metre in discharge areas, and 1.5 m in typical recharge areas. The shallow groundwater levels mean that there will be a strong interaction between evapotranspiration, soil moisture and groundwater. Diurnal fluctuations of the groundwater levels, driven by evapotranspiration cycles, were evident in the data from many of the groundwater monitoring wells in the QD.

Direct recharge from precipitation is obviously the dominant source of groundwater recharge. However, the groundwater level measurements in the vicinity of Lake Bolundsfjärden and Lake Eckarfjärden show that the lakes may act as recharge sources to the till aquifers in the immediate vicinity of the lakes during summer. While the groundwater levels are well above the lake water levels during most of the year, they are considerably below the lake water levels under dry summer conditions. However, due to the low permeability of the bottom sediments, the resulting water fluxes can be assumed to be relatively small.

Similar to the external boundaries of the model area, the internal surface water divides and the groundwater divides of the groundwater systems in the QD are assumed to coincide. The strong correlation between the mean groundwater elevations observed in the till and the ground surface elevation means that the average vertical hydraulic flux at some point below the surface is smaller than the net infiltration into the saturated zone of the till. The decrease in hydraulic conductivity with depth and the anisotropy of the till, with $K_v < K_h$ (where K_v and K_h are the vertical and horizontal hydraulic conductivities, respectively), are plausible explanations, but a contribution from a contrast in vertical hydraulic conductivity between the till and the bedrock is also possible (with the uppermost bedrock having a lower K_v).

The small-scale topography and the hydraulic conductivity profile of the tills imply that many small catchments will be formed with local shallow groundwater flow systems in the QD, and that a dominating part of the groundwater will move along these shallow flow paths. According to the conceptual model, the horizontal hydraulic conductivity of the till dominating the area decreases from more than 10^{-5} m/s in the uppermost part of the profile to c.10^{-6} and 10^{-7} m/s deeper down in the profile for coarse and fine-grained till, respectively. Similarly, the specific yield decreases from 0.15–0.20 to 0.03–0.05.

The local, small-scale recharge and discharge areas only involving groundwater flow systems restricted to the QD overlay the more large-scale flow systems associated with groundwater flow at greater depths. Within the tectonic lens, the measured groundwater levels in the till are considerably higher than those in the bedrock. The differences between the levels in till and rock are generally much larger than between different sections in the bedrock boreholes sealed off by packers. In general, the groundwater levels in the bedrock are still above the QD/rock interface, indicating that no unsaturated zone exists below this interface.

The groundwater levels in the till and the bedrock are well correlated. The natural groundwater level fluctuations are, however, smaller in the bedrock, but still to a great extent controlled by the annual precipitation and evapotranspiration cycles. The conditions prevailing within

the northern part of the tectonic lens, with a lower groundwater level in bedrock than in the QD, mean that the groundwater flow has a downward component at the studied locations and consequently an inflow from the till to the bedrock.

A probable explanation for the generally low levels measured in the bedrock boreholes is that these intersect one/some of the highly conductive horizontal to sub-horizontal zones shown to exist in the shallow bedrock in the Forsmark area. The highly transmissive shallow bedrock acts a drain for water coming from above as well as from below. The available data indicate that flow systems involving the bedrock do not have discharge areas on land in the northern part of the tectonic lens but discharge into the sea. The only occasions when data from this area show a continuous upward flow gradient are during dry summers when the groundwater level in the QD decreases below the levels in the bedrock.

Interestingly, the lake level and the groundwater level in till in the middle of Lake Bolundsfjärden are considerably higher than the groundwater levels in the bedrock below the lake (i.e. in borehole HFM32). The levels are lowest in the two deepest sections of the bedrock borehole. The difference between these two sections is small but after density correction of the measured heads the second deepest section has the lowest head. This indicates that the fractures in this section act as drains for water coming from above as well as from below. During a pumping test in bedrock in a well 500 m away, the responses were strongest in the two deepest well sections, but were also obvious in the upper two sections and also in the monitoring well in the till above.

The borehole HFM32 has the lowest point water head of all the percussion-drilled boreholes around Lake Bolundsfjärden. Only boreholes at the inlet of the cooling water canal and on the SFR peninsula have occasionally point water heads at the same low level or below. The groundwater level in HFM32 was below the sea level during the summer and autumn of 2006. Two possible, perhaps superimposed, phenomena could explain this: (i) the groundwater level in the bedrock is indirectly influenced by evapotranspiration extracting water from the groundwater zone in the QD, thereby inducing an upward flow from the bedrock, and/or (ii) the borehole is influenced by the drainage pumping in the SFR facility (c. 6 L/s).

An influence from evapotranspiration requires that the groundwater level in the bedrock is above the QD/rock interface, which is the case in the low-lying areas surrounding Lake Bolundsfjärden. The MIKE SHE hydrological simulations, with field-based parameter setting, showed a clear upward flow gradient from the bedrock to the QD in the littoral zone of Lake Bolundsfjärden during the dry summer of 2006.

An influence from the pumping at SFR requires a good hydraulic contact all the way to SFR. From a pumping test in the HFM33 borehole, immediately west of SFR, it is known that quick and strong responses were observed in site investigation boreholes located c. 1.5 km SW of the pumping well. Pumping tests in HFM14 have also shown quick and strong responses in other quite distant HFM-wells (c. one km away), confirming the high transmissivity and low storativity of the upper bedrock. The prevailing situation, with in general relatively low groundwater levels in the shallow bedrock within the northern parts of the tectonic lens, may partly be caused by the pumping at SFR. However, no definite conclusions on this issue can be drawn based on existing data.

The lake water level-groundwater level relationship indicates that the lake sediments, the underlying till, and/or the uppermost bedrock have low vertical hydraulic conductivities. If the surface water-groundwater hydraulic contact had been good, the situation with groundwater level drawdown from evapotranspiration extending below the lakes, and the quick and extensive drawdowns from the pumping tests in percussion-drilled boreholes HFM14 and HFM33 in the rock below Lake Bolundfjärden and the sea, would not appear. The flow systems around and below the lakes appear to be quite complex. The chemistry of the waters below the lakes indicates a very limited flow since relict marine water is found.

During the MIKE SHE modelling there was a general problem with too high simulated groundwater levels in the bedrock, whereas there was a good agreement between measured

and simulated groundwater levels in the QD. Furthermore, with the original parameter settings the model was unable to simulate the drawdowns in the pumping tests in borehole HFM14. To overcome these problems, several test simulations were conducted with different combinations of increased horisontal hydraulic conductivity of the bedrock and decreased vertical hydraulic conductivity of the bedrock and the QD, and a decreased specific storage of the bedrock compared with the data set obtained from the bedrock hydrogeology modelling.

The outcome of these tests was that the specific storage had to be lowered considerably from the values used initially (varying from $1 \cdot 10^{-7}$ m^{-1} to $1 \cdot 10^{-5}$ m^{-1}) to obtain a good match between measured and simulated responses in the pumping tests. In the final calibrated model a value of $5 \cdot 10^{-8}$ m^{-1} was used. Furthermore, an increase of the horizontal hydraulic conductivity of the sheet joints, as implemented in the upper bedrock part of the model, by a factor of 10 compared to the delivered bedrock parameterisation and a decrease of the vertical hydraulic conductivity of the upper 200 m of the bedrock by a factor of 10 were found to be necessary to obtain a good fit between measured and simulated pumping test responses. A further decrease of the vertical hydraulic conductivity of the QD turned out to have only a marginal effect on the groundwater levels.

However, the problem with the generally too high groundwater levels in the bedrock was only partly solved by the changes made. As a final test, the drainage pumping in the SFR facility was introduced in quite a simplistic manner, i.e. as a well screened between c. 40 and 140 m depth. The introduction of this sink drastically improved the agreement between measured and simulated groundwater levels in the bedrock, with the mean absolute error and mean error for all monitoring sections in rock decreasing from 0.68 m to 0.41 m and from –0.65 m to –0.05 m, respectively (a negative mean error indicates that the simulated level is too high). Most sections showed errors of c. ±0.2 m. Of the boreholes within the northern part of the tectonic lens, only HFM16 and HFM32 showed considerably larger errors with an overestimation and underestimation of c. one metre, respectively.

Particle tracking simulations were performed using the final calibrated MIKE SHE model. When particles were released at c. 140 m below sea level inside the area corresponding to the planned repository, only 10% of the particles had left the model volume after 300 years and all these particles had gone to the sea. When pumping at SFR, 18% of the particles had left the model volume through the pumping in SFR. The rest of the particles were still in the model. In both cases, the particles concentrated to the sheet joint layer at 110 m below sea level and the horizontal transport was dominating. Above this level only a few cells were passed by a particle. When pumping at SFR, no particles reached higher than 70 m below sea level. Thus, there were no exit points at the surface after 300 years of simulation when pumping at SFR. When the SFR-pumping was not activated, a few particles reached the sea with exit points close to the shoreline.

Since many particles were still in the model volume after 300 years, an additional longer simulation was run for 5,000 years. The transport times were long and even after 5,000 years 81% of the particles were still in the model volume. No exit points were found in the terrestrial part of the model area. All the particles exited the model volume at sea. It was also found that 5% of the introduced particles were stuck in the marine sediments. Apart from them, no particles were left in the upper calculation layers. All the particles that were left in the model after 5,000 years were found in the deeper bedrock, between 110 and 600 m below sea level.

Although providing potentially important information guiding further analyses, the particle tracking results presented should be interpreted with great caution. The results depend heavily on the geometry and hydraulic properties of the hydrogeological structures of the upper part of the bedrock, which are implemented in the model in quite a simplistic way.

In the MIKE SHE modelling, the water balance was calculated for the four-year period September 2003–August 2007 for the terrestrial part of the model area (i.e. excluding the sea). The mean annual precipitation for this period was 533 mm and the mean annual actual evapotranspiration was 405 mm. The annual total interception was 122 mm/year, the transpiration from plants 169 mm/year, and the calculated runoff (discharge) 144 mm/year. The infiltration

to the unsaturated zone was 351 mm/year, whereas the groundwater recharge from the unsaturated zone to the uppermost calculation layer of the saturated zone was 124 mm/year. The flow to the second calculation layer in QD, at 2.5 m depth, was c. 45 mm. There are many local recharge and discharge areas within in this layer; 41 mm was transported back to the uppermost QD layer. Only c.11 mm was flowing down to the uppermost bedrock. The upward flow from the rock to the QD corresponded to some 8–9 mm, which means that the net downward flow was only 2–3 mm.

The comprehensive investigation and monitoring programme forms a strong basis for the developed conceptual and descriptive model of the hydrological and near-surface hydrological system of the site investigation area. However, there are some remaining uncertainties regarding the interaction of deep and near-surface groundwater and surface water of importance for the understanding of the system:

- The groundwaters in till below Lake Eckarfjärden, Lake Gällsboträsket, Lake Fiskarfjärden and Lake Bolundsfjärden have high salinities. The hydrological and hydrochemical interpretations indicate that these waters are relict waters of mainly marine origin. From the perspective of the overall water balance, the water below the central parts of the lakes can be considered as stagnant. However, according to the hydrochemical interpretation, these waters also contain weak signatures of deep saline water. Rough chloride budget calculations for the Gällboträsket depression also raise the question of a possible upward flow of deep groundwater. No absolute conclusion can be drawn from the existing data analyses regarding the key question of whether there is a small ongoing upward flow of deep saline water. However, Lake Bolundsfjärden is an exception where the clear downward flow gradient from the till to the bedrock excludes the possibility of an active deep saline source.
- The available data indicate that there are no discharge areas for flow systems involving deep bedrock groundwater in the northern part of the tectonic lens, where the repository is planned to be located (the so-called “target area”). However, it can not be excluded that such discharge areas exist. Data indicate that the prevailing downward vertical flow gradients from the QD to the bedrock are highly dependent on the very transmissive horizontal and sub-horizontal fractures of the uppermost bedrock and that evapotranspiration induced flow may change these directions under dry conditions in some areas.
- Data as well as the simulations with MIKE SHE raise the question if the prevailing groundwater levels in the northern part of the tectonic lens are influenced by the pumping for the drainage of the SFR facility (c. 6 L/s). Another possibly influencing sink is the pumping for drainage of the Forsmark nuclear plant reactor buildings 1 and 2 (c. 1–2 L/s). These sinks may influence the vertical flow gradients in some parts of the investigation area, and it is strongly recommended that additional investigations are performed to resolve this uncertainty.

Sammanfattning

Svensk Kärnbränslehantering AB (SKB) har genomfört platsundersökningar på två platser, Forsmark och Laxemar-Simpevarp, för lokalisering av ett slutförvar för använt kärnbränsle. Denna rapport redovisar modellering av ythydrologi och ytnära hydrogeologi utförd som en del av den sista platsbeskrivande modell av Forsmark som redovisas under platsundersökningsskedet, ”SDM-Site Forsmark”.

Forsmark ligger vid kusten, ca 120 km norr om Stockholm. Platsundersökningsområdet har en flack, småskalig topografi och nästan hela området ligger lägre än 20 m över havet. Skogsbruk är den dominerande markanvändningen. De större sjöarna i området, Fiskarfjärden, Bolundsfjärden, Eckarfjärden och Gällsboträsket, är alla mindre än en kvadratkilometer och grunda. Det rinner inga större vattendrag genom de centrala delarna av platsundersökningsområdet. Våtmarker förekommer rikligt och täcker mer än 25 % av ytan i vissa delavrinningsområden. Morän är den dominerande jordarten och täcker ca 75 % av landytan. Berg i dagen återfinns på många ställen men täcker endast ca 5 % av ytan. Jordlagren är tunna, oftast mindre än 5 m tjocka. Den största jordmäktigheten som konstaterats vid borrning är 16 m. I våtmarkerna är de organiska jordlagren antingen avsatta direkt på moränen eller underlagrade av sand och lera ovanpå moränen.

Under tiden för platsundersökningarna var nederbörden nära den beräknade normalnederbörden för området, vilken av SMHI (Sveriges meteorologiska och hydrologiska institut) har uppskattats till 559 mm/år. Medelvärdet av de lokala mätningarna under fyraårsperioden juni 2003–maj 2007 var 563 mm. Den beräknade årliga potentiella evapotranspirationen för samma period var 526 mm. Vattenbalansen för platsundersökningsområdet kan uppskattas utgående från normalnederbörden under 30 år vid SMHI:s kringliggande nederbördsstationer och de relativt korta meteorologiska och hydrologiska tidsserierna från platsundersökningarna: nederbörd = 560 mm/år, verklig evapotranspiration = 400–410 mm/år och avrinning = 150–160 mm/år.

Berggrunden i området domineras av granitiska bergarter. De hydrogeologiska förhållandena i berggrunden uppvisar tydlig anisotropi i den tektoniska lins som utgör den centrala delen av platsundersökningsområdet. De översta ca 150 m av berggrunden innehåller högtransmissiva horisontella sprickor/bankningsplan. Under detta djup försvinner denna typ av sprickor och sprickfrekvensen totalt blir väldigt låg liksom sprickornas transmissivitet. I några av de 1 000 m långa kärnborrhålen saknas flödande sprickor under 150 m djup nästan helt.

Den starka korrelationen mellan landytans topografi och grundvattennivån i jordlagren betyder att ytvattendelarna och grundvattendelarna för jordgrundvattnet kan antas sammanfalla. Vad gäller grundvattennivåerna i det ytliga berget finns inte motsvarande starka korrelation. Detta är tydligast i den tektoniska linsen som innehåller de ytliga högtransmissiva horisontella och subhorisontella sprickorna. Utanför linsen, stiger grundvattennivåerna i berget och indikerar att grundvattensystemen i det ytliga berget har en vattendelare som sammanfaller med den topografiska ytvattendelaren mot Forsmarksån.

Av förhållandet att ytvattendelarna och grundvattendelarna för grundvattensystemen som begränsas till jordlagren sammanfaller följer att dessa system endast har ett direkt utflöde till havet i restavrinningsområdena närmast havet som saknar vattendrag. För de flödessystem som också inkluderar det ytliga berget är förhållandena annorlunda, vilket beror på de högtransmissiva horisonella och subhorisontella sprickzoner som sträcker sig ut under havet. Den vertikala kontakten mellan dessa zoner och havet, direkt eller via vertikala sprickor, bestämmer randvillkoren för dessa system. De ytliga bankningsplanen har en tendens att följa bergytans topografi vilket gör att direkt kontakt med havet bedöms som mindre vanlig.

Vid tillfällen med mycket höga havsvattennivåer rinner havsvatten in i flera av sjöarna (Norra Bassängen, Puttan, Bolundsfjärden, Lillfjärden och Fiskarfjärden). Vid dessa tillfällen påverkas

yt- och grundvattensystemen i och omkring sjöarna naturligtvis starkt av det inträngande havsvattnet.

Jordlagrens infiltrationskapacitet överstiger med få undantag nederbördens och snösmältningens intensitet. Grundvattennivån i många av observationsrören i jord ligger närmare markytan än en meter under hela året och som medeltal för samtliga observationsrör låg nivån närmare markytan än 0,7 m under halva året. Även i områden som bedöms som typiska inströmningsområden låg grundvattenytan i medeltal inte mer än 1,2 m under markytan. Grundvattennivåns årsvariation är oftast mindre än en meter i utströmningsområden och ca 1,5 m i typiska inströmningsområden. Det ytnära grundvattnet innebär att det blir en stark interaktion mellan evapotranspiration, markvatten och grundvatten. Tydliga dygnsfluktuationer i grundvattennivån, orsakade av evapotranspirationens dygnsvariationer, kunde konstateras i många av observationsrören i jordlagren.

Grundvattenbildning direkt från nederbörden dominerar, men mätningar av grundvattennivåerna runt Bolundsfjärden och Eckarfjärden visar att sjöarna kan utgöra grundvattenbildningsområden under sommaren. Grundvattennivåerna runt sjöarna ligger högre än sjönivåerna under större delen av året, men under torra somrar ligger de betydligt lägre än sjönivåerna. Bottensedimentens låga vattengenomsläpplig medför emellertid att de flöden som dessa omvända gradienter orsakar kan antas vara relativt små.

Liksom för modellområdets yttre gränser, kan det antas att de interna ytvattendelarna och grundvattendelarna för de grundvattensystem som är begränsade till jordlagren sammanfaller. Den starka korrelationen mellan topografin och grundvattenytan i jordlagren visar att på någon nivå under markytan är det vertikala grundvattenflödet lägre än nettoinfiltrationen till den mättade zonen i moränen. Den konstaterade minskningen av den hydrauliska konduktiviteten med djupet och anisotropin, med $K_v < K_h$ (K_v är den vertikala och K_h den horisontella hydrauliska konduktiviteten), är de troliga huvudorsakerna, men en kontrast i vertikal hydraulisk konduktivitet mellan moränen och det ytliga berget (där det ytliga berget har lägre K_v) skulle också kunna bidra.

Den småskaliga topografin och att den hydrauliska konduktiviteten i moränen minskar med djupet medför att många små avrinningsområden med lokala ytliga grundvattensystem i jordlagren bildas, och att den dominerande delen av vattenomsättningen sker i dessa system. Enligt den konceptuella modellen minskar den hydrauliska konduktiviteten i den morän som dominerar i området från över 10^{-5} m/s i den översta delen av jordprofilen till ca 10^{-6} och 10^{-7} m/s djupare ner för den mer grovkorniga respektive finkorniga moränen. På liknande sätt minskar den effektiva porositeten med djupet från 0,15–0,20 till 0,03–0,05.

De lokala småskaliga in- och utströmningsområdena i grundvattensystemen i jordlagren överlagrar flödessystemen för det djupare grundvattnet. Inom den tektoniska linsen ligger grundvattennivåerna betydligt högre i jordlagren än i berget. Skillnaden mellan dessa nivåer är i allmänhet betydligt större än nivåskillnaderna mellan olika djup i berget. Grundvattennivån i berget ligger dock oftast ovanför bergets överyta vilket betyder att det inte finns någon omättad zon i berget.

Grundvattennivåernas variationer i moränen och i berget är välkorrelerade. De naturliga grundvattennivåvariationerna är mindre i berget men styrs också de i huvudsak av de årliga variationerna i nederbörd och evapotranspiration. De förhållanden som råder i den norra delen av den tektoniska linsen, där grundvattennivån i berget ligger lägre än i jordlagren, betyder att grundvattenflödet här har en nedåtriktad komponent och därmed en flödesriktning från moränen till berget.

En trolig förklaring till de uppmätta låga grundvattennivåerna i observationshålen i berget i den tektoniska linsen är att borrhålen korsar en eller flera av de högkonduktiva horisontella till subhorisontella sprickzoner som påvisats i det ytliga berget. Det högtransmissiva ytliga berget dränerar både vatten som kommer uppifrån och nerifrån. Tillgängliga data indikerar att de flödessystem som involverar berget inte har några utströmningsområden i den norra delen av den tektoniska linsen utan att utströmningen sker till havet. De enda tillfällen då data från vissa punkter i det här området visar en kontinuerlig uppåtriktad gradient är under torra somrar när grundvattennivån i jordlagren kan sjunka under nivån i berget.

Det är intressant att konstatera att sjönivån och grundvattennivån i moränen i mitten av Bolundsfjärden är avsevärt högre än grundvattennivåerna i berget under sjön (uppmätta i borrhål HFM32). Nivåerna är lägst i de två djupaste sektionerna av HFM32. Nivåskillnaden mellan dessa två sektioner är liten men efter densitetskorrektion av uppmätta trycknivåer har den näst djupaste sektionen lägst nivå, vilket visar att sprickorna i denna sektion dränerar vatten såväl uppifrån som nerifrån. Vid en provpumpning av ett borrhål i berg ca 500 m bort erhölls de starkaste responserna i de djupaste två sektionerna, men de var tydliga också i de två övre sektionerna och i moränen.

Borrhålet HFM32 har den lägsta grundvattennivån av alla berghål runt Bolundsfjärden. Det är bara i borrhålen vid inloppet till kylvattenkanalen och på SFR-halvön som lika låga eller lägre grundvattennivåer periodvis har uppmätts. Grundvattennivån i HFM32 var lägre än havsnivån under sommaren 2006. Två möjliga, kanske överlagrande, orsaker till detta är att (i) grundvattennivåerna i berget indirekt påverkas av att grundvattennivån i jordlagren sänks genom evapotranspiration vilket i sin tur medför ett uppåtriktat vattenflöde från berget, och/eller (ii) borrhålet påverkas av pumpningen i SFR (ca 6 L/s).

En påverkan från evapotranspirationen kräver att att grundvattennivån i berget ligger ovanför bergets överyta vilket är fallet i de lågt liggande områdena runt Bolundsfjärden. De hydrogeologiska simuleringarna med MIKE SHE, vilka baseras på i fält mätta parametrar, visade en tydlig uppåtriktad flödesgradient från berget till jordlagren i den littorala zonen runt Bolundsfjärden under den torra sommaren 2006. En påverkan från pumpningen i SFR kräver en god hydraulisk kontakt med SFR. En provpumpning i borrhål HFM33, omedelbart väster om SFR, gav snabba och tydliga responser i platsundersökningsborrhål som ligger ca 1,5 km SV om pumpbrunnen. Provpumpningar i HFM14 har också visat på snabba och tydliga responser i andra bergborrhål på stort avstånd (ca en kilometer bort), vilket konfirmerar den höga transmissiviteten och den låga specifika magasinskoefficienten i det ytliga berget. Den rådande situationen, med generellt låga grundvattennivåer i det ytliga berget i den norra delen av den tektoniska linsen, kan delvis orsakas av pumpningen i SFR. Definitiva slutsatser gällande detta kan dock inte dras baserat på existerande underlag.

Relationerna mellan sjöarnas vattennivåer och grundvattennivåerna indikerar att bottensedimenten, den underliggande moränen och/eller det övre berget har låga vertikal hydrauliska konduktiviteter. Om det hade varit god kontakt mellan yt- och grundvattnet skulle inte de påvisade förhållandena med en grundvattennivåavsänkning under sjöarna orsakad av evapotranspiration eller snabba och omfattande avsänkningar från provpumpningar som sprids under Bolundsfjärden och havet kunna uppstå. Generellt verkar flödessystemen kring sjöarna att vara komplexa. Grundvattenkemin under sjöarna indikerar ett mycket begränsat flöde eftersom relikt marint vatten påträffats.

Vid grundvattensimuleringarna med MIKE SHE var det generellt problem med för höga simulerade grundvattennivåer i berget medan det var god överensstämmelse mellan mätta och simulerad grundvattennivåer i jordlagren. Det var också omöjligt att på ett bra sätt simulera avsänkningarna från provpumpningarna i HFM14 med den först använda parameteruppsättningen. För att lösa dessa problem gjordes flera testsimuleringar med olika kombinationer av ökad horisontell hydraulisk konduktivitet i berget och minskad vertikal hydraulisk konduktivitet i berget och i jordlagren, liksom med minskad specifik magasinskoefficient jämfört med de data som erhölls från bergmodelleringen.

Resultatet av dessa tester var att den specifika magasinskoefficienten måste minskas jämfört med de inledningsvis ansatta värdena (som låg i intervallet $1 \cdot 10^{-7}$ m^{-1} till $1 \cdot 10^{-5}$ m^{-1}) för att erhålla en god passning mellan mätta och simulerade responser från provpumpningarna. I den slutligt kalibrerade modellen användes värdet $5 \cdot 10^{-8}$ m^{-1}. Därutöver var det också nödvändigt att öka den horisontella hydrauliska konduktiviteten i de horisontella sprickzonerna, som de var ansatta i den övre delen av berget, med en faktor 10 och samtidigt minska den vertikala hydrauliska konduktiviteten i de övre 200 m av berget med en faktor 10 för att få en god passning mellan mätta och simulerade responser.

Problemet med de generellt för höga grundvattennivåerna i berget kvarstod dock till stora delar även efter att de ovan beskrivna ändringarna gjorts. Som ett slutligt test inkluderades därför pumpningen i SFR i simuleringarna genom en brunn med ett vattenintag mellan ca 40 och 140 m djup. Denna sänka förbättrade överensstämmelsen mellan mätta och simulerade grundvattennivåer i berget drastiskt; det absoluta medelfelet och medelfelet minskade från 0,68 m till 0,41 m respektive från –0,65 m till –0,05 m (negativt medelfel indikerar för höga simulerade nivåer). I de flesta borrhålen var medelfelet ca ± 0,2 m. Av borrhålen i norra delen av den tektoniska linsen var det bara HFM16 och HFM32 hade väsentligt större fel med en överskattning respektive underskattning av nivåerna med ca en meter.

Simuleringar med partikelspårning utfördes med den slutligt kalibrerade MIKE SHE-modellen. När partiklar släpptes på ca 140 m djup i det planerade förvarsområdet var det endast 10 % av partiklarna som hade lämnat modelvolymen efter 300 år och alla dessa partiklar hade transporterats till havet. När SFR-pumpningen inkluderades i motsvarande simulering transporterades 18 % av partiklarna till denna sänka medan resten av partiklarna var kvar i modellen. I båda fallen koncentrerades partiklarna till en sprickzon på 110 m djup och den horisontella transporten dominerade. Ovanför denna nivå var det endast enstaka modellceller som passerades av en partikel. När pumpningen i SFR inkluderades var det inga partiklar som nådde ovanför nivån 70 m under havets nivå. Inga partiklar transporterade alltså till ytan. Utan pumpning i SFR nådde ett fåtal partiklar havet nära strandkanten.

Eftersom så många partiklar var kvar i modellen efter 300 års simulering gjordes en ytterligare simulering för en tidsperiod av 5 000 år. Transporttiderna var långa och efter 5 000 år var fortfarande 81 % av partiklarna kvar i modellvolymen. Inga partiklar hade nått ytan på land utan alla partiklar som lämnat modellen hade transporterats till havet. Det kunde också konstateras att 5 % av de introducerade partiklarna hade fastnat i de marina sedimenten. Utöver dessa partiklar fanns inga partiklar i det översta beräkningslagret utan alla partiklar som var kvar i modellen efter 5 000 år fanns djupare ner i berget mellan lager 8 och lager 14, d v s mellan 110 och 600 m under havets nivå.

Resultaten från partikelspårningen är intressanta och ger underlag för fortsatta analyser men de skall tolkas med stor försiktighet. Resultaten beror till stor del på geometrin och de hydrauliska egenskaperna hos de relativt ytliga geologiska strukturer som har implementerats på ett mycket förenklat sätt i modellen.

Vattenbalansen från MIKE SHE-modelleringen beräknades för fyraårsperioden september 2003–augusti 2007 för landdelen av modellområdet. Den årliga nederbörden var 533 mm och den årliga verkliga evapotranspirationen 405 mm. Den årliga interceptionen var 122 mm, transpirationen 169 mm och avrinningen 144 mm. Infiltrationen till den omättade zonen var 351 mm/år medan grundvattenbildningen från den omättade zonen till grundvattenzonen var 124 mm/år. Flödet till modellens näst översta beräkningslager, på 2,5 m djup, var ca 45 mm/år. I detta lager finns många lokala in- och utströmningsområden och 41 mm/år flödade tillbaka till det översta beräkningslagret. Endast ca 11 mm/år strömmade ner till det översta berglagret. Det uppåtriktade flödet från berget till jordlagren var 8–9 mm/år, vilket betyder att det nedåtriktade nettoflödet var endast 2–3 mm/år.

Det omfattande undersöknings- och mätprogrammet utgör en god grund för den konceptuella modellen avseende platsundersökningsområdets hydrologi och ytnära hydrogeologi. Det kvarstår dock några osäkerheter gällande interaktionen mellan det djupa och ytnära grundvattnet och ytvattnet som är viktiga för förståelsen av systemet:

- Morängrundvattnen under Eckarfjärden, Gällsboträsket, Fiskarfjärden och Bolundsfjärden har höga salthalter. De hydrogeologiska och hydrokemiska analyserna indikerar att dessa vatten är relikta och av i huvudsak marint ursprung. Ur ett övergripande vattenbalansperspektiv kan vattnen under de centrala delarna sjöarna betraktas som stagnanta. Enligt tolkningarna av de hydrokemiska data har emellertid dessa vatten också svaga signaturer av ett djupt salint vatten. Grova kloridbudgetberäkningar för Gällsboträsksänkan reser också frågan om det finns ett litet uppåtriktat flöde av djupt salint vatten. Ingen definitiv slutsats kan dras från

befintliga data gällande denna nyckelfråga. Bolundsfjärden är dock ett undantag där en tydligt nedåtriktad flödesgradient utesluter möjligheten till en aktiv tillförsel av djupt salint vatten till moränen eller sjön.

- Tillgängliga data indikerar att det inte finns några utströmningsområden för flödessystem som inkluderar djupt berggrundvatten i den norra delen av den tektoniska linsen där slutförvaret planeras. Det kan emellertid inte uteslutas att sådana områden finns. Data indikerar att den rådande nedåtriktade flödesgradienten från jordlagren till berget är starkt beroende av de högtransmissiva horisontella och subhorisontella sprickzonerna i den övre delen av berggrunden och att evapotranspirationen kan ge uppåtriktat flöde under torra sommarförhållanden i vissa områden.
- Data, liksom simuleringarna med MIKE SHE, reser frågan om de rådande grundvattennivåerna i berget, framförallt i den norra delen av den tektoniska linsen, påverkas av pumpningen för dräneringen av SFR (ca 6 L/s). En annan möjlig sänka är den pumpning som görs för dräneringen av kärnkraftsverkets reaktorbyggnader 1 och 2 (ca 1–2 L/s). Dessa sänkor kan påverka de vertikala flödesgradienterna i delar av platsundersökningsområdet och det rekommenderas starkt att denna osäkerhet löses genom kompletterande undersökningar.

Contents

1 Introduction

1.1 Background

The Swedish Nuclear Fuel and Waste Management Company (SKB) has conducted site investigations at two different locations, the Forsmark and Laxemar-Simpevarp areas, with the objective of siting a geological repository for spent nuclear fuel. The investigations were divided into two phases referred to as *Initial site investigation phase* and *Complete site investigation phase*, respectively /SKB 2001/. The results from the investigations at the sites are used as input to the site descriptive modelling. A *Site Descriptive Model (SDM)* is an integrated description of the site and its regional setting, covering the current state of the geosphere and the biosphere as well as ongoing natural processes of importance for long-term safety. The SDM shall summarise the current state of knowledge of the site, and provide parameters and models to be used in further analyses within Safety Assessment, Repository Design and Environmental Impact Assessment.

The first steps of the site descriptive modelling of the Forsmark area were taken with versions 0, 1.1 and 1.2 of the Forsmark site descriptive model reported in /SKB 2002, 2004, 2005a/, respectively. The final SDM, which is version 2.3 in the series of SDM's produced, is based on data available up to March 31, 2007. This SDM is designated "SDM-Site Forsmark" to mark that it provides the Forsmark site data to be used within the SR-Site safety assessment. The present report on hydrology and near-surface hydrogeology is a background report to SDM-Site Forsmark.

Forsmark is located in the municipality of Östhammar in eastern central Sweden, c. 120 km north of Stockholm. The location of the Forsmark site investigation area and the surface areas covered by the site descriptive models are shown in Figure 1-1. Specifically, models are developed on a regional scale (hundreds of square kilometres) and on a local scale (tens of square kilometres). These model areas include the candidate area, within which most of the deep rock boreholes are located.

1.2 Physiographic setting

The regional model area shown in Figure 1-1 includes a part of Öregrundsgrepen, which is a part of the Baltic Sea. The land area within the site investigation area is characterized by a low relief with a small-scale topography. The study area is almost entirely below 20 m RHB70, see Figure 1-2.

There is a relatively strong west-east gradient in precipitation in the region. The highest precipitation occurs some distance inland from the coast. For example, the mean annual precipitation at Lövsta, c. 15 km inland, is 690 mm, which can be compared with the corresponding value of 492 mm measured on the island of Örskär, c. 15 km northeast of the study area. These values are mean values for the period 1994–2006 obtained from the Swedish Meteorological and Hydrological Institute (SMHI) and stored in the SKB Sicada database. The precipitation data are corrected for wind losses etc by 9% and 16% for Lövsta and Örskär, respectively, according to /Wern and Jones 2006/. Some 25–30% of the annual precipitation falls in the form of snow. The locations of the meteorological stations are shown in Figure 2-2 below.

From regional data the mean annual precipitation in the Forsmark site investigation area has been estimated to 559 mm for the period 1961–1990 by SMHI, see Appendix 1. The average corrected precipitation for 2004–2006 at the two stations within the site investigation area was 537 mm/year. During the same period the potential evapotranspiration was calculated to 509 mm/year based on data from the two same stations. The winters are slightly milder at the

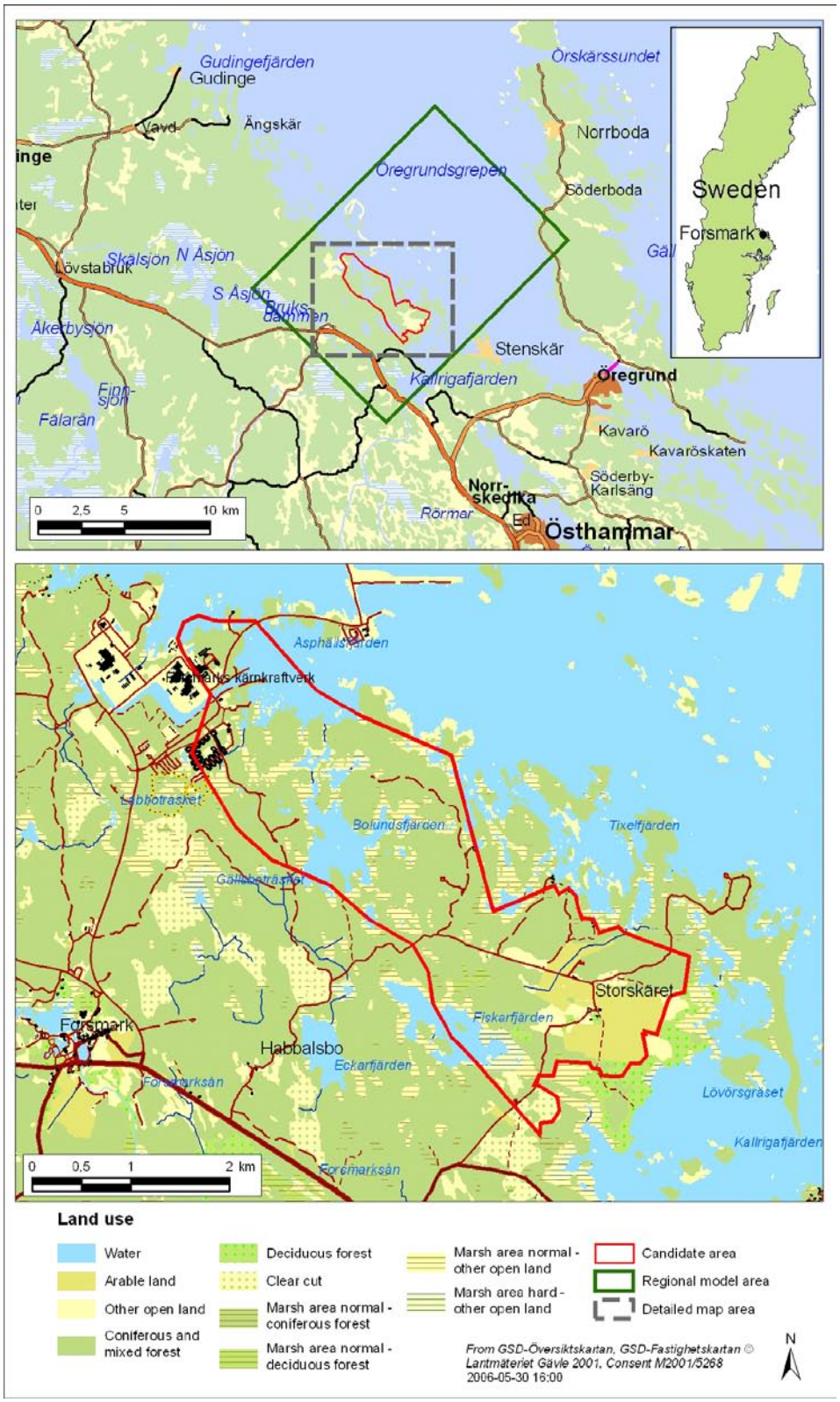

Figure 1-1. *Overview of the Forsmark area and identification of the regional model area and the candidate area.*

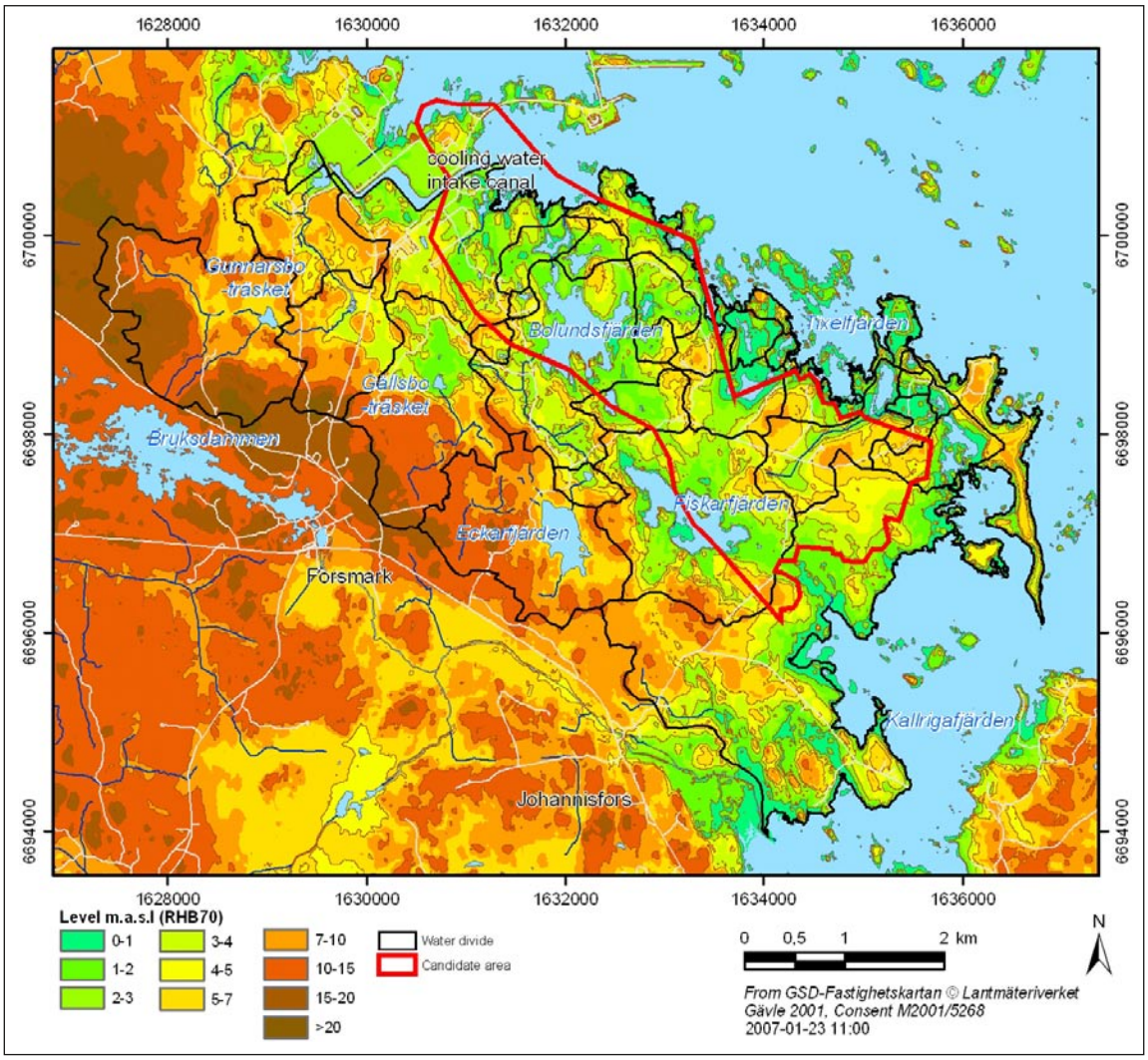

Figure 1-2. *Topographical map of the candidate area and its surroundings with surface water divides indicated.*

coast than inland. The mean annual temperatures at Örskär and Films kyrkby were 5.5 and 5.0°C, respectively for the period 1961–1990. During 2004–2006 the mean annual temperatures were higher, 7.1, 6.9 and 6.1°C at Örskär, Forsmark and Films kyrkby, respectively. The vegetative period, defined as the period with daily mean temperatures exceeding 5°C, was approximately 180 days for 1961–1990 compared approximately 210 during 2004–2006. Based on the synoptic observations at Örskär, the mean annual global radiation was calculated to 930 kWh/m^2 for the period 1961–1990. At Forsmark, the mean annual global radiation was 949 kWh/m^2 during 2004–2006.

As described by /Brunberg et al. 2004/, 25 “lake-centered” catchments and sub-catchments have been delineated, ranging in size from 0.03 km^2 to 8.67 km^2. Forest is dominating and covers approximately 70% of the total catchment areas. Only in the southeast, at Storskäret, agriculture is an important landuse, see Figure 1-1. The main lakes are Lake Fiskarfjärden (0.752 km^2), Lake Bolundsfjärden (0.609 km^2), Lake Eckarfjärden (0.282 km^2) and Lake Gällsboträsket (0.185 km^2). The lakes are shallow with mean depths and maximum depths ranging from approximately 0.1 to 0.9 m and 0.4 to 2.2 m, respectively /Brunberg et al. 2004/. Sea water flows into the most low-lying lakes during events of high sea water levels.

No major water courses flow through the catchment areas delineated in Figure 1-2. The brooks downstream Lake Gunnarsboträsket, Lake Eckarfjärden and Lake Gällsboträsket carry water most of the year, but can still be dry for long time periods during dry summers and early autumns such as in 2003 and 2006. Many brooks in the area have been deepened for considerable distances for draining purposes. However, the riparian zones are still wide at many locations and relatively large areas are inundated during periods of high water flows. Surface discharge is measured at four stations within the site investigation area. If the full 3-year period of April 15, 2004 until April 14, 2007, for which discharge measurements are available from the station with the largest catchment is considered, the corrected mean precipitation was 546 mm/year while the mean specific discharge of the largest catchment of 5.6 km^2 was 154 mm/year.

From a comparison of groundwater and surface water levels at the start and end of the period it can be concluded that the these storages were a little smaller at the end of the period but only corresponding to a difference of c. 5 mm/year. The mean precipitation was 13 mm/year lower than the 30-year normal precipitation estimated by SMHI (see Appendix 1). Since approximately 2/3 of the precipitation goes to evapotranspiration, the precipitation deficit should correspond to a discharge deficit of approximately 5 mm/year. These estimates of storage changes and precipitation deficit indicate that the measured 3-year mean discharge should be close the longterm normal discharge. A rough estimate of the longterm overall water balance of the area is then as follows: P (precipitation) = 560 mm/year, ET (actual evapotranspiration) = 400–410 mm/year, and R (runoff) = 150–160 mm/year.

Wetlands are frequent and cover more than 25% of some sub-catchments /Johansson et al. 2005/. Bogs are found in the most elevated parts of the area only. These bogs are small and the peat cover is not very thick (< 3 m) /Fredriksson 2004/. Fens and marshes are frequent in the more low-lying parts of the area. The peat in the wetlands can rest directly on till, or be underlain by gyttja and/or sand and clay above the till. This means that the hydraulic contact with the surrounding groundwater system varies among the wetlands in the area.

A map of the Quaternary deposits in the central terrestrial part of the site investigation area is shown in Figure 1-3. From this map, it is obvious that till is the dominating Quaternary deposit, covering approximately 75% of the terrestrial area. Bedrock outcrops are frequent, but constitute only approximately 5% of the area. Wave-washed sand and gravel, clay, gyttja clay and peat

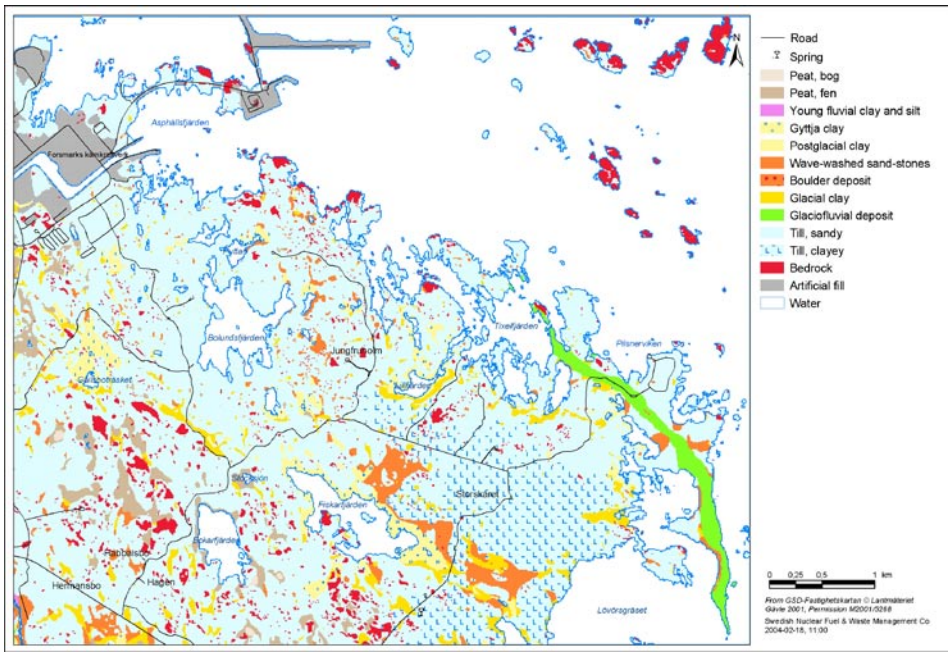

Figure 1-3. *Detailed map of Quaternary deposits /Sohlenius et al. 2004/.*

cover 3–4% each. The only glaciofluvial deposit, the Börstilåsen esker, runs in a north-south direction along the coast (cf. the "green belt" on the map, Figure 1-3). The Quaternary deposits are shallow, usually less than 5 m deep /Hedenström et al. 2008/. The greatest depth to bedrock recorded in a drilling southeast of Lake Fiskarfjärden was 16 m.

The hydraulic properties of the till are mainly determined by the grain size distribution, the compactness, and structures such as lenses of sorted material. From generic and site-specific data it is known that in the uppermost part of the till, the hydraulic conductivity and specific yield are much higher than further down the profile, see e.g. /Lind and Lundin 1990, Lundin et al. 2005/. This is mainly due to soil forming processes, probably with ground frost as the single most important process, resulting in higher porosity and formation of macro-pores. However, wave washing also implies that the till at exposed locations is coarser at the ground surface, and at some locations coarse out-washed material has been deposited.

Based on generic and site specific data, the saturated hydraulic conductivity in the uppermost part of the till can be estimated to 10^{-5}–10^{-4} m/s and the specific yield to between 10 and 20%, with the higher values close to the surface. The total porosity can typically be estimated to 30–40% mainly depending on depth. Below the depth interval strongly influenced by the soil forming processes, the hydraulic conductivity and the porosity of the till are considerably lower. The results from the slug tests indicate a higher hydraulic conductivity at the Quaternary deposit/bedrock interface than in the till itself, with geometric mean values of $1.2 \cdot 10^{-5}$ m/s and $1.3 \cdot 10^{-6}$ m/s, respectively (see section 3.4.1 of the present report). From site specific and generic data, the total porosity and specific yield of the till below the upper c. 0.5 metre can be estimated to 20–30% and 2–5%, respectively /Johansson 1987ab, Lundin et al. 2005/. The hydraulic conductivity values given for till below the uppermost c. 0.5–1 m are horizontal conductivities. The site-specific measurements indicate a K_h/K_v-ratio of approximately 30 below this depth (see section 3.4.1).

For the only glaciofluvial deposit in the area, the Börstilåsen esker, the obtained hydraulic conductivity of $2 \cdot 10^{-4}$ m/s is relatively low, and the storativity of $2 \cdot 10^{-3}$ indicates mainly confined conditions /Werner et al. 2004/. Site-specific hydraulic data for clay, gyttja and peat are relatively sparse /Johansson 2004, Werner and Lundholm 2004a, Alm et al. 2006/. However, the available data indicate a horizontal hydraulic conductivity of c. $3 \cdot 10^{-7}$ m/s below the uppermost 0.5–1 m of the soil profile for all three deposits. Also for these deposits a K_h/K_v-ratio of approximately 30 was obtained.

The stratigraphy of bottom sediments in lakes has been investigated, and typical profiles have been identified for some of the lakes /Hedenström 2003, 2004a, Vikström 2005/. Typically, the sediment stratigraphy from down and up is glacial and/or postglacial clay, sand and gravel, and nested layers of gyttja in different fractions. The clay layer is missing in parts of the area below Lake Bolundsfjärden. However, pumping tests in the vicinity of this lake still indicate a very limited hydraulic contact between the lake and the groundwater in till below the lake /Werner and Lundholm 2004a, Gokall-Norman and Ludvigson, 2007ab/.

The bedrock hydrogeology reveals a significant hydraulic anisotropy within the tectonic lens, which covers the body of the candidate area. The upper c. 150 m of bedrock contains high-transmissive horizontal fractures/sheet joints. These fractures/sheet joints occur at different elevations in the percussion drilled boreholes, but are found to interconnect hydraulically across large distances (2 km). The bedrock in between the horizontal fractures/sheet joints, however, is considerably less conductive (hydraulic conductivity c. $1 \cdot 10^{-11}$ –$1 \cdot 10^{-8}$ m/s) except where it is intersected by transmissive steeply-dipping or gently-dipping deformation zones.

Below the uppermost c. 150 m of bedrock there are no high-transmissive horizontal fractures/sheet joints and the conductive fracture frequency becomes very low and the fractures fairly low-transmissive. In some of the 1,000 m deep cored boreholes there are almost no flowing fractures observed below c. 150 m depth

1.3 Objectives and scope

The general objectives of the site descriptive modelling of the Forsmark area and the specific objectives of the SDM-Site modelling are presented in the SDM-Site Forsmark report /SKB 2008/. The present report is a background report describing hydrology and near-surface hydrogeology in support of the SDM-Site model. Concerning these disciplines, it may be noted that they were covered by a background report also in the Forsmark version 1.2 modelling /Johansson et al. 2005/ and that analyses and presentations based on meteorological, hydrological and hydrogeological monitoring data have been reported separately in both the 2.1 and 2.3 modelling stages /Juston et al. 2007, Werner et al. 2007, Johansson and Öhman 2008/.

The objectives of the data analysis and modelling reported in this document are to:

- present and analyse data available in the Forsmark 2.3 dataset,
- update the conceptual and descriptive model presented in model version Forsmark 1.2 /SKB 2005a/,
- present the results of the quantitative surface water and near-surface groundwater modelling performed in order to support the site description,
- summarise and present the results in the form of an updated site description of hydrology and near-surface hydrogeology including a discussion of uncertainties.

After Forsmark model version 1.2 was produced, a considerable amount of new site-specific data concerning meteorology, hydrology and near-surface hydrogeology have become available, including information from additional discharge gauging stations, groundwater level monitoring wells in Quaternary deposits and hydraulic tests. Furthermore, an additional 32 months of time series data from monitoring points already existing at the data freeze of model version Forsmark 1.2 (July 31, 2004) were available at the time for the Forsmark 2.3 data freeze (March 31, 2007). Extensive new datasets are also available from other disciplines of the site investigation, including geology, deep-rock hydrogeology, and hydrogeochemistry.

The updated site description presented in this report should give supporting information on meteorology, hydrology and near-surface hydrogeology primarily to the following related activities:

- the deep-rock groundwater modelling (upper boundary condition and hydraulic properties of the Quaternary deposits),
- the ecosystem modelling (the water balance and its components),
- the SR-Site safety assessment (hydrogeological parameters and flow modelling results used as direct inputs to dose models),
- other transport modelling performed to support site descriptive and safety assessment modelling,
- the Environmental Impact Assessment (flow model and hydrological-hydrogeological data for use in the assessment of hydrological-hydrogeological effects and their consequences).

1.4 Methodology, terminology and organisation of work

1.4.1 Methodology

The overall methodology of the modelling of hydrology and near-surface hydrogeology is presented in Figure 1-4. As reflected in the present report, a relatively strong emphasis was put on the evaluation of field data from the site, especially the relations between different types of monitoring (time series) data, and the construction of a conceptual model based on site data. This conceptual model was then tested by flow modelling resulting in the final hydrological-hydrogeological site description.

A preliminary conceptual model, mainly based on the data gathered and analysed in the Östhammar pre-study /Follin et al. 1996, SKB 2000/, was the starting point for the design of the investigation

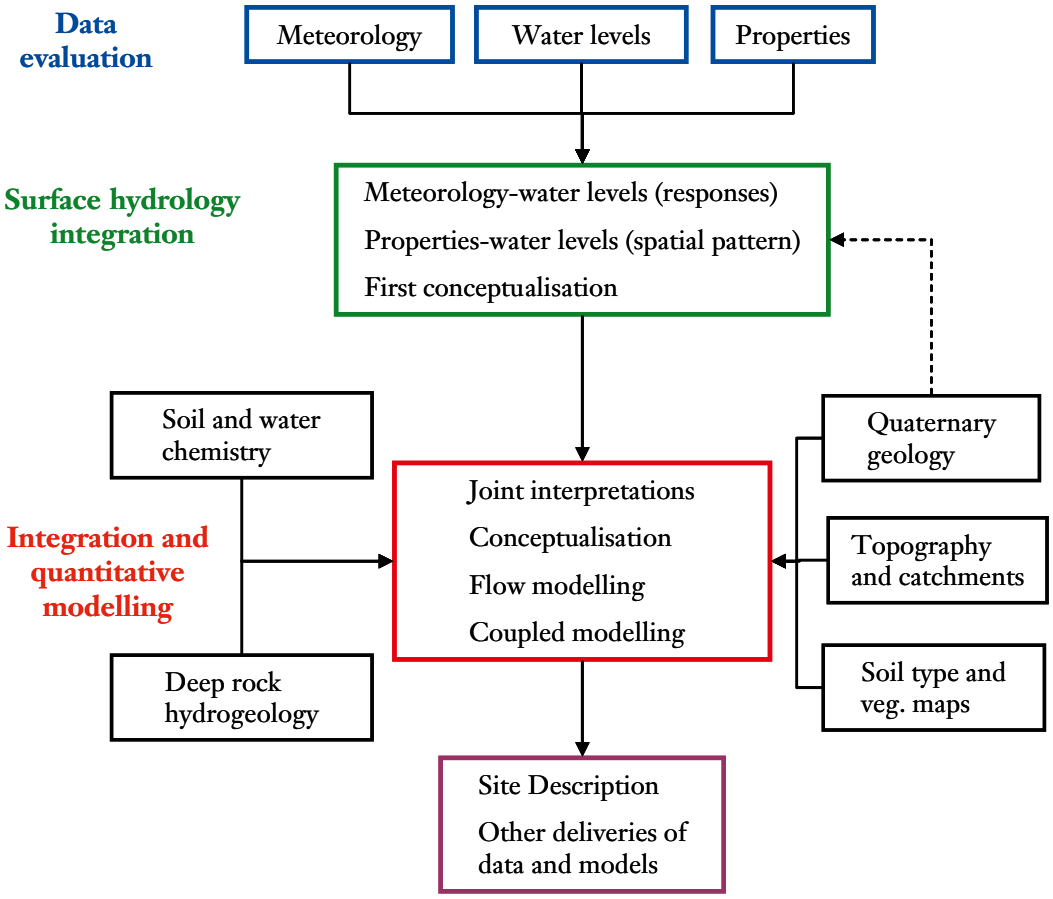

Figure 1-4. *Overall description of the methodology of the hydrological and near-surface hydrogeological modelling work performed within the Forsmark site investigation /Johansson et al. 2005/.*

programme /SKB 2001/. The successive data evaluations and modelling coupled to the data freezes applied in the site investigation methodology, and input from internal and external reviews, have resulted in revisions and additions to the originally proposed programme /SKB 2005b/.

The data evaluation presented in this report includes meteorological data, surface water levels and discharge, groundwater levels, and properties of the involved hydraulic domains. These data sets were first evaluated separately and then subject to an integrated analysis. This integrated analysis, supported by data from related site investigation disciplines and generic data, formed the basis for the elaboration of a site-specific conceptual and descriptive model followed by quantitative flow modelling. The procedure has been iterative and repeated for the different model versions.

1.4.2 Terminology

Main hydrological and hydrogeological definitions

/Rhén et al. 2003/ established the terminology to be used within the site descriptive hydrogeological modelling. The *conceptual model* should define the framework in which the problem is to be studied, the size of the modelled volume, the boundary conditions, and the equations describing the processes. The (hydrogeological) *descriptive model* defines, based on a specified conceptual model, geometries of domains and parameters assigned to these domains.

Since the term "hydrology" often refers to all aspects of the hydrological cycle, i.e. atmospheric, surface and subsurface processes and parameters, it should be noted that the following distinction is made between "hydrology" and "hydrogeology" in the data handling within SKB's site investigation programme:

- *Hydrology* refers to the surface water system only; hydrological data include surface water divides and the associated catchments and sub-catchments and water levels and flow in water courses and lakes.
- *Hydrogeology* refers to the subsurface system, i.e. the water below the ground surface, including the unsaturated and saturated parts of the subsurface; hydrogeological data include groundwater levels and hydraulic parameters for unsaturated and saturated flow.

Thus, the terminology is clear as far as the input data are concerned; hydrological data are obtained on the ground surface and in surface waters, and hydrogeological data from the subsurface, primarily from drillings and observation wells (sampling for analysis of hydraulic properties has also been made in pits and trenches).

In the site descriptive modelling it was found practical to make a distinction between *near-surface* and *deep-rock (bedrock) hydrogeology*. The main reason was the high resolution in time and space needed in the description of the surface and near-surface system. Shallow flow paths dominate the water balance of the area and data from this part of the system are important for the ecosystem modelling. The surface water and groundwater interaction is a main issue of the near-surface hydrogeology.

Obviously, there is an overlap between "near-surface" and "deep rock" hydrogeological models, since they must incorporate components of each other in order to achieve an appropriate parameterisation and identification of boundary conditions. In the present report, groundwater level data from the percussion-drilled boreholes, i.e. from the upper highly transmissive c. 150 m of the bedrock is included. For a detailed conceptual and descriptive model of the shallow as well as the deep bedrock the reader is referred to /Follin et al. 2007a/.

In the different disciplines of the site investigation, several terms for the unconsolidated deposits overlying the rock are used, such as *Quaternary deposits, overburden, soil, regolith* and *hydraulic soil domain (HSD)*. In this report, the term *Quaternary deposits*, often abbreviated as *QD*, is used when discussing and describing the unconsolidated deposits. Other terms, e.g. soil and HSD, are here used for more specific purposes.

In SKB's systems approach to hydrogeological modelling three hydraulic domains/flow domains are defined, (*i*) hydraulic soil domains (HSD), (*ii*) hydraulic conductor domains (HCD), and (*iii*) hydaulic rock domains (HRD). For surface water the flow domains are (i) overland flow, (ii) water courses, (iii) lakes, and (iv) the sea. Wetlands are described separately in the report but are not considered as a separate flow domain.

Groundwater recharge is defined as "Process by which water is added from outside to the zone of saturation of an aquifer, either directly into a formation, or indirectly by way of another formation" /UNESCO 1992/. A *groundwater recharge area* may be defined as an area where water flows from the unsaturated zone to the saturated zone or from a groundwater flow perspective, as an area where the shallow groundwater flow has a downward flow component. In the same way a *groundwater discharge area* may be defined as an area where water leaves the saturated zone or from a groundwater flow perspective as an area where the groundwater flow has an upward component /Grip and Rodhe 1985/.

In the present report the definitions of groundwater recharge and discharge areas as areas where groundwater has a downward and upward flow component, respectively, is adopted. Groundwater is very shallow in large parts of the site investigation area meaning that vegetation water uptake take place from the groundwater zone, directly or indirectly by inducing capillary rise, especially during periods of dry conditions. Under such conditions these areas, from the definition used, will be characterised as groundwater discharge areas.

There are no major water courses in the central part of the site investigation area. The term *brook* is used for the small, mainly natural water courses appearing whereas the term *ditch* is used for man-made features dug for draining purposes.

Groundwater head definitions in variable-density systems

The term *groundwater level* is used as a common term for the position of the groundwater table in unconfined aquifers and the potentiometric head in confined aquifers. However, due to considerable differences in groundwater salinity with depth and thereby in density, the measured groundwater levels in some of the bedrock boreholes should be regarded as point water heads. For a correct interpretation of groundwater flow gradients, point water heads should be re-calculated to fresh water heads (for the horizontal flow component) or to environmental water heads (for the vertical flow component) /Lusczynski 1961, Post et al. 2007/. A short summary of the theory of the transfer of point water heads to fresh water heads and environmental water heads is presented below, as well of the methodology adopted in the present report; the summary is extracted from /Juston et al. 2007/.

The illustration in Figure 1-5 shows a groundwater monitoring well, which is open in its lower end. The pressure at the opening is denoted by p_i. The fluid density in the well is constant and has the same value as the density at the point in the aquifer where the opening is. If the groundwater in the aquifer is fresh, the groundwater level (GWL) can be regarded as a fresh water head. In the general case of brackish groundwater of variable density, the groundwater level (GWL) should instead be regarded as a point water head where the height of the water column is determined by the density at the opening at *i*.

The fresh water head at any point *i* in groundwater of variable density is defined as the water level in a well filled with fresh water from *i* to a level high enough to balance the existing pressure at *i*, i.e. p_i. From Figure 1-5 it can be concluded that this pressure is given by $\rho_i\, g\, (H_{ip} - Z_i)$ when the point water head (H_{ip}) and density (ρ_i) at *i* in the well are used. Similarly, the pressure is given by $\rho_f\, g\, (H_{if} - Z_i)$ when the fresh water head at *i* (H_{if}) and the fresh water density (ρ_f) are used. From the equality of these two expressions for the pressure at *i*, the fresh water head may be expressed in terms of the point water head as:

$$\rho_f\, H_{if} = \rho_i\, H_{ip} - Z_i\, (\rho_i - \rho_f),$$

where

ρ_f = density of fresh water,

ρ_i = density of water at *i*,

H_{if} = fresh water head at *i*,

H_{ip} = point water head at *i*,

Z_i = elevation of point *i*; elevation measured positively upward.

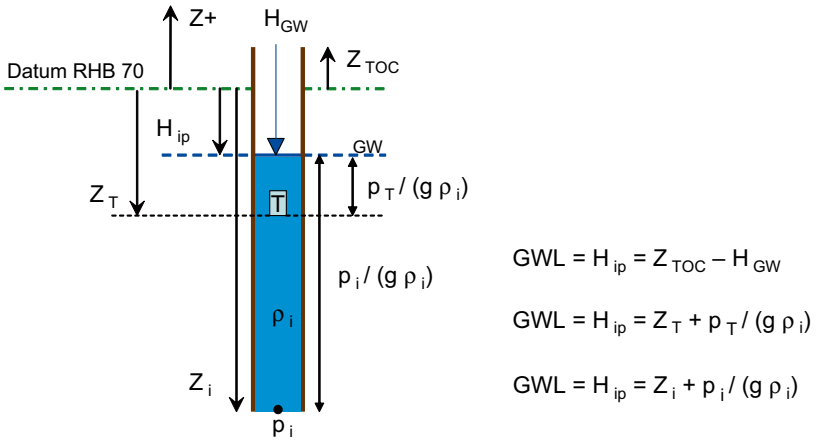

Figure 1-5. *Definition of groundwater level. The pressure at the well opening is denoted by p_i. The fluid density in the well is constant and has the same value as in the in aquifer where the opening is. A pressure transducer (T) is located at elevation Z_T (TOC = top of casing) /Juston et al. 2007/.*

If one wants to understand the prevailing directions of flow in a variable-density groundwater flow system based on head measurements it is necessary to transfer point water heads to fresh water heads and environmental water heads. Fresh water heads are useful for a discussion about the horizontal component of the hydraulic gradients between different points in the horizontal plane, whereas environmental water heads are useful for a discussion about the vertical components of the hydraulic gradients. The relation between fresh water head and environmental water head (H_{in}) is given by

$$\rho_f \, H_{in} = \rho_f \, H_{if} - (\rho_f - \rho_a)(Z_i - Z_r),$$

and the relation between environmental water head and point water head is expressed by

$$\rho_f \, H_{in} = \rho_i \, H_{ip} - Z_i(\rho_i - \rho_a) - Z_r(\rho_a - \rho_f),$$

where

ρ_a = average density of water between Z_r and i, as defined by $\frac{1}{Z_r - Z_i} \int_{Z_i}^{Z_r} \rho \, dz$,

H_{in} = environmental water head at i,

Z_r = elevation of reference point from which the average density of water to point i is determined and above which water is fresh; elevation measured positively upward.

The hydraulic gradient for any point i in groundwater of variable density is

$$\rho_f \, \nabla H_{in} - (Z_i - Z_r)\left[\frac{\partial(\rho_a)}{\partial x}\mathbf{i} + \frac{\partial(\rho_a)}{\partial y}\mathbf{j}\right] = \rho_f \, \nabla H_{if} + (\rho_i - \rho_f)\,\mathbf{k}$$

Along a vertical, the left hand side of the equation reduces to $\rho_f (\partial H_{in}/\partial z)$, which is simply a product of fresh water density and a gradient defined by environmental water heads. Along any horizontal, the right hand side of the equation reduces to $\rho_f (\partial H_f/\partial x)$, which is simply a product of fresh water density and a gradient defined by fresh water heads. Because environmental water heads define hydraulic gradients along a vertical, they are comparable along a vertical, e.g. a borehole with multiple packer sections

Figure 1-6 shows the point water heads and water densities associated with the multiple packer system in the percussion-drilled borehole HFM19 together with the point water head and water density in the nearby monitoring well in the Quaternary deposits, SFM0058 (for locations of the wells see Figures 2-7 and 2-10). HFM19 has three monitoring intervals, HFM19:1-3, where HFM19:1 is the deepest. HFM19:1 to HFM19:3 have transmissivities of $2.8 \cdot 10^{-4}$ m^2/s, $2.2 \cdot 10^{-5}$ m^2/s and $4.2 \cdot 10^{-5}$ m^2/s, respectively.

When the difference in density is large and the borehole sections are long, the way of construction of a continuous density profile may be important for the interpretation of the flow gradients. A sensitivity analysis of three different ways to construct the density profile has been conducted, see Figure 1-6.

In the most common case with the water density continuously increasing with depth, the largest differences between the measured point water head and calculated fresh and environmental water heads are obtained when the densitities are linearly interpolated setting each section's density as a point value at the top of the section. However, in the boreholes analysed in the present report the differences between the different methods for construction of the density profiles are small and of no practical importance. For simplicity only fresh and environmental water heads calculated from constant densities in sections are presented and discussed in this report.

For some wells the influence of the vertical density gradient is so large that the *point water heads* should be transformed to *freshwater and/or environmental water heads* for interpretation of flow directions (see Section 3.4.2 and Appendix 2).

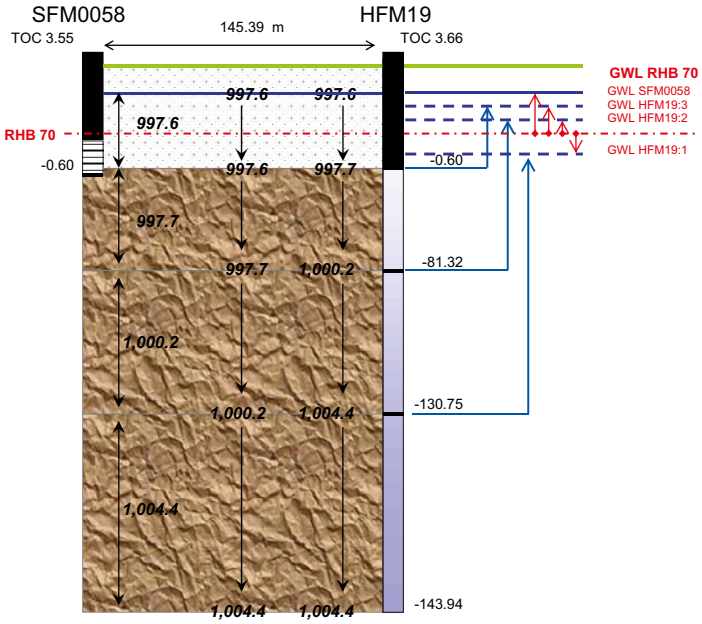

Figure 1-6. *Point water heads and water densities associated with the multiple packer system in the percussion-drilled borehole HFM19 together with the point water head and water density in the nearby monitoring well in the Quaternary deposits, SFM0058. Datum is RHB70. TOC = top of casing. Water densities between packers are treated in three ways; either uniform (constant) between packers (left), linearly increasing between packers with the section's density set at the bottom of the section (middle) or at the top of the section (right) (revised from Juston et al. 2007).*

1.4.3 Organisation of work

The modelling of hydrology and hydrogeology within and related to the surface system has been performed as part of the SurfaceNet project. This project incorporates all site descriptive modelling of the surface system, i.e. both abiotic aspects such as hydrology and hydrogeology, and models of the biotic parts of the system. A project group with representatives for all the surface system modelling disciplines was formed early in the process. Most disciplines have had additional modellers associated with the project group.

The interactions with related modelling disciplines, primarily the hydrogeological and hydrogeochemical modelling of the deep rock, have taken place both by informal contacts and discussions and by participation in project meetings with the HydroNet and ChemNet teams. Interactions between surface and bedrock modelling have also been handled in connection with meetings within the Forsmark site descriptive modelling project (PFM). In a similar manner, the integration and interactions witin the surface system modelling have been taken care of by means of both informal contacts and SurfaceNet project meetings.

The SurfaceNet modelling for SDM-Site Forsmark is reported in /Lindborg (ed.) 2008/. Furthermore, the contents of the present report are used in the overall conceptual and descriptive model of the hydrogeology at Forsmark /Follin et al. 2007a, 2008/. The contents of the SurfaceNet report and the Hydrogeology report are then summarised in the SDM report /SKB 2008/. The structure of the SDM-Site Forsmark reporting is illustrated in Figure 1-7. In this structure, the surface system (SurfaceNet) report is referred to as a "level II" report, whereas the present report is "level III".

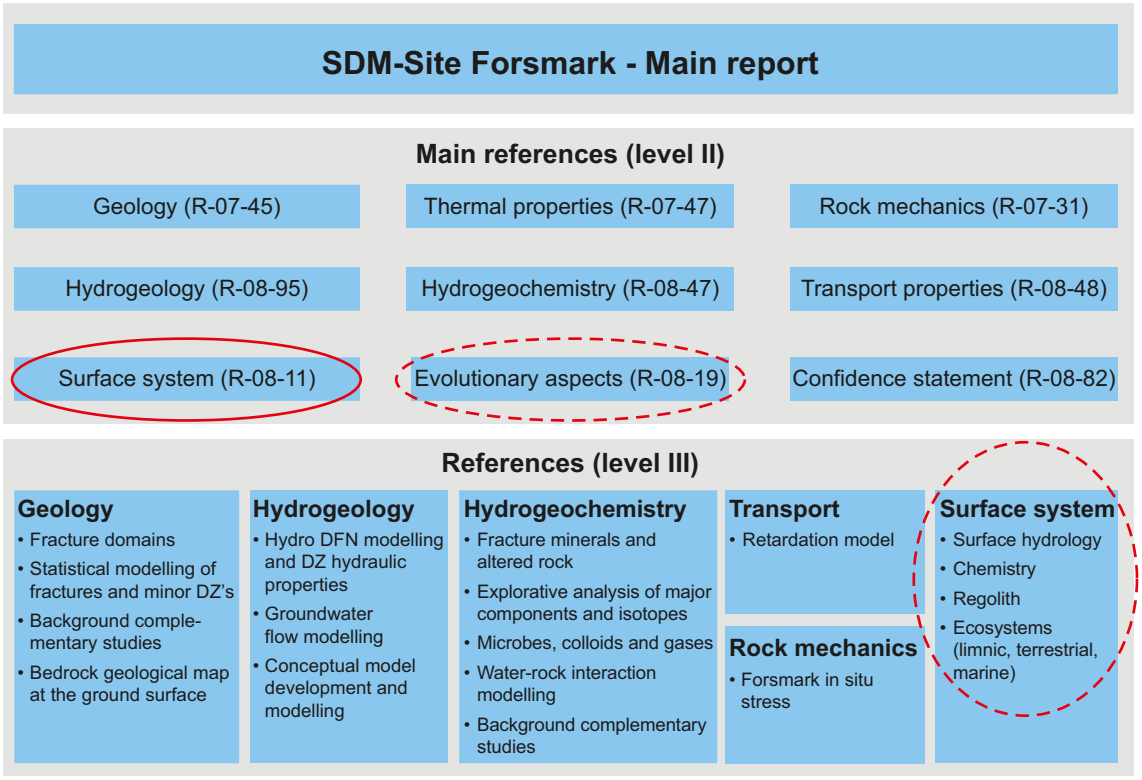

Figure 1-7. *The SDM-Site Forsmark report structure /Lindborg (ed.) 2008/. The present report is a level III report ("Surface hydrology") primarily providing input to the "Surface system" level II report, which, in turn, is one of the main references used in the SDM-Site report.*

1.5 Model structure and contents of report

1.5.1 Structure of SKB hydrogeological models

The present report provides a conceptual and descriptive model of the hydrological and near-surface hydrogeological system of the Forsmark area. The model, based on site-specific, regional and generic data, describes this system and includes quantitative flow modelling.

The model of the system includes descriptions of:

- boundaries,
- flow domains and their interfaces,
- infiltration and groundwater recharge,
- flow systems and discharge.

Figure 1-8 illustrates SKB's systems approach to hydrogeological modelling; this modelling approach is described in detail in the hydrogeological modelling strategy report /Rhén et al. 2003/. The division into three types of hydraulic domains (QD, rock mass, and conductors in rock) constitutes the basis for the quantitative models. From a hydrogeological perspective, the geological data and related interpretations constitute the basis for the geometrical modelling of the different hydraulic domains. Thus, the investigations and documentation of the QD and the bedrock provide input to:

- the distribution of QD (HSD), including genesis, composition, stratification, thickness and total depth,
- the geometry of deterministic fracture zones, or lineaments, if needed (HCD), and the bedrock in between (HRD).

In the present context, where the HSDs are investigated in detail, a further division is made of the near-surface hydrogeology (in terms of domains and interfaces) than shown in Figure 1-8.

A complete conceptual and descriptive model of the hydrology and the hydrogeology at a site involves a description of the integrated (continuous) hydrological-hydrogeological system, i.e. surface waters, groundwater in QD and groundwater in bedrock. The focus of the modelling presented here is on the surface and near-surface conditions. The hydrogeological properties of the bedrock and the lower boundary condition used in the quantitative modelling are therefore just described very briefly in this report and reference is made to /Follin et al. 2007abc and Follin et al. 2008/.

1.5.2 This report and its background reports

The disposition of this report follows the overall disposition of the SDM reports: first, data presentation and evaluation, followed by conceptual, descriptive and quantitative flow modelling, and finally the resulting site description. The database for the conceptual and descriptive model is mainly the data referred to and presented in Chapter 2. In Chapter 3 the overall conceptual and descriptive model is presented as derived from site-specific field observations, and regional and generic data. The hydrological objects/flow domains and their hydraulic interaction are presented and analysed. Examples are also given of supporting evidence from other disciplines of the site investigation.

In Chapter 4 the quantitative flow modelling is presented; this includes the transfer of the conceptual and descriptive model developed in Chapter 3 to quantitative models, description of water modelling tools, presentation and interpretation of modelling results. Furthermore, the results of the quantitative modelling are compared with the conceptual and descriptive model based on field observations, and agreements, deviations and uncertaities are discussed. Finally, the resulting site description is presented in Chapter 5, including identification of remaining important uncertainties.

The present report is associated with a set of background reports where more detailed descriptions of certain parts of the modelling work are given. Specifically, the available data, the data evaluations and the numerical modelling are detailed in background reports, as follows:

- Presentation and evaluation of meteorological, hydrological and hydrogeological monitoring data: SKB R-08-10 /Johansson and Öhman 2008/.
- Numerical modelling of surface water and groundwater flow: SKB R-08-09 /Bosson et al. 2008/.
- Numerical modelling of solute transport: SKB R-08-106 /Gustafsson et al. 2008/.

As indicated above, also data and models from other modelling disciplines are used in the work presented herein. In addition to the hydrogeological background reports to SDM-Site Forsmark referred to above, results from backgrounds reports from other surface system disciplines are referred to in the present report /Tröjbom et al. 2007, Hedenström and Sohlenius 2008, Hedenström et al. 2008, Strömgren and Brydsten 2008/.

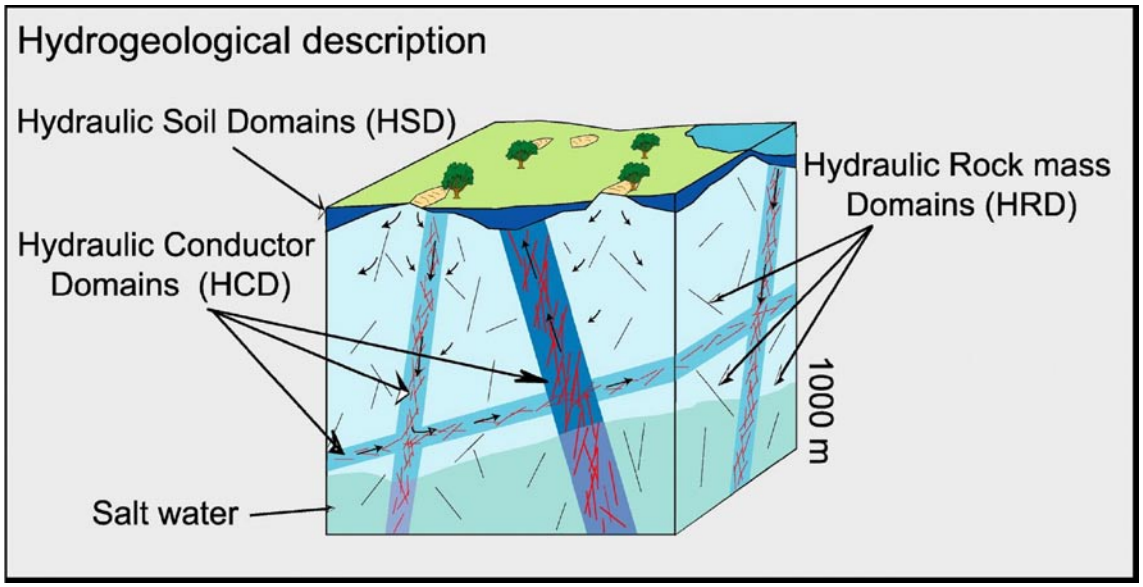

Figure 1-8. *Division of the QD and the bedrock into hydraulic domains representing the QD (HSD) and the rock domains (HRD) between fracture zones modelled as conductor domains (HCD). Within each domain the hydraulic properties are represented by mean values, or by statistical distributions /Rhén et al. 2003/.*

2 Presentation of site investigations and available data

2.1 Previous investigations

Three preliminary site descriptive models (SDM) of the Forsmark area have been presented before the present version: version 0 (F0) /SKB 2002/, version 1.1 (F1.1) /SKB 2004/, and version 1.2 (F1.2) /SKB 2005a/. F0 was developed before the start of the site investigations and was mainly based on data compiled for the Östhammar feasibility study /SKB 2000/ and related background reports. This model was developed at a regional scale and covered a rectangular area, 15 km by 11 km, surrounding the area identified in the feasibility study as favourable for further study. This area was called the Forsmark regional model area.

The information that provided the basis for the F0 model was mainly 2D in nature (surface data) and general and regional, rather than site specific, in character. However, 3D (depth) information was available from boreholes, shafts and tunnels from the construction of the Forsmark nuclear power plant and the underground storage facility for low to medium active radioactive waste (SFR).

Meteorological and hydrological data were compiled from nearby stations operated by the Swedish Meteorological and Hydrological Institute (SMHI) /Lindell et al. 2000, Larsson-McCann et al. 2002/, whereas data on catchments were obtained from /SMHI 1985/ and /Brunberg and Blomqvist 1998/. The description of the Quaternary deposits (QD) in the feasibility study /SKB 2000/ formed the basis for the conceptualisation of the hydrogeology of the QD. However, no site-specific data on hydraulic properties or groundwater levels in the QD were presented in F0.

At the time for the F1.1 data freeze, i.e. April 30, 2003, the site investigations in terms of hydrology and near-surface hydrogeology included:

- delineation of catchment areas in the field in the central parts of the model area,
- manual discharge measurements at 8 locations,
- installation of surface water level gauges, drilling of boreholes and excavation of pits in QD,
- installation of groundwater monitoring wells in QD,
- hydraulic tests (slug tests) in these groundwater monitoring wells.

Local meteorological and hydrological stations were not established before the F1.1 data freeze, and there was no time to collect time series of surface water and groundwater levels. The still very limited amount of site specific data implied that also F1.1 was mainly based on generic and/or regional data regarding meteorology, hydrology and near-surface hydrogeology.

The preliminary SDM version 1.2 was based on data available up to July 31, 2004. Compared with the site specific data available at data freeze F1.1, the following additional meteorological, hydrological and near-surface hydrogeological data were available:

- local meteorological data from two stations,
- surface water and groundwater levels from additional monitoring points and longer time series from monitoring points existing already at data freeze F1.1,
- additional hydraulic tests from pumping wells and monitoring wells.

However, still no local surface discharge data were available. The first surface discharge gauging station was put into operation in April 2004, meaning that the time series was too short to be used in the analysis.

2.2 Overview of meteorological, hydrological and hydrogeological investigations in the Forsmark area

The meteorological, hydrological and near-surface hydrogeological investigations have comprised the following major components:

- establishment of two meteorological stations and collection of meteorological data,
- monitoring of snow depth, snow water content, ground frost and ice cover,
- identification and description of surface water catchments,
- establishment of four surface discharge gauging stations for automatic collection of water level, electrical conductivity, temperature and discharge data,
- survey of lake thresholds, lake bathymetry, and brook gradients and cross-sections,
- installation of surface water level gauges and collection of water level data,
- installation of groundwater monitoring wells and pumping wells in QD and collection of groundwater level data,
- slug tests and pumping tests in wells in QD,
- installation of BAT-type filter tips and permeability tests and pore pressure data collection in the tips.

In addition to the investigations listed above, the modelling in the present report is based on data from the SKB databases Sicada and SKB-GIS on:

- topographical and other geometrical conditions,
- surface-based geological investigations of QD and soil type mapping,
- composition and stratigraphy of QD from boreholes, pits and trenches,
- hydrogeological properties of the bedrock and groundwater levels from the percussion-drilled boreholes,
- soil and water chemistry.

There are five principal datasets of time series used for the modelling presented in this document. Those are time series of meteorological data, surface water levels, surface water discharge, and groundwater levels in the QD and in the bedrock. The installation of instruments to collect these time series has been an ongoing process in the Forsmark site investigation. Figure 2-1 gives an historical overview of the number of available data records for each dataset from January 2003 up to the March 2007 data freeze 2.3, which is the last data freeze providing input data to the SDM-Site modelling.

The short-term variations in the number of available data are due to malfunctions of equipments and specific tests in some wells. It is seen in Figure 2-1 that most of the datasets are fairly stable after an initial build-up phase. The main exception is the “point water head in bedrock” dataset, which increases during most of the investigation period. One reason for this is that early groundwater level data from the rock to large extent are disturbed by various drilling and testing activities, and therefore excluded from the dataset used in the modelling (see Chapter 3).

Table 2-1 gives references to site investigation reports and other sources that have provided the meteorological, hydrological and near-surface hydrogeological data used in the SDM-Site modelling. Table 2-2 lists the corresponding information with respect to other disciplines and types of investigations. The site investigation data are available in SKB’s Sicada and GIS databases.

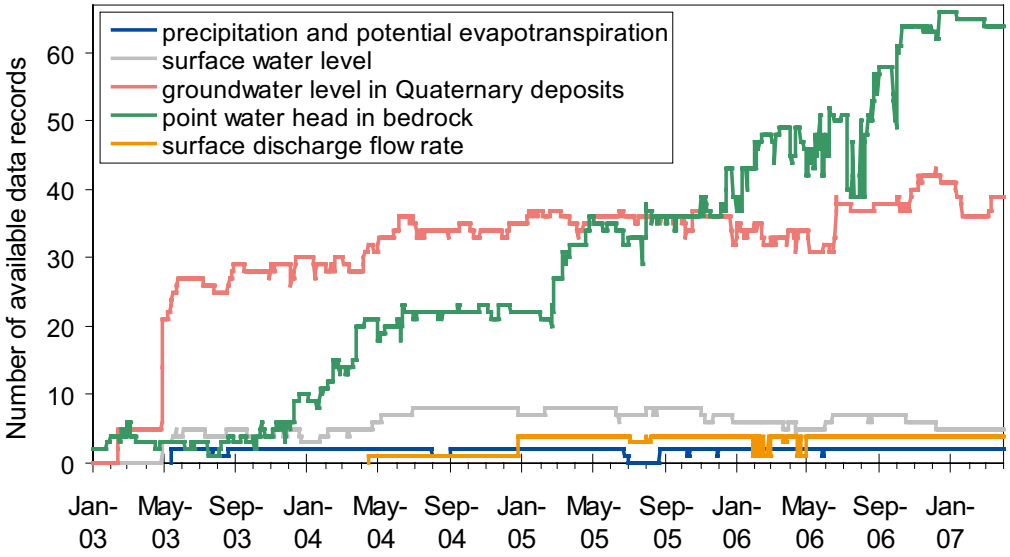

Figure 2-1. *Overview of the availability of data from time series of meteorological data, surface water levels, surface discharge, and groundwater levels in the Quaternary deposits and in the bedrock.*

Table 2-1. Available meteorological, hydrological and near-surface hydrogeological data and their handling in the SDM-Site modelling.

Available site data Data specification	Ref.	Usage in SDM-Site Analysis/Modelling	Cf. Section
Meteorological data			
Regional data			
Precipitation, temperature, wind, humidity and global radiation up to March 2007	/Lindell et al. 2000/ /Larsson-McCann et al. 2002/ /Wern and Jones 2006/ /Wern and Jones 2007ab/ Sicada	Basis for general description and quantitative modelling of surface water and groundwater flow. Comparison with local meteorological data for extention of time series.	1.2 2.2.1 3.5.1 Ch. 4, 5 App. 1
Site Investigation data			
Precipitation, temperature, wind, humidity, global radiation and potential evapotranspiration June 2003 – March 2007 from the meteorological stations at Högmasten and Storskäret	/Juston and Johansson 2005/ /Wern and Jones 2006/ /Wern and Jones 2007ab/ Sicada	Basis for site-specific description of the meterological conditions, and conceptual, descriptive and quantitative modelling of surface water and groundwater flow. Comparison with regional meteorological data for extention of time series.	1.2 2.2.1 3.5.1 Ch. 4, 5
Snow depth, ground frost and ice cover	/Aquilonius and Karlsson 2003/ /Heneryd 2004/ /Heneryd 2005/ /Heneryd 2006/ /Heneryd 2007/	Validation of snow routine in quantitative modelling	2.2.1 3.5.1 Ch. 4, 5
Hydrological data			
Regional data			
Regional discharge data	/Lindell et al. 2000/ /Larsson-McCann et al. 2002/ Sicada	Specific discharge in initial conceptual, descriptive and quantitative modelling	

Available site data Data specification	Ref.	Usage in SDM-Site Analysis/Modelling	Cf. Section
Site Investigation data			
Geometric data on catchment areas, lakes and water courses	/Brunberg et al. 2004/ /Brydsten and Strömgren 2005/ SKB GIS	Delineation and characterisation of catchment areas and lakes, geometrical input to the MIKE SHE modelling	1.2 2.2.2 3.3.1 3.3.2 3.3.3 Ch. 4, 5
Installation of automatic discharge gauging stations	/Johansson 2005a/	Basis for measurements of discharge, electrical conductivity and temperatures at four locations in brooks	2.2.2 3.3.3
Automatic discharge measurements	/Johansson and Juston 2007/ Sicada	Data for site-specific description and water balance, conceptual and descriptive modelling, and for calibration of quantitative water flow modelling	1.2 2.2.2 3.3.3 3.5.3 Ch. 4, 5
Manual discharge measurements	/Nilsson et al. 2003/ /Nilsson and Borgiel 2004/ /Johansson 2005b/ /Nilsson and Borgiel 2005a/ /Nilsson and Borgiel 2007/ Sicada	General description of temporal variability in surface water discharge	
Installation of surface water level gauges	/Johansson 2003/ /Werner and Lundholm 2004b/	Basis for surface water level measurements	2.2.2
Level measurements in lakes and the sea	/Nyberg et al. 2004/ /Nyberg and Wass 2005/ /Nyberg and Wass 2006/ /Nyberg and Wass 2007/ Sicada	Surface water-groundwater level relations, conceptual and descriptive modelling, and calibration of quantitative modelling with MIKE SHE	1.2 2.2.2 3.3.2 3.5.3 Ch. 4, 5
Hydrogeological data			
Inventory of private wells	/Ludvigson 2002/	Description of available hydrogeological information	2.2.4
Installation of groundwater monitoring wells, abstraction wells and BAT filter tips	/Johansson 2003/ /Johansson 2004/ /Werner et al. 2004/ /Werner and Lundholm 2004b/ /Werner et al. 2006/	Description of QD type and depth to bedrock, basis for groundwater level measurements and hydraulic tests	2.2.3
Hydraulic conductivity of QD	/Werner and Johansson 2003/ /Johansson 2004/ /Werner 2004/ /Werner and Lundholm 2004a/ /Werner et al. 2004/ /Alm et al. 2006/	Basis for assigning hydraulic conductivity of QD in conceptual and quantitative models	1.2 2.2.3 3.4.1 3.5.3 Ch. 4, 5
Groundwater levels in QD	/Nyberg et al. 2004/ /Nyberg and Wass 2005/ /Nyberg and Wass 2006/ /Nyberg and Wass 2007/ Sicada	Conceptual and descriptive modelling, and calibration of quantitative models	1.2 3.3.3 3.5.3 Ch. 4, 5

Table 2-2. Input data from other disciplines and their handling in the Forsmark SDM-Site modelling.

Available site data Data specification	Ref.	Usage in SDM-Site Analysis/Modelling	Cf. Section
Topographical and other geometrical data			
Digital Elevation Model (DEM)	/Brydsten 2004/ /Brydsten and Strömgren 2004/ /Strömgren and Brydsten 2008/ SKB GIS	Conceptual, descriptive, and quantitative modelling (MIKE SHE)	1.2 Ch. 3–5
Vegetation and land use data			
Vegetation map	/Boresjö Bronge and Wester 2003/ /Löfgren (ed.) 2008/ SKB GIS	Conceptual, descriptive, and quantitative modelling	1.2 3.2 3.3.1 Ch. 4, 5
Surface-based geological data			
Soil type map	/Lundin et al. 2004/ SKB GIS	Conceptual, descriptive, and quantitative modelling with MIKE SHE	3.2 3.3–3.5 Ch 4, 5
Geological map of QD	/Sohlenius and Rudmark 2003/ /Sohlenius et al. 2003/ /Sohlenius et al. 2004/ /Hedenström and Sohlenius 2008/ SKB GIS	Basis for the conceptual hydrogeological model of QD and for the quantitative modelling (MIKE SHE)	1.2 3.2 Ch. 4, 5
Geophysical data	/Bergman et al. 2004/ /Chyssanthakis and Tunbridge 2005abc, 2006/ /Gustafsson and Gustafsson 2004/ /Juhlin and Bergman 2004/ /Marek 2004a/ /Marek 2004b/ /Nissen 2004/ /Isaksson and Keisu 2005/ /Toresson 2005/ /Toresson 2006/	Conceptual, descriptive and quantitative modelling with MIKE SHE	3.2 Ch. 4, 5
Geological data from boreholes and pits			
Stratigraphical data of QD	/Hedenström 2003/ /Fredriksson 2004/ /Hedenström 2004ab/ /Hedenström et al. 2004/ /Sundh et al. 2004/ /Albrecht 2005/ /Lokrantz and Hedenström 2006/ /Forssberg et al. 2007/ /Petersson et al. 2007/	Basis for the conceptual hydrogeological model of QD and for the quantitative modelling (MIKE SHE)	3.4.1 3.3.4 Ch. 4, 5
Hydrochemical data			
Surface water	/Nilsson et al. 2003/ /Nilsson and Borgiel 2004/ /Nilsson and Borgiel 2005/ /Nilsson and Borgiel 2007/	Conceptual and descriptive modelling	3.5.4
Shallow groundwater	/Nilsson and Borgiel 2005b/ /Berg et al. 2006/	Conceptual and descriptive modelling	3.4.2 3.5.4
Groundwater in near-surface bedrock (< c. 150 m depth)	Sicada	Conceptual and descriptive modelling	3.4.2 3.5.4
Hydrogeological data of the bedrock			
Hydraulic properties of the near-surface bedrock (< c. 150 m depth)	/Follin et al. 2007a/ /Follin et al. 2008/		3.4.2 3.5.3 Ch. 4, 5
Groundwater levels in bedrock	Sicada		3.4.2 3.5.3
Modelled hydraulic conductivity and pressure distributions in the upper part of the rock – results from ConnectFlow, stage 2.2	/Follin et al. 2007a/	Quantitative modelling (MIKE SHE) – boundary conditions and parameterisation	Ch. 4, 5

2.2.1 Meteorological data

Figure 2-2 shows locations of Högmasten and Storskäret meteorological stations in the Forsmark site investigation area, as well as for several nearby SMHI stations.

The following parameters are measured at Högmasten and Storskäret:

- Precipitation
- Air temperature
- Barometric pressure (only at Högmasten)
- Wind speed and direction
- Air humidity
- Global radiation (only at Högmasten)

The wind is measured at 10 m above ground level and the other parameters at 2 m. Data are collected every half-hour. The data values of the different parameters are valid for the following time periods:

- **Precipitation:** Accumulated sum of precipitation every 30 minutes. The 30-minutes precipitation value is the difference between two adjacent accumulated precipitation sums.
- **Air temperature:** 30-minutes mean of one-second values.
- **Barometric pressure:** 30-minutes mean of one-second values.

Figure 2-2. *SKB's two meteorological stations, Högmasten and Storskäret, within the Forsmark site investigation area, and nearby SMHI stations.*

- **Wind speed and wind direction:** The last 10-minutes mean value for the preceding 30 minutes. Hence, for the 10:00 data the measurement is from 09:51 to 10:00.
- **Relative humidity:** 30-minutes mean of one-second values.
- **Global radiation:** 30-minutes mean of one-second values.

All precipitation data presented in this report are corrected for losses (i.e. precipitation is increased) according to /Alexandersson 2003/ (general methodology) and /Wern and Jones 2007a/ (SKB stations). The corrections largely compensate for wind losses. The monthly and annual corrections for the different stations are shown in Tables 2-3 and 2-4.

The potential evapotranspiration, $E_{p,}$ is calculated from the Penman equation:

$$E_P = \left(\frac{\Delta \cdot (R_n - G)}{(\Delta + \gamma) \cdot L} + \frac{\gamma \cdot f(u) \cdot (e_s - e)}{(\Delta + \gamma)}\right) \cdot tstep$$

where

Δ	proportionality constant
R_n	net radiation flux density
G	heat flux density into ground
γ	psychrometric constant
$f(u)$	function of wind speed
e_s	saturated water vapor pressure
e	water vapor pressure
L	latent heat of vaporisation
$tstep$	time step

The method is described in detail in /Eriksson 1981/. Measured data every 30-minutes of temperature, relative humidity, wind speed and global radiation are required as input data to the equation to calculate the potential evapotranspiration. The wind speed is measured at 10 m above the ground but for the estimation of potential evapotranspiration the wind speed is re-calculated to a value representing 2 m above the ground. This is done by multiplying the

Table 2-3. Corrections of measured precipitation (increases, in percent) at SMHI's stations according to /Alexandersson 2003/.

	Jan	Feb	Mar	Apr	May	Jun	Jul	Aug	Sep	Oct	Nov	Dec	Year
Örskär A	19	22	23	15	15	13	13	15	14	15	17	20	16
Östhammar	9	13	10	9	9	12	8	9	8	7	8	10	9
Lövsta	10	9	12	10	11	12	8	8	8	8	9	9	9
Risinge	11	12	10	11	13	12	8	8	8	9	8	9	9
Film Kyrkby A	13	16	19	15	13	14	11	13	13	13	14	16	14
Söderby-Karlsäng D	10	11	10	10	12	12	9	9	8	8	8	9	10

Table 2-4. Corrections of measured precipitation (increases, in percent) at SKB's stations according to /Wern and Jones 2007a/.

	J	F	M	A	M	J	J	A	S	O	N	D	Year
Högmasten	13	14	13	11	10	10	10	10	10	10	11	12	11
Storskäret	13	14	13	11	10	10	10	10	10	10	11	12	11

measured value by a factor of 0.8. The net radiation is calculated from the measured global radiation and the albedo is set to 0.12 when the ground is not covered with snow and to 0.5 when there is a snow cover. The applied method included heat storage in the ground.

In general the meteorological measurements at Högmasten and Storskär have worked well. The only longer period of data loss was when the precipitation gauges were out of function from end of June until mid August 2005.

In addition to the monitoring at the two meteorological stations, a set of meteorological winter parameters, i.e. snow depth, ground frost penetration depth and ice cover, have been measured and observed. In addition to these parameters, the water content of the snow was calculated from the weight of a snow sample at every measurement. The snow depth and ice cover measurements started the winter 2002/2003 while the ground frost and snow water content measurements started the winter 2003/2004. The ground frost measurements were stopped after the season 2005/2006. The measurements and observations were carried out weekly during the season. The locations of the monitoring points are shown in Figure 2-3.

2.2.2 Hydrological data

Water levels have been monitored in six lakes and at two locations in the Baltic Sea during the site investigation, see Figure 2-4. The pressure transducers used for the monitoring were installed in stand pipes drilled into the bottom of the lakes and the sea for all locations except for PFM010038. Due to ice-lifting of the stand pipes, the two stations in the sea in Kallrigafjärden (SFM0043) and in Lake Lillfjärden (SFM0066) were abandoned in Nov. 2005 and Dec. 2006, respectively. In the analysis in the present report only the sea levels monitored at PFM010038 are used.

Figure 2-3. *Locations of monitoring points for meteorological winter parameters.*

Figure 2-4. *Locations of the surface water level gauges.*

Measurements of the water levels are made with 5 to 10 minutes intervals. Measurements are not stored unless they differ by more than 0.05 m from the previous measurements. In addition to this, a value is stored every two hours.

Four surface water discharge gauging stations were installed in the central part of the site investigation area (Figure 2-5). Long-throated flumes were selected for the discharge measurements, mainly due to the limitations set by the flat landscape, the need for accurate measurements, and the desire to avoid migration obstacles for the fish. Long-throated flumes give accurate measurements over relatively wide flow ranges and work under a high degree of submergence. At three of the four discharge gauging stations, two flumes, with different measurement ranges, were installed to obtain good accuracy data over the full flow range. At all four stations water levels, electrical conductivities, temperatures and discharges were monitored. Water electrical conductivity was measured at one additional station, at the outlet of Lake Bolundsfjärden (PFM002292), see Figure 2-5.

Measurements of water levels, electrical conductivities and temperatures were made every 10 minutes. However, if the difference from the previous measurement was small, not all data were stored. However, mostly the storing interval was less than one hour and at least one value was stored every two hours.

For the calculation of discharge, quality assured water level data from the flumes were taken from the Sicada database. The calculation procedure included consolidation of the time series to hourly averages, screening of data for removal of short-term spikes, noise and other data that were judged erroneous. Data gaps were filled by manual measurements when available. After the calculations were performed, the results were delivered to Sicada. The procedure for calculation of discharge is described in detail in /Johansson and Juston 2007/. The sizes of the catchment areas associated to the four discharge gauging stations are given in Table 2-5.

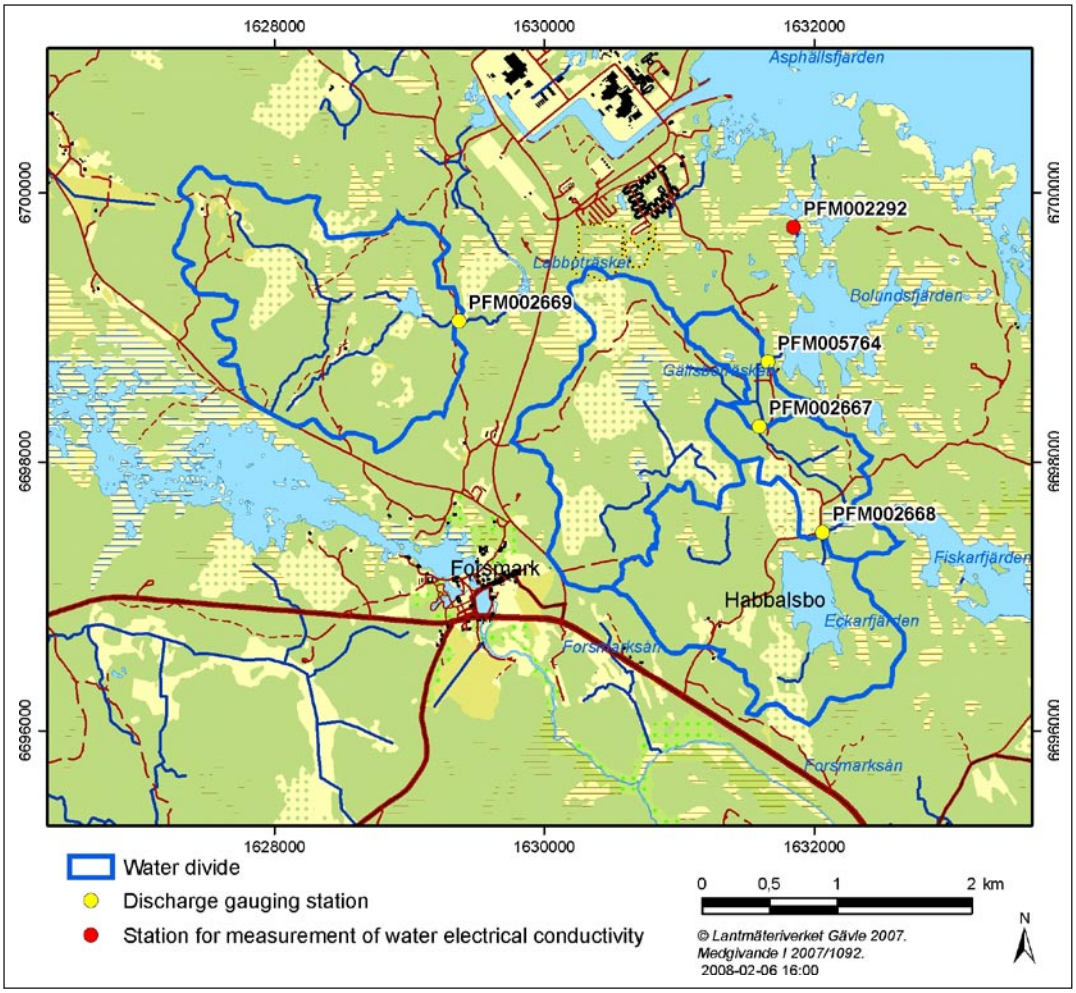

Figure 2-5. *Map showing locations of the four surface water discharge gauging stations, their associated catchment areas, and the station for continuous measurements of electrical conductivity only.*

Table 2-5. Sizes of catchment areas associated with the automatic discharge gauging stations.

Gauging station ID-code	Catchment area ID-code	Catchment area (km²)
PFM005764	AFM001267	5.59
PFM002667	AFM001268	3.01
PFM002668	AFM001269	2.28
PFM002669	AFM001270	2.83

2.2.3 Hydrogeological data

A total number of 74 groundwater wells have been installed in Quaternary deposits (69 monitoring wells and 5 pumping wells). Their locations and at what stage of the investigations they were installed are shown in Figure 2-6. In 51 of these wells the groundwater level has been registered automatically, see Figure 2-7.

In addition, BAT-type filter tips have been installed in low-permeable Quaternary deposits to measure pore pressure and hydraulic conductivity (10), and for water sampling (10), see Figure 2-8. In the seven filter tips for pore pressure measurements belonging to data freeze 2.2, pore pressure was measured twice a month.

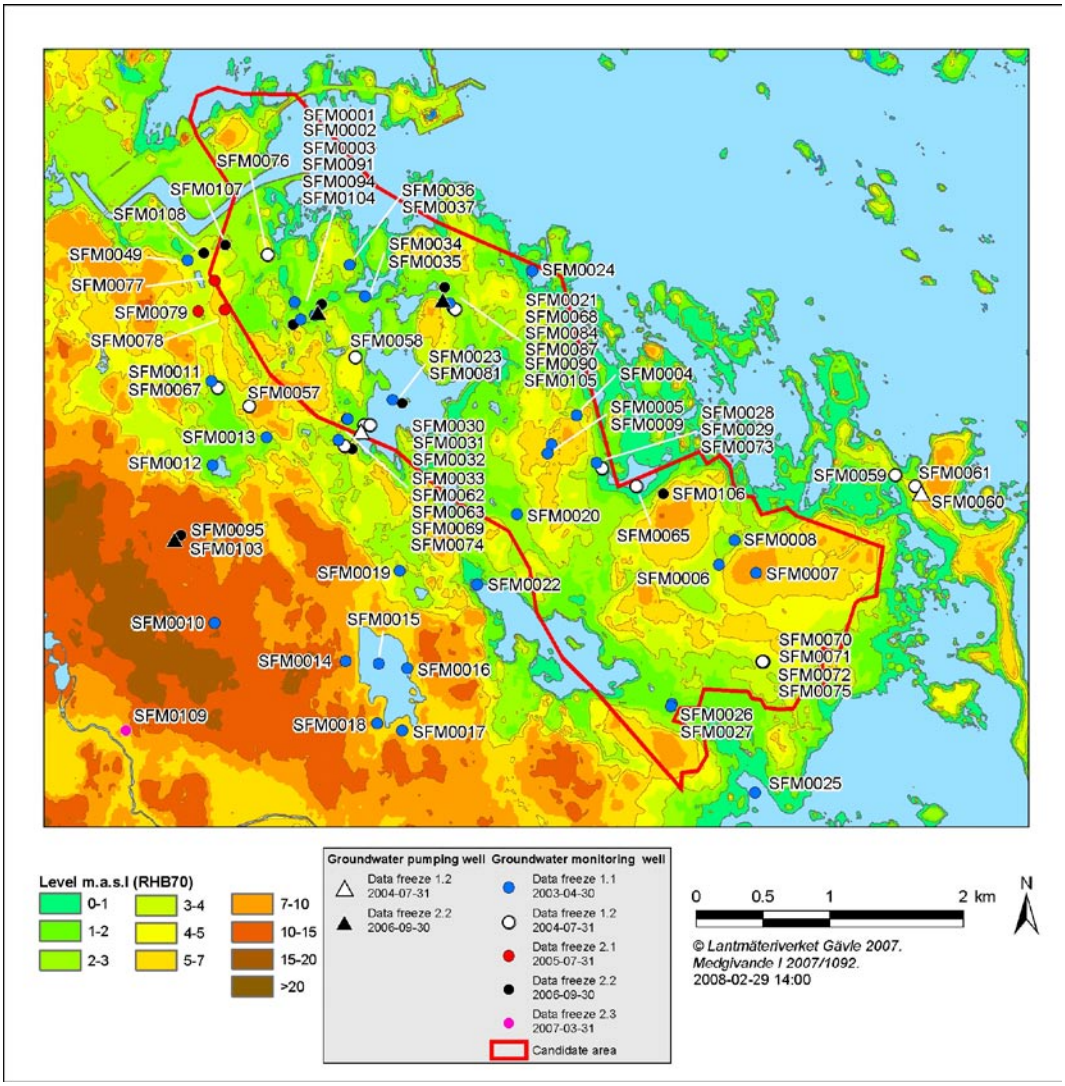

Figure 2-6. *Locations of groundwater wells in Quaternary deposits and at what stage of the investigation the wells were installed.*

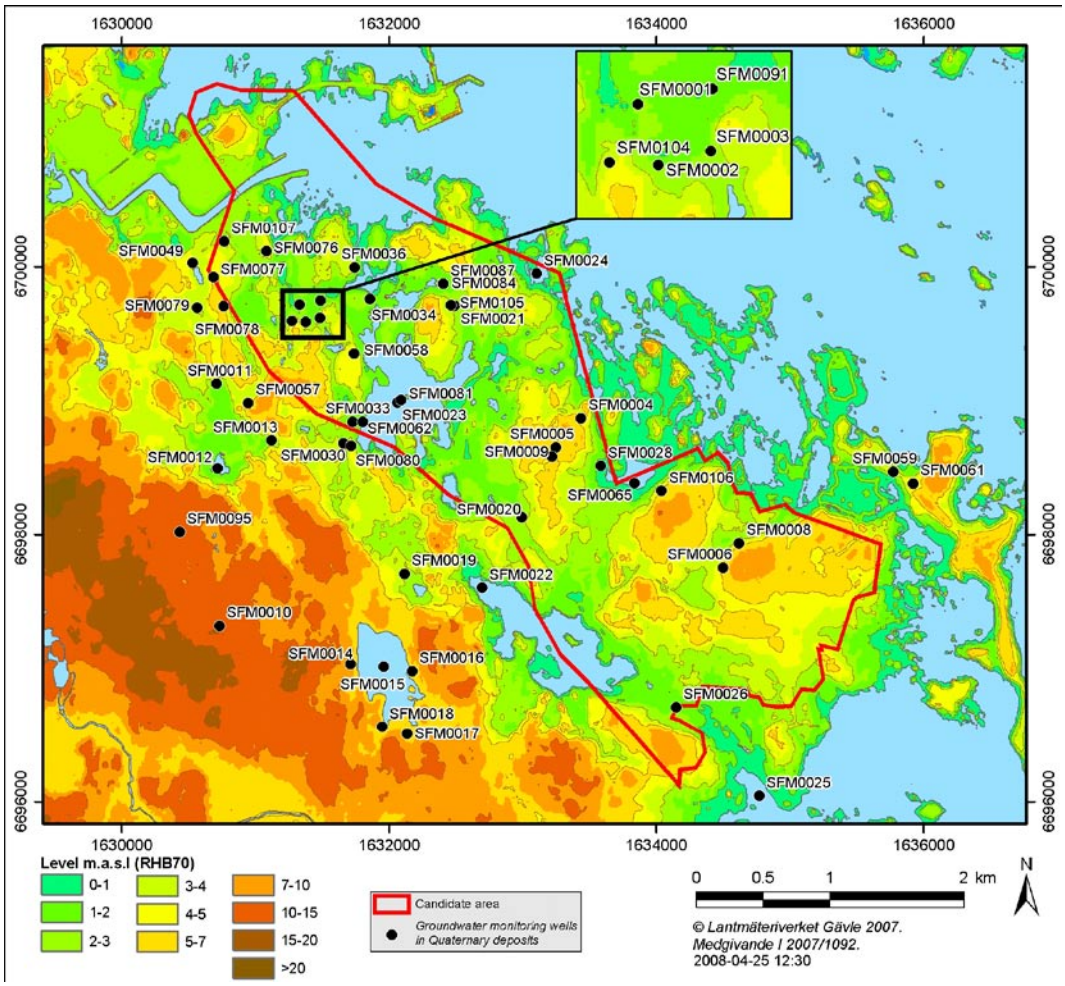

Figure 2-7. *Locations of groundwater monitoring wells in Quaternary deposits with automatic registration of groundwater levels.*

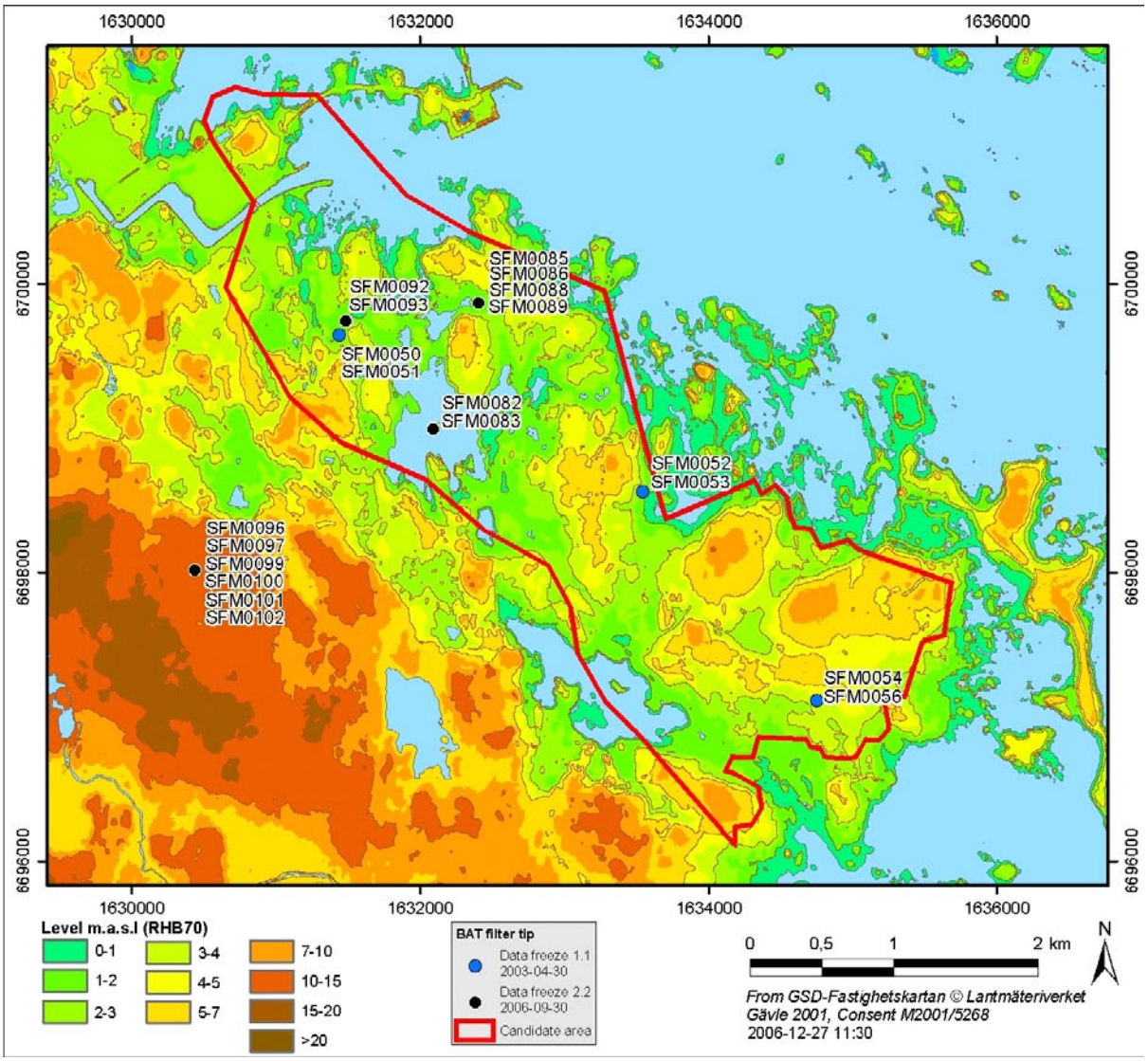

Figure 2-8. *Locations of BAT-type filter tips used in low-permeable Quatarnary deposits to measure pore pressure and hydraulic conductivity, and for water sampling.*

The number of groundwater wells and BAT-type filter tips installed with regard to the different data freezes is summarised in Table 2-6 and the type and number of hydraulic tests are shown in Table 2-7.

Table 2-6. List of installed groundwater wells and BAT filter tips with regard to the different data freezes (DF) in Forsmark (K denotes hydraulic conductivity).

Type of installation	DF 1.1 2003-04-30	DF 1.2 2004-07-31	DF 2.1 2005-07-31	DF 2.2 2006-09-30	DF 2.3 2007-03-31	Total
Monitoring wells for gw levels and K on land	32	13	3	10	1	59
Monitoring wells for gw levels and K below surface water	6	3	–	1	–	10
Pumping wells	–	2	–	3	–	5
BAT filter tips for pore pressure and K	3	–	–	7	–	10
BAT filter tips for water sampling	3	–	–	7	–	10

Table 2-7. List of completed hydraulic tests in Quaternary deposits with regard to the different data freezes (DF) in Forsmark.

Type of installation	DF 1.1 2003-04-30	DF 1.2 2004-07-31	DF 2.1 2005-07-31	DF 2.2 2006-09-30	DF 2.3 2007-03-31	Total
BAT tests	3	–	–	7	–	10
Slug tests	36	12	–	11	–	59
Pumping tests	–	2	–	3	–	5

The present report focuses on the near-surface hydrogeology in Quaternary deposits. However, groundwater levels (point water, fresh water and environmental water heads) in the upper c. 150 m of the bedrock are analysed together with groundwater levels in the Quaternary deposits for interpretation of the interaction between groundwater flow in the two flow domains. The locations of the percussion-drilled boreholes are shown in Figure 2-9. For more information on the bedrock hydrogeology the reader is referred to /Follin et al. 2007abc, 2008/.

Groundwater level time series from the percussion-drilled boreholes show frequent intervals of high amplitude disturbances that are related to core drilling acitivities and other pumping activities. The network of groundwater wells in the bedrock responded differently to activities at different locations, thus suggesting that these disturbance intervals contain valuable information on interconnectivity in the bedrock. Accordingly, these intervals were analysed to identify which wells responded and to what extent for different sources of disturbance.

The disturbances were oscillatory and with high amplitude and tended to obscure more subtle groundwater level changes in response to infiltration and sea level changes. Therefore, a thorough data screening was performed to produce a second "clean" data set with no visible artefacts from disturbing activities.

2.2.4 Water related activities not connected to the site investigation

Drainage of SFR and at the nuclear plant

For drainage of the SFR repository, located below the sea at Forsmark Harbour, a pumping of approximately 6 L/s is necessary. The pumping is conducted from two sumps at two different levels, 88 and 140 m below the sea level. The amounts pumped from the two levels are approximately 1.2 and 4.8 L/s, respectively (Levén, pers. comm.). For analyses of the possible influence of this pumping on the hydrogeology of the site investigation area, see Sections 3.5.3, 3.5.4 and 4.3.4.

For drainage of of the Forsmark nuclear plant reactor buildings 1 and 2, a pumping of c. 1-2 L/s is conducted (Levén, pers. comm.). The sump is located at an elevation of c. –20 m RHB70.

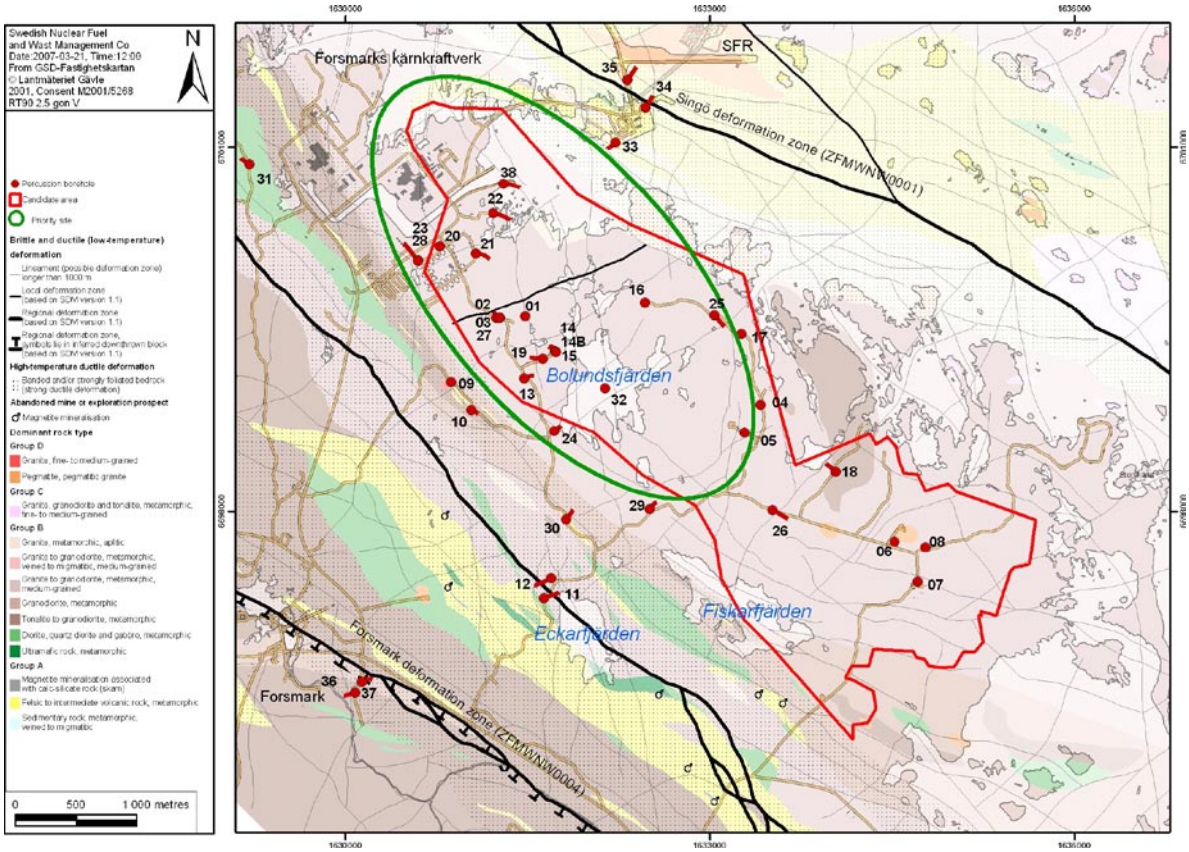

Figure 2-9. *Locations of all percussion-drilled boreholes in bedrock; the numbers refer to the ID numbers of the boreholes (e.g. 32 is HFM32).*

Water supply

The water supply for the nuclear plant, including the accomodation area and the SFR facilities, is based on surface water from Bruksdammen at Forsmark (see Figure 2-10 for location of Bruksdammen).

Private wells and water prospecting wells in the Forsmark area were investigated by /Ludvigson 2002/. A total of 40 wells (27 private wells and 13 water prospecting wells) were identified. The locations of the identified wells are shown in Figure 2-10. The investigation included a gathering of basic well data, field checks, and water sampling in 25 of the private wells. Also included was a summary of geological and hydrogeological investigations, performed in Forsmark prior to the site investigations /Ludvigson 2002/.

The private wells include 15 wells drilled into the bedrock, and 12 dug wells in Quarternary deposits. As shown in Figure 2-10, most of these wells are located in, or immediately outside of, the western part of the candidate area, or south of this area. Only one well was found in the central part of area considered in the hydro(geo)logical modelling. This well is situated just south of Lake Bolundsfjärden, but is now abandoned. Furthermore, some wells are located in the area west of Lake Eckarfjärden. It should also be noted that no private wells were found in the central and northwestern parts of the candidate area.

The water prospecting wells were drilled by Vattenfall/Forsmarks Kraftgrupp in connection with investigations performed in order to find a new freshwater supply to the Forsmark nuclear power plant. These investigations are summarised by /Ludvigson 2002/. Most of the water prospecting wells are located in an area northwest of Lake Gällsboträsket.

The water sampled in 25 of the private wells was analysed for chemical and microbiological parameters. According to the results of the analyses, the water quality shows large variations between different wells. The water from some of the wells can be used as drinking water, whereas the water quality is poor in other wells.

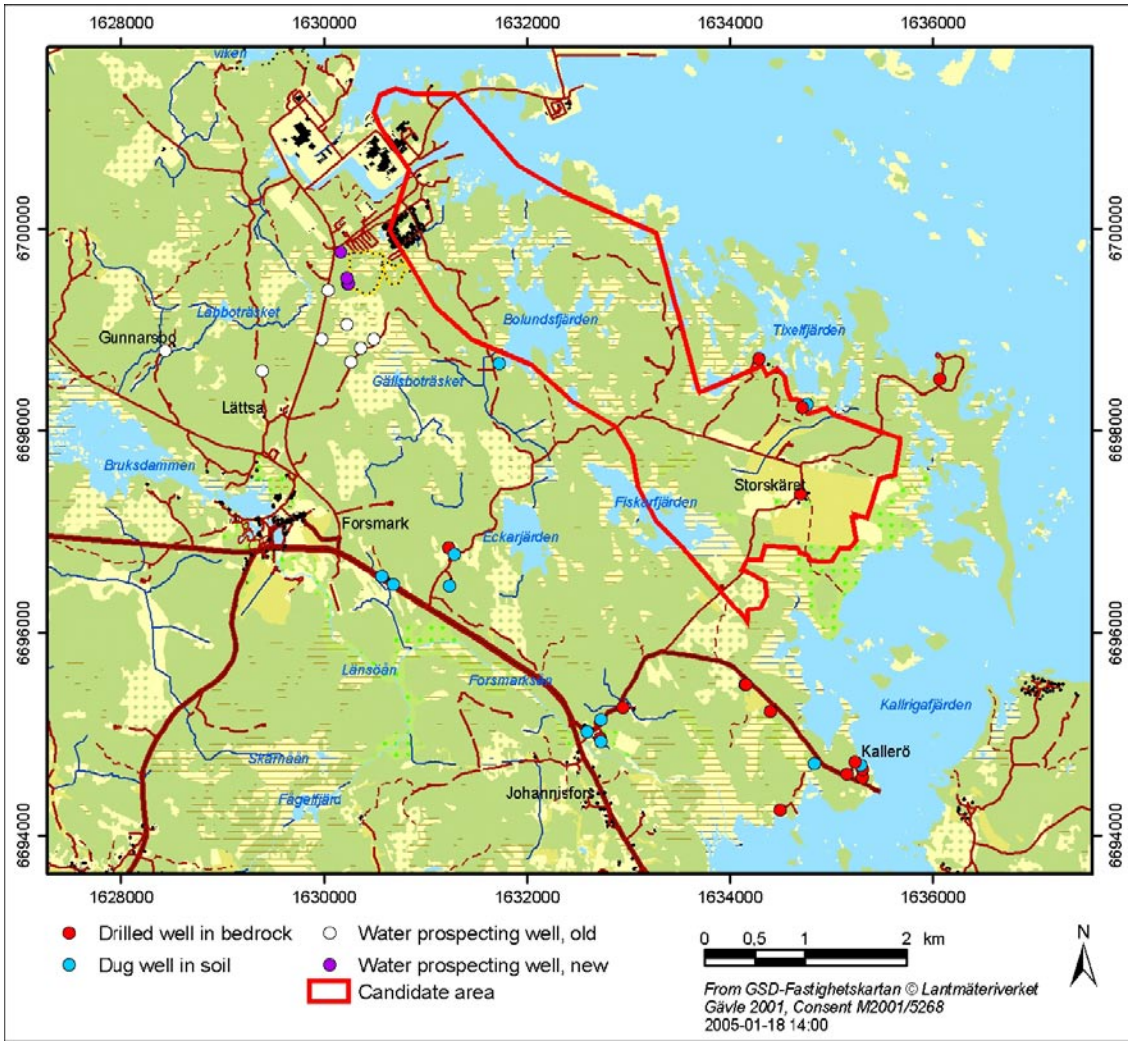

Figure 2-10. *Locations of identified private wells and water prospecting wells in the Forsmark area.*

Cooling water for the power plant is withdrawn via an open canal from Asphällsfjärden, see Figures 1-1 and 1-2 for location. The maximum withdrawal rate is c. 130 m^3/s. The cooling water is released in the so-called Biotestsjön , an artificial lake c. 3 km NNW of the power plant that is separated from the surrounding coastal basins by embankment dams. The water passes through Biotestsjön and is let out via a canal towards north. See Section 3.3.5 for further aspects of the cooling water use.

Sewage water

The sewage water from the nuclear plant, including the accomodation area, and the SFR-facilities are treated in a sewage treatment plant located south of the cooling water canal. The plant has mechanical, biological and chemical treatment (dimensioned for 1,000 persons). The treated sewage water is released into Asphällsfjärden.

The private houses in the area have their own separate sewage treatment facilities.

Storm water

The storm water system for water from paved areas and roofs covers a total area of 0,19 km^2. After check of radioactivity also the groundwater drained from the reactor and turbine buildings are released to the storm water system as well as groundwater drained from culverts and service buildings. The storm water is released in the intake part of the cooling water canal. Some stormwater from the accomodation area is also released to Asphällsfjärden.

3 Conceptual and descriptive model of surface and near-surface water flow at the Forsmark site I: Field observations

3.1 Overall conceptual model

In Figure 3-1 the overall conceptual model of the near-surface hydrogeology is illustrated. Direct groundwater recharge from precipitation is the dominating source of recharge. However, due to vegetation water uptake groundwater levels are lowered in the vicinity of the lakes during dry summer conditions converting the lakes from groundwater discharge areas to recharge areas. The infiltratration capacity of the upper QD is so high that overland flow rarely occurs except in areas where the groundwater level reaches the ground surface.

The runoff in the brooks is dominated by water of groundwater origin. Overland flow contributes to the runoff mainly during extended periods of wet conditions during autumn and winter and in connection to snow melt in spring. The lakes in the area are shallow and the turn-over times are short.

The surface water and near-surface groundwater divides of the model area, both the outer and the internal ones, are assumed to coincide. The small-scale topography implies that many small catchments are formed with local, shallow groundwater flow systems in the QD. The decreasing hydraulic conductivity with depth and the anisotopy ($K_h > K_v$) of the tills dominating in the area, mean that a dominating part of the groundwater will move along very shallow flow paths. Groundwater levels in the QD are very shallow with mean levels within less than a metre below the ground in most of the area and the groundwater level is highly correlated with the topography of the ground surface.

The local, small-scale recharge and discharge areas will overlay the more large-scale flow systems associated with groundwater flow at greater depths. The high transmissivity of the upper c. 150 m of the bedrock means that the relatively small flow of water occuring from the QD to the bedrock is easily transmitted in the upper bedrock already at low gradients. While the groundwater level in the QD follows the topography of the ground surface, the groundwater level in the upper bedrock is very flat and approximately at c. 0.5 m RHB70 within the candidate area which largely coincides with a tectonic lens.

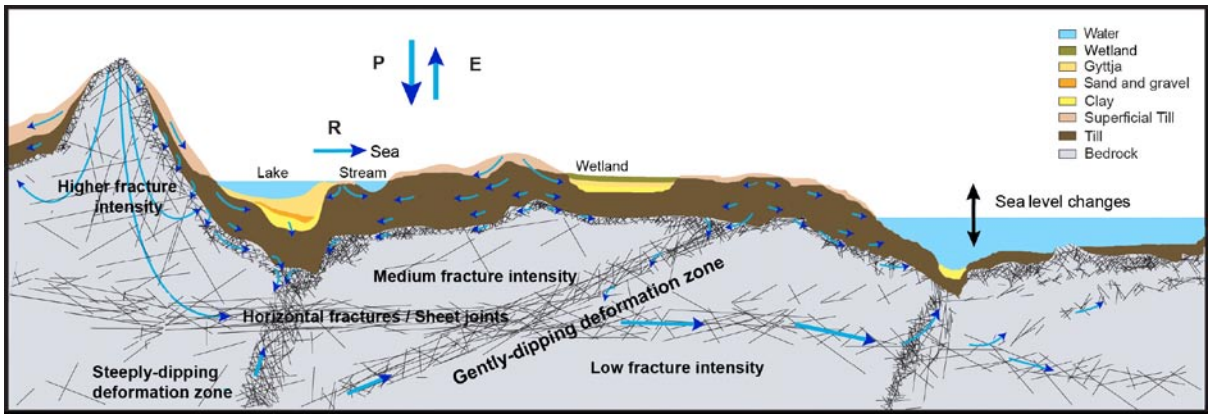

Figure 3-1. *Section illustrating the conceptual hydrogeological model of the Quaternary deposits and the upper bedrock.at the Forsmark site /Follin et al. 2007a/.*

Where groundwater levels are measured in the QD and in the bedrock at the same location, the groundwater levels in the bedrock are mostly considerably lower than in the QD. The dominating horizontal and sub-horizontal fracture zones in the upper bedrock give rise to a relatively strong anisotropy ($K_h > K_v$) which means that long, shallow flowpaths dominate. The highly transmissive horizontal and sub-horizontal fracture zones in the upper bedrock also collect groundwater flow from below and to a great extent prevent deeper groundwater to discharge within the central part of the site investigation area. Instead, the deeper groundwater discharges into the Baltic Sea.

3.2 Supporting data and models from other disciplines

The conceptual and descriptive model of the hydrology and near-surface hydrogeology to be presented here is supported by data and models from other disciplines of the site investigation:

- **Digital Elevation Model (DEM)**
  Detailed DEM's have been developed for the site investigation area based on various sources. Only the source judged to be of highest quality was used for areas with overlapping data. The first DEM for the Forsmark area has a cell size of 10×10 m and is classified due to national security reasons /Brydsten and Strömgren 2004/. A new non-classified DEM in lower resolution (20×20 m) was constructed later /Strömgren and Brydsten 2008/. The new DEM also includes additional input data for the interpolation. In the present work, topographical data have been used directly as well as other quantities derived from the DEM's (i.e. slopes and higher order derivatives), e.g. in the conceptualisation and modelling of groundwater recharge and discharge areas. The DEM is an important input when constructing numerical models for groundwater and surface water flow.
- **Geological map of Quaternary Deposits**
  A detailed mapping of the Quaternary deposits of the central land parts of the site has been performed, see Figure 1-3 /Sohlenius et al. 2004/. The mapping included extensive field work. A map covering the whole regional modelling area (including its offshore part) has also been constructed based on various data sources /Hedenström and Sohlenius 2008/. In the conceptual, descriptive and quantitative water flow modelling, the QD geological map has been used for classification and assignment of hydraulic properties.
- **The regolith depth and stratigraphy model**
  Based on the DEM, drillings and geophysical investigations, a model of the depth and the stratigraphy of the Quaternary deposits has been developed within the site descriptive modelling /Hedenström et al. 2008/. In this context, the model has been used for conceptualisation of flow patterns and for assignment of hydraulic properties. Since the depth and stratigraphical model is very important for the conceptual, descriptive and quantitative modelling of the near-surface hydrogeology, the model is described in some detail in Section 3.2.1 below.
- **Soil map**
  The soil map /Lundin et al. 2004/ has been used qualitatively in the conceptual modelling. For example, the wetness index produced in connection with the soil mapping has been used as one indicator of depth to groundwater and in the interpretation and classification of recharge and discharge areas.
- **Vegetation map**
  The vegetation map /Boresjö Bronge and Wester 2003/ has been used specifically as a basis for the modelling of the evapotranspiration processes, but also as a qualitative indicator in the interpretation and classification of recharge and discharge areas.
- **Bedrock hydrogeological conceptual and descriptive model**
  The bedrock hydrogeological conceptual and descriptive model of the site investigation is presented in /Follin et al. 2007abc, 2008/. This model, especially the upper c. 150 m of the model, is of great importance for the conceptualisation of the near-surface hydrogeology and a short description of the model is given in Section 3.2.2.

- **Hydrochemical data and modelling**
  The hydrochemistry of surface water and shallow groundwater has been analysed and modelled in /Tröjbom et al. 2007/. The spatial and temporal distributions of "water types" and specific components are used to infer information on the flow pattern and reference will be given to hydrochemical data and models as support for the conceptual and descriptive model of the hydrology and near-surface hydrogeology (see Section 3.5.4).

3.2.1 Regolith depth and stratigraphy model

/Hedenström et al. 2008/ present a depth and stratigraphy model of the regolith (QD, HSD). The model is geometrical and the topography of the ground surface, and lake and sea bottom from the DEM forms the upper boundary of the model while the bedrock topography, derived from the extensive drillings and geophysical investigations conducted in the site investigation, constitutes the bottom boundary. The conceptual model for the construction of the different layers is based on knowledge from the site as well as a general geological model of the Quaternary deposits in this part of Sweden. The principle of the definition of the layers and lenses is illustrated in Figure 3-2.

The model is subdivided into ten layers or units according to the conceptual understanding of the Forsmark site. The layers are named Z1-Z6 (where Z4 is divided into two layers, Z4a and Z4b) and L1-L3. As indicated in Figure 3-2, all layers are not present everywhere; a layer may have zero thickness in parts of the model area. The model presents the geometry of the lower level for each layer, given as elevation above sea level (RHB70). The model has a spatial resolution of 20×20. The lower level of Z5 is interpolated from the data set of information of depth of the Quaternary deposits as well as the bedrock outcrops; thus, the lower level of Z5 represents the bedrock surface regardless if it is covered by deposits or not. The bottom layer, Z6, is characterized by fractured bedrock and is in the model considered to be a part of the rock and not a part of the regolith. The layer is included since high hydraulic conductivity has been observed in the contact zone between bedrock and Quaternary deposits (see Section 3.4.1).

Below the lakes, the stratigraphical information was sufficient for modelling of three separate lenses, L1-L3. However, the lenses are only modelled below eight lakes in the area. In the areas where these lenses appear they replace the occurrence of Z1, Z2, Z3, Z4a and Z4b. Therefore, Z5 and/or Z6 exist also below the lenses. In the wetlands the information was not sufficient for modelling of lenses. The layers in the model are summarized and explained in Table 3-1.

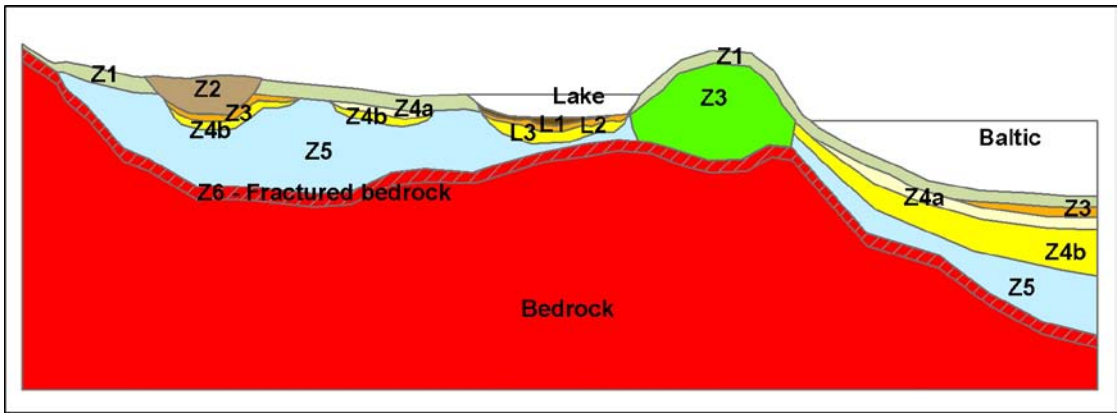

Figure 3-2. *Conceptual model of the regolith depth and stratigraphy model /Hedenström et al. 2008/. For definition and description of the layers, see Table 3-1.*

Table 3-1. Deposits, codes and occurrence of the seven layers and three lenses of the regolith depth and stratigraphy model of the Forsmark site /Hedenström et al. 2008/.

Description of layer/lens	Simplified Code	Description/Occurrence
Gyttja (algal gyttja, calcareous gyttja, clay gyttja-gyttja clay), Peat	L1	Present inside the boundaries of the lakes. When peat is present as surface layer within the lake area, this is included in the L1 lens. The sediments in L1 and Z4a partly consist of the same geological units.
Postglacial sand and/or gravel	L2	Present inside the boundary of the lakes. The sediments in L2 and Z3 consist of the same geological unit.
Clay (glacial and postglacial)	L3	Present inside the boundaries of the lakes. The sediments in L3 and Z4a and Z4b consist of the same geological unit.
Surface layer	Z1	The layer is affected by surface processes, e.g soil forming processes in the terrestrial parts or sedimentation/transport/ersion in the limnic/marine parts. This layer is present within the entire modelled area, except where the surface is covered by peat or where the model has a lens (below lakes). On bedrock outcrops, the layer is 0.1 m thick and 0.6 m in other areas. If the total modelled regolith depth is less than 0.6 m, Z1 will be the only layer. The layer can be connected to a GIS application such as the map of Quaternary deposits or soil type map and assigned properties in accordance to the properties of the deposits.
Peat	Z2	This layer is only present where peat is shown in the QD map. Calculated average depths are used for the layer since too few observations are available for interpolation. The average depth used for peat above and below the 5 metres above sea level contour line , is 1.4 m and 0.4 m, respectively. Postglacial sand (Z3) always underlies Z2. If peat is intersecting glacial clay or sand on the QD map, Z4b underlies Z3.
Postglacial sand/gravel, glaciofluvial sediment and artificial fill	Z3	The layer is only present where the surface layer consists of postglacial sand/gravel, glaciofluvial sediment or artificial fill. The layer geometry is interpolated from input data and average values. This may result in a discrepancy between the modelled Z3 and the marine geological map. In the terrestrial parts, Z3 is assigned average depth values for postglacial sand, artificial fill and glaciofluvial sediment. The glaciofluvial sediment and artificial fill are modelled to always be situated directly on bedrock. Z3 as sand is always present under peat (Z2).
Postglacial clay including gyttja clay	Z4a	Z4a is present in the marine area where postglacial clay is the surface layer. In the marine areas, the layer geometry is interpolated from input data and average values. This may result in a discrepancy between the modelled Z4a and the marine geological map. When average values are used, Z4a is always underlain by Z4b.
Glacial clay	Z4b	Z4b is present where glacial clay is the surface layer. Additionally, Z4b is present under Z3 when peat is located next to sand or glacial clay and when sand is located next to glacial clay. In the marine area, the layer geometry is based on interpolation from input data and average values. In the terrestrial area, the layers are assigned calculated average depth values. In the marine area, interpolated Z4b values >0.5 m are rejected in areas where the geological map shows till or glaciofluvial sediment. This may result in a discrepancy between the modelled Z4b and the marine geological map.
Till	Z5	This layer is present in a major part of the model area. The thickness of the layer is based on interpolation from input data and average values. Z5 is 0 at bedrock outcrops, if the total QD depth is <0.6 m, or if the layers/lenses are located directly on the bedrock surface. The lower limitation of Z5 represents the bedrock surface, i.e. Z5 represents a Digital Elevation Model for the bedrock surface.
Fractured bedrock	Z6	This layer has a constant depth of 0.6 m and represents the bedrock upper part, calculated from the interpolated Z5.The layer represents a highly conductive zone that has been observed in many of the hydraulic tests in Forsmark.

3.2.2 Bedrock hydrogeological conceptual and descriptive model

The hydrogeological conceptual and descriptive model of the bedrock is stongly coupled to the deformation zones and fracture domains of the geological model, see Figure 3-3.

The bedrock hydrogeology reveals a significant hydraulic anisotropy within the tectonic lens, which covers the body of the candidate area. The upper c. 150 m of bedrock contains high-transmissive horizontal fractures/sheet joints. These fractures/sheet joints occur at different elevations in the percussion drilled boreholes, but are found to interconnect hydraulically across large distances (2 km) /Gokall-Norman et al. 2005, Gokall-Norman and Ludvigson 2007ab, 2008/. The horizontal fractures/sheet joints have transmissivities in the range c. $1{\cdot}10^{-6}$ –$1{\cdot}10^{-3}$ m^2/s (hydraulic conductivity c. $1{\cdot}10^{-6}$ –$1{\cdot}10^{-3}$ m/s). The bedrock in between the horizontal fractures/sheet joints, however, is considerably less conductive (hydraulic conductivity c. $1{\cdot}10^{-11}$ –$1{\cdot}10^{-8}$ m/s) except where it is intersected by transmissive steeply-dipping or gently-dipping deformation zones.

Below the uppermost c. 150 m of bedrock there are no high-transmissive horizontal fractures/ sheet joints and the conductive fracture frequency becomes very low and the fractures fairly low-transmissive (fracture transmissivity c. $1{\cdot}10^{-10}$ –$1{\cdot}10^{-7}$ m^2/s). In some of the 1,000 m deep cored boreholes there are almost no flowing fractures observed below c. 150 m depth, which is exceptional in a national perspective given the experiences from SKB's investigations at Äspö, Stripa, Laxemar-Simpevarp and the many study sites investigated in the 1970's and 1980's.

3.3 Description of hydrological objects/flow domains

3.3.1 Catchment areas

The entire Forsmark area is situated within the SMHI catchment no. 54/55, i.e. in the area between River Tämnarån (SMHI catchment no. 54) and River Forsmarksån (SMHI catchment no. 55). A total of eight catchments, with sub-catchments, have been identified that are situated partly or

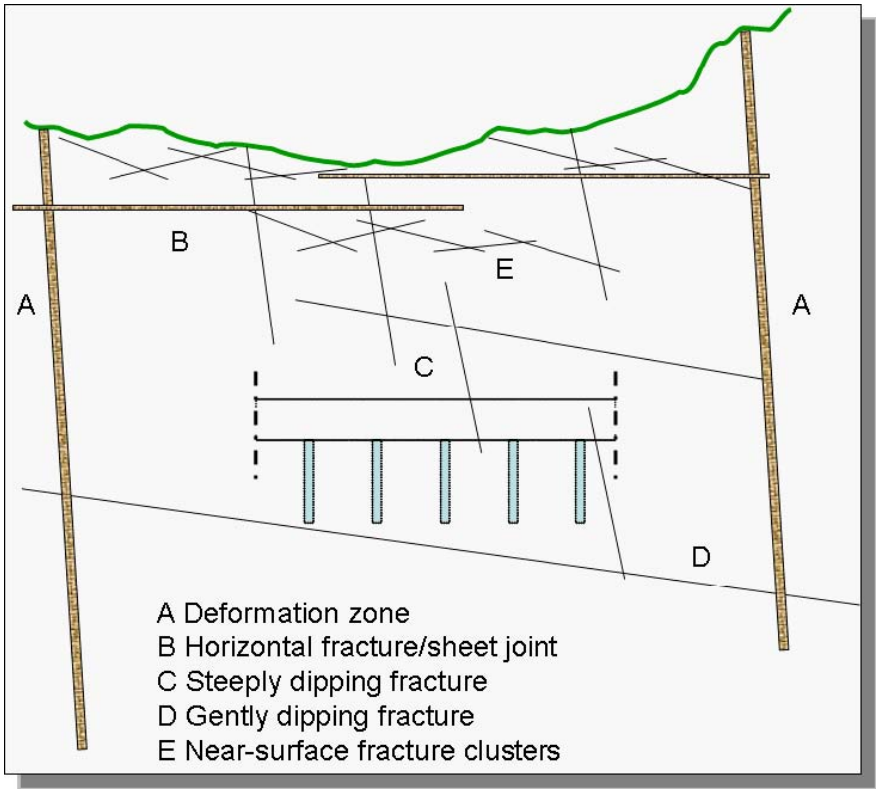

Figure 3-3. *Simplified conceptual model of the bedrock hydrogeology in Forsmark (Follin et al. 2007a).*

entirely within the SKB site investigation area. These eight catchments have outlets to the Baltic Sea. Between these catchments, coastal areas without lakes or larger brooks are formed, which are delineated by the water divides of the catchments and the coastal shoreline, Figure 3-4.

N.B! A major revision of the water divides of catchments 2:3, 2:8, 2:9 and 2:10 has been made since version 1.2 of the SDM. A small brook draining to Eckarfjärden that had been overlooked in the original investigation was identified, which required a revision of the delineation of catchment areas.

The sizes and landuse of the catchments are shown in Tables 3-2 and 3-3. Additional information on the delineated catchments, i.e regarding distributions of QD and morphometrical parameters, can be found in /Brunberg et al. 2004/. (Note that the report by Brunberg et al. has been updated with the new catchment area delineation near Lake Eckarfjärden (revision dated December 2007), but that the report in accordance with the SKB procedure for revisions of existing reports still is referred to as /Brunberg et al. 2004/.)

The catchment areas of the four surface water discharge gauging stations are used in the evaluation of measured discharges. These catchment areas are shown in Figure 2-6, and their sizes are given in Table 2-5.

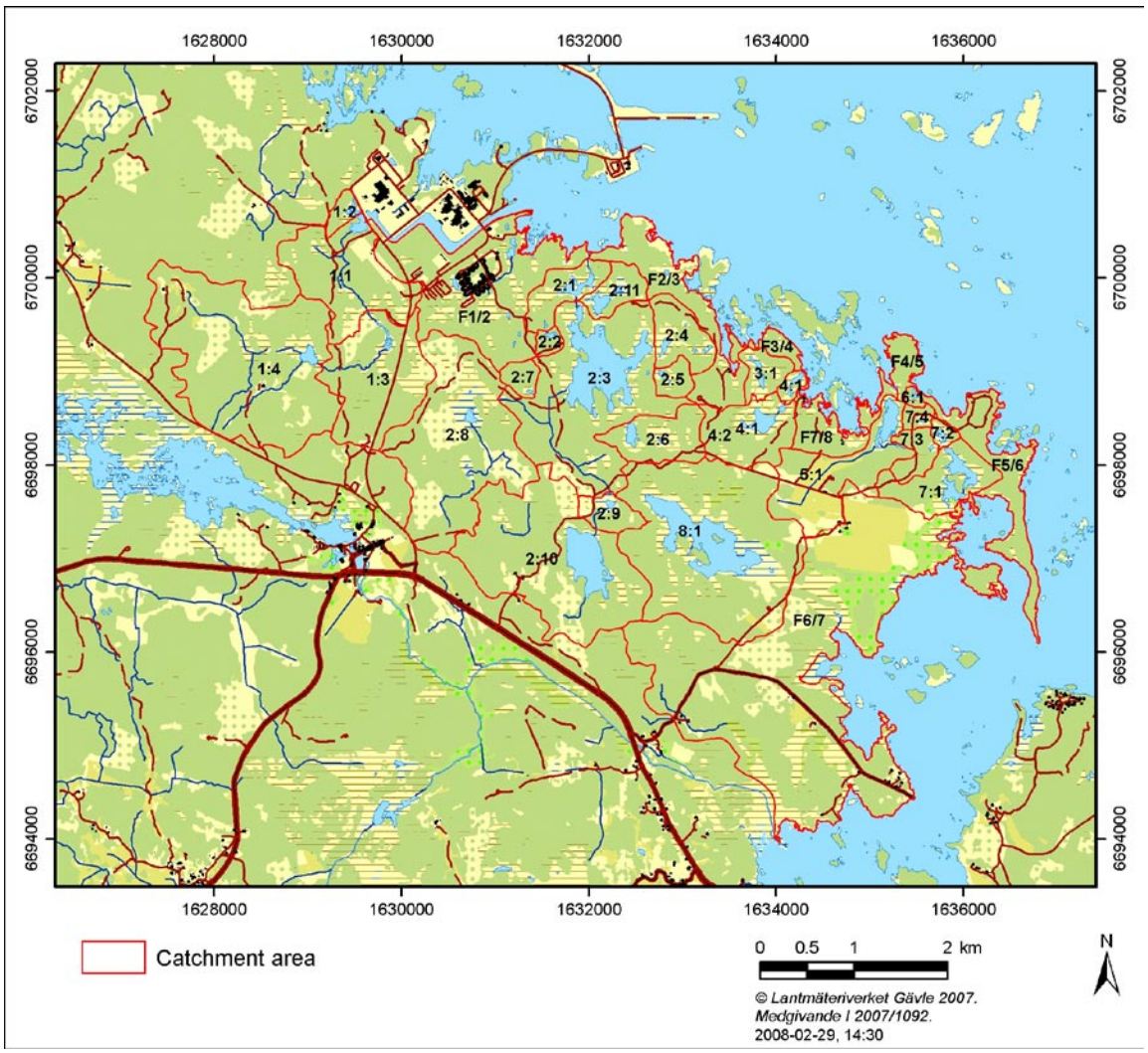

Figure 3-4. *Delineated catchment areas, including updates in the vicinity of Lake Eckarfjärden (see text) /Brunberg et al. 2004/.*

Table 3-2. Size and land use of delineated catchment areas /Brunberg et al. 2004/.

ID Code	Catchment number	Name	Area Km^2	Water surface MA1 [%]	Coniferous- and mixed forest MA2 [%]	Agriculture land MA4 [%]	Remaining open land MA5 [%]	Cut forest MA6 [%]	Industrial area MA15 [%]	Remaining open land without forest contour MA17 [%]	Deciduous forest MA19 [%]	Wetland (VEG 61-64, 72 and 74-79) [%]
	1	***Forsmark 1***										
AFM000073	1:1-4	Gunnarsbo - Lillfj. (south)	5.120	1	73	1	7	11	0	8	0	10
AFM001099	1:1	*Sub-area: Gunnarsbo-Lillfj. (south)*	1.088	2	62	0	17	8	0	10	0	12
AFM000096	1:2	Gunnarsbo - Lillfj. (north)	0.104	9	81	0	2	0	0	8	0	18
AFM000048	1:3-4	Labboträsket	3.928	1	75	1	4	11	0	7	0	10
AFM001100	1:3	*Sub-area: Labboträsket*	1.194	1	70	0	1	15	0	13	0	15
AFM000095	1:4	Gunnarsboträsket	2.734	1	78	1	6	10	0	5	0	7
	2	***Forsmark 2***										
AFM000074	2:1-11	Norra Bassängen	8.668	10	69	0	1	9	0	10	0	12
AFM001101	2:1	*Sub-area: Norra bassängen*	0.350	13	60	0	0	10	0	18	0	21
AFM000092	2:2	Lake 2:2	0.071	9	45	0	0	46	0	0	0	0
AFM000050	2:3-10	Bolundsfjärden	8.003	9	70	0	1	9	0	10	0	11
AFM001103	2:3	*Sub-area: Bolundsfjärden*	2.002	20	57	0	0	12	0	11	0	13
AFM000087	2:4-5	Graven	0.529	5	74	0	0	0	0	21	0	22
AFM001104	2:4	*Sub-area: Graven*	0.390	6	71	0	0	0	0	23	0	24
AFM000088	2:5	Fräkengropen	0.139	4	80	0	0	0	0	16	0	16
AFM000089	2:6	Vambörsfjärden	0.484	5	70	0	0	10	0	15	0	17
AFM000093	2:7	Kungsträsket	0.126	3	69	0	0	24	0	3	0	3
AFM000094	2:8	Gällsboträsket	2.141	1	89	0	1	0	0	10	0	11
AFM000090	2:9-10	Stocksjön	2.477	9	65	1	4	16	0	5	0	6
AFM001105	2:9	*Sub-area: Stocksjön*	0.209	3	77	0	1	0	0	18	0	18
AFM000010	2:10	Eckarfjärden	2.268	10	64	1	4	18	0	4	0	5
AFM000091	2:11	Puttan	0.244	17	58	0	0	0	0	25	0	25
	3	***Forsmark 3***										
AFM000086	3:1	Tallsundet	0.215	11	58	0	0	0	0	31	0	35
	4	***Forsmark 4***										
AFM000085	4:1-2	Lake 4:1	0.689	13	64	0	1	0	0	23	0	23
AFM001106	4:1	*Sub-area: 4:1*	0.068	17	45	0	0	0	0	38	0	38
AFM000049	4:2	Lillfjärden	0.621	12	66	0	1	0	0	21	0	21
	5	***Forsmark 5***										
AFM000052	5:1	Bredviken	0.944	7	49	28	11	0	0	4	0	4
	6	***Forsmark 6***										
AFM000084	6:1	Simpviken	0.035	11	89	0	0	0	0	0	0	0
	7	***Forsmark 7***										
AFM000080	7:1-4	Lake 7:1	0.895	13	70	0	2	0	0	14	1	14
AFM001107	7:1	*Sub-area: 7:1*	0.558	18	64	0	3	0	0	13	2	14
AFM000081	7:2-4	Märrbadet	0.337	5	81	0	0	0	0	15	0	15
AFM001108	7:2	*Sub-area: Märrbadet*	0.068	17	47	0	0	0	0	36	0	36
AFM000082	7:3	Lake 7:3	0.192	1	93	0	0	0	0	6	0	6
AFM000083	7:4	Lake 7:4	0.077	2	81	0	0	0	0	17	0	17
	8	***Forsmark 8***										
AFM000051	8:1	Fiskarfjärden	2.926	14	68	1	4	0	0	13	0	16

"MA": Layers of the digital topographic map. "VEG": Layers of the SKB´s digital vegetation map.

Table 3-3. Size and land use of delineated rest-catchments /Brunberg et al. 2004/.

ID Code	Catchment number	Name	Area Km^2	Water surface MA1 [%]	Coniferous- and mixed forest MA2 [%]	Agriculture land MA4 [%]	Remaining open land MA5 [%]	Cut forest MA6 [%]	Industrial area MA15 [%]	Remaining open land without forest contour MA17 [%]	Deciduous forest MA19 [%]	Wetland (VEG 61-64, 72 and 74-79) [%]
		Forsmark 1/2										
AFM001109	1/2	"Rest catchment area"	1.862	3	63	0	14	3	0	10	0	11
		Forsmark 2/3										
AFM001110	2/3	"Rest catchment area"	0.837	4	84	0	3	0	0	9	0	9
		Forsmark 3/4										
AFM001111	3/4	"Rest catchment area"	0.107	1	98	0	0	0	0	0	0	0
		Forsmark 5/6										
AFM001112	5/6	"Rest catchment area"	0.701	4	92	0	0	0	0	3	0	3
		Forsmark 6/7										
AFM001113	6/7	"Rest catchment area"	5.561	4	91	0	0	0	0	5	0	5
		Forsmark 7/8										
AFM001114	7/8	"Rest catchment area"	0.389	1	64	10	5	1	0	13	6	17
		Forsmark 4/5										
AFM001115	4/5	"Rest catchment area"	0.178	2	88	0	0	0	0	10	0	13

"MA": Layers of the digital topographic map. "VEG": Layers of the SKB´s digital vegetation map.

3.3.2 Lakes

Most of the lakes in the Forsmark area are small and shallow. The average lake depth is typically less than 1 m and the maximum depth c. 2 m. The typical lake shore is shallow (in the order 0–0.25 m deep) and reed covered. The largest lakes are Lake Fiskarfjärden, Lake Bolundsfjärden and Lake Eckarfjärden (Figure 2-4 and Table 3-4). Distinguishing between lakes, wetlands and water courses with a diffuse furrow is in many cases not a simple task, which makes it a question of definition.

Due to the limited depth, the vertical mixing is likely to be complete (driven mainly by wind shear) with a homogeneous water in the vertical direction. In the horizontal plane the inlet and outlet are usually located at opposite ends of the lakes and the lakes may also be assumed to be well mixed in the horizontal (driven by flow and wind shear). The risk of more stagnant water occurring is highest in the shallow reed covered areas and it may be necessary to estimate an effective volume (the volume that is active) for lakes where a substantial part of the area is shallow and covered by reed. The degree of mixing must, however, be related to the flow which is generally small; thus, velocities induced by flow will also be small compared to for example velocities induced by wind shear, which supports the notion of well mixed lakes.

Morphometrical data

Morphometrical data for the lakes are summarised in Table 3-4 (see Figure 3-4 for the location of the lakes). For a more detailed description of the lakes, see /Brunberg et al. 2004/. Several lakes have water levels close to the Baltic Sea level. During events of high sea levels, water

Table 3-4. Morphometrical data for the lakes in the Forsmark area.

No. in Figure 3-4	Name	Lake threshold (m RHB70)	Area (m^2)	Max. depth (m)	Mean depth (m)	Volume (m^3)	Theoretical turnover time (days)
1:1	Gunnarsbo-Lillfjärden (södra)	1.92	33,107	2.22	0.70	23,110	11
1:2	Gunnarsbo-Lillfjärden (norra)	1.07	23,148	0.90	0.30	6,870	161
1:3	Labboträsket	2.65	60,042	1.07	0.27	15,950	10
1:4	Gunnarsboträsket	5.68	67,453	1.29	0.51	34,040	30
2:1	Norra Bassängen	0.19	76,070	0.88	0.31	23,650	7
2:2	Lake 2:2	1.77	9,921	0.60	0.29	2,860	98
2:3	Bolundsfjärden	0.28	611,312	1.81	0.61	373,950	114
2:4	Graven	0.44	50,087	0.35	0.12	5,920	27
2:5	Fräkengropen	No data	19,423	0.79	0.19	3,660	64
2:6	Vambörsfjärden	1.02	49,577	0.98	0.43	20,550	103
2:7	Kungsträsket	2.31	7,733	0.54	0.20	1,550	30
2:8	Gällsboträsket	1.47	187,048	1.51	0.17	32,100	38
2:9	Stocksjön	2.70	36,480	0.82	0.22	8,030	8
2:10	Eckarfjärden	5.15	283,850	2.12	0.91	257,340	276
2:11	Puttan	0.48	82,741	1.29	0.37	30,150	301
3:1	Tallsundet	–0.23	79,414	0.80	0.23	18,350	208
4:1	Lake 4:1	–0.34	35,058	1.53	0.38	13,000	46
4:2	Lillfjärden	–0.35	161,269	0.89	0.29	47,030	184
5:1	Bredviken	–0.26*	97,664	1.72	0.74	72,010	186
6:1	Simpviken	–0.32	9,119	1.80	0.50	5,000	348
7:1	Lake 7:1	–0.47*	163,052	1.07	0.32	52,570	143
7:2	Märrbadet	–0.29	23,611	1.01	0.36	8,500	61
7:3	Lake 7:3	0.17	6,393	0.70	0.25	1,620	21
7:4	Lake 7:4	No data	9,312	0.81	0.24	2,250	71
8:1	Fiskarfjärden	0.28	754,303	1.86	0.37	274,450	228

from the sea may intrude into these lakes. For example, sea water relatively frequently flows into Lake Bolundsfjärden. The theoretical turnover times presented in Table 3-4 are based on the ratio of the lake volume and the catchment area with a specific discharge of 150 mm/year. For the low-lying lakes, occasionally intruded by sea water, no account is taken for this water in the values presented in Table 3-4.

Surface water level time series

Time series of surface water levels of the major lakes and the Baltic Sea are shown in Figure 3-5. The time series for Lillfjärden (SFM0066) indicate that the lake level is mainly determined by the sea level. The lake levels of Norra Bassängen (SFM0039) and Bolundsfjärden (SFM0040) are also quite low (close to the sea water level), but these levels seem to be determined mainly by the lake thresholds and the surface water and groundwater inflows from inland.

Occasionally the sea level rises high enough for direct sea water intrusion to the lower elevation lakes in the site investigation area. During the two major storms in Jan. 2005 and Jan. 2007 (named "Gudrun" and "Per", respectively) the sea water level also rose well above of the level of Lake Fiskarfjärden which has a mean water level of +0.55 m. The two major events of salt water intrusion into Lake Norra Bassängen and Lake Bolundsfjärden coupled to "Gudrun" and "Per" are shown in Figure 3-6.

The highest recorded half-hour value of the sea level, 1.40 m RHB70, was during the "Per" storm, which can be compared with 0.94 m during "Gudrun" (the corresponding maximum daily averages were 0.99 and 0.75 m, respectively). For comparison the mean sea water level during the whole monitoring period was –0.04 m and the minimum recorded half-hour value –0.68 m (minimum daily average –0.55 m).

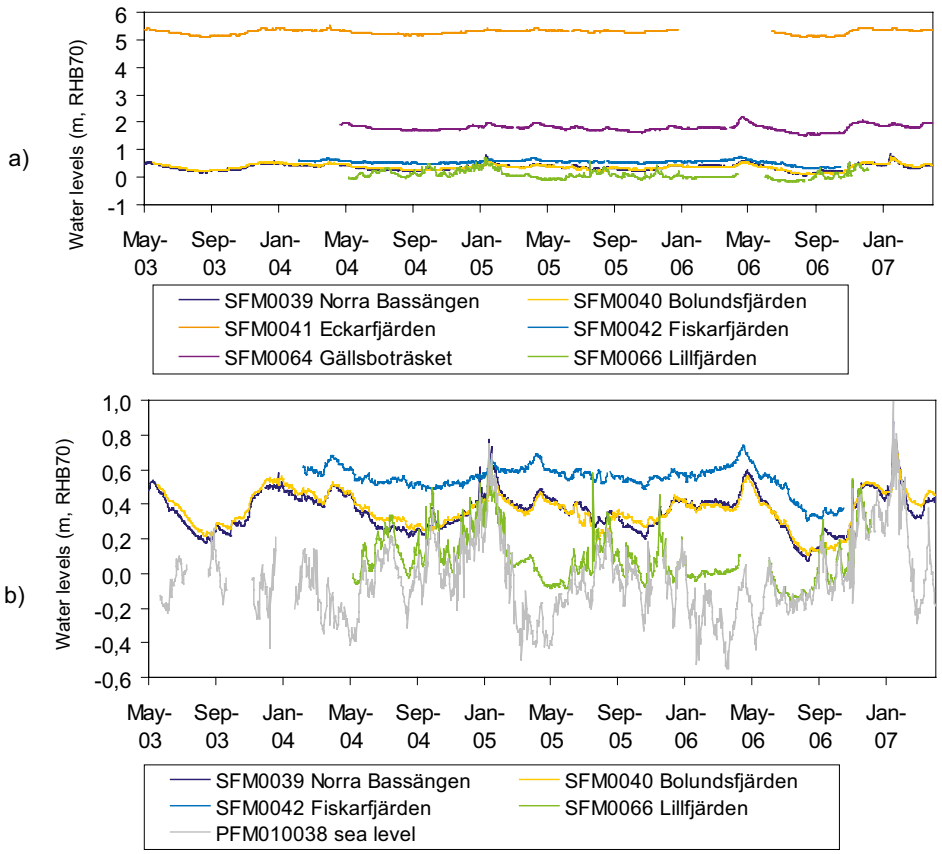

Figure 3-5. *Daily average surface water levels in the Baltic Sea and the larger lakes in the study area shown for all in a) and in close-up for the four lakes with the lowest levels in b). (Tick marks on the x-axis indicate the first date of labelled months.)*

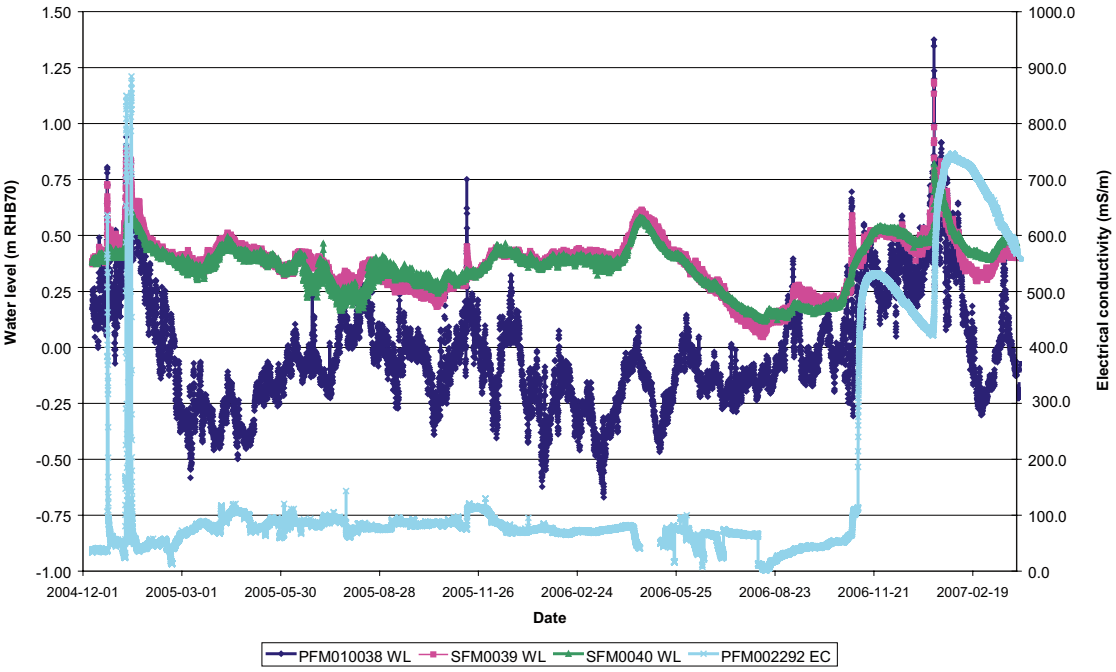

Figure 3-6. *The water levels in the Baltic Sea (PFM010038), Lake Norra Bassängen (SFM0039) and Lake Bolundsfjärden (SFM0040) plotted together with the electrical conductivity in the channel connecting the two lakes (PFM002292).*

From Figure 3-6 it is obvious that the development over time of the electrical conductivity (EC) was quite different in the channel between Lake Norra Bassängen and Lake Bolundsfjärden during the two storms. During "Gudrun" the EC peak was very distinct with a highest value of almost 900 mS/m, which is approximately the same as the EC of the sea water. However, already after less than two days the EC of the flow from Lake Bolundsfjärden to Lake Norra Bassängen was well below 100 mS/m.

This is explained by a distinct density layering in the ice-covered lake during "Gudrun", resulting in only low-salinity water flowing out of the lake. Figure 3-7 complements these observations with electrical conductivity profiles from lake water in Lake Bolundsfjärden taken at three occasions during 2005. The first occasion (Jan. 31, 2005) was approximately 3 weeks after the sea water intrusions and shows the settling of saline waters at the lake bottom. Two months later

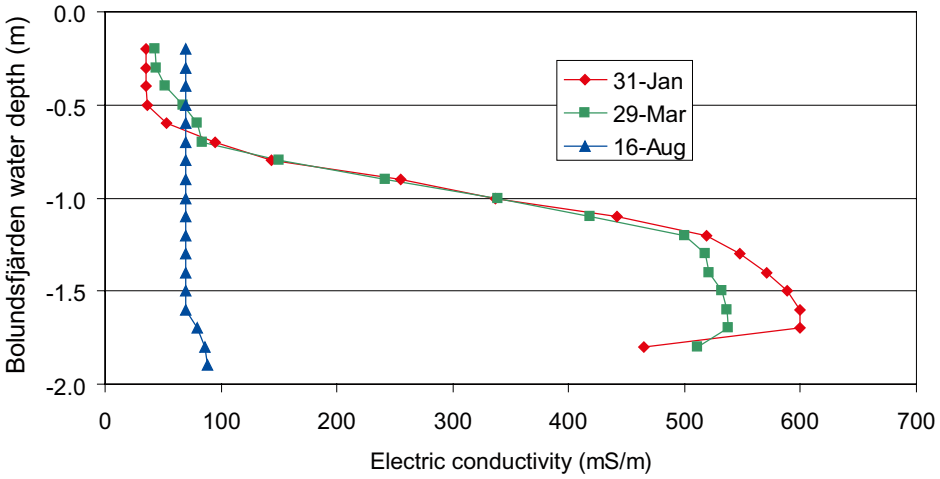

Figure 3-7. *Electrical conductivity profiles in Lake Bolundsfjärden measured during winter, early spring, and summer, 2005.*

(March 29, 2005), the conductivity profile was virtually identical. At that time the lake was still covered by ice preventing wind-driven water mixing. However, the summer measurement of Aug. 16 showed profiles indicating well-mixed conditions.

During 2006/2007 the conditions were quite different. A major inflow of sea water appeared already in the beginning of Nov. 2006. The water levels in Lake Norra Bassängen and Lake Bolundsfjärden were at that occasion still low after the very dry summer and early autumn of 2006. Since the lakes were not ice-covered the water body was completely mixed resulting in a continuously high but slowly decreasing EC in the outflow from Lake Bolundsfjärden after this event. Then another major sea water intrusion took place during "Per". The peak EC was somewhat lower than during "Gudrun", c. 750 mS/m.

Based on the water level changes in Lake Bolundsfjärden, information of the bathymetry, and the EC-measurements, the inflow of chloride to the lake has been estimated to c. 40 tonnes during "Gudrun" and during "Per", c. 250 tonnes. The difference is mainly explained by the considerably higher sea water levels during "Per".

3.3.3 Brooks and other surface drainage systems

There are no large water courses within the study area. The catchment areas are typically dewatered by small brooks that are periodically dry. The major brooks are shown in Figure 2-5 together with the installed surface discharge gauging stations.

The digital elevation model (DEM), in the form of a regular grid with a resolution of 10 m, does not describe the brooks with an adequate accuracy for the quantitative surface water flow modelling. In particular, brooks have been deepened for drainage purposes, which may lead to significant differences between their bottom elevations and the surrounding topography described by the DEM. Man-made alterations of the drainage system may also have changed the overall discharge directions from some sub-catchments, as compared to those inferred directly from the DEM.

In order to obtain a better description of the brooks in the area, field surveying was performed of cross-sections at regular distances along the major brooks within the central parts of the model area, see Figure 3-8 and /Brydsten and Strömgren 2005/. Furthermore, these brooks were characterised regarding bottom substrate, vegetation and technical encroachments in /Carlsson et al. 2005/.

General characteristics of brooks

The brooks in the study area pass through varying types of landscape and typically they exhibit a well defined furrow for some stretches and a more diffuse path where the furrow is difficult to distinguish in areas that can be characterized as wetlands. Figure 3-9 shows a schematic sketch of these types of landscapes. Figures 3-10 to 3-12 show photos of some typical brook sections.

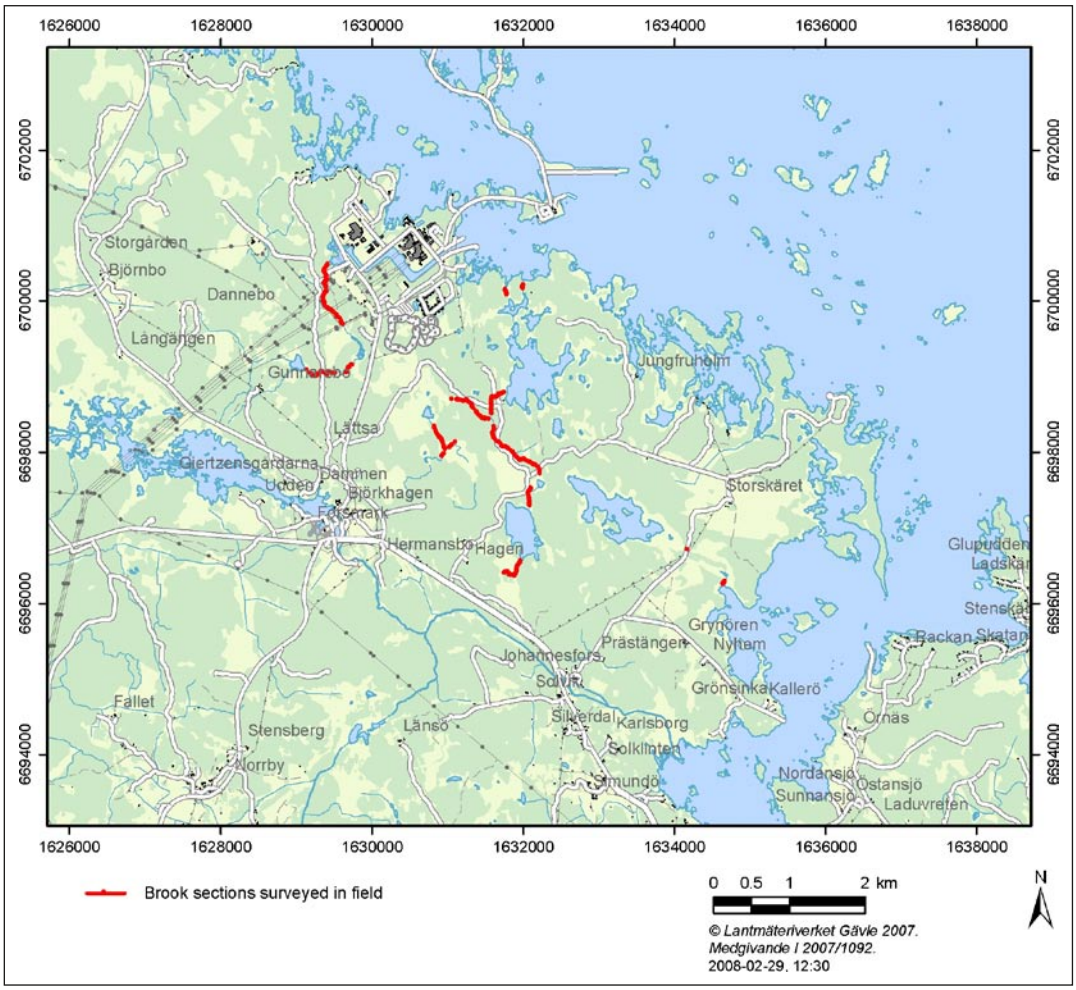

Figure 3-8. *The brook stretches where cross-sections were measured by field surveying.*

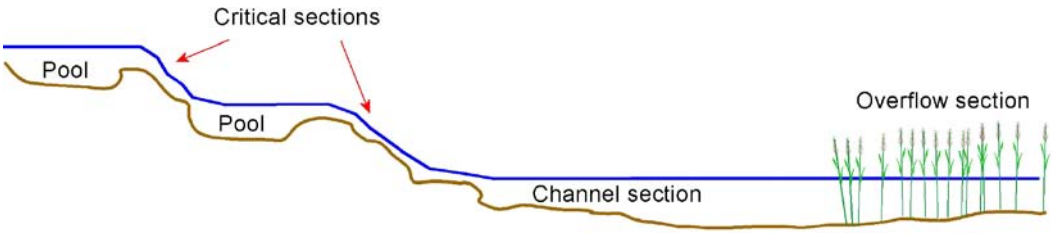

Figure 3-9. *Schematic sketch of a brook showing various section types.*

Figure 3-10. *Brook section downstream from discharge station PFM002668.*

Figure 3-11. *Brook from Lake Fiskarfjärden as seen from downstream.*

Figure 3-12. *Brook between Lake Norra Bassängen and the Baltic Sea with a well defined furrow at low flows.*

Brook properties

Figures 3-13 and 3-14 show the bottom elevations along the two major brooks in the central part of the investigation area, the brook from Eckarfjärden to the Baltic Sea, and that from about 400 m upstream of Gällsboträsket to the conjunction with the brook from Eckarfjärden, respectively (cf. Figure 3-8).

Observations describing the occurrence of overflow/wetland areas, cross-sectional geometry parameters, and bottom substrate are useful for describing the hydraulic properties of the brooks. Below, the classification of dominating bottom substrate and abundance of vegetation is compared to the bed gradient /Brydsten and Strömgren 2005, Carlsson et al. 2005/.

The brook between Lake Eckarfjärden and Lake Bolundsfjärden

The whole brook section has been substantially excavated except for a part of the stretch upstream of Lake Eckarfjärden which has been moderately excavated according to the classification in /Carlsson et al. 2005/. Bottom substrate and vegetation coverage are shown in Figures 3-15 and 3-16. Coarser bed material is found along stretches where the gradient is comparatively steeper, which is due to higher flow velocities removing fine material that is more readily scoured.

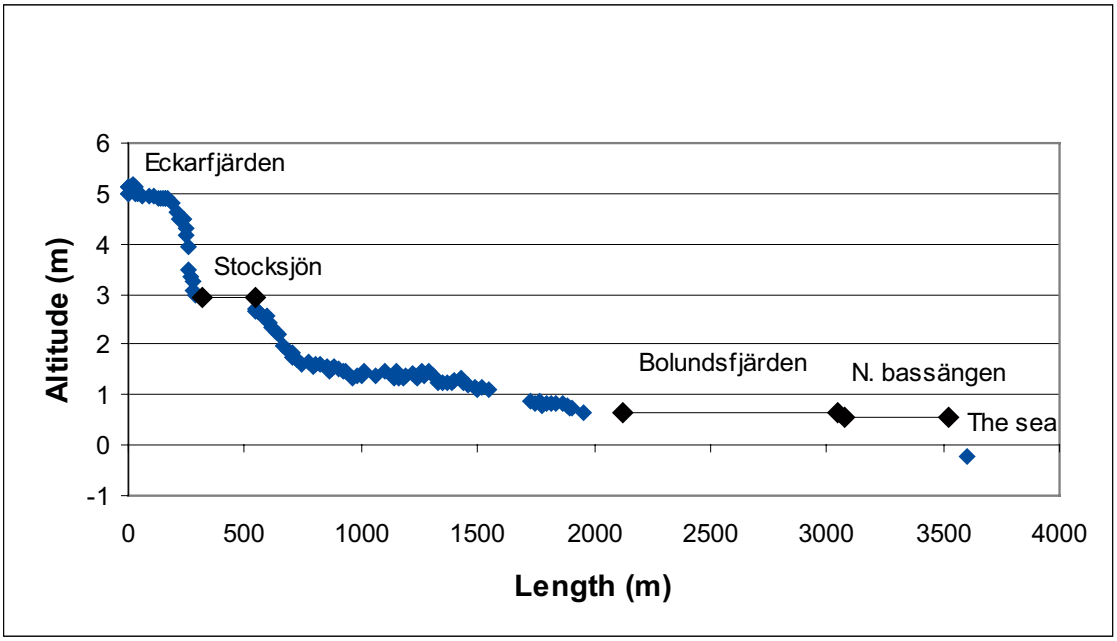

Figure 3-13. *The bottom elevation of the brook between Lake Eckarfjärden and the Baltic Sea.*

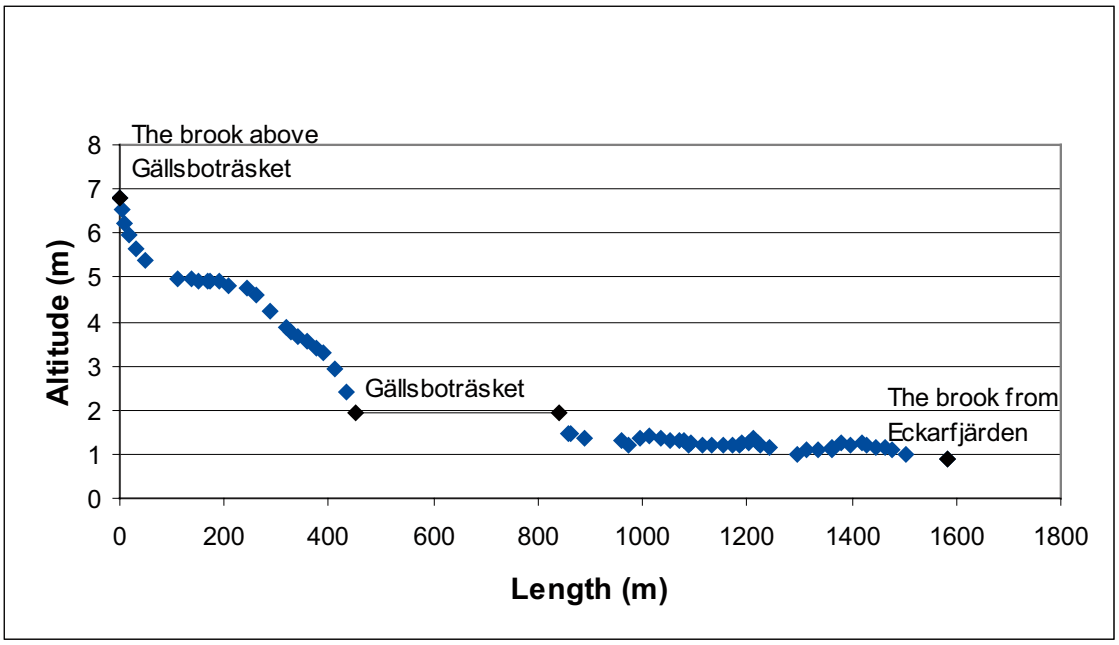

Figure 3-14. *The bottom elevation of the brook between a point 400 m upstream of Lake Gällsboträsket and the conjunction with the brook from Lake Eckarfjärden.*

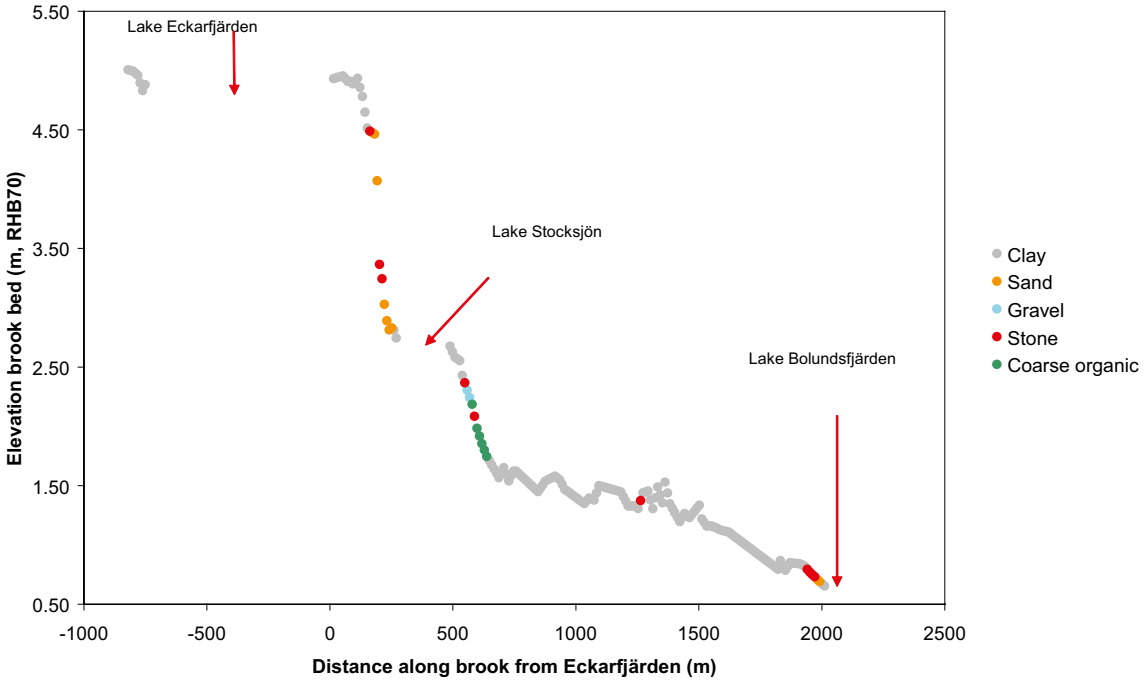

Figure 3-15. *Dominating bottom substrate in the brook from Lake Eckarfjärden to Lake Bolundsfjärden. The origin of the x-axis is placed at the stream outlet from Lake Eckarfjärden. Missing bed elevation values were interpolated in places where information on bottom substrate was available.*

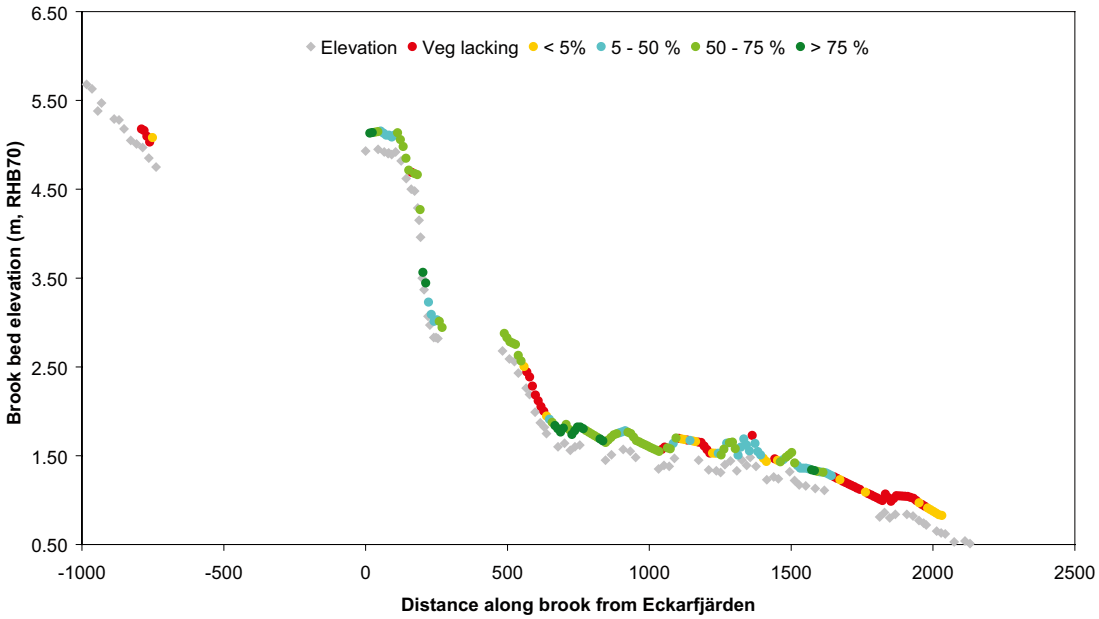

Figure 3-16. *Vegetation coverage along the brook from Lake Eckarfjärden to Lake Bolundsfjärden. Note that an offset has been applied to the dots showing vegetation abundance in order to discriminate them from dots showing the elevation.*

The brook through Lake Gällsboträsket and to the junction with the brook from Lake Eckarfjärden.

Approximately 80% of the brook section through Lake Gällsboträsket and to the junction with the brook from Lake Eckarfjärden has been substantially excavated and the rest (approximately half of the stretch downstream of Lake Gällsboträsket) moderately excavated, according to the classification in /Carlsson et al. 2005/. The bottom substrate, including and excluding organic material, and the vegetation coverage, are shown in Figures 3-17 to 3-19.

The coarseness of the dominating bed material shows no discernable pattern when compared to the gradient. Generally the bottom substrate in the reach upstream of Lake Gällsboträsket is comprised of fine organic material (and a short stony stretch) while the stretch downstream of Lake Gällsboträsket is comprised of clay. Plotting the dominating substrate when organic material is excluded, however, shows a clearer picture where the bed material in the steeper upper reach is comprised of stone and gravel.

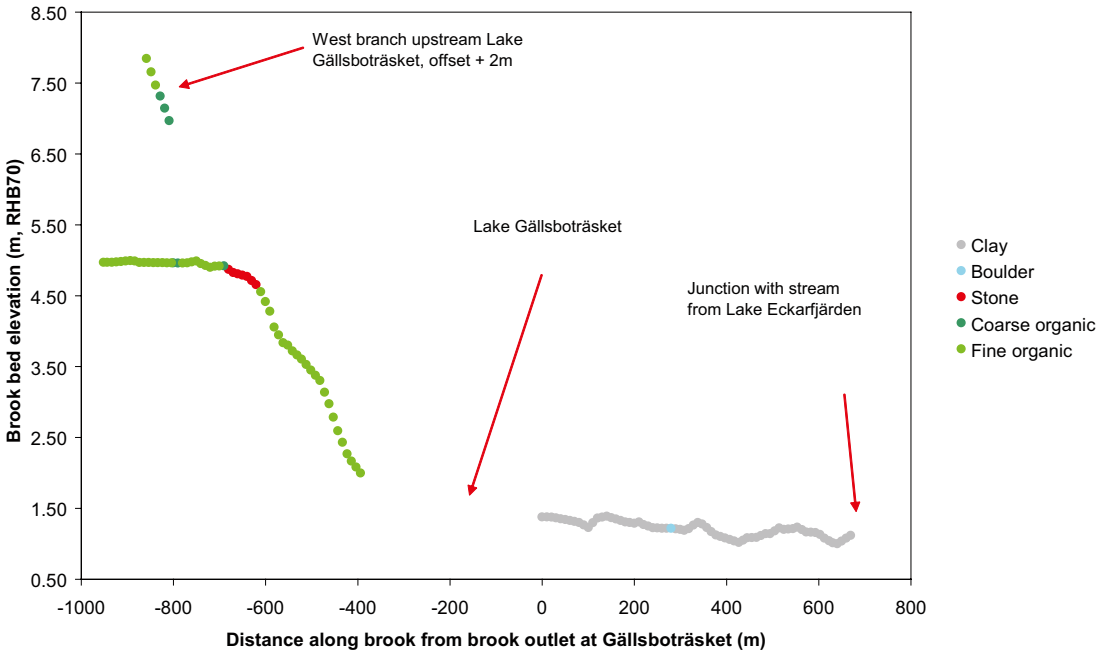

Figure 3-17. *Dominating bottom substrate along the brook that passes Lake Gällsboträsket and down to the junction with the brook from Lake Eckarfjärden. Note that an offset of +2 m has been added to the western branch of the stream upstream Lake Gällsboträsket in order to discriminate it from the eastern branch.*

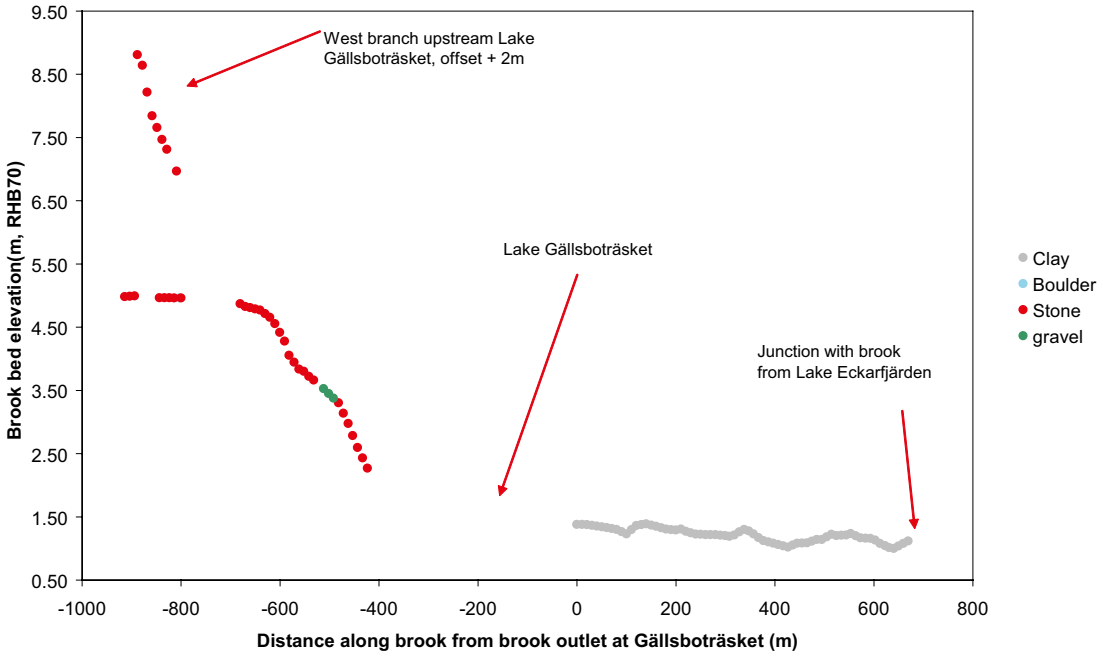

Figure 3-18. *Dominating substrate excluding organic material along the brook that passes Lake Gällsboträsket and down to the junction with the brook from Lake Eckarfjärden. Note that an offset of +2 m has been added to the western branch of the stream upstream Lake Gällsboträsket in order to discriminate it from the eastern branch.*

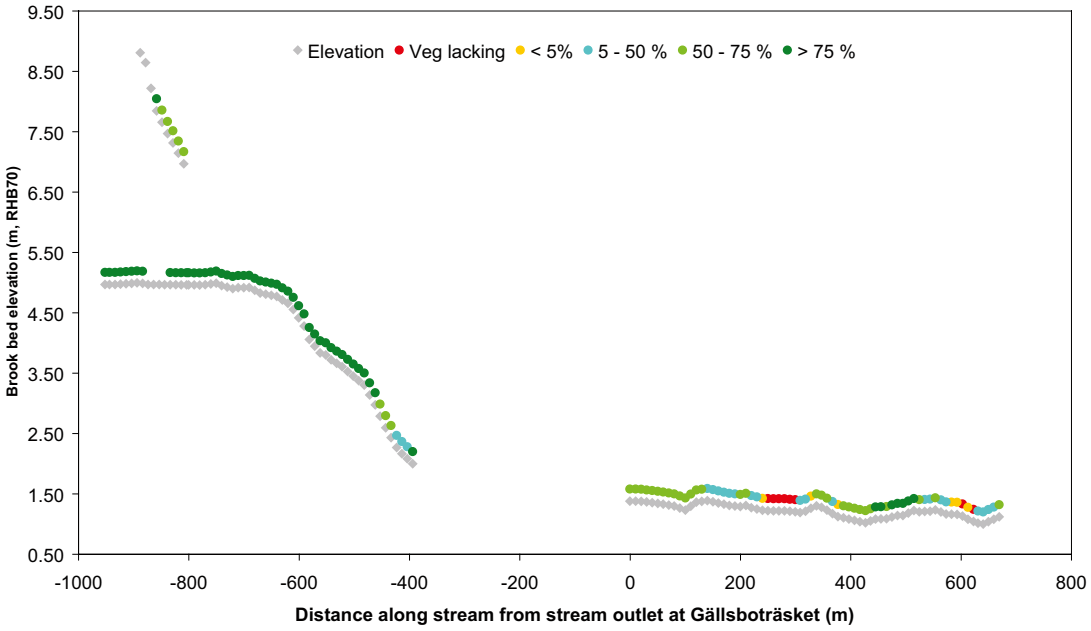

Figure 3-19. *Vegetation coverage along the brook that passes Lake Gällsboträsket and down to the junction with the brook from Lake Eckarfjärden. Note that an offset of +2 m has been added to the western branch of the stream upstream Lake Gällsboträsket in order to discriminate it from the eastern branch, and that an offset also has been applied to the dots showing vegetation abundance in order to discriminate them from dots showing the elevation.*

Discharge and surface water level elevations

Lake Eckarfjärden, SFM0041 to PFM002668

The stream between the Lake Eckarfjärden outlet and the discharge station PFM002668 is approximately 200 m long. The elevation of the lake threshold is +5.15 m RHB70 (cf. Table 3-4) and the level of the discharge station +4.29 m. Thus, the average bed gradient is $4.3 \cdot 10^{-3}$. The relationship between the level of Lake Eckarfjärden and the discharge in PFM002668 is shown in Figure 3-20.

The measured discharge and the theoretical discharge curve show a good general agreement, which mainly tells that the discharge station is fairly well adjusted to the brook geometry at the outlet section from Lake Eckarfjärden. For low flows, however, the agreement is less good and there seems to be a small flow volume, occurring mainly during autumn, which is not related to the upstream water level in the same way as larger flow volumes. This could be due to a critical section formed when the flow depth is approximately 0.1 m (threshold level 5.15 m), which implies that the flow describes a transformation from subcritical to the supercritical flow regime when the flow depth becomes more shallow. This is reasonable for a natural channel with a rough bottom.

Comparing discharge between seasons for the same level in Lake Eckarfjärden shows that there is a variation with a higher flow during winter, which is reasonable presuming that the stream is congested by reeds and similar during spring to autumn. This seasonal variation may be attributed solely to varying stream roughness, assuming that the geometry and bed gradient is unchanged.

PFM002668 to PFM002667

The brook between discharge stations PFM002668 and PFM002667 is comprised of two sections, firstly the part between PFM002668 and Lake Stocksjön, which has a steep gradient, and secondly the part between Lake Stocksjön and PFM002667, which is initially comparatively steep with a smaller gradient further downstream.

The first reach from PFM002668 to Lake Stocksjön is approximately 160 m long. The outlet threshold at Lake Stocksjön is at level +2.70 m RHB70 and the flume PFM002668 bottom at +4.29 m, which makes the average bed gradient approximately $9.9 \cdot 10^{-3}$ (assuming that pressure gradient losses in the lake are negligible the outlet threshold is applicable as inflow threshold).

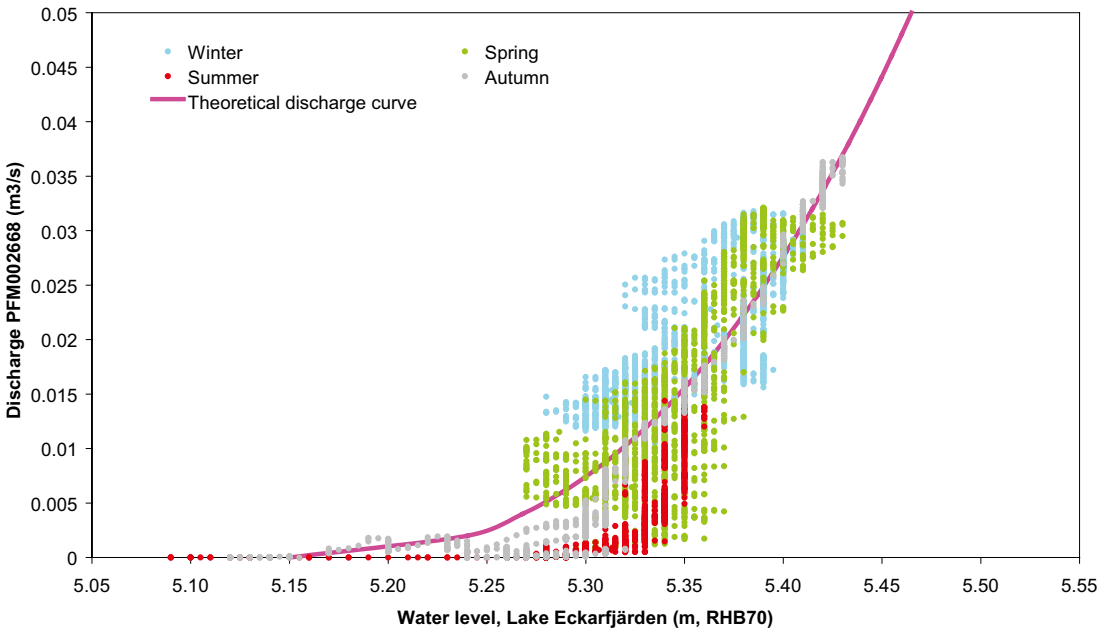

Figure 3-20. *Discharge curve divided by season and the theoretical discharge curve of the station PFM002668.*

The distance between Lake Stocksjön and PFM002667 is approximately 990 m and the bed level at PFM002667 is approximately +1.50 making the average bed gradient $1.2 \cdot 10^{-3}$. This part of the brook has been described as having a generally well-defined geometry although in parts with a less well-defined furrow in reaches where the water sometimes overflows the stream banks.

A comparison of the normalised discharge from PFM002667 with the upstream station PFM002668 is made in Figure 3-21, with the data divided into periods of increasing and decreasing discharge at the upstream discharge station PFM002668.

The normalized discharge from the downstream measuring station PFM002667 is at times larger during periods when the discharge is increasing. The standard deviation of the normalized discharge at PFM002667 is also approximately 7% larger for periods when the flow is increasing as compared to periods when the flow is decreasing. Physically the difference may be due to Lake Eckarfjärden which is comparatively large and close upstream of the discharge station PFM002668 and likely to dampen out quick variations in discharge. During periods when the discharge is decreasing the normalized discharge is more or less the same for both stations.

PFM002667 to junction with brook from Lake Gällsboträsket to PFM005764

The brook between discharge stations PFM002667 (+1.50 m RHB70) and PFM005764 (+0.90 m) is approximately 570 m long making the mean bed gradient $1.1 \cdot 10^{-3}$. This part of the stream has been described as having a generally well-defined geometry although in parts with a less well-defined furrow in reaches where water sometimes overflows the banks. The largest overflow area is located at the junction between this brook and the brook from Lake Gällsboträsket, starting approximately 100 m upstream and ending approximately 100 m downstream of the junction.

The discharge normalized with the average discharge for each respective station is shown in Figure 3-22. In the figure the data is divided into periods of increasing and decreasing discharge at the upstream discharge station, PFM002667. The normalized discharge from the downstream measuring station PFM005764 is occasionally smaller during periods when the discharge is increasing indicating that the degree of retention is higher for the catchment area affecting station PFM005764 than for the catchment area affecting PFM002667. Physically it may be due to the large wetland area near the junction as well as the discharge from Lake Gällsboträsket. During periods when the discharge is decreasing the normalized discharge is more or less the same for both stations.

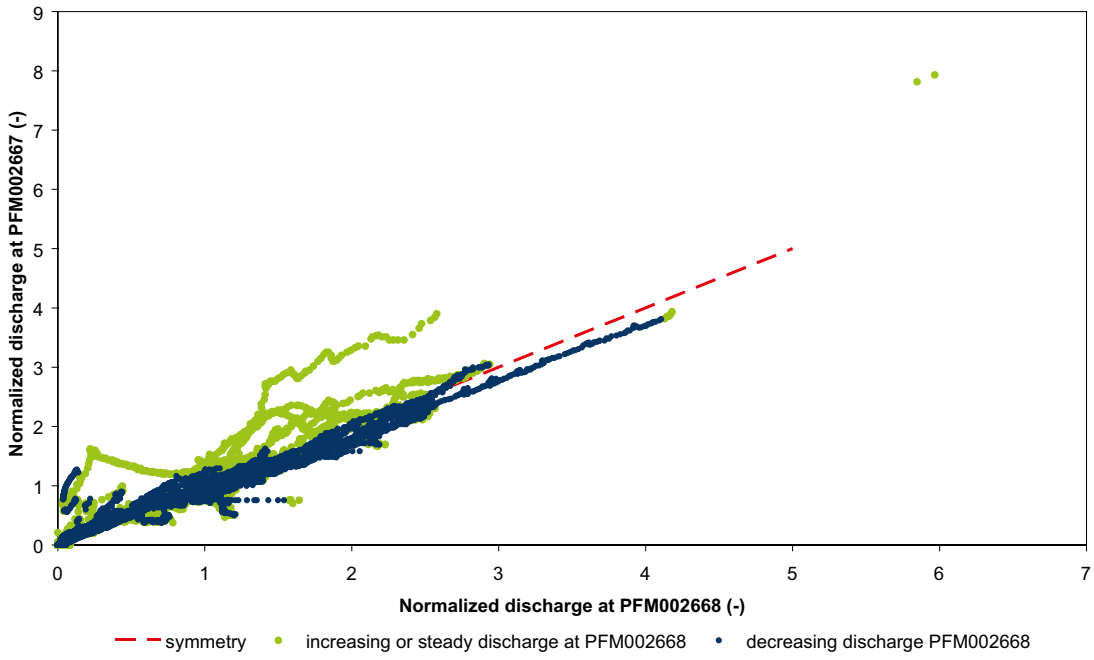

Figure 3-21. *Normalized discharge at PFM002668 and PFM002667.*

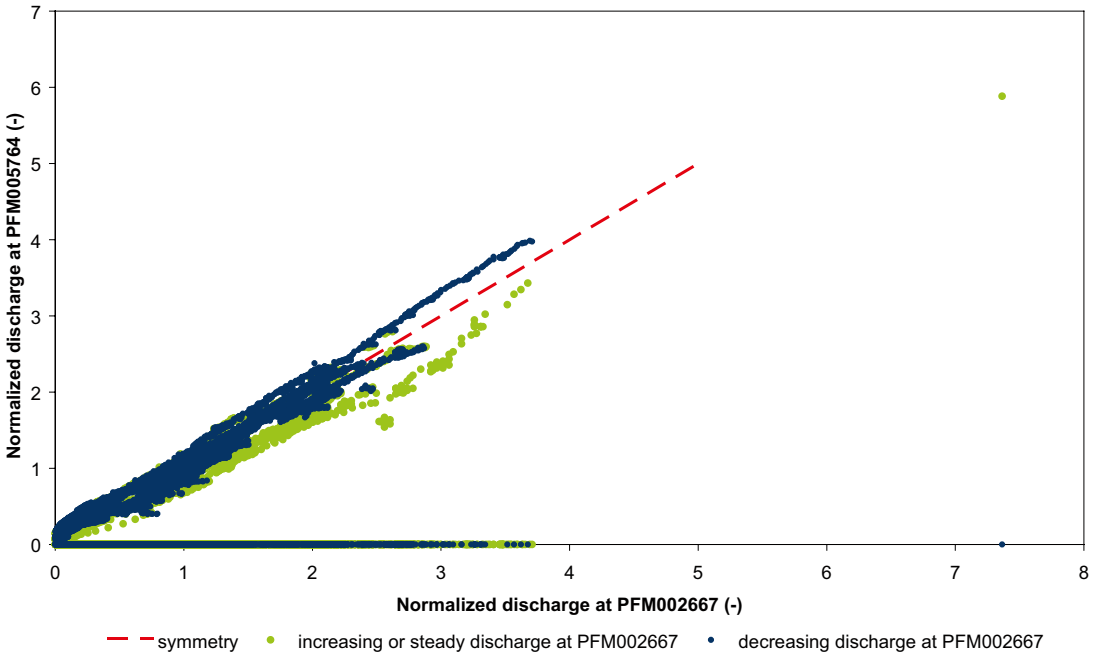

Figure 3-22. *Normalized discharge from PFM002667 and PFM005764.*

PFM005764 to Lake Bolundsfjärden, SFM0040

The brook reach between the discharge station PFM005764 and Lake Bolundsfjärden is approximately 150 m long and has a bed gradient of $4.1 \cdot 10^{-3}$ assuming that the lake inlet is at the same level as the lake threshold (+0.28 m), which is slightly steeper than the gradient in the upstream stretch between station PFM005764 and PFM002667.

The measured discharge and the water levels in Lake Bolundsfjärden vary independently since the measuring flume produces a critical section, which by definition is unaffected by the water level downstream. The variations in water level and discharge are, however, correlated to a degree with a correlation coefficient of 0.77 (Figure 3-23).

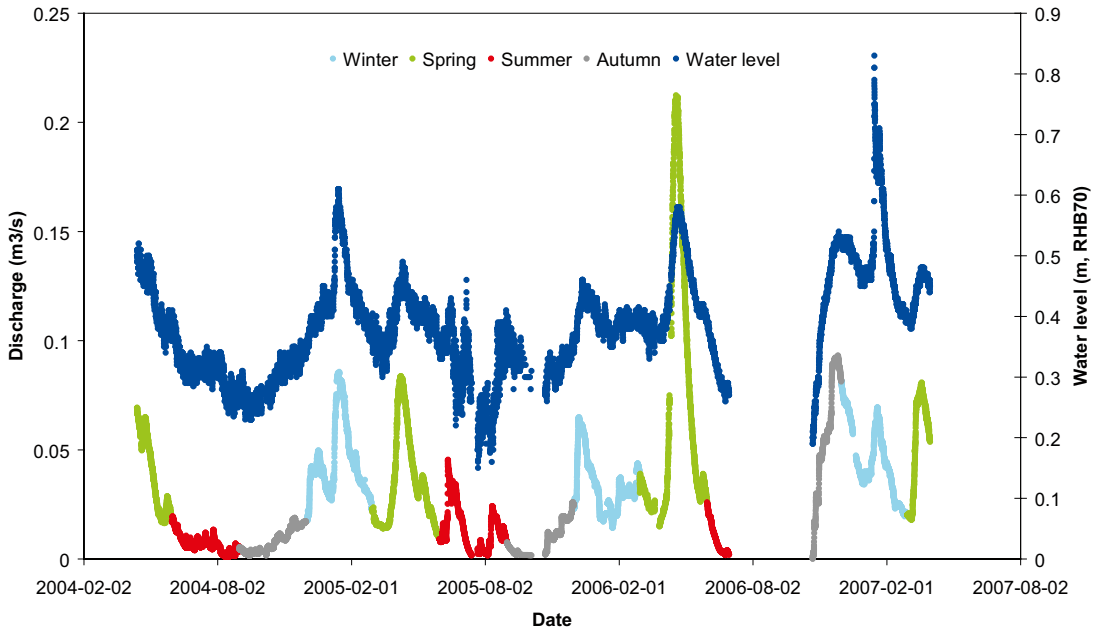

Figure 3-23. *Measured discharge at PFM005764 and water level in Lake Bolundsfjärden, SFM0040.*

Lake Gällsboträsket to the junction with the brook from Lake Eckarfjärden to PFM005764

The brook between the lake threshold from Lake Gällsboträsket (+1.47 m RHB70) and the discharge station PFM005764 (+0.90 m) is approximately 1,050 m long and has an average gradient of $0.54 \cdot 10^{-3}$. The section between Lake Gällsboträsket and the junction with the brook from Lake Eckarfjärden has a well defined furrow, occasionally with banks as high as 2 m, until approximately 30 m upstream of the junction were the stream discharges into a wetland area. The relationship between discharge and water level in Lake Gällsboträsket (SFM0064) is shown in Figure 3-24.

The discharge-water level relationship shows no clear seasonal variation like the one from Lake Eckarfjärden. This may be due to the smaller gradient, which leads to lower flow velocities, which in turn entails smaller losses due to stream roughness. The discharge shows no discernable pattern when divided into periods with increasing and decreasing water levels.

Lake Bolundsfjärden (SFM0040) to Lake Norra Bassängen (SFM0039) to the Baltic Sea (PFM010038)

The stream between Lake Bolundsfjärden and Lake Norra Bassängen has a distinct furrow during low flows. During higher flow, the water flows through a wide reed covered area with a stony bottom. Between Lake Norra Bassängen and the Baltic Sea there are two brook outlets (with different threshold levels). They are described as reed covered areas with a bottom substrate of stony till (see Figure 3-12 showing photos of the eastern outlet with the lower threshold level).

Stream roughness

It is not possible to estimate any specific friction coefficient from the performed measurements and observations since the flow regime and the occurrence of critical sections are unknown. There may also be a fairly clear seasonal variation in flow resistance as shown in Figure 3-20, where the same upstream lake level may result in significantly different discharges.

A comprehensive table of Manning's roughness coefficients related to stream properties that can serve as some guidance can be found in, for example, /Chow 1959/. One of the prerequisites of the Manning equation is that the flow is steady and only slightly non-uniform. In the study area, however, critical brook sections are likely to be fairly common, particularly in the steeper sections.

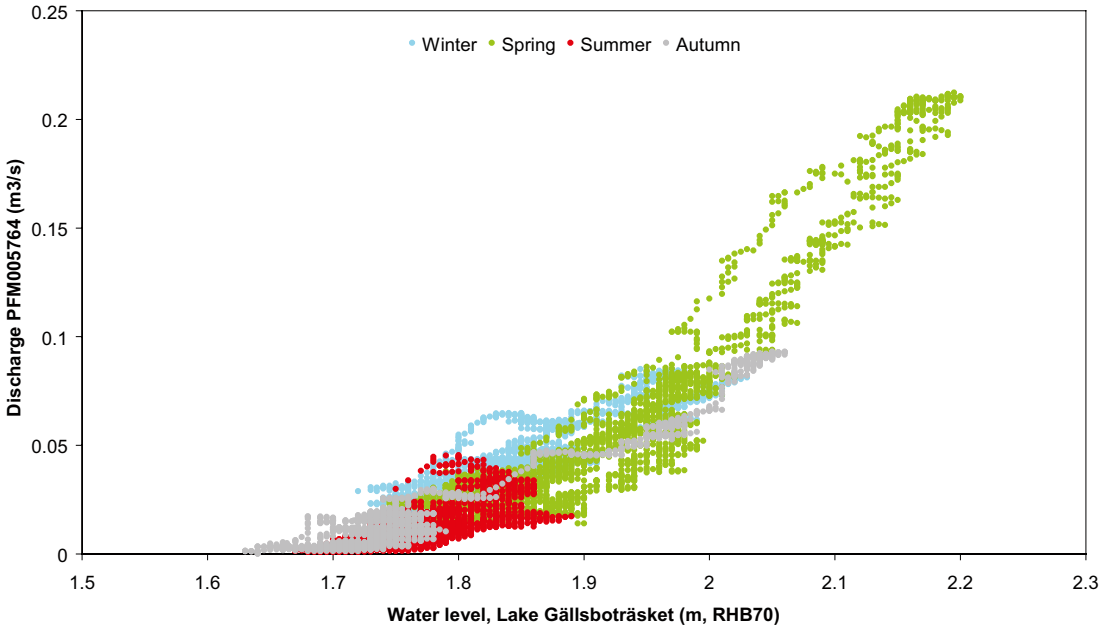

Figure 3-24. *Discharge at PFM005764 compared to the water level at Lake Gällsboträsket, SFM0064.*

Surface discharge time series

Time series of surface water discharge at the four installed gauging stations are shown in Figure 3-25 (for locations of the stations and sizes of upstream catchments see Figure 2-5 and Table 2-5). The highest recorded discharge from the catchments at stations PFM005764, PFM002667, PFM002668 and PFM002669 were 212 L/s (38.0 L/s/km^2), 131 L/s (43.4 L/s/km^2), 75.9 L/s (33.3 L/s/km^2), and 183 L/s (64.5 L/s/km^2), respectively. All stations had zero discharge for relatively long periods in late summers and early autumns, especially during 2006.

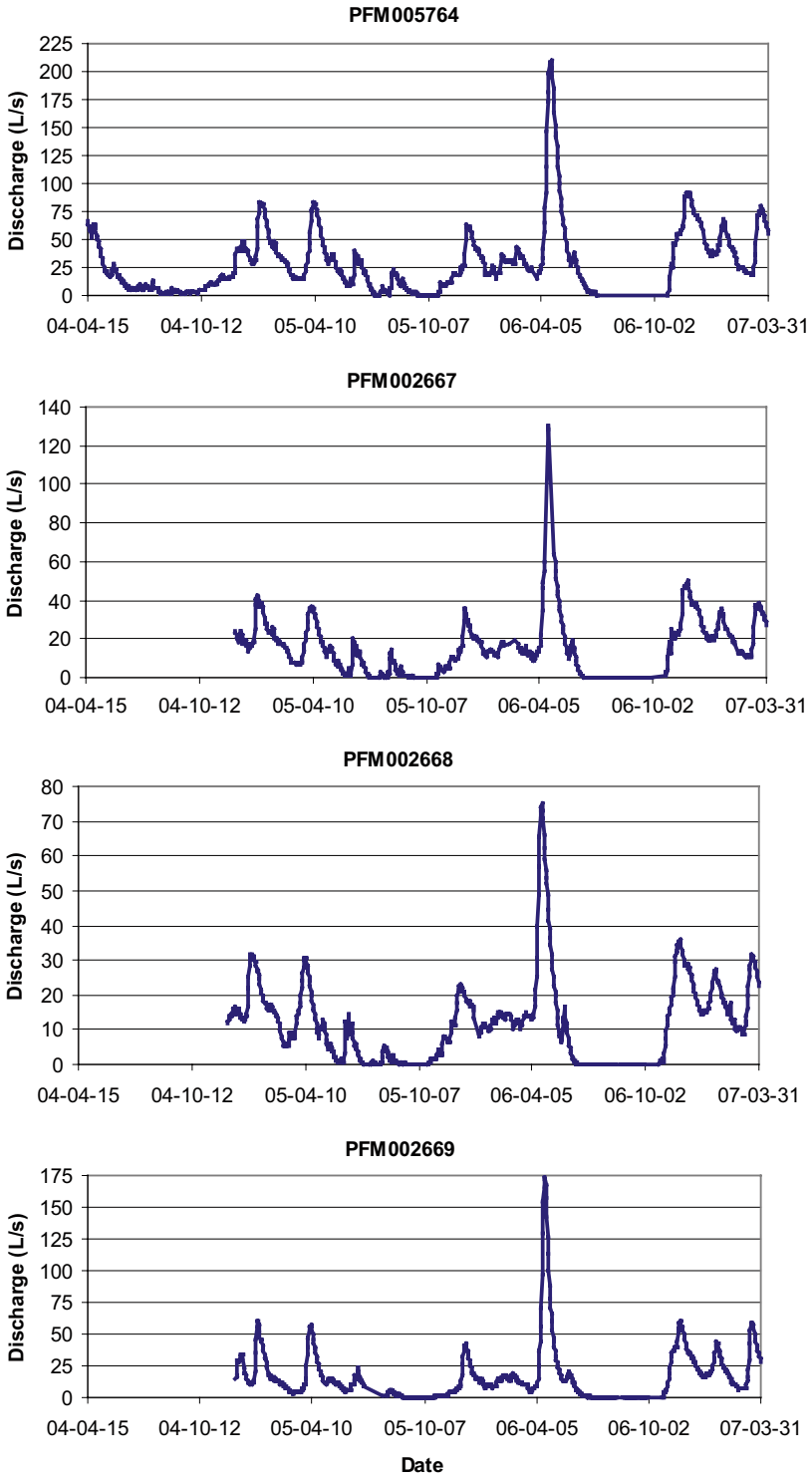

Figure 3-25. *Surface discharge time series at the four automatic gauging stations (daily means). Note the different scale of the discharge axes.*

The relatively short time series available imply that it is difficult to draw any definite conclusions on longterm mean specific discharge. This is illustrated by the mean values for various time periods presented in Table 3-5. The mean specific discharge for the largest catchment, which had a 35.5 months' time series, was 4.87 L/s/km^2 (154 mm/year). The variation of specific discharge for a specific station for the time periods selected for comparison was 30–35%, whereas the variation between stations for the same time period was 10–17%.

If the full 3-year period of April 15, 2004 until April 14, 2007 is considered the corrected mean precipitation was 546 mm/year while the mean specific discharge of the largest catchment of 5.6 km^2 was 154 mm/year. From a comparison of groundwater and surface water levels at the start and end of the period it can be concluded that the these storages were a little smaller at the end of the period but only corresponding to a difference of c. –5 mm/year.

The mean precipitation was 13 mm/year lower than the 30-year normal precipitation estimated by SMHI (see Appendix 1). Since approximately 2/3 of the precipitation goes to evapotranspiration, the precipitation deficit should correspond to a discharge deficit of approximately 5 mm/year. These estimates of storage changes and precipitation deficit indicate that the measured 3-year mean discharge should be close the longterm average discharge. A rough estimate of the longterm overall water balance of the area is then: P (precipitation) = 560 mm/year, ET (evapotranspiration) = 400–410 mm/year, and R (runoff) = 150–160 mm/year.

Table 3-5. Discharge characteristics for the four gauging stations for various time periods (* total available time series for PFM00576, ** total available time series for PFM002667, PFM002668 and PFM002669).

	PFM005764	PFM002667	PFM002668	PFM002669
Apr 15, 2004–Mar 31, 2007*				
Mean discharge (L/s)	27.2			
Min. discharge (L/s)	0.00			
Max. discharge (L/s)	212			
Specific discharge (L/s/km^2)	4.87			
Specific discharge (mm/yr)	154			
Dec 8, 2004–Mar 31, 2007**				
Mean discharge (L/s)	31.0	15.6	11.6	15.8
Min. discharge (L/s)	0.00	0.00	0.00	0.00
Max. discharge (L/s)	212	131	75.9	183
Specific discharge (L/s/km^2)	5.54	5.19	5.07	5.57
Specific discharge (mm/yr)	175	164	160	176
Jan 1–Dec 31, 2005				
Mean discharge (L/s)	25.2	12.1	9.09	11.6
Min. discharge (L/s)	0.00	0.00	0.00	0.00
Max. discharge (L/s)	85.3	43.7	31.8	60.7
Specific discharge (L/s/km^2)	4.51	4.01	3.99	4.10
Specific discharge (mm/yr)	142	127	126	129
Jan 1–Dec 31, 2006				
Mean discharge (L/s)	32.9	17.1	12.1	17.4
Min. discharge (L/s)	0.00	0.00	0.00	0.00
Max. discharge (L/s)	212	131	75.9	183
Specific discharge (L/s/km^2)	5.89	5.67	5.31	6.13
Specific discharge (mm/yr)	186	179	167	193
Oct 1, 2004–Sep 30, 2005				
Mean discharge (L/s)	24.7			
Min. discharge (L/s)	0.00			
Max. discharge (L/s)	85.3			
Specific discharge (L/s/km^2)	4.42			
Specific discharge (mm/yr)	139			
Oct 1, 2005–Sep 30, 2006				
Mean discharge (L/s)	27.3	14.3	10.3	14.1
Min. discharge (L/s)	0.00	0.00	0.00	0.00
Max. discharge (L/s)	212	131	75.9	183
Specific discharge (L/s/km^2)	4.88	4.74	4.53	4.96
Specific discharge (mm/yr)	154	149	143	157

3.3.4 Wetlands

Different types of wetlands occur frequently within the Forsmark site investigation area. In Figure 3-26, the different wetlands types, as presented in the ground layer of the vegetation map /Boresjö Bronge and Wester 2003, Löfgren (ed.) 2008/, are shown. Wetlands cover 10%, 12% and16% of the major catchments Forsmark 1, 2 and 8, respectively. For some of the sub-catchments, wetlands cover between 25% and 40% (Tables 3-2 and 3-3).

From a hydrological point of view, it is useful to distinguish between bogs, fens and marshes /Kellner 2004/. Bogs are peat covered areas where the precipitation falling within the area is the only source of water for the vegetation (ombrotrophic). Bogs are found in the most elevated parts of the site investigation area only. These bogs are small and the peat cover is not very thick (< 3 m) /Fredriksson 2004/.

Fens are peat covered areas where the vegetation at least partly is supplied by inflowing surface water and/or groundwater. Marshes are wetlands with little or no peat. Fens and marshes are frequent in the more low-lying parts of the area.

The lithostratigraphies of the bogs, fens and marshes are decisive for their hydraulic contact with the surrounding groundwater system. From existing borings /Johansson 2003, Werner and Lundholm 2004b, Lokrantz and Hedenström 2006/, it is known that the peat and gyttja in the

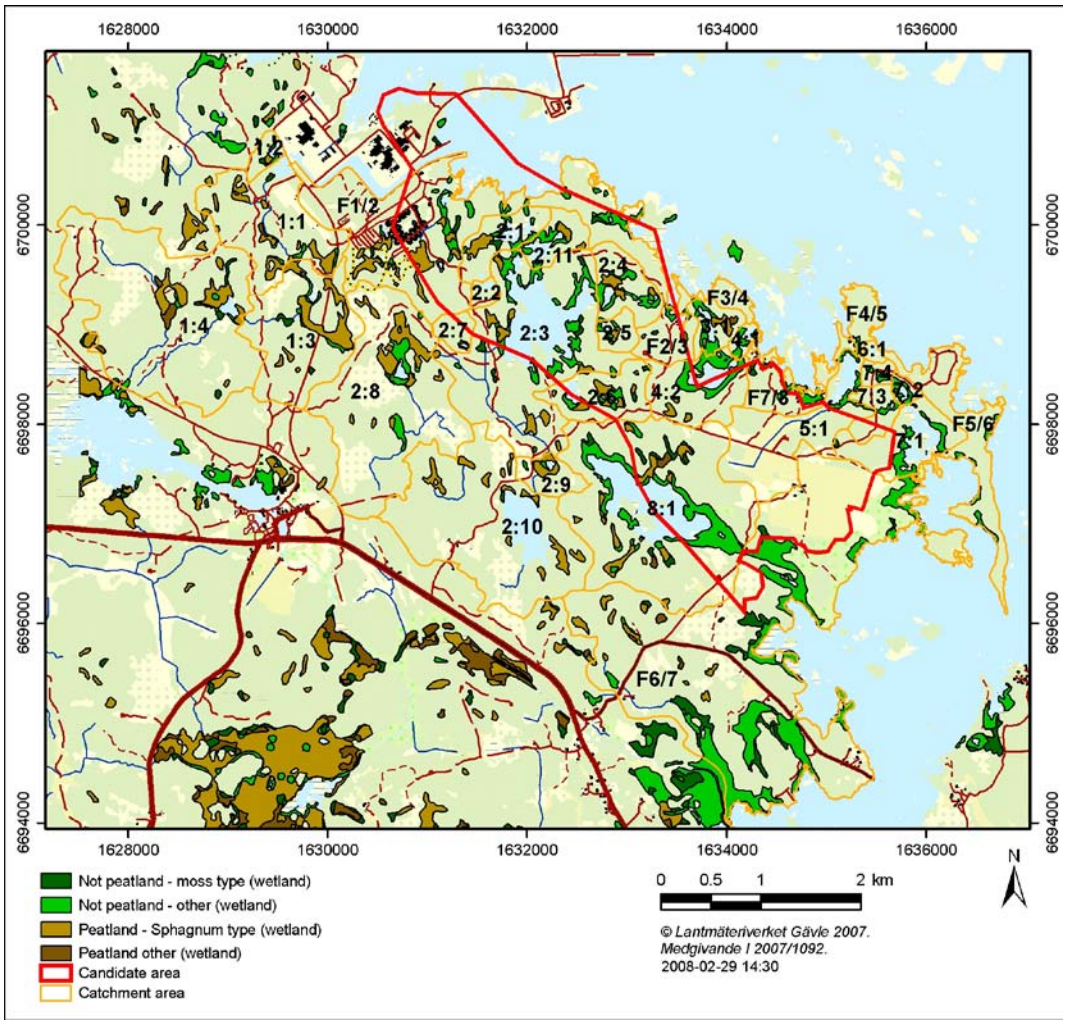

Figure 3-26. *Wetlands of different types within the Forsmark area, based on the vegetation map /Boresjö Bronge and Wester 2003/.*

wetlands can rest directly on till, or be underlain by clay and sand above the till. In Figure 3-27 presence/absence of a clay layer is shown from an inventory of 25 wetlands in the central part of the site investigation area. In summary, 13 sites contain a clay layer and at 12 sites the organic sediment is resting directly on coarse minerogenic material, often till /Lokrantz and Hedenström 2006/.

In Table 3-6 generalised lithstratigraphies of three wetlands are presented; two fens and one bog. The investigations regarding hydraulic properties of the wetland sediments as well as groundwater levels are presented in Section 3.4.1.

Table 3-6. Generalised lithostratigraphy of three wetlands. For locations of the coring sites, see Figure 2-7.

Deposit	SFM0084 (fen)	SFM0091(fen)	SFM0095 (bog)
Peat thickness	None	none	0.10–1.65 m/1.55 m
Gyttja (depth interval/thickness)	0.35–0.80 m/0.45 m	0.45–0.82 m/0.37m	1.65–1.85 m/0.20 m
Clayey gyttja (depth interval/thickness)	0.80–1.29 m/0.49 m	0.82–1.15 m/0.33m	1.85–2.12 m/0.27 m
Sand (depth interval/thickness)	1.29–1.74 m/0.45 m	1.15–1.25 m/0.10m	patchy
Clay (depth interval/thickness)	1.74–2.46 m/0.72 m	1.25–1.31 m/0.06m	2.12–2.96 m/0.84 m
Till (depth interval/thickness)			3–5 m

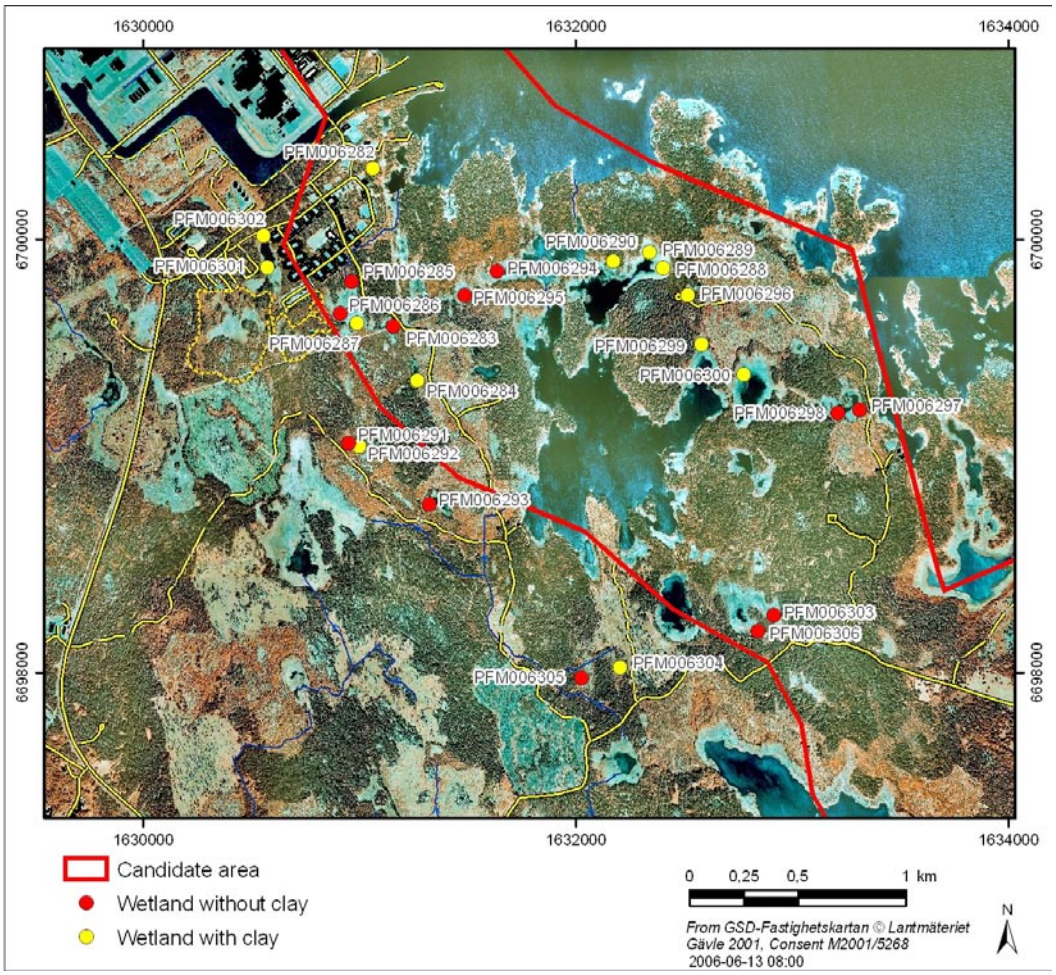

Figure 3-27. *Absence or presence of a stratum of clay in 25 wetlands in the central part of the site investigation area /Lokrantz and Hedenström 2006/.*

3.3.5 Coastal basins

The coastal marine system of the site investigation area is located in Öregrundsgrepen. Öregrundsgrepen is an open-ended embayment with a wide and deep boundary towards north and a narrow and shallower strait towards south, which connects to an archipelago that gives a buffer zone before the southern seaward boundary. A deep channel runs in the north-south direction in the eastern part of the embayment. The southern strait has a sill at approximately 25 m depth (Figure 3-28).

The water exchange of semi-enclosed coastal basins is controlled by a number of forcing variables acting at different spatial and temporal scales (Table 3-7). Tides are insignificant in the Baltic Sea. Instead, the dominant cause of water exchange in semi-enclosed Baltic coastal basins is often density fluctuations at the seaward boundary /Engqvist and Omstedt 1992/. With strong freshwater discharge, estuarine (baroclinic) circulation can also be an important mode of water exchange. Atmospheric heat transfer act stabilizing (heating) or destabilizing (cooling) on the stratification. Wind shear acts to increase the depth of the well-mixed surface layer, and large-scale wind patterns can also cause up- or down-welling events through Ekman dynamics.

Due to the wide open boundary towards north, Öregrundsgrepen is strongly affected by the large-scale circulation and dynamics of the Baltic Sea, and notably by the southbound coastal current, with seasonal density fluctuations due to variations in the collective discharge to the Bothnian Bay by the major rivers in northern Sweden and Finland.

The local freshwater discharge to Öregrundsgrepen is moderate with the streams Forsmarksån and Olandsån discharging about 3 and 6 m^3/s, respectively, as an annual average to the southern part of Öregrundsgrepen. In the central parts only minor brooks, that are periodically dry, and diffuse groundwater discharge contribute to the natural freshwater supply, see Sections 3.3.3 and 3.4. The freshwater discharge is not sufficiently strong for large-scale estuarine circulation to establish in Öregrundsgrepen.

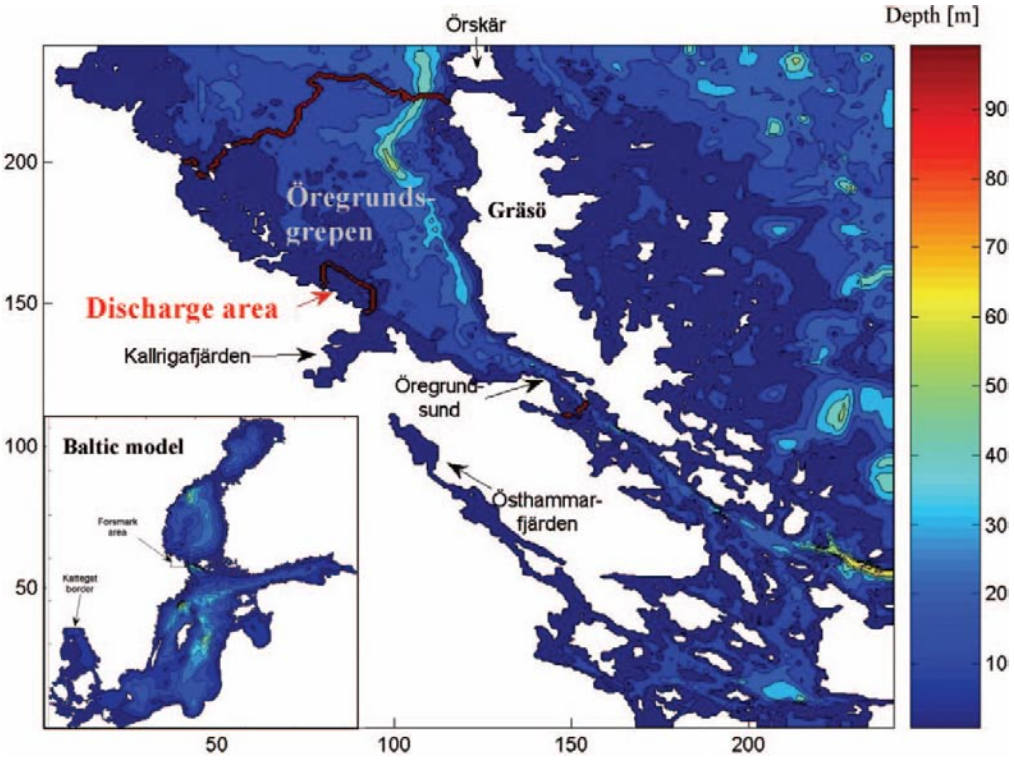

Figure 3-28. *Bathymetric map of the Forsmark coastal area.*

Table 3-7. Coastal and archipelago water exchange processes and typical time scales of forcing (solid lines) and basin response (dashed) /Engqvist and Stenström 2004/.

Forcing	Mediating processes	Basin response	Time scale s min h day week month
Boundary fluctuations			
- Sea level	Long surface waves	Filling/ emptying	
- Density	Long internal waves	Adjusted stratification	
Freshwater discharge			
- Mass and mom. transfer	Long surface waves	Filling	
	Horizontal jets	Horizontal currents	
	Turbulent mixing	Deepened surface layer	
- Buoyancy flux	Long internal waves	Baroclinic circulation	
		Enhanced vertical density gradient	
Atmospheric heat transfer			
- Differential cooling/heating	Long internal waves	Baroclinic circulation	
- Surface cooling	Penetrative convect.	Vertical mixing	
- Surface heating	Enhanced vertical density gradient	Stabilized stratification	
Wind shear			
- Energy transfer	Turbulent mixing	Deepened surface layer	
- Surface drag	Surface currents	Surface setup/ -down	
		Pycnocline setup/ -down	
Tides	Long surface waves	Filling/ emptying	
	Seiches	Filling/ emptying	
Propeller energy	Turbulent mixing	Deepened surface layer	
	Horizontal jets	Horizontal currents	

Salinity and temperature measurements indicate that stratification is strengthened during the heating period from April to August, with the thermocline occasionally interrupted by strong vertical mixing events or by possible up- or downwelling episodes. During the cooling period from September to April, vertically well-mixed conditions prevail down to 25 m depth /Engqvist and Andrejev 2008/.

Cooling water for the power plant is withdrawn via an open canal from Asphällsfjärden, just east of the nuclear power plant (Basin 120 in Figure 3-31). The maximum withdrawal rate is c. 130 m^3/s. The withdrawal strongly affects the water exchange of Asphällsfjärden. The cooling water is released with an over-temperature of about 10°C northeast of the power plant, in the so-called Biotestsjön, an artificial lake that is separated from the surrounding coastal basins by embankment dams. The water passes through Biotestsjön and is let out via a canal towards north (Basin 108). The discharge creates a thermal plume in the surface layer in the central part of the modelling area. However, the natural water exchange rate of the basins north of Biotestsjön is about 10–20 times greater than the discharge rate, so the effect of the discharge is small.

The coastline of the modelling area is flat and the lakes close to the coast are subject to saltwater intrusion during periods with high seawater level (see Section 3.3.2). The seabed has been mapped with regard to the horizontal and vertical distribution of Quaternary deposits in large parts of Öregrundsgrepen /Elhammer and Sandqvist 2004/, (Figure 3-29), and in the whole modelling area (i.e. without internal "white areas") based on complementary interpretations of the data /Hedenström and Sohlenius 2008/ (Figure 3-30). Offshore Quaternary deposits are dominated by glacial and post-glacial clay, together covering about 55% of the area covered by the map of Figure 3-29. The thickness of the offshore Quaternary deposits varies considerably from less than 2.5 m to more than 10 m. Differences between land and water deposits indicate that there is substantial erosion and re-deposition of finer material on the seabed in the area.

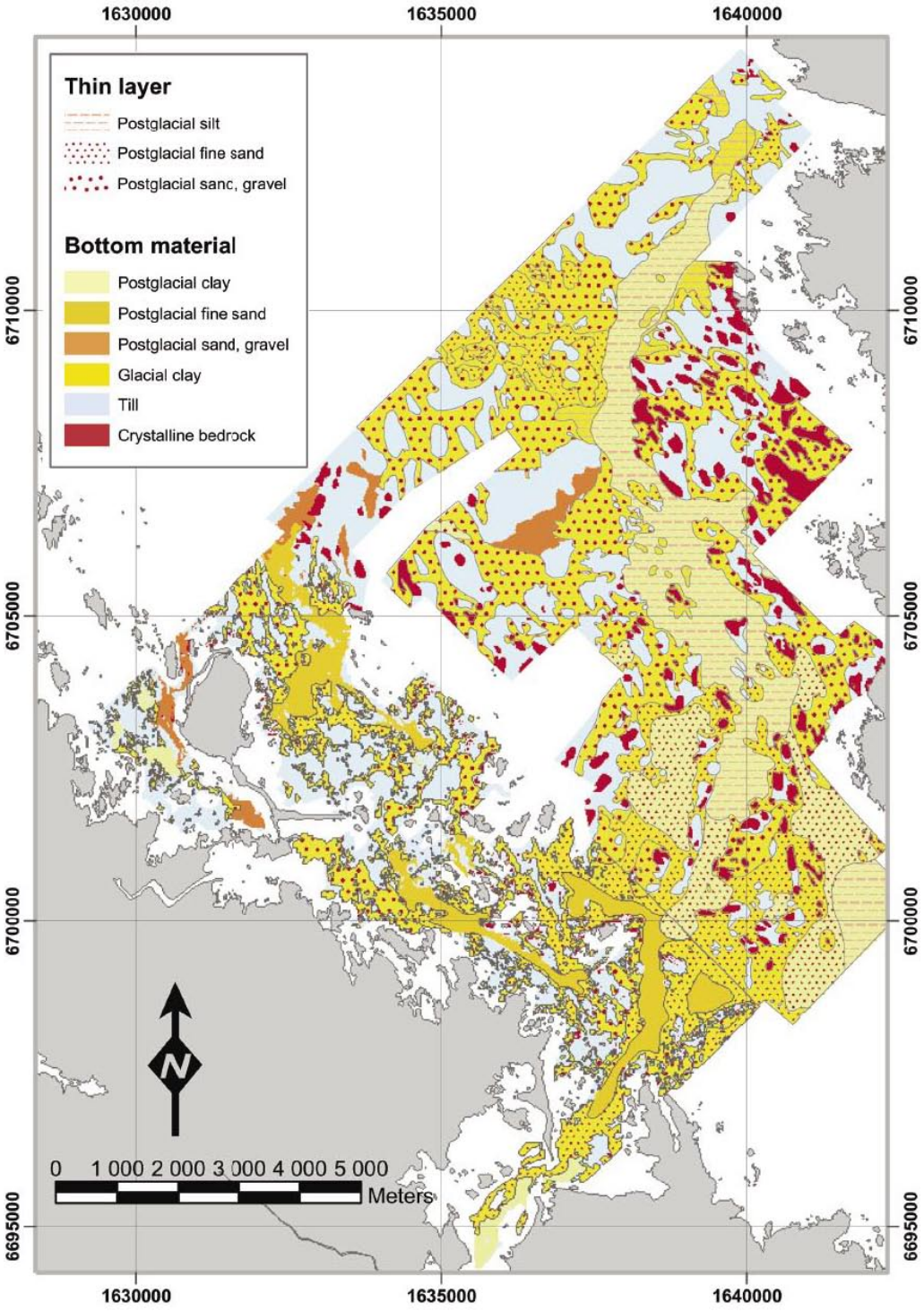

Figure 3-29. *Spatial distribution of bedrock exposures and Quaternary deposits on the seabed outside Forsmark /Elhammer and Sandkvist 2004/.*

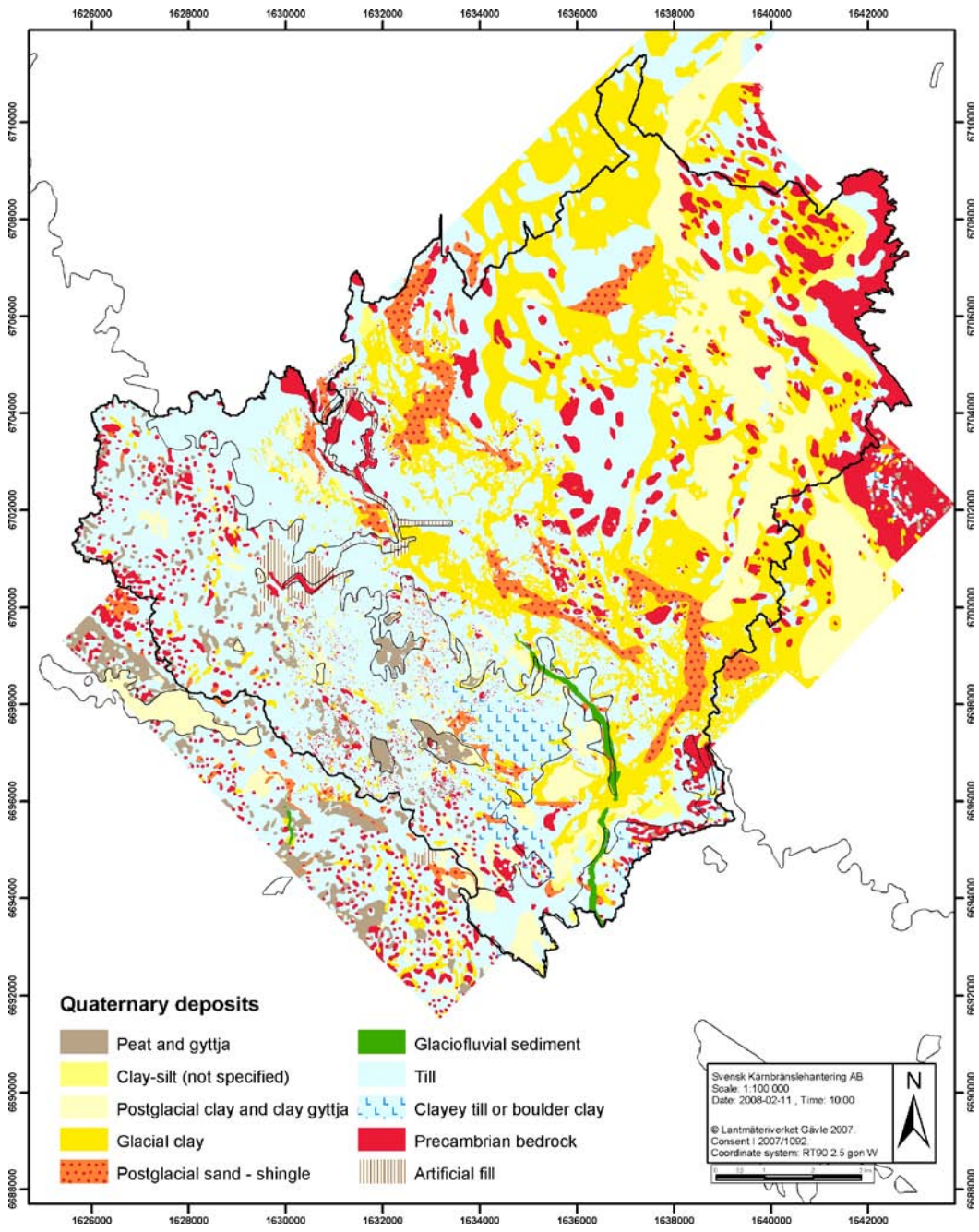

Figure 3-30. *Geological map of Quaternary deposits in the regional modelling area of the site investigation /Hedenström and Sohlenius 2008/.*

For modelling purposes, the Forsmark coastal area has been subdivided into a number of sub-basins (Figure 3-31), see /Wijnbladh et al. 2008/. The delineation is made based on the identification of bathymetric features that are projected to play a successively greater role in controlling water exchange within the area, due to the ongoing land rise /Brydsten 2006a/. Hypsographic data for the basins in Figure 3-31 are presented in Table 3-8.

Water exchange modelling

Nested models

Water exchange modelling has been made with the three-dimensional hydrostatic numerical model AS3D /Andrejev and Sokolov 1997/, with some simplifications concerning heat exchange with the atmosphere and ice formation and melting processes /Lindborg (ed.) 2005, Section 3.5/. The model has been set up at two different grids, one fine-resolution grid (0.1×0.1 nautical miles) that covers Öregrundsgrepen and the archipelago south of Öregrundsgrepen, and one coarse-resolution grid (2×2 nautical miles) that covers the entire Baltic Sea and provides boundary conditions when running the model at the fine-resolution grid.

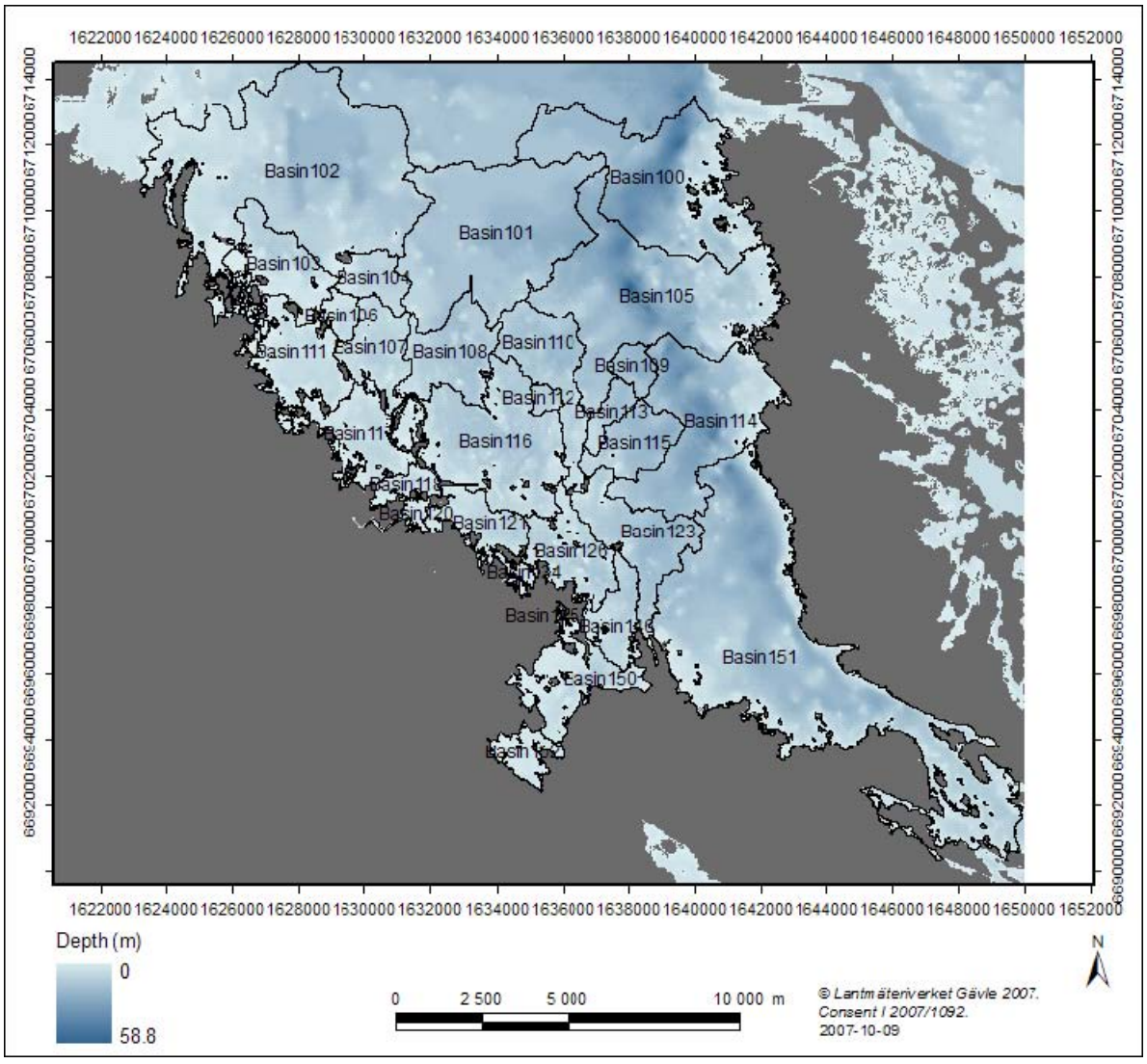

Figure 3-31. *Basin delineation of the Forsmark coastal area.*

Table 3-8. Hypsographic data for the sub-basins of Öregrundsgrepen.

Basin no.	Area $[m^2]\times10^6$	Mean depth [m]	Volume $[m^3]\times10^6$
100	18.6	19.4	360.0
101	21.8	16.1	351.9
102	34.4	10.9	373.2
103	5.8	5.5	31.9
104	2.7	7.6	20.7
105	22.8	18.2	414.5
106	1.4	4.5	6.3
107	4.7	7.0	32.6
108	7.2	10.6	77.0
109	1.5	19.3	29.3
110	7.1	12.4	88.2
111	7.0	3.3	23.0
112	0.7	10.9	7.6
113	1.6	12.5	20.0
114	14.1	19.4	274.1
115	4.2	16.1	67.7
116	13.6	9.5	128.9
117	5.9	3.7	21.9
118	1.5	3.1	4.5
120	0.8	2.5	1.9
121	3.8	5.5	20.8
123	7.3	13.6	99.3
126	5.5	7.5	41.3
134	0.7	1.8	1.2
146	3.4	7.7	26.5
150	6.0	3.6	21.6
151	42.5	13.2	561.4

The year 1988 was chosen as a typical year for running the models. The aim of the modelling was primarily to estimate the average age of the water (AvA, see below). Validation has also been made for a 12-month period 2004/2005 /Engqvist and Andrejev 2008/. In the type-year simulation, the dynamics induced by the withdrawal and discharge of cooling water for the power plant were not included, since the aim of this simulation was to characterise the water exchange of Öregrundsgrepen on a longterm basis. In the validation simulation, however, the cooling water dynamics had to be included.

Data

Input data for the typical year 1988 were:

- Synoptically gridded so-called Mueller-data from which wind components, air pressure and air temperature were extracted every 3 hours.
- Sea level data gauged both on the Swedish and on the Danish side of the model boundary at Kattegatt. The difference between these levels provides an estimate of the geostrophically adjusted flow.
- Seasonally averaged salinity and temperature at the model border at Kattegatt.
- Freshwater discharge of the two streams Forsmarksån and Olandsån calculated from the HBV-model by SMHI.
- Estimates of the average freshwater discharge of the major rivers around the Baltic Sea.

Average age, exchange flow and turnover time

The characteristic water exchange of the different sub-basins is described through the concept of average age (AvA). The age is the time a particular water parcel has spent within a specified body of water, at a given instant in time. The AvA represents the ensemble average for all particles.

In the three-dimensional model, the age is implemented as a passive tracer that is advected and diffused just as any other passive tracer. At every grid cell within the model domain, the age is increased by one time step unit for every time step. Water entering the domain over an open boundary or as discharge is assigned the age 0. Given slowly varying forcing, a quasi-steady equilibrium between renewal over boundaries and aging within the domain, will be attained over time.

In addition to AvA, the exchange flow (m^3/day) and the turnover time (days) was calculated for each basin. The exchange flow for a given basin is the sum of all advective inflows from (or outflows to) the adjacent basins. The turnover time (days) is the basin volume divided by the exchange flow. There is no simple general relationship between AvA and turnover time. For a large basin it is possible for water to flow back and forth over the boundaries without causing renewal in the interior of the basin. The exchange flow will then be large and the estimated turnover correspondingly short, whereas the AvA may be large.

On the other hand, small, shallow land-locked basins can be dominated by horizontal diffusion rather than by advective water exchange. The exchange flow will then be small and the turnover time correspondingly long, whereas the AvA will be small. Neither AvA nor turnover time hence perfectly characterises the renewal of water in a coastal basin, particularly not when a 3D model with a fixed coefficient of horizontal diffusion is used, as is the case here. This coefficient tends to over-estimate the diffusive flow at smaller scales.

Results and discussion

Table 3-9 presents the results of the modelling of the typical year 1988 for the sub-basins of Öregrundsgrepen. The longest turnover times are calculated for the land-locked basins (111, 117, 118, 120, 134 and 150) and the large southernmost basin (151) bordering to the southern archipelago. This is due to the comparatively low advective flow into and out of these basins. The AvA is, however, small for these basins, reflecting a dominance of horizontal diffusion. The model probably over-estimates the horizontal diffusion. The calculated AvA hence indicates a larger water exchange for these land-locked basins than the factual. The turnover time, on the other hand, takes only advection into account and hence under-estimates the water exchange.

Basin 134 has an exchange flow very close to zero and hence a turnover time that goes towards infinity. This is probably due to insufficient resolution of the model for the smallest land-locked basins. For the large basins of Öregrundsgrepen, the AvA and the turnover time are of the same order of magnitude, and generally shorter than one day. Öregrundsgrepen is hence very well ventilated. Advective flows dominate and both AvA and turnover time should be good proxies for the water renewal of these basins.

The water exchange of Asphällsfjärden (Basin 120) is strongly dependent on the withdrawal of cooling water to the power plant (maximum c. 130 m^3/s). With only the natural water exchange, the average volume flux between Asphällsfjärden and the next basin seaward of Asphällsfjärden is in the order of 1 m^3/s, corresponding to a turnover time in the order of 20 days. Taking the withdrawal of 130 m^3/s into account, the turnover time decreases to just a few hours. The modelling for the typical year 1988 does not take the cooling water into account. The validation simulation, however, includes the cooling water.

The effect of the release of the cooling water via Biotestsjön to Basin 108 is hardly noticeable since the natural exchange flow is about 10–20 times greater. The water is released with an over-temperature of 10°C. The resulting thermal plume is noticeable only very locally (a few grid cells in the model).

Table 3-9. Modeled average age (AvA) and calculated exchange flow and turnover time for the sub-basins of Öregrundsgrepen (typical year 1988).

Basin no.	AvA [days]	Exchange flow [m^3/day]×10^6	Volume [m^3]×10^6	Turnover time [days]
100	0.34	750.2	360.0	0.5
101	0.39	547.6	351.9	0.6
102	0.68	400.6	373.2	0.9
103	0.13	86.1	31.9	0.4
104	0.07	64.7	20.7	0.3
105	0.49	643.6	414.5	0.6
106	0.14	23.7	6.3	0.3
107	0.22	59.7	32.6	0.5
108	0.19	165.0	77.0	0.5
109	0.04	122.8	29.3	0.2
110	0.12	239.9	88.2	0.4
111	0.99	9.2	23.0	2.5
112	0.02	35.9	7.6	0.2
113	0.03	119.5	20.0	0.2
114	0.44	422.6	274.1	0.6
115	0.12	202.7	67.7	0.3
116	0.74	142.8	128.9	0.9
117	1.41	4.8	21.9	4.5
118	0.67	0.6	4.5	7.2
120	0.33	0.1	1.9	26.2
121	0.27	22.1	20.8	0.9
123	0.12	228.3	99.3	0.4
126	0.24	60.8	41.3	0.7
134	0.02	–	1.2	inf.
146	0.09	63.5	26.5	0.4
150	0.69	9.2	21.6	2.4
151	4.52	200.1	561.4	2.8

In summary, the modelling shows that Öregrundsgrepen is well ventilated with a typical turnover time shorter than 1 day for the basins in the central parts. For the smaller, shallow, land-locked basins, the modelling results are a bit misleading. The turnover time represents an under-estimation of the water exchange since horizontal diffusion across the boundary is neglected. The AvA, on the other hand, over-estimates the water exchange since it includes a horizontal diffusion that probably is over-estimated in the model.

3.4 Description of hydrogeological objects/flow domains

3.4.1 Quaternary deposits

Hydraulic properties

The hydraulic properties of the Quaternary deposits (QD) and/or the QD/rock interface have been calculated from slug tests, pumping tests, and BAT-filter tip permeability tests (see Figures 2-6 and 2-8 and Table 2-7 for the locations and number of tests). Furthermore, permeameter tests were performed in the laboratory on undisturbed samples (19 samples, sample size Ø 7.2 cm, length 5.0 cm) and hydraulic conductivities (K) were also calculated from grain size distributions (74 samples).

The data from the slug tests were evaluated using three separate methods: the Cooper et al. method, the Hvorslev method, and the Bouwer & Rice method /Butler 1998/. For most wells a good to acceptable fit to the type curves of the Cooper et al. method was obtained when applying a fixed α (corresponding to a storativity (S) of 10^{-5}). Figure 3-32 shows the hydraulic conductivities on a map of the area. The data presented are all from the evaluation by the Cooper et al. method with a fixed α.

Figure 3-33 shows a histogram of the hydraulic conductivities from tests in till (57 of the total of 59 tests). The histogram shows that most hydraulic conductivity values are in the range 10^{-7}–10^{-4} m/s; the measured hydraulic conductivities vary between $2.0 \cdot 10^{-8}$ and $7.0 \cdot 10^{-4}$ m/s. The geometric mean is $5.4 \cdot 10^{-6}$ m/s (arithmetic mean $5.3 \cdot 10^{-5}$ m/s, median $5.7 \cdot 0^{-6}$ m/s) and the standard deviation of $\log_{10}$(K) is 1.06, which corresponds to 2.45 if the natural logarithm is used. Assuming a log-normal distribution, the 95% confidence interval for the geometric mean is $2.9 \cdot 10^{-6}$–$1.0 \cdot 10^{-5}$ m/s, and the 95% confidence interval for a new observation is $4.5 \cdot 10^{-8}$–$6.5 \cdot 10^{-4}$ m/s.

The relatively high degree of spatial variability reflects the fact that the dataset includes K-values associated with different types of till and depths, as well as values from well screens at and across the till/bedrock interface. The geometric mean of the K-values from wells in till only is $1.3 \cdot 10^{-6}$ m/s, whereas it is $1.2 \cdot 10^{-5}$ m/s in wells at and across the till/bedrock interface. Thus, the hydraulic conductivity is on average one order of magnitude higher at the till/bedrock interface than in the till.

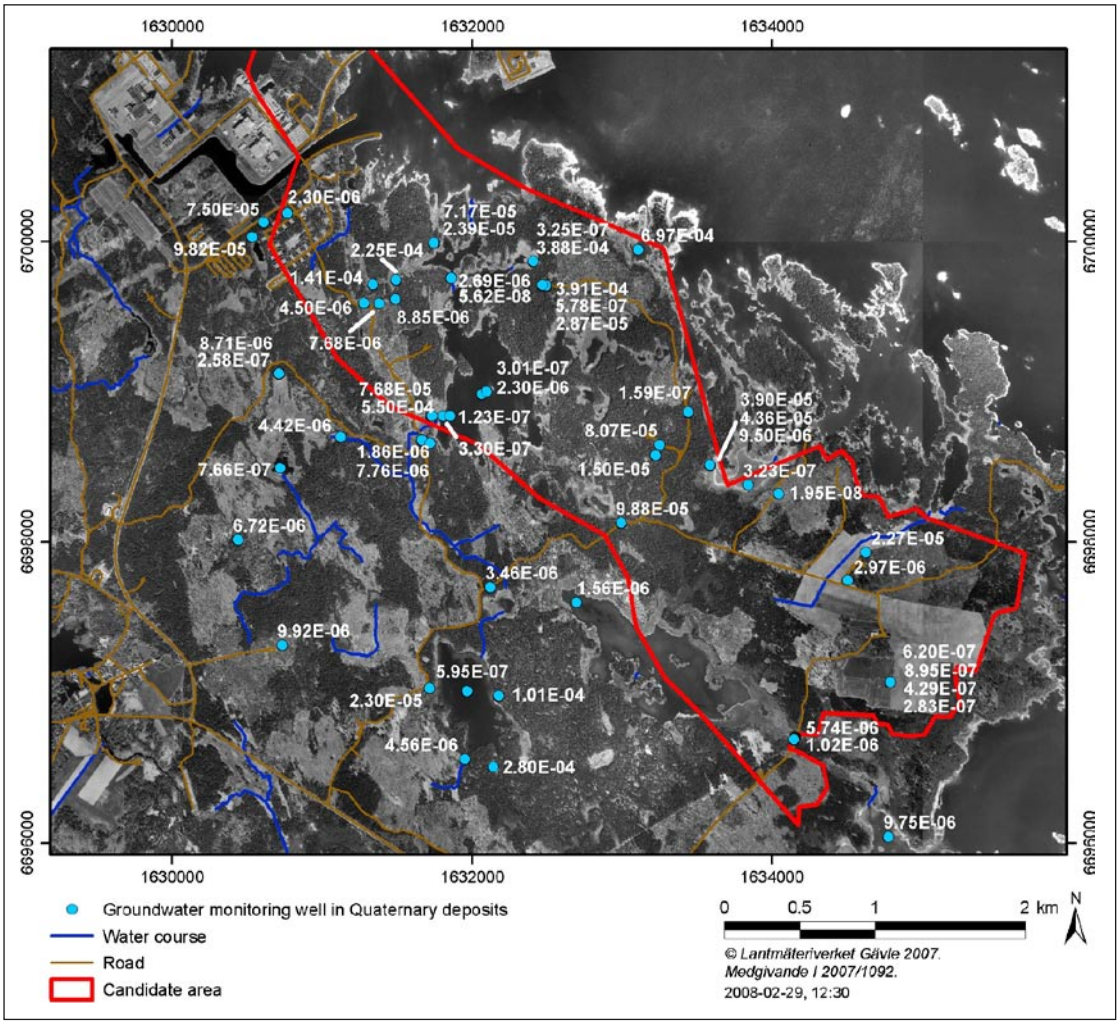

Figure 3-32. *Hydraulic conductivities obtained from slug tests evaluated by the Cooper et al method /Butler 1998/.*

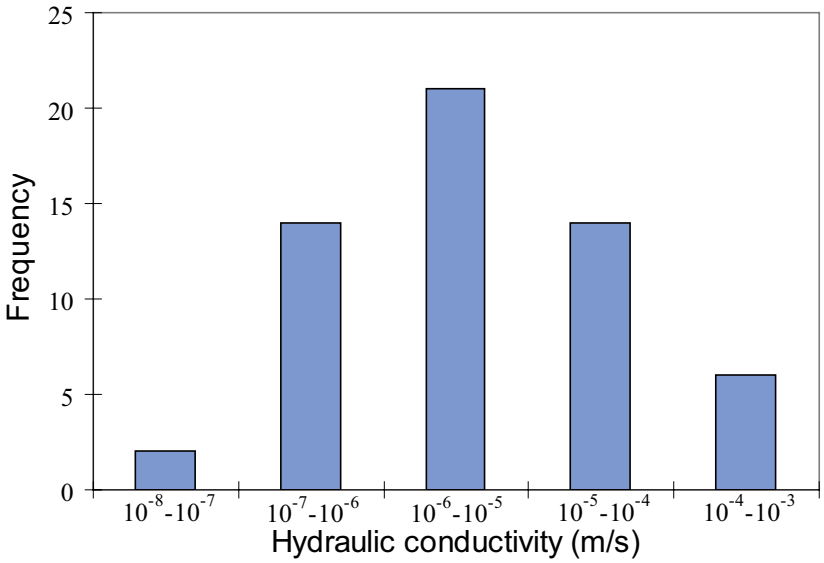

Figure 3-33. *Histogram for the hydraulic conductivities of till, obtained from slug tests in 57 groundwater monitoring wells /Werner and Johansson 2003, Werner 2004, Alm et al. 2006/*

In Figure 3-34 a comparison of the evaluated hydraulic conductivity values as a function of the screen depth is shown, also taking into consideration whether the screen is placed at the till/bedrock interface. The linear fits in Figure 3-34 indicate a decrease in conductivity by approximately half an order of magnitude over a depth interval of 8 m for wells with the screen in till only. However, it should be noted that no slug tests are available from the uppermost c. one metre of the soil profile.

The potential influence of the well-installation technique on the estimations of hydraulic properties that are obtained from the slug tests is an important issue. In order to investigate this issue, the hydraulic conductivities obtained from slug tests in groundwater monitoring wells installed in till only by air rotary-casing driver were compared to the corresponding values obtained from wells installed by hammer drilling. The geometric means of for the two groups of wells are $1.4 \cdot 10^{-6}$ m/s and $1.3 \cdot 10^{-6}$ m/s, respectively. Hence, the well installation technique is not considered to have a large influence on the evaluated hydraulic parameters. The two slug tests performed in sand gave hydraulic conductivities of $2.3 \cdot 10^{-4}$ m/s and $3.9 \cdot 10^{-4}$ m/s.

Grain-size analyses were performed on a large number of QD samples. The resulting particle-size distribution curves (PSD) were used to estimate the hydraulic conductivity using three different methods: the equations presented by Hazen and Gustafson, respectively /Andersson et al. 1984/, and the Fair-Hatch equation /Freeze and Cherry 1979/. The results obtained from the Fair-Hatch equation are summarised in Table 3-10.

The hydraulic conductivity of the till, as obtained from the PSDs, is on the order of 10^{-6} for the gravelly-sandy till types, and on the order of 10^{-7} m/s for the clayey till types. Figure 3-35 shows a comparison between hydraulic conductivity values obtained from slug tests and those obtained from PSDs. The analysis includes only the PSDs that are sampled within the same depth interval as where the corresponding well screen is located; in some cases, there is only a small overlap between the sampling interval and the well screen depths for the data shown in the figure.

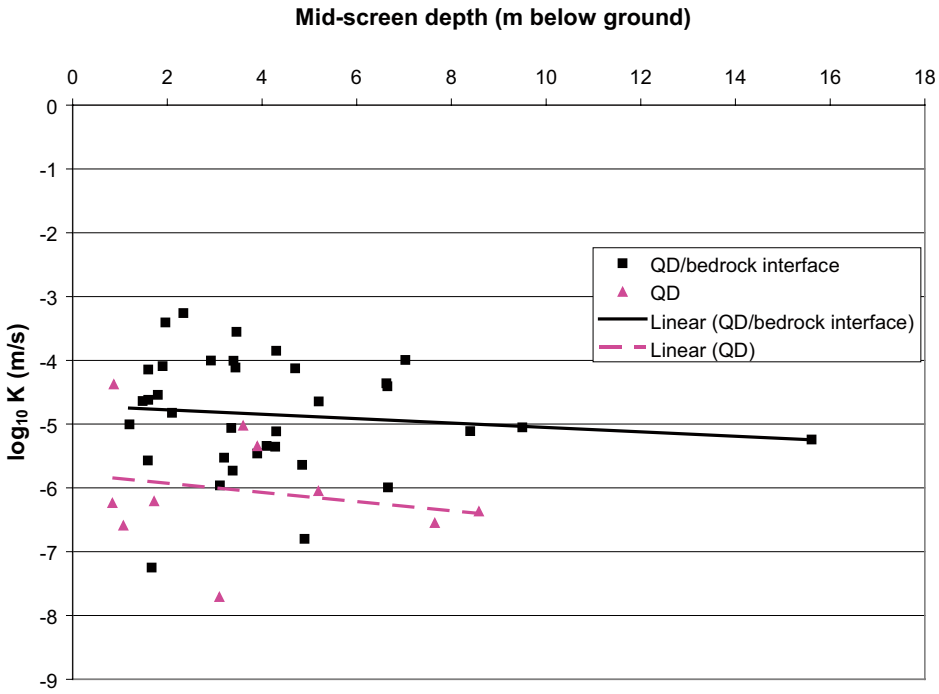

Figure 3-34. *Hydraulic conductivities (logarithmic scale) of the QD obtained from slug tests in wells installed on land (i.e., wells installed below open water are not included). The data are plotted as a function of depth (metres below ground level). The lines are linear fits to the measured data.*

Table 3-10. Statistical analysis of hydraulic conductivity K (m/s) obtained from evaluation of particle-size distribution curves by the Fair-Hatch equation. The available number of K-values for each QD type is shown within parentheses.

	Gravelly till, sandy till (32)	Clayey sandy-silty till, clayey sandy till, clayey gravelly till (33)	Sand, sandy gravel (5)	Boulder clay (3)	Silty sand (1)
Arithmetic mean of log-K	–6.09	–6.60	–4.30	–6.74	–6.05
Standard deviation of log-K	0.56	0.43	0.94	0.19	–
Geometric mean of K	$8.23 \cdot 10^{-7}$	$2.52 \cdot 10^{-7}$	$5.06 \cdot 10^{-5}$	$1.81 \cdot 10^{-7}$	$8.97 \cdot 10^{-7}$
Arithmetic mean of K	$1.77 \cdot 10^{-6}$	$3.62 \cdot 10^{-7}$	$3.22 \cdot 10^{-4}$	$1.94 \cdot 10^{-7}$	$8.97 \cdot 10^{-7}$
Median of K	$9.65 \cdot 10^{-7}$	$2.77 \cdot 10^{-7}$	$2.35 \cdot 10^{-5}$	$1.42 \cdot 10^{-7}$	$8.97 \cdot 10^{-7}$
95% confidence interval for K	$5.25 \cdot 10^{-7}$ – $1.29 \cdot 10^{-6}$	$1.79 \cdot 10^{-7}$ – $3.54 \cdot 10^{-7}$	$7.58 \cdot 10^{-6}$ – $3.38 \cdot 10^{-4}$	$1.10 \cdot 10^{-7}$ – $2.98 \cdot 10^{-7}$	–
95% confidence interval for a new observation/measurement	$6.51 \cdot 10^{-8}$ – $1.04 \cdot 10^{-5}$	$3.59 \cdot 10^{-8}$ – $1.77 \cdot 10^{-6}$	$7.25 \cdot 10^{-7}$ – $3.54 \cdot 10^{-3}$	$7.60 \cdot 10^{-8}$ – $4.30 \cdot 10^{-7}$	–

For those wells where the screen is located across the till/bedrock interface, Figure 3-35 shows that the hydraulic conductivities obtained from slug tests generally are higher compared to the corresponding values obtained from the PSDs. The deviations are larger for those wells where the till consists of clayey till. Furthermore, the results show that there is no correlation between grain size distribution and hydraulic conductivity for wells where the screen is located across the QD/bedrock interface, but some correlation for well in till only.

Pumping tests were performed in wells SFM0061, SFM0074, SFM0090, SFM0094 and SFM0103 /Werner et al. 2004, Werner and Lundholm 2004a, Alm et al. 2006/. The hydraulic conductivity values evaluated from the pumping tests are presented in Table 3-11.

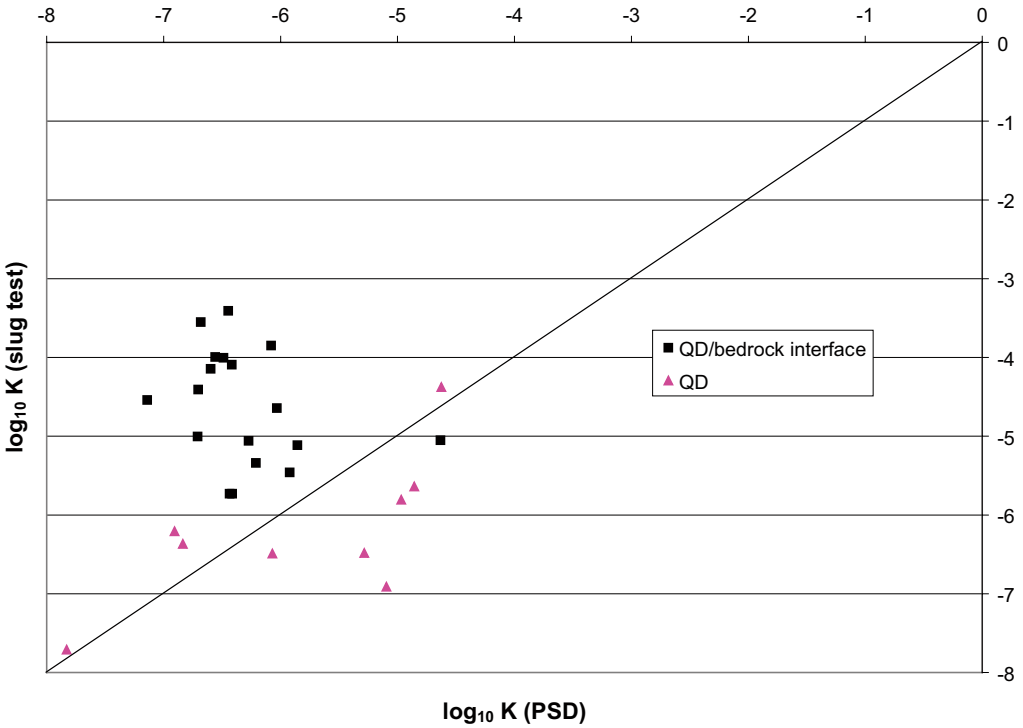

Figure 3-35. *Hydraulic conductivities (logarithmic scale) of the till obtained from slug tests plotted versus corresponding values obtained from particle-size distribution curves (PSD). The solid line represents a perfect correlation between the two datasets.*

Table 3-11. Evaluated hydraulic conductivity data from pumping tests /Werner et al. 2004, Werner and Lundholm 2004a, Alm et al. 2006/ (see Figure 2-6 for the locations of the wells).

Pumping well	Observation well	Hydraulic conductivity (m/s)	Storage coefficient (-)
SFM0061 (glaciofluvial mtrl)		$2.1 \cdot 10^{-4}$	
	SFM0060 (glaciofluvial mtrl)	$1.3 \cdot 10^{-4}$	$4.0 \cdot 10^{-3}$
SFM0074 (till/bedrock)		$5.6 \cdot 10^{-5}$	
	SFM0031 (till)	$5.6 \cdot 10^{-4}$	$1.0 \cdot 10^{-3}$
	SFM0032 (till)	$5.6 \cdot 10^{-5}$	$2.5 \cdot 10^{-4}$
	SFM0062 (till)	$5.5 \cdot 10^{-5}$	$1.8 \cdot 10^{-3}$
	SFM0063 (till)	$3.7 \cdot 10^{-4}$	$1.6 \cdot 10^{-3}$
SFM0090 (till/bedrock)		$3.6 \cdot 10^{-6}$	
SFM0094 (till/bedrock)		$6.7 \cdot 10^{-6}$	
SFM0103 (till/bedrock)		$9.1 \cdot 10^{-5}$	
	SFM0095 (till)	$7.6 \cdot 10^{-5}$	$3.1 \cdot 10^{-4}$

The pumping well SFM0061 and its observation wells (SFM0059 and SFM0060) are located in a glaciofluvial deposit, the Börstilåsen esker, and the material consists of sand, gravel and stones. The well SFM0074 is installed across the till/bedrock interface immediately west of Lake Bolundsfjärden, whereas the observation wells for that pumping test are installed in till (SFM0031 and –32 on land and SFM0062 and –63 below open water). The evaluation of the pumping test in SFM0074 also included an analysis of the impact of hydraulic boundaries and lake water leakage. The results showed that there is a limited hydraulic contact, potentially determined by low-permeable lake sediments, between Lake Bolundsfjärden and the pumped aquifer. The evaluation of the vertical leakage through the gyttja sediments indicates a vertical K of the gyttja of 10^{-8} to 10^{-9} m/s. However, it should be noted that these values are quite uncertain.

With the objective to explore the hydraulic contact between wetlands and their surrounding groundwater systems, three pumping tests were conducted with pumping in wells installed across the QD/bedrock interface at the fringes of three wetlands and with observation wells in the different wetland sediments and in the till below the wetlands, see Figure 3-36 for an illustration of the test set up. However, due to insufficient spreading of the cone of depression in the till, evaluation of drawdowns in the monitoring wells was only possible at the site shown in Figure 3-36 (see Figures 2-6 and 2-8 for the locations of these monitoring wells).

The hydraulic conductivities evaluated from the pumping tests, which represent larger aquifer volumes than the slug tests, are approximately 2-3 orders of magnitude larger than the corresponding values from the slug tests for wells SFM0031 and SFM0062-63, whereas the values are approximately equal for well SFM0032 and SFM0095. Furthermore, an evaluation of the vertical leakage through the peat/gyttja/clay sediments when pumping in well SFM0103 indicates a vertical harmonic mean K-value of the sediments of $4.8 \cdot 10^{-8}$ m/s.

The hydraulic conductivity has also been measured in BAT filter tips at 10 locations /Johansson 2004, Alm et al. 2006/. The results of these measurements are shown in Table 3-12. The hydraulic conductivities obtained from the filter-tip tests in till concern fine-grained tills, and can be expected to be low. However, the K-values from the BAT filter tips in till are much lower than those from slug tests in similar geological materials. The reasons for this difference could be related to scale effects or to methodological differences. The obtained values on the order of 10^{-7} m/s are close to the upper limit of values than can be measured by the BAT-equipment.

The K-values obtained from the laboratory permeameter tests, conducted on undisturbed samples from the uppermost part of the till are presented in Figure 3-37 /Lundin et al. 2005/. It should be noted that these tests measure vertical hydraulic conductivities. However, it can be assumed that the difference between horizontal and vertical K are less pronounced in the upper part of the soil profile (c. 1 m) due to impact from soil forming processes.

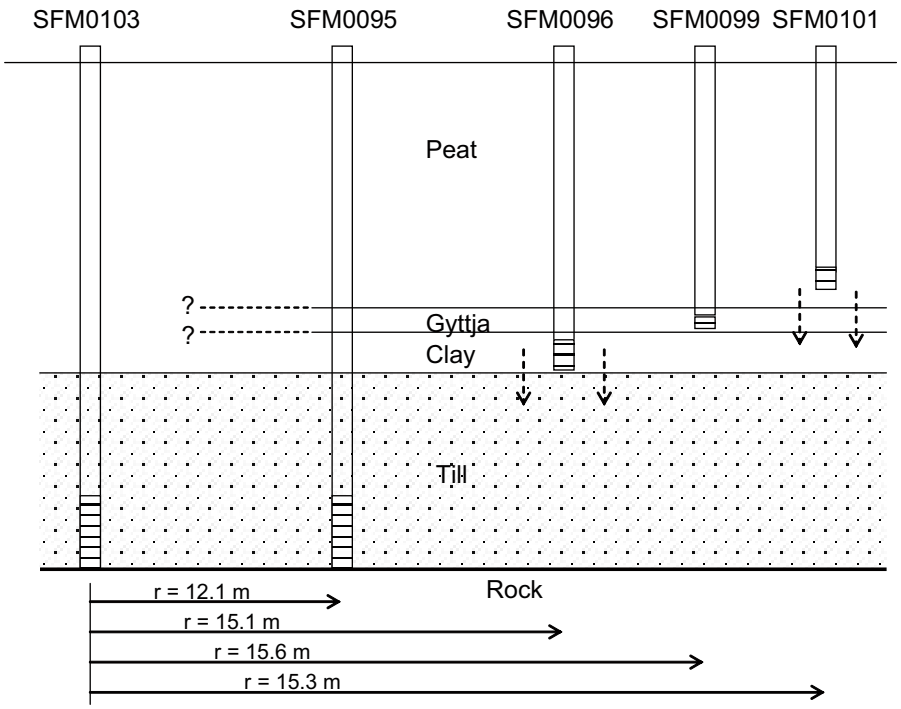

Figure 3-36. *A conceptual model of the pumping well (SFM0103) and the four monitoring wells /Alm et al. 2006/. Note that the figure is not in scale.*

Table 3-12. Measurements of hydraulic conductivity in BAT filter tips /Johansson 2004, Alm et al. 2006/.

Station	Hydraulic conductivity (m/s)	Deposit
SFM0050	$(4.0–4.3)\cdot10^{-8}$	Sandy till
SFM0052	$4.0\cdot10^{-9}$	Clayey, sandy, silty till
SFM0054	$(8.5–8.8)\cdot10^{-9}$	Boulder clay
SFM0082	$3.2\cdot10^{-7}$	Gyttja
SFM0085	$2.6\cdot10^{-7}$	Clay
SFM0088	$3.3\cdot10^{-7}$	Clayey gyttja
SFM0092	$3.4\cdot10^{-7}$	Gyttja
SFM0096	$2.9\cdot10^{-7}$	Clay
SFM0099	$3.2\cdot10^{-7}$	Gyttja
SFM0101	$3.3\cdot10^{-7}$	Peat

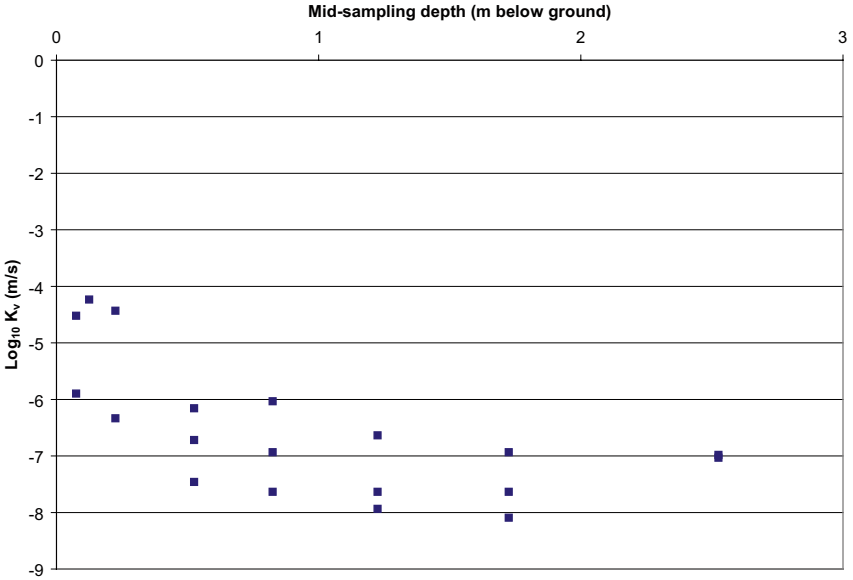

Figure 3-37. *Vertical hydraulic conductivities in till from laboratory permeameter tests on undisturbed samples /Lundin et al. 2005/.*

From Figure 3-37 it is clear that the hydraulic conductivities are considerably higher in the uppermost c. half metre of the soil profile. The difference, due to impact of soil forming processes, is 2 to 3 orders of magnitude. These observations are in agreement with several other investigations of hydraulic properties of till, see /Lind and Lundin 1990/. Total porosities and specific yield (S_y) also show clear trends with depth below ground /Lundin et al. 2005/. The total porosity in the uppermost 0.25 m of profile is 30–40% and then decreases down to c. 20% below a depth of c. one metre. S_y decreases from almost 20% in the uppmost part of the profile down to c. 5% below one meter's depth. The field capacity (water holding capacity at 100 cm suction) is, however, almost constant over depth, c. 15%.

In Table 3-13 best estimates of hydraulic parameters of Quaternary deposits in Forsmark are presented. When sufficient site specific data are available these are used as a basis for the best estimate, while when site specific data are scarce or missing generic data are also used as support for the estimates. Due to the influence of soil forming processes on the uppermost part of the soil profile, a differentiation of the hydraulic properties has been made between the upper 0.6 metre of the profile and the deeper part of the profile for some of the Quaternary deposits. The change in hydraulic properties in the uppermost part of the soil profile is gradual towards depth. The division into two distinct layers is made to facilitate the transfer of the conceptual model to the three-dimensional numerical flow model.

Table 3-13. Best estimates of hydraulic parameters of Quaternary deposits in Forsmark based on site specific data and supported by generic data when site specific data are scarce. The K-values given are for the horizontal direction (K_h).

Deposit	K_h (m/s)	Total porosity (–)	Specific yield (–)
Peat	Depth < 0.6 m: $1.0 \cdot 10^{-6}$ Depth > 0.6 m: $3.0 \cdot 10^{-7}$	Depth < 0.6 m: 0.60 Depth > 0.6 m: 0.40	Depth < 0.6 m: 0.20 Depth > 0.6 m: 0.05
Gyttja, Clay-gyttja, Gytttja-clay	$3.0 \cdot 10^{-7}$	0.50	0.03
Glaciofluvial and postglacial sand	$1.5 \cdot 10^{-4}$	0.35	0.20
Clay (glacial and post-glacial)	Depth < 0.6 m: $1.0 \cdot 10^{-6}$ Depth > 0.6 m: $1.5 \cdot 10^{-8}$	Depth < 0.6 m: 0.55 Depth > 0.6 m: 0.45	Depth < 0.6 m: 0.05 Depth > 0.6 m: 0.03
Till	Till (fine and coarse), Depth < 0.60: $1.5 \cdot 10^{-5}$ Depth > 0.6 m: Fine-grained: $1.0 \cdot 10^{-7}$ Coarse: $1.5 \cdot 10^{-6}$	Depth < 0.60 m: 0.35 Depth > 0.60 m: 0.25	Depth < 0.6 m: 0.15 Depth > 0.6 m: Fine-grained: 0.03 Coarse: 0.05
Till/bedrock interface	$1.5 \cdot 10^{-5}$	0.25	0.05

The K-values given in Table 3-13 are horizontal conductivities. The only vertical K-values from till are from the laboratory permeameter tests. The geometric mean of these tests for samples below one metre were approximately $4.4 \cdot 10^{-8}$ m/s while the geometric mean of till from the slug tests is $1.3 \cdot 10^{-6}$ m/s. This corresponds to a K_h/K_v ratio of about 30. However, this result should be used with caution since the scales of the tests are not the same. The vertical K-values for gyttja and peat/gyttja/clay obtained from leakage coefficients from the pumping tests were approximately $1 \cdot 10^{-8}$ m/s. Also for these tests the vertical K-values are about 30 times lower than the K_h-values given for these deposits in Table 3-13.

Groundwater level time series

Groundwater levels in Quaternary deposits were automatically registered in 51 groundwater monitoring wells. Figure 2-7 shows a map of the locations of these wells.

Figure 3-38 presents daily average groundwater levels expressed as a) elevations (RHB70) and b) depth below ground surface for the 42 wells situated on land. Measured groundwater elevations in Quaternary deposits range from about –1 m in SFM0030 to +13 m in SFM0010 (Figure 3-38a). However, there is only about a 5.5 m range in groundwater levels when represented as depths below ground surface (Figure 3-38b). The majority of wells form a tight-packed cluster with reported groundwater levels in the range of approximately +0.25 to –1.5 m relative to the surface. These wells typically show a strong uniformity in their responses to drier summer conditions in July and August. Similarly, these wells also display uniformity in response to recharge events following major precipitation and snowmelt events.

SFM0026, which is located in a confined till aquifer at the outlet of Lake Fiskarfjärden, reveals clear artesian conditions with a groundwater level up to approximately one metre above ground. The deepest observed groundwater levels are from two wells situated in Börstilåsen (SFM0059 and SFM0061), which is a glaciofluvial deposit. The wells SFM0006, SFM0008 and SFM0058, which also have relatively deep groundwater levels, are located in till in locally elevated areas, i.e. in typical groundwater recharge areas. The very low groundwater levels during the dry summers of 2003 and 2006 are believed to be caused by root water uptake, indirectly and directly, from the groundwater zone.

Numerous combinations of wells in the Quaternary deposits indicated similar time series responses. The time series from groundwater wells in Quaternary deposits were analysed to identify wells with high covariance ($R^2 > 0.9$) and similar range of variation (± 10%). Sets of wells in close proximity as well as wells further apart demonstrated nearly identical groundwater level variation patterns /Juston et al. 2007/.

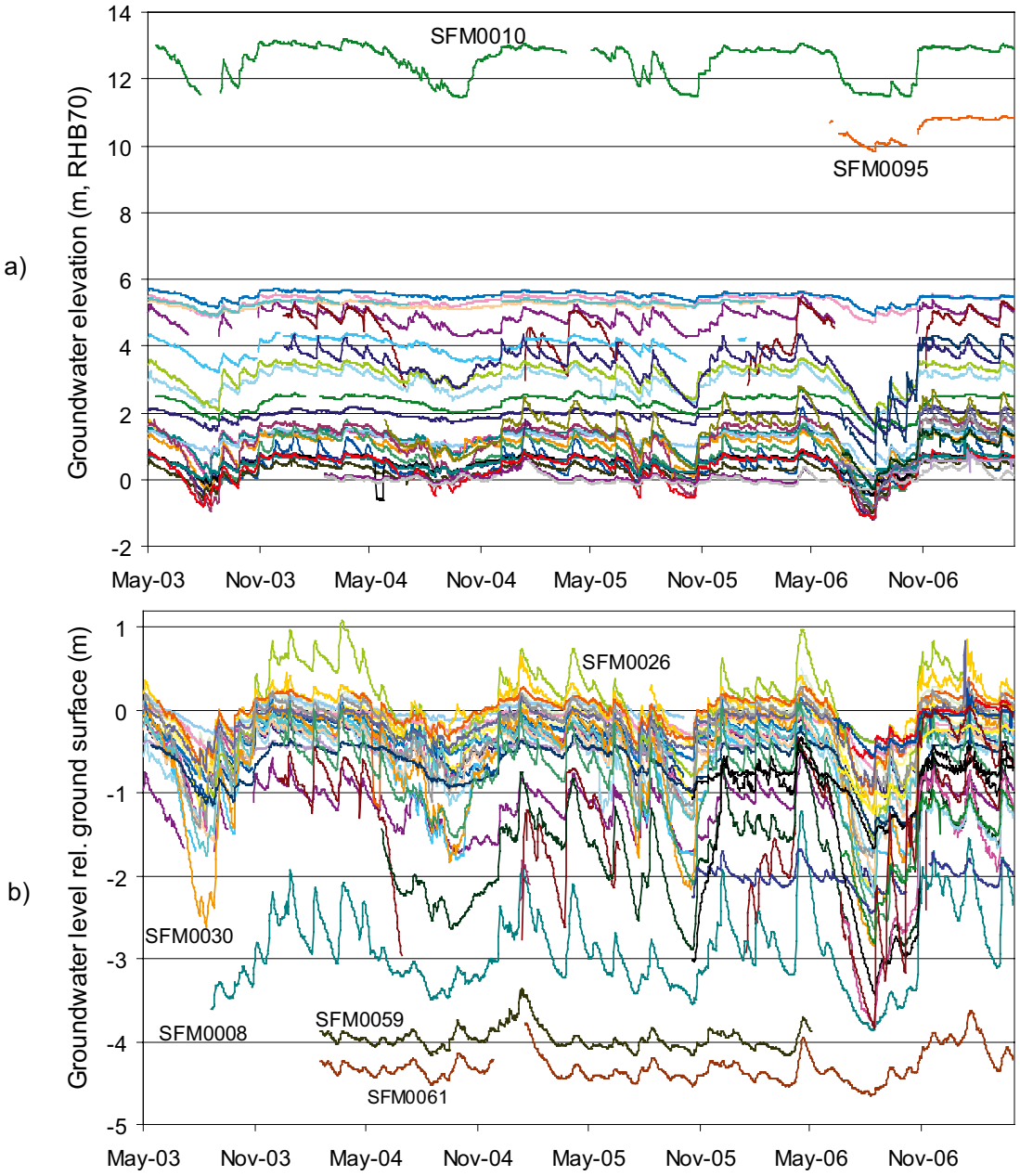

Figure 3-38. *Daily average groundwater levels expressed as a) absolute elevations (RHB70) and b) relative to ground surface for 42 monitoring wells in Quaternary deposits on land.*

Figure 3-39 shows plots of cumulative frequency distributions of the data presented in Figure 3-38b. Two different methodologies for calculating distributions yield two different curves, but they have similar interpretations. If a daily average groundwater level in Quaternary deposits relative to ground surface is first calculated from the 42 well time series (the orange curve in Figure 3-39), the cumulative distribution of that average time series indicates that 80% (between the 10th to 90th percentiles) of the site average groundwater levels were between 0.4 and 1.2 m below ground surface. If instead the cumulative distribution is based on pooled analysis of the 42 individual well time series (the blue curve), then 80% of measured groundwater levels were between 0 and 2.2 m below ground surface. In either case, it can be concluded that groundwater in Quaternary deposits is shallow in observation wells across the site investigation area.

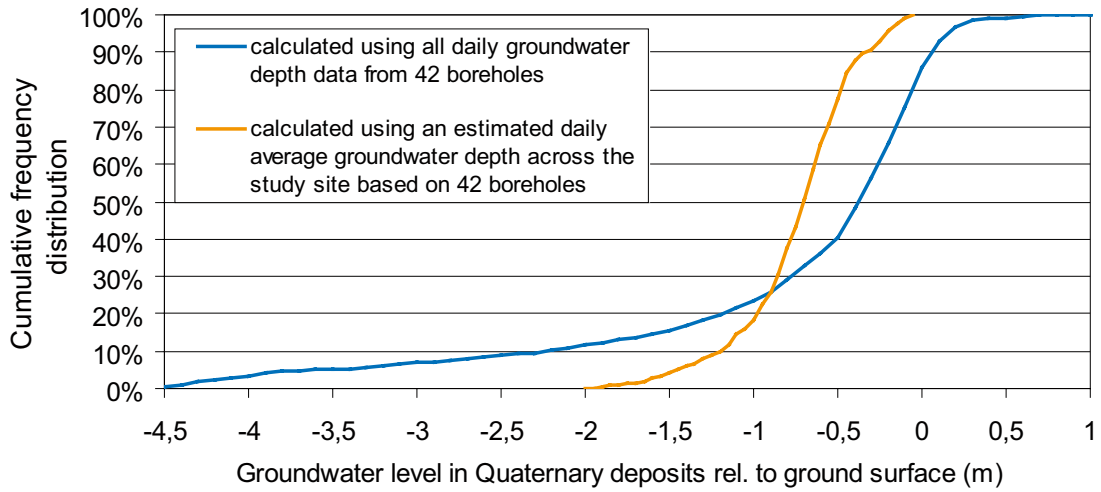

Figure 3-39. *Cumulative frequency distribution of groundwater depth in Quaternary deposits from 42 monitoring wells in the Forsmark site investigation area.*

To facilitate comparisons between well locations, Figure 3-40 shows summaries of the groundwater level in Quaternary deposits time series in terms of means and observed ranges. Figure 3-40a shows the mean and range of groundwater depths in the Quaternary deposits, co-plotted with bedrock depth at each site, and shown ranked according to increasing groundwater depths. In Figure 3-40b the same data are presented ranked according to bedrock depth. Finally, Figure 3-40c shows the mean and range of groundwater elevations, co-plotted with bedrock and ground surface elevations at each site, and shown ranked according to bedrock elevations. All wells exhibited mean groundwater elevations above 0.0 m RHB70. However, 14 of the 40 wells exhibited minimum groundwater elevations less than 0.00 m, with the lowest reported level of –1.18 m in SFM0030.

Figures 3-41 and 3-42 summarise the strong correlation that was observed between mean observed groundwater and ground surface elevations in the Quaternary deposits. With a few exceptions, it can be stated that the average position of the groundwater level in the Quaternary deposits appears to be largely determined by the local ground surface elevation. In other words, the three-dimensional shape of the groundwater surface in Quaternary deposits appears to generally follow that of the ground surface. There are some outliers indicated by well IDs in Figure 3-41. The most pronounced outliers, SFM0059 and SFM0061, are located below the ridge of the glaciofluvial deposit Börstilåsen, while SFM0008, SFM0058, SFM0077, SFM0080, SFM0104 and SFM0107 are located in till in typical recharge areas and with one exception (SFM0107) in locally elevated areas.

3.4.2 Rock

Hydraulic properties

The bedrock hydrogeology reveals a significant hydraulic anisotropy within the tectonic lens, which covers the body of the candidate area. The upper c. 150 m of bedrock contains high-transmissive horizontal fractures/sheet joints. These fractures/sheet joints occur at different elevations in the percussion drilled boreholes, but are found to interconnect hydraulically across large distances (2 km) /Gokall-Norman et al. 2005, Gokall-Norman and Ludvigson 2007ab, 2008/. The horizontal fractures/sheet joints have transmissivities in the range c. $1{\cdot}10^{-6}$ –$1{\cdot}10^{-3}$ m^2/s (hydraulic conductivity c. $1{\cdot}10^{-6}$ –$1{\cdot}10^{-3}$ m/s). The bedrock in between the horizontal fractures/sheet joints, however, is considerably less conductive (hydraulic conductivity c. $1{\cdot}10^{-11}$ –$1{\cdot}10^{-8}$ m/s) except where it is intersected by transmissive steeply-dipping or gently-dipping deformation zones.

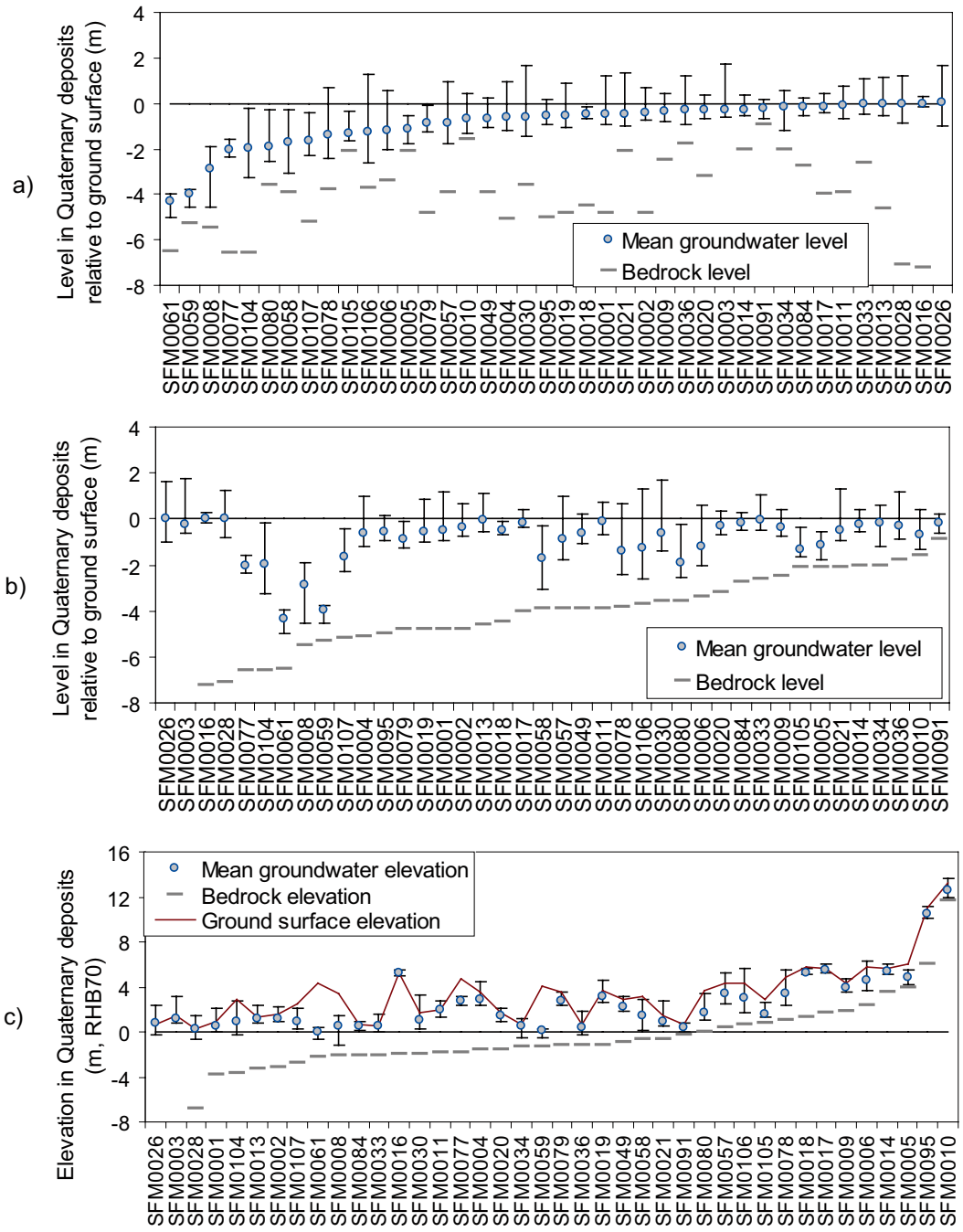

Figure 3-40. *Summary of mean and range of groundwater levels in the Quaternary deposits shown as a) level relative to ground surface ranked accordingly, b) level relative to ground surface ranked by depth to bedrock and c) levels RHB70 ranked by bedrock elevation. In all figures, bedrock surface levels at SFM0026 (–15.4 m RHB70 and 16.1 m below surface) and SFM0003 (–8.7 m RHB70 and 10.2 m below surface) are not shown to increase resolution on the remaining data. (Note that wells below open water and wells with time series <150 days are not included.)*

Below the uppermost c. 150 m of bedrock there are no high-transmissive horizontal fractures/ sheet joints, and the conductive fracture frequency becomes very low and the fractures fairly low-transmissive (fracture transmissivity c. $1{\cdot}10^{-10}$ –$1{\cdot}10^{-7}$ m²/s). In some of the 1,000 m deep cored boreholes there are almost no flowing fractures observed below c. 150 m depth, which is exceptional in a national perspective given the experiences from SKB's investigations at Äspö, Stripa, Laxemar-Simpevarp and the many study sites investigated in the 1970's and 1980's. For a comprehensive description of the hydraulic properties of the rock the reader is referred to /Follin et al. 2007abc, 2008/.

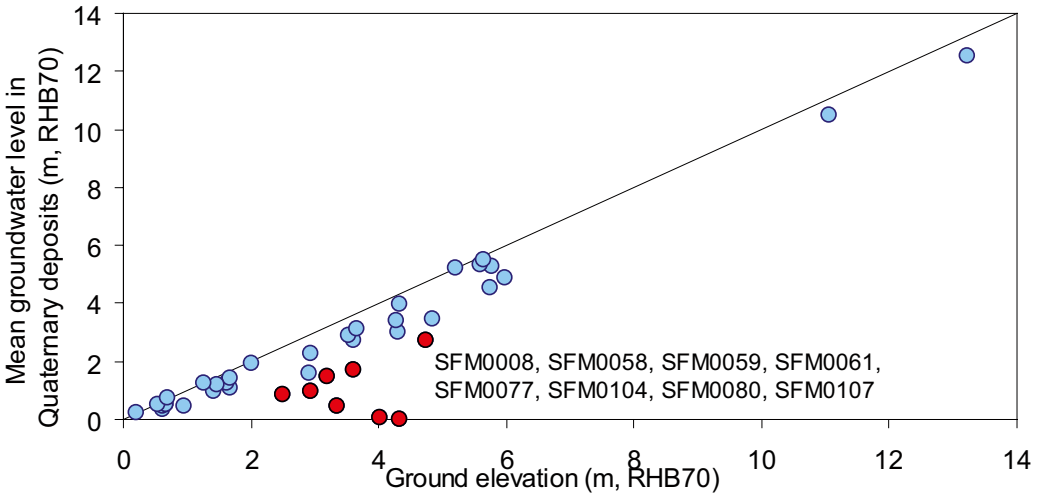

Figure 3-41. *Cross-plot of average groundwater level elevations in Quaternary deposits versus ground elevations. The red dots represent outliers; the well IDs of these are listed in the figure.*

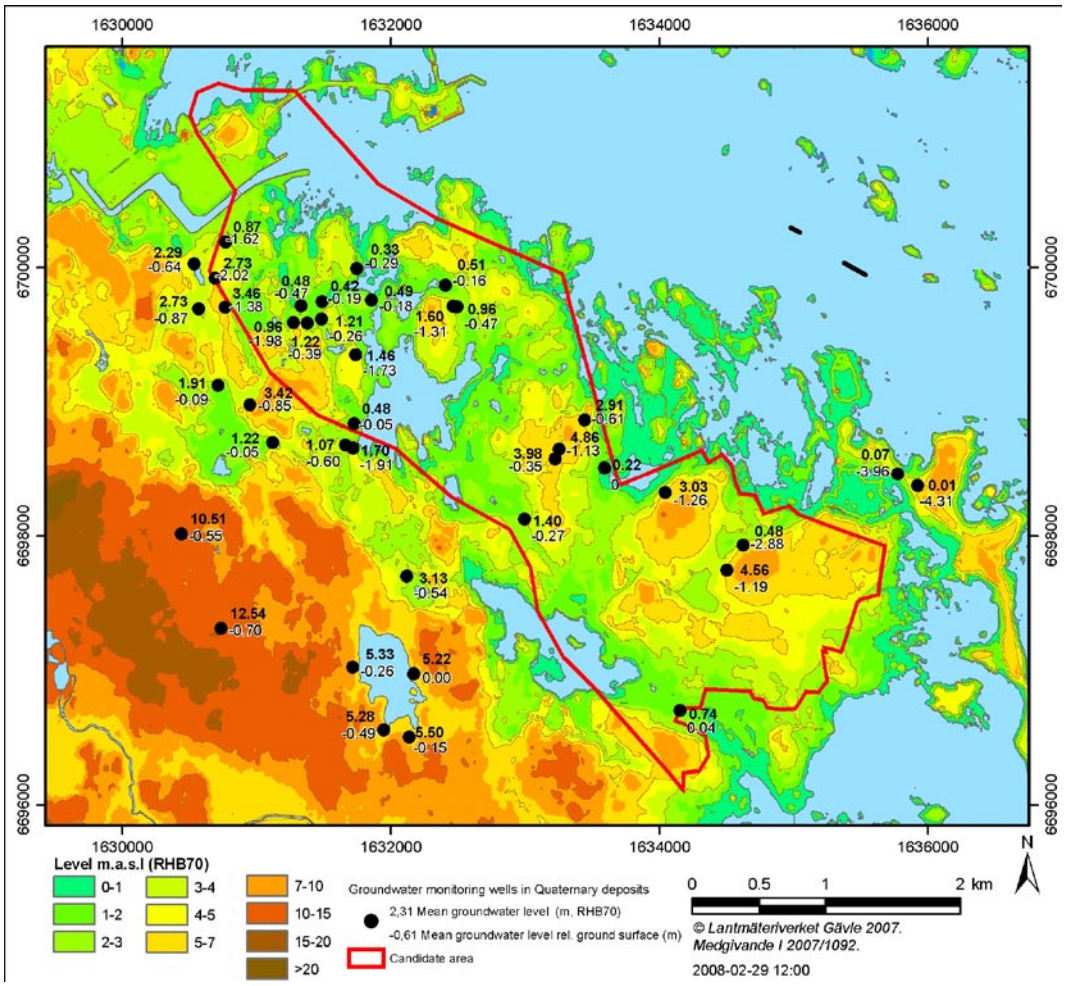

Figure 3-42. *Mean groundwater level elevations and depths below ground in monitoring wells in Quaternary deposits.*

Point water heads and environmental water heads

In Table 3-14 all the sections in the percussion-drilled boreholes are listed where the difference between mean measured point water heads and calculated environmental water heads is > 0.1 m; for definitions of heads and a description of the method applied for calculation of environmental head from point water head see Section 1.4.2. In Appendix 2 figures with full time series of point and environmental water heads of the HFM-boreholes represented in Table 3-14 are shown as well as vertical flow directions between borehole sections based on point water heads and environmental heads for all HFM-boreholes.

Figure 3-43 illustrates measured groundwater levels, i.e. point water heads, and the calculated environmental heads in HFM19 and SFM0058. Both point and environmental water heads suggest that the site is a recharge area for most of the period. The heads in QD are well above the point and environmental water heads in the bedrock borehole sections except during dry summer months. Due to evapotranspiration the groundwater level in the QD during dry summer conditions drops below the point water head in the two uppermost borehole sections HFM19:2 and 3 and below environmental water heads in all sections. The groundwater level in QD is also well above the sea water level and the level of Lake Bolundsfjärden except during the dry summer of 2006.

On average the environmental heads of HFM19:1 and HFM19:2 are 0.76 and 0.21 m higher than the point water heads, respectively, whereas average point and environmental water heads are the same for the uppermost section. When comparing the HFM-sections internally, the deepest section, HFM19:1, always shows the lowest point water head, while the uppermost sections shows the lowest environmental head.

The example illustrates the complexity in the interpretation of vertical gradients in an environment with water density varying with depth. If densities are not considered the flow gradient is downward all the way down to the deepest borehole section at a depth of –131 to –144 m RHB70. If the difference in density is taken into account the calculated environmental heads instead indicate that water flows both from above and below to the uppermost borehole sections with its bottom at –81 m. However, it should be noted that the differences between the environmental water heads in the three borehole sections are quite small.

A vital uncertainty in the calculation of environmental heads is the assumption of the density profile in the bedrock outside the borehole compared with that measured in the borehole sections. The fact that a fractured medium is considered implies that water density in a single fracture crossing a borehole section may have a dominating influence on the density obtained for that section. It may also very well be so that there is no continuous vertical hydraulic contact in the bedrock outside the borehole. Furthermore, there is always a risk that the drilling of the borehole, in spite of the packer installations, creates a vertical contact that does not exist naturally. However, if there is a natural vertical contact, the environmental heads should give an indication of the vertical flow direction between the frequent horizontal and sub-horizontal fracture zones existing in the upper c. 150 m of the bedrock in the candidate area. This information is of major interest in discussions of groundwater recharge and discharge.

Table 3-14. HFM-borehole sections with a difference between measured point water head (PWH) and calculated environmental water head (EWH) > 0.1m.

HFM-borehole	Section No. (of total)	Difference EWH-PWH (m)
HFM02	1(3)	0.12
HFM08	1(2)	0.68
HFM10	1(2)	0.51
HFM13	1(3)	0.83
HFM19	1(3)	0.76
HFM19	2(3)	0.21
HFM27	1(4)	0.14
HFM27	2(4)	0.12
HFM32	1(4)	0.10

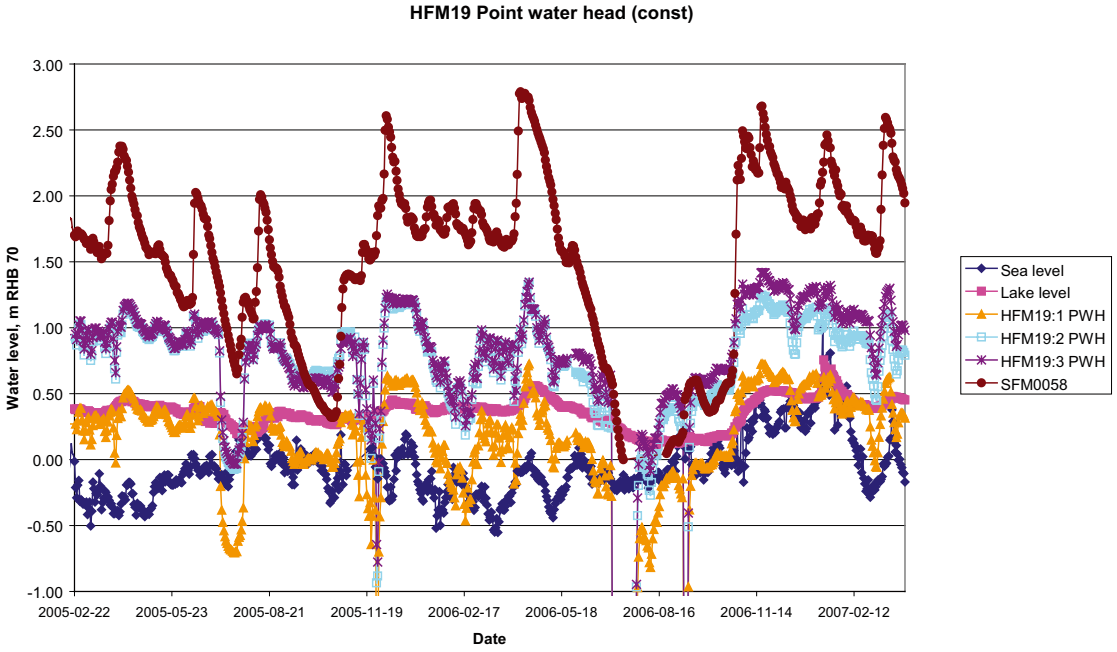

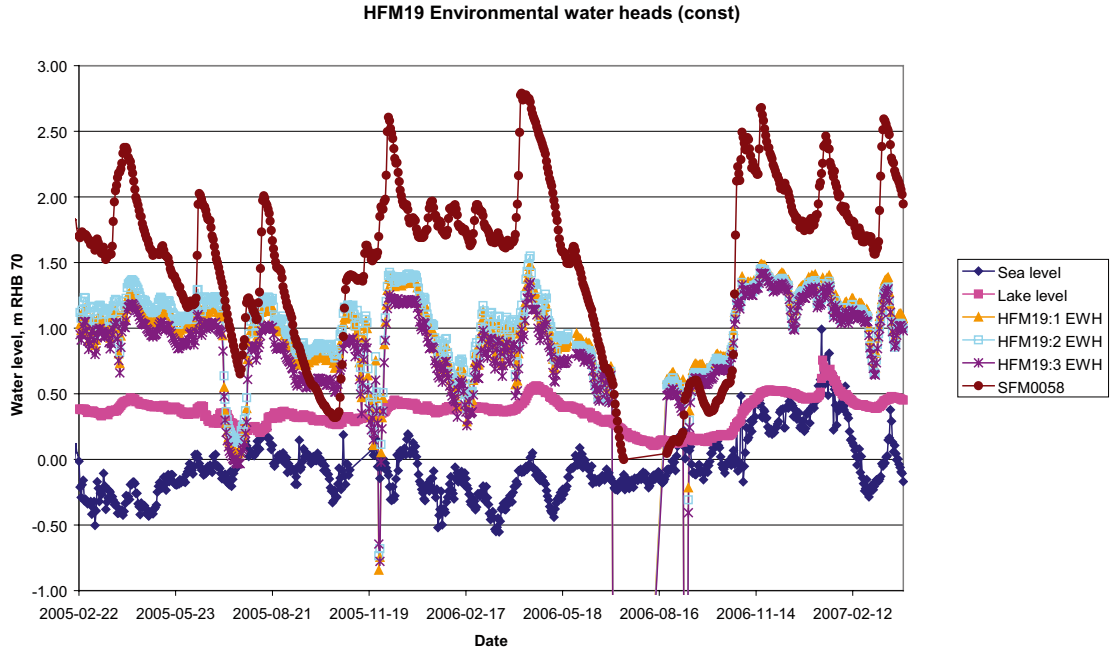

HFM19 (Constant) QD =SFM0058

Section	Min		Percentil 0.02		Ave		Percentil 0.98		Max		Section	Difference EWH-PWH mean
QD	PWHQD	EWHQD	PWHQD	EWHQD	PWHQD	EWHQD	PWHQD	EWHQD	PWHQD	EWHQD	QD	
	-5,63 ↓	-5,63 ↓	-2,5 ↓	-2,5 ↓	-0,8 ↓	-0,8 ↓	0,26 ↓	0,26 ↓	0,44 ↓	0,44 ↓		
3	PWH3	EWH3	PWH3	EWH3	PWH3	EWH3	PWH3	EWH3	PWH3	EWH3	3	0,00
	-0,43 ↓	-0,15 ↓	-0,26 ↓	-0,01 ↓	-0,07 ↓	0,13 ↓	0,06 ↓	0,26 ↓	0,09 ↓	0,27 ↓		
2	PWH2	EWH2	PWH2	EWH2	PWH2	EWH2	PWH2	EWH2	PWH2	EWH2	2	0,21
	-0,78 ↓	-0,24 ↓	-0,64 ↓	-0,09 ↓	-0,51 ↓	-0,03 ↓	0,32 ↑	0,08 ↑	0,35 ↑	0,12 ↑		
1	PWH1	EWH1	PWH1	EWH1	PWH1	EWH1	PWH1	EWH1	PWH1	EWH1	1	0,76

Figure 3-43. *Plot of groundwater levels, i.e. measured point water heads and calculated environmental heads, in HFM19 and SFM0058 and water levels in the sea and Lake Bolundsfjärden. The inset at the bottom shows the level difference between nearby sections (blue = downward gradient, level diff. > 0.05 m, yellow = level diff. less than 0.05 m, red = upward gradient, level diff. > 0.05 m).*

Groundwater level time series

From Table 3-14, listing the 9 borehole sections where the difference between measured point water head and calculated environmental head is > 10 cm, it is clear that for most borehole sections the difference is small and will not influence the interpretation of vertical groundwater flow gradients. In the following, the presented groundwater levels are measured point water heads unless otherwise stated.

As mentioned in Section 2.2.3, groundwater level time series from the percussion-drilled boreholes show frequent intervals of high amplitude disturbances related to core drilling acitivities and other pumping. While these disturbances could give valuable information on interconnectivity in the bedrock, they also tend to obscure more subtle groundwater level changes in response to infiltration and sea level changes. Therefore, a thorough data screening was performed to produce a second "clean" data set with no visible artefacts from disturbing activities, see Figure 3-44.

Natural conditions

Figure 3-45 shows summaries of undisturbed groundwater levels in the bedrock in terms of means and observed ranges. Note that it is difficult to establish meaningful comparisons of time series summary statistics when the time series themselves are so unevenly populated (Figure 3-44b). For this reason, the summary values shown in Figure 3-45 should be considered "best available". In the figure only data series with more than 150 days are presented. The data points are colour-coded to indicate the variable populations used in the mean and range calculations. In the notations used for the percussion-drilled boreholes, HFMXX.Y, XX is the borehole number and Y is the borehole section number, with the numbering of the sections starting from the bottom of the borehole.

Figure 3-45a shows the mean and range of groundwater point water heads in the bedrock (topmost section of HFM-borehole or open borehole), co-plotted with bedrock and ground surface elevations at each site, and shown ranked according to increasing bedrock elevations. Two well sections exhibit mean groundwater point water heads below 0.0 m RHB70 (HFM34.3: –0.47 and HFM35.4: –0.72). Four more wells show minimum values extending below 0.0 m RHB70 (HFM07, HFM17, HFM27 and HFM32). The number of wells with means and minimums below 0.0 m RHB70 is not changed if point water heads are transformed to environmental water heads.

For the conceptual modelling, it is interesting to note that 23 of the 36 boreholes demonstrate point water heads above local bedrock levels. As was evident in the undisturbed time series (Figure 3-44c), most wells had mean point water heads within a close range (between 0.0 and 1.0 m RHB70). Of the wells located within the geologic tectonic lens constituting the candidate area, all wells but two have mean point water heads below 1.5 m RHB70. These two borehole sections (HFM07 and HFM13:3) have very low transmissivity and do not appear to be affected by any of the highly transmissive horizontal fracture zones/sheet joints, see Figure 3-45c.

Figure 3-45b shows these same data plotted as point water heads in relation to ground surface, co-plotted with bedrock depth below ground surface, and ranked according to decreasing depth to bedrock. It is obvious that the strong coupling between groundwater level and topography found for the well in till does not exist for the point water heads in bedrock. This is illustrated in Figures 3-46 and 3-47.

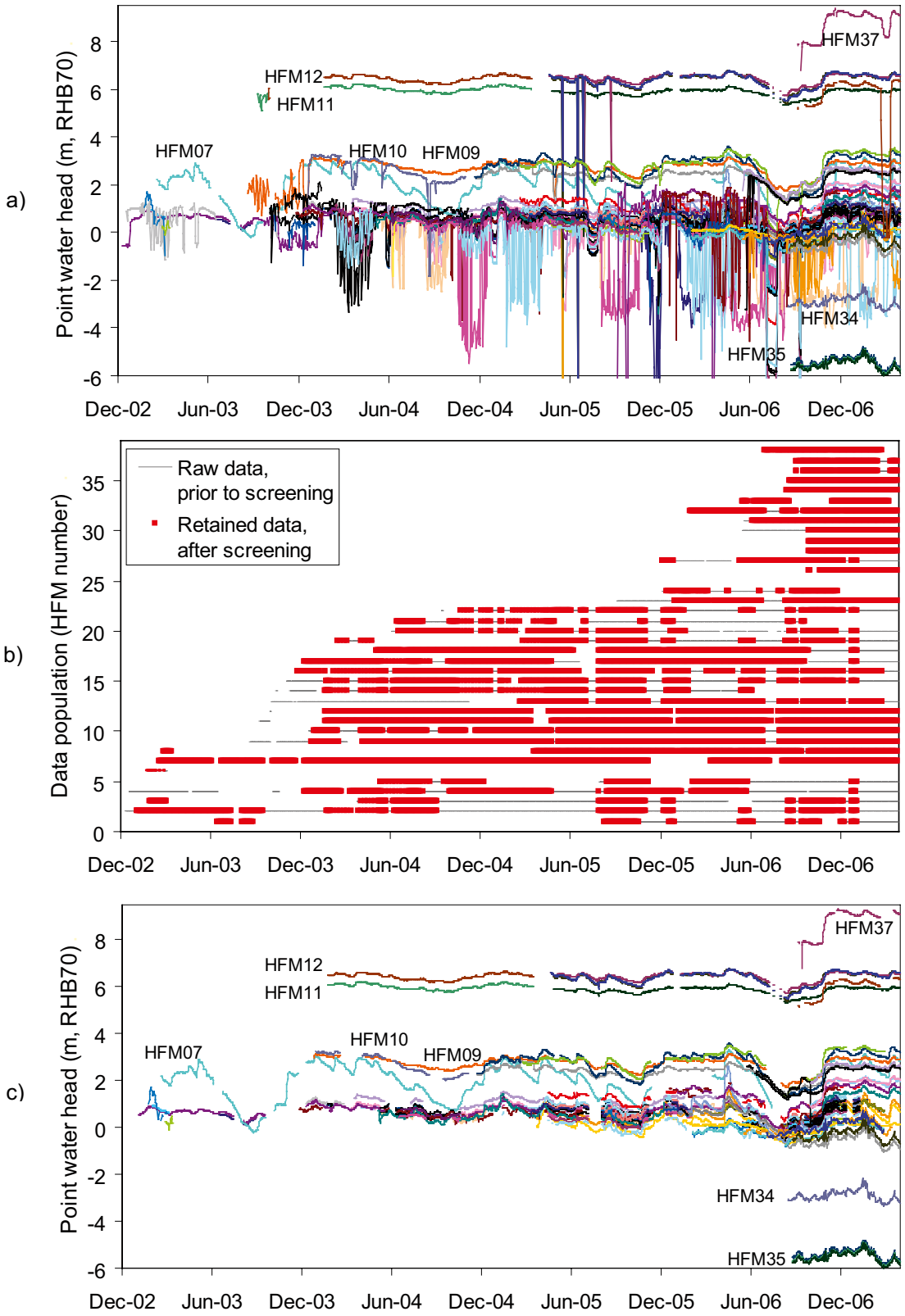

Figure 3-44. *Daily averages of point water heads in 37 percussion-drilled boreholes in bedrock. Raw data is shown in a) and include numerous disturbance intervals. Data population is shown in b) with data judged as undisturbed by site investigation activities marked in red. In c) the retained data set after the screening is shown.*

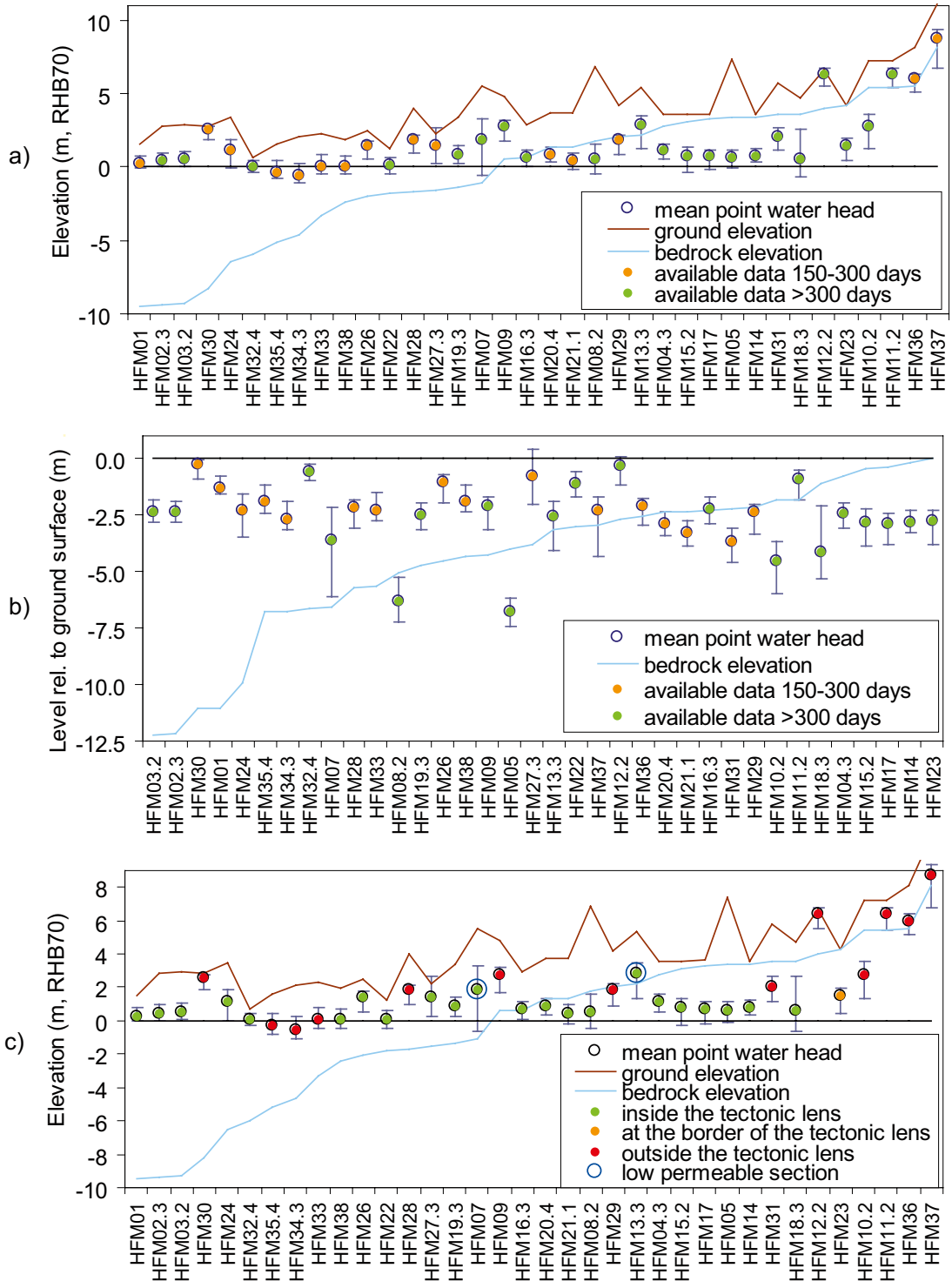

Figure 3-45. *Mean groundwater point water heads in bedrock with observed ranges based on available "clean" data plotted as a) point water head elevations ranked according to bedrock elevations, b) point water head relative to ground surface ranked by depth to bedrock, and c) point water heads ranked according to bedrock elevation as in a) but with colour-coding to show the well location related to the tectonic lens. Data are from the topmost section in wells with packers or open boreholes for wells with no packers.*

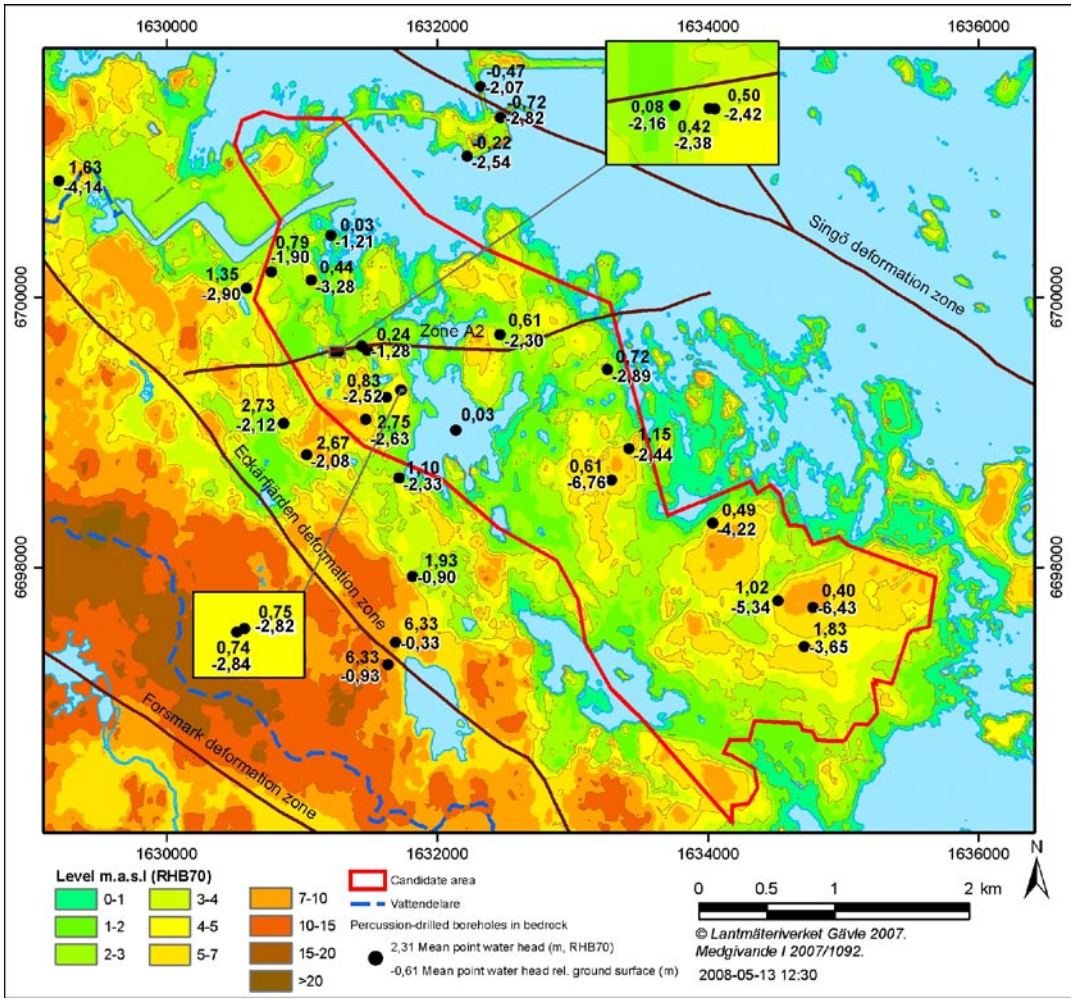

Figure 3-46. *Map indicating the mean point water heads in bedrock (RHB70) and the corresponding head related to ground surface.*

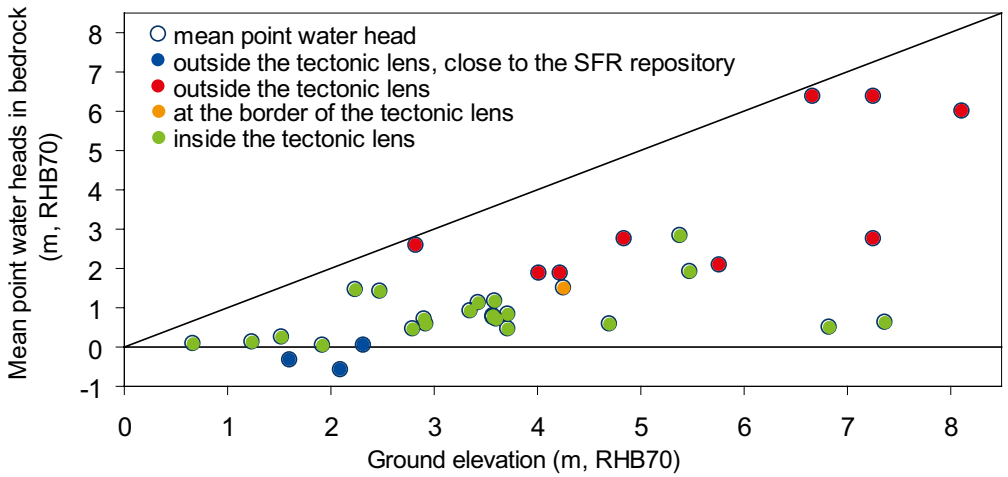

Figure 3-47. *Cross-plot of mean groundwater point water heads in bedrock versus ground surface elevations.*

Figure 3-48 shows multiple point water head time series measured in HFM04 at sections separated by packer installations. These data suggest downward vertical gradients in point water heads in the bedrock penetrated by HFM04 (in this borehole there is no salinity gradient which means that point and environmental water heads are the same).

Figure 3-49 shows average differences in mean point water heads between neighbouring sections for the boreholes that have multiple sections (packers); the borehole locations are shown in Figure 2-9. In most wells there is a downward gradient between the two uppermost borehole sections (for point water heads in 14 of 17 wells and for environmental heads in 11 of 17 wells). In six of the boreholes there are differences in vertical direction of the gradient in one or more sections if point and environmental water head data are compared (HFM08, HFM10, HFM13, HFM16, HFM19 and HFM32). If environmental heads are considered, there is a continuous downward gradient in six wells (HFM01, HFM03, HFM11, HFM15, HFM18 and HFM34) while there is a continuous upward gradient in four wells (HFM02, HFM08, HFM10, HFM12).

Disturbed conditions

In Figures 3-50 and 3-51 the responses in groundwater levels in bedrock wells in the central part of the site investigation area on pumping by c. 6 L/s in HFM14 during 3 weeks in the summer of 2006 are shown /Gokall-Norman and Ludvigson 2007a/. The widespread and fast respones indicate very high transmissivities in combination with low storativities.

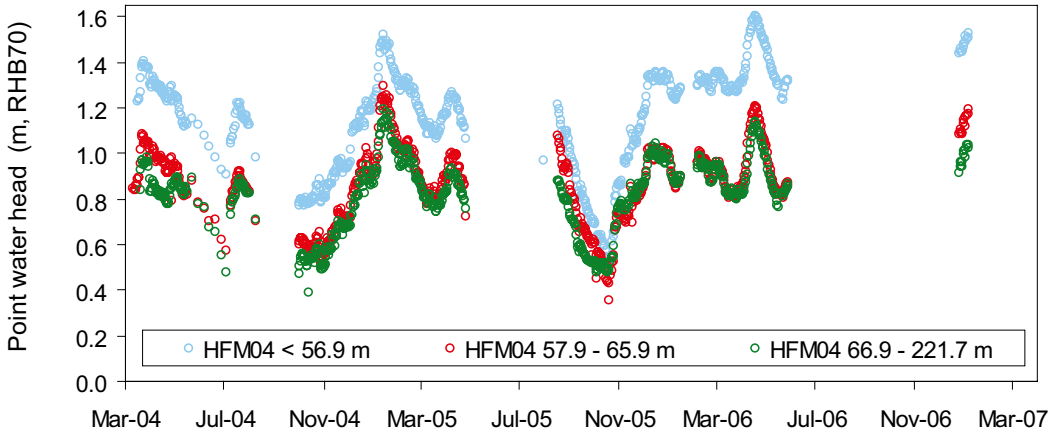

Figure 3-48. *An example of vertical groundwater point water head differences in three sections at HFM04.*

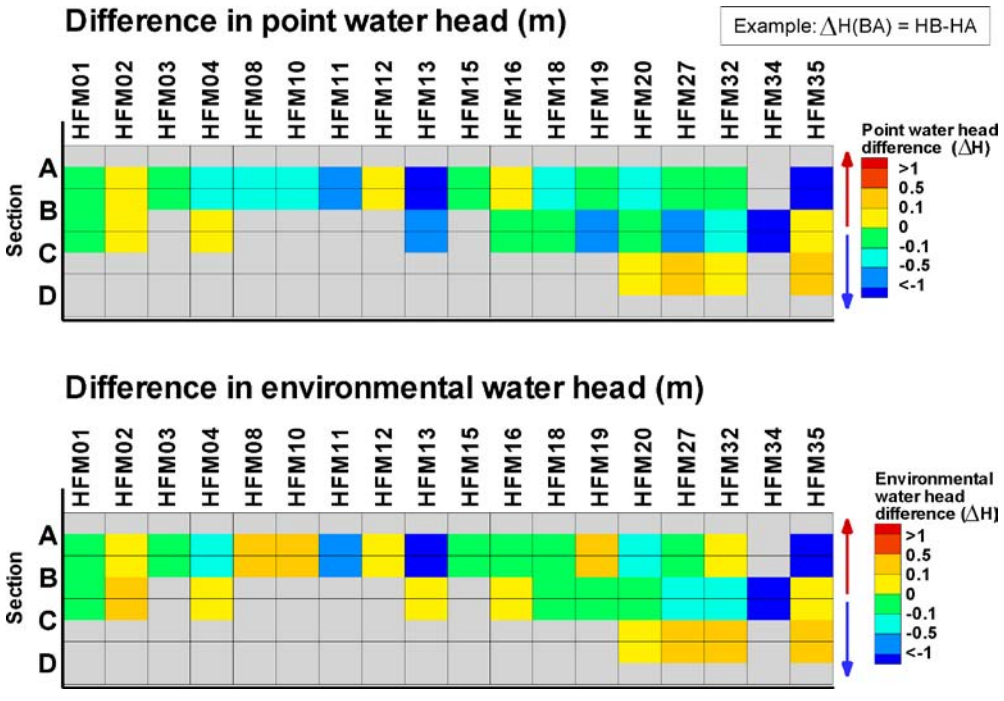

Figure 3-49. *Summary of a) mean difference in point water head and b) environmental water head in the percussion-drilled boreholes with packers separating the boreholes into several intervals.*

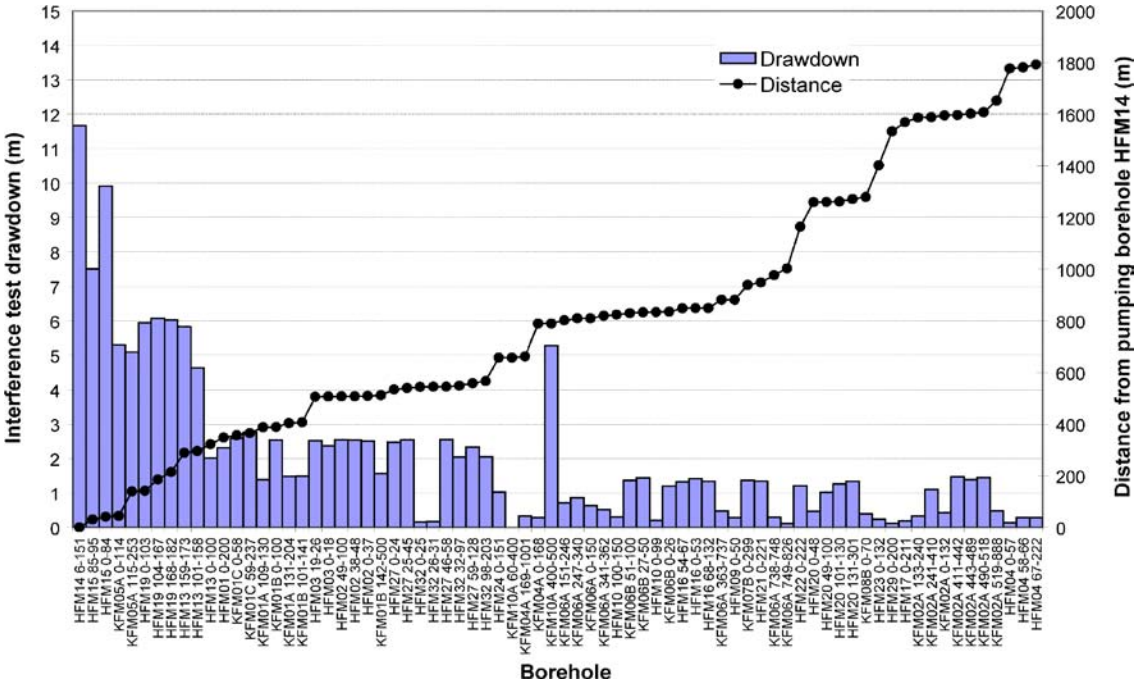

Figure 3-50. *Plot of observed drawdowns at the end of the 2006 interference test in HFM14. Monitoring intervals are sorted by distance from the abstraction well /Follin et al. 2007a/.*

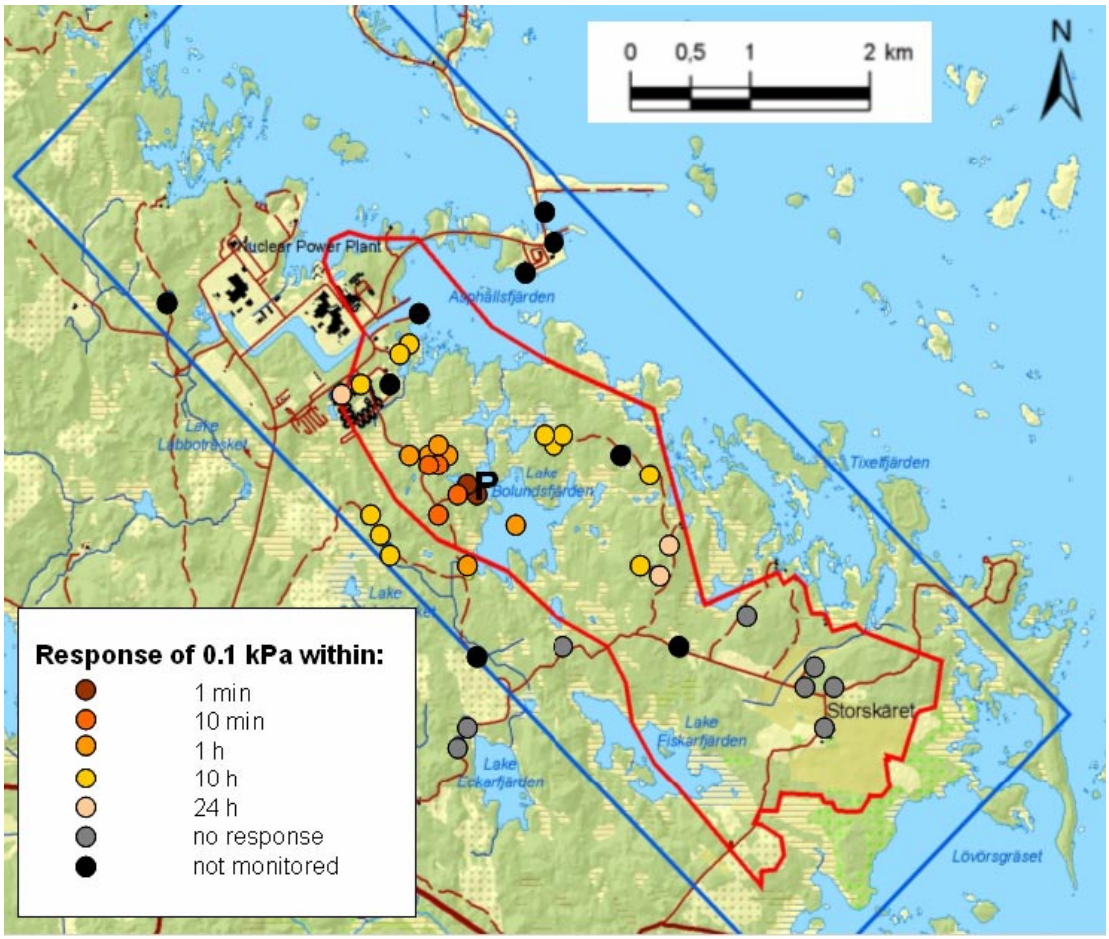

Figure 3-51. *Map showing response times in the bedrock to the 2006 interference test conducted in HFM14. The test responses were monitored at 71 "observation points". In boreholes with more than one section, the section with the fastest response is shown /Follin et al. 2007a/.*

3.5 Joint description of the flow system

In this section a systems approach is used to describe the hydrological and near-surface hydrogeological flow system of the site investigation area. The description joins the hydrological and hydrogeological objects/flow domains described in Sections 3.3 and 3.4. The flowing water is the primary target of the description, i.e. the main functional units are the flow system and its sub-systems, not the water courses, lakes or aquifers. The groundwater flow systems connect recharge areas with discharge areas. Such systems may use only a part of an aquifer or may cut across aquifers.

A groundwater flow system is characterised by boundary types, geometry, volume, energy conversion capacity, system flux and hierarchical place /Engelen and Jones (eds.) 1986/. The systems approch, focussing on the flow system and its sub-systems, is considered to facilitate the transfer of the conceptual model to the quantitative numerical flow modelling to be conducted.

3.5.1 External boundary conditions

Top boundary

The meteorological conditions constitute the top boundary of the hydrological and near-surface hydrogeological system. Water is added to the system by rainfall and snowmelt and abstracted by evapotranspiration. (All precipitation data presented here are corrected for wind losses, see Section 2.2.1.)

In northeastern Uppland, where the site investigation area is located, there is a relatively strong west-east gradient in precipitation. In Figure 3-52 the annual precipitation at the SMHI-stations surrounding the site investigation area is shown for the years 2004–2006 together with an average of the 13 years of data available in the SKB Sicada database (see Figure 2-2 for the locations of the stations). The average annual precipitation at Lövsta, approximately 15 km west of Forsmark, was 690 mm, as compared with 492 mm at Örskär, a small island approximately 15 km northeast of Forsmark.

In Figure 3-53 annual precitation from SKB's stations in Forsmark, Högmasten and Storskäret, are presented together with data from the SMHI-stations, for the three full years of available data up to data freeze 2.3. Data for both hydrological and calendar years are shown (hydrological years Oct. 2003–Sep. 2006, and calendar years 2004–2006). Missing data at the SKB stations were estimated by regression analysis where the SMHI-stations Lövsta, Östhammar and Örskär were used.

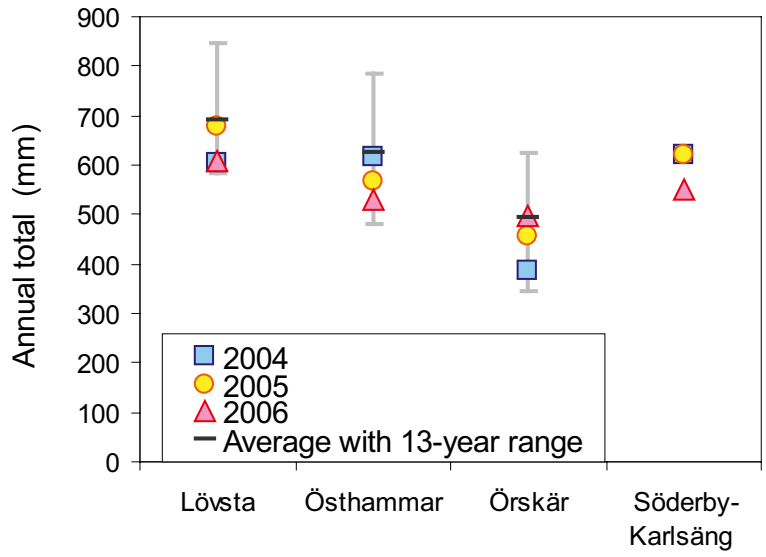

Figure 3-52. *Precipitation data from SMHI-stations surrounding the site investigation area (Söderby-Karlsäng is a recently established station).*

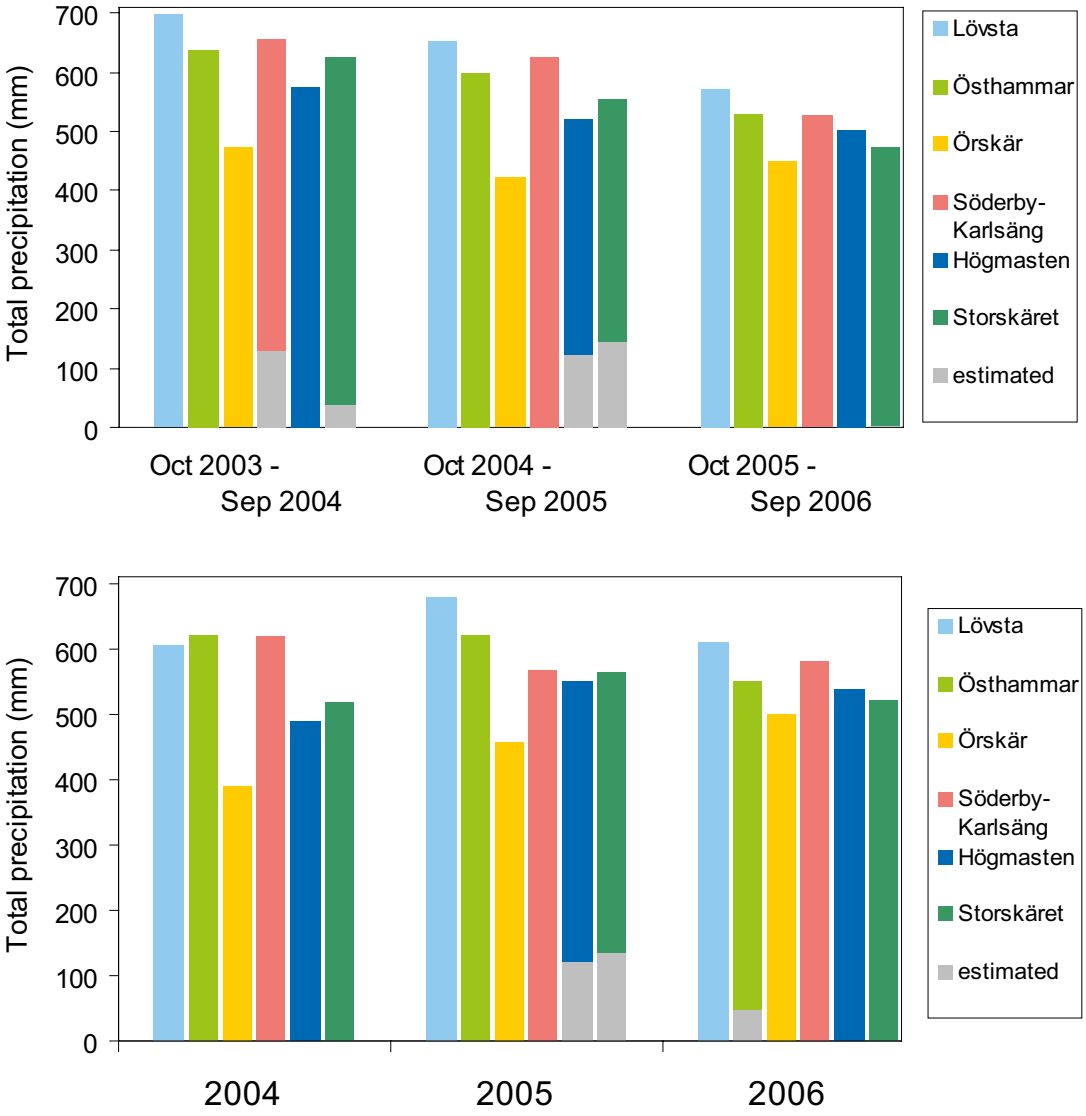

Figure 3-53. *Comparison of annual precipitation at the SKB stations, Högmasten and Storskäret, and at surrounding SMHI-stations.*

Table 3-15 presents annual precipitation data from Forsmark (averages of the Högmasten and Storskäret stations) for the same three-year periods as in Figure 3-53. In addition, data for the four-year period of June 2003–May 2007 are presented to make maximum use of site specific data.

From regional data the mean annual precipitation in the Forsmark site investigation area has been estimated to average to 559 mm (standard deviation of 106 mm) for the period 1961–1990 by the Swedish Meteorological and Hydrological Institute (SMHI), see Appendix 1. From Table 3-15 it can be concluded that the precipitation during the site investigation has been quite close to the longterm average.

In Table 3-16 the annual "potential evapotranspiration" for a short crop, calculated by the Penman equation, is given for the same time periods as for precipitation in Table 3-15. The calculation method is described in Section 2.2.1.

A simple snow-routine, based on the degree-day factor approach, has been calibrated to the site measurements of snow water content /Johansson and Öhman 2008/. Based on the results a time series of daily values could be constructed of the water added to the system in liquid form. In Figure 3-54 monthly sums of this time series are shown together with the potential evapotranspiration from the start of the measurements up to data freeze 2.3 (March 31, 2007).

Table 3-15. Annual, corrected, average precipitation at Forsmark (average of the Högmasten and Storskäret stations) for three different time periods.

Time period	Corrected precipitation (mm)
Jan. 2004–Dec. 2006	537
Oct. 2003–Sep. 2006	536
June 2003–May 2007	563

Table 3-16. Calculated potential evapotranspiration at Forsmark (Högmasten) for three different time periods.

Time period	Potential evapotranspiration (mm)
Jan. 2004–Dec. 2006	509
Oct. 2003–Sep. 2006	507
June 2003–May 2007	526

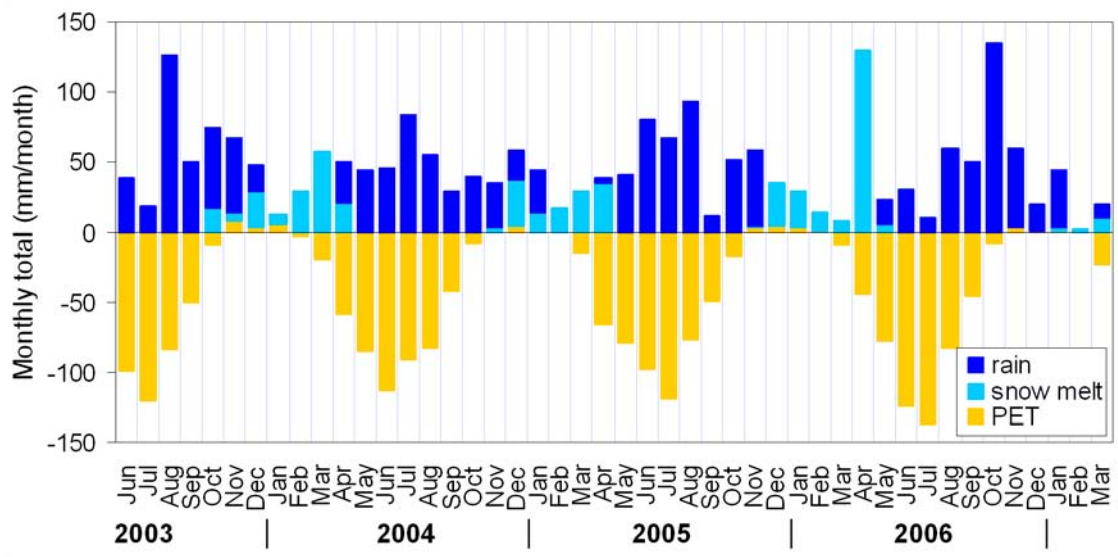

Figure 3-54. *Monthly values of rainfall+snowmelt and potential evapotranspiration (PET).*

Inland boundary

The close correlation between the topography of the ground surface and the groundwater level in the Quaternary deposits, shown in Figures 3-38 to 3-42, means that surface water and groundwater divides for the QD can be assumed to coincide. Regarding groundwater levels in the upper bedrock there is not a similar strong coupling to the topography of the ground surface, see Figures 3-45 to 3-47. This is most evident in the central part of the site investigation area, i.e. within the tectonic lens, where the upper c. 150 m of the bedrock is known to have frequent horizontal and sub-horizontal highly transmissive fractures. However, Figure 3-46 also indicates a trend with westward increasing groundwater levels in the bedrock outside the tectonic lens. Furthermore, no major fracture zones crossing the inland surface water divide towards River Forsmarksån are known, with exception of Eckarfjärdszonen crossing south of Lake Eckarfjärden.

The conclusion is that the water divides of the flow systems in QD, where the major part of the groundwater flow takes place, coincide with the surface water divides. It can also be assumed that the water divides of the flow systems involving the near-surface bedrock follow the surface water divide of River Forsmarksån, i.e. the topography can be used for delineation of the inland boundary.

Sea boundary

From the conclusion that groundwater divides for the shallow groundwater systems limited to QD (till), where most of the water flow takes place, coincide with the surface water divides follows that such systems only may have lateral boundaries to the sea in the rest catchments with no surface discharge in water courses (see Figure 3-4). For the flow systems involving also the near-surface bedrock the situation is different due to the highly transmissive horizontal and sub-horizontal fracture zones extending below the sea /Follin et al. 2007a, 2008/. The vertical contact between these zones and the sea (via outcropping or indirectly via vertical fractures) will determine the boundary conditions of these systems. The superficial horizontal sheet joints have a tendency to follow the topography of the bedrock surface implying that direct hydraulic contact with the sea via outcropping is considered to be less common /Follin et al. 2007a, 2008/.

From Figures 3-29 and 3-30 it can be seen that the sea bottom is to a great extent covered by fine sediments (silt and clay) and till. However, areas with coarse sediments and also outcropping bedrock are frequent. The described features will determine the boundary conditions and the degree of hydraulic contact between the sea and the flow systems involving the near-surface bedrock. In Figure 3-55 sea levels are plotted with groundwater levels in QD and bedrock.

The correlation between the three data sets has been investigated by several methods, including linear regression of mean values for different time intervals and displacement in time, principal component analysis (PCA), independent component analysis (ICA) and partial least squares modelling (PLS) /Juston et al. 2007/. In Figures 3-56 and 3-57 the regression coefficients for the QD and bedrock wells, respectively, are shown. The time intervals and displacements in time demonstrating the highest regression coefficients are shown.

As anticipated the regression coefficients for the groundwater levels in QD with the sea were very low with exception of the two wells SFM0059 and SFM0061 located in glaciofluvial material (Börstilåsen) within 100 m from the sea. The regression coefficients of the bedrock boreholes were also quite low with exception for boreholes located at the SFR-peninsula, i.e. HFM33, –34 and –35 (Figure 3-57). The time series in these boreholes are comparatively short. However, it is assumed that the high regression coefficients in these wells will remain also when longer time series become available.

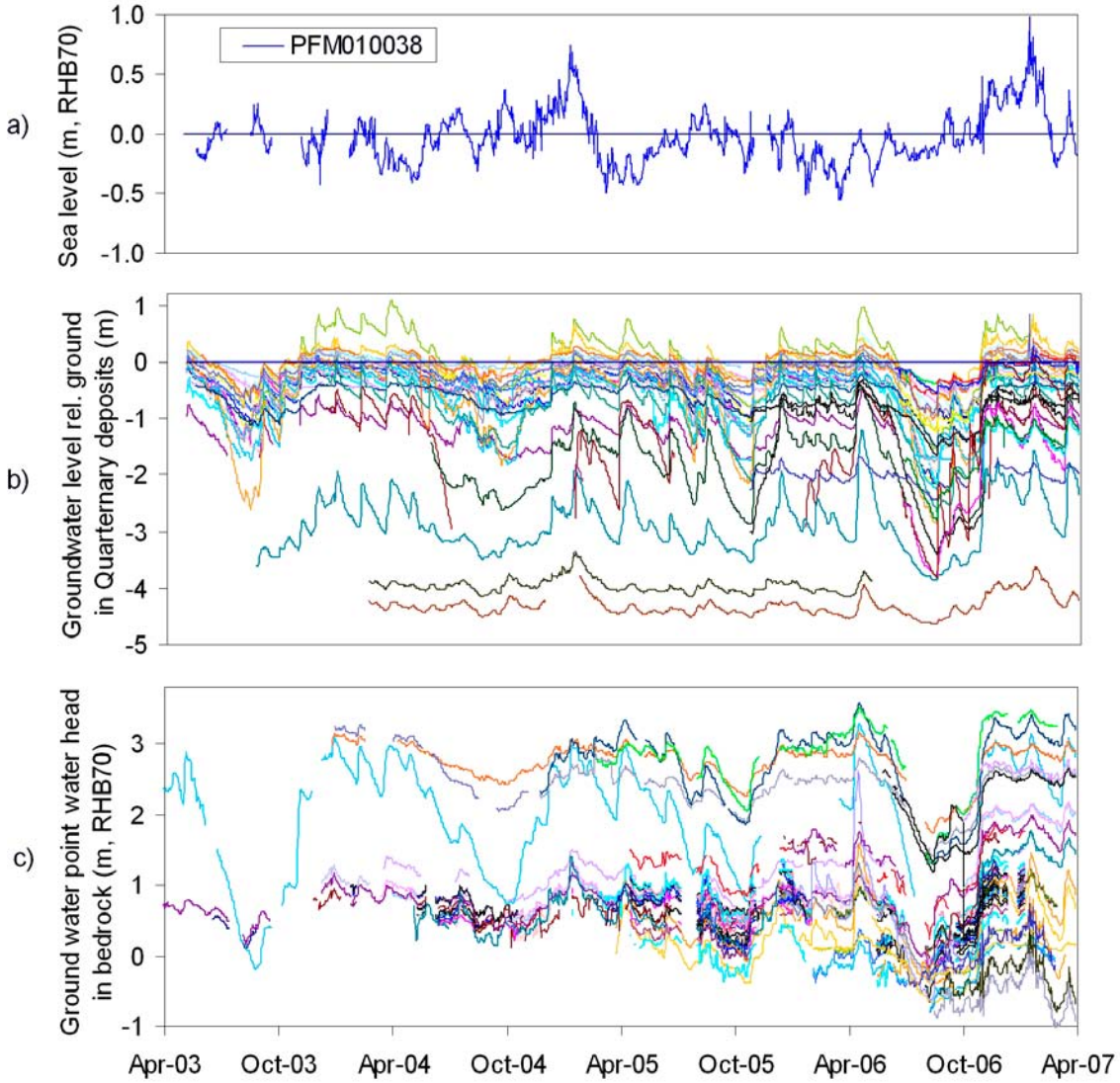

Figure 3-55. *Comparison of sea water levels (a) and groundwater levels in QD (b) and in bedrock (c). In c) HFM11, 12, 34:2, 35:1–3, 36 and 37 have been excluded to enable a better resolution of the y-axis.*

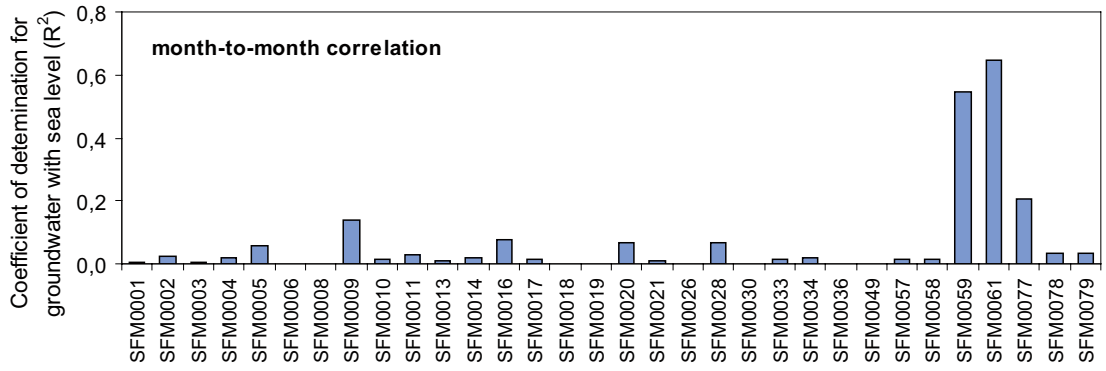

Figure 3-56. *Correlation between sea water level and groundwater levels in monitoring wells in QD on land with more than one year of data.*

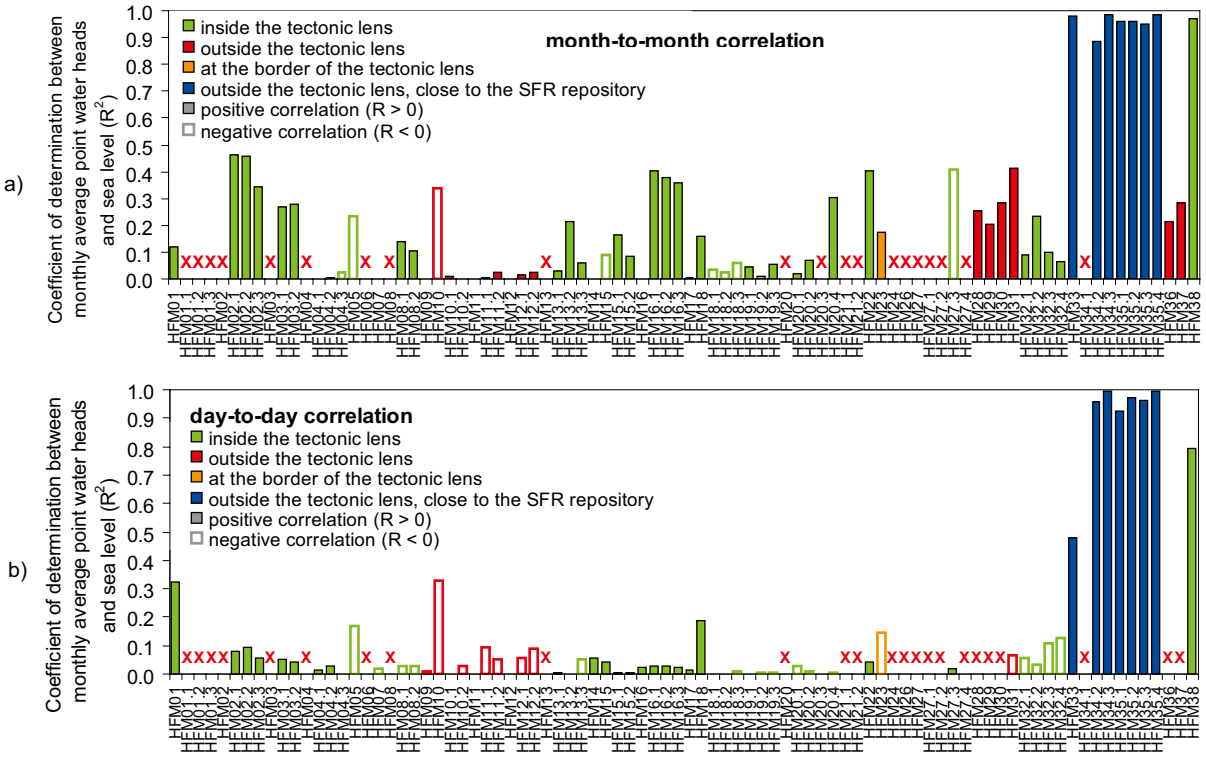

Figure 3-57. *Correlation between sea water level and point water heads in bedrock (HFM-borehole sections). The month to month correlation is presented for sections with more than 6 months of data with at least 15 days of data per month. For the day-to-day correlation, sections with more than 6 months of data are included.*

The very low regression coefficients for most of the bedrock boreholes were not expected. To further explore the relationship between the sea level and the groundwater levels in the bedrock PCA (Principal Component Analysis), ICA (Independent Component Analysis) and PLS (Partial Least Squares) analyses were conducted. The PCA and ICA analyses indicated that the seasonal rain + snowmelt and evapotranspiration variations describe about 80% of the total variation, while sea water level explains less than 10% of the variation /Juston et al. 2007/. However, the fact that the sea water level covariates with the occurrence of low pressures and accompanying precipitation makes the correlation difficult to elucidate.

Figure 3-58 shows the sea water level plotted together with the mean of measured groundwater levels in all HFM-boreholes and a groundwater level simulated by a simple tank model. The level in the groundwater storage was assumed to be a function of daily infiltration (corrected precipitation and difference in snow storage minus potential evapotranspiration), and an outflow function proportional to the groundwater level. A constant of the outflow function was calibrated to meet the assumption of zero change of groundwater storage during March 2005 to February 2007. There is a good match between the modelled groundwater level (green) and the mean variation in all percussion boreholes (red) according to Figure 3-58, indicating that the annual cycle is mostly controlled by variations in evapotranspiration /Johansson and Öhman 2008/.

The PLS regression technique, which is a multivariate regression technique related to PCA and suitable to explore the correlation structure between two matrices, was applied on selected time series of groundwater point water heads, sea level, air pressure and modelled groundwater level. Here, one matrix contains the time-series of sea level, air pressure and modelled groundwater level, and the second matrix the time-series of groundwater point water heads.

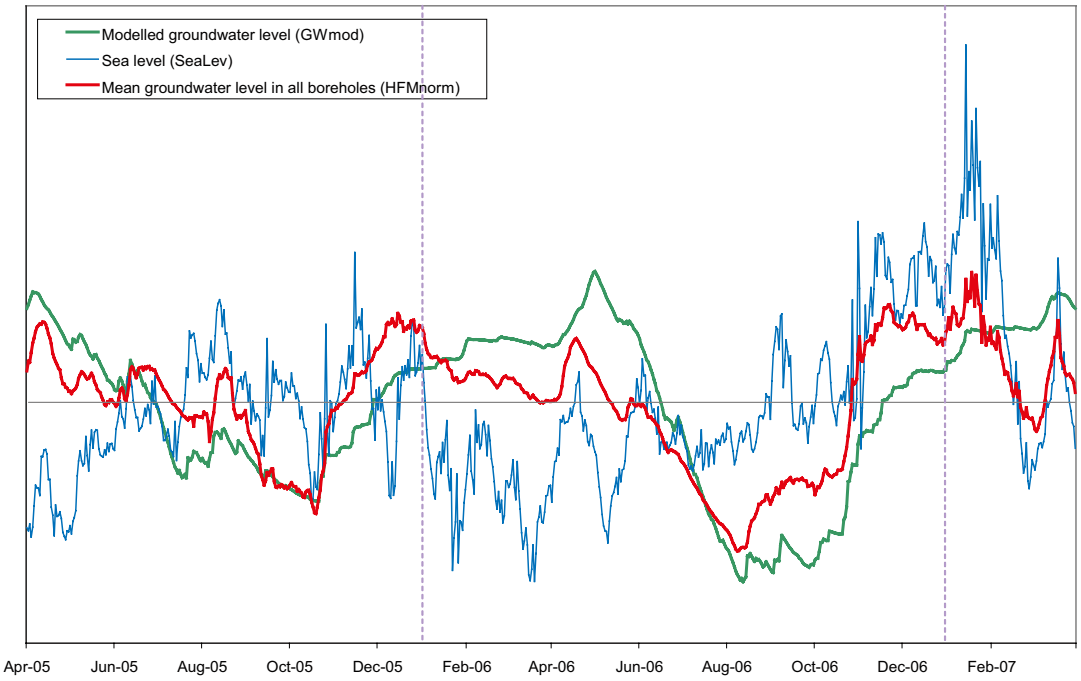

Figure 3-58. *Time-series showing sea level and modelled groundwater level together with the mean groundwater level in all percussion-drilled boreholes (HFM) (mean of individually normalised time series). All time series are standardised to zero mean and equal variance.*

The resulting components of the PLS-model reveal underlying factors common to both matrices (i.e. common to both sea level, air pressure and modelled groundwater level, and groundwater point water heads), and may have an explicit interpretation. In all models the first component describes the overall seasonal pattern closely coupled to GWmod, whereas the second component is mainly coupled to variations in sea level and air pressure. The graphical output of these multivariate models is analogous to the "loading plot" of the PCA, in the respect that variables located close to each other are correlated, whereas variables located on opposite sides of the origin are inversely correlated. Variables located close to the origin show little connection to the selected components.

In order to describe the relative influence of the sea level (SeaLev), air pressure and modelled groundwater level (Gwmod) on the observed groundwater level variation in each borehole, the distance to SeaLev and GWmod was calculated according to the schematic picture in Figure 3-59. This projected measure (ζ) is used to summarise all models in Table 3-17 and finally to achieve a compact spatial visualisation of the relative influence of the variations in sea level in Figure 3-60.

In all analyses, two-component PLS-models are used, where about 70–80% of the variation in groundwater point water heads are explained by the selected variables. In Table 3-17 a rough statistical classification in three classes denoted "no influence", "possible influence" and "probable influence" is introduced to facilitate interpretations. It should be noted that both limits and denominations of these classes are chosen rather arbitrarily.

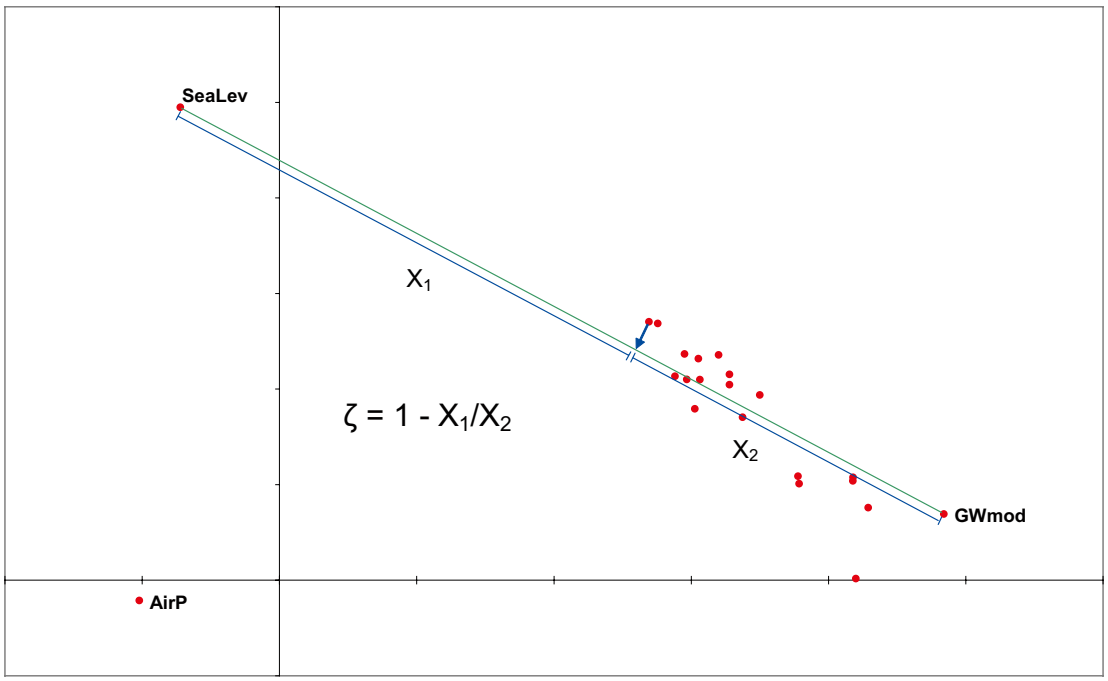

Figure 3-59. *Schematic description of how the relative distance to the SeaLev "pole" (ζ) is calculated from the perpendicular projection to the line that connects SeaLev and GWmod.*

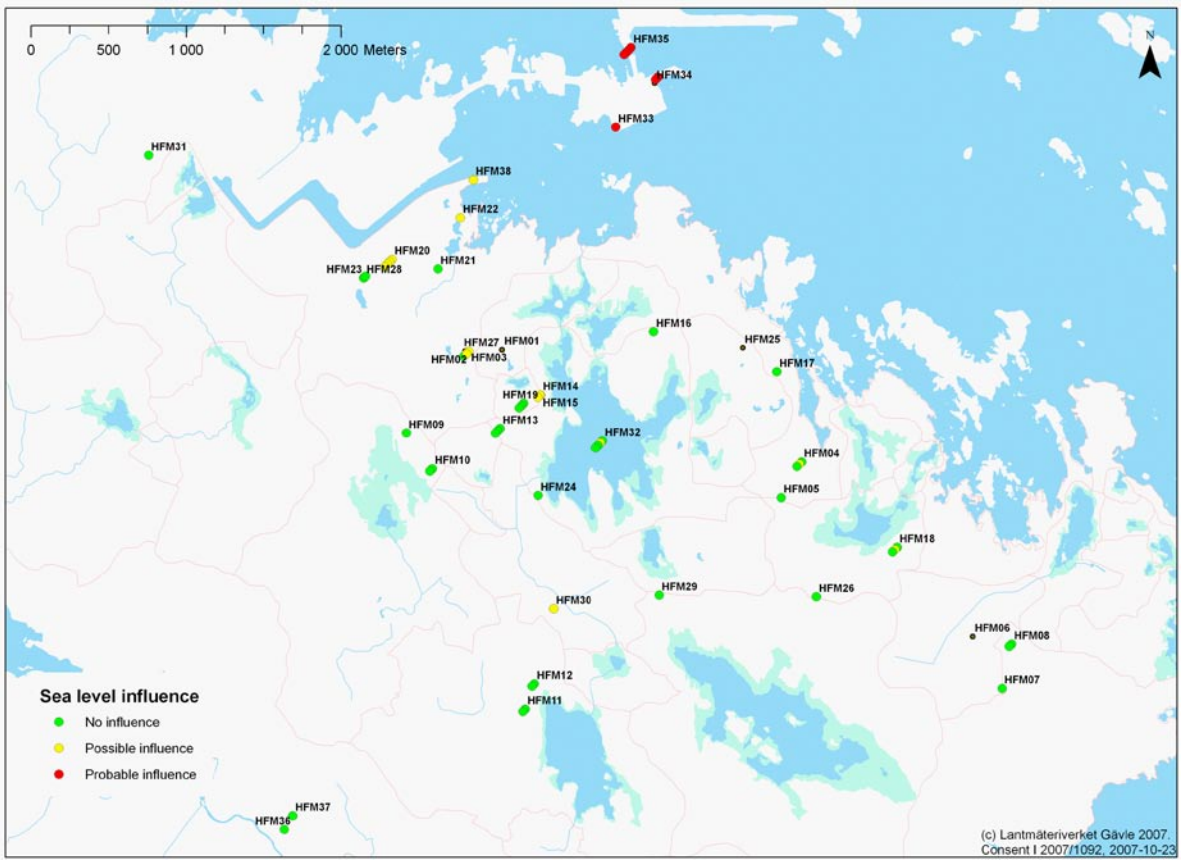

Figure 3-60. *The spatial distribution of the three classes representing "no influence", "possible influence" and "probable influence" from variations in sea water level. In case of several sections per borehole, the uppermost section is plotted on top and the deepest section at the bottom of the pile.*

Table 3-17. Compilation of results from the correlation analysis of sea water level influence on percussion-drilled boreholes. The analysis has been conducted on individual borehole sections (denoted HFMXX.Y with the section numbering (Y) starting from the deepest section). The ζ-parameter ranging from 0 to 1 represents the relative association with the SeaLev and GWmod variables (1 indicates strong association with SeaLev). To facilitate interpretations three colour coded classes denoted 'no influence' (green), 'possible influence' (yellow) and 'probable influence' (pink) have been marked in the table. A0-G are sub-series of data used to make maximum use of available data.

Borehole	Data selection										Classification	
Idcode	A0	B0	C0	A	B	C	D	E	F	G	Mean	Class
HFM02.1			0.40				x				0.40	Possible influence
HFM02.2			0.63				x				0.63	Possible influence
HFM02.3			0.32				x				0.32	No influence
HFM03.1			0.43				x				0.43	Possible influence
HFM03.2			0.42				x				0.42	Possible influence
HFM04.1	0.27				0.30						0.28	No influence
HFM04.2	0.27				0.40						0.34	Possible influence
HFM04.3	0.20				0.16						0.18	No influence
HFM05					0.17						0.17	No influence
HFM07	0.11	0.02	0.00	0.01			x	0.27	0.14		0.09	No influence
HFM08.1		0.07		0.15	0.29	0.37	x	0.39	0.26	0.29	0.26	No influence
HFM08.2		0.07		0.15	0.30	0.35	x	0.41	0.24	0.27	0.25	No influence
HFM09	0.09	0.06	0.00	0.11	0.16	0.11	x	0.26	0.11	0.12	0.11	No influence
HFM10.1	0.08	0.07	0.00	0.11	0.15	0.10	x	0.26	0.11	0.13	0.11	No influence
HFM10.2		0.02		0.07	0.11	0.14	x	0.21	0.09	0.12	0.11	No influence
HFM11.1	0.29	0.01	0.00		0.13	0.08	x	0.30	0.11	0.11	0.13	No influence
HFM11.2			0.00		0.21	0.17	x	0.37	0.17	0.16	0.18	No influence
HFM12.1	0.17	0.10			0.23	0.16	x	0.34	0.14	0.14	0.18	No influence
HFM12.2					0.16	0.08	x	0.37	0.15	0.16	0.18	No influence
HFM13.1		0.23		0.35			x				0.29	No influence
HFM13.2		0.31		0.29			x				0.30	No influence
HFM13.3		0.21		0.26	0.17	0.18	x		0.17	0.17	0.19	No influence
HFM14	0.34	0.33	0.42	0.42							0.38	Possible influence
HFM15.1	0.36	0.24	0.40	0.33			x				0.33	Possible influence
HFM15.2		0.31		0.41			x				0.36	Possible influence
HFM16	0.32	0.25	0.37								0.31	No influence
HFM17	0.23		0.25		0.32	0.19	x				0.25	No influence
HFM18	0.39	0.13	0.54	0.32			x				0.35	Possible influence
HFM18.1						0.32	x				0.32	No influence
HFM18.2						0.35					0.35	Possible influence
HFM18.3						0.32					0.32	No influence
HFM19.1		0.24		0.36							0.30	No influence
HFM19.2		0.23		0.34							0.29	No influence
HFM19.3		0.20		0.30							0.25	No influence
HFM20.1		0.60		0.30			x				0.45	Possible influence
HFM20.2		0.47					x				0.47	Possible influence
HFM20.3		0.42					x				0.42	Possible influence
HFM20.4		0.33					x				0.33	No influence
HFM21.1				0.25			x				0.25	No influence
HFM22		0.65		0.33			x				0.49	Possible influence
HFM23						0.29	x	0.33	0.31		0.31	No influence
HFM24						0.03					0.03	No influence

Borehole	Data selection										Classification	
Idcode	A0	B0	C0	A	B	C	D	E	F	G	Mean	Class
HFM26							x	0.25			0.25	No influence
HFM28							x	0.27			0.27	No influence
HFM29								0.23			0.23	No influence
HFM30								0.35			0.35	Possible influence
HFM31							x	0.20			0.20	No influence
HFM32.1						0.19	x		0.27		0.23	No influence
HFM32.2						0.31	x		0.35		0.33	Possible influence
HFM32.3						0.12					0.12	No influence
HFM32.4						0.07		0.32	0.16		0.19	No influence
HFM33								1.00			1.00	Probable influence
HFM34.2							x	1.00			1.00	Probable influence
HFM34.3							x	0.96			0.96	Probable influence
HFM35.1							x	1.00			1.00	Probable influence
HFM35.2								1.00			1.00	Probable influence
HFM35.3							x	1.00			1.00	Probable influence
HFM35.4							x	0.97			0.97	Probable influence
HFM36								0.05			0.05	No influence
HFM37								0.21			0.21	No influence
HFM38							0.63				0.63	Possible influence

With the selected class limits there is a tendency of stronger sea level influence in the northern and northwestern part of the Forsmark area. This pattern is most evident near the SFR repository (note the red points at the peninsula in the north), where all observations are classified as "probable influence" from sea level fluctuations (HFM33, HFM34, HFM35). Also a number of boreholes located on the mainland show "possible influence" indicating that groundwater in the bedrock in this area is influenced from sea level fluctuations, e.g. HFM02, HFM03, HFM14, HFM15, HFM20, HFM22 and HFM38.

Except for the boreholes in the northwest, there are a two boreholes near the coast (HFM04 and HFM18) that are classified as "possible influence", as well as one borehole (HFM30) located more distant from the sea. In the case of HFM18 there are several indications of "possible influence" that strengthen the conclusion, whereas the classification of the latter borehole, HFM30, which is only represented in one time-series, most probably is a coincidence.

It should, be noted that there are many uncertainties associated with the analysis and precise conclusions should not be drawn about specific boreholes. There are several examples of borehole sections that are classified both as "no influence" and "possible influence", e.g. HFM08, HFM11 and HFM12, indicating that there is a substantial noise in the classification.General spatial trends shown by several boreholes based on different time series may on the other hand give indications that there is a real phenomenon behind the pattern rather than a coincidence. For example, this is the case in the northwestern part of the area. The spatial pattern formed by the boreholes in the northwestern part of the area, demonstrating possible influence from sea water fluctuations according to the correlation analysis (e.g. HFM02, HFM03, HFM14, HFM15, HFM20, HFM22 and HFM38), may reflect structural properties of the bedrock in this area.

During events of very high sea water levels, sea water flows into several of the lakes (Norra Bassängen, Puttan, Bolundsfjärden, Lillfjärden and Fiskarfjärden), see Section 3.3.2 and Figures 3-6 and 3-7. During these events the sea obviously has an impact on both surface and groundwater flow systems in these lakes and their surroundings. This will be discussed in Section 3.5.2.

3.5.2 Infiltration and groundwater recharge

With few exceptions, the infiltration capacity of the soils in the area exceeds the rainfall and snowmelt intensity. The highest recorded daily rainfall and snowmelt of 27 and 8.6 mm equal $3 \cdot 10^{-7}$ and $1 \cdot 10^{-7}$ m/s, respectively, which can be compared with the measured saturated hydraulic conductivity of approximately $1.5 \cdot 10^{-5}$ m/s of the uppermost part of the till dominating the area. However, unsaturated (Hortonian) overland flow may appear over short distances, mainly on agricultural land covered with clayey till/boulder clay and on frozen ground where the soil water content was high during freezing. Also on outcropping bedrock unsaturated overland flow may appear, but just over very short distances before the water reaches open fractures or the contact zone between the bedrock and the QD.

The shallow groundwater levels mean that there will be a strong interaction between evapotranspiration, soil moisture and groundwater. The time series presented in Figure 3-38 and Figure 3-39 show that the groundwater levels in many monitoring wells were within one metre below the ground surface all the year, and that the groundwater level on average was less than 0.7 m below ground during 50% of the time. Also in what can be considered as typical recharge areas the average groundwater level was not more than 1.2 metres below ground. Only in locally elevated areas with relative steep slopes, considerably deeper groundwater levels can be assumed to exist, see e.g. the results for SFM0008 in Figure 3-38. The annual variation in the groundwater level is mostly less than one metre in discharge areas, and 1.5 m in typical recharge areas. Figure 3-61 shows the average daily groundwater level for wells in till in recharge and discharge areas. The method used for classification of the wells is described in /Werner et al. 2007/.

Diurnal fluctuations of the groundwater levels, driven by evapotranspiration cycles, were evident in the data from many of the groundwater wells in Quaternary deposits. Figure 3-62 shows two examples of diurnal ET-driven cycles for the wells SFM0033 and SFM0030 with very shallow and somewhat deeper groundwater levels, respectively; one-hour resolution data for a three-week period in August 2006 (see Figure 2-7 for the location of the wells). As would be expected, the well with shallower groundwater depth exhibited a stronger diurnal response (~10 cm), as compared to the location with deeper groundwater (~5.0 cm). Additionally, the shallow system exhibited a sharper response to the precipitation beginning on August 15. During the period August 15–17 the total rainfall was 35 mm.

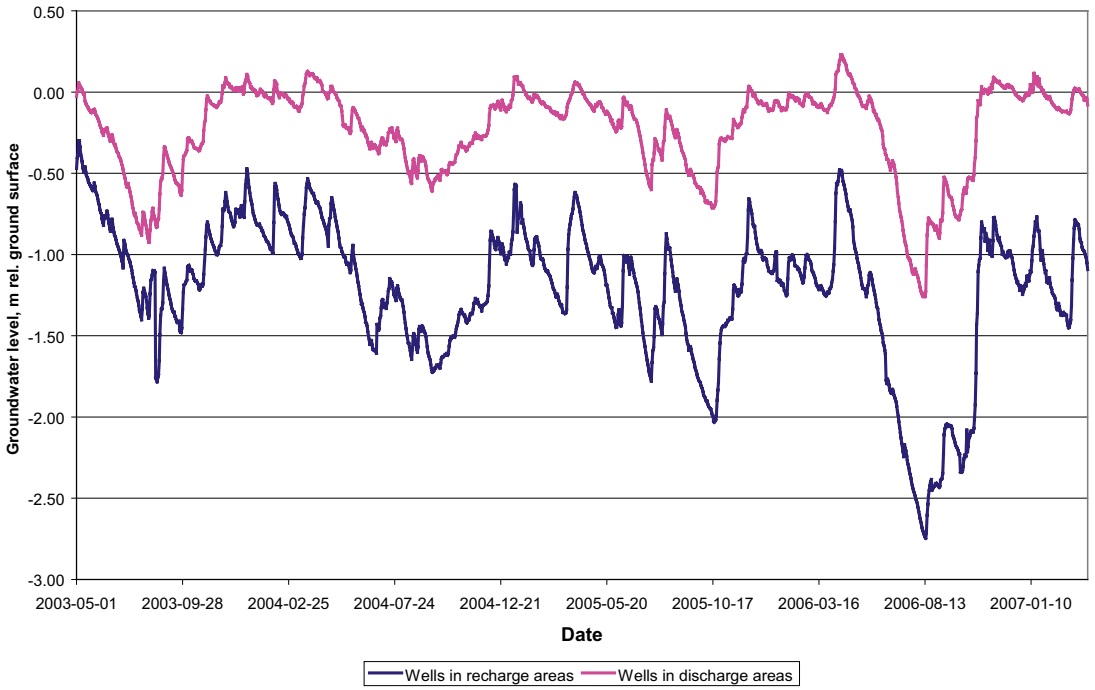

Figure 3-61. *Average daily groundwater levels in relation to ground surface in wells in recharge and discharge areas in till.*

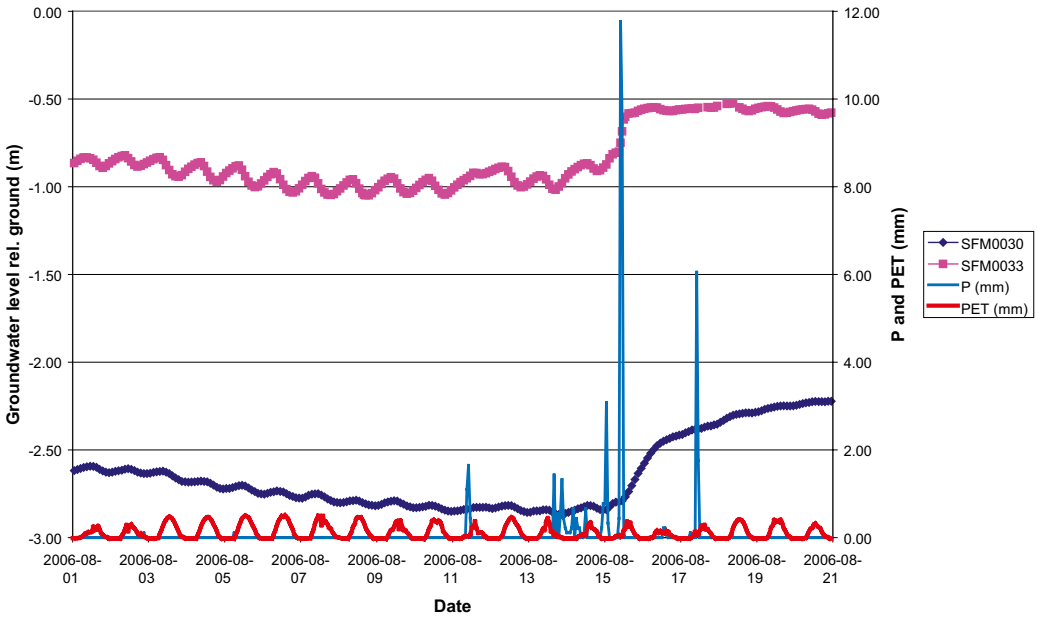

Figure 3-62. *Diurnal groundwater level fluctuations in an area with very shallow groundwater (represented by well SFM0033) and in an area with somewhat deeper groundwater (represented by well SFM0030).*

In Figure 3-63 the accumulated sum of rain and snowmelt (R + S) minus potential evapotranspiration is plotted together with the average groundwater level in all wells in till. The direct response on rainfall and the stong impact of evapotranspiration can be clearly seen. The very fast and strong responses of the groundwater level to rainfall also when the level is relatively deep below the ground and the unsaturated zone water deficit could be assumed to be relatively large, as in the summer/autumn of 2005 and 2006, indicate some kind of by-pass flow and/or a small specific yield.

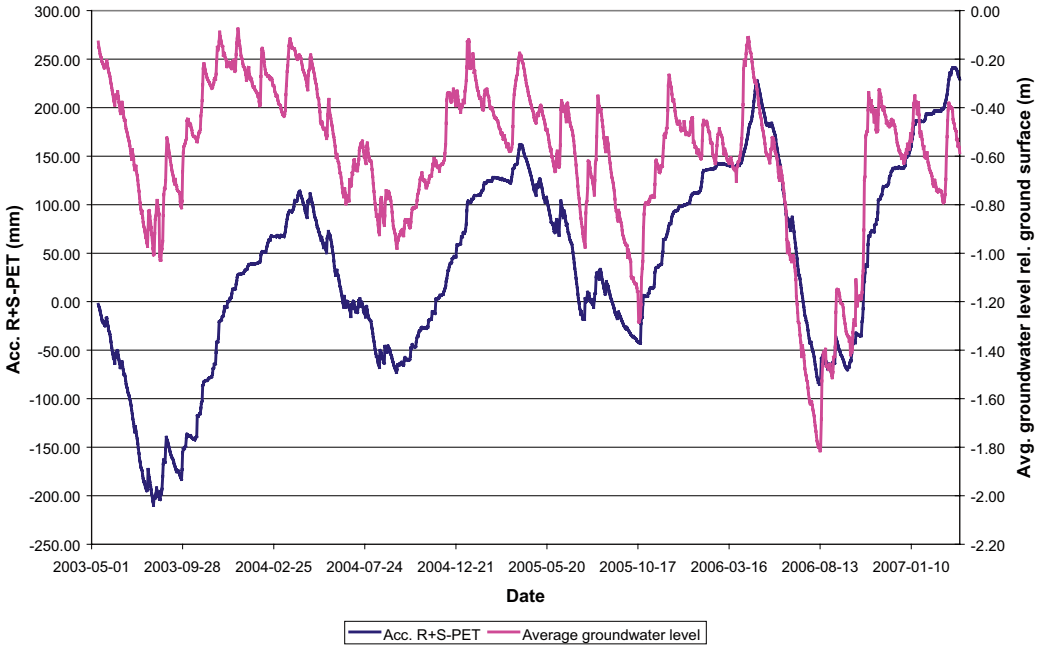

Figure 3-63. *Rain and snowmelt (R+S) minus potential evapotranspiration PET is plotted together with the average groundwater level in all wells in till.*

In Figure 3-64 groundwater level rises after a long dry period are shown for three monitoring wells categorised as situated in typical groundwater recharge areas. The rainfall of 32 mm during Sep. 25–Oct. 11, causing a minor rise in groundwater levels, was followed by an 11-day period without any significant rainfall. During this period the rise of the groundwater level stopped and it can be assumed that the water storage in the unsaturated zone was close to field capacity when a period of heavy rainfall started on Oct. 21. During Oct.21 to Oct. 27, the rainfall was 76 mm. This rainfall caused a rise in groundwater levels of 0.60 m, 0.76 m and 1.43 m in the wells SFM0004, SFM0019 and SFM0104, respectively.

If all the rain is assumed to replenish the groundwater storage, these rises in groundwater level correspond to specific yields of 12%, 10% and 5.3%. If the rise is transferred to mm water by use of a function of the specific yield varying with depth (an exponential function fitted to the measurements by /Lundin et al. 2005/) 63 mm, 86 mm and 66 mm are obtained for the three wells, i.e. the average of added water for the three wells is almost the same as the rainfall during the period. The evapotranspiration was insignificant during the period.

Direct recharge from precipitation is obviously the dominant source of groundwater recharge. However, the groundwater level measurements in the vicinity of Lake Bolundsfjärden and Lake Eckarfjärden presented in Figures 3-65 and 3-66 show that the lakes may act as recharge sources to the till aquifers in the immediate vicinity of the lakes during summer. While the groundwater levels are well above the lake water levels during most of the year, they are considerably below the lake water levels during dry summer conditions. This is very clear close to the lake shores, but also below the middle of the lakes the groundwater levels are slightly below the lake levels under such conditions. Although small, the differences are well outside the probable measurement errors.

The gradients from the lakes to the surrounding areas are created by direct and indirect groundwater abstraction by evapotranspiration. Due to the low permeability of the bottom sediments, the resulting water fluxes can be assumed to be small. Also the Baltic Sea can potentially act as a source of groundwater recharge, especially during periods of high sea water levels. However, as illustrated in Figure 3-56 there is no correlation between the sea water level and the groundwater levels on land for most monitoring wells. Therefore, the influence of this recharge can be assumed to be restricted to areas below the sea and areas in the immediate vicinity of the coast line.

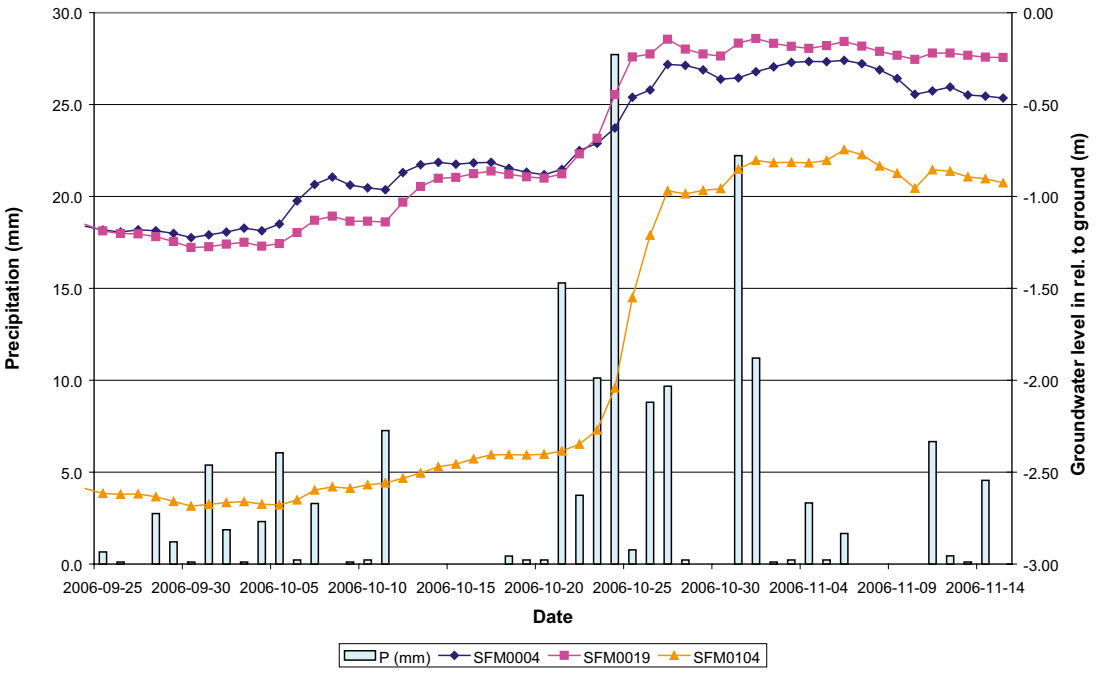

Figure 3-64. *Groundwater level responses on precipitation in three wells in typical groundwater recharge areas during autumn 2006.*

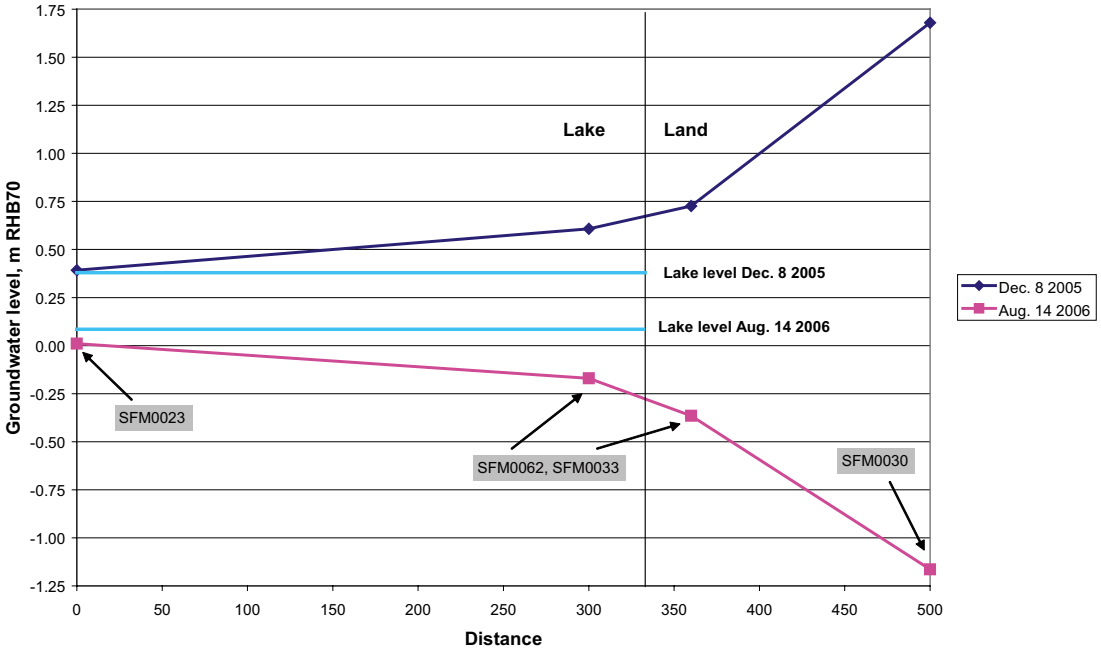

Figure 3-65. *Lake water level and groundwater profiles from an average winter situation (Dec. 8, 2005) and from dry summer conditions (Aug. 14, 2006). See Figure 2-7 for the locations of the wells.*

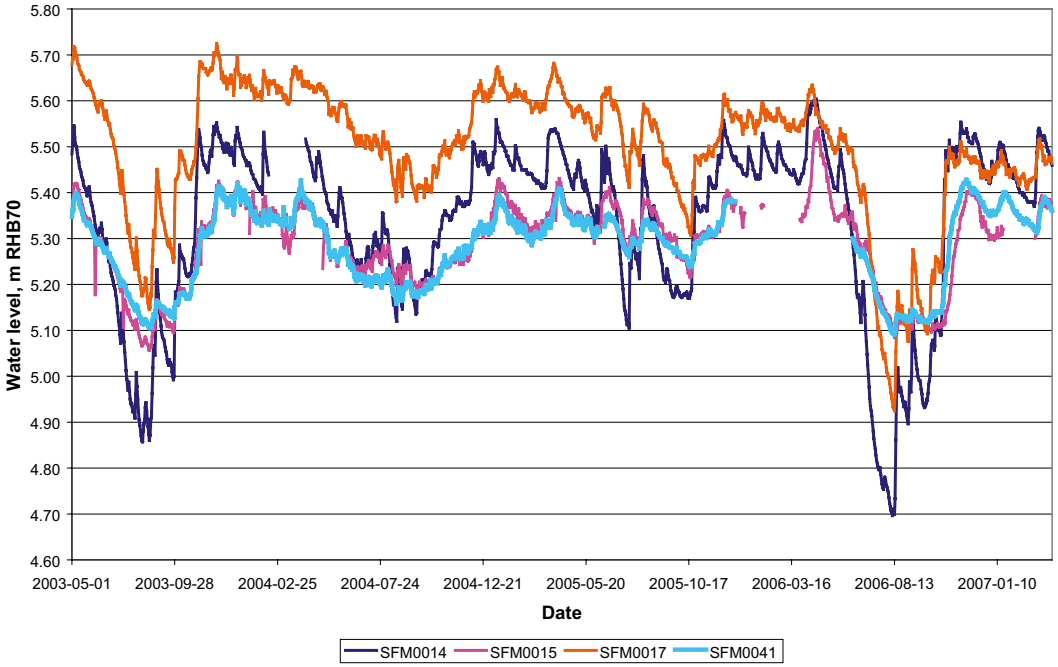

Figure 3-66. *Lake water level and groundwater levels at Lake Eckarfjärden.SFM0041 is the lake level, SFM0015 a well in till below the lake, and SFM0014 and SFM0017 are wells in till approximately 50 and 80 m from the lake shore, respectively. See Figure 2-7 for the locations of the wells.*

Special conditions occur in the areas flooded during extremely high sea water levels, e.g. during the storm "Per" in January 2007. Figure 3-67 shows groundwater levels in SFM0033, –34 and –36 located around Lake Norra Bassängen (lake threshold 0.19 m RHB70) and Lake Bolundsfjärden (lake threshold 0.28 m RHB70) together with the levels of the sea and Norra Bassängen (see Figure 2-7 for locations of the wells). The ground level at these wells is 0.5–0.7 m RHB70, i.e. the ground was flooded during "Per". In the figure the groundwater level variations of the inland well SFM0019 are shown as a reference; to enhance the resolution of the y-axis the groundwater level of this well is shown with an offset of –3 m.

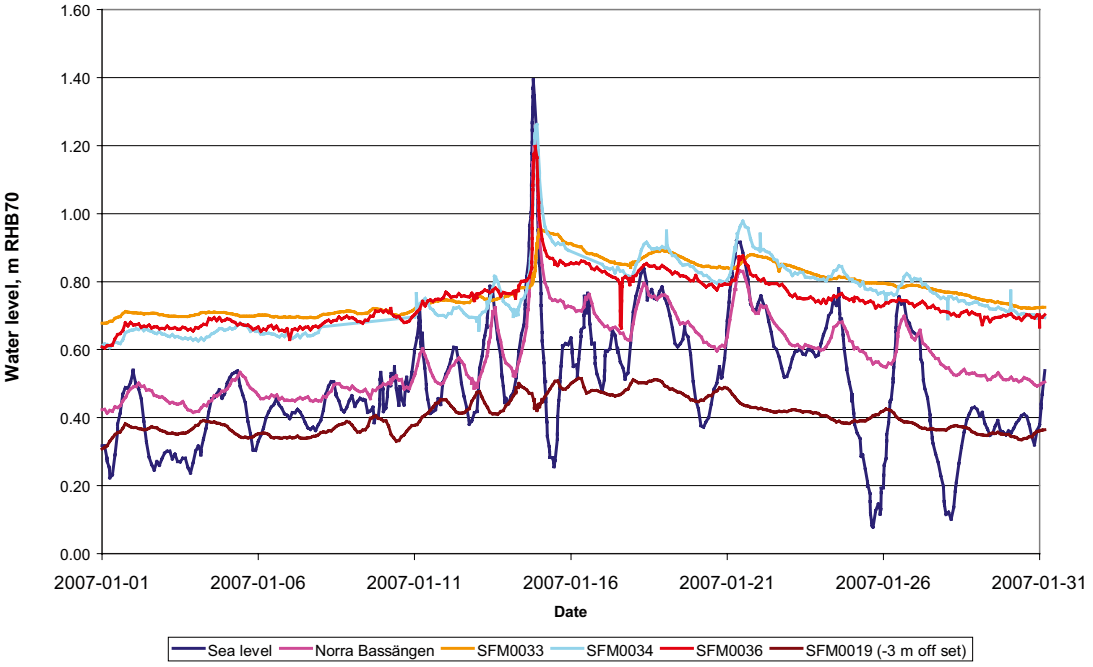

Figure 3-67. *Water levels in the Baltic and Lake Norra Bassängen during the storm "Per" plotted with groundwater levels close to the lake (SFM0033, –34 and –36) and the groundwater level at the inland well SFM0019 as a reference (the groundwater level of SFM0019 is plotted with an off set of –3 m).*

At SFM0034 the till aquifer, in which the groundwater level is measured, is unconfined, while at SFM0033 and –36 the till is covered by 0.7 and 0.25 m of gyttja, respectively. At SFM0034 the flooding water can infiltrate directly to the till aquifer, while at least at SFM0033 the groundwater level rise mainly may be an effect of the weight load of the flooding water. In SFM0034 the groundwater level increased more than 0.5 m within 12 hours.

The prevailing conditions, with a strong interaction between evapotranspiration and the groundwater, imply that a clear definition of groundwater recharge is required. The definition provided in Section 1.4.2 was:

"Process by which water is added from outside to the zone of saturation of an aquifer, either directly into a formation, or indirectly by way of another formation".

In the present situation, however, with very shallow groundwater, there is a large difference between gross and net recharge to the QD. The diurnal groundwater level fluctuations shown in Figure 3-62 clearly illustrate the influence of evapotranspiration on the groundwater zone during dry periods. Of course, this influence is most accentuated in locations with very shallow groundwater, but it is also evident in some areas where the groundwater table is more than two metres below the ground surface.

3.5.3 Sub-flow systems and discharge

Similar to the external boundaries of the model area, the internal surface water divides and the groundwater divides of the groundwater systems restricted to QD are assumed to coincide. The strong correlation between the mean groundwater elevations observed in the till and ground surface elevation data shown in Figures 3-40 to 3-42 means that the average vertical hydraulic flux at some point below the surface is less than the net infiltration into the saturated zone of the till. The decrease in hydraulic conductivity with depth and the anisotropy with $K_v<K_h$ of the till are a plausible explanations, but a contribution from a contrast in vertical hydraulic conductivity between the till and the bedrock is also possible (the uppermost bedrock having a lower K_v). The small-scale topography and the hydraulic conductivity profile of the tills, dominating in the area, imply that many small catchments will be formed with local, shallow groundwater flow systems in the QD, and that a dominating part of the groundwater will move along these shallow flow paths.

In Figure 3-68 and Figure 3-69 mean groundwater depths are plotted against a field classification of local geomorphology and groundwater recharge-discharge conditions /Werner et al. 2007/. Figure 3-68 shows that groundwater depth below ground is more variable and generally larger in locally elevated areas, while no clear coupling can be seen between absolute groundwater elevation and local geomorphology. From Figure 3-69 it is obvious that depth to groundwater varies considerably within typical recharge areas, whereas the variations are small and the groundwater level close to the ground surface in discharge areas. No coupling can be seen between groundwater elevation and the classification in recharge-discharge areas. The two figures support the concept that groundwater flow in the Quaternary deposits is mainly governed by local topography and forms small local flow systems.

The permeability and storage characteristics of the till profile mean that very little water needs to be added to raise the groundwater table below a depth of approximately one metre. A groundwater recharge of 10 mm will give an increase in the groundwater level of c. 20 cm. During periods of abundant groundwater recharge the groundwater level, also in most recharge areas, reaches the shallow part of the QD-profile where the hydraulic conductivity is much higher and a significant lateral groundwater flow will take place. However, the transmissivity of this upper layer is so high that the groundwater level does not reach much closer to the ground surface than 0.5 m in typical recharge areas.

The local, small-scale recharge and discharge areas only involving groundwater flow systems restricted to QD will overlay the more large-scale flow systems associated with groundwater flow at greater depths. Interesting observations were made in groundwater level time series from nearby wells in till and bedrock, as illustrated in Figures 3-70 to 3-79. Specifically, the groundwater level in the till seems to be considerably higher than that in the bedrock in the central part of the site investigation area (within the tectonic lens). This difference exists even though most of the screens of the wells in till are installed at or across the QD/rock interface. The differences between the levels in till and rock are generally much larger than between different sections in the bedrock boreholes sealed off by packers. However, the groundwater levels

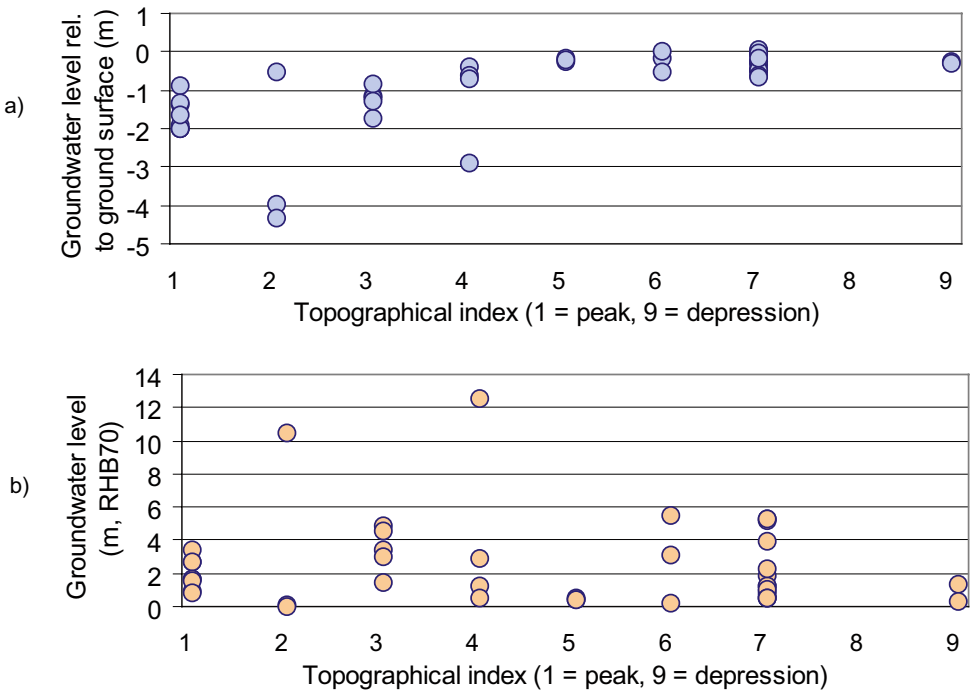

Figure 3-68. *Mean a) groundwater depths and b) elevations as a function of a topographic index based on in-field assessments /Werner et al. 2007/. Numeric categories were defined as follows: 1 = peak, 2 = ridge, 3 = upper slope, 4 = mid slope, 5 = pass, 6 = lower slope, 7 = flat, 8 = channel, 9 = regional depression.*

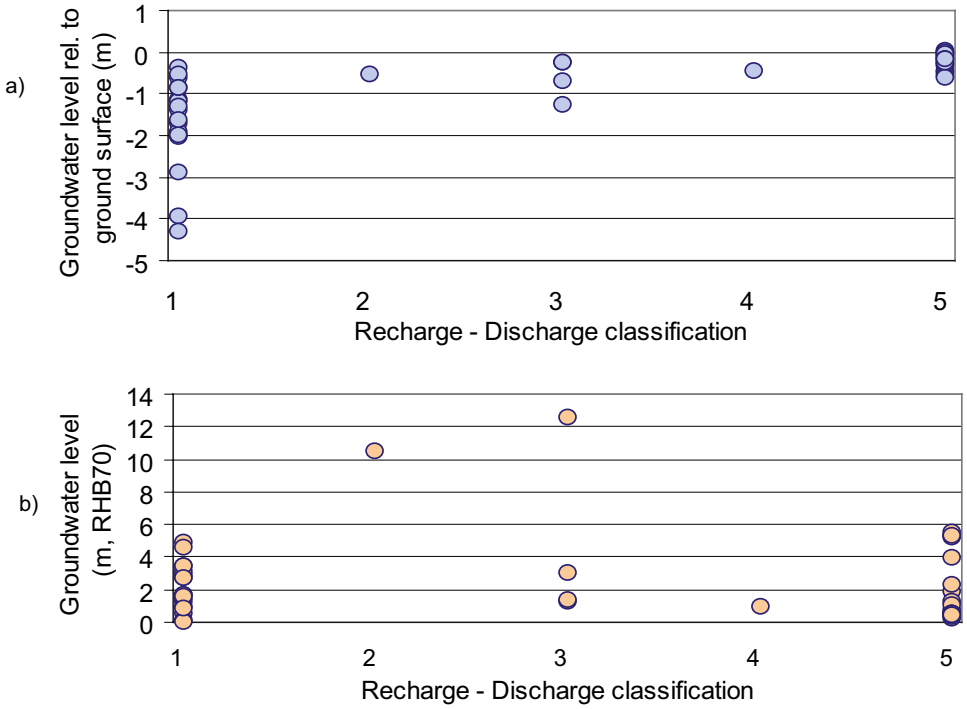

Figure 3-69. *Mean a) groundwater depths and b) elevations as a function of a recharge-discharge classification based on in-field assessments /Werner et al. 2007/. Numeric categories were defined as follows: 1 = recharge area, 2 = probable recharge area, 3 = varying, 4 = probable discharge area, 5 = discharge area.*

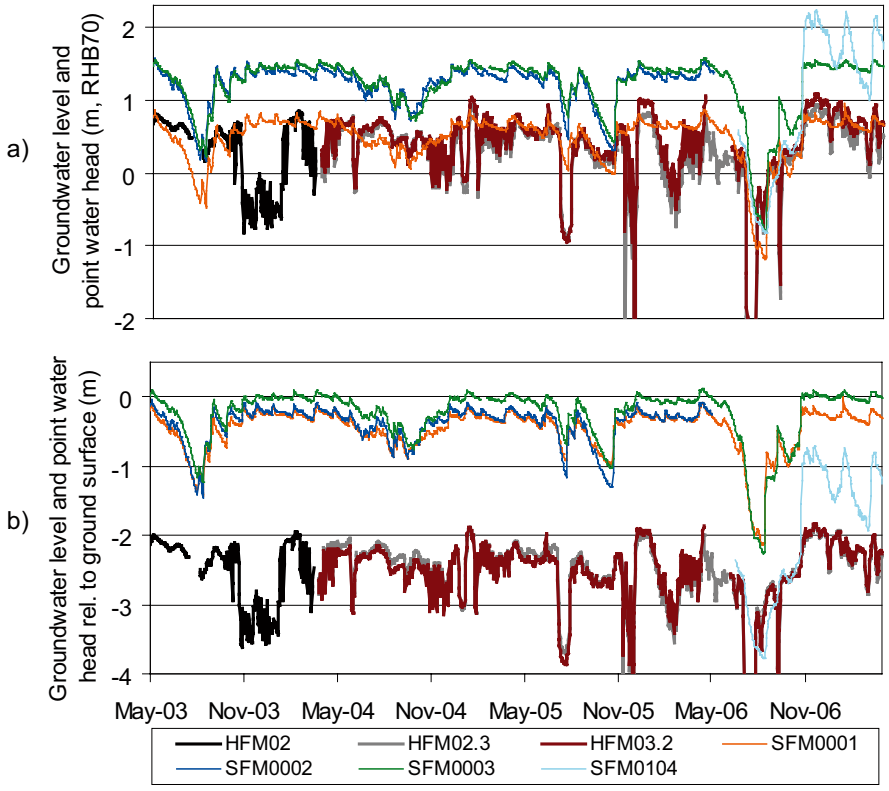

Figure 3-70. *Comparison of groundwater levels in wells in Quaternary deposits (SFM0001-3 and SFM0104) and point water heads in bedrock (HFM02.3 and HFM03.2) at Drill site 1 in terms of a) metres above sea level and b) depth below ground surface. The head differences between HFM-sections are within a few centimetres. See Figures 2-7, 2-9 and 3-71 for the locations of the wells.*

in the presented bedrock boreholes are still above the QD/rock interface under undisturbed conditions, indicating that no unsaturated zone exists below the interface. In Figure 3-70, the groundwater levels in wells in QD and bedrock at Drill site 1 are shown.

Absolute groundwater levels in QD are well above the point water heads in bedrock except during dry summer conditions (see the summers 2003 and 2006). In the summer of 2006, a pumping test was performed in HFM14, situated at Drill site 5 approximately 400 m to the southeast of Drill site 1. The bedrock wells (HFM02 and HFM03) responded to the pumping, but no impact could be seen in the QD-wells. In general, there is no discernable response in the groundwater levels in QD to disturbances in the groundwater levels in the bedrock. On the other hand both groundwater levels in QD and bedrock are correlated to rainfall + snowmelt and evapotranspiration.

In Figures 3-72 and 3-73 groundwater wells close to Drill site 2 are presented. The absolute groundwater levels in QD are also here well above those in bedrock. In difference to the bedrock wells at Drill site 1, no response to the pumping in HFM14 in the summer of 2006 can be seen in the bedrock wells at Drill site 2 (Figure 3-72c).

Figure 3-74, from Drill site 5, again shows the situation with groundwater levels in QD well above those in bedrock. However, during dry summer conditions the QD-levels may fall below the groundwater levels in bedrock. During summer 2006, the groundwater level in SFM0058 fell below the till/rock interface and the uppermost part of the bedrock profile was here unsaturated.

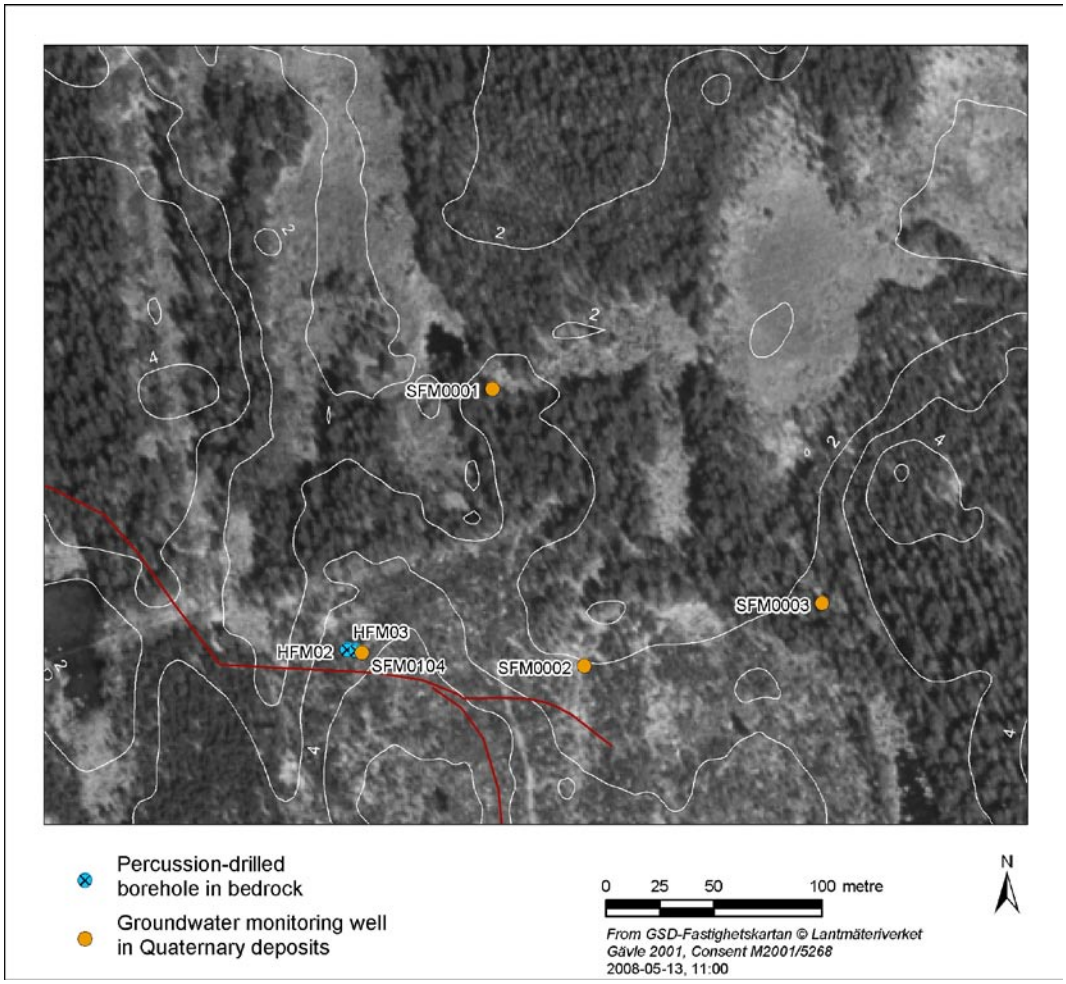

Figure 3-71. *Groundwater monitoring wells in Quaternary deposits (SFM) and percussion-drilled boreholes in bedrock (HFM) at Drill site 1.*

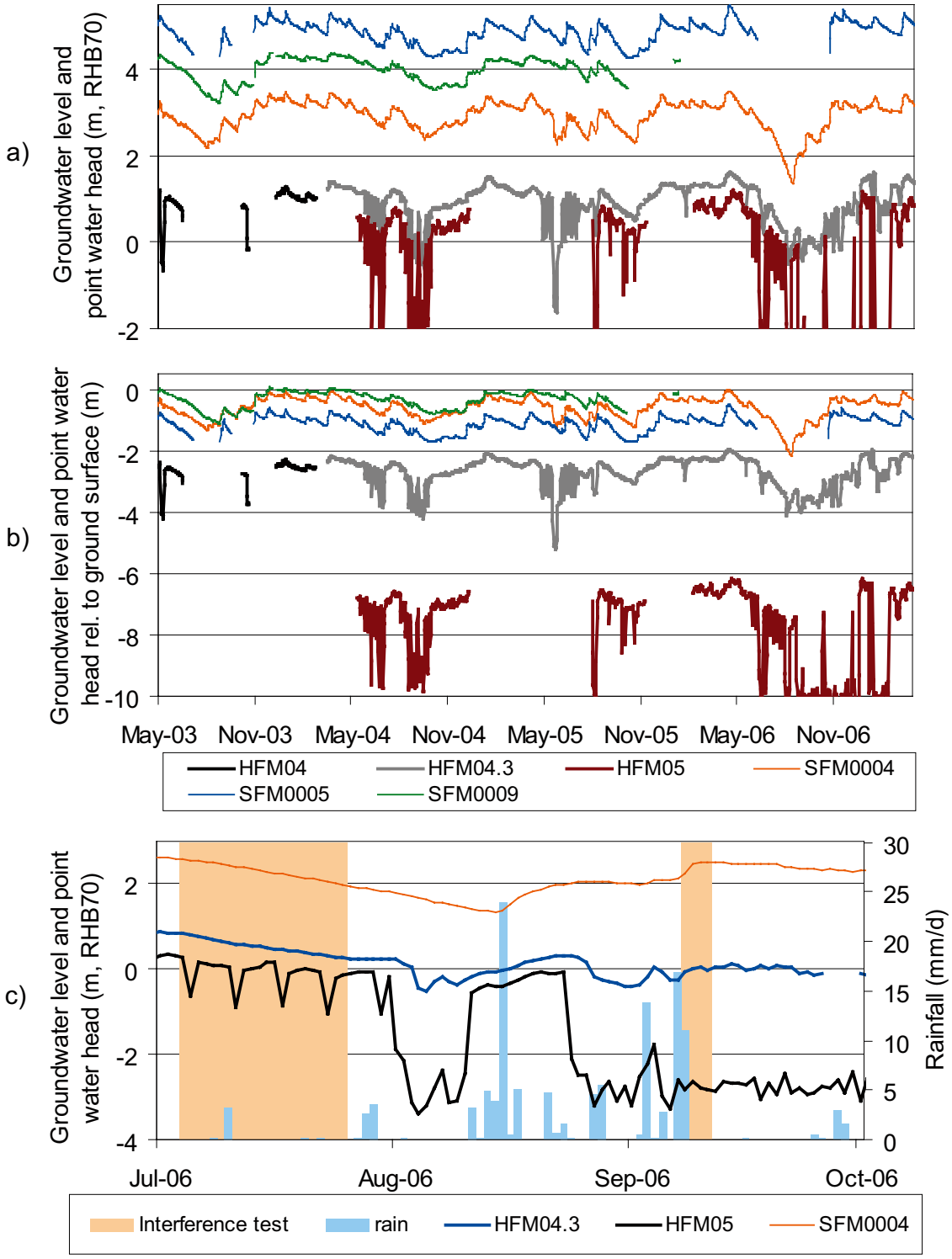

Figure 3-72. *Comparison of groundwater levels in Quaternary deposits (SFM) and point water heads in bedrock (HFM, uppermost section) at Drill site 2 in terms of a) metres above sea level, b) depth below ground surface, and c)groundwater levels and point water heads co-plotted with rainfall during July–Oct. 2006 (see Figures 2-7, 2-9 and 3-73 for the locations of the wells).*

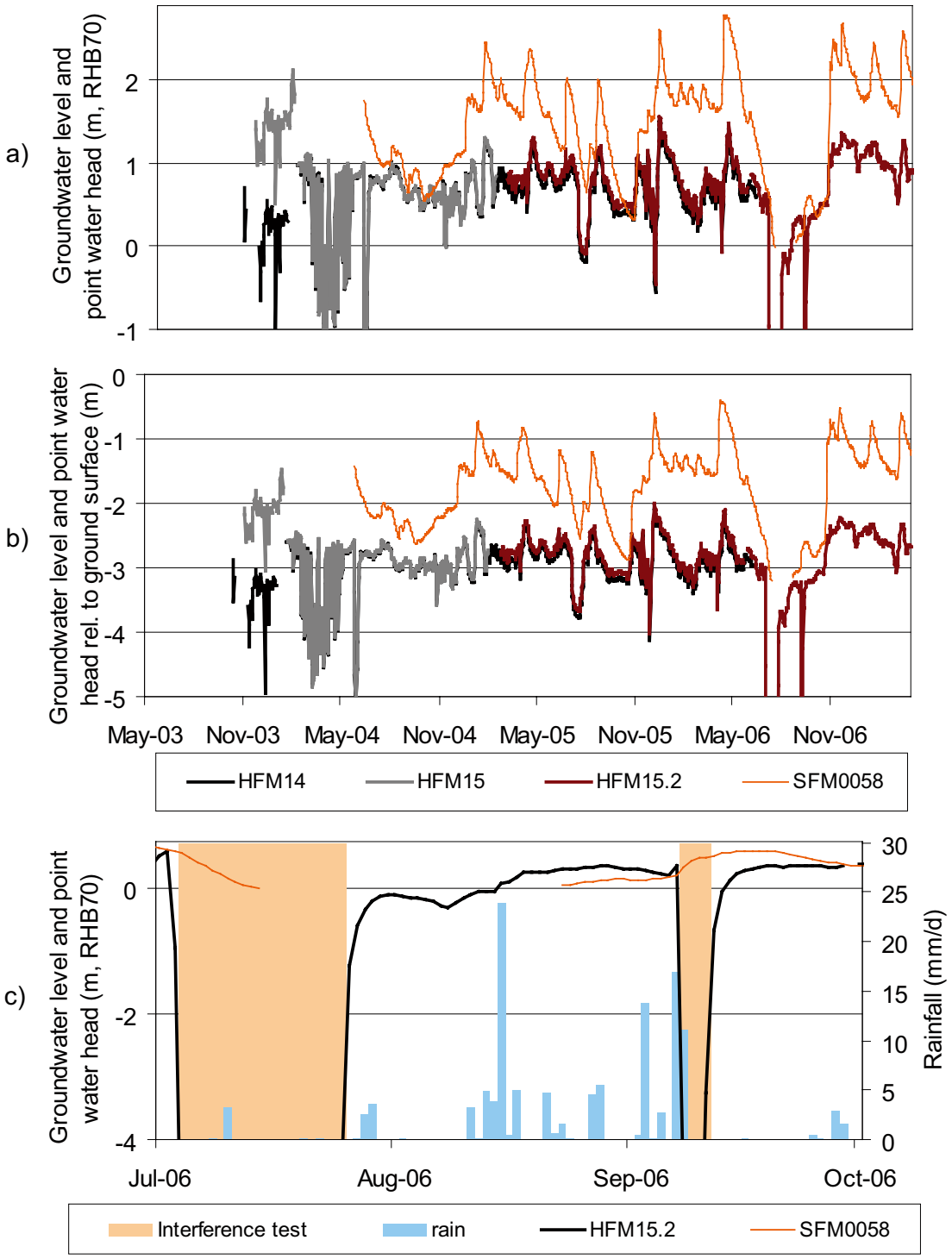

Figure 3-74. *Comparison of groundwater levels in wells in Quaternary deposits (SFM0058) and point water heads in bedrock (HFM14 and 15) at Drill site 5 in terms of a) metres above sea level, b) depth below ground surface, and c) groundwater levels and point water heads co-plotted with rainfall during July–Oct. 2006. HFM14 is an open borehole and HFM15.2 is the uppermost section of the well. However, the head difference between sections is within a few centimetres (see Figures 2-7, 2-9 and 3-75 for the locations of the wells).*

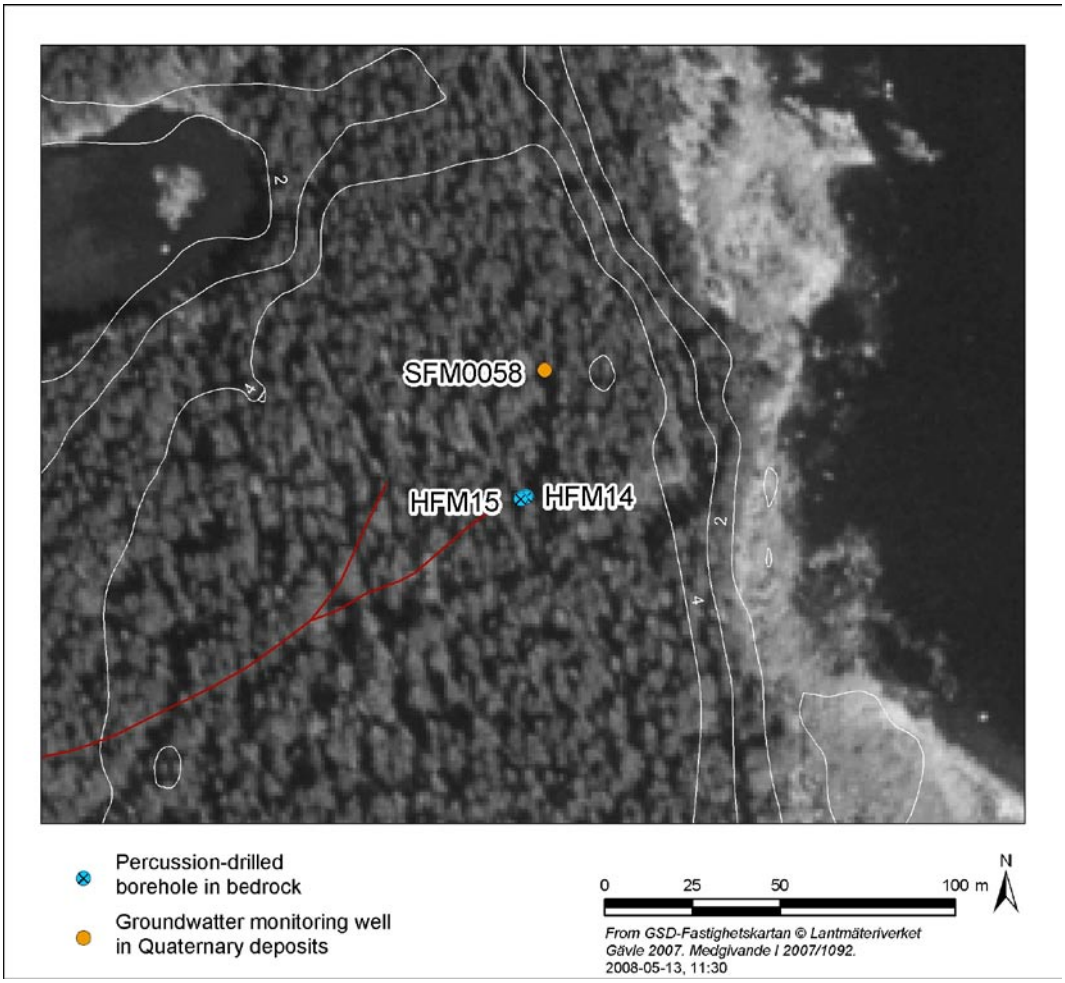

Figure 3-75. *Groundwater monitoring wells in Quaternary deposits (SFM) and percussion-drilled boreholes in bedrock (HFM) at Drill site 5.*

The co-variation of the groundwater levels in QD and bedrock, due to rainfall+snowmelt and evapotranspiration is obvious. However, the hydraulic contact between groundwater in the QD and the bedrock seems to be limited, which is clear from the second pumping test in HFM14 in Sep. 2006 (Figure 3-74c) when the groundwater level in QD (SFM0058) increases due to rainfall despite a drawdown by several meters in the groundwater level in bedrock (HFM15).

A co-variation of groundwater levels in QD and bedrock is also obvious at Drill site 6, see Figure 3-76. As at the other drill sites within the tectonic lens, the groundwater level in QD is well above the groundwater level in bedrock. However, the groundwater level in QD is below the one in bedrock during dry summer conditions. The response in the bedrock well HFM16 to the pumping tests in HFM14 in summer/autumn 2006 is also very clear. The distance to the pumping well exceeds 800 metres. The drawdown extended below Lake Bolundsfjärden and was approximately one metre in HFM16.

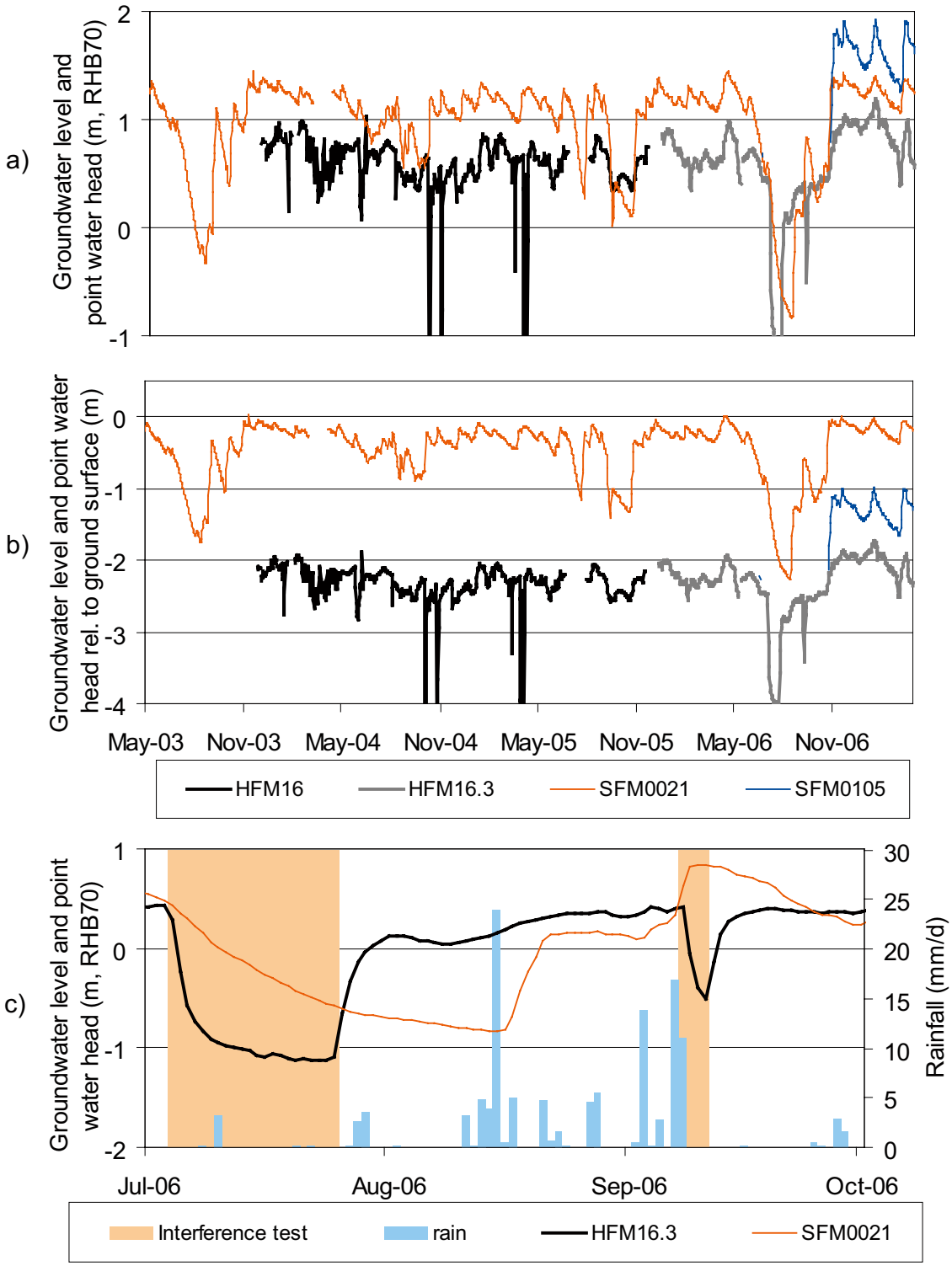

Figure 3-76. *Comparison of Quaternary deposit (SFM) and bedrock (HFM) groundwater level data at Drill site 6 in terms of a) metres above sea level, b) depth below ground, and c) groundwater levels and point water heads co-plotted with rainfall during July–Oct. 2006 (see Figures 2-7, 2-9 and 3-77 for the locations of the wells).*

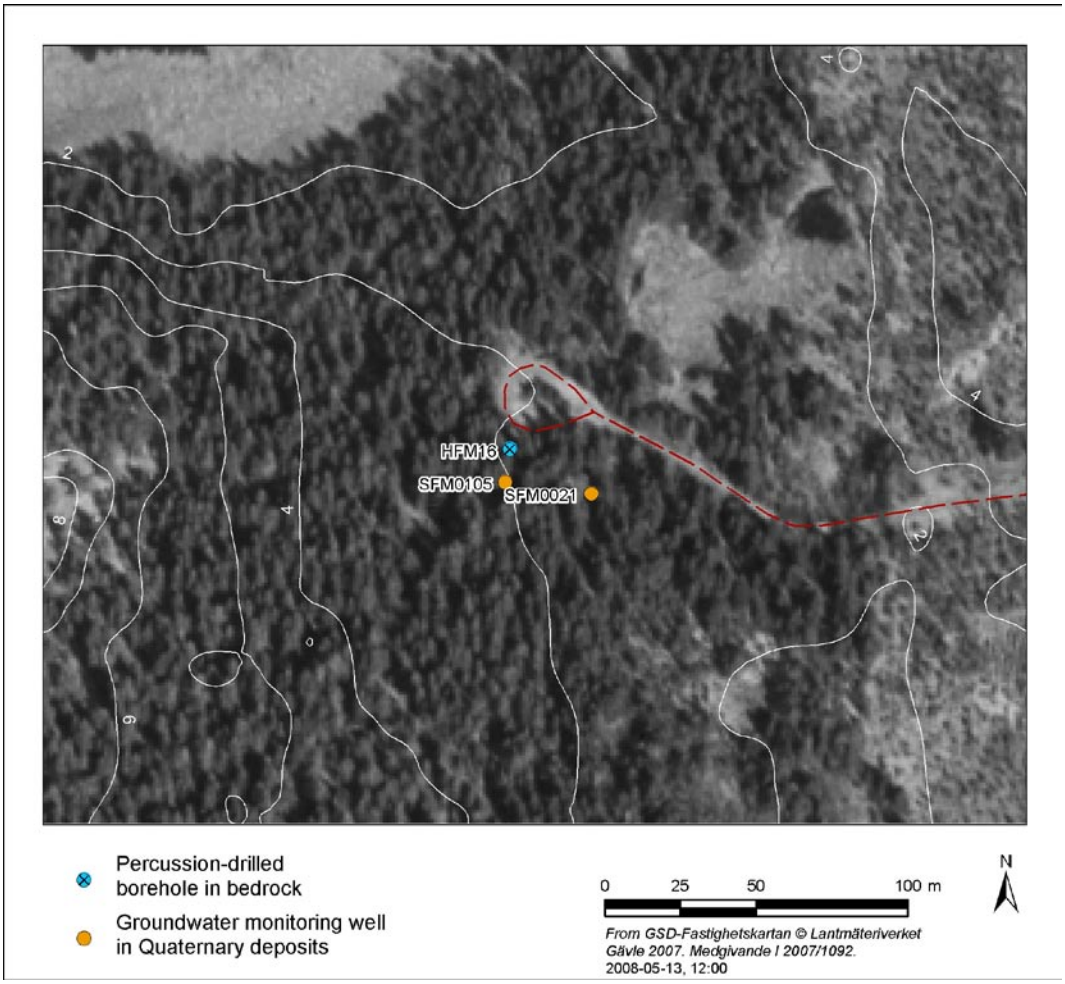

Figure 3-77. *Groundwater monitoring wells in Quaternary deposits (SFM) and percussion-drilled boreholes in bedrock (HFM) at Drill site 6.*

As shown in Figure 3-78, the conditions at Drill site 4, located outside the tectonic lens, are quite different from those at the drill sites discussed above. The absolute groundwater levels in the bedrock wells are higher, c. 2.5 m RHB70 and also well above the groundwater levels in QD in the Gällsboträsket depression (SFM0011 and SFM0013, see Figures 2-7, 2-9 and 3-79 for the locations of the wells). Furthermore, the bedrock wells (HFM09 and HFM10) did not show any response to the pumping tests in HFM14 in summer/autumn 2006.

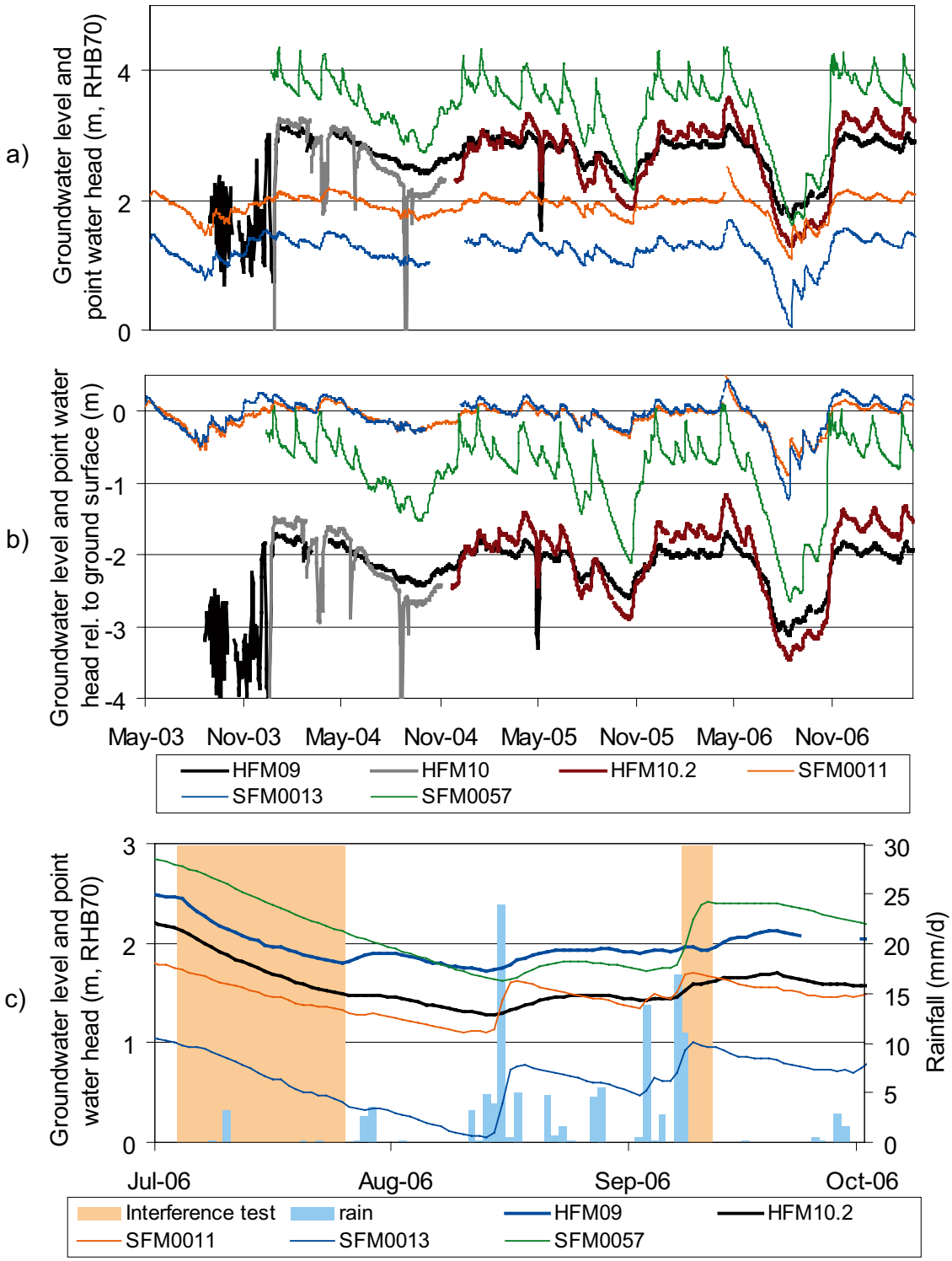

Figure 3-78. *Comparison of Quaternary deposit (SFM) and bedrock(HFM) groundwater level data at Drill site 4 in terms of a) metres above sea level, b) depth below ground, and c) groundwater levels and point water heads co-plotted with rainfall during July–Oct. 2006. Data for the lowermost section in HFM10 are shown because it is longer in duration than the uppermost section (see Figures 2-7, 2-9 and 3-79 for location of the wells).*

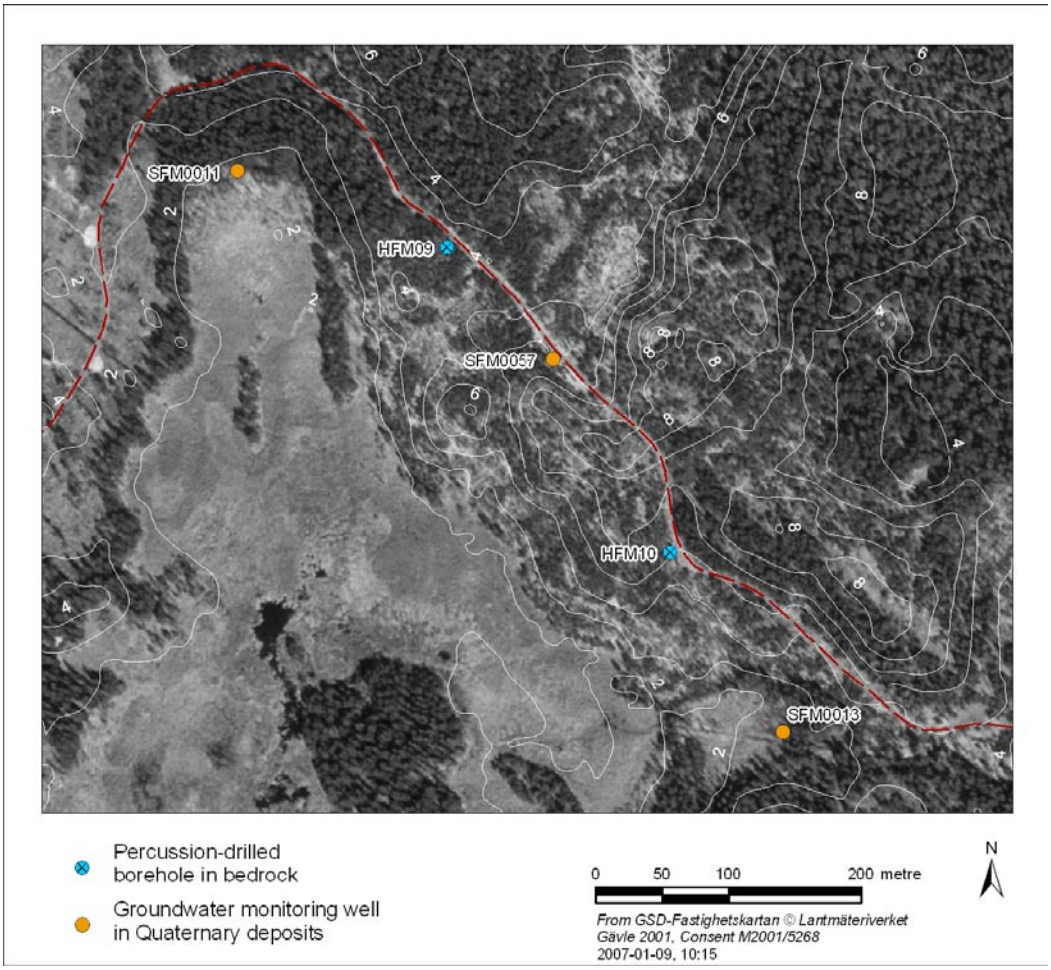

Figure 3-79. *Groundwater monitoring wells in Quaternary deposits (SFM) and percussion-drilled boreholes in bedrock (HFM) at Drill site 4.*

Figure 3-80 shows the groundwater levels in a monitoring well in till below the middle of Lake Bolundsfjärden (SFM0023) and a nearby percussion-drilled borehole (HFM32) located on a small island in the lake. Water levels in the sea and in the lake are also shown in the figure. The lake level and the groundwater level in till are considerably higher than the levels in the four sections of HFM32. The HFM-levels shown are point water heads. However, the density differences between the borehole sections are small; only in the deepest section the calculated environmental head is more than 0.1 m higher than the point water head, while the differences between the two head types are insignificant for the other sections.

The heads are lowest in the two deepest sections. The difference between these two sections is small but after re-calculation to environmental head the second deepest section has the lowest head, i.e. the fractures in this section act as drains for water coming from above as well as from below. The results indicate a downward flow gradient from the lake and QD to the bedrock. In Figure 3-81 the levels are shown during two pumping tests in HFM14 (see Figures 2-7 and 2-9 for well locations). The responses were strongest in the two deepest well sections, but are also obvious in the upper two sections and interestingly also in the till well (SFM0023). The response in SFM0023 is best seen at the start of the July pumping test. The very large drawdawn following the intial phase is coupled to water sampling and not to the pumping test.

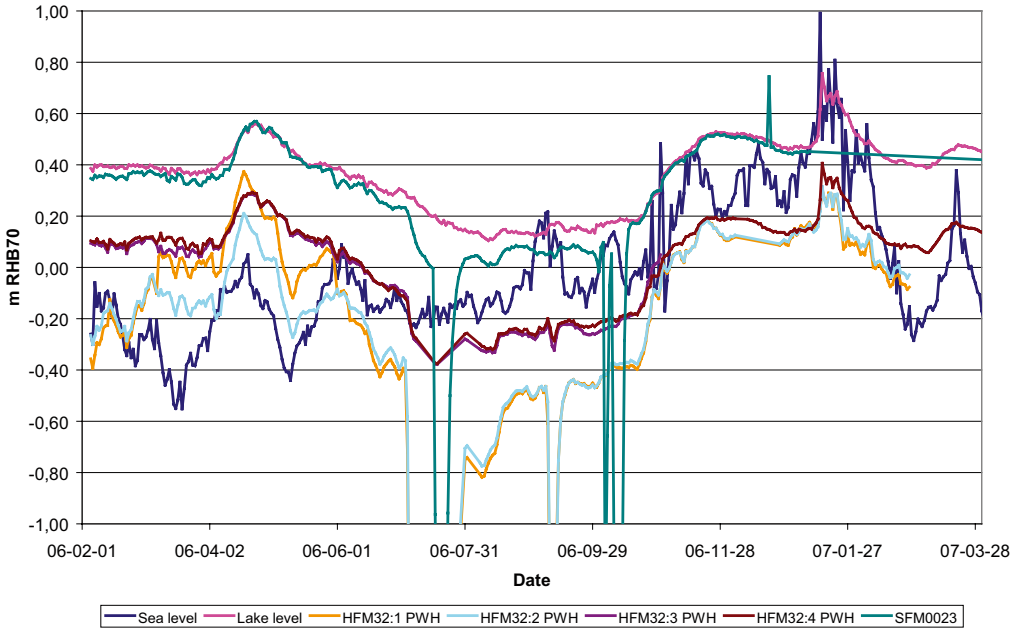

Figure 3-80. *Water levels in the Baltic Sea and Lake Bolundsfjärden plotted together with groundwater levels in till below the lake (SFM0023) and in sections in the bedrock borehole HFM32 (elevations in m RHB70: HFM32:1: –198.75 to –96.27; HFM32:2: –95.27 to –30.95; HFM32:3: –29,95 to 24,97; HFM32:4: –23.97 to 0.97).*

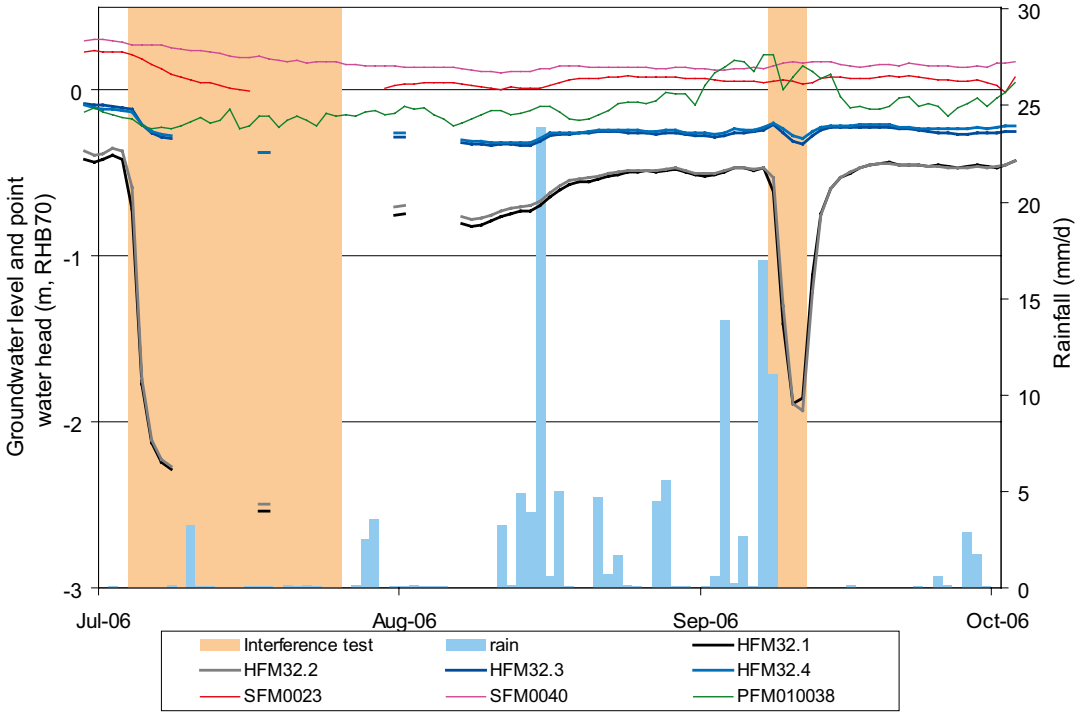

Figure 3-81. *Water levels in the Baltic Sea (PFM010038) and in Lake Bolundsfjärden (SFM0041), and groundwater levels in till below the lake (SFM0023) and in different depth intervals in the bedrock (HFM32:1–4). Rainfall and duration of pumping tests in HFM14 are also shown. (See Figure 3-80 for the levels of the borehole sections of HFM32.)*

Figure 3-82 shows the point water heads in percussion-drilled boreholes surrounding Lake Bolundfjärden plotted with the sea water level and the accumulated rainfall + snowmelt – potential evapotranspiration. The point water head in HFM33, located close to SFR, is also inclued in the figure. The borehole section with the lowest point water head in each borehole is shown (see Figure 2-9 for the locations of the boreholes); the differences between point water heads and environmental water heads are insignificant.

HFM32 has the lowest point water head. Only HFM33 and HFM38 have occasionally point water heads at the same level or below. The head variations are mainly controlled by the annual precipitation-evapotranspiration cycle, represented by R+S-PET in the figure, and the sea water level. The sea water level has a stronger influence on HFM33 and HFM38 than on HFM32. The groundwater level in HFM32 is below the sea level during the summer and autumn of 2006. Two possible, perhaps superimposed, phenomena could explain this: (i) the groundwater level in the bedrock is indirectly influenced by evapotranspiration extracting water from the groundwater zone in the QD thereby inducing an upward flow from the bedrock, and/or (ii) the borehole is influenced by the pumping at SFR (approximately 6 L/s).

An influence from evapotranspiration requires that the groundwater level in the bedrock is above the QD/rock interface, which is the case in the low-lying areas surrounding Lake Bolundsfjärden, so that no unsaturated zone exists in the bedrock. An influence from the pumping at SFR requires a good hydraulic contact all the way to SFR. From a pumping test in HFM33, immediately west of SFR, it is known that quick and strong responses were observed in in e.g. HFM02 (c. 0.3 m) and HFM15 (c. 0.1 m) located c. 1.5 km inland from the pumping well. The pumping rate in HFM33 was approximately 3.8 L/s /Gokall-Norman and Ludvigson 2008, Follin et al. 2008/. Pumping tests in HFM14 have also shown quick and strong responses in other quite distant HFM-wells (c. 1 km away, such as HFM16 and HFM38), confirming the high transmissivity and low storativity of the upper bedrock.

Figures 3-70, 3-72, 3-74, 3-76, 3-78 and 3-80 show that the groundwater levels in the till and the bedrock are correlated. The natural groundwater level fluctuations are, however, smaller in the bedrock but still to a great extent controlled by the annual precipitation and evapotranspiration cycles. The conditions prevailing within the northern part of the tectonic lens, with a lower

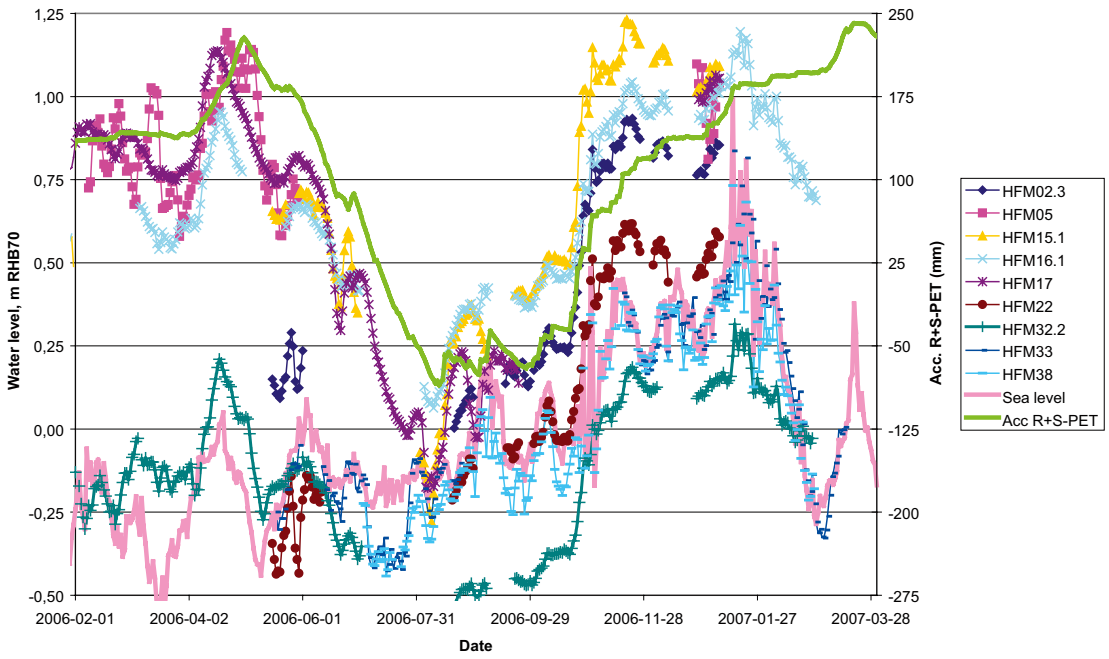

Figure 3-82. *Point water heads in bedrock wells surrounding Lake Bolundsfjärden plotted with the sea level and accumulated values of rainfall (R) + snowmelt (S) minus potential evapotranspiration (PET).*

groundwater level in bedrock than in QD, mean that the groundwater flow has a downward component at the sites studied, i.e. there is an inflow from the till to the bedrock. The difference between the levels in till and bedrock indicates a limited hydraulic contact between QD and rock.

A probable explanation for the generally low levels measured in the bedrock boreholes is that these intersect one or some of the highly conductive horizontal to sub-horizontal zones shown to exist in the shallow bedrock in the Forsmark area /Follin et al. 2007a, 2008/. The highly transmissive shallow bedrock acts a drain for water coming from above as well as from below. The principle is illustrated in Figure 3-83, where the draining effect of a sub-horizontal zone is shown using an illustrative generic simulation with an analytical model /Werner et al. 2007/. The available data indicate that flow systems involving the bedrock do not have discharge areas in the northern part of the tectonic lens but discharge into the sea. The only occasions when data from this area show a continuous upward flow gradient are during dry summers when the groundwater level in QD decrease below the levels in the bedrock. However, it should be noted that the periods with uptake of water, and hence also of dissolved substances, in the vegetation are of specific interest for the safety assessment dose calculations.

The situation prevailing in Forsmark, with relatively low groundwater levels in the shallow bedrock within the northern parts of the tectonic lens, may partly be caused by the pumping at SFR. However, no definite conclusions on this issue can be drawn based on existing data. This is further discussed in Chapters 4 and 5. Outside the tectonic lens, as illustrated by the situation at Drill site 4 (see Figure 3-78) and in the area around Lake Eckarfjärden (HFM11 and 12), the groundwater level in the bedrock may be well above the groundwater levels in QD in nearby low-lying areas, implying that flow systems involving the bedrock may have local discharge areas.

The lake water level-groundwater level relationships indicate that the lake sediments, the underlying till and/or the uppermost bedrock have low vertical hydraulic conductivities. If the surface water-groundwater hydraulic contact had been good, the situation with groundwater level drawdown from evapotranspiration extending below the lakes, and the quick and extensive drawdowns from the pumping tests in HFM14 and HFM33 below Lake Bolundfjärden and the sea, should not appear.

The flow systems around and below the lakes seem quite complex. The chemistry of the water below the lakes indicates a very limited flow since relict water of marine origin is found. Chemical data as support for the hydrological and hydrogeological model is discussed in Section 3.5.4.

In discharge areas, by definition no groundwater recharge takes place. However, not all discharge areas are saturated up to the ground surface, but water flows in the uppermost most permeable part of the soil profile. In unsaturated discharge areas, the soil water deficit is usually very small and in these areas water levels respond quickly to rainfall and snowmelt and contribute to runoff generation. So called saturated overland flow appears in discharge areas where the groundwater level reaches the ground surface. This type of discharge areas is quite common in the flat landscape of the site investigation area.

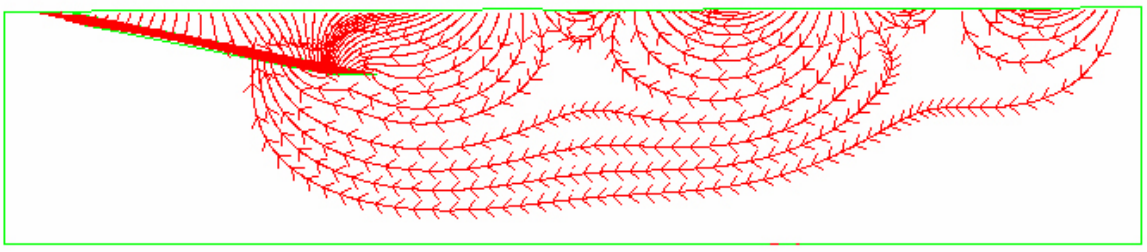

Figure 3-83. *Visualization of stationary flow paths along a regional slope in a groundwater basin with a high-permeable sub-horizontal layer. The length and depth of the basin is 3.7 km and 750 m, respectively, and the amplitude of the hummocky groundwater table is 1.5 m. The hydraulic conductivity contrast between the layer and the rest of the basin is 100 to 1 /Werner et al. 2007/.*

The brooks are considered as permanent discharge areas, although dry during parts of the year. The wetlands can either be in direct contact with the groundwater zone and constitute typical discharge areas or be separate hydrological systems with low-permeable bottom materials and with little or no hydraulic contact with the underlying aquifer. The flat terrain and the shallow groundwater within the area imply that the spatial extents of recharge and discharge areas may vary during the year.

The strong correlation between groundwater levels and surface discharge was earlier analysed and described in /Juston et al. 2007/. In Figure 3-84 time series of the average groundwater level in relation to ground surface and discharge for the catchment area of discharge gauging station PFM005764 are shown. The two time series are obviously correlated, although the quantitative coupling appears to vary a lot among the various hydrological events.

3.5.4 Hydrochemical data for interpretation of the flow systems

In this section, water chemical analyses of precipitation, surface water, and groundwater from QD and different depths in the bedrock are interpreted as support for the conceptual hydrological and hydrogeological model. For detailed descriptions of the water chemistry the reader is referred to /Tröjbom and Söderbäck 2006/, /Tröjbom et al. 2007/ and /Laaksoharju et al. 2008/, of which the first and the second are focused on the surface system and the third on the deep rock.

/Laaksoharju et al. 2008/ uses the concept of "end-members" to describe a number of ideal water types. Observed water compositions in water samples are then interpreted as mixtures of the different end-members. The end-members used in the Forsmark 2.2 reporting stage are shown in Table 3-18.

/Tröjbom et al. 2007/ applied principal component analysis (PCA) to establish an ion-source model for the Forsmark data. In a first step, only data from percussion-drilled and core-drilled boreholes were used to optimize a model for separating the groundwater types found in the bedrock. This model was then applied on observations of surface water and groundwater in QD, revealing similarities in hydrochemical composition between these observations and the main patterns found in the groundwater in the bedrock.

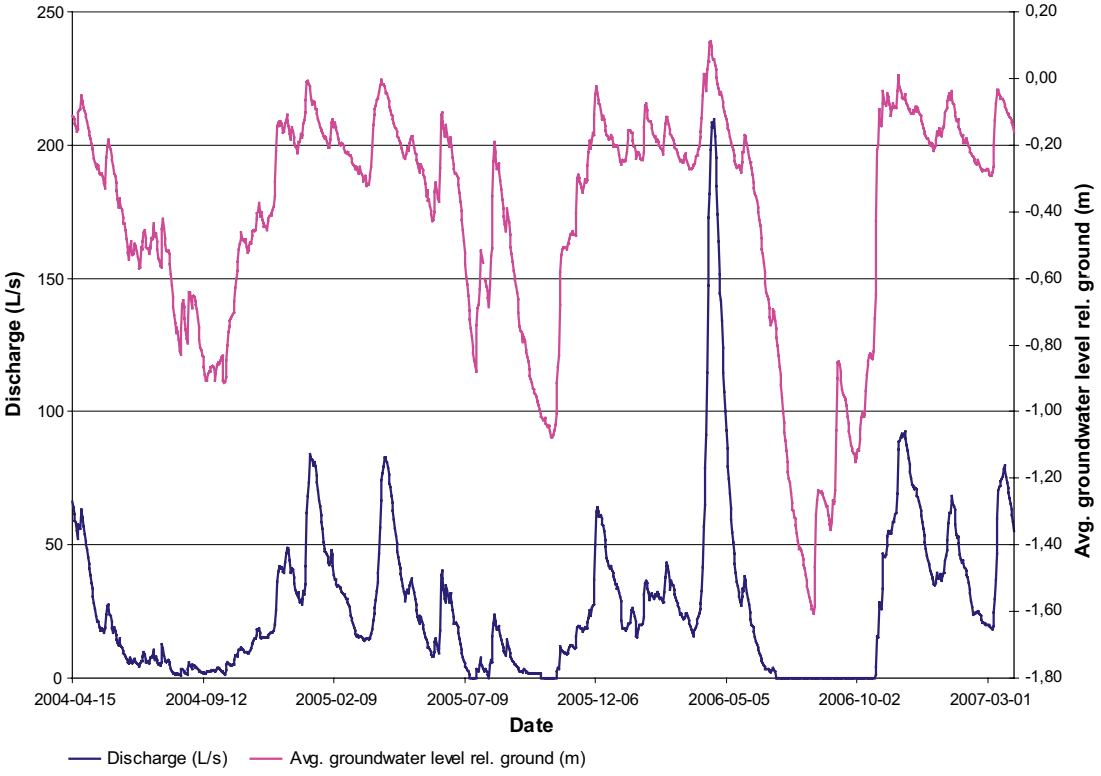

Figure 3-84. *Average groundwater level and surface discharge for the catchment area of discharge gauging station PFM005764.*

Table 3-18. End-members used in the Forsmark 2.2 modelling stage /after Laaksoharju et al. 2008/.

End-member	Na mg/L	K mg/L	Ca mg/L	Mg mg/L	HCO_3 mg/L	Cl mg/L	SO_4 mg/L	Br mg/L	δ^2H ‰SMOW	^3H TU	$\delta^{18}O$ ‰SMOW
Brine	8,200	45.5	19,300	2.12	14.1	47,200	10		–44.9		–8.9
Littorina Sea	3,674	134	151	448	92.5	6,500	890		–37.8		–4.7
Dilute Granitic GW	274	5.6	41.1	7.5	466	181	85.1	0.572	–80.6	12.1	–11.1
Glacial	0.17	0.4	0.18	0.1	0.12	0.5	0.5		–158		–21
Meteoric	0.4	0.29	0.24	0.1	12.2	0.23	1.4		–80		–10.5
Baltic	1,960	95	93.7	234	90	3,760	325		–53.3		–5.9

In Figure 3-85 the ion-source model is shown for labelled monitoring wells in QD with different possible ion sources and possible groundwater types. Five major water types are identified:

- *Modern sea water.*
- *Water influenced by relict marine water (Littorina)*.
- *Deep saline water,* which is significantly influenced by shield brine (shield brine is a highly saline groundwater present at great depths in the granitic environment of the Scandinavian shield).
- *Altered meteoric water*, which is of meteoric origin but significantly altered by processes in the QD.
- *Fresh waters* include both surface water and shallow groundwater, showing "immature" ion signatures from biogenetic CO_2 and calcite dissolution.

Most of the samples are classified as belonging to the *fresh water* and *altered meteroric groundwater* groups. Among the samples in the *fresh water* group are many samples from wells classified as located in typical recharge areas in the hydrogeological classification, e.g. SFM0005 and SFM0020, but also some wells at the shores of Lake Eckarfjärden and Lake Bolundsfjärden and classified as located in discharge areas (SFM0014, SFM0016, SFM0032 and SFM0074). The hydrogeological interpretation of the hydrochemical composition of water from these wells is that the wells are placed in very shallow flow systems with short residence time.

For the wells close to the lakes, a potential influence from recharging lake water during dry summers can not be excluded. The classification of water from the wells SFM0028 and SFM0029 as belonging to the *fresh water* group is surprising from a hydrogeological point of view. These wells are located in till below a 1.5 m thick confining layer of gyttja and clay close to Lake Lillfjärden and relatively distant from unconfined aquifer conditions where groundwater recharge can take place.

The wells placed in till below the lakes and the sea show a quite different chemical composition compared with the other wells placed in QD. In general the waters from these wells have a high salinity, including a high chloride content. The well below Lake Gällsboträsket (SFM0012) and the other wells located in the Gällsboträsket depression (SFM0011 and SFM0013) are classified as belonging to the *influence from relict marine water* group and have chloride contents of approximately 2,000 mg/L. Interestingly, SFM0057 located at the edge of the Gällsboträsket depression has a signature indicating an influence from deep saline water and shows similarities with the signatures of HFM11 and HFM12 located at Lake Eckarfjärden and in the large fracture zone, Eckarfjärdszonen, which also goes through Lake Gällsboträsket. The water in SFM0057 is, however, quite diluted with an average chloride content of c. 250 mg/L.

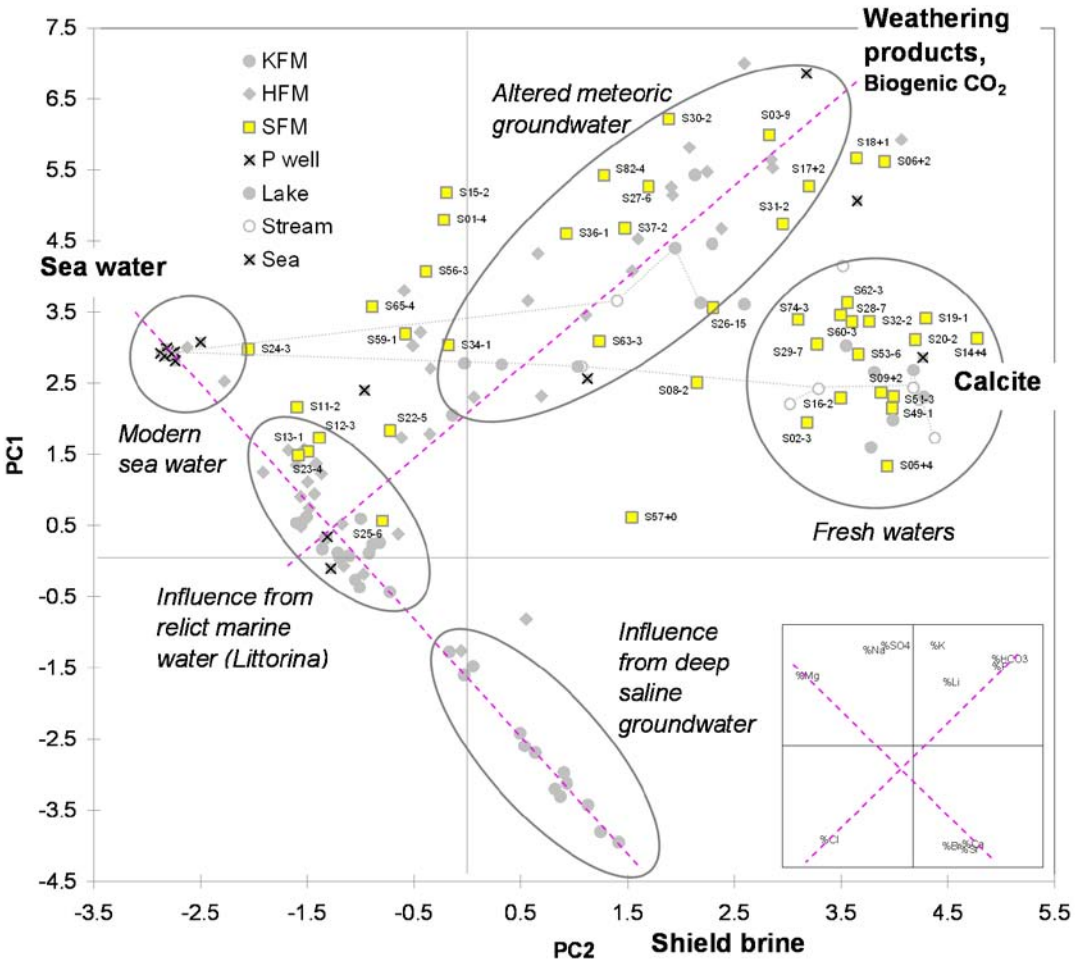

Figure 3-85. *The ion-source model showing labelled monitoring wells in QD with different possible ion sources and possible groundwater types. Note that FM and two zeros have been deleted from the well ID numbers and that the last part of the displayed well number is the elevation of the sampling point (e.g. S02-3 means that data come from SFM0002 where sampling was was made at –3 m RHB70).*

The well in the middle of Lake Bolundsfjärden (SFM0023) also belongs to the *influence from relict marine water* group and has a chloride concentration of c. 3,775 mg/L. The chloride concentration is approximately the same as in the nearby percussion-drilled borehole HFM32 down to a depth of c. 100 m. Also the well SFM0022 below Lake Fiskarfjärden shows a chemical signature clearly influenced by relict marine water. The water from the well below Lake Eckarfjärden (SFM0015), however, shows a quite different chemical composition and is in the ion-source model closest to the group *altered meteoric water*. The chloride content in the well is c. 300 mg/L. The waters in the two wells placed in till below the sea, SFM0024 and SFM0025, belong to the *modern sea water* and i*nfluence of relict marine water* groups, respectively.

The occurrence of water belonging to the group *influenced by relict marine water (Littorina)* below Lake Bolundsfjärden, Lake Fiskarfjärden and Lake Gällsboträsket is a strong indication of very low flow rates in the flow systems involving these parts of the investigation area. In perspective of the total annual water balance of the area, the water can be considered as stagnant. At Lake Bolundsfjärden, no flow from below reaches the till at present according to the groundwater levels measured in QD and bedrock (see Figures 3-80 and 3-81). The water composition indicates that the leakage from the lake through the sediments is very small, i.e. the small gradients shown in Figures 3-80 and 3-81 are combined with a low K_v (vertical K) of the sediments and the till below the lake.

The water *influenced by relict marine water* in the well in the middle of the lake should be compared with waters belonging to the *altered meteoric groundwater* and *fresh water* groups found in wells below the lake close to the shore and on the shore, i.e. SFM0062, –63, –32 and –33 (see Figures 2-6 and 2-7 for locations of the wells). The hydrogeological and hydrochemical interpretations indicate that shallow groundwater flow systems involving only QD have discharge areas around the lake and in the near-shore parts of the lake, while deeper systems are drained by the highly transmissive shallow bedrock.

Figure 3-86 shows a Piper plot of the SFM wells divided according to the hydrogeological recharge-discharge area classification /Werner et al. 2007/. Recharge wells should be low in chloride. Discharge wells could have either low or high chloride concentrations; low if located in discharge areas of small and shallow flow systems and high in discharge areas of flow systems involving deeper flow paths and in areas affected by relict and modern sea water. The two wells deviating from this pattern are SFM0057 and SFM0059. As discussed above SFM0057 shows an influence from deep groundwater, however, quite diluted perhaps by modern recharge. SFM0059 is located in the glaciofluvial deposit, Börstilåsen, quite close to the sea and is most probably influenced by modern sea water infiltrating during events of high sea water levels.

The water chemistry of the water flowing out of Lake Eckarfjärden and Lake Gällsboträsket gives an opportunity to investigate to what extent relict marine water and deep saline groundwater are present in the flow systems generating surface discharge. Chloride is considered as

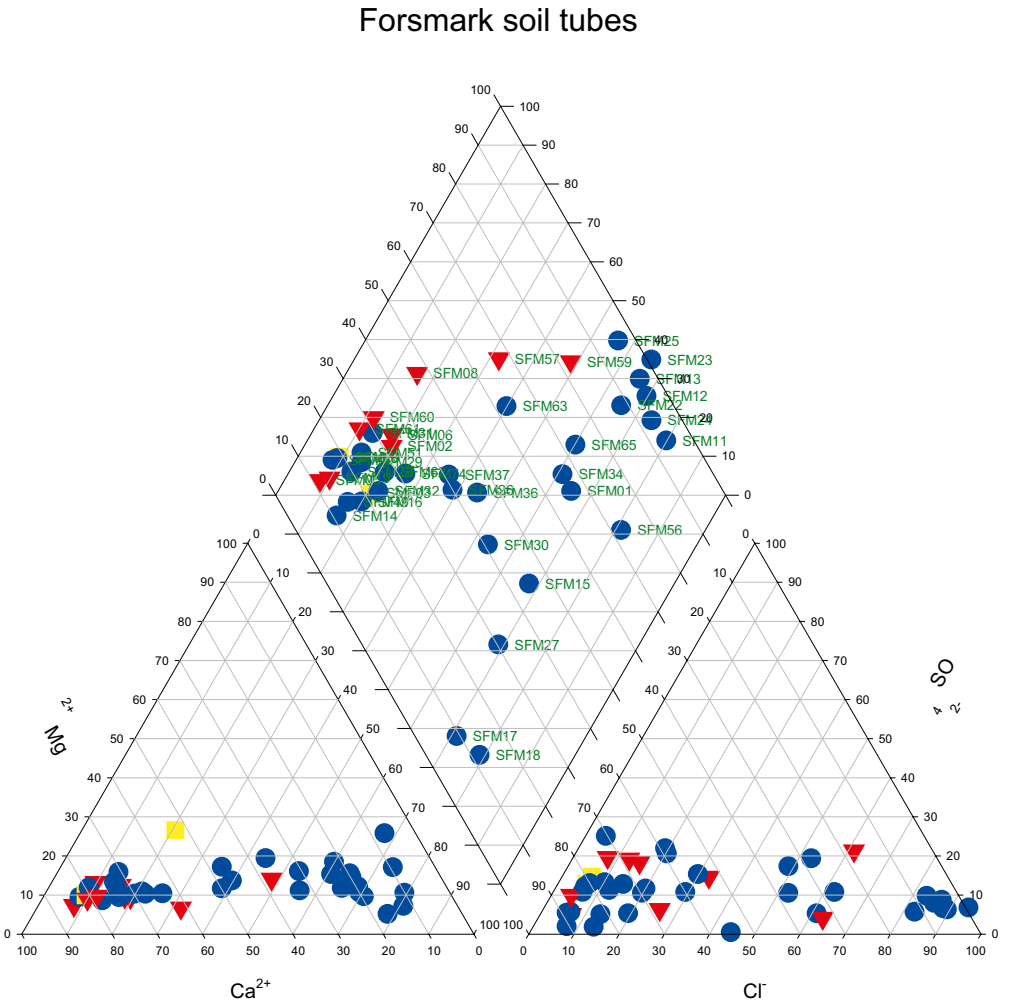

Figure 3-86. *Piper plot of water samples from wells in QD subdivided according to the hydrogeological classification of their locations in recharge areas (red), areas of varying recharge/discharge conditions (yellow) and discharge areas (blue) /Tröjbom et al. 2007/.*

a good tracer as it follows the water and as there is a big difference in chloride concentration between water with chloride only from atmospheric deposition and relict marine and deep saline waters (see Table 3-18).

The measurements of the chemical composition of the precipitation performed within the site investigation in open land, with lower dry deposition than in forest, show an average chloride concentration of 0.95 mg/L (n = 31) (SKB's Sicada database). At Järinge, a station included in the Swedish National Environmental Monitoring Programme and run by IVL Swedish Environmental Research Institute, approximately 45 km SSE of the site investigation area, the ratio between the atmospheric deposition in spruce forest and in open land was approximately 1.6 during 2001–2002 when measurements from both type of land use are available. If this ratio is used in the site investigation area the atmospheric deposition in the catchment areas of Lake Eckarfjärden and Lake Gällsboträsket, which are totally dominated by forest, should be approximately 1.5 mg/L.

According to Section 3.3.3 the average precipitation is c. 560 mm/year, the evapotranspiration 400–410 mm/year, and the specific surface discharge 150–160 mm/year. The concentration in surface discharge of water in which the atmospheric deposition is the only source of chloride should then be slightly more than 5 mg/L. This concentration agrees very well with the concentrations found in QD-wells, classified to be located in typical recharge areas and/or in local discharge areas of shallow flow systems and at an elevation where enough time has passed for flushing of marine water since the area rose above the sea level. The average Cl-concentration in the wells SFM0005, SFM0009, SFM0019, SFM0095, SFM0102 and SFM0103 was 5 mg/L.

The average Cl-concentration at the outlet of Lake Eckarfjärden was 5.1 mg/L (n = 68) (min. = 2.3 and max. = 7.6 mg/L). Thus, the chloride concentration corresponds to what can be assumed to originate from atmospheric deposition. Even a very small contribution from relict marine water or deep saline groundwater should give a noticeable increase of the chloride concentration. For example, a contribution of 2.7 mm/year to the specific discharge or in total 0.2 L/s from a water of the Cl-concentration found in till below the lake should double the concentration in the discharge to 10 mg/L.

The chloride concentration in the discharge from Lake Gällsboträsket, measured upstream the conjunction with the brook from Lake Eckarfjärden, is considerably higher and an additional source beside atmospheric deposition has to exist. The average chloride concentration in the discharge is 29 mg/L (n = 73) (min. = 4.2, max. = 59). By using the continuous discharge and electrical conductivity (EC) measurements at PFM002667 and PFM005764, and the correlation between EC and the chloride concentration, daily values of the transport of chloride from Lake Gällsboträsket have been calculated. The average annual chloride transport for the period Dec. 8, 2004–March 31, 2007 was c. 9,900 kg. The annual atmospheric deposition in the catchment area was c. 1,800 kg, leaving approximately 8,000 kg originating from another source.

From the regolith depth and stratigraphy model /Hedenström et al. 2008/, the volume of the QD-layers in the Gällsboträsket depression below 2.5 m RHB70 has been calculated and, by use of the values of the total porosity in Table 3-13, the total water volume in QD. From this volume and the mean chloride concentration of c. 2,000 mg/L in the three QD-wells in the depression (SFM0011, SFM0012 and SFM0013) the storage of chloride in the QD can be estimated to c. 500 tonnes, i.e. with the current transport rate the storage will be depleted in approximately 60 years. The lake threshold of Lake Gällsboträsket (1.47 m RHB70) rose above the average sea level about 225 years ago.

The correlation between discharge and chloride is shown in Figure 3-87. To investigate if the hydrochemical signatures are different depending on discharge, the available samples were divided into classes based on the discharge when they were taken and plotted in the ion-source model, Figure 3-88. Interestingly, there is a tendency of the hydrochemical signatures with decreasing discharge in the direction towards SFM0057 and HFM11 and HFM12 indicating an influence of deep saline water. This, together with the current outflow rate compared with estimated storage in QD, raises the question of whether an additional source of chloride besides atmospheric deposition and relict marine water exists, i.e. an upward flow of deep saline groundwater.

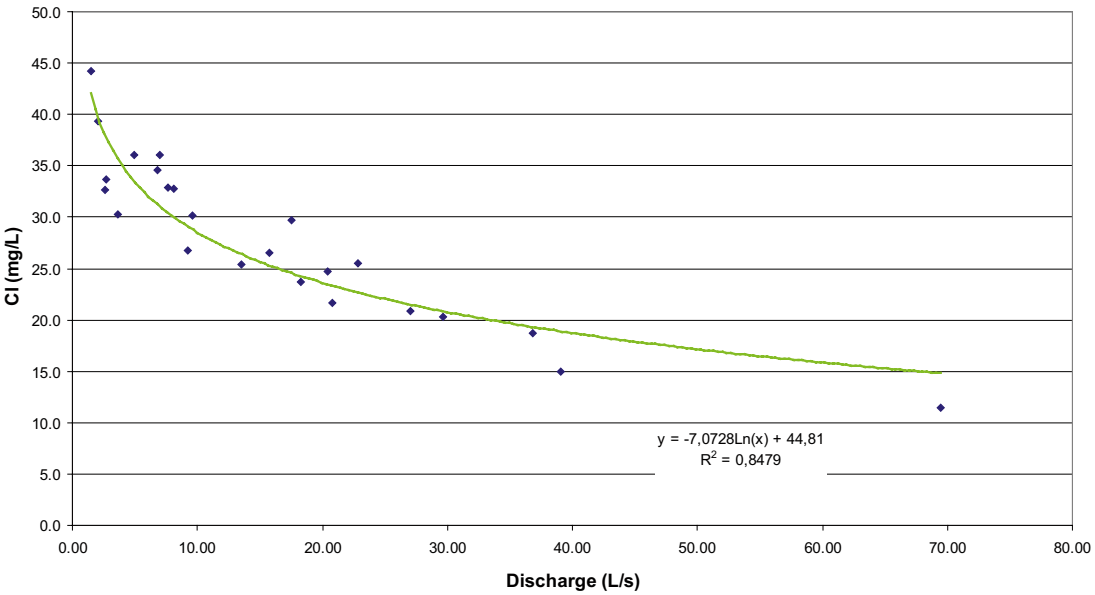

Figure 3-87. *Relationship between discharge and chloride concentration in water from Lake Gällsboträsket.*

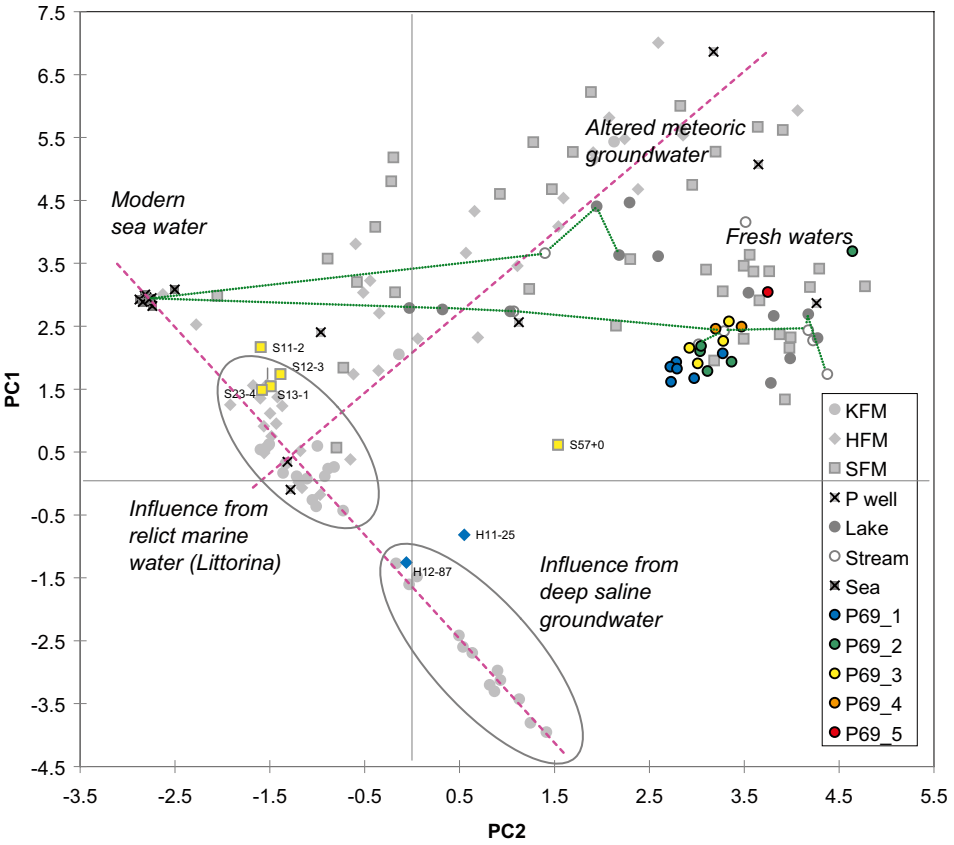

Figure 3-88. *Mean chloride concentrations in the outflow from Lake Gällsboträsket (P69) for different discharge intervals plotted in the ion-source model (P69_1 blue = 0–5, P69_2 green = 5–10, P69_3 yellow = 10–25, P69_4 orange = 25–50, and P69_5 red>50 L/s).*

In Figure 3-89 the ion-source model is shown for labelled surface water sampling points. The dotted green lines show flow paths (i) from a small brook upstream Lake Eckarfjärden (PW71) – Lake Eckarfjärden (PL117) – the outlet from Eckarfjärden (PW70) – branch from Lake Gällsboträsket (PW69) – the inlet to Lake Bolundsfjärden (PW68) – Lake Bolundsfjärden (PL107) – the outlet of Lake Bolundsfjärden (PW67) – Lake Norra Bassängen (PL097) – the Baltic Sea, and (ii) Lake Fiskarfjärden (PL135 /NW part/, PL127 /SE part/) – outlet from Lake Fiskarfjärden (PW72) – the Baltic Sea.

The parameters ^{3}H, ^{2}H, and $\delta^{18}O$, as well as the absolute concentration of chloride, may contain information on the sources of the dissolved ions that is not used in the ion-source model. These parameters are plotted on the ion-source model in Figure 3-90. Specifically, the three wells below Lake Bolundsfjärden (SFM0023), Lake Eckarfjärden (SFM0015), and Lake Gällsboträsket (SFM0012) are labelled. In general, SFM0012 and SFM0023 show similarities for the presented parameters. The ^{3}H-values indicate a mixture of submodern and modern water (TU 0.8–4), the slightly low ^{18}O and ^{2}H excess values may indicate an effect of evaporation from relict marine water. SFM0015, below Lake Eckarfjärden, deviates significantly from SFM0012 and SFM0023, with slightly higher ^{18}O and lower ^{2}H excess values as well as considerbly lower chloride concentration. The combined picture is difficult to interpret but may be a result of a mixed water with components exposed to evaporation.

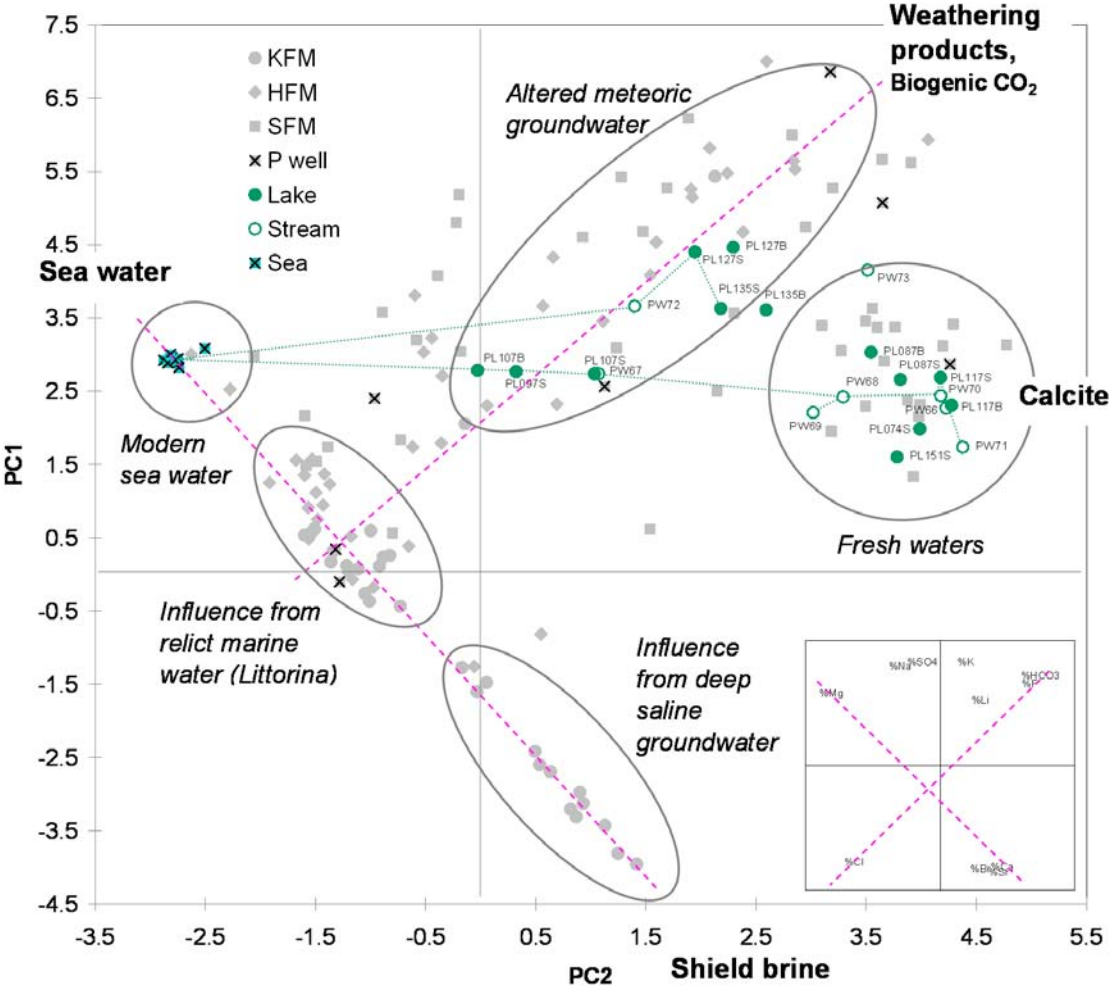

Figure 3-89. *Surface water samples plotted on the ion-source model. The dotted green lines show flow paths from upstream Lake Eckarfjärden (PW71) to the sea, and from Lake Fiskarfjärden (PL135) to the sea.*

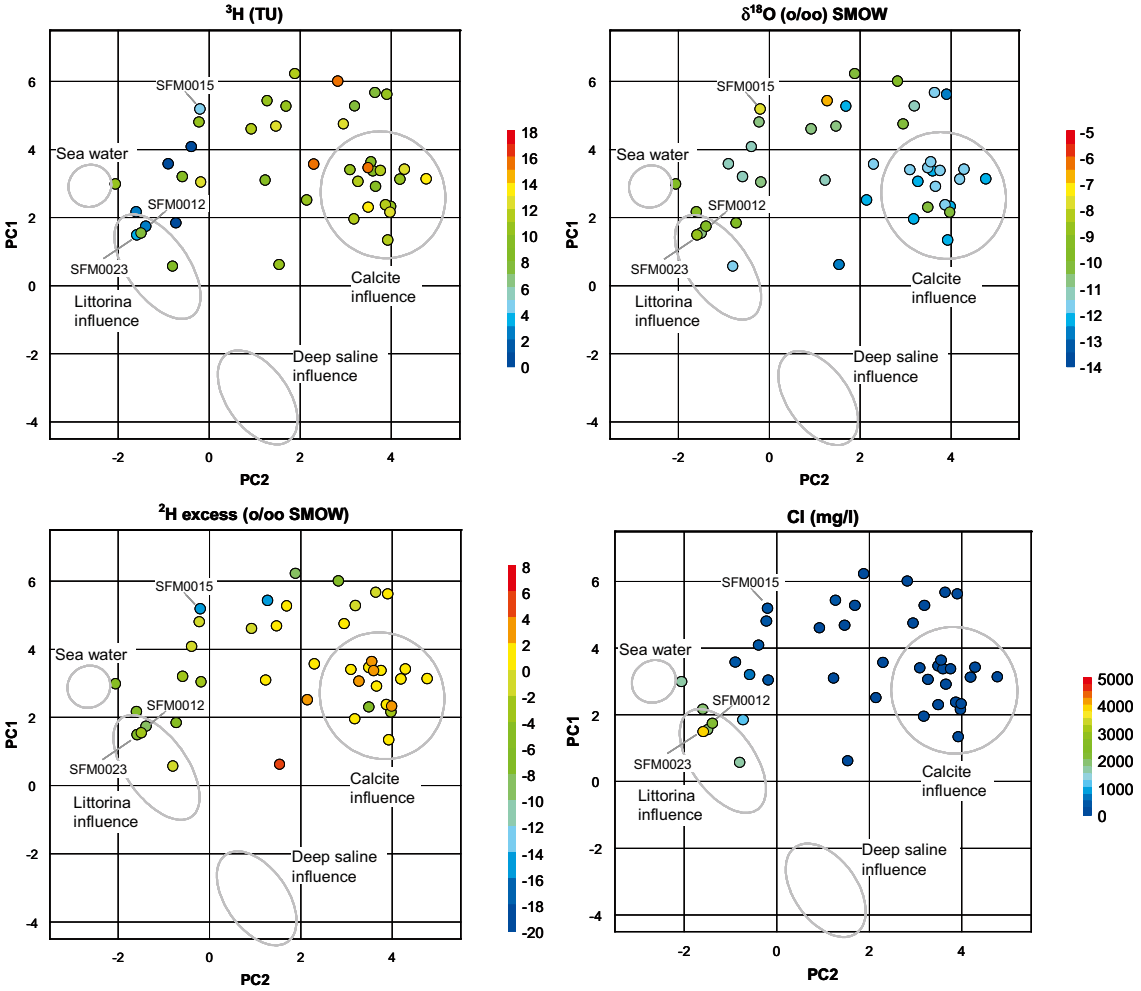

Figure 3-90. *The parameters ^{3}H, ^{2}H, $\delta^{18}O$, and the absolute concentration of chloride of the QD-wells plotted on the ion-source model, with SFM0012, SFM0015 and SFM0023 labelled.*

Figure 3-91 shows the ion-source model with two samples of the water pumped out of SFR, from the upper and lower pump sump respectively, as well as samples from the SFR boreholes. In general, the SFR-samples plot along a line indicating a mixture of marine and deep saline water. The positions of the two samples from the pump sumps indicate waters of mainly marine origin, but with a deep saline component. Compared with the HFM- and SFM-sampling points of the site investigation, the composition of the water pumped out of SFR is most similar to the water from HFM32 (especially the upper three sections), HFM08 and HFM22 in the bedrock and to SFM0023 in the QD.

Of the HFM-boreholes closest to SFR, the waters of HFM34 and HFM35, located to the east of the Singö zone, are more similar to sea water than the water pumped out of SFR (see Figure 2-9 for the locations of the wells). The water in HFM34 is totally dominated by modern sea water. On the other hand, the water in HFM33, located to the west of the Singö zone, shows a pronounced deep saline component which is quite similar to the water of the deepest section in HFM32.

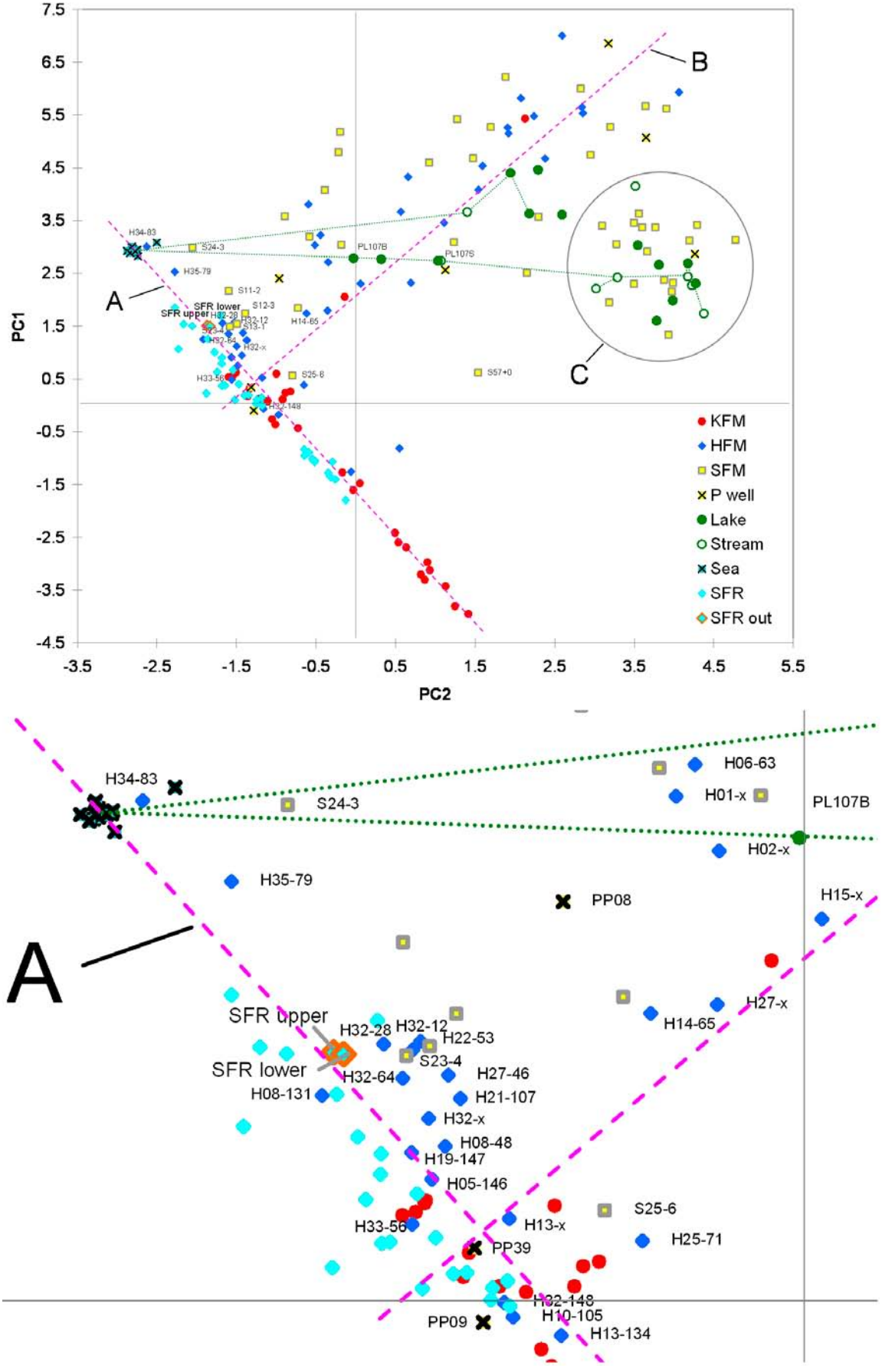

Figure 3-91. *The ion-source model with water samples from SFR included. SFR out are water pumped out of SFR from the upper and lower pump sumps. In the labelling of the HFM-boreholes, the last figures give the sampling depths (m, RHB70). Note that FM has been deleted from the well ID.*

4 Conceptual and descriptive model of water flow at the Forsmark site II: Quantitative water flow modelling

4.1 Water flow modelling tools used in the site investigation

Several tools have been applied for modelling of the surface hydrology and/or the near-surface hydrogeology of the Forsmark area.

The main modelling work has been performed by use of MIKE SHE, which is a dynamic, physically based modelling tool that describes the main processes of the land phase of the hydrological cycle. A comprehensive summary of this work based on the detailed presentation of the MIKE SHE modelling in /Bosson et al. 2008/ is presented in Section 4.3.

In Section 4.2, the results of modelling by a customised HBV-model for exploration of relationships between precipitation, evapotranspiration, groundwater levels in Quaternary deposits and surface discharge are presented. These results have not been published before in the SKB report series, motivating a thorough presentation here, but earlier simulations with a slightly different model and based on shorter time series have been presented in /Juston et al. 2007/. For a description of the HBV-model the reader is referred to /Bergström 1976/ and /Lindström et al. 1997/.

In the Forsmark 1.2 stage, GIS-based modelling with the ArcGIS extension "Hydrological modelling" was performed. The modelling used a digital elevation model which was the basis for flow direction and flow accumulation calculations. By use of a "direction grid" the number of upstream cells generating flow in a specific cell and a specific discharge, the flow in each cell can be calculated. The specific objective of this modelling was to roughly calculate the spatial distribution of total runoff for use in the early phases of the ecological systems modelling. Furthermore, based on limits set on the number of upstream cells a preliminary division of the area into recharge and discharge areas was suggested. The reader is referred to /Johansson et al. 2005/ for a comprehensive description of the methodology and results of this GIS-based modelling.

In the Forsmark 1.2 stage also another GIS-based modelling tool, PCRaster-POLFLOW, providing extended capabilities for hydrological modelling, was applied /Jarsjö et al. 2005, Johansson et al. 2005/. PCRaster-POLFLOW allows for analyses of spatially varying flow and transport processes. In the Forsmark application, the PCRaster-POLFLOW modelling approach used empirical equations and data for quantification of the specific discharge and its distribution on surface and sub-surface flows. Specifically, the input data included the digital elevation model, and spatially variable meteorological, geological and land use parameters, which are used either in emprical equations or as a basis for a classification of different subareas within the model area. The reader is referred to /Jarsjö et al. 2005/ and /Johansson et al. 2005/ for a comprehensive description of the methodology and results of the PCRaster-POLFLOW modelling. Recently, the PCRaster-POLFLOW modelling of the Forsmark area has been extended to include solute transport /Jarsjö et al. 2007/.

In /Brydsten 2006b/ a topographical modelling study is presented for identification of recharge and discharge areas. The identification contained five classes:

- *Most likely recharge areas* (areas identified as peaks and ridges by means of geomorphological classification using the Landserf software /www.landserf.org/).
- *Most likely discharge areas* (areas identified by the "Basin fill" and "Flow accumulation" functions of ArcGIS /www.esri.com/software/arcgis/).
- *Probable recharge areas*, *Undefined areas*, and *Probable discharge areas* (areas defined by topographical wetness indices (TWI) as defined by /Beven and Kirkby 1979/).

The reader is referred to /Brydsten 2006b/ and /Werner et al. 2007/ for a comprehensive description of the methodology and results of the topographical modelling of recharge and discharge areas, and for a comparison of these results with results from the MIKE SHE modelling, respectively.

The hydrogeological modelling including the deep bedrock is performed with the modelling tool CONNECTFLOW which contains also a simplified description of the Quaternary deposits. In the more recent SDM models, the upper boundary of the model is a flux boundary defined by an annual average groundwater recharge. For a description of the modelling performed with CONNECTFLOW the reader is referred to /Follin et al. 2007abc, 2008/.

4.2 Catchment-based simulation of surface discharge and groundwater depths

The strong correlations between rainfall + snowmelt – evapotranspiration, groundwater levels in Quaternary deposits and surface discharge in brooks have been described in Sections 3.5.2 and 3.5.3 and illustrated in e.g. Figures 3-63 and 3-84. The relation between these parameters has also been described earlier in /Juston et al. 2007/. To further explore these relationships, catchment-based simulations of surface discharge and groundwater depths were conducted by a one-dimensional model. Simulations were conducted for the four catchments equipped with automatic discharge gauging stations, see Figure 2-5 for the locations of the catchment areas and the gauging stations. Three of these discharge stations are located at different distances along the brook between Lake Eckarfjärden and Lake Bolundsfjärden. These three catchments are nested and their hydrological responses are sequentially coupled. The fourth catchment is located along the brook discharging Lake Gunnarsboträsket, and is independent from the other three. Separate calibrations and simulations were conducted for these four catchments.

The model used for the simulations was a site-specific customization of the HBV model /Bergström 1976, Lindström et al. 1997/ and was named the Forsmark-HBV model in recognition of this relationship. As with HBV, Forsmark-HBV is a one-dimensional conceptual model. The model uses daily input data for precipitation (P), temperature (T), radiation (R), and potential evapotranspiration (PET) time series data to predict discharge (Q), catchment-averaged groundwater depths (X), and snow accumulations (S). Model parameter values were tuned within the framework of a selective Monte Carlo analysis, as described below, to calibrate predictions against measured data.

Earlier efforts with Forsmark-HBV have been reported twice before /Johansson et al. 2005, Juston et al. 2007/. However, there are several features that distinguish the effort reported here from the previous ones:

- The available time series are considerably longer. Here, simulations used data through April 30, 2007.
- The model structure has been further refined to eliminate redundancy (over-parametization) in the groundwater storage relationship, and to improve model fit during snow melt events.
- Also for the first time, the calibration results are presented in the context of an uncertainty analysis, such that suitable parameter values are represented with distributions rather than deterministic point values, and simulated time histories are represented with credibility bands rather than singular trends.

4.2.1 Methods

Model structure and parameter description

The structure of the Forsmark-HBV model is shown schematically in Figure 4-1. This structure is a further evolution of the HBV-derived model that has been previously applied to the same

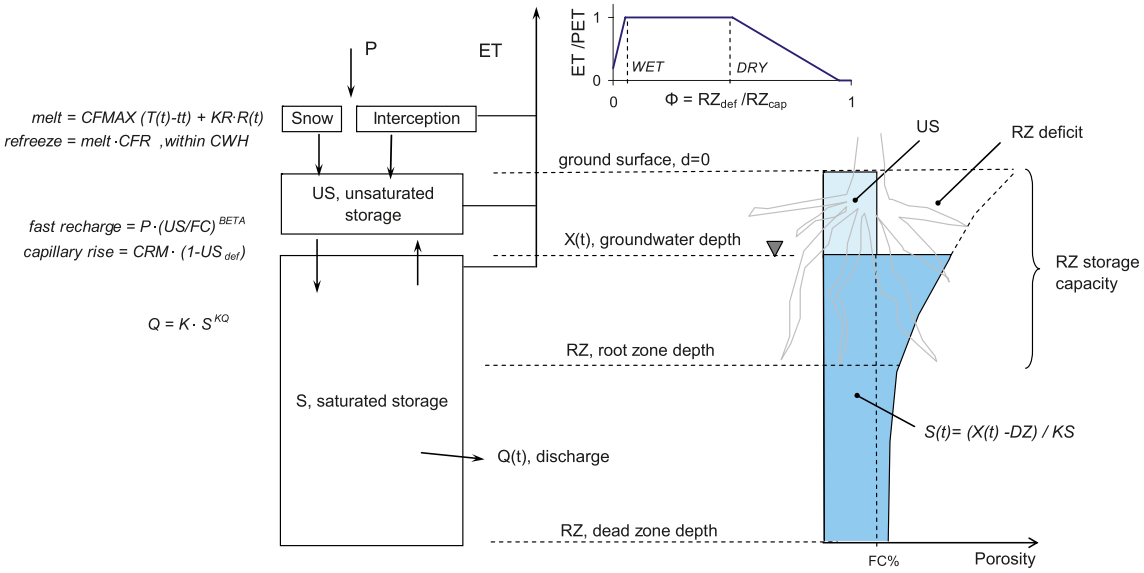

Figure 4-1. *Schematic diagram of Forsmark-HBV model structure with key equations.*

catchments /Johansson et al. 2005, Juston et al. 2007/. The changes introduced compared with the original HBV-model were based on site specific characteristics as presented in Chapter 3, with the shallow groundwater as the single most important factor. Parameter name definitions are given in Table 4-1 using names from the traditional HBV formulation /Lindström et al. 1997/ where possible. Compared to the last presentation of this model /Juston et al. 2007/, the structure presented here incorporates the following refinements:

- The interception storage was eliminated.
- A radiation term was added to the degree-day formulation in the snow melt routine.
- The fast recharge flux ($F_{flow\text{-}through}$) was eliminated, while the capillary flux was retained.
- The groundwater storage function was simplified to a linear depth-storage equation, thus reducing the number of parameters required to specify groundwater storage from four to two.

These refinements were aimed at either improving model fit or removing redundancies where possible. Although not presented here, the analytical justifications for these modifications were based on a similar methodology as the uncertainty analyses described below.

The model uses a one-dimensional catchment-averaged water balance based around three conceptual water storages: QD unsaturated and saturated zones, and above ground water content in snow and ice accumulation. Interception storage was included in the original conceptualization of the model and is shown in Figure 4-1, but was later deemed insignificant in reducing predictive uncertainty and was therefore eliminated.

The saturated storage (S) was modeled with a linear depth-storage relationship. This linear relationship was based on an analysis of porosity profiles in soil cores from the site, see Section 3.4.1, /Lundin et al. 2005/ and /Juston et al. 2007/. HBV does not usually simulate groundwater levels, but similar storage functions have been used with HBV on occasions in past studies /Bergström and Sandberg 1983, Seibert 2000/. The same soil core data indicated an approximately constant water holding capacity of 15% at pF 2, independent of depth and sample location. Therefore, the field capacity of the unsaturated zone (US) in Forsmark-HBV was calculated dynamically as 15% of the simulated depth to groundwater. This is also a change from the typical HBV formulation and is well-suited to the shallow groundwater depths in Quaternary deposits found throughout the study area.

Table 4-1. Parameter descriptions and ranges of prior distributions for uncertainty analysis.

Parameter	Description	Fixed value	Min. range	Max. range	Unit
Snow and interception					
CFMAX	Degree-day constant for melting		1	5	mm/°C/d
tt	Threshold temperature for melting		0	2.5	°C
KR	Radiation constant for melting		0	0.15	mm/W/m^2
CWH	Water holding capacity	0.10	–	–	%
CFR	Refreezing coefficient	0.05	–	–	–
Subsurface fluxes					
CRM	Maximum capillary rise		0	15	mm/d
K	Discharge scalar		50	500	1/d
KQ	Discharge exponent		2	8	–
Breakpoints in ET soil moisture function					
ETM	Min. evap. when saturated	0.2	–	–	
WET	Threshold for moisture limited	0.1	–	–	
DRY	Threshold for deficit limited		0.3	0.7	mm/mm
Lumped physical constants					
RZ	Root zone depth		–0.3	–0.9	mm
DZ	Dead zone depth		–0.9	–1.2	mm
KS	Inverse storage constant		1.5	3.5	mm/mm

Water flow through the model was simulated as follows. Precipitation entered the snow storage (SNOW) if daily temperatures were less than 0°C, or was treated as rainfall above 0°C. Snow melt was calculated from the sum of a standard degree-day formulation plus a new (to HBV) radiation term /Hock 2003/. The radiation term (KR) was added during the model structure identification process and proved useful for improving model fit during late season snow melts, such as the one in April 2006. As in the original HBV formulation, a fraction of the freezing capacity (CFR) was retained (refrozen) during melt events in the existing snow storage, but only within a preset storage limit (CWH).

Snowmelt and rainfall were simulated to enter directly to the unsaturated zone storage. No overland flow processes were simulated, as they were not deemed significant in the area. When the unsaturated storage exceeded field capacity, the excess water was added to the saturated zone. A capillary rise term provided a return water flux from the groundwater to the unsaturated zone. Discharge was dependent on an active saturated storage volume, specified as the saturated storage above a dead-zone depth (DZ), and was calculated with a power-law equation.

Evapotranspiration (ET) was modelled as a function of daily PET and a root zone (RZ) moisture deficit index. Obviously, the ET sub-model was an aggregation of complex root zone processes. However, as with other process representations in HBV-Forsmark, a simpler ET sub-model was adhered to with the purpose to keep the overall model structure as simple as possible.

Input data time series

The model required input time series for daily precipitation, potential evapotranspiration, air temperature, and solar radiation. Time series of meteorological data from Högmasten and Storskäret were available from May 2003, and these data were complemented with earlier data from SMHI for several regional sites to provide a complete input time series from January 1, 2002 (see Section 2.2.1 for available meteorological data). All simulations were run beginning from this date.

Observation data for model calibration

Simulated model responses for discharge, catchment-average groundwater depth, and snow accumulation were compared to observed data from the study site. Discharge and groundwater level time series were used for model calibration, while snow accumulation data were used for comparison (validation) only.

Discharge data from the four gauging stations, and hence for the four catchment outflows, were discussed in detail in Section 3.3.3. Groundwater data for all wells in Quaternary deposits in the study site were presented in Section 3.4.1. As described below, only a small subset of these wells were used for model calibrations. Data from the two snow measurement stations in forest (AFM000072 and AFM001172) were pooled and used for validation of model predictions (see Figure 2-3 for location of the stations).

The discharge gauging stations had different start dates for data availability: April 15, 2004 for PFM005764 and December 8, 2004 for the other three stations. Groundwater level data were typically available from spring 2004 and therefore May 1, 2004, was chosen at the start date for the data comparison intervals. Daily simulations between January 1, 2002 and the differing start dates of the discharge time series were used for starting up the model and initializing model storages before the data comparison intervals (Table 4-2).

In the data comparison intervals, observed data were divided into calibration and validation periods for split-sample comparisons as shown in Table 4-2. As noted, simulations were run with the validation period proceeding the calibration period. The reason for this was that it was desirable to calibrate the four catchments to identical time intervals of data for meaningful comparisons of parameter distributions. Since the start dates of available discharge data were not the same in all four catchments, the usual order of calibration and then validation periods was reversed. Calibration intervals for all catchments were from August 1, 2005 through April 30, 2007 and enclosed two complete winter seasons. The durations of validation intervals were shorter and variable amongst catchments (Table 4-2).

As described above, the Forsmark-HBV model functioned on an aggregated catchment scale, and simulated groundwater depths represented catchment-average responses. The catchment-averaged groundwater depths for comparison to the simulations were estimated from the available network of groundwater wells in Quaternary deposits (Figure 2-7). For each catchment, a group of 8–9 wells were selected as representative for that catchment. The wells selected for each catchment are listed in Table 4-3. Where possible, the representative wells were enclosed by the catchment boundary. For example, all eight wells used to represent the aggregated response in PFM005764 were enclosed within the catchment boundary. On the other hand, no wells were enclosed within PFM002669 and only 1–2 wells were enclosed within the other two catchments.

The supplemental wells (those from outside the catchment boundary) were chosen to be representative of the range of recharge and discharge conditions that might be expected in the catchments. The group of representative wells for PFM002667, PFM002668, and PFM002669 was the same. Therefore, for each of the two different groupings, an average groundwater depth time series was calculated using the representative wells. Additionally, standard deviation time series were calculated as measures of uncertainty. These values were combined into a performance measure for calibration as described in the next section.

Table 4-2. Summary of calibration and validation intervals for the four catchments.

Catchment	Simulation start date	Validation start date	Calibration start date	Simulation end date	Calibration days	Validation days
PFM005764	Jan. 1, 2002	May 1, 2004	Aug. 1, 2005	Apr. 30, 2007	638	457
PFM002667	Jan. 1, 2002	Dec. 8, 2004	Aug. 1, 2005	Apr. 30, 2007	638	236
PFM002668	Jan. 1, 2002	Dec. 8, 2004	Aug. 1, 2005	Apr. 30, 2007	638	236
PFM002669	Jan. 1, 2002	Dec. 8, 2004	Aug. 1, 2005	Apr. 30, 2007	638	236

Table 4-3. Wells used for estimating an averaged groundwater response in each catchment. Well descriptors in bold type were enclosed within the respective catchments' boundaries.

Catchment	Groundwater wells in Quaternary deposits used for calibrating simulated groundwater
PFM005764	**SFM0010**, **SFM0011**, **SFM0013**, **SFM0014**, **SFM0017**, **SFM0019**, **SFM0030**, **SFM0057**.
PFM002667	SFM0003, SFM0004, SFM0010, **SFM0014**, **SFM0019**, SFM0021, SFM0033, SFM0049, SFM0057.
PFM002668	SFM0003, SFM0004, SFM0010, **SFM0014**, SFM0019, SFM0021, SFM0033, SFM0049, SFM0057.
PFM002669	SFM0003, SFM0004, SFM0010, SFM0014, SFM0019, SFM0021, SFM0033, SFM0049, SFM0057.

Calibration objectives

Performance measures were defined for simulated discharge and groundwater time series. Calibration objectives were defined with stepwise criteria:

1. Solutions were accepted if the cumulative error in simulated discharge was within ± 15% of the observed total over the calibration interval.
2. Within the subset of solutions that satisfied this water balance criterium, solutions were further screened with a threshold criterium on performance index for simulated discharge and groundwater time series.

Simulated discharge time series were evaluated with the Nash-Sutcliffe efficiency (N-S) /Nash and Sutcliffe 1970/. It is expressed as one minus the quotient of the sum of squared model errors divided by the observed data variance. Calculated values for N-S can vary between one for a perfect simulation (zero error) and large negative numbers for highly imperfect simulations.

The performance index for simulated groundwater depth time series followed a methodology proposed by /Beven 2006/ that has proven useful for calibrating to uncertain targets. Here, the calculated mean and standard deviation time series from the representative wells for each catchment (Table 4-3) were used to define a window of acceptability for simulated values. At each daily time step in the calibration periods, simulated groundwater depths were compared to the mean and standard deviation of the representative observations. If the simulated value was within one-half standard deviation of the observed mean, then full credit (value = 1) was given for that day. If the simulated value was outside one S.D. of the mean, then no credit (value = 0) was given. Simulated values between one-half and one-full S.D. were given credit graded linearly between one and zero.

The net score for a simulated time series was the average of all daily scores. In this way, a perfect score of 1.0 implied all simulated values were at least within one-half standard deviation of the mean time series, while scores less than one reflected the degree to which the simulated time series adhered to the target range. Other studies have used similar approaches for defining windowed and/or fuzzy targets to uncertain targets /Seibert 2000, Freer et al. 2004, Beven 2006/.

Uncertainty Analysis

All calibrations were conducted within the framework of a Monte Carlo analysis using the GLUE methodology /Beven and Binley 1992, Beven and Freer 2001/. For each catchment simulation, two million combinations of randomly selected parameter values were evaluated within the predefined ranges (Table 4-1). For each parameter set in the Monte Carlo samples, model output was compared to measured data using the calibration objectives described in the previous section. Desirable parameter sets were first screened from the Monte Carlo runs based on the ± 15% error constraint on the simulated water balance, and then with a user-defined

threshold on the combined (averaged) criteria for discharge and groundwater simulations. In the vocabulary of the GLUE methodology, the accepted solutions (those that passed these screening criteria) are referred to as the "behavioral" simulations. Information from behavioral simulations (parameter sets and simulated time series) was retained for post-processing after the Monte Carlo run was completed.

In GLUE, the number of accepted behavioral solutions is directly controlled by the magnitude of the user-defined threshold criteria. Lower thresholds for acceptance imply more behavioral solutions, higher thresholds imply fewer, and clearly calibrations to different time series could respond differently to the same threshold criteria. Therefore, in order to provide a basis of comparison amongst the different catchment simulations, the acceptance threshold was varied for each catchment such that each Monte Carlo run produced approximately the same number of behavioral solutions (N = c. 100 of the two million runs). In this way, post-processing comparisons were made amongst similar sample sizes representing only the upper echelons of achievable simulations with Forsmark-HBV in each catchment.

Variations in parameter sets and time series simulations in the behavioral solutions were used to express predictive uncertainty. For uncertainty in time series simulations, "credibility bands" were estimated from the range of simulated values in all behavioral simulations on each day. To account for variations introduced by unequal sample sizes and the possibility of outliers, the credibility bands were represented as the 5^{th} and 95^{th} percentiles of the range of behavioral values at each time step.

Cumulative distribution functions (CDFs) were calculated from the behavioral parameter sets for each parameter value. CDFs were presented instead of probability distribution functions (PDFs) since the relatively small sample size of accepted solutions resulted in lumpy PDFs (but smooth CDFs). Here, only marginal distributions are presented, but co-variation can also exist between various parameters.

It is important to keep in mind when evaluating the results presented below that uncertainty in the GLUE method is conditioned on several user-defined parameters, such as the likelihood measures and acceptance threshold defined above. Changing those parameters (and the modeler is free to do that in GLUE) would change the represented uncertainties. Therefore, to high degree, these results represent the best judgment of the modelers with regard to their experience with the Forsmark data and the Forsmark-HBV model.

4.2.2 Results

Time series

Credibility bands for time series simulations of discharge, groundwater depth, and snow water content are shown in Figures 4-2, 4-3, 4-4 and 4-5 for PFM005764, PFM002667, PFM002668, and PFM002669, respectively. Performance measures from the simulations are summarized in Table 4-4. The table shows ranges for N-S efficiencies for discharge, cumulative flow errors, and groundwater acceptability indices for calibration and validation intervals for each catchment. All results in this section were derived from the set of behavioral solutions (sample size between 90 and 105) from two million random variations of the predefined parameter space (Table 4-1). Since the simulation results for individual catchments share many similarities, they will be discussed together.

Simulated discharges during the calibration intervals were generally quite good. Nash-Sutcliffe efficiencies typically varied between 0.82–0.92 for accepted solutions in each catchment (Table 4-4), with the average of this range being approximately 0.87 for all catchments. Simulated discharges during the validation range were less accurate. The average N-S efficiencies for accepted solutions during validation intervals were 0.53, 0.44, 0.66, and 0.16 for PFM005764, PFM002667, PFM002668, and PFM002669, respectively.

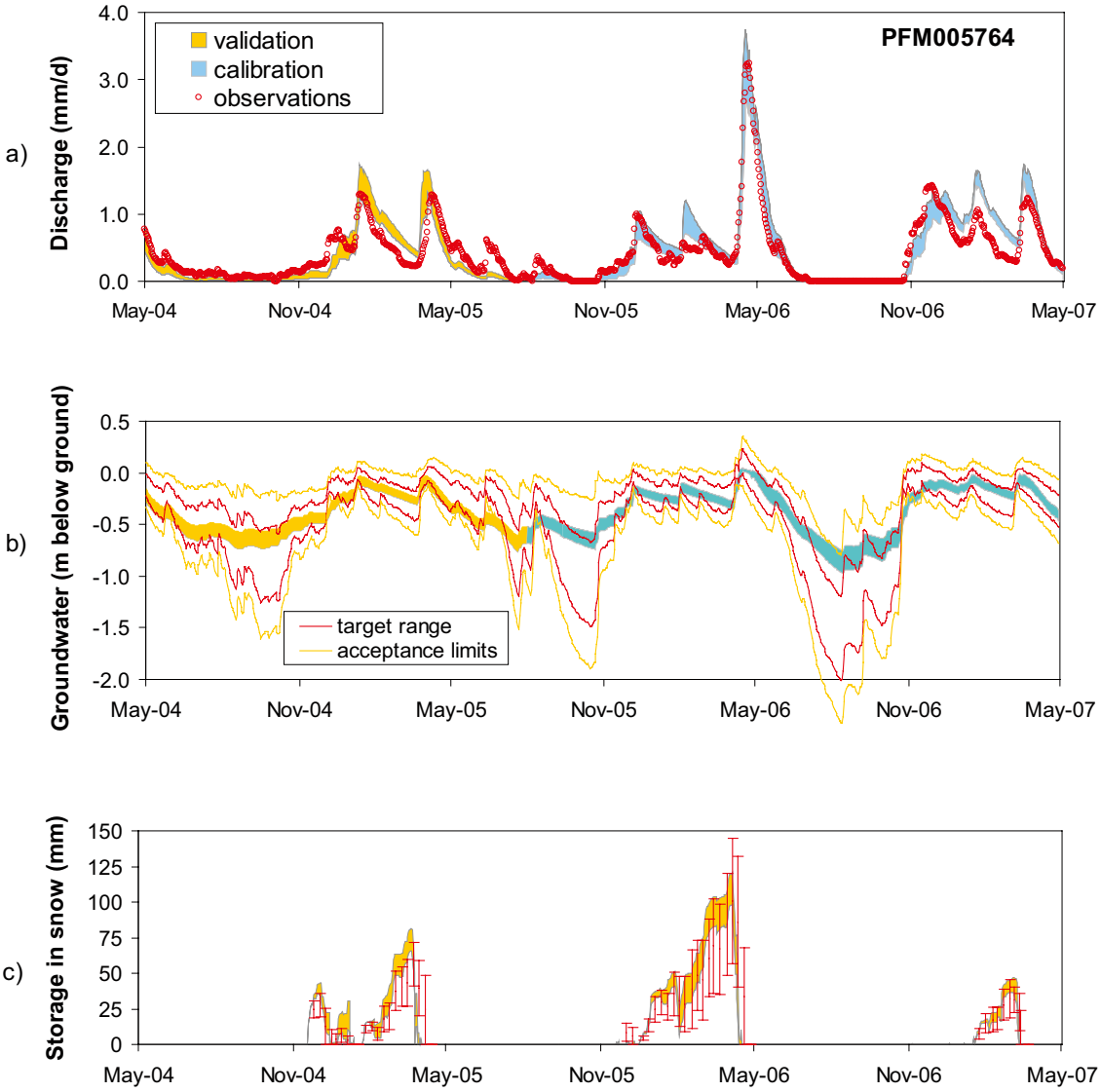

Figure 4-2. *Credibility bands and calibration targets for hydrological simulations of the PFM005764 catchment for a) discharge, b) catchment-average groundwater depth, and c) water storage in snow. In the graph for groundwater simulations, the "target range" indicates a plus and minus one-half standard deviation range around the mean time series calculated from the representative wells for that catchment (see Table 4-3), and the "acceptability range" indicates a full standard deviation range. In the snow accumulation graph, the error bars indicate a range of the observations from two nearby stations.*

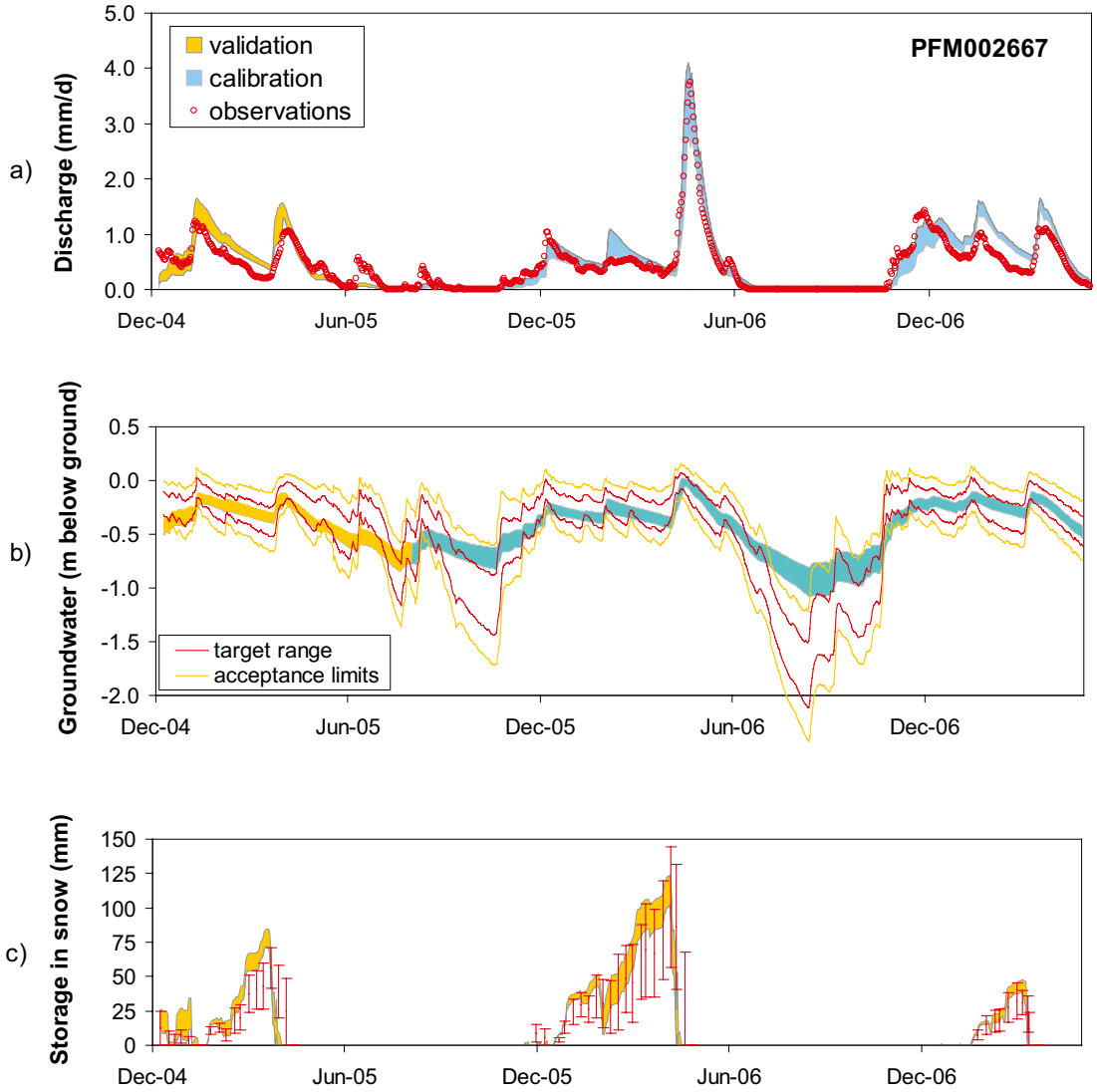

Figure 4-3. *Credibility bands and calibration targets for hydrological simulations of the PFM002667 catchment for a) discharge, b) catchment-average groundwater depth, and c) water storage in snow, see Figure 4-2 for explanations of "target range" and "acceptability range" in b) and the error bars in c).*

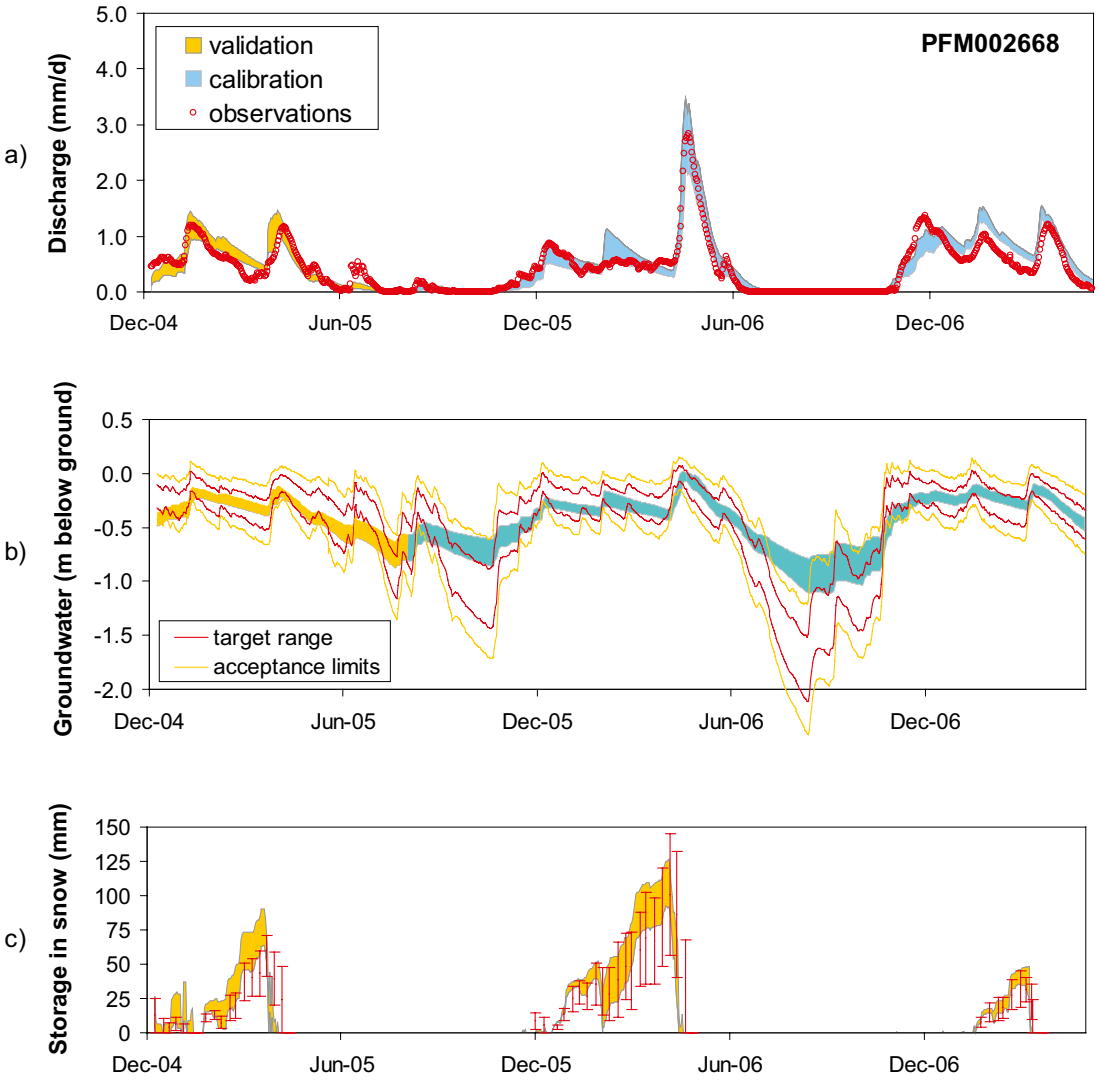

Figure 4-4. *Credibility bands and calibration targets for hydrological simulations of the PFM002668 catchment for a) discharge, b) catchment-average groundwater depth, and c) water storage in snow, see Figure 4-2 for explanations of "target range" and "acceptability range"in b) and the error bars in c).*

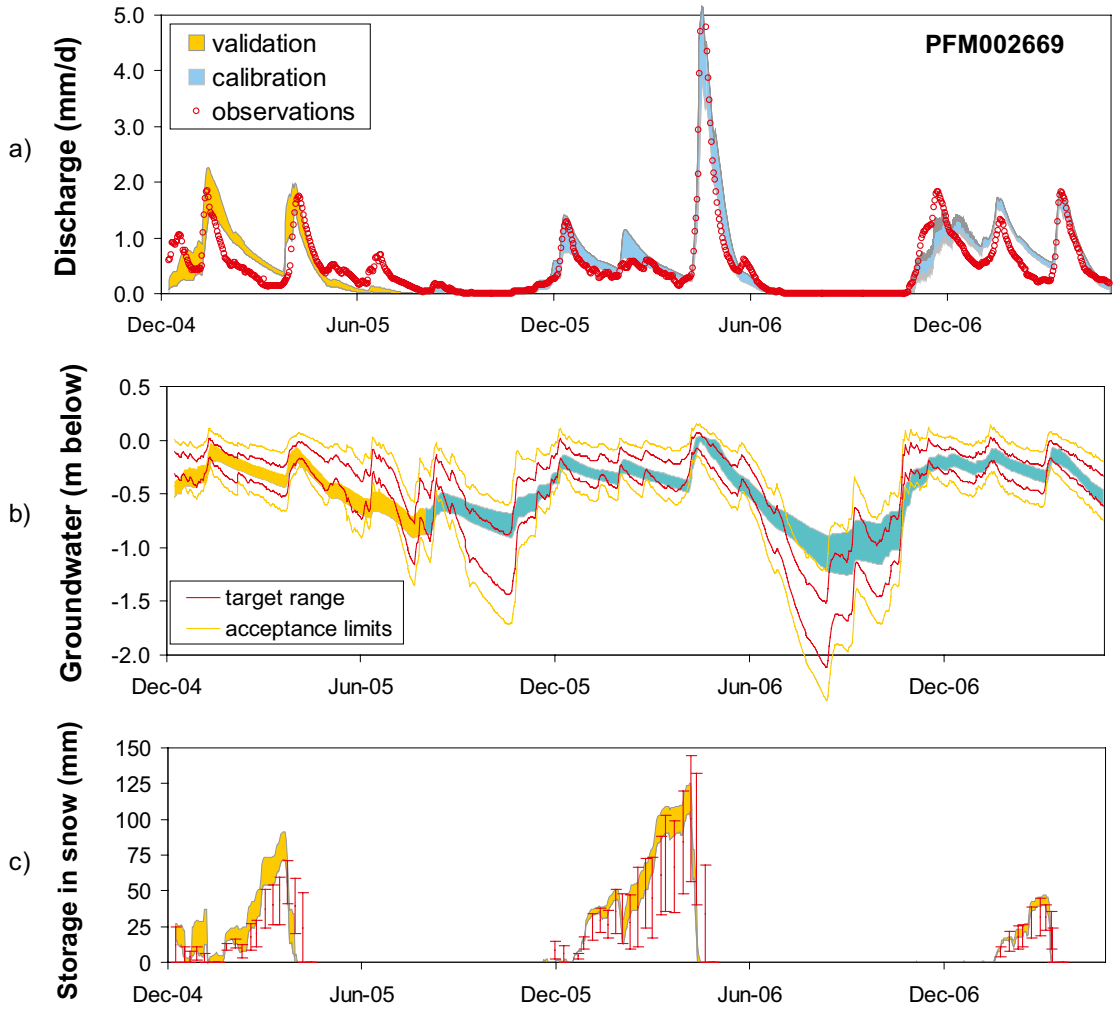

Figure 4-5. *Credibility bands and calibration targets for hydrological simulations of the PFM002669 catchment for a) discharge, b) catchment-average groundwater depth, and c) water storage in snow, see Figure 4-2 for explanations of "target range" and "acceptability range"in b) and the error bars in c).*

Table 4-4. Summary of performance indices for calibration and validation intervals.

Catchment	Interval	Nash-Sutcliffe efficiency (Discharge)	Cumulative flow error (%) (Discharge)	Window of Acceptability Score (Groundwater)
PFM005764	Calibration	0.82–0.90	4–15	0.83–0.92
	Validation	0.18–0.71	(–25)–1	0.75–0.94
PFM002667	Calibration	0.82–0.89	(–1)–15	0.74–0.86
	Validation	0.23–0.60	(–8)–23	0.67–0.95
PFM002668	Calibration	0.82–0.90	0–15	0.73–0.85
	Validation	0.46–0.79	(–11)–16	0.66–0.94
PFM002669	Calibration	0.83–0.92	2–15	0.76–0.89
	Validation	–0.40–0.37	(–14)–9	0.64–0.92

Cumulative flow error was constrained to be less than 15% for all accepted solutions as part of the acceptance criteria. Therefore, it is no surprise that the average cumulative flow error during the calibration interval was approximately +10% in all catchment simulations. During the validation interval, average cumulative flow errors were –14%, 10%, 3%, and –1% for PFM005764, PFM002667, PFM002668, and PFM002669, respectively. Therefore, although the N-S efficiencies were less satisfactory during the validation interval, the simulation errors appear more related to timing rather than quantity of discharges.

The largest discharge event in all four time series occurred during the late season snow melt in April 2006 (Figures 4-2a, 4-3a, 4-4a and 4-5a). This peak was more than two times larger than the next highest peaks in each catchment and was well simulated by Forsmark-HBV in all cases. This, however, is also not a surprise since since minimising errors in peak events is an efficient path towards maximising Nash-Sutcliffe efficiencies.

Interestingly, many other qualities of the discharge simulations amongst the four catchments are also quite similar. None of the simulated credibility bands completely enveloped the observed data for any catchment. The falling limb of the January 2005 snow melt event was consistently simulated for all catchments with a 1–2 week delay compared to the measured data. Conversely, the subsequent rising limb of the April 2005 snow melt event was consistently simulated with a several day lead compared to the data. The June 2005 rainfall event was underestimated in all catchment simulations. The rainfall-driven peak in December 2005 was generally well simulated in all catchments, but all catchment simulations created a peak in February 2006 that was not as prevalent in the measured data. As discussed above, the large late season snow melt event in April 2006 was well-simulated in all catchments. Both the rising and falling limbs of the rainfall-driven peak in December 2006 were lagging in the simulations compared to the data. The subsequent January 2007 snow melt event was not very well simulated in any of the catchments, but the final March 2007 snow melt looked better in all.

Simulated groundwater depths were also acceptable in all catchments (Figures 4-2b, 4-3b, 4-4b and 4-5b). The average score of the window of acceptability target, as described above, was 0.88, 0.80, 0.80, and 0.83 for PFM005764, PFM002667, PFM002668, and PFM002669, respectively. These scores suggest that on average between 80–88% of the simulated groundwater depths fell within the desired target range. Scores for the simulated groundwater depths were closer in calibration and validation intervals than they were for discharge (Table 4-4).The most noticeable issue in the groundwater simulations, and this was consistent amongst catchments, was that the depth of simulated groundwater during the dry summer seasons was substantially underestimated. For instance, the range of simulated groundwater depths in all catchments in August 2006 did not dip below approximately 1.1 m below ground, whereas the average observed data in each grouping of observed wells (Table 4-3) were often up to a full metre deeper.

Simulated water storage in snow also looked good compared to the measured data (Figures 4-2c, 4-3c, 4-4c and 4-5c). Recall that the snow data was not used for calibration and was for validation only. In all catchments, simulated water storage in snow was close to the upper boundary of the data range reported from the two measurement stations. The upper boundary in the measured data was in all cases from AFM000072. This station is an inland station located in the forest in very close proximity to the discharge gauging station at PFM005764 (see Figures 2-4 and 2-6). The other station is located closer to the sea. It seems sensible that the simulated water storage in snow closer followed the inland upstream station's data.

4.2.3 Parameter distributions

Figure 4-6 summarizes cumulative distribution functions (CDFs) calculated for each model parameter (see Table 4-1) from the subset of accepted behavioral parameter sets and for each catchment simulation. There are many interesting features of these distributions. Distributions for most parameters, with the exception of depth to dead zone (DZ), were refined during calibration (Figure 4-6); prior distributions would appear as corner-to-corner straight lines in these plots. In other words, the behavioral solutions demonstrated focused regions within the initial parameter ranges that produced the best simulations.

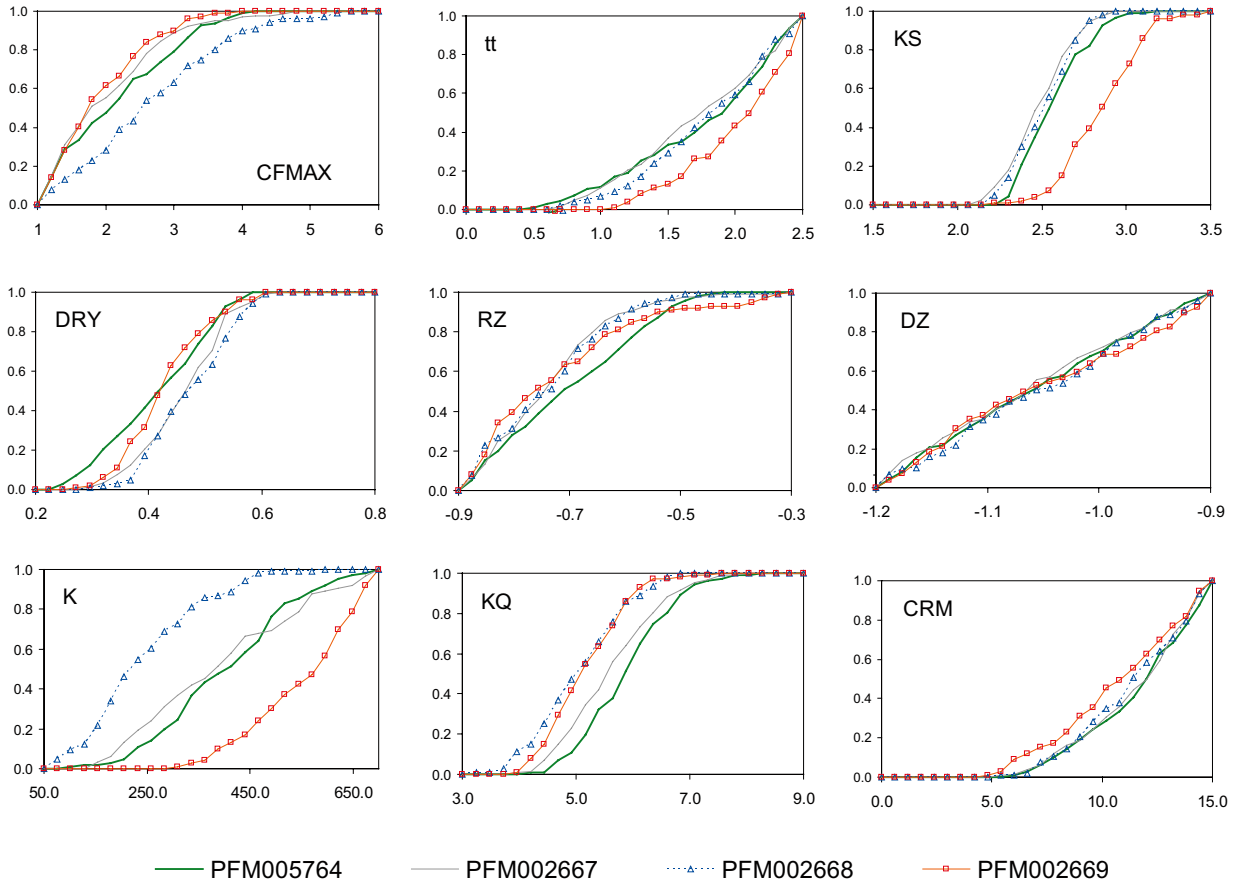

Figure 4-6. *Cumulative marginal probability distributions for the accepted behavioral model parameters for Forsmark-HBV from each catchment simulation.*

In the context of the model structure, differences in the hydrological performance of the four catchments seemed to be attributable to differences in four model parameters: the degree-day constant for snow melt (CFMAX), the inverse groundwater storage constant (KS), and the constant and exponent that defined the discharge relationship (K and KQ). This is evident in substantial differences in CDF's between catchments for these parameters. CDFs for the other five model parameters (tt, DRY, RZ, DZ, and CRM) were comparatively similar amongst catchments.

Interestingly, the parameter distributions for PFM005764 and PFM002667 were virtually indistinguishable for all parameters. This suggests very similar conditions in the catchments, which is sensible given that PFM002667 is nested within PFM005764 and comprises 54% of its area. PFM002668 is also nested within both PFM002667 and PFM005764, and parameter distributions were also quite similar here except for the two parameters that defined the discharge response, K and KQ. Perhaps these differences reflect the larger influence of the lake response (Lake Eckarfjärden) in the smaller PFM002668 catchment compared to the other two. Direct discharge from lakes was not explicitly modeled in Forsmark-HBV, and instead this response was aggregated within the storage-discharge equation (Figure 4-1).

PFM002669 also shared similar parameter ranges compared to the other three catchments, but differed substantially in terms of both the inverse storage constant (KS) and discharge scalar (K). It is difficult to assess these differences since the PFM002669 catchment contained no groundwater wells itself. Recall that the calibration target for simulated groundwater in this catchment was synthesized from a grouping of external wells (Table 4-3). Therefore, these differences could reflect either a rather sensible outcome if the synthesized calibration target was indeed fairly accurate, or a direct inference of an erroneous assumption regarding the synthesized calibration target. It is impossible to tell with no data for reference.

4.2.4 Simulated annual ET

Figure 4-7 shows simulation results for predicted annual ET on rolling basis for the four catchments. As above, results are presented as credibility bands produced from the range of predicted values in accepted simulations from the Monte Carlo runs. Annual totals are shown from January 2005 onward for consistent comparison amongst catchments.

As seen, annual total ET varies in time in all catchments, depending on the antecedent years' moisture conditions. The average annual total ET (calculated for all behavioral simulations and all annual totals between January 2004 and April 2007) was 400, 409, 413, and 396 mm/yr for PFM005764, PFM002667, PFM002668, and PFM002669, respectively. The average width of the credibility band around the mean predicted annual ET time series was 36, 43, 43, and 42 mm/yr, respectively, corresponded to approximately ± 5% uncertainty on the mean simulated series.

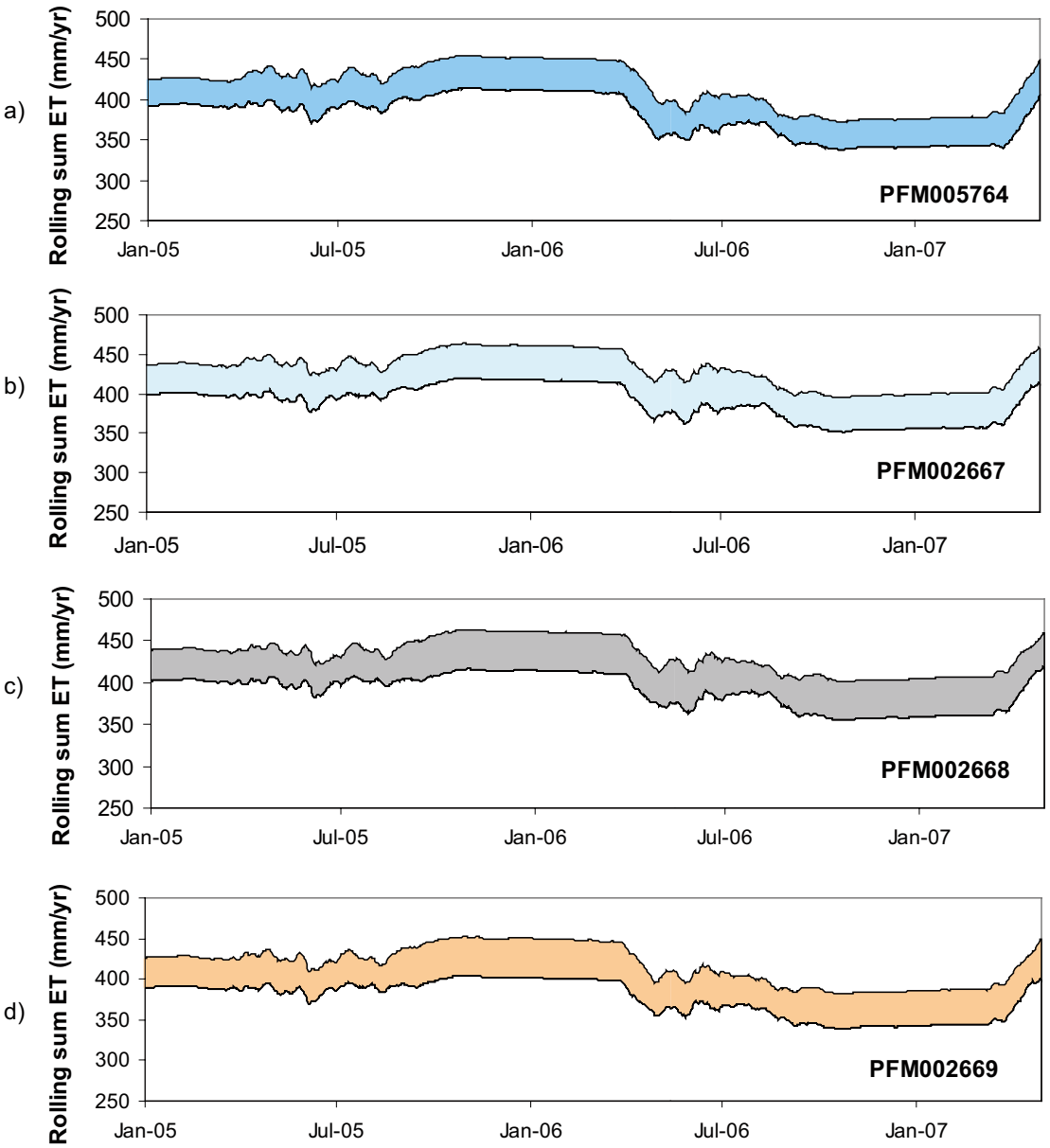

Figure 4-7. *Credibility bands for rolling annual total ET, as simulated for a) PFM005764, b) PFM002667, c) PFM002668, and d) PFM002669.*

4.2.5 Discussion

The Forsmark-HBV model provided good simulation results of discharge and aggregated groundwater responses in four catchments within the Forsmark study site. Discharge time series from the four catchments were simulated with Nash-Sutcliffe efficiencies that averaged 0.87 and groundwater time series were simulated with average acceptability scores of 0.83 (1.0 is max). Although there were consistent deficiencies amongst the four catchment simulations, seasonal and event dynamics in discharge and groundwater time series were generally very well-replicated by model predictions. This is a good result that reinforces the conceptual understanding of the near-surface hydrology in the area.

Calibration of the Forsmark-HBV model within the framework of an uncertainty analysis provided several important insights:

- Credibility bands on time series simulations showed remarkably consistent patterns for the four catchment simulations, in terms of well simulated behavior. The uncertainty analysis was a powerful tool for highlighting the positive aspects of the model capabilities.
- There were also consistent patterns of error in the simulations amongst catchments and this suggests structural errors in the model that may be amendable with future refinements. Indeed, all models introduce some form of error and here again the uncertainty analysis was a powerful tool for exposing those in Forsmark-HBV. Since some efforts have already been undertaken to optimize Forsmark-HBV (not reported here), it seems that these remaining issues may reflect the somewhat expected and inherent limitations of applying an aggregated, one-dimensional, 14-parameter model to complex catchment-scale responses.
- Distributions of parameters from accepted "behavioral" simulations were also remarkably similar amongst the four catchment simulations. This is a credible finding given the largely similar topographic and land cover characteristics in the catchments. Where parameter distributions differed amongst catchments, they differed in ways that seemed credible and that provided insight for explaining differing hydrological responses in the catchments.

An important question that remains after a modeling effort is to what extent additional data could help refine the model or decrease predictive uncertainty. Here, it seems doubtful that increased duration in the pre-existing time series would contribute significantly to resolving modeling errors or further reducing parameter uncertainties. On the other hand, if future efforts are planned for modelling on the catchment scale in the Forsmark study site, then an increased density of snow and/or near-surface groundwater monitoring points in the catchments of interest could indeed provide useful information for reducing uncertainty and possibly improving simulations. In particular, the Forsmark-HBV model would likely benefit from data collection focused to refine the storage-discharge relationship.

4.3 MIKE SHE modelling

In this section a summary of the MIKE SHE modelling conducted as a part of Forsmark SDM-Site is presented. For a detailed description of the modelling the reader is referred to /Bosson et al. 2008/. MIKE SHE is a dynamic, physically based, modelling tool that describes the main processes of the land phase of the hydrological cycle /DHI Software 2007/. It has been used in previous stages of the Forsmark and Laxemar-Simpevarp modelling for site descriptions and safety assessments, /Johansson et al. 2005, Bosson and Berglund 2006/ and /Werner et al. 2005ab/, respectively.

4.3.1 Overview of the modelling tool

The model structure of MIKE SHE is shown in Figure 4-8. In the model, precipitation can be either intercepted by vegetation or fall to the ground. The water on the ground surface can infiltrate, evaporate or form overland flow. Once the water has infiltrated into the soil, it enters the unsaturated zone. In the unsaturated zone, it can be either extracted by roots and leave the system as transpiration, or it can percolate down to the saturated zone. MIKE SHE is fully integrated with a channel-flow code, MIKE11. The exchange of water between the two modelling tools takes place during the whole simulation, i.e. the two programs run simultaneously.

MIKE SHE is developed primarily for modelling of groundwater flow in porous media. However, in the present modelling the fractured bedrock is also included. The bedrock was parameterised by use of data from the deep-rock modelling performed with the CONNECTFLOW modelling tool,which involved a transformation of data on fractures and deformation zones to a continuum ("porous medium") model /Follin et al. 2007a, 2008/. Hydrogeological parameters were imported from this continuum description in CONNECTFLOW, in some cases after up- or downscaling to overcome differences in grid resolution, to the elements in the MIKE SHE model /Bosson et al. 2008/.

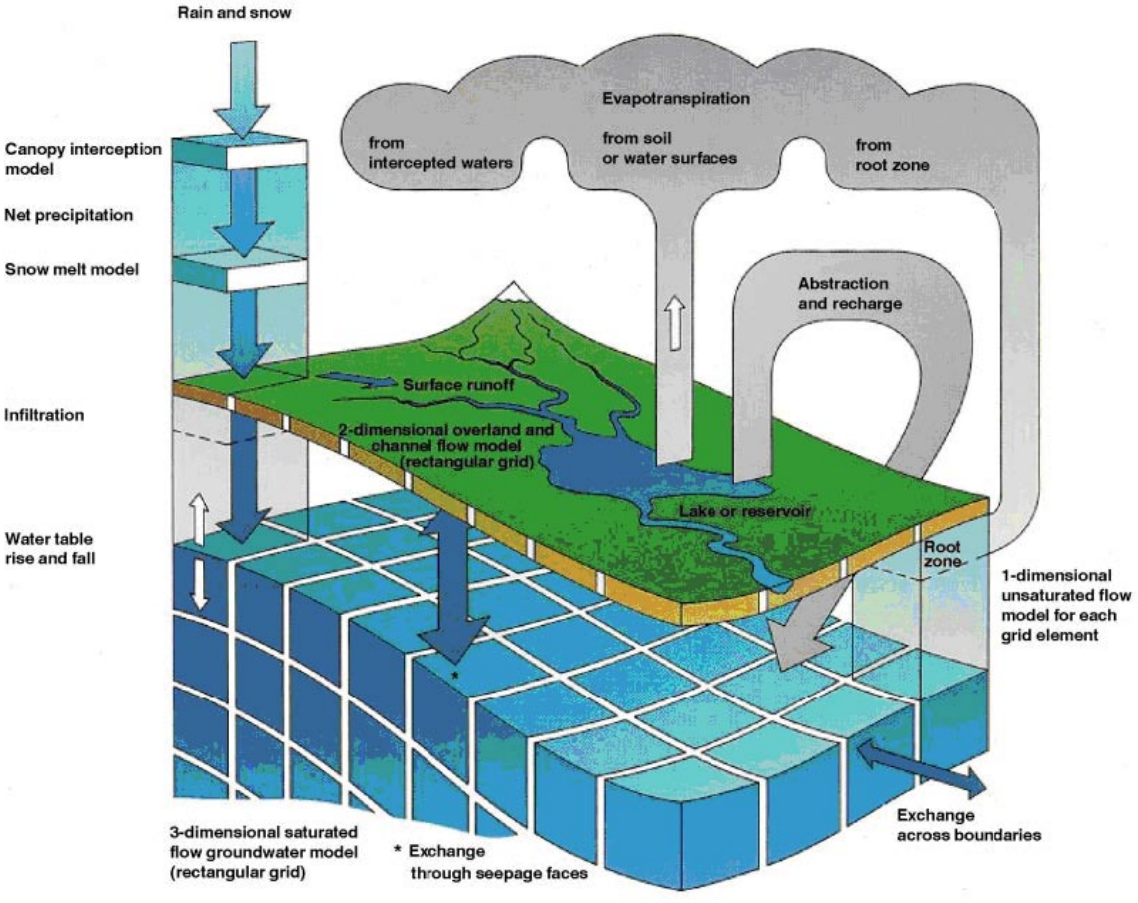

Figure 4-8. *Overview of the model structure and the processes included in MIKE SHE /DHI Software 2007/.*

MIKE SHE consists of the following model components:

- Precipitation (rain or snow).
- Evapotranspiration, including canopy interception, which is calculated according to /Kristensen and Jensen 1975/.
- Overland flow, which is calculated with a 2D finite difference diffusive wave approximation of the Saint-Venant equations, using the same 2D mesh as the groundwater component. Overland flow interacts with rivers, the unsaturated zone, and the saturated (groundwater) zone.
- Channel flow, which is described through the river modelling component, MIKE11, a modelling system for river hydraulics. MIKE11 is a dynamic, 1D modelling tool for the design, management and operation of river and channel systems. MIKE11 supports any level of complexity and offers simulation tools that cover the entire range from simple Muskingum routing to high-order dynamic wave formulations of the Saint-Venant equations.
- Unsaturated water flow, which in MIKE SHE is described as a vertical soil profile model that interacts with both the overland flow (through ponding) and the groundwater model (the groundwater table is the lower boundary for the unsaturated zone). MIKE SHE offers three different modelling approaches, including a simple 2-layer root-zone mass balance approach, a gravity flow model, and a full Richards's equation model. The last option was used in the present application.
- Saturated (groundwater) flow allowing for 3D flow in a heterogeneous aquifer, with conditions shifting between unconfined and confined. The spatial and temporal variations of the dependent variable (the hydraulic head) are described mathematically by the 3D Darcy equation and solved numerically by an iterative implicit finite difference technique.

The code used in this project is software release versions 2007 and 2008. For a detailed description of the processes included in MIKE SHE and MIKE11, see /Werner et al. 2005a, DHI Software 2007, 2008/.

4.3.2 Implementation of the field observation-based conceptual model

Model domain and grid

Most of the on-land part of the Forsmark regional model area is included in the MIKE SHE model area. However, the upstream (inland) boundary follows the surface water divide towards River Forsmarksån catchment, rather than the boundary of the regional model area. The MIKE SHE model area, which has a size of 37 km^2, is shown in Figure 4-9. It can be seen that the southwestern part of the regional model area is excluded, and that the eastern part of the candidate area also is outside the model area. The MIKE SHE model area extends some distance into the sea, but its offshore part is much smaller than that of the regional model area.

When defining the horizontal extent of the model area, the candidate area, the surface water divides, and the regional fracture zones were taken into consideration. The surface water divide towards River Forsmarksån is a natural boundary for the southwestern part of the model area. In addition, the field-checked catchment area boundaries were used to determine the position of the on-land part of the northwestern boundary. Previous particle tracking simulations, where particles have been released inside the area of the planned repository, indicated that the near-shore bays might be discharge areas for the repository. Therefore, it was decided to include parts of the sea in the model. The Singö deformation zone is a major hydrogeological structure at sea, and the MIKE SHE model area was extended approximately one kilometre beyond this zone. The main deformation zones, the Forsmark and the Eckarfjärden deformation zones in the southwest, and the Singö deformation zone (in the northeast at sea), are also shown in Figure 4-9. The reason for using the bedrock geology when defining the model boundaries is that the major deformation zones also constitute major hydrogeological structures, that may act as boundaries for horizontal flow and transport, see e.g. /Follin et al. 2007a/.

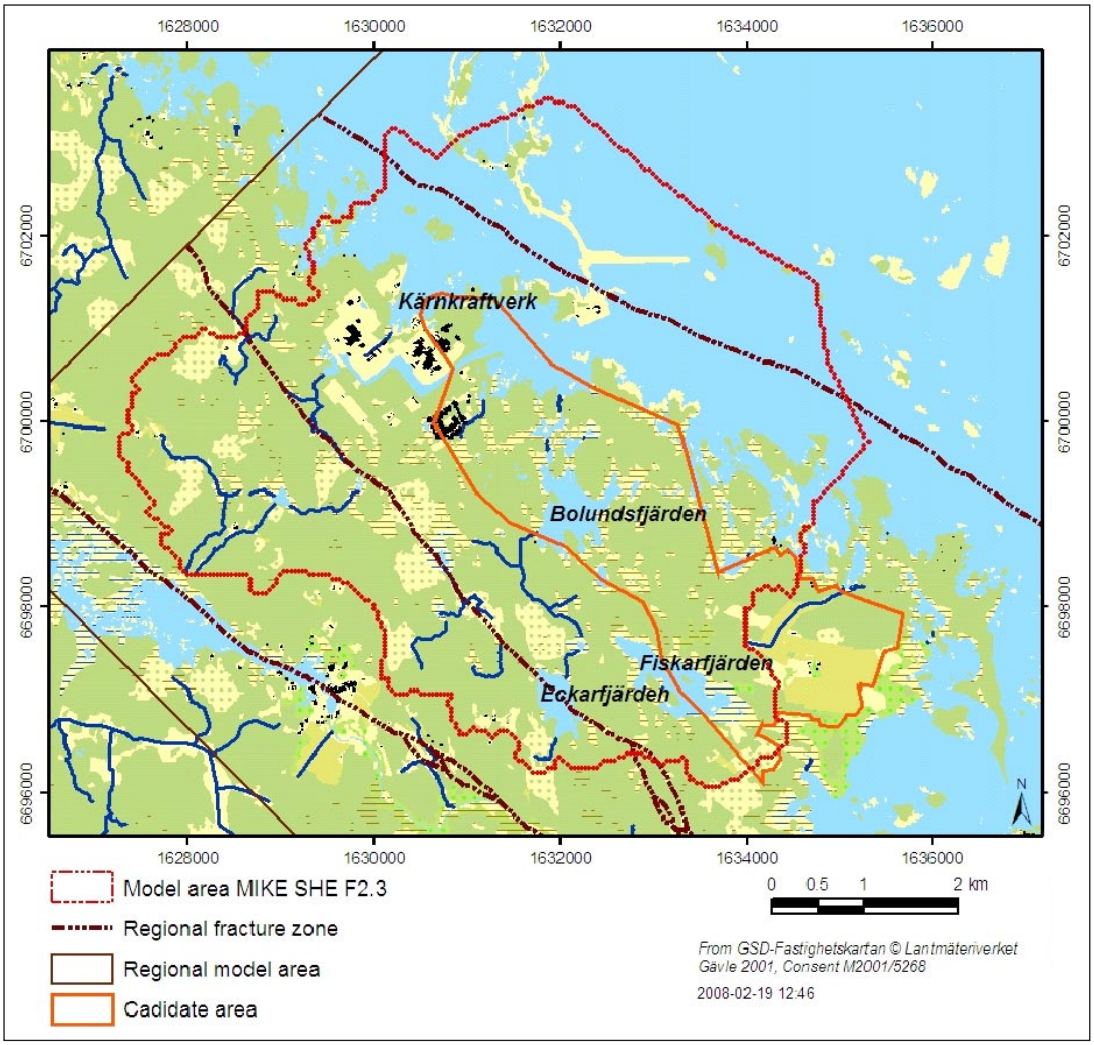

Figure 4-9. *The MIKE SHE model area, the regional model area in Forsmark and the candidate area. The regional deformation zones (from southwest to northeast: the Forsmark zone, the Eckarfjärden zone and the Singö zone) are marked in the figure /Bosson et al. 2008/.*

The vertical extent of the base setup of the model was from the ground surface down to 150 m.b.s.l. After analysing the effect of the position of the bottom boundary and the bottom boundary condition in a sensitivity analysis during the calibration process, it was decided to extend the final model down to 600 m.b.s.l.

The horizontal resolution of the calculation grid is 40 × 40 m in the whole model area, and it is applied to all of the flow components in MIKE SHE, i.e. the overland flow, the unsaturated zone (incl. evapotranspiration), and the saturated zone. The unsaturated zone, which is a 1D vertical model description, is however treated in a semi-distributed manner, see below. Hydrogeological input data for the bedrock and the Quaternary deposits, and geometrical data for the bedrock and QD-layers are given on a 20 m × 20 m grid. An arithmetic mean of four data points is used in the pre-processing of data converting the 20 × 20 m grid to the 40 × 40 m model grid.

The vertical resolution varies with depth, both for the unsaturated and the saturated zone, according to the description below. The vertical geologic distribution is interpolated to the vertical grid as follows:

- In each horizontal model grid cell, the vertical geological model is scanned downwards and the properties from the geological model are assigned to the cell. The properties are based on the average of the values found in the cell, weighted by the thickness of each geological layer /DHI Software 2007/. For the vertical hydraulic conductivity a harmonic mean is used.
- In the Quaternary deposits several geological layers might be included in the same calculation layer. The calculation layers in the bedrock follow the geological layers given in the CONNECTFLOW modelling /Follin et al. 2008/.

Boundary conditions, initial conditions and time step

The groundwater divides are assumed to coincide with the surface water divides, see Figure 3-4. Thus, a no-flow boundary condition is used for the on-land part of the model boundary. The sea forms the uppermost calculation layer in the off-shore parts of the model. Since large volumes of overland water can cause numerical instabilities, the sea is described as a geological layer consisting of highly permeable material. The hydraulic conductivity of this material is set to 0.001 m/s. The sea part of the uppermost calculation layer has a head boundary condition. The measured sea level time series are used as input data.

The top boundary condition is expressed in terms of the precipitation and potential evapotranspiration.The precipitation is assumed to be uniformly distributed over the model area, and is given as a time series. The actual evapotranspiration is calculated during the simulation.

In the base set up, the bottom boundary condition was a fixed-head condition at 150 m.b.s.l. Model results from the Forsmark 2.2 CONNECTFLOW groundwater flow modelling /Follin et al. 2007a/ were used as input data when setting the bottom boundary condition. The calculated hydraulic head from 150 m.b.s.l. was imported to the MIKE SHE model. The time step used in the CONNECTFLOW simulations was much longer than that in the MIKE SHE modelling, which implies that short-term temporal variations cannot be captured. Thus, the bottom boundary condition in the MIKE SHE model was assumed to be constant with time. In later simulations a no-flow boundary was set at 600 m.b.s.l.

The calibration period is from May 15, 2003, through July, 2005. The simulations use a so called hot start, which constitutes the initial conditions. Data representing the May 4, 2005, were sed as initial conditions. The initial conditions were updated before the final version of the model was run.

In MIKE SHE, a maximum time step is defined for each compartment of the model. During the simulation the time step may be reduced. The maximum time steps for each compartment are listed in Table 4-5.

Table 4-5. Maximum time steps for the different compartments of the MIKE SHE-MIKE 11 model /Bosson et al. 2008/.

Compartment	Maximum time step
Over land	1 h
Unsaturated zone	1 h
Saturated zone	3 h
MIKE 11, water courses	5 s

Geometrical and hydraulic properties of objects/flow domains

Streams and lakes

The length of the surface stream network described in MIKE11 is c. 20 km, which is divided into 96 calculation nodes for discharge and 119 calulation nodes for the water level. This gives an average length between calculation nodes for flow of 208 m and for water level 168 m. Cross-sections are given at the majority of the head calculation nodes.

The surface stream network in MIKE11 is laterally communicating with the overland flow component and the saturated zone in MIKE SHE. Lakes are not geometrically specified in the model input, but are created during the simulation by ponding water in topographical depressions.

Unsaturated zone

In order to speed up the simulation, only a number of grid cells are simulated in the unsaturated zone. The selection is done through a special classification system where the unsaturated zone columns having the same conditions (i.e. the same land use, soil profile, and approximate groundwater depth) are grouped together. From each group, only one column, randomly selected, is simulated. In the Forsmark model, an exception from this is made in areas with ponding water on the surface, i.e. lakes and wetland areas, excluding the sea. In these areas, the unsaturated zone simulation is executed in all grid cells.

The vertical discretization is the same for all soil profiles, see Table 4-6.

Saturated zone

MIKE SHE distinguishes between geological layers and calculation layers. The geological layers (cf. Section 3.1, Figure 3-1, Section 3.2.1, Figure 3-2 and Table 3-1, and Section 3.4.2) are the basis for the model parameterisation, which means that the hydrogeological parameters are assigned to the different geological layers. The calculation layers are the units considered in the numerical flow model. In cases where several geological layers are included in one calculations layer, the properties of the latter are obtained by averaging of the properties of the former. The base set up of the present model consisted of 10 calculation layers (total model depth 150 m). During the calibration process, the vertical extent of the model was increased. The final model consisted of 14 calculation layers and had a total depth of c. 600 m.

In general, the calculation layers follow the geological layers. However, the Quaternary deposits and lake sediments are included in the two uppermost calculation layers. The uppermost calculation layer has a minimum thickness of two metres (2.5 metres in the final simulations) and the other calculation layers have a minimum thickness of one metre. The lake sediments are included in the uppermost calculation layer, thus if the thickness of the lake sediments are more than two metres (2.5 metres), the lower level of calculation layer 1 follows the lower level of the lake sediments (cf. Figure 3-2).

Table 4-6. Vertical discretization of the unsaturated zone (metres) /Bosson et al. 2008/.

From depth	To depth	Cell height	Number of cells
0	1	0.1	10
1	5	0.5	8
5	10	1	5
10	20	2	5

In the sea, the lower boundary of the uppermost calculation layer follows the sea bottom. Modelling large volumes of overland water is very time-consuming in MIKE SHE and may cause numerical instabilities. Therefore, the sea is described as a geological layer filled with gravel of high hydraulic conductivity. The "sea-gravel" is present from the sea bottom up to the level of the lowest measured sea-level during the simulation period.

The "sea-gravel" is included in the uppermost calculation layer; therefore, the model topography is flat at the sea. The reason why the minimum sea level is chosen as the upper limit for the "sea gravel" is that the littoral zone in the model should be able to vary with time. When the measured sea level rises above the minimum sea level, overland water is built up in the littoral zone and the water level/the sea can rise and move towards land during periods of high water levels.

The model topography (i.e. the upper boundary of the uppermost calculation layer) is defined as follows:

If DEM (Digital elevation model) > minimum sea level → Topography = DEM
If DEM < minimum sea level → Topography = minimum sea level

The part of calculation layer 1 containing the sea has an internal boundary condition with a prescribed time-varying head given by the measured sea-level. Since the internal boundary is set from the sea bottom up to the minimum sea-level, the littoral zone may vary during the simulation. The lower layer of calculation layer one is calculated in six steps:

1. If lake sediment is present → Lower level = Lower level of L3.
2. If **Topography** > minimum sea level → Lower level = Topography – 2 m.
3. If **Topography** < minimum sea level → Lower level = Sea bottom (DEM).
4. Calculate the thickness, T, of calculation layer one based on step 1 and 2.
5. Correct for the littoral zone: If T < 2 m → set T to 2 m.
6. Lower level of calculation layer 1 = **Topography** – T

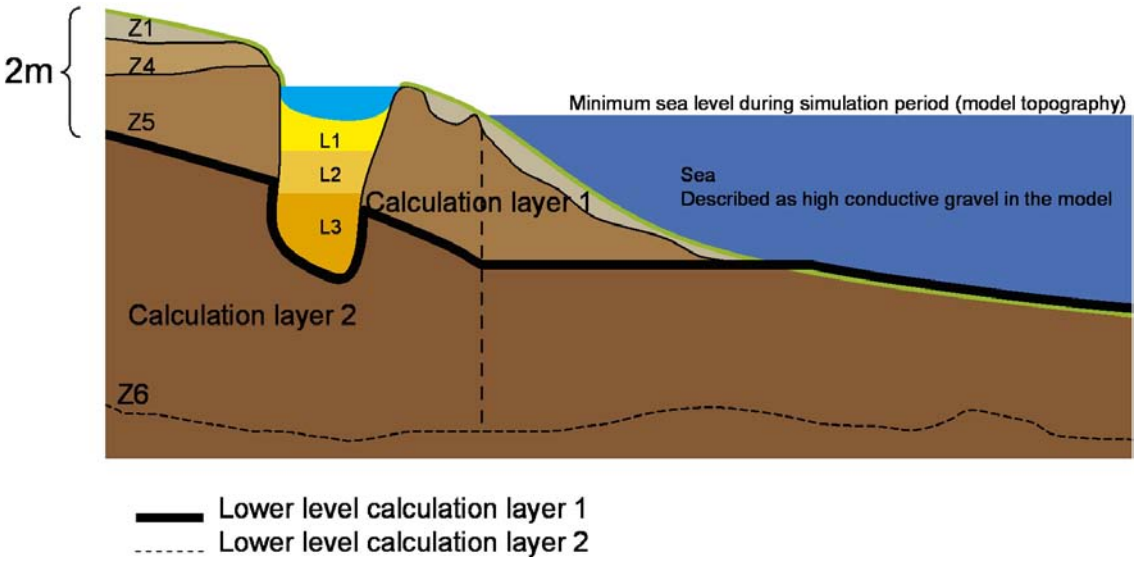

Figure 4-10. *Illustration of the calculation layers in Quaternary deposits /Bosson et al. 2008/.*

The lower layer of calculation layer 2 follows the lower level of Z6, with the condition that the minimum thickness of the layer has to be one metre. In areas where the thickness is less than one metre, calculation layer 2 enters the uppermost geological bedrock layer (with a maximum of one metre). Since all the geological bedrock layers are 20 m or thicker, the impact from calculation layer 2 is only affecting the uppermost bedrock layer. For all the other bedrock layers geological layers and the calculation layers coincide.

4.3.3 Calibration and sensitivity analyses

A summary of the calibration and sensitivity analyses is given below. For a more detailed description the reader is referred to /Bosson et al. 2008/.

Strategy and procedure

The calibration and sensitivity analyses were performed in *two phases*. Figure 4-11 summarises the calibration process and all the steps taken to reach the final calibrated model of *Phase 1*. The period May 15, 2003, through July, 2005, was used for calibration while Aug., 2005 through March, 2007, was used for validation.The procedure was an iterative process since each action taken resulted in changed conditions in many processes. Figure 4-11 illustrates the main sub-versions of the model during *Phase 1*, main actions taken in each step, and the target of each calibration step.

An extensive sensitivity analysis was conducted. Since the focus of the MIKE SHE modelling was to describe the dynamics of the surface waters, the groundwater - surface water interaction, and the near surface groundwater dynamics, the sensitivity analysis was focused on the hydraulic properties of the Quaternary deposits and the unsaturated zone parameters. Only a few sensitivity simulations were performed in order to analyse the hydraulic properties of the bedrock. The model was, however, not calibrated to the results of these analyses of the bedrock, i.e. the hydraulic properties of the bedrock was not updated even if some sensitivity cases generated better results compared with observed groundwater levels in the bedrock than the original properties.

In the middle of the calibration process of *Phase 1* a new version of the bedrock hydrogeology dataset with lower conductivity values of the rock was delivered. The vertical flow through the bedrock had so far in the modelling process supplied water to the surface and contributed to the discharge in the brooks. Once the new conductivity values were implemented, the surface water discharge was reduced. Previous analyses had shown that the only way to reach a considerable increase of the surface water discharge was to decrease the potential evapotranspiration. The main reason for this is that wetlands dominate the area, which means that the modelled actual evapotranspiration can be expected to be controlled by the potential evapotranspiration. Thus, the potential evapotranspiration was reduced by 15% compared to the original values, as illustrated by the dotted arrows in Figure 4-11.

Five main sub models were defined during the calibration process of *Phase 1*. The *Base model,* the *Base case surface water* with updated parameters as a result of the analysis of the surface water dynamics, the *Base case groundwater* containing updated properties of the till and the surface bedrock, and the *Base case groundwater 2* containing the updated version of the bedrock properties and the additional reduction of the potential evapotranspiration. *The Final calibrated model* is the resulting model after all the sensitivity analyses and calibration steps. This model was validated using data from the period Sep, 2005, through March, 2007.

In the final calibrated model of *Phase 1*, there were still some discrepancies compared with the conceptual model and field observations which were considered to be important:

- the underestimated and delayed surface water dynamics in the spring and autumn of 2006,
- the dynamics of groundwater levels in some wells in Quaternary deposits in the summer of 2006,
- the overestimated groundwater levels in the bedrock.

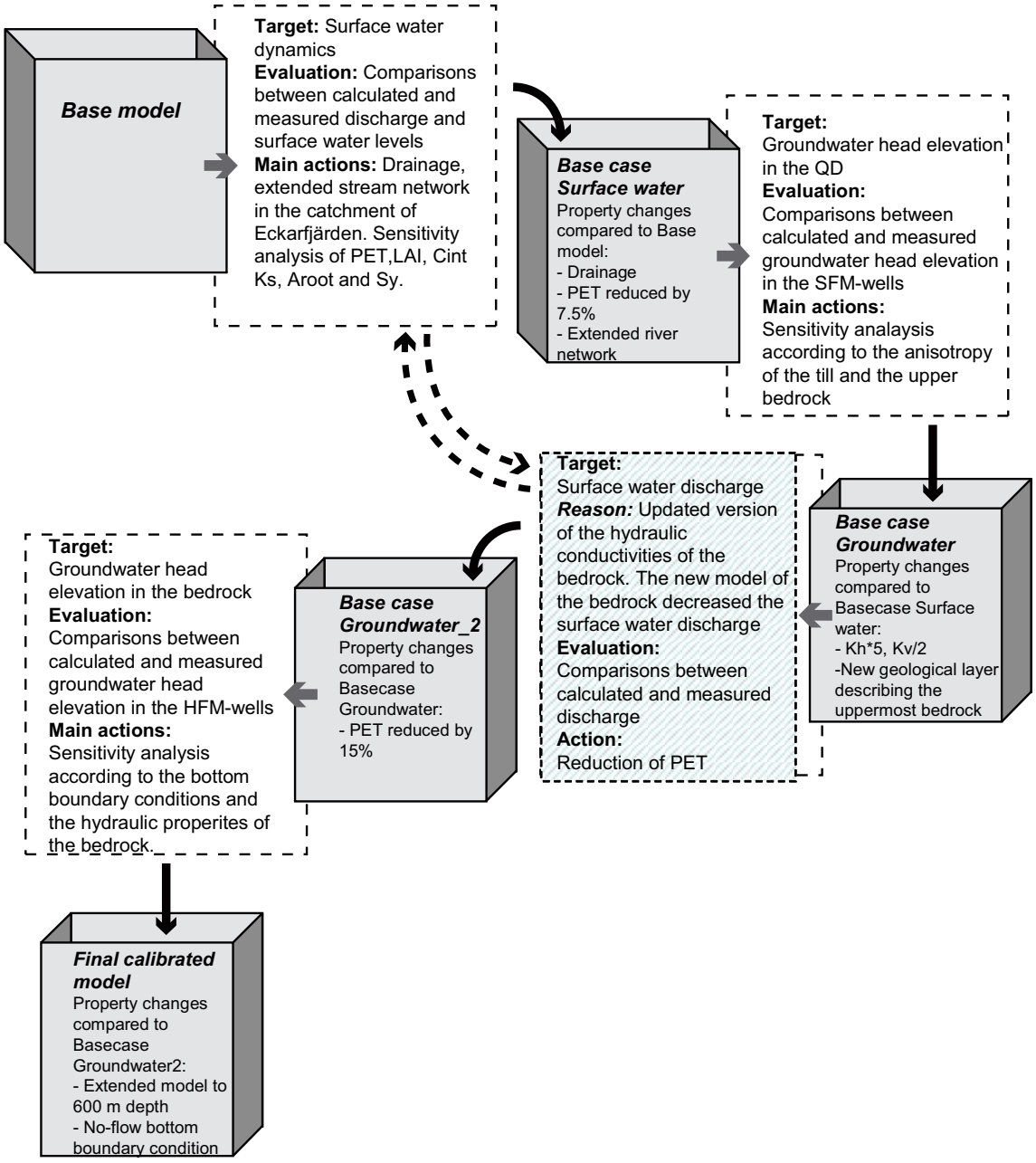

Figure 4-11. *Summary of the calibration steps and sensitivity analysis performed in order to reach the Final calibrated model of Phase 1 /Bosson et al. 2008/.*

The overestimation of the groundwater levels in the bedrock (mean absolute error: 0.75 m) was considered the most important of these discrepancies. This deviation implied that in some central parts of the site investigation area the model showed upward flow from the bedrock to the Quaternary deposits, whereas the field observations indicated the opposite. Thus the model indicated discharge areas and the measurements recharge areas. Furthermore, the model was not able to simulate the pumping tests in HFM14 in an acceptable way; the responses were too slow and too small.

It was therefore decided to perform complementary calibration and sensitivity analyses in a *Phase 2*, see Figure 4-12. Furthermore, in *Phase 2* a new revised model of the stratigraphy and depth of the Quaternary deposits was implemented, see /Hedenström et al. 2008/. However, since it was found that the revision of the QD model had only small effects on the results /Bosson et al. 2008/, the effect of the revised model is not discussed in detail here.

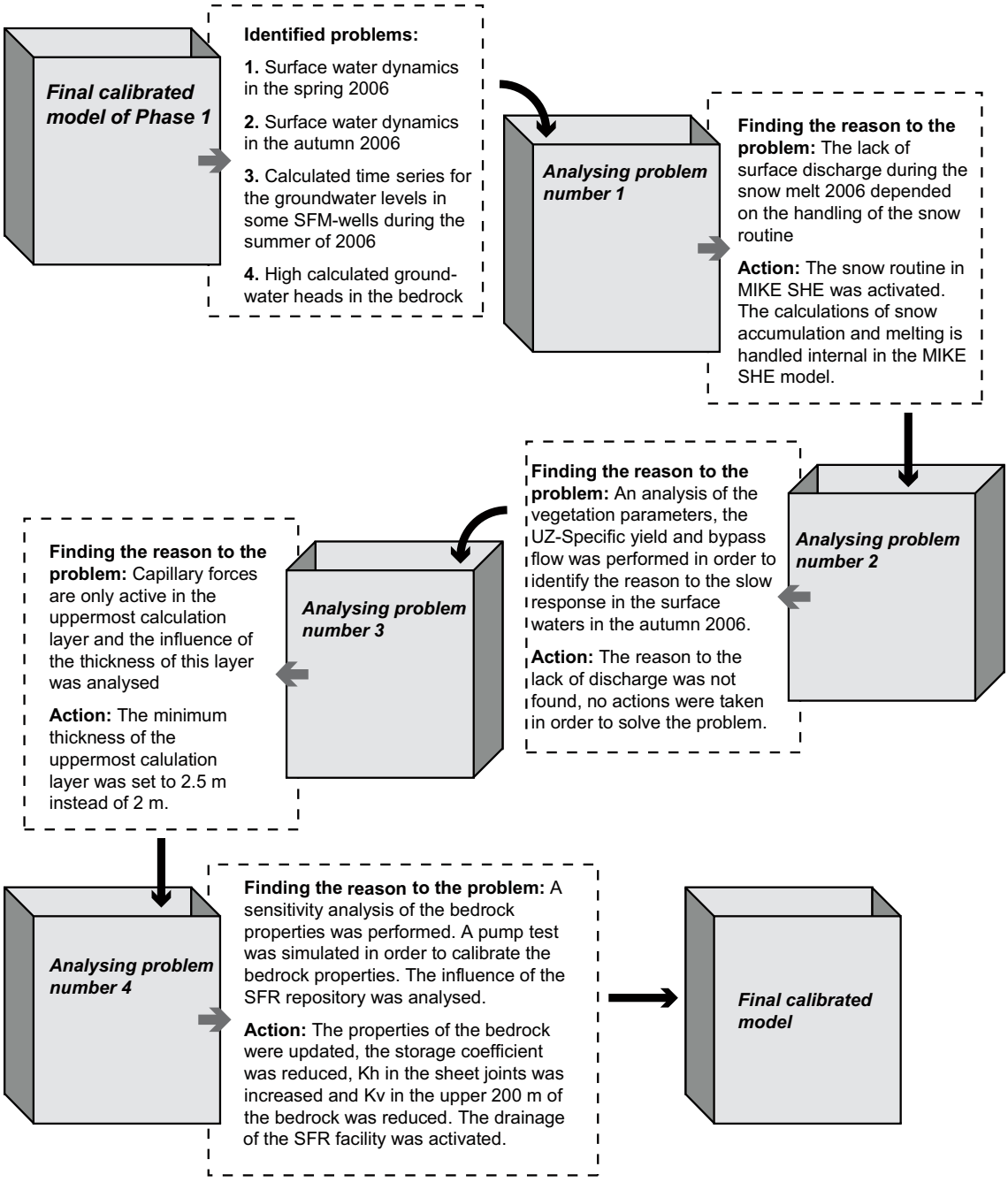

Figure 4-12. *The calibration steps and sensitivity analyses performed in Phase 2 in order to improve the agreement between simulated and observed surface water dynamics in the summer and autumn of 2006, groundwater dynamics in QD in the summer and autumn of 2006, and groundwater levels of the bedrock (after Bosson et al. 2008/.*

Boundary conditions

One important discovery in the calibration process was the outcome of the analysis of the bottom boundary condition. This analysis showed that the bottom boundary condition used in the base setup of the model generated input of water to the model, resulting in too high vertical groundwater fluxes, compared with the CONNECTFLOW simulations, and too high groundwater elevations in the bedrock. After this analysis the model was extended to 600 m depth and a no-flow boundary was used at the bottom of the model.

The effect of different bottom boundary conditions on the vertical flow is shown in Figure 4-13. The percolation from the unsaturated zone to the saturated zone was not influenced by the bottom boundary condition and the groundwater conditions in the Quaternary deposits seemed to be independent of the bottom boundary condition of the model. However, the vertical flow in the bedrock was highly dependent on whether there was a no-flow boundary or an open (prescibed head) boundary at the bottom of the model. The calculated vertical groundwater fluxes in mm/year at the depth 150 m.b.s.l. are presented in Figure 4-13. In the model *Base case groundwater 2* of *Phase 1,* the net vertical flow was 11 mm/year directed upwards. The corresponding net calculated flow at the same depth in CONNECTFLOW modelling was almost zero, 1 mm up and 1 mm down. When a no-flow boundary at 600 m depth was introduced in the MIKE SHE model almost the same flux was obtained at 150 m depth as in the CONNECTFLOW modelling.

The fact that the best overall performance was obtained for the model with a no-flow boundary at 600 m.b.s.l. implied that the original approach to couple the deep hydrogeological model (CONNECTFLOW) and the near-surface groundwater model (MIKE SHE) by a prescribed head at the bottom boundary of the latter was abandoned. Instead, the coupling is obtained by comparing the calculated fluxes in the bedrock at 150 m.b.s.l. and updating the MIKE SHE model to improve the agreement, if needed.

Surface water

Phase 1

Simulated lake water levels were in good agreement with observed levels already for the *Base model*. However, initial simulations by the *Base model* showed a lack of runoff in the surface water system for all stations, especially for the surface discharge station at the outlet of Lake Eckarfjärden. Also, the discharge peaks were too narrow, i.e. the model response was too quick. Furthermore, in contrary to the field-based conceptual model, substantial overland flow appeared in the simulations.

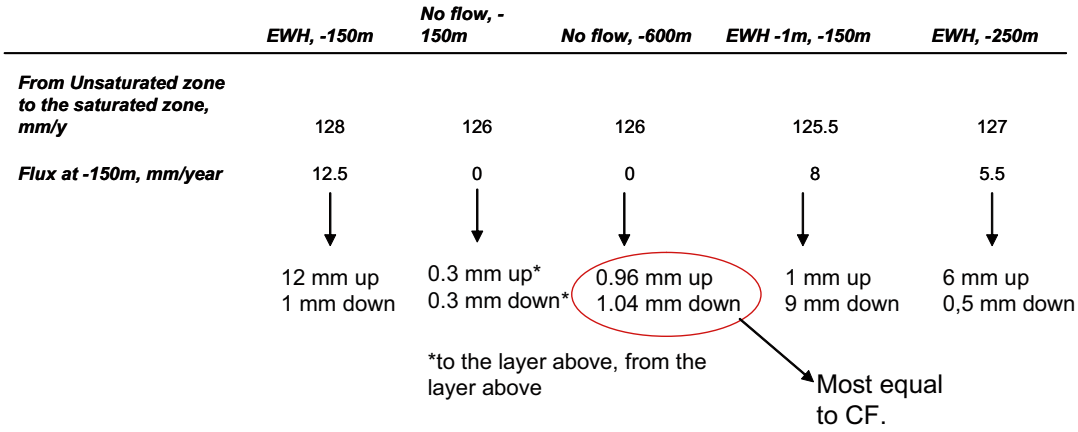

Figure 4-13. *Vertical flux, in mm/year, at the depth of 150 m in the Base case groundwater 2 model of calibration phase 1 (EWH=environmental water head) /Bosson et al. 2008/.*

The calibration and sensitivity analysis contained the following steps:

- variation of the Manning number (to investigate the reasons for the too quick discharge responses),
- activation and calibration of a sub-surface drainage function at a depth of 0.5 m below ground to enhance the hydraulic conductivity of the uppermost part of the QD profile (to study the influence of allowing a quick discharge response generated by an increase in groundwater levels instead of overland flow),
- extension of the MIKE 11 stream flow system upstream Lake Eckarfjärden (the simulated discharge from Lake Eckarfjärden was much too low indicating that water was diverted to areas downstream of the discharge station at the outlet of the lake),
- sensitivity analyses of the vegetation parameters root distribution, interception storage and leaf area index (to investigate possible reasons for the lack in surface discharge quantities),
- sensitivity analysis testing a reduction of the potential evapotranspiration (to investigate possible reasons for the underestimated surface discharge).

In summary the changes made from the base model to the *Base case surface water* were:

- inclusion of subsurface drainage as a representation of high-conductive top soil layers,
- extension of the surface stream network upstream Lake Eckarfjärden,
- reduction of the potential evapotranspiration rates (with 7.5%).

Phase 2

During the model validation procedure of the final calibrated model from *Phase 1*, two major problems were identified: the underestimation of the surface discharge during the fast and distinct snowmelt in the spring of 2006 and the inability to simulate the first run-off event in the autumn after the dry summer of 2006, see Figure 4-14 where an example from PFM005764 (upstream of Lake Bolundsfjärden) is shown. During the snowmelt in April 2006, approximately 30% of the observed run-off was not captured by the model. The response of the surface water dynamics in the model was somewhat slow and only 50% of the first run-off in the autumn was captured. The same pattern was shown at all discharge stations.

In *Phase 1*, the description of snow accumulation and melting was managed outside the MIKE SHE model code by a simple degree-day approach. In this approach, accumulation and melting started at certain temperature thresholds and a certain melting intensity (the degree-day-coefficient) was applied, see /Juston et al. 2007/. The output from this snow routine was used as precipitation input in MIKE SHE. However, it was discovered that this procedure gave too large evaporation losses from intercepted water. Because of this, the approach for snow handling was changed to be included and managed fully by the MIKE SHE code.

The snow routine inside MIKE SHE is also based on the degree-day method, but melted water from the internal snow routine goes directly to the ground surface in the model, without passing the canopy storage, and consequently without any interception losses. In the MIKE SHE model version 2008 used in *Phase 2* /DHI Software 2008/, the description of snow melt also includes a possibility to set a maximum wet snow fraction. The wet snow fraction is the amount of wet snow divided by the total amount of snow storage. When the maximum wet snow fraction is exceeded, any excess melted snow will be converted to ponded water. The ponded water is then available for infiltration, evapotranspiration, or overland runoff.

Simulated discharge peaks in April 2006 are shown in Figure 4-15 for PFM005764, the station immediately upstream of Lake Bolundsfjärden. Now the simulation of the peak, including the snow fraction parameter, was acceptable containing approximately the correct volume of water but still the peak was somewhat delayed.

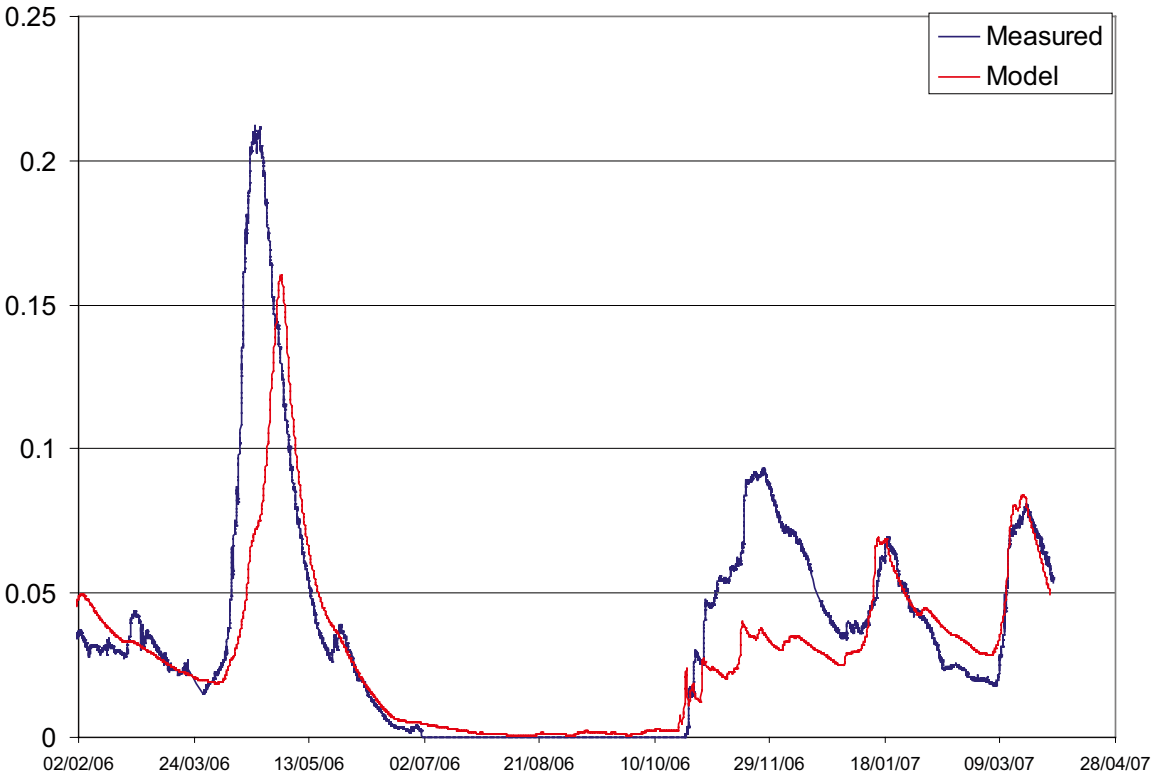

Figure 4-14. *Discrepancy between measured and calculated discharges by the Final calibrated model of Phase 1 in PFM005764, upstream Lake Bolundsfjärden /Bosson et al. 2008/.*

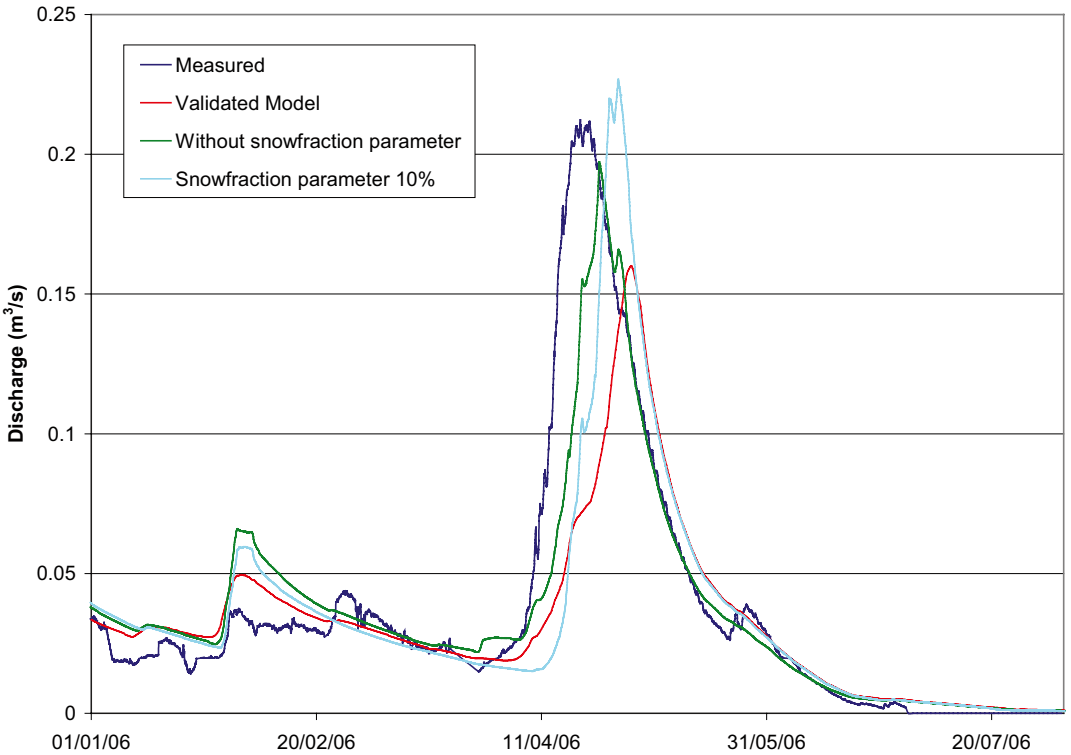

Figure 4-15. *Measured and simulated discharge peaks at the station PFM005764, immediately upstream of Lake Bolundsfjärden. The addition of the snow fraction parameter considerably improved the simulation /Bosson et al. 2008/.*

After the dry summer of 2006 the model response to the rain seems to be too slow with regard to the surface water discharge. Several sensitivity simulations were performed in order to improve the model response after the summer, including by-pass flow in the unsaturated zone, changes in leaf area index and decrease of specific yield. However, none of the simulations resulted in any significant improvement of the first surface discharge peak after the summer. Figure 4-16 shows the results from the sensitivity analysis for the gauging station immediately upstream of Lake Bolundsfjärden. All the stations showed similar patterns.

Groundwater

Phase 1

Most of the area is covered by a layer of till. Hence, a sensitivity analysis of the conductivity of the till layer was an important step in the groundwater modelling, including the introduction of an anisotropy (in the original model setup the vertical and horizontal conductivities were set equal). An introduction of an anisotropic hydraulic conductivity in the Quaternary deposits is in line with the indications found in the site specific measurements presented in Section 3.4.1 under *Hydraulic properties*.

When evaluating the results from the simulations it was noted that the *Base model* was not describing the dynamics of the groundwater correctly in areas with bedrock outcrops or in areas with a thin QD layer. According to the CONNECTFLOW model /Follin et al. 2008/, this layer describes the bedrock in an appropriate way from approximately 20 m below ground surface up to 4 m below ground surface. It was decided to make a test with an additional, thinner layer in the uppermost bedrock.

The head values at the bottom boundary in the original model were fresh water head values. To see the impact of using fresh water head or environmental heads on the simulation results, simulations were made with both types of head bottom boundaries. Based on the earlier

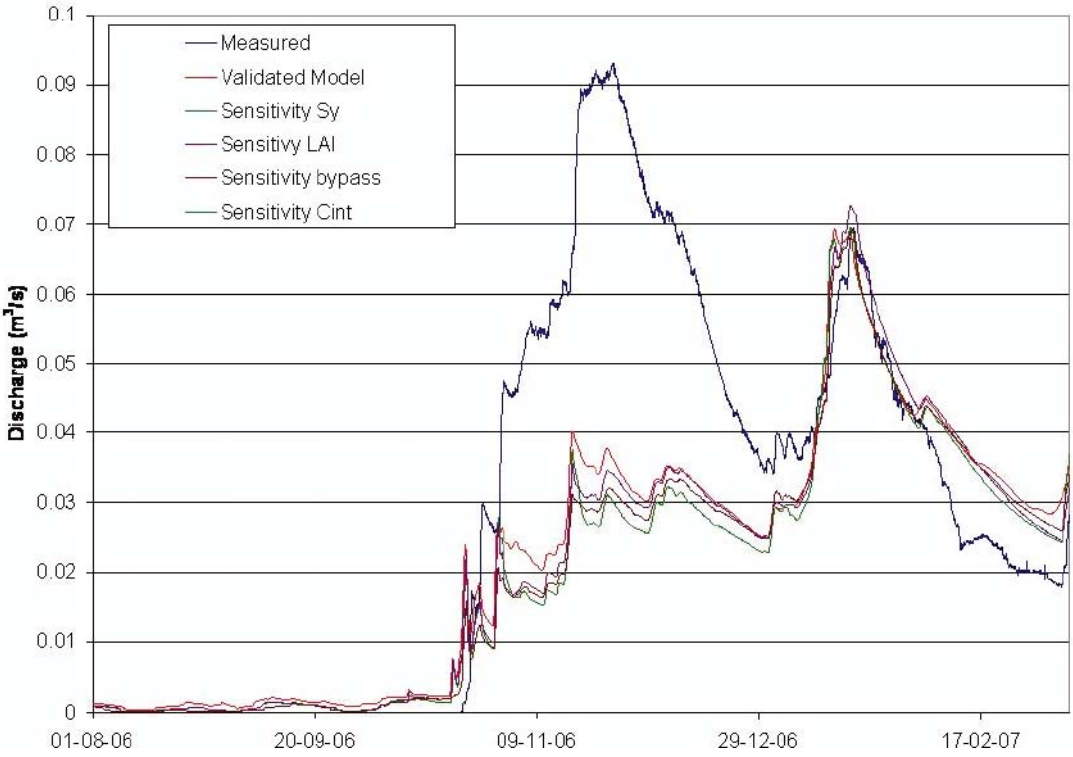

Figure 4-16. *Results from the calibration and sensitivity analyses conducted to improve the simulation of the discharge peaks in the autumn of 2006 at PFM005764, immediately upstream of Lake Bolundsfjärden /Bosson et al. 2008/.*

sensitivity analysis of till hydraulic conductivity and the unsaturated zone specific yield it was indicated that different monitoring points react differently in the sensitivity analysis. Hence, a regionalisation of the these parameters was tested.

When the calibration proceeded to the groundwater levels in the bedrock, a new version of the data set for hydraulic conductivities, porosities and calculated heads was delivered from the CONNECTFLOW modelling /Follin et al. 2008/. The new lower vertical hydraulic conductivities resulted in a reduced vertical flow in the bedrock and in a reduced discharge in the brooks.

Based on the above-mentioned observations, the calibration and sensitivity analysis of the groundwater components of the model contained the following steps:

- Test of an anisotropy in the hydraulic conductivity of the Quaternary deposits.
- Test of the effect of the introduction of a new geological layer describing the uppermost bedrock in areas with a thin overburden.
- Simulations in order to evaluate the sensitivity of the different bottom boundary heads and the hydraulic conductivity of the new surface bedrock layer.
- Test of a regionalisation of the hydraulic conductivities and specific yield of till.
- Test of further reduction of potential evapotranspiration to compensate for decreased surface discharge due to the lower vertical hydraulic conductivities of the new hydrogeological bedrock model.
- Test of a no-flow boundary at 600 m.b.s.l.

The calibration and sensitivity analysis gave as a result that the following changes were made in the calibrated *Base case groundwater* model:

- Introduction of hydraulic anisotropy in saturated zone QD layers (horizontal conductivities increased by a factor 5 of and vertical hydraulic conductivities reduced by a factor of 2).
- Introduction of a new surface bedrock geological layer (isotropic conductivity with $K_h = K_v = 1 \cdot 10^{-7}$ m/s).
- Regionalisation of till hydraulic conductivities and specific yields with increased values at locally elevated areas in the vicinity of SFM0004, SFM0005 and SFM0009, and in the catchment of Lake Eckarfjärden (the horizontal hydraulic conductivity in the till was increased by a factor of 10 and the specific yield was increased by a factor of 1.5).
- Implementation of a new version of the data set for hydraulic conductivities, storage properties, and calculated heads in the bedrock.
- Reduction of the potential evapotranspiration by 15% compared with the original SMHI dataset.
- Extention of the model by moving the bottom boundary to 600 m.b.s.l. where a no-flow boundary was applied.

A final sensitivity analysis in *Phase 1* was conducted with regard to the hydraulic parameters of the bedrock. Five sensitivity cases were defined in which the horizontal and/or vertical hydraulic conductivities were changed; two cases where all the geological layers concerning the bedrock were modified and three cases where the hydraulic properties of the upper 200 m of the bedrock were modified.

The SFM-wells were found to be almost independent of the changes in the hydraulic conductivities of the bedrock. Minor changes of the mean absolute error (MAE) were noticed in some wells. However, the average value of all the MAE was not changed in the different sensitivity cases. In the bedrock, however, there were considerable effects on the groundwater levels. The best agreement with observed levels was obtained in the case where the horizontal hydraulic conductivity of the upper 200 m of the bedrock was multiplied by a factor of 50.

The MAE in seven selected percussion-drilled boreholes was 0.39 m and the mean error (ME) was –0.21 m in this case (negative ME means that the simulated groundwater levels were too high). When using the values delivered from CONNECTFLOW the corresponding errors were 0.79 and –0.78 m, respectively. However, in *Phase 1* no changes were made of the bedrock data set delivered from the CONNECTFLOW deep-rock modelling, implying that in the *Final calibrated model* no changes were made of the hydraulic conductivities of the bedrock.

Phase 2

In some of the monitoring wells in QD it was noted that the simulated groundwater levels during the dry summer of 2006 were very flat (i.e. constant in time). An interpretation of these results revealed that the groundwater levels reached the bottom level of the upper calculation layer and did not decrease further. As a consequence, the upper calculation layer thickness was increased from 2 m to 2.5 m in *Phase 2* to enable deeper root water uptake. No effects on accumulated discharges were seen due to the increased layer thickness.

To further test the final calibrated model of *Phase 1,* a simulation was made of the pumping test in HFM14 performed July 4–25, 2006. Figure 2-9 shows the locations of the bedrock wells and the drawdown data are presented in Section 3.4.2 (Figures 3-50 and 3-51) and Section 3.5.3 (Figures 3-72, 3-74, 3-76, 3-78 and 3-81). The simulated response of the pumping in HFM14 was too slow and the calculated drawdowns in the majority of the HFM-wells were more than 50% less than the observed. In agreement with the changes of the bedrock properties made in the CONNECTFLOW modelling during the calibration, the specific storage (S_s) was set to a homogenous value of $5 \cdot 10^{-9}$ 1/m (in the base model, S_s was based on a relationship with hydraulic conductivity defined by /Rhen et al. 1997/ and varied between $1 \cdot 10^{-7}$ and $1 \cdot 10^{-5}$ 1/m). The response of the pumping was better captured by the model with the lower S_s-value, but still the drawdown was too small.

Since the calculated drawdown in the pumping test was too small and the problem with the generally too high groundwater levels in the bedrock still was not solved, additional sensitivity analyses of the hydraulic properties of the bedrock were performed. Eight cases were defined where S_s was set to $5 \cdot 10^{-9}$ 1/m in all cases. The horizontal hydraulic conductivities (K_h) of the sheet joints in the upper rock (implemented in the calculation layers at 10–30, 50–70 and 90–110 m.b.s.l) were modified in combination with different combinations of modification of K_v in the bedrock and K_v in the lake sediments and the layer of the QD-model in direct contact with the bedrock. Also, a modification of K_h of all bedrock above 200 m.b.s.l. was tested.

The best overall performance of the model compared with measured surface discharge, surface water levels and groundwater levels in QD and bedrock was obtained when K_h of the sheet joints was increased by a factor of 10 and K_v in the upper 200 m of the bedrock was reduced by a factor of 10, while the K-values of the QD were kept unchanged.

The surface discharge, surface water levels and the groundwater levels in QD were only marginally affected by these changes in K-values and the performance of the revised model was very similar to the final calibrated model of *Phase 1*. Groundwater levels in bedrock were more affected and the MAE of the HFM-wells was decreased from 0.75 to 0.67 m, but still the simulated groundwater levels in bedrock were generally too high (ME: –0.63 m). However, the revised model showed a dramatically improved performance with regard to the simulation of the pumping test in HFM14, see the example in Figure 4-17.

Despite the improved ability of the model to mimic field observations, the problem of too high groundwater levels in the bedrock in central parts of the site investigation area remained. In /Follin et al. 2007a/ and in Section 3.5.3 of the present report it is discussed if one possible explanation to the observed very low groundwater levels and the downward gradient from the

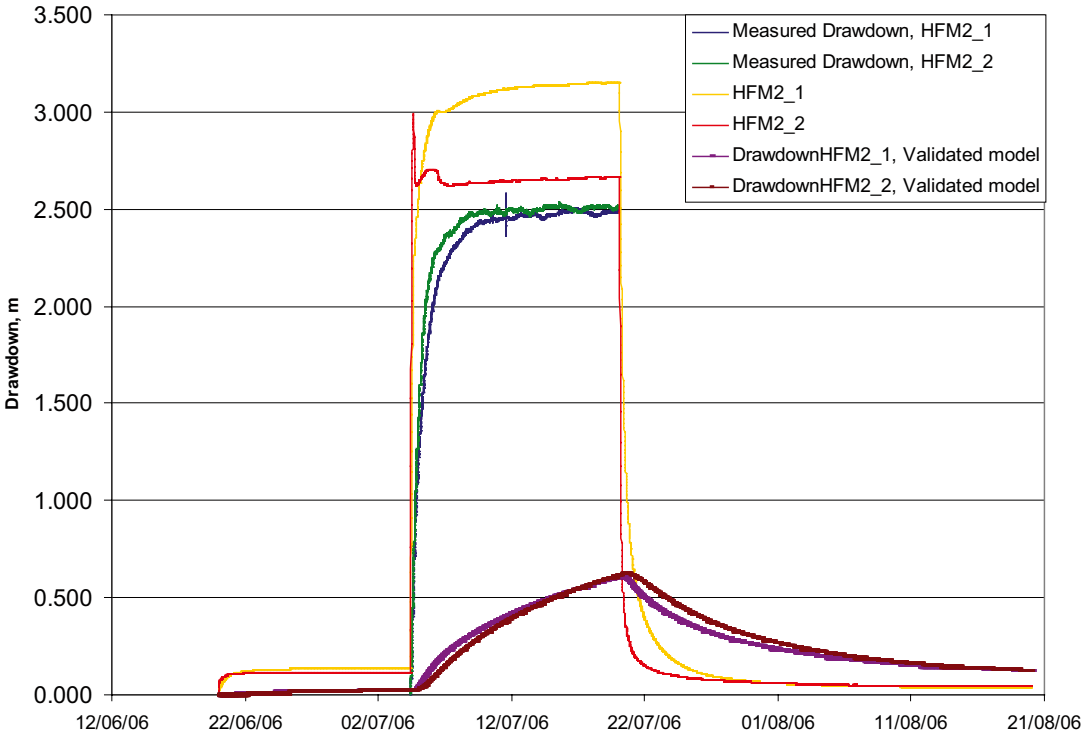

Figure 4-17. *Comparison of measured and calculated drawdowns in HFM2, section 1 and 2, the calculated curves,"HFM2_1" and "HFM2_2", represent the pumping test for the revised model (case 5), while the two curves for the "Validated model" are from the final model of Phase 1 /Bosson et al. 2008/.*

central parts of Lake Bolundsfjärden to the QD and further to the near-surface bedrock could, at least partly, be the pumping for drainage of SFR (c. 6 L/s) below the sea at Forsmark Harbour (cf. Figures 3-80 to 3-82). To investigate whether the drainage of the SFR facility can influence the hydrogeology of the site investigation area an additional simulation with the revised model was conducted.

The sink at SFR was introduced in a fairly simplistic way in the model as a pumping well screened from 40 to 140 m.b.s.l. The pumping at SFR caused numerical instabilities in MIKE SHE and therefore the storage coefficient (S_s) was multiplied by a factor of ten. This change gave a numerically stable model without having any negative influence on the simulations of undisturbed conditions and the pumping tests in HFM14. Consequently, the SFR-pumping simulation was run with a storage coefficient of $5 \cdot 10^{-8}$ 1/m.

The introduction of the pumping at SFR had a strong influence on the simulated groundwater levels in the bedrock in the central parts of the site investigation area, especially in the northern part of the tectonic lens. The MAE and ME in simulated groundwater levels in the HFM-wells decreased to 0.41 and –0.05 m, respectively (negative mean error indicating too high simulated groundwater levels). Most wells showed errors of c. ± 0.2 m. Of the wells within the northern part of the tectonic lens, only HFM16 and HFM32 showed considerably larger errors with an overestimation and underestimation of the groundwater levels by c. one metre, respectively.The QD-wells were not affected by the pumping. The simulated drawdowns at 100 m.b.s.l., i.e. the difference in head at that level between simulations with and without pumping, are shown in Figure 4-18.

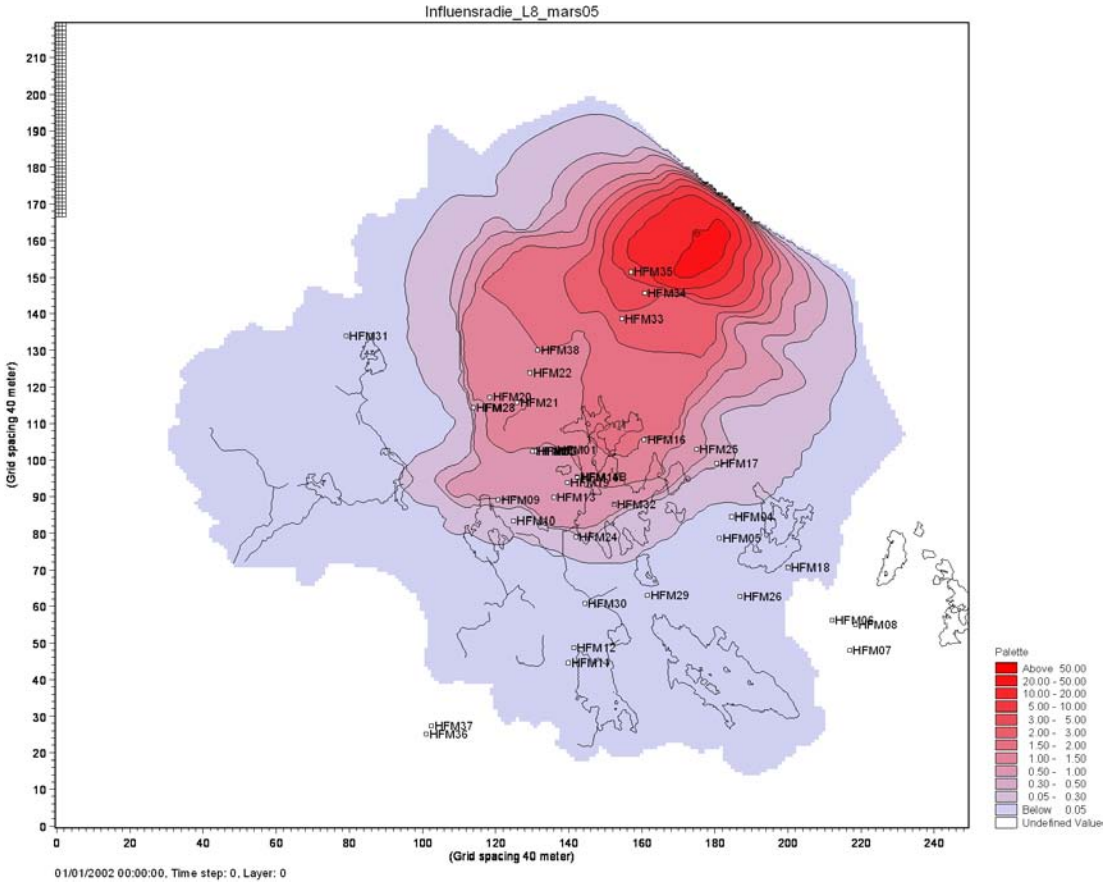

Figure 4-18. *Simulated drawdown (metres) at 100 m.b.s.l. caused by the pumping in SFR /Bosson et al. 2008/.*

4.3.4 Interpretation of modelling results

Performance of the final model

The performance of the final model resulting from the calibrations and sensitivity analyses in *Phase 1* and *Phase 2* is presented below. In many figures comparisons are made between measurements and the performance of the final model of *Phase 1* (called Validated model), and the final model after the *Phase 2* calibration without and with the pumping at SFR (called Case 5 and Case 5 with SFR, respectively).

Surface water levels and surface water discharge

There is a good agreement between measured and simulated surface water levels during the calibration period (May 15, 2003 until July 31, 2005) as well as during the validation period (Aug. 1, 2005 until March 31, 2007). The MAE between measured and simulated water levels for all the lakes during the combined calibration and validation period was 0.06 m. Concerning lake water levels there was no difference between the final models of *Phase 1* and *2*. The time series from Lake Bolundsfjärden are shown in Figure 4-19 as an example (from the final model of *Phase 1*).

Comparisons of measured and simulated surface discharges from two of the four discharge gauging stations are shown in Figures 4-20 and 4-21. The major discharge peaks in April 2006, due to snowmelt, are much better simulated in the final model of *Phase 2*, but still the first discharge peaks in November and December 2006 are underestimated. The accumulated discharge at the discharge station immediately upstream of Lake Bolundsfjärden (PFM005764) is shown in Figure 4-22, and in Table 4-7 accumulated calculated and measured discharge are compared for all four discharge gauging stations.

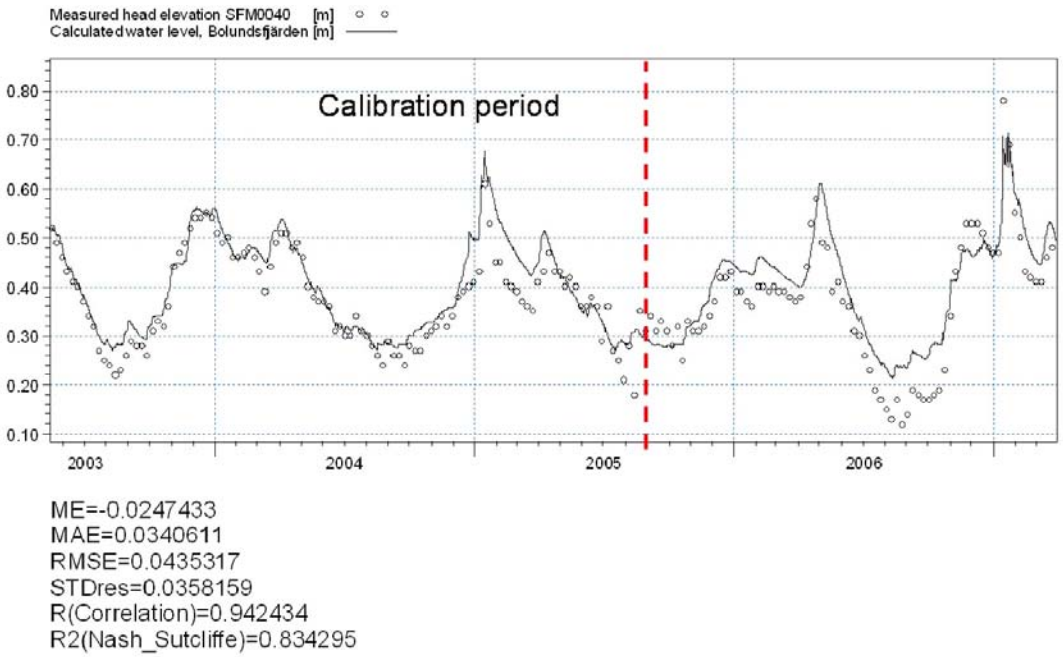

Figure 4-19. *Calculated and measured water levels in Lake Bolundsfjärden (from the final model of Phase 1) /Bosson et al. 2008/.*

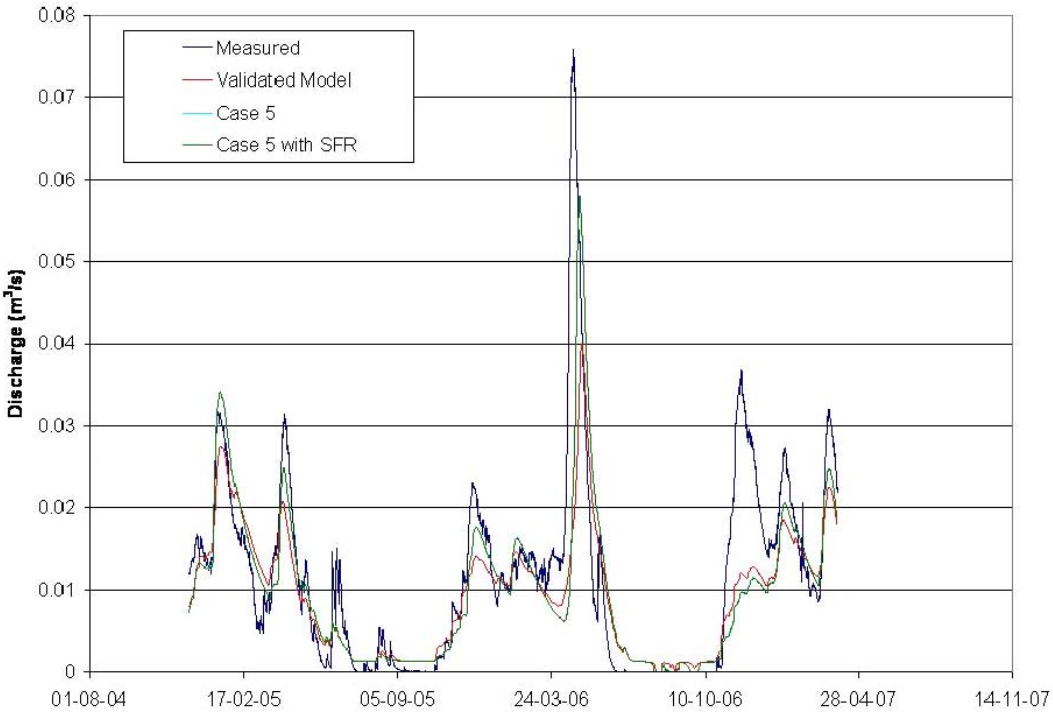

Figure 4-20. *Comparison between measured and calculated discharges in PFM002668, downstream of Lake Eckarfjärden (the curves of Case 5 and Case 5 with SFR are identical, why only one of them can be seen in the figure) /Bosson et al. 2008/.*

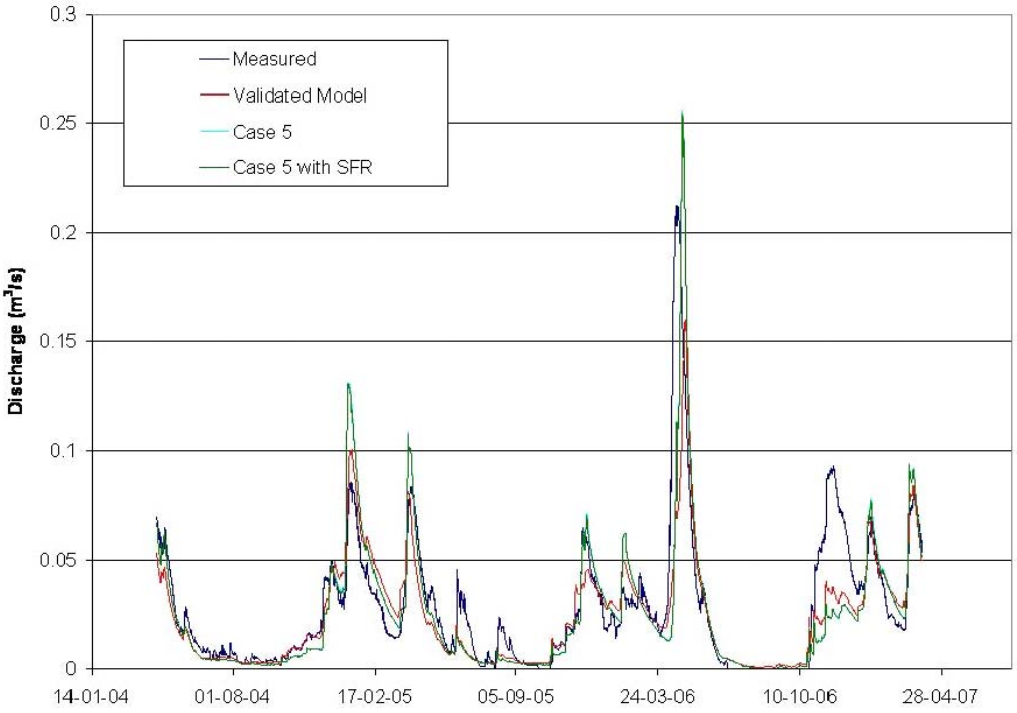

Figure 4-21. *Comparison between measured and calculated discharges in PFM005764, upstream of Lake Bolundsfärden (the curves of Case 5 and Case 5 with SFR are identical, why only one of them can be seen in the figure) /Bosson et al. 2008/.*

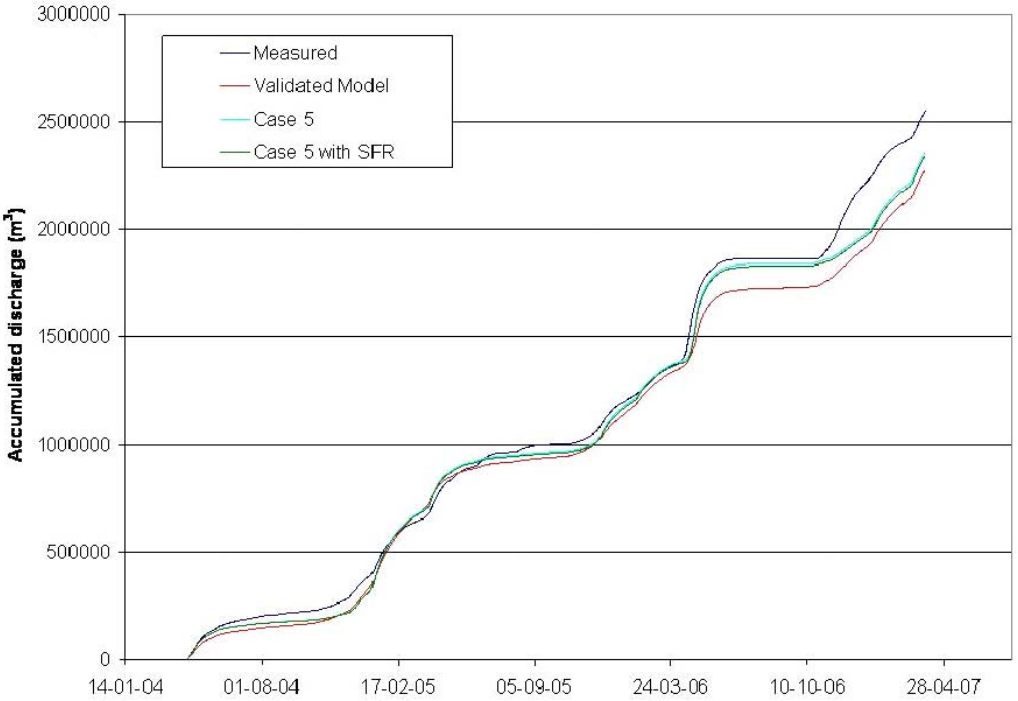

Figure 4-22. *Accumulated measured and calculated discharges at gauging station PFM005764, immediately upstream of Lake Bolundsfjärden /Bosson et al. 2008/.*

Table 4-7. Comparison of calculated and measured accumulated discharges at the four gauging stations (see Figure 2-5 for the locations of the stations) /Bosson et al. 2008/.

Station	Period for comparison	Calculated accumulated surface discharge in % of measured accumulated discharge		
		Validated model	Case 5	Case 5 with SFR
PFM002668 (Lake Eckarfjärden)	041208–070331	83	87	87
PFM002667 (Lake Stocksjön)	041208–070331	86	92	92
PFM002669 (Lake Gunnarsboträsket)	041208–070331	79	83	83
PFM005764 (Lake Bolundsfjärden)	040414–070331	89	92	92

Groundwater levels

In general, the correspondence was good between measured and simulated groundwater levels in Quaternary deposits. The effects of the model changes between the final models of *Phase 1* and *2* were small, both on the mean absolute error and mean error, see Table 4-8. Note that whereas most of the comparisons between measured and calculated heads are made in terms of absolute head elevations (i.e. heads expressed in RHB70), depths below ground surface are used for some monitoring wells. In Figure 4-23 a cross-plot of measured and simulated groundwater levels are shown from the final model of *Phase 1*.

The observed levels during the summer of 2006 were considerably lower than the calculated ones in some boreholes. This implies that the effects of the very dry summer were not fully described by the model. The groundwater levels in some areas reached the bottom of the uppermost calculation layer in the *Phase 1* modelling. To overcome this problem, simulations with an uppermost calculation layer of 2.5 m were made to enable deeper root water uptake. No negative effects of this increase of the depth were found, and consequently a 2.5 m uppermost calculation layer was used in the final model of *Phase 2*.

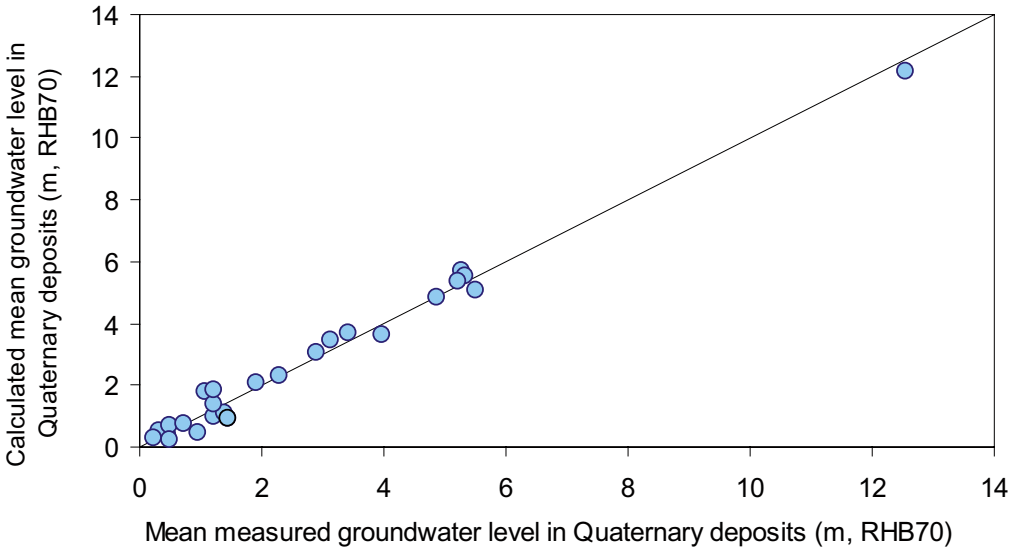

Figure 4-23. *Correlation between measured and calculated mean groundwater levels (based on the period May 15, 2003–March 31, 2007) /Bosson et al. 2008/.*

Table 4-8. Mean absolute error (MAE) and mean error (ME) of simulated groundwater levels by the final models of Phase 1 (validated model) and Phase 2 (Case 5) in wells in Quaternary deposits /Bosson et al. 2008/.

ID code SFM-well	Validated model		Case 5	
Calculated head	MAE	ME	MAE	ME
SFM0003	0.21	–0.20	0.19	–0.09
SFM0004	0.23	–0.12	0.21	–0.01
SFM0005	0.21	–0.11	0.21	–0.15
SFM0012	0.08	–0.05	0.08	0.01
SFM0013	0.23	–0.07	0.27	0.00
SFM0014	0.24	–0.24	0.34	–0.34
SFM0015	0.09	–0.08	0.09	–0.08
SFM0016	0.15	–0.15	0.14	–0.14
SFM0017	0.37	0.37	0.63	–0.63
SFM0019	0.51	0.51	0.53	0.53
SFM0022	0.05	–0.02	0.06	–0.02
SFM0023	0.07	–0.06	0.07	–0.05
SFM0026	0.34	–0.04	0.32	–0.09
SFM0030	0.74	–0.74	0.76	–0.76
SFM0033	0.32	0.24	0.35	0.32
SFM0034	0.28	–0.25	0.29	–0.10
SFM0036	0.26	–0.22	0.24	–0.15
SFM0039	0.04	–0.03	0.05	–0.03
SFM0057	0.31	–0.27	0.63	–0.59
SFM0062	0.11	0.04	0.11	0.05
SFM0065	0.20	–0.07	0.21	–0.08
SFM0066	0.11	0.02	0.12	0.03
Depth to phreatic surface				
SFM0001	0.16	0.08	0.21	0.16
SFM0002	0.28	0.27	0.37	0.37
SFM0009	0.38	0.36	0.36	0.35
SFM0010	0.39	0.37	0.31	0.29
SFM0011	0.11	–0.11	0.10	–0.09
SFM0018	0.17	–0.05	0.17	–0.04
SFM0019	0.32	–0.31	0.32	–0.29
SFM0020	0.22	–0.22	0.26	–0.26
SFM0021	0.53	0.53	0.48	0.48
SFM0028	0.16	–0.05	0.15	–0.04
SFM0030	0.61	0.52	0.63	0.61
SFM0049	0.19	–0.03	0.20	0.01
SMF0058	0.57	0.58	0.43	–0.28
MEAN SFM	**0.26**	**0.01**	**0.28**	**–0.03**

In Figure 4-24 a comparison between simulations of groundwater levels in SFM0036 with uppermost calculation layer thicknesses of 2.0 and 2.5 m is shown (see Figure 2-7 for the location of the well). The flat curve in the summer of 2006 indicates that the bottom of the calculation layer was reached with an uppermost calculation layer thickness of 2.0 m.

The hydraulic contact between the lakes and the underlaying till seemed well described by the model. Figures 4-25 and 4-26 show the calculated surface water level and groundwater level in the till below Lake Eckarfjärden and Lake Bolundsfjärden, respectively. The limited hydraulic contact between the lakes and the till due to low-permeable sediments of gyttja and clay, which was indicated by pumping tests and effects of evapotranspiration (cf. Sections 3.4.1 and 3.5.2), was implemented in the model via the low hydraulic conductivities of clay ($1 \cdot 10^{-8}$ m/s) and gyttja ($1 \cdot 10^{-7}$ m/s). There was no need for changes of these values during the calibration process.

The final model after the calibration in *Phase 2* was run both without and with the SFR-pumping. Table 4-9 shows the mean absolute errors and mean errors in simulated groundwater levels in HFM-boreholes in these two simulations.

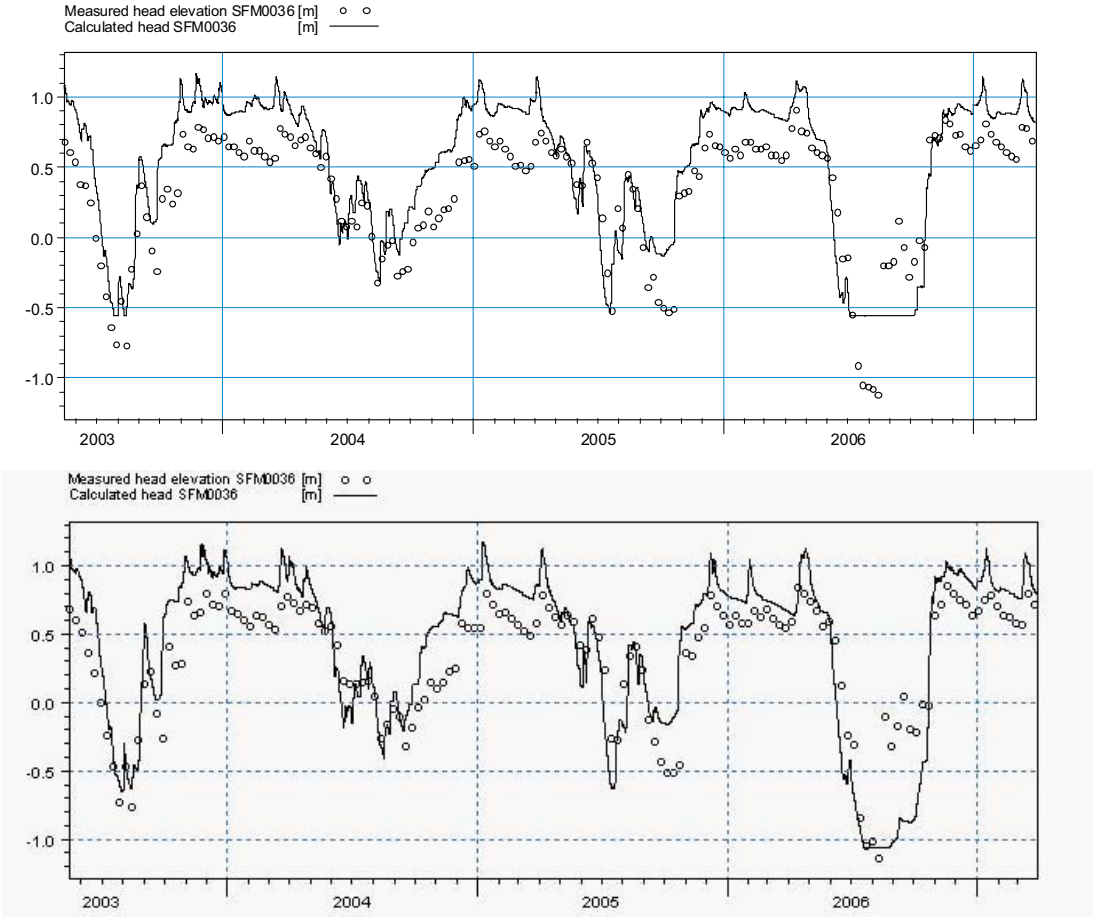

Figure 4-24. *Comparison of measured and simulated groundwater levels in well SFM0036 with an uppermost calculation layer of 2.0 m (top) and 2.5 m (bottom) /Bosson et al. 2008/.*

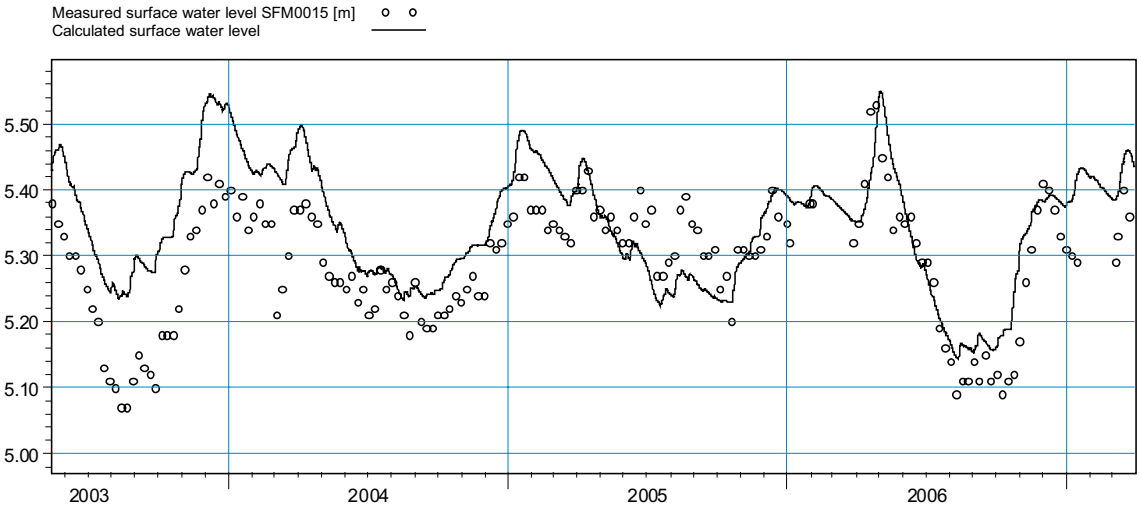

ME=-0.0792843
MAE=0.0877464
RMSE=0.0992607
STDres=0.0597218
R(Correlation)=0.770746
R2(Nash_Sutcliffe)=-0.453664

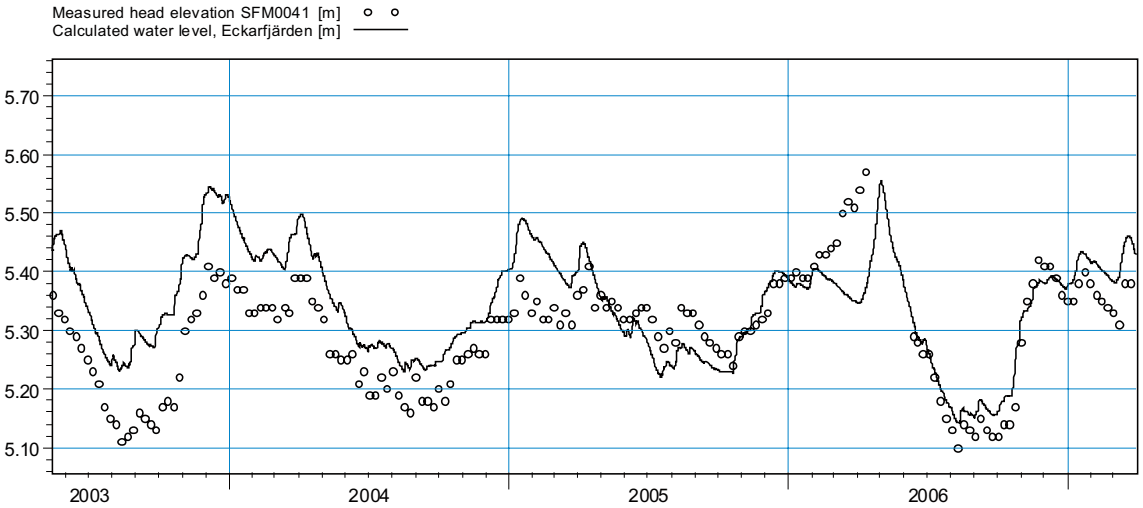

ME=-0.025771
MAE=0.0715902
RMSE=0.0827709
STDres=0.0786567
R(Correlation)=0.643092
R2(Nash_Sutcliffe)=0.00798512

Figure 4-25. *Comparison between measured and simulated groundwater levels in the till (SFM0015) below Lake Eckarfjärden and measured and simulated surface water levels (SFM0041) /Bosson et al. 2008/.*

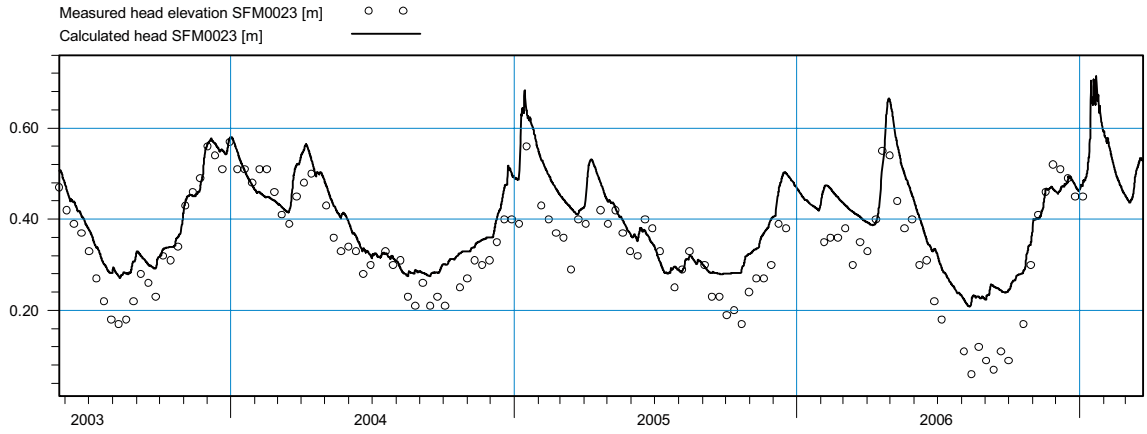

ME=-0.0565516
MAE=0.0714796
RMSE=0.190508
STDres=0.181921
R(Correlation)=0.612194
R2(Nash_Sutcliffe)=0.270634

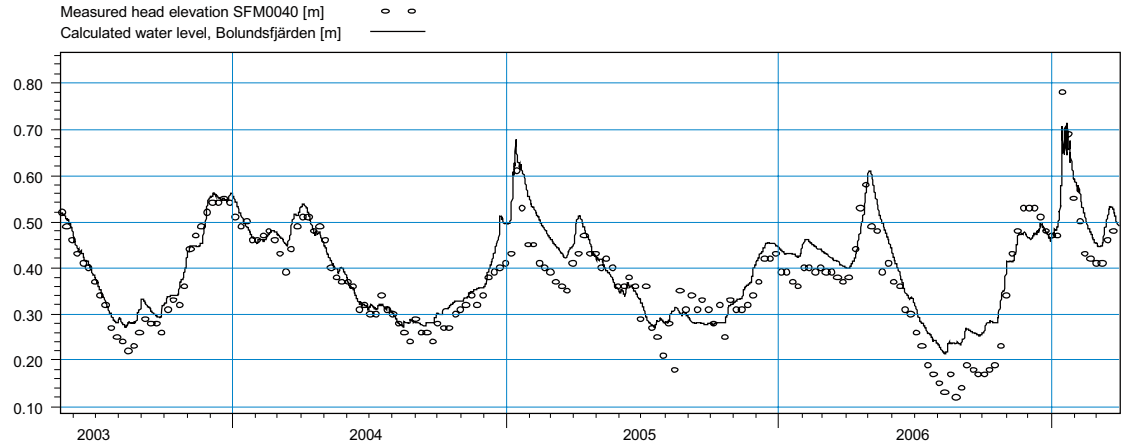

ME=-0.0247433
MAE=0.0340611
RMSE=0.0435317
STDres=0.0358159
R(Correlation)=0.942434
R2(Nash_Sutcliffe)=0.834295

Figure 4-26. *Comparison between measured and simulated groundwater levels in the till (SFM0023) below Lake Bolundsfjärden and measured and simulated surface water levels (SFM0040). The low measured levels in SFM0023 during the summers of 2005 and 2006 are in some cases caused by test pumpings during the site investigations /Bosson et al. 2008/.*

Table 4-9. MAE and ME for the HFM-wells in Case 5, with and without pumping at SFR /Bosson et al. 2008/.

ID code HFM-well	Case 5		Case 5 with SFR	
Calculated head	MAE	ME	MAE	ME
HFM01_1	0.81	–0.81	0.28	0.28
HFM01_2	0.89	–0.89	0.26	–0.26
HFM02_1	0.82	–0.82	0.25	0.19
HFM02_2	0.78	–0.78	0.22	–0.14
HFM02_3	0.81	–0.81	0.21	–0.16
HFM03_1	0.75	–0.75	0.39	–0.39
HFM03_2	0.74	–0.74	0.38	–0.38
HFM04_1	0.08	–0.01	0.09	0.06
HFM04_2	0.15	–0.12	0.13	–0.09
HFM9	0.18	–0.16	0.13	0.07
HFM10_1	0.39	–0.39	0.23	–0.22
HFM10_2	0.27	–0.22	0.22	–0.09
HFM11_1	0.28	–0.28	0.28	–0.27
HFM11_2	0.26	–0.22	0.25	–0.22
HFM12_1	0.24	–0.04	0.24	–0.04
HFM12_2	0.17	–0.01	0.17	–0.01
HFM13_2	0.28	–0.24	0.66	0.66
HFM13_3	0.32	–0.17	0.38	0.28
HFM14	0.71	–0.71	0.21	0.19
HFM15_1	0.68	–0.68	0.25	0.23
HFM15_2	0.62	–0.62	0.30	0.28
HFM16_1	0.40	–0.40	1.02	1.02
HFM16_2	0.47	–0.47	0.54	0.54
HFM16_3	0.56	–0.56	0.22	0.16
HFM19_2	0.57	–0.57	0.37	0.37
HFM19_3	0.47	–0.47	0.24	–0.11
HFM20_2	0.48	–0.48	0.71	0.71
HFM20_3	0.44	–0.44	0.76	0.76
HFM20_4	0.79	–0.79	0.43	–0.34
HFM24	0.23	–0.07	0.25	0.14
HFM26	0.50	–0.50	0.50	–0.50
HFM30	0.23	–0.07	0.23	–0.07
HFM32_1	1.38	–1.38	0.78	–0.78
HFM32_2	1.43	–1.43	0.94	–0.94
HFM32_3	1.32	–1.32	0.98	–0.98
HFM32_4	1.37	–1.37	0.77	–0.77
HFM34_2	3.89	–3.89	0.77	–0.77
HFM34_3	1.09	–1.09	0.45	–0.45
MEAN HFM	**0.68**	**–0.65**	**0.41**	**–0.05**

The model performance was considerably improved when the SFR-pumping was included. Figure 4-27 shows graphs of a number of wells in the central part of the site investigation area where a very good agreement is reach between measured and simulated groundwater levels in bedrock when the SFR-pumping is included. In Figure 4-28 graphs from the HFM16 and HFM32 wells are shown. In these wells, an improvement is achieved when the SFR-pumping is included but the groundwater level in the deepest section of HFM16 is underestimated while the groundwater levels in HFM32 are overestimated for all sections (only the deepest and shallowest sections are shown in the figure).

Correlation plots of measured and simulated groundwater levels in the HFM-boreholes from the final model without and with SFR-pumping are shown in Figures 4-29. The correlation is improved when the SFR-pumping is included with R^2 increasing from 0.89 to 0.95.

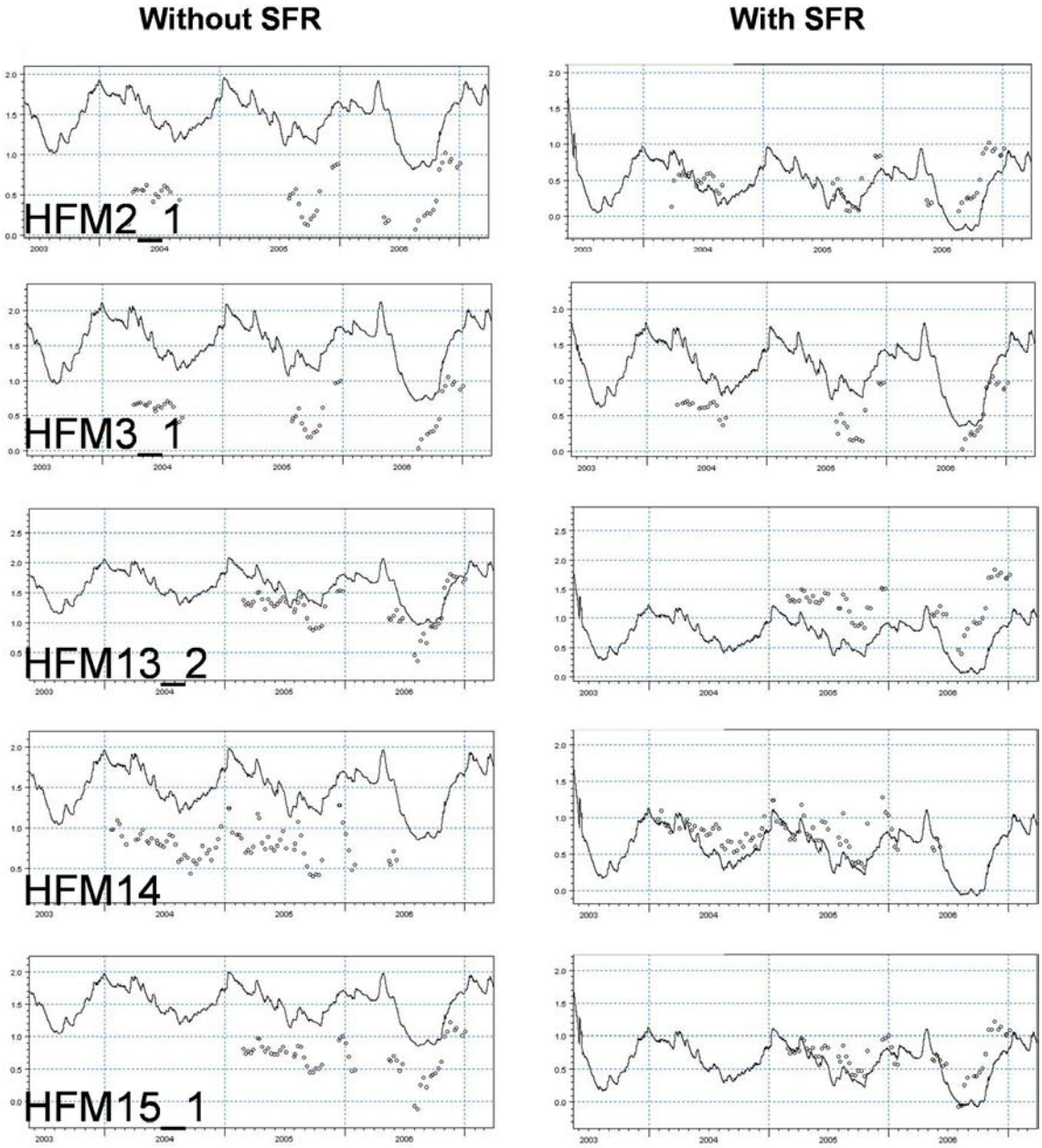

Figure 4-27. *Measured and simulated groundwater levels in the HFM borehole sections HFM02_1, HFM03_1, HFM13_2, HFM14 and HFM15_1 /Bosson et al. 2008/.*

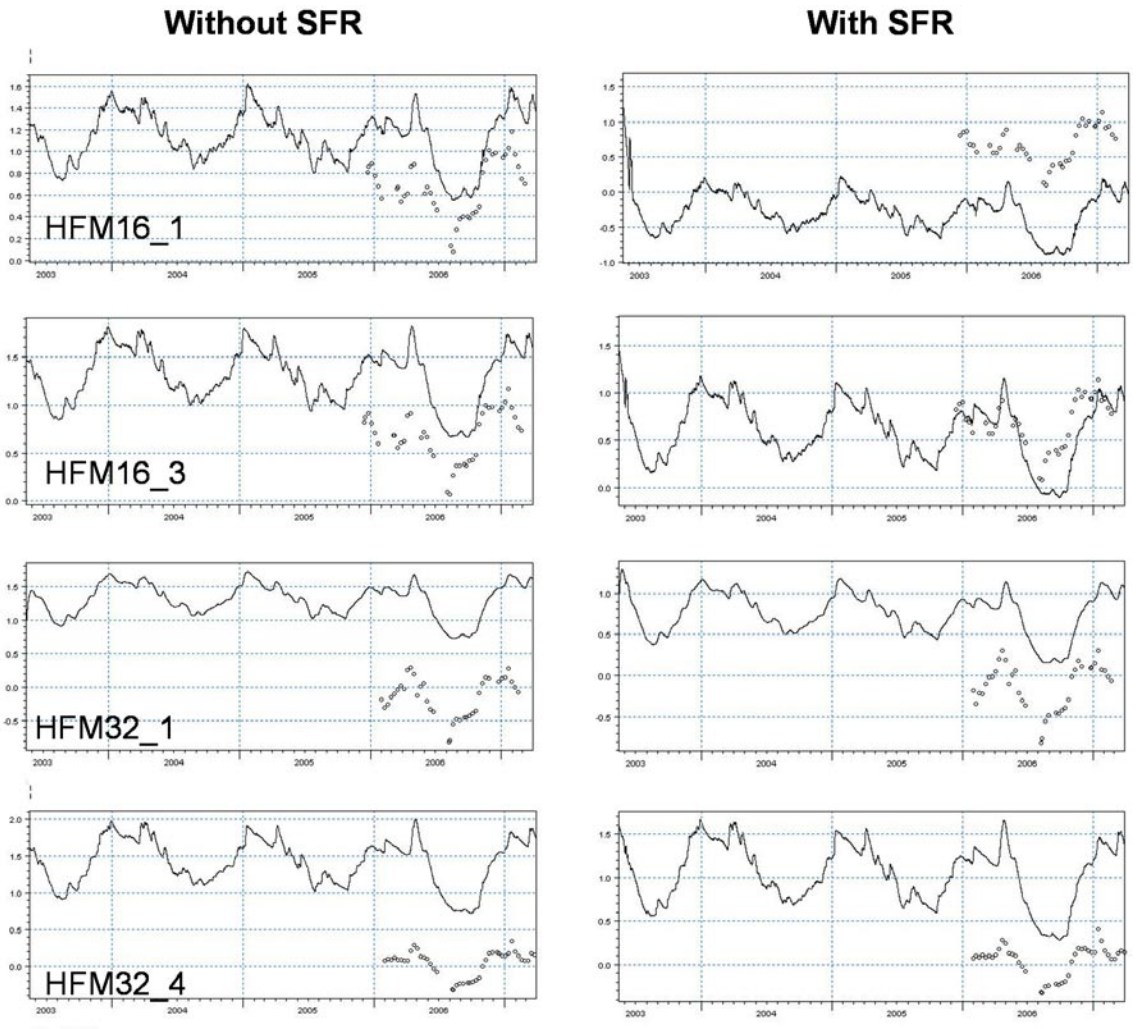

Figure 4-28. *Measured and simulated groundwater levels in HFM borehole sections HFM16_1, HFM16_3, HFM32_1 and HFM32_4 /Bosson et al. 2008/.*

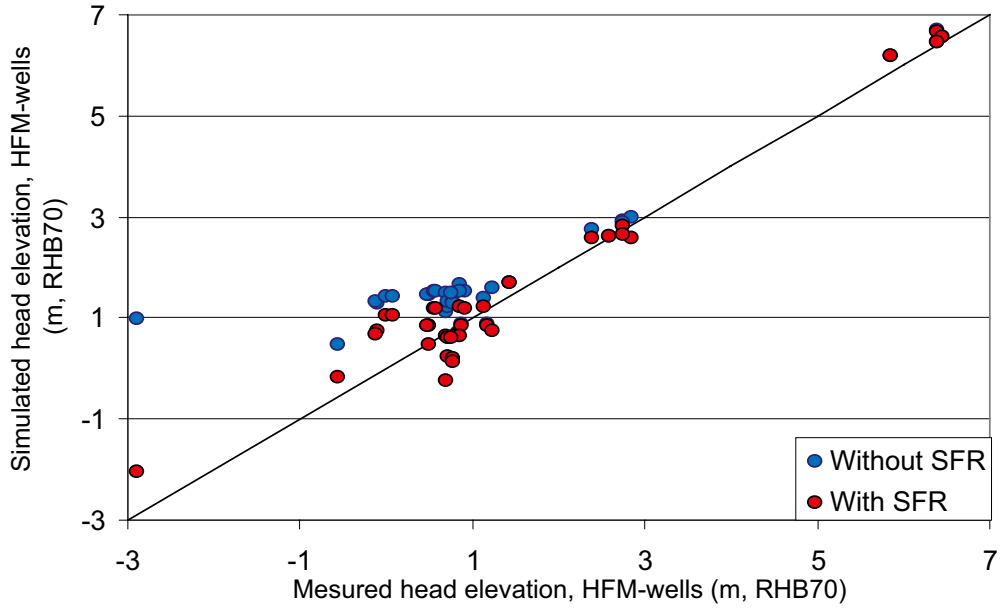

Figure 4-29. *Correlation plot of measured and simulated groundwater levels in HFM-boreholes without and with inclusion of the SFR-pumping /Bosson et al. 2008/.*

Recharge and discharge areas

The distribution of recharge and discharge areas was explored in the final calibrated model of *Phase 2*. In this context the groundwater head difference between calculation layer 1 and 2 was used for the definition of recharge and discharge areas; i.e. areas where the head was higher in layer 1 than in layer 2 were defined as recharge areas and vice versa for discharge areas. Furthermore, a comparison was performed between the heads in calculation layers 4 and 5 (between c. 20 and 40 m depth), in order to investigate the head differences in the upper bedrock.

The mean situation of the period Sep.1, 2003 to Sep. 1, 2006 is presented in Figures 4-30 and 4-31. The sea, the brook valleys and the lakes are discharge areas in the Quaternary deposits and these areas also have an upward gradient in the upper bedrock. In the QD, the local topography creates a split pattern of recharge and discharge areas, while the areas with upward gradient in the upper bedrock are concentrated close to and below the lakes. The depressions along the brooks also have upward gradients in the upper bedrock. The head differences within the Quaternary deposits are somewhat smaller than the difference between the two layers in the upper bedrock. The mean head difference in the recharge areas in QD was 0.05 m between layers 1 and 2, and 0.34 m between layers 4 and 5. The mean head difference in the discharge areas in QD is –0.02 m between layers 1 and 2 and –0.14 m in the bedrock between layers 4 and 5.

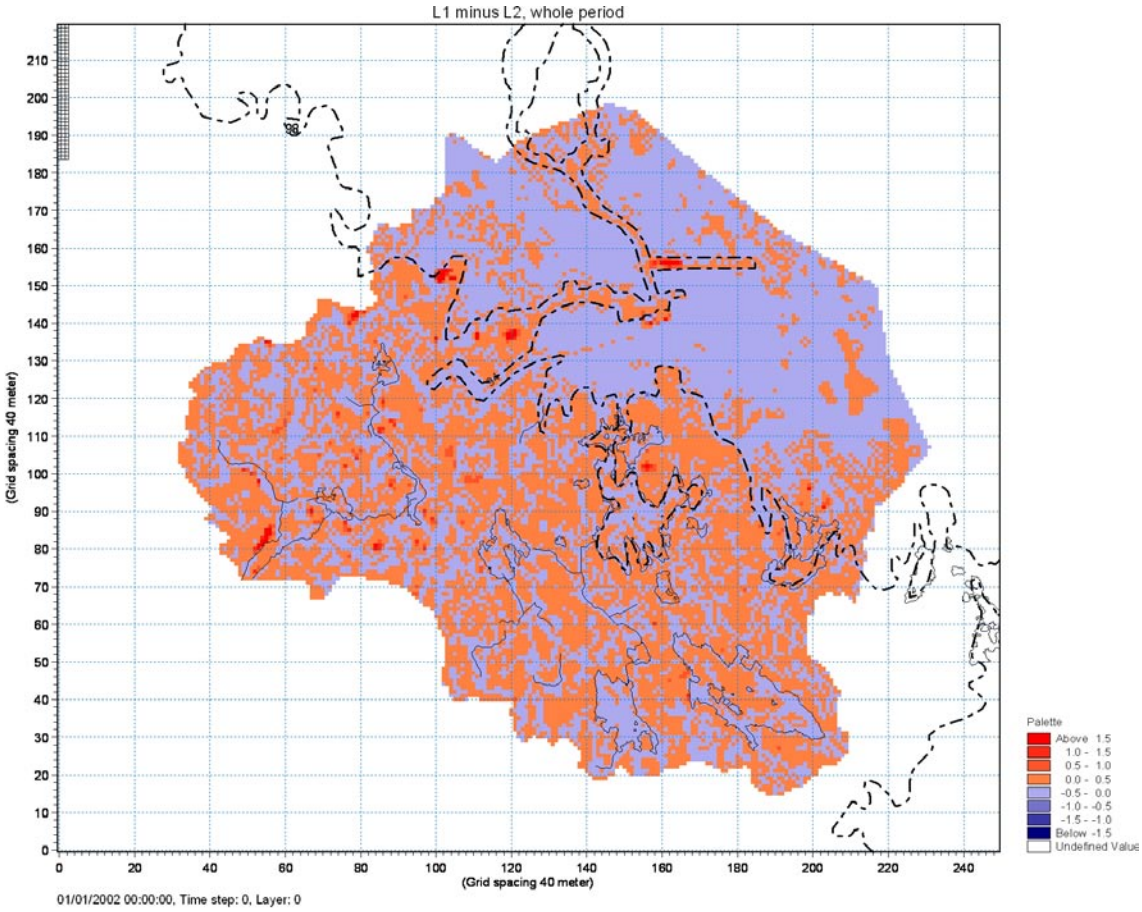

Figure 4-30. *Mean head difference between calculation layers 1 and 2 in the Quaternary deposits for the whole period Sep. 1, 2003 to Sep. 1, 2006 (positive values indicate recharge areas and negative values indicate discharge areas) /Bosson et al. 2008/.*

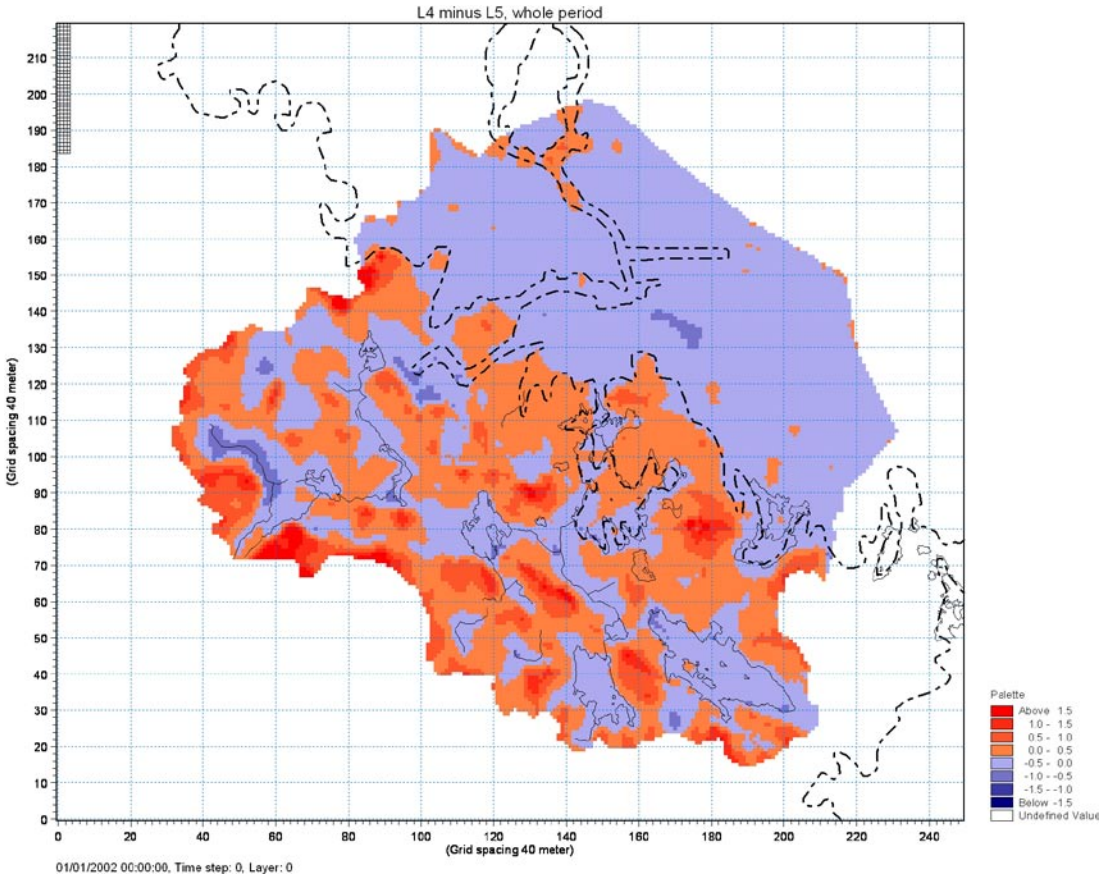

Figure 4-31. *Mean head difference between calculation layers 4 and 5 in the upper bedrock (between c. 20 and 40 depth) for the whole period Sep. 1, 2003 to Sep. 1, 2006 (positive values indicate downward gradients) /Bosson et al. 2008/.*

In order to analyse the changes in recharge and discharge areas in QD and in the vertical flow direction in the upper bedrock between dry and wet conditions, the distribution of areas was evaluated during two different periods. The dry conditions are represented by the mean head gradient during July 10–25, 2006, and the wet condition by the mean head gradient during March 15–30, 2004.

During the dry period, the overall pattern of recharge and discharge areas in the QD was similar to that of the average conditions, see Figure 4-32. However, the total size of discharge areas in the QD increased during dry conditions. This is due to the strong impact of transpiration on the vertical gradient between the two uppermost layers in the QD. Thus, upward flow is created by the water uptake of the vegetation, especially in areas with very shallow groundwater.

In Lake Fiskarfjärden there is a big difference where areas simulated as recharge areas during average conditions are converted to discharge areas during dry conditions. Conversely, an area in the southwestern part of Lake Eckarfjärden is turned into a recharge area under dry conditions. In the bedrock, the pattern during dry conditions is very similar to the mean situation. However, in an area to the west of Lake Bolundfjärden the vertical gradient is turned from downward to upward during the dry period, see Figure 4-33.

During the wet period some discharge areas in the Quaternary deposits turn into recharge areas, see Figure 4-34. This is in contradiction to the common concept of expanding discharge areas during wet conditions. Again, the explanation is the shallow groundwater and the influence of transpiration. In some areas transpiration causes an upward flow during dry condition as well as during average conditions. That is, the area is a discharge area with the definition used of discharge as water leaving the saturated zone, while during periods of abundant precipitation these areas are recharge areas.

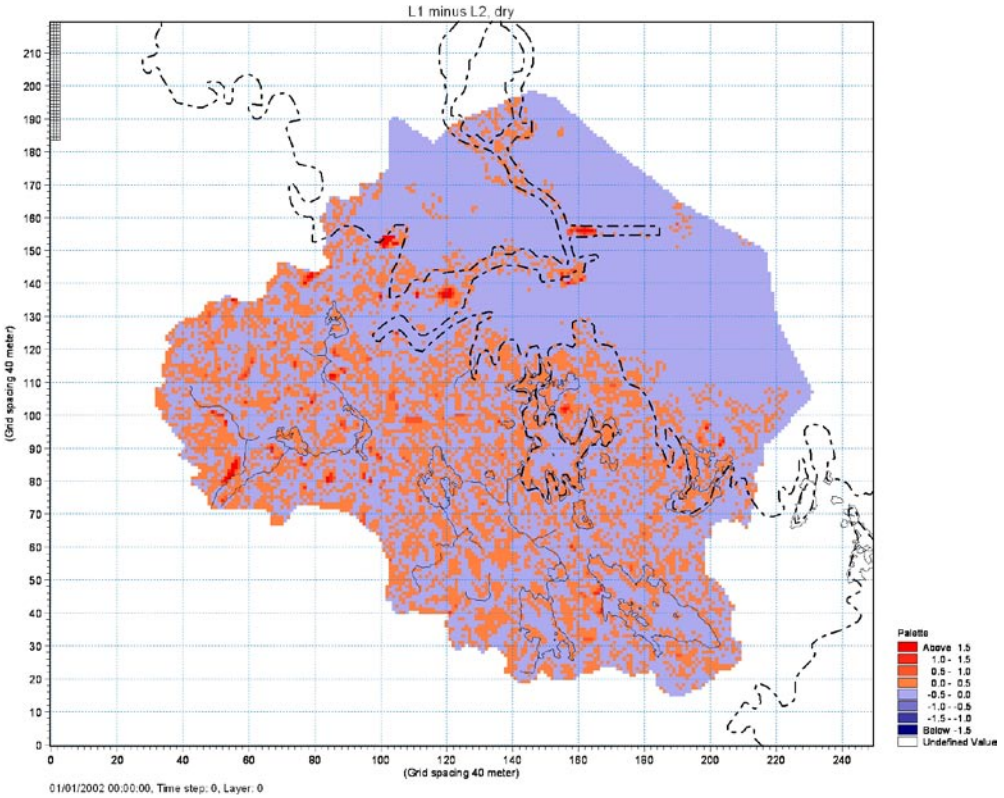

Figure 4-32. *Mean head difference between layer 1 and 2 in the Quaternary deposits during a period of dry conditions (positive values indicate recharge areas and negative values indicate discharge areas) /Bosson et al. 2008/.*

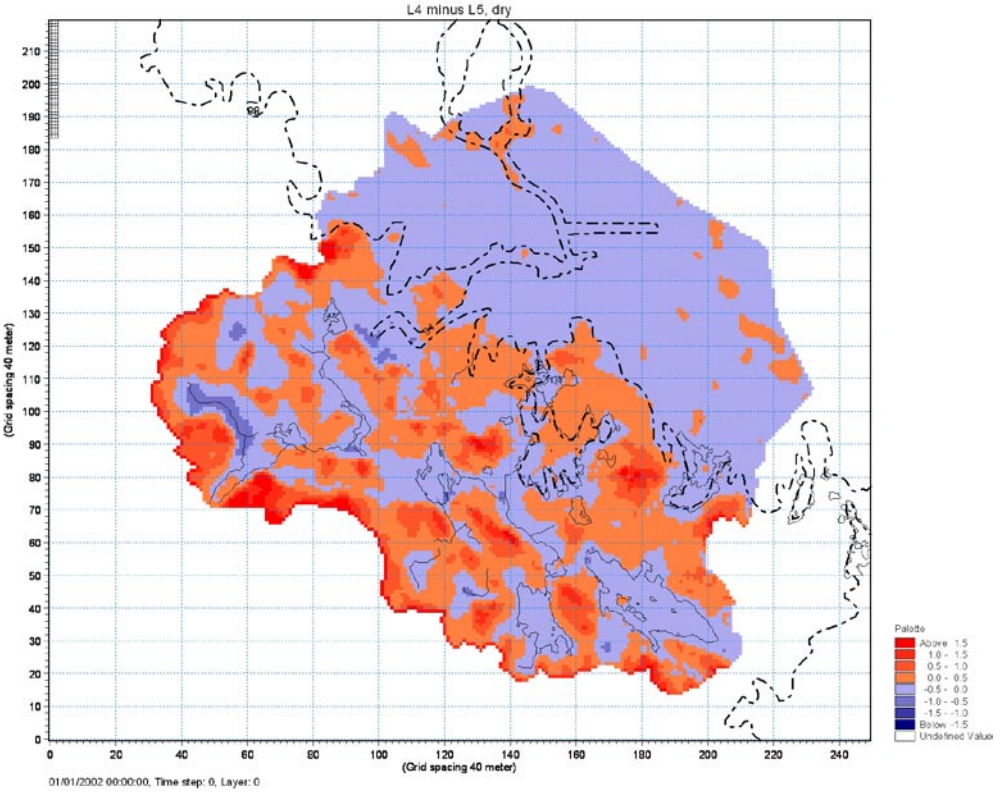

Figure 4-33. *Mean head difference between calculation layers 4 and 5 in the upper bedrock (between c. 20 and 40 depth) during a period of dry conditions (positive values indicate downward gradients) /Bosson et al. 2008/.*

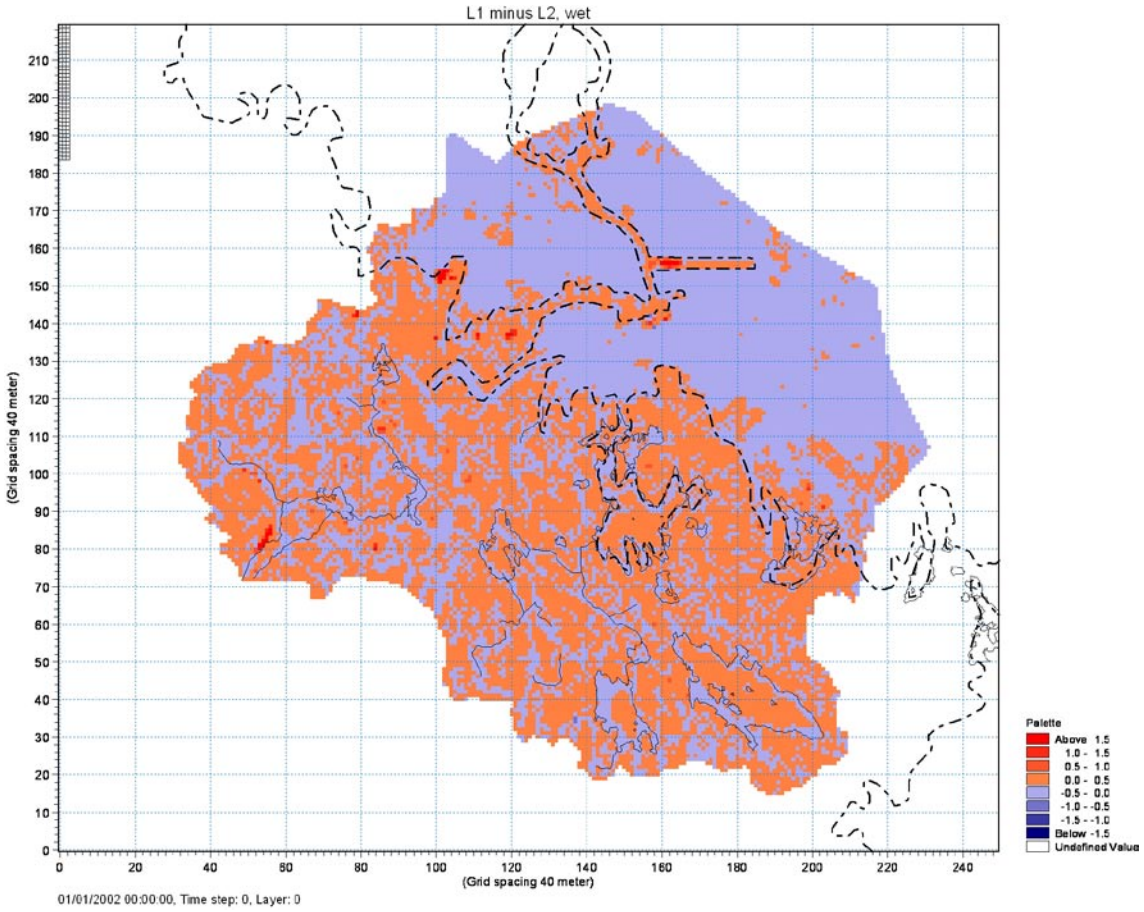

Figure 4-34. *Mean head difference between calculation layers 1 and 2 in the Quaternary deposits during a period of wet conditions (positive values indicate recharge areas and negative values indicate discharge areas) /Bosson et al. 2008/.*

Furthermore, the simulated water levels in the lakes become higher than the groundwater heads in the underlying till during wet periods, i.e the lakes turn into recharge areas. This result is in contradiction to the field observations, which show slightly higher groundwater levels compared with lake levels during wet periods and slighly lower during dry periods, cf. Section 3.5.2 (Figures 3-65 and 3-66). The pattern of vertical gradients in the upper bedrock (between c. 20 and 40 m depth) under wet conditions is almost identical to the pattern under average conditions, see Figure 4-35.

Tables 4-10 and 4-11 summarise Figures 4-30 to 4-35. Table 4-10 shows how the sizes of recharge and discharge areas in Quaternary deposits are varying with the weather conditions. Since the sea is mostly a discharge area that shows small changes between the various cases studies, and hence mainly obscures the changes in the on-land part of the model area, results are shown both for the whole model area and the on-land part only. The difference between the sizes of recharge and discharge areas of the three averaging periods are most obvious for the dry situation. The discharge areas in Quaternary deposits increase by 30% during the dry period for the whole area compared with the average conditions, and by 44% if only the on-land part is considered.

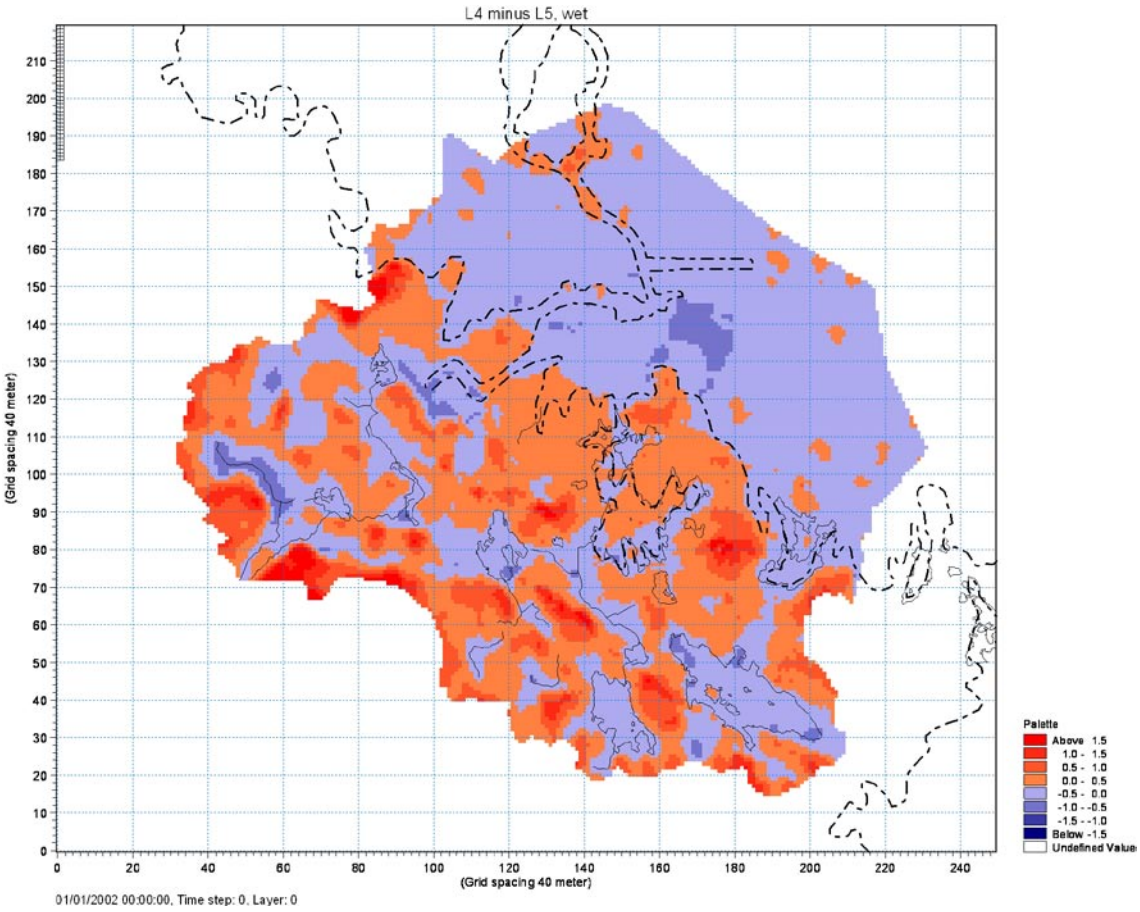

Figure 4-35. *Mean head difference between calculation layers 4 and 5 in the upper bedrock (between c. 20 and 40 depth) during a period of wet conditions (positive values indicate downward gradients) /Bosson et al. 2008/.*

Table 4-10. The sizes of recharge and discharge areas in the Quaternary deposits during mean, wet, and dry conditions /Bosson et al. 2008/.

	Recharge area, km²		Discharge area, km²	
	Whole model area	On-land part	Whole model area	On-land part
Mean	16.91	14.91	19.10	9.90
Wet	16.79	16.16	19.17	8.64
Dry	11.26	10.54	24.71	14.26

Table 4-11. The distribution of areas with downward and upward gradients in groundwater heads between calculation layers 4 and 5 in shallow bedrock at c. 40 m depth during mean, wet, and dry conditions /Bosson et al. 2008/.

	Downward gradien, km²		Upward gradient, km²	
	Whole model area	On-land part	Whole model area	On-land part
Mean	14.48	14.21	21.49	10.60
Wet	15.39	15.01	20.58	9.80
Dry	14.21	13.60	21.76	11.21

Overall water balance

The calculated water balance of the simulation is shown in Figure 4-36. The numbers are based on annual mean values for the period Sep.1, 2003–Sep. 1, 2006. The water balance is calculated for the on-land part of the model area, including the littoral zone. The red figures represent the situation when the SFR-pumping is not active and the blue figures represent the calculations when this pumping is activated. The SFR-pumping does not have a strong influence on the overall water balance.

The mean annual precipitation was 533 mm and the total annual evapotranspiration was 405 mm. The total evapotranspiration is a sum of the different evaporation components and transpiration. The transpiration from plants was 169 mm/year, the evaporation from soil was 56 mm/year and the evaporation from flooded areas was 28 mm/year. The amount of water intercepted by plant leaves was calculated to 122 mm/year and the evaporation from the saturated zone was 30 mm/year. The annual runoff in the brooks was calculated to 144 mm.

In the model, the water in saturated areas is classified as "overland water". Therefore, a large amount of water (74 mm) is transported from the overland compartment (OL) to the brooks (i.e. the MIKE 11 model). This should not be interpreted as Hortonian overland flow. Instead, the water is transported in the saturated zone (SZ) towards the river links in MIKE SHE. The cells in direct contact with MIKE 11 are often saturated or flooded. In the water balance calculation, MIKE SHE does not take this into consideration and the water transported from SZ to the brooks via the OL compartment is classified as flow "from overland to river".The annual infiltration from the OL compartment to the unsaturated zone is 351 mm and the net groundwater recharge, defined as net the water flow from the unsaturated to the saturated zone, is 124 mm/year.

The water balance shown in Figure 4-36 is made for the area with a higher altitude than the minimum sea level during the simulation, i.e the land parts and the littoral zone of the model area. Due to the boundary condition at the coastline, overland water is produced in the littoral zone and the depth of this water is varying with the sea water level. This causes a water exchange between the overland compartment and the saturated zone and also a net outflow of water to the sea. Thus the numbers 437 mm from SZ to OL, 358 mm from OL to SZ, and 42 mm net out flow to the sea, are water fluxes due to the boundary condition. The average storage in

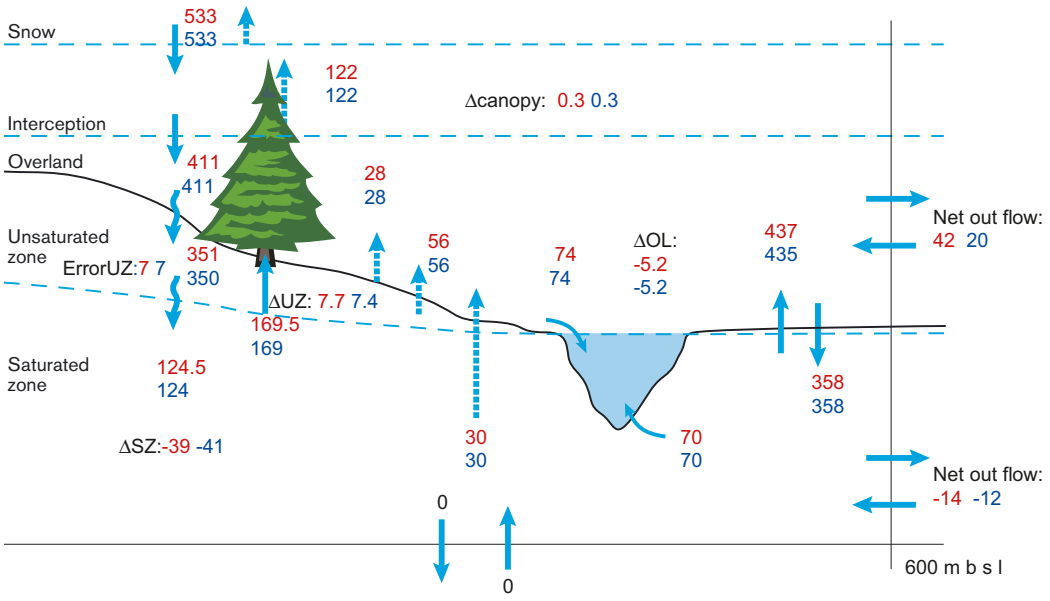

Figure 4-36. *Mean annual water balance in mm for the period Sep. 1 2003–Sep. 1, 2006 (also storage changes are given in mm/year). Red and blue figures show the results of the simulations without and with the SFR-pumping activated, respectively /Bosson et al. 2008/.*

SZ is decreased by c. 40 mm/year during the simulation period. This is mainly due to the very dry summer of 2006.

The annual water balance for each layer in the saturated zone is presented in Figure 4-37. The figures shown only represent the on-land part of model area. All the flows outside the saturated zone except for the infiltration from the unsaturated zone are removed from the figure. The average net groundwater recharge from the unsaturated zone to the uppermost calculation layer containing the Quaternary deposits is 124 mm. The flow to the second calculation layer in QD, at 2.5 m depth, is c. 45 mm. There are many local recharge and discharge areas within this layer; 41 mm was transported back to the uppermost QD layer.

Only c.11 mm was flowing down to the uppermost bedrock, calculation layer 3. The upward flow from the rock to the QD corresponds to some 8–9 mm, which means that the net downward flow is only 2–3 mm. In the uppermost c. 100 m there is a slight increase of the downward flow when the SFR-drainage is included in the simulation, 1–2 mm/year. The pumping is active down to 140 m.b.s.l. and below this level the effects of the SFR-pumping are insignificant. (The SFR-pumping has a stronger influence on the flow in the bedrock below the sea but this area is not included in water balance in Figure 4-37.) The vertical groundwater flow at the level of –150 m, which was the original bottom boundary level, was 0.3 mm downward and 0.2 mm upward. This implies a net flow in the same range as the calculated flow at the corresponding level in the CONNECTFLOW model /Follin et al. 2008/.

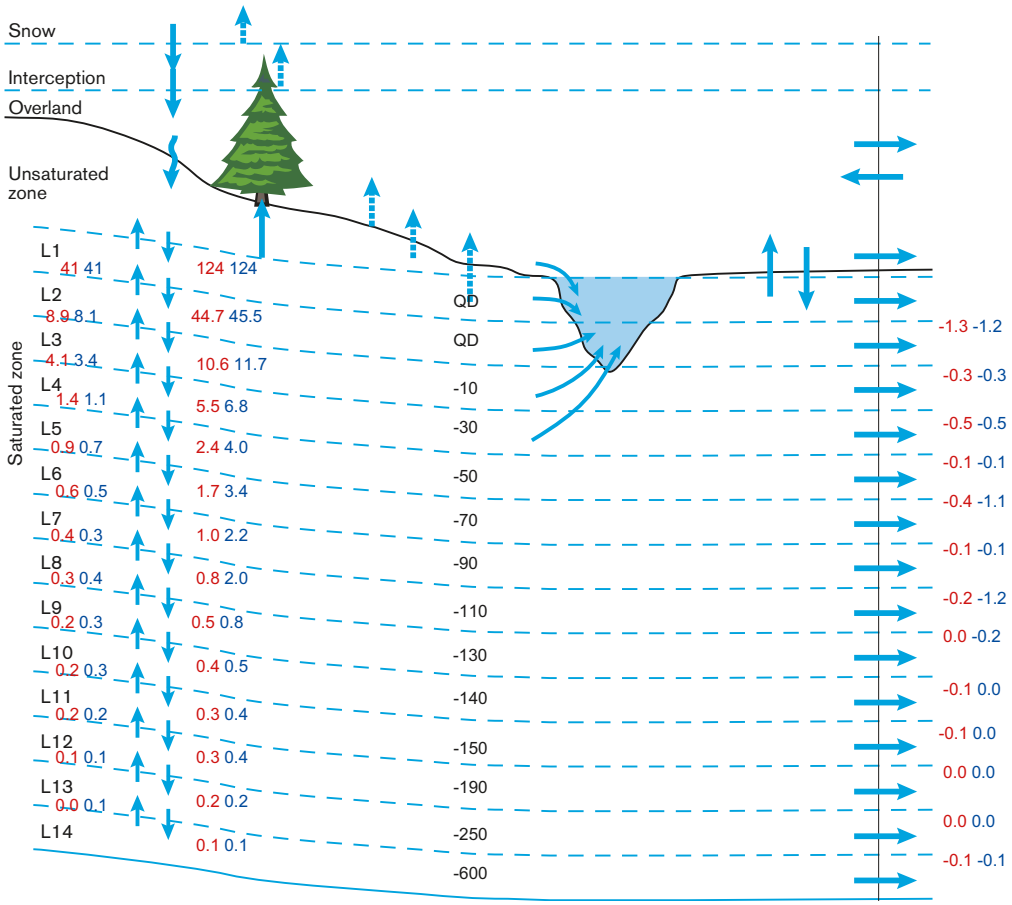

Figure 4-37. *The annual average water balance for each layer in the saturated zone (in mm/year), vertical flows between each calculation layer and horizontal flows at the coastline (only the on-land part of the model area included). The mean lower boundary of each calculation layer is marked in the middle of the figure. Red and blue figures show values from the simulation without and with SFR-drainage included, respectively /Bosson et al. 2008/.*

Gradient between different model compartments

The gradients between different model compartments in the flow model are crucial for any kind of transport analyses. The conditions around the lakes are of specific interest because they may act as discharge areas for sub-flow systems restricted to QD but also for sub-systems involving the bedrock to different depths (cf. Section 3.5.3). The spatial and temporal distributions of the vertical flow directions in the bedrock and up to the QD are most important, but also the horizontal gradients around the lakes in the QD and the upper bedrock are of interest. Unless explicitly stated, all of the simulated results in this section are with the SFR-pumping included in the model.

Figure 4-38 shows the simulated and observed groundwater levels around Lake Eckarfjärden and Lake Bolundsfjärden. In the Lake Eckarfärden area, two of the QD-wells are located on each side of the lake in the littoral zone, SFM0014 on the western side and SFM0016 on the eastern side, and one in the centre of the lake, SFM0015. The modelled horizontal gradient directions coincide with the observed ones during most of the year, with a gradient from the west of the lake to the centre and further from the centre to the east.

At Lake Bolundsfjärden, one of the QD-wells is located on the western side of the lake, in the littoral zone (SFM0033), one well 100 m out in the lake (SFM0062), and one well in the centre of the lake (SFM0023). During wet periods, the observed direction of the gradient is from the littoral zone to the centre of the lake, and vice versa during dry conditions (cf. Figure 3-65). In the simulation there is a gradient from the littoral zone only during very short periods. Furthermore, the simulated head difference between the two boreholes in the lake is much smaller than the observed.

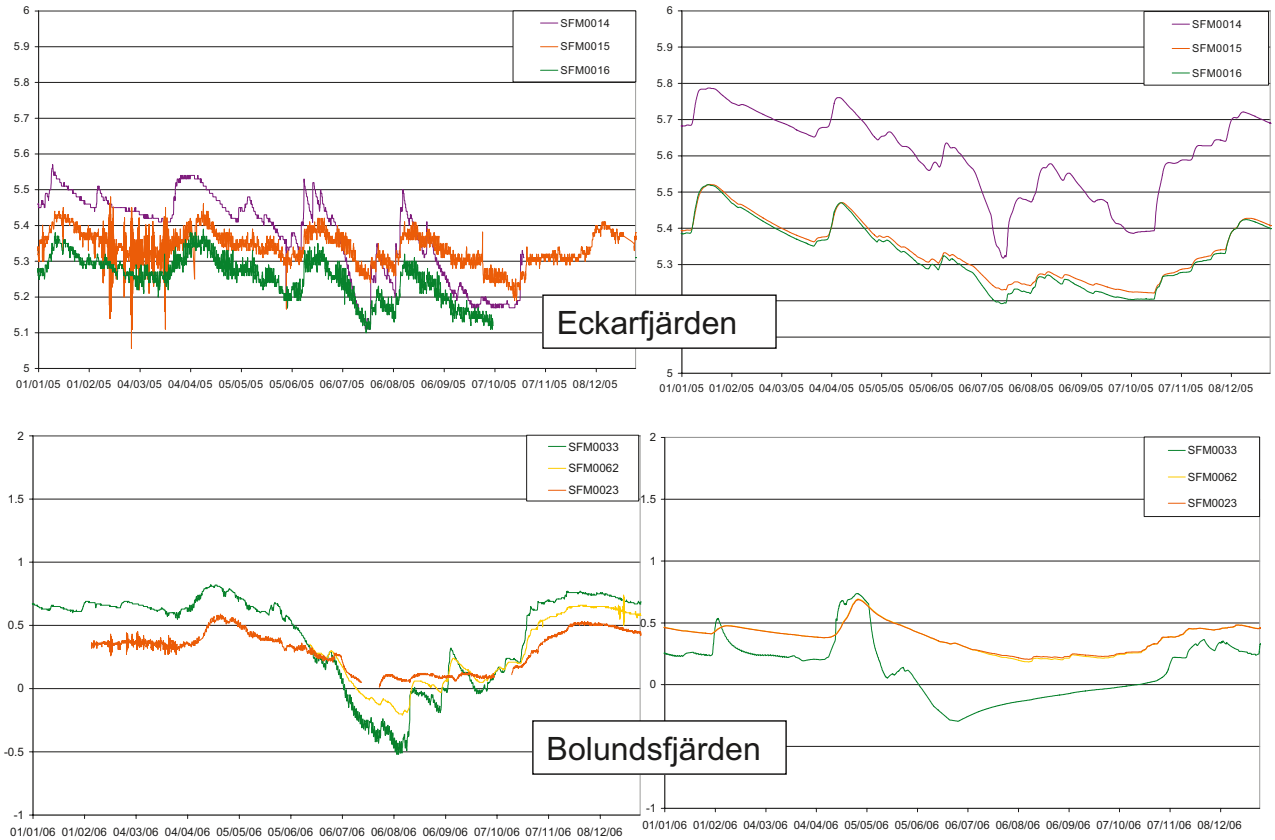

Figure 4-38. *Comparison of measured (left) and simulated (right) groundwater levels at Lake Eckarfjärden and Lake Bolundsfjärden for the period Jan. 1–Dec. 31, 2006 /Bosson et al. 2008/.*

Figure 4-39 shows the surface water levels in Lake Eckarfjärden and Lake Bolundsfjärden as well as the groundwater levels in QD and bedrock below the central parts of the lakes (only measured groundwater level in QD was available below Lake Eckarfjärden). The observed surface water level in Lake Eckarfjärden and the groundwater level below the lake show an upward gradient during all seasons in 2006 except for some short periods during the summer, which was dry that year (cf. Figure 3-66; during long periods, the level difference is within the measurement error limits). The same pattern as observed in the data from the site can be seen in the model results, with a few short periods of fast level increases as exceptions. The differences during these periods are due to slightly faster responses in the simulated surface water level compared with the simulated groundwater level. Differences are also observed during the short summer periods with downward gradient.

Regarding the surface water level in Lake Bolundsfjärden and the groundwater level in the QD below the lake, the level difference is very small, mostly within the measurement error limits. However, during the dry summer of 2006 there is a downward gradient; the difference is considered to be well outside the measurement error limits. In the simulation, no difference can be seen between the surface water level and the groundwater level in QD below the lake (i.e. these two curves are identical in the figure).

For the observed groundwater levels in the bedrock below Lake Bolundsfjärden, there is a continuous downward gradient all the way down to the deepest well section below –96 m RHB70, although the level difference is small between the two lowest well sections (HFM32-1 and HFM32-2). If the measured point water heads are re-calculated to environmental water heads the gradient is actually upward from the lowest to the next lowest section of the well,

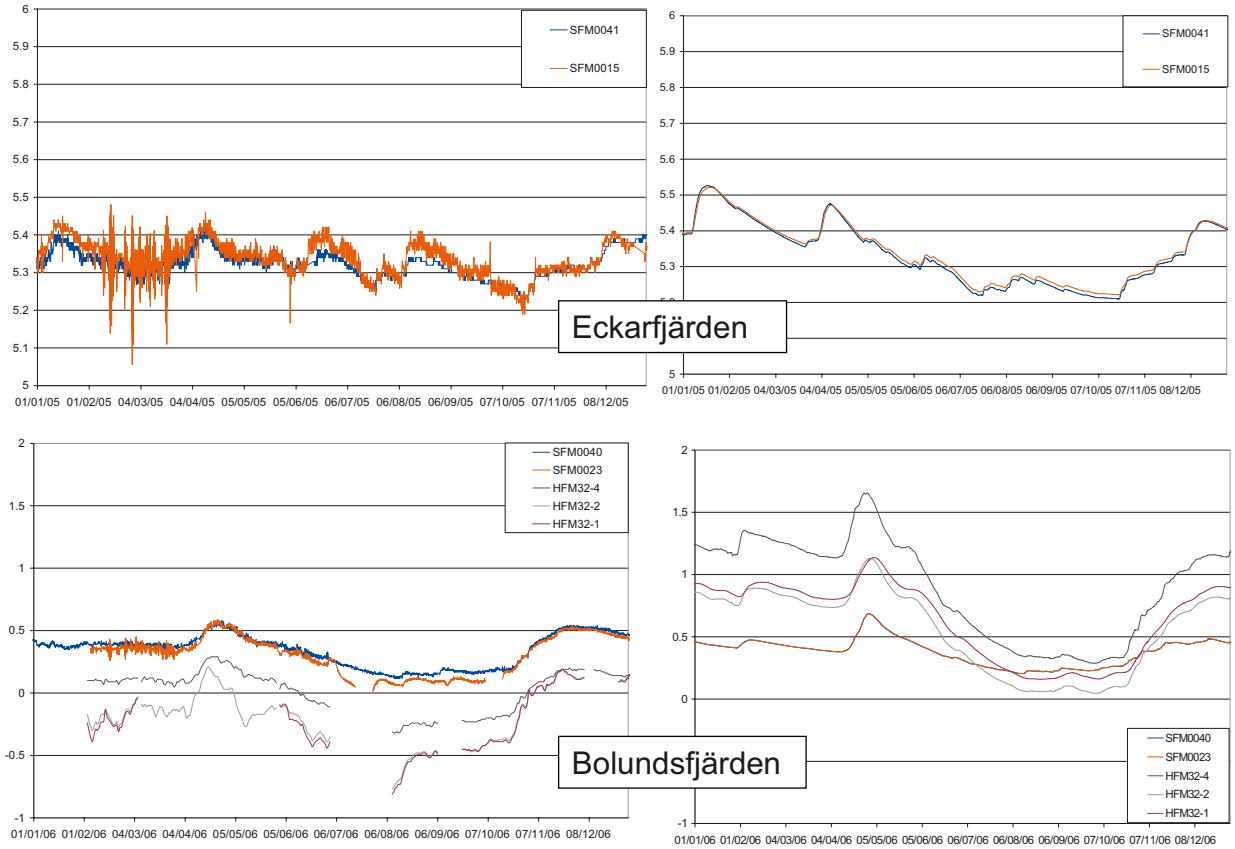

Figure 4-39. *Lake water levels and groundwater levels below the central parts of the lakes in Lake Eckarfjärden and Lake Bolundfjärden for the period Jan. 1–Dec. 31, 2006. Observed levels are shown to the left and simulated levels to the right.The borehole sections of HFM32 are numbered starting with 1 for the deepest section /Bosson et al. 2008/.*

see Appendix 2. The simulated groundwater levels in the bedrock are generally too high even when the SFR-pumping is active and higher than the lake water level and the groundwater level in QD most of the time. Section HFM32-2 has the lowest simulated head indicating both an upward and downward gradient toward this section. However, the head difference between the uppermost bedrock section and the QD is larger than between the uppermost and the second uppermost bedrock section.

Figure 4-40 shows the observed and simulated vertical gradients at two locations in the vicinity of Lake Bolundsfjärden; observations wells SFM0058 and HFM15, 100 m west of the lake, and SFM0004 and HFM04, 1,000 m southeast of the lake (see Figures 2-7 and 2-9 for locations of the wells). At both locations, a clear downward gradient can be seen from the QD, both in observed and simulated levels, and the downward gradient continues within the bedrock. The observed groundwater levels indicate, however, a smaller downward gradient between the QD and the bedrock during the dry summer months and for one period even an upward gradient. This seems to be an effect of direct or indirect (via capillary rise) root water uptake in the QD.

The present version of the MIKE SHE model code supports these processes in the upper saturated zone layer only, why the response from these phenomena cannot be fully developed in the model. Because of this, the drawdown in the QD during very dry periods, like in the summer of 2006, may be underestimated by the model.

In Figures 4-41 and 4-42 the impact of evapotranspiration is illustrated by presentation of accumulated net flow between unsaturated zone and saturated zones in 120 × 120 m squares at SFM0011 and SFM0019, classified as located in typical discharge and recharge areas, respectively. A considerable upward flow from the saturated to the unsaturated zone takes place at both sites during the dry summer of 2006 according to the modelling. In the figures also the accumulated direct root water uptake from the saturated zone is shown.

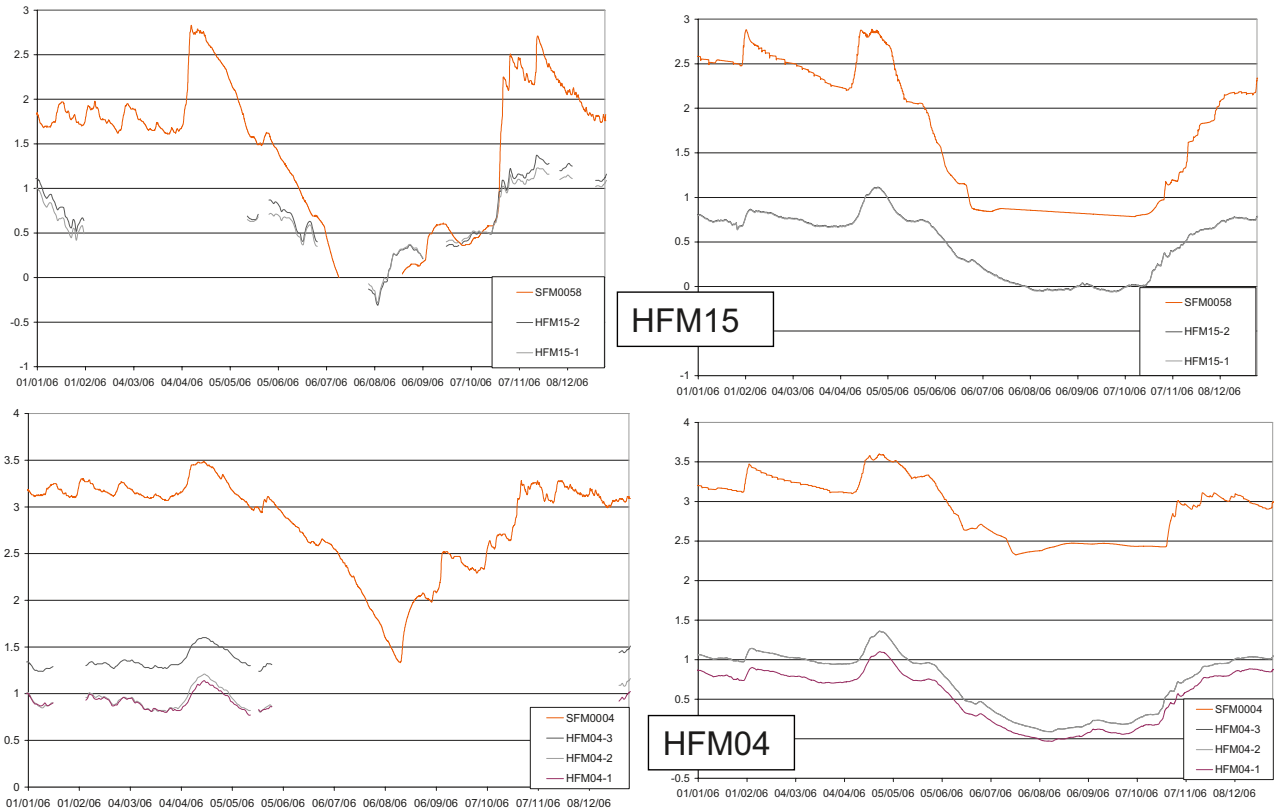

Figure 4-40. *Observed (left) and simulated (right) groundwater levels in HFM04 and HFM15 in bedrock and in nearby monitoring wells in Quaternary deposits, SFM0004 and SFM0058, respectively (lowest HFM-well index indicate the deepest section) /Bosson et al. 2008/.*

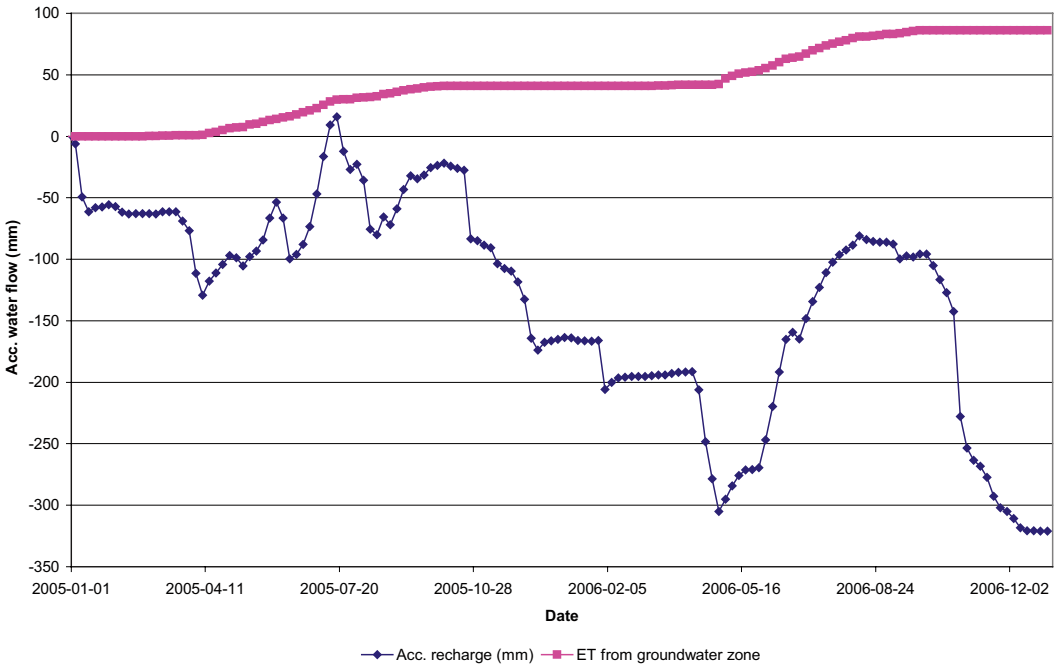

Figure 4-41. *Accumulated net flow between unsaturated and saturated zones in a 120 × 120 m area at SFM0011, classified as located in a typical discharge area. Increasing negative values indicate downward flow (recharge) and consequently a rising curve indicates upward flow (discharge). In the figure also accumulated direct groundwater root water uptake is shown.*

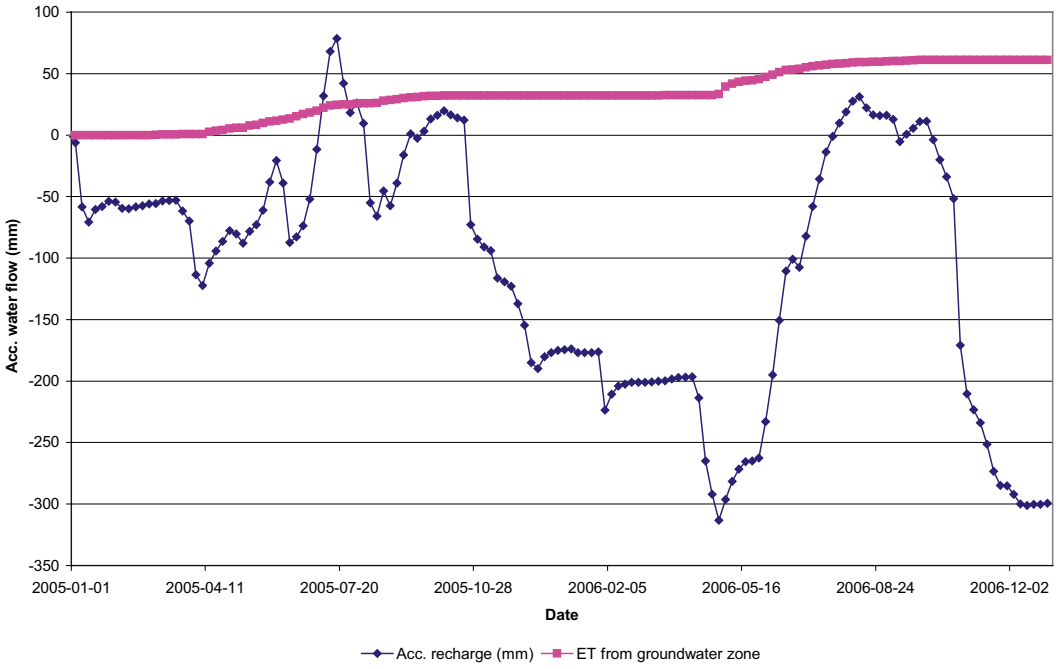

Figure 4-42. *Accumulated net flow between unsaturated and saturated zones in a 120 × 120 m area at SFM0019, classified as located in a typical recharge area. Increasing negative values indicate downward flow (recharge) and consequently a rising curve indicates upward flow (discharge). In the figure also accumulated direct groundwater root water uptake is shown.*

Figure 4-43 shows a summary of the simulated and observed vertical gradients in four HFM-wells; HFM32, HFM16, HFM15 and HFM04, and in adjacent monitoring wells in QD, which are all located in the vicinity of Lake Bolundsfjärden. Results are shown for April 2006, being a wet period, and August the same year, being a dry period. In April, the simulated gradients give the same flow directions as the observed, except between the upper part of the bedrock in HFM32 and the QD in SFM0023 (represented as "QD" in the HFM32 section), where the simulated groundwater levels in the bedrock are too high.

In August, the simulated gradients in HFM04 are still correct, while some deviations appear in the other wells. The levels in the bedrock at HFM32 are still too high. The observed level in

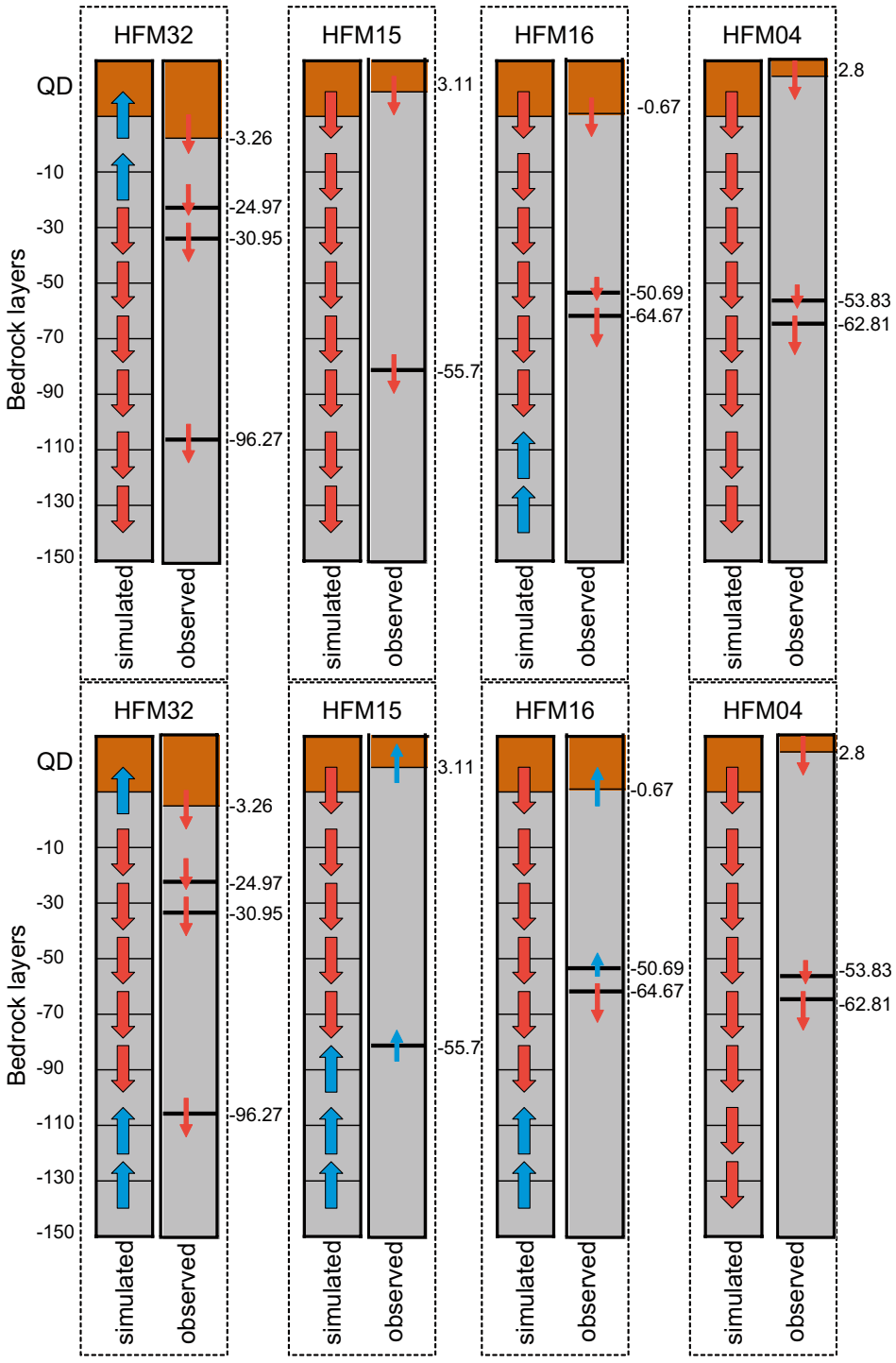

Figure 4-43. *Comparison of measured and simulated direction of the vertical gradients in HFM32, HFM15, HFM16 and HFM04 in April and August 2006 (upper and lower graphs, respectively) /Bosson et al. 2008/.*

the lowest section is lower than higher up, which is not the case in the model. However, if the observed point water heads are re-calculated to environmental heads, the level in the lowest section is higher than in the section above.

In HFM15 and HFM16, the gradients are switched from downward in April to upward in August, according to observed gradients in Figure 4-43. This is most likely due to root water uptake in the QD. In the model, these processes are limited to the upper layer of the saturated zone, being 2.5 m in most parts of the model.

Figure 4-44 shows simulated groundwater levels in a west-east profile through Lake Eckarfjärden at SFM0015 (see Figure 2-7 for well location). In the upper graph the conditions in

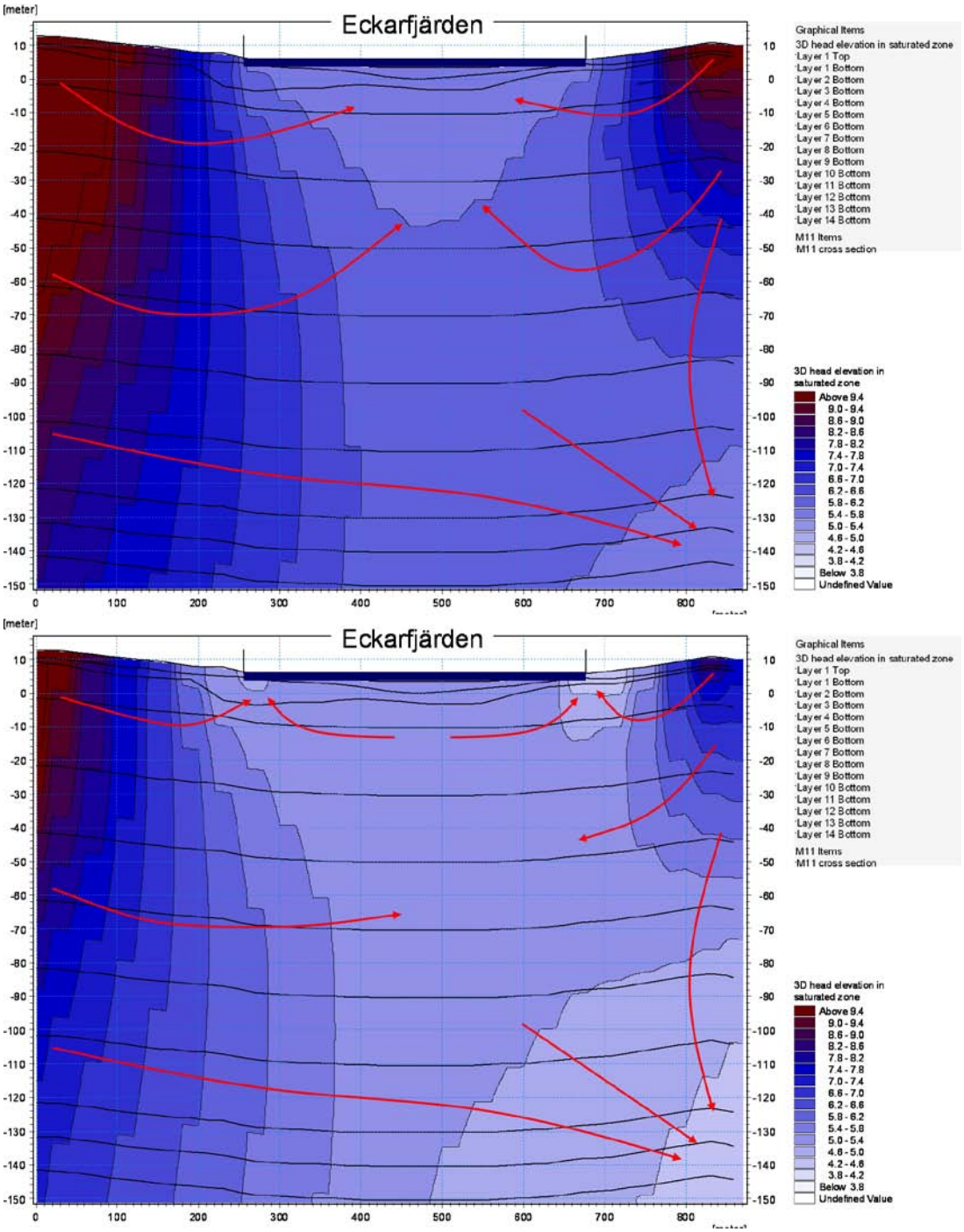

Figure 4-44. *Simulated groundwater heads in a west-east profile crossing Lake Eckarfjärden at SFM0015 in April and August 2006 (upper and lower graphs, respectively) /Bosson et al. 2008/.*

April 2006 (a wet period) are shown, and in the lower graph the conditions in August 2006 (a dry period). The red arrows in the figure indicate the prevailing flow directions. Under wet conditions, Lake Eckarfjärden acts as discharge area for the upper parts of the profile, quite weak though with higher gradients in the horizontal direction. Deeper down in the profile, a downward gradient to the east can be seen.

During the period of dry conditions, the principal flow directions are to a large extent the same as under wet conditions, with the difference that during the dry period the effect of transpiration on the gradients in the littoral zones results in upward gradients along the lake perimeter inducing a flow both from the land and the lake side.

In Figure 4-45 the simulated accumulated net flow through the bottom of Lake Eckarfjärden is shown. Specifically, it shows the average net flow within the area with a water depth of > 0.5 m; the accumulated flow increases when discharge takes place. The recharge of water from the lake to the groundwater zone during the dry summer of 2006 is clearly seen as a drop in the cumlative discharge.

In Figure 4-46, a profile of simulated groundwater heads in a west-east profile across Lake Bolundsfjärden at SFM0023 is shown (see Figure 2-7 for well location). Under wet conditions, also Lake Bolundsfjärden acts as discharge area for the upper parts of the bedrock according to the model. The comments to Figures 4-39, 4-40 and 4-43 above, however, make it clear that observed data do not support this. The reason for the discrepancy is that the simulated heads in the bedrock are higher than the observed levels. In the model, the simulated gradients in the upper part of Figure 4-46 show that layer 4 (c. 10–30 m.b.s.l), being part of the high-conductive sheet joints in this area, transports water from the higher altitude areas around the lake in under the lake.

During the period of dry conditions, the effect of transpiration on the gradients in the littoral zones is even more pronounced at Lake Bolundsfjärden than at Lake Eckarfärden. At the eastern side of the lake, a significant upward gradient is simulated by the model, i.e. according to the model the root water uptake together with the capillary forces are important sinks. This is the case not only for the QD but also for the upper bedrock, especially in the littoral zones around the lakes.

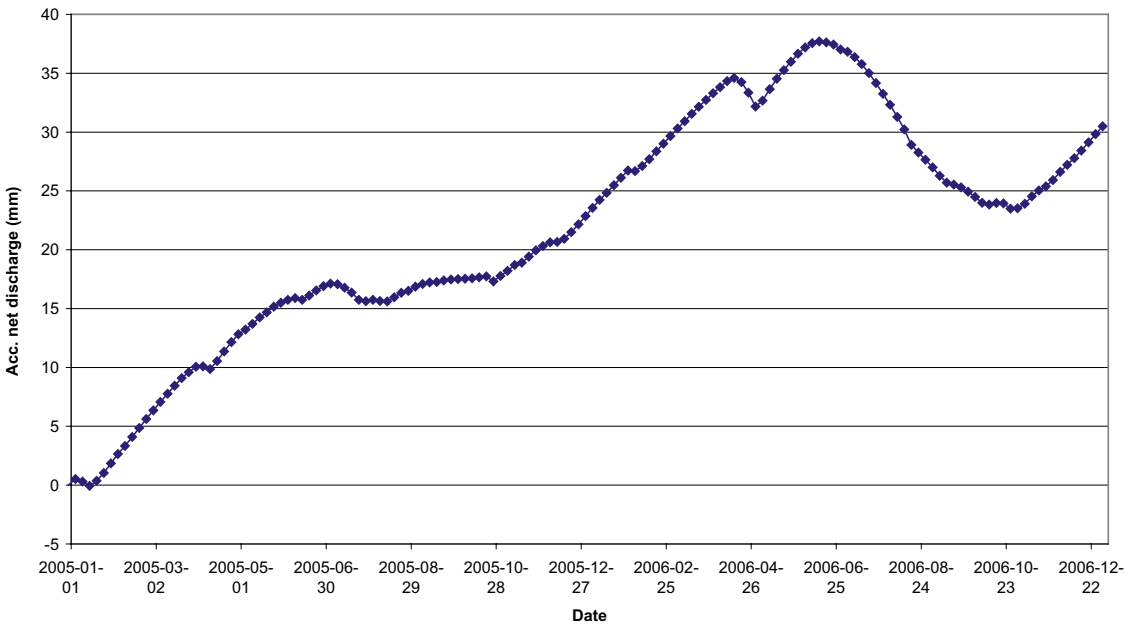

Figure 4-45. *Accumulated net discharge from the groundwater zone through the bottom of Lake Eckarfjärden (within the area of water depth > 0.5 m).*

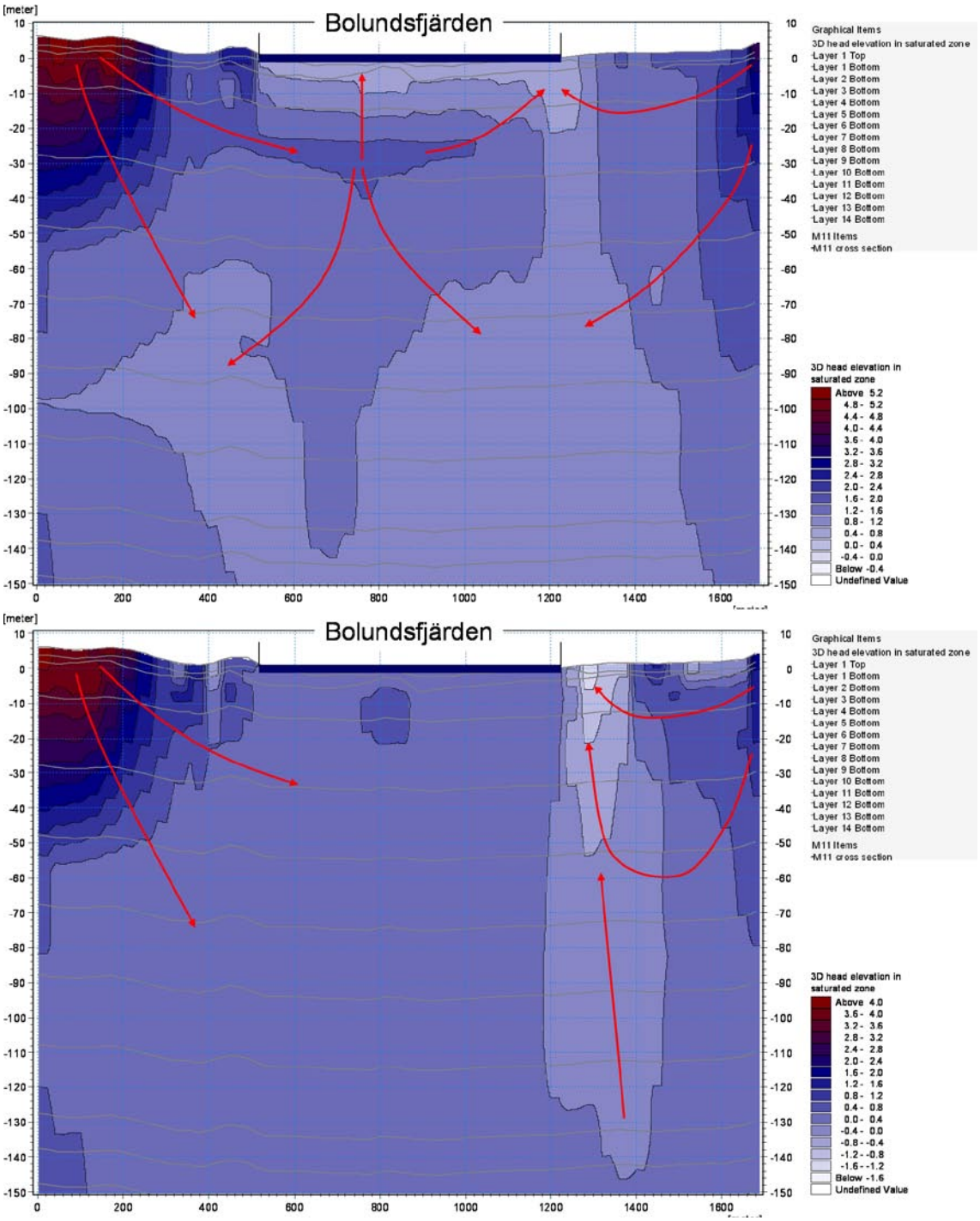

Figure 4-46. *Simulated groundwater heads in a west-east profile crossing Lake Bolundsfjärden at SFM0023 in April and August 2006 (upper and lower graphs, respectively) /Bosson et al. 2008/.*

In Figure 4-47 the effect of the SFR-pumping on the simulated vertical gradients at four HFM-wells (HFM32, HFM16, HFM15 and HFM04), all in the vicinity of Lake Bolundsfjärden, are shown (see Figure 2-9 for well locations). The influence on the flow directions during wet periods, like in April 2006 (shown in the upper graph of Figure 4-47), is minor. However, it is interesting to note the change from downward to upward flow direction deep down in HFM16. The simulated downward flow directions below –110 m are reversed due to the drawdown caused by the highly conductive sheet joints connecting to the SFR-pumping at this depth in the model.

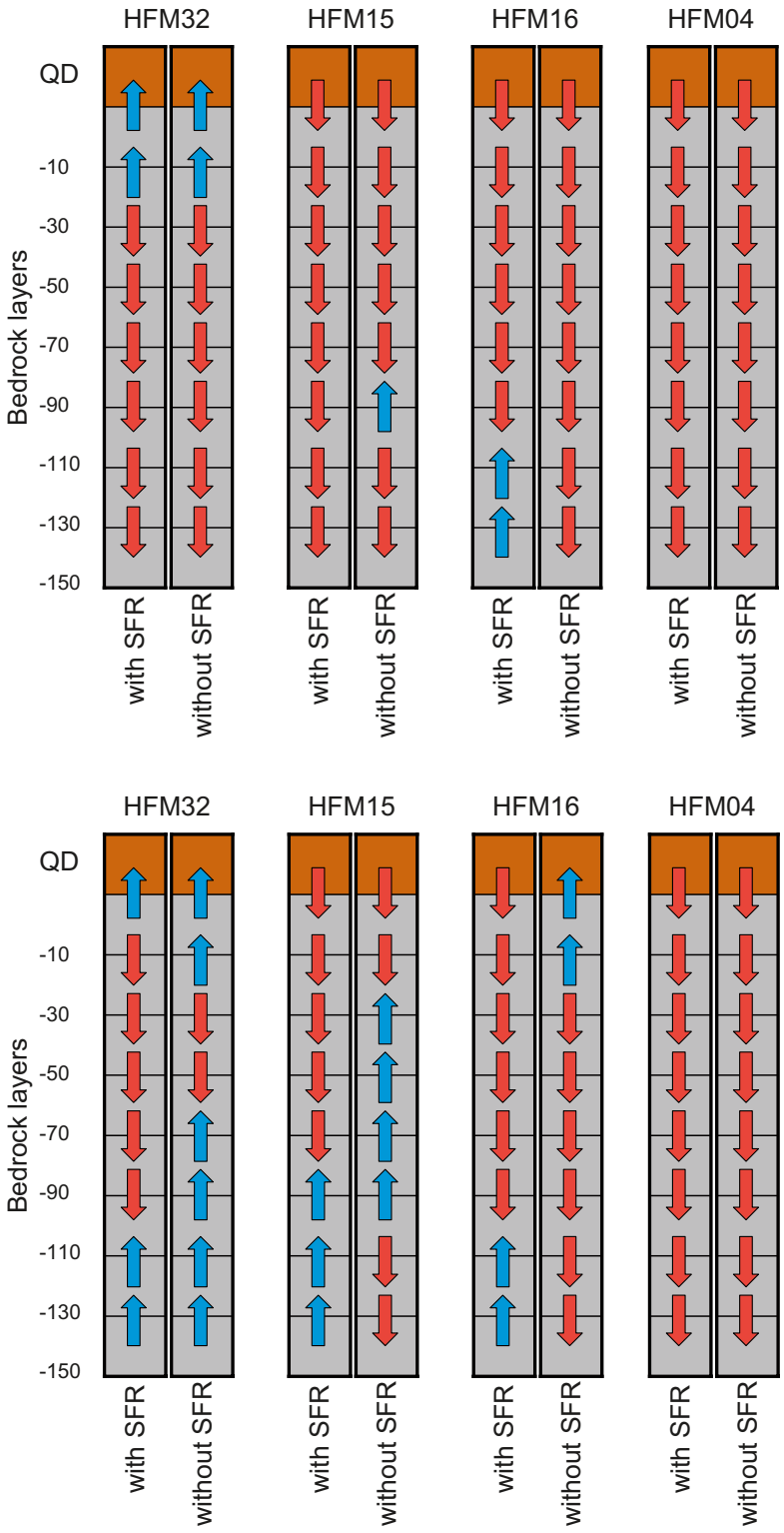

Figure 4-47. *Simulated vertical groundwater flow directions without and with the SFR-pumping included in the model during April and August 2006 (upper and lower graph, respectively) /Bosson et al. 2008/.*

The flow directions during dry periods, here exemplified by August 2006 (shown in the lower part of Figure 4-47), are much more influenced than those under wet conditions. The only borehole where the flow directions are unchanged is HFM04. The pattern at the other locations is a switch to a downward flow direction to the layer where the deepest sheet joints are located (at c. 90 to 110 m.b.s.l.), and a switch to an upward direction to the same layer from the deeper bedrock layers below the sheet joints.

Figures 4-48 and 4-49 show simulated groundwater levels in a south-north profile from the location of HFM32 in Lake Bolundsfjärden, through Lake Puttan, to the location of HFM34 (see Figure 2-9 for well locations). In Figure 4-48 the conditions in April 2006 are shown. The upper graph shows the simulated conditions without the SFR-pumping and the lower one shows the conditions with the SFR-pumping. The lakes and the sea act as quite strong discharge areas when SFR is not included. When the SFR-pumping is included a pronounced downward and northeast-directed gradient is created, leaving smaller and weaker discharge areas. The same holds for the conditions in August 2006, shown in Figure 4-49, but even more pronounced, with almost no upward directed gradients when SFR is included.

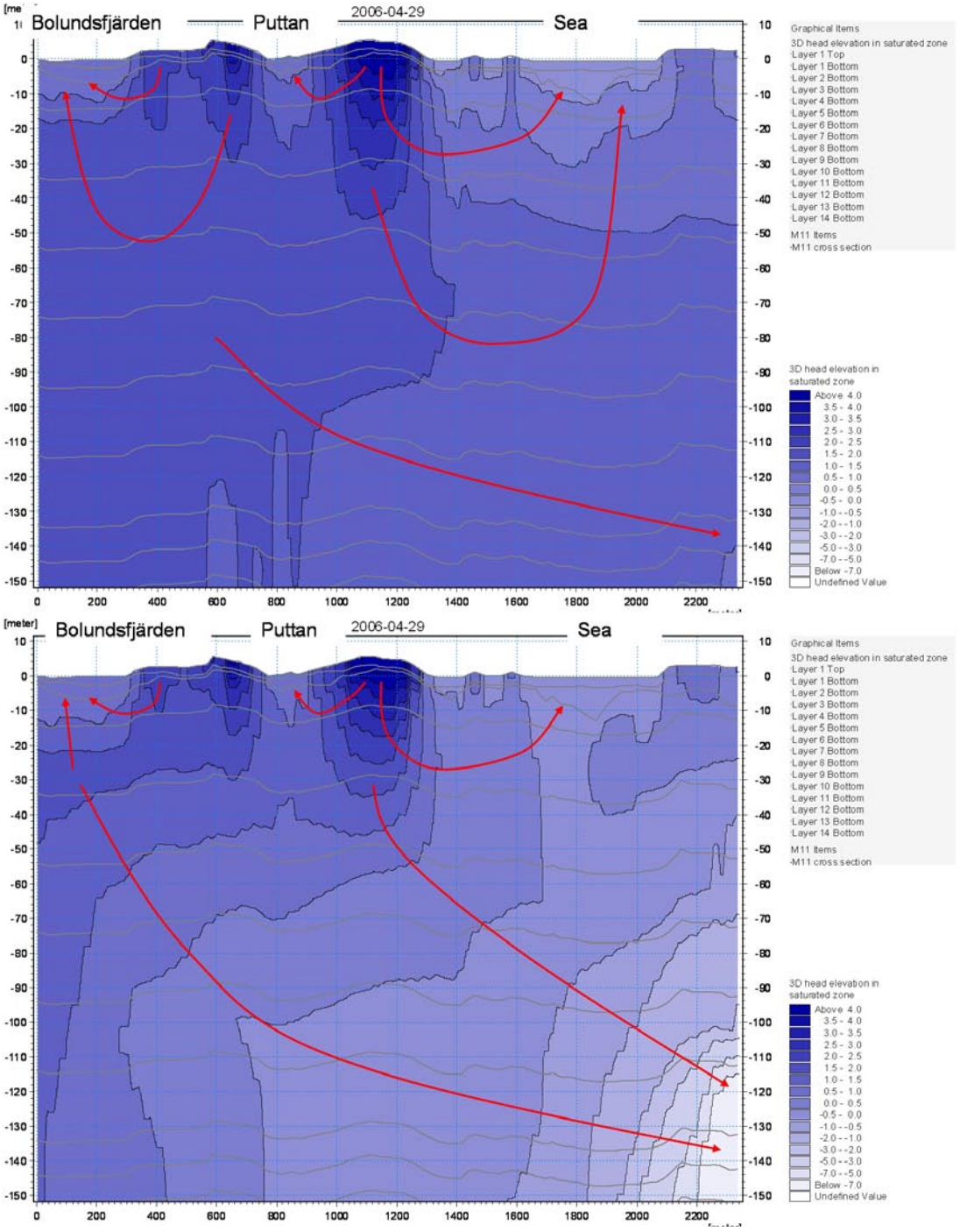

Figure 4-48. *SW-NE profile from HFM32 to HFM34 showing simulated groundwater heads in April 2006 without (upper graph) and with (lower graph) the SFR-pumping included in the model /Bosson et al. 2008/.*

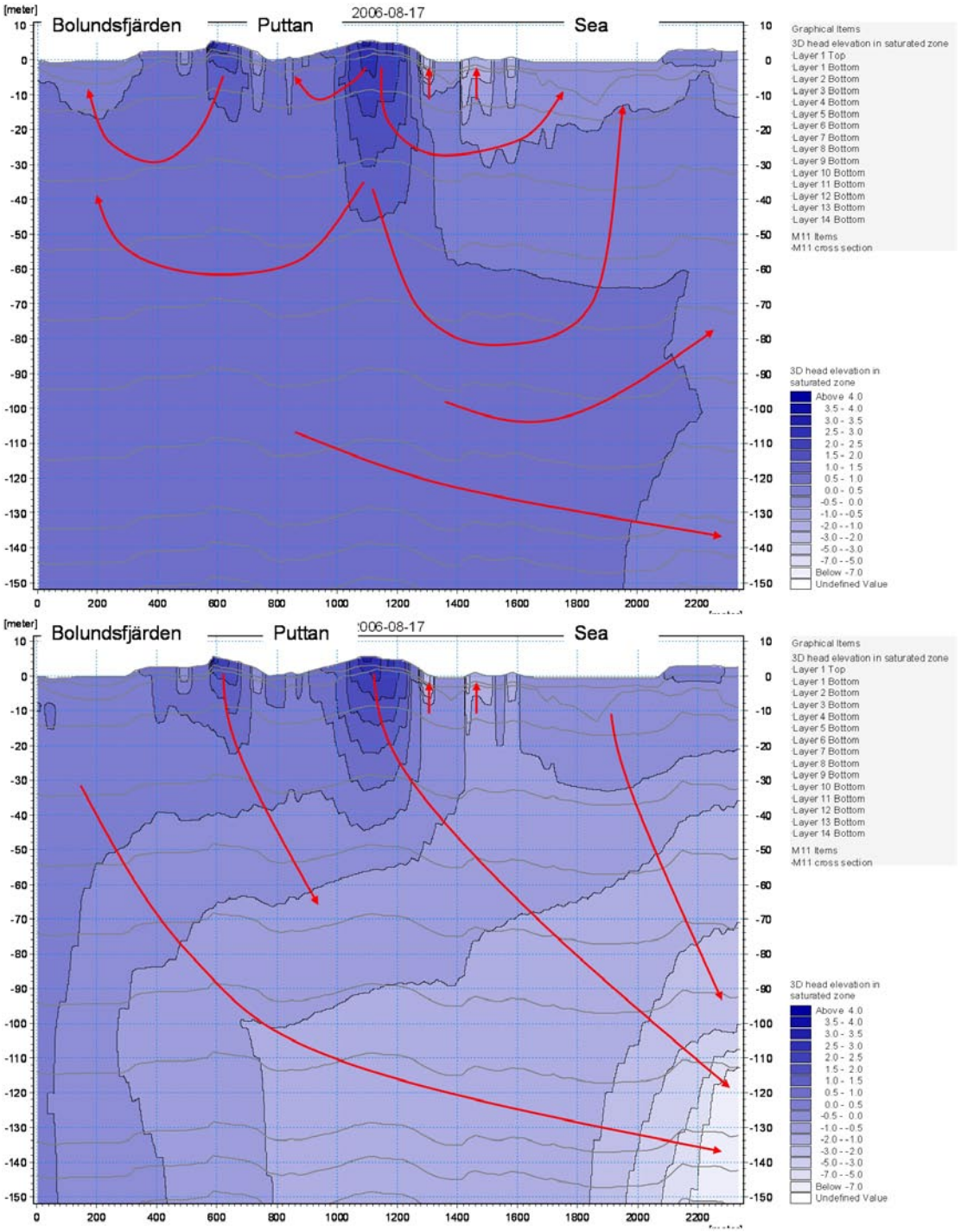

Figure 4-49. *SW-NE profile from HFM32 to HFM34 showing simulated groundwater heads in August 2006 without (upper graph) and with (lower graph) the SFR-pumping included in the model /Bosson et al. 2008/.*

Transport modelling

Both particle tracking and advection-dispersion modelling were performed using the final three-dimensional flow fields simulated by MIKE SHE. Only the results of the particle tracking will be summarised here. For a more detailed presentation of the particle tracking and the advection-dispersion modelling the reader is referred to /Bosson et al. 2008/ and /Gustafsson et al. 2008/.

Particle tracking was performed based on the final model from *Phase 2* of the calibration, both without and with the SFR-pumping activated in the model. For each of these two cases, two particle release cases were simulated:

- **PT5-allover**: One particle was introduced in each cell at 140 m.b.s.l. in the whole MIKE SHE model area.
- **PT5_repository**: One particle was introduced in all cells at 140 m.b.s.l. within an area corresponding to that of the planned repository (the repository is planned to be built at 500 m.b.s.l.).

The selected simulation time was 300 years, using the transient flow modelling results obtained for the simulated one-year period of Oct. 2003–Sep. 2004 as input. This means that the model results from the MIKE SHE flow field simulation for this one-year period were cycled 300 times. The overall results for *PT5_allover* with and without the SFR-pumping, expressed in terms of where the particles left the saturated zone (i.e. to which other model compartments or boundaries they went), are summarised in Table 4-12.

According to the simulations, the dominating sink without SFR is the combined unsaturated zone/overland compartment. (It is not possible to separate these two sinks in the model.) At the end of the simulation, 65% of the particles were still in the model volume, i.e. it took less than 300 years for 35% of the particles to reach the ground surface or the sea from 150 m depth. When pumping at SFR, the sink "particles removed by wells" (i.e. SFR) was the dominating sink with 15% of the particles leaving the model volume through the pumping at SFR. Only 5% of the particles moved to the sea when pumping at SFR, compared with 14% when the SFR-pumping was not active.

When pumping at SFR, 66% of the particles were still in the model volume after 300 years. Illustrations of the numbers in Table 4-12 are shown in Figures 4-50 and 4-51. The figures shows the position of each particle where it left the saturated zone and moved to a specific sink. Results are shown both without (Figure 4-50) and with (Figure 4-51) the SFR-pumping activated. The different sinks are marked with different colours. The blue dots represent the particles that moved to the combined unsaturated zone/overland sink. Since the majority of these dots are situated in the lakes and close to the brooks, i.e in saturated areas, the majority of the particles registered in this sink have moved to the overland compartment. When pumping at SFR, the majority of the particles that have gone to sinks outside the on-land part of the model area have been removed by this pumping.

Table 4-12. List of particle sinks and the distribution of particles on the sinks in the PT5_allover modelling without and with the SFR-pumping activated /Bosson et al. 2008/.

Sink	PT5-allover, no SFR Number of particles	%	PT5-allover, SFR Number of particles	%
Particles removed to OL-UZ*	3,460	15	2,480	11
Particles removed directly to brooks	817	4	468	2
Particles removed by drain to brooks	415	2	352	1
Particles gone to the sea	3,349	14	1,149	5
Particles removed by wells	0	0	3,404	15
Particles left in model	14,826	65	15,014	66
Sum	22,867	100	22,867	100

*OL-UZ is the combined Overland flow-Unsaturated zone sink.

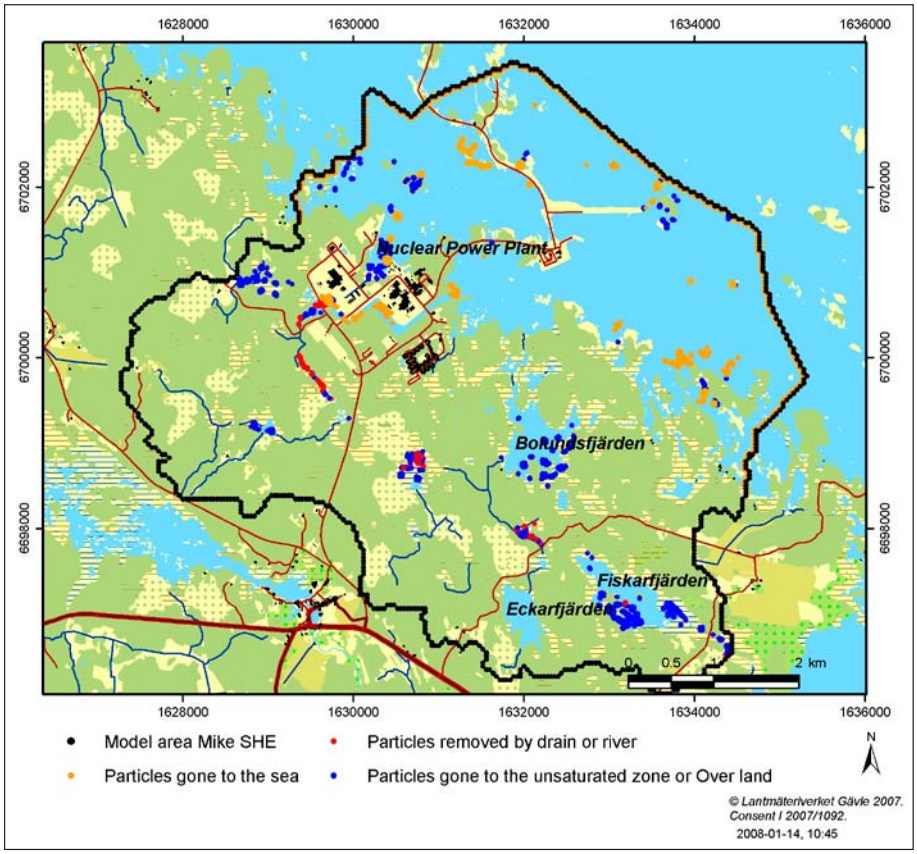

Figure 4-50. *Sinks for the particles in PT5_allover without the SFR-drainage /Bosson et al. 2008/.*

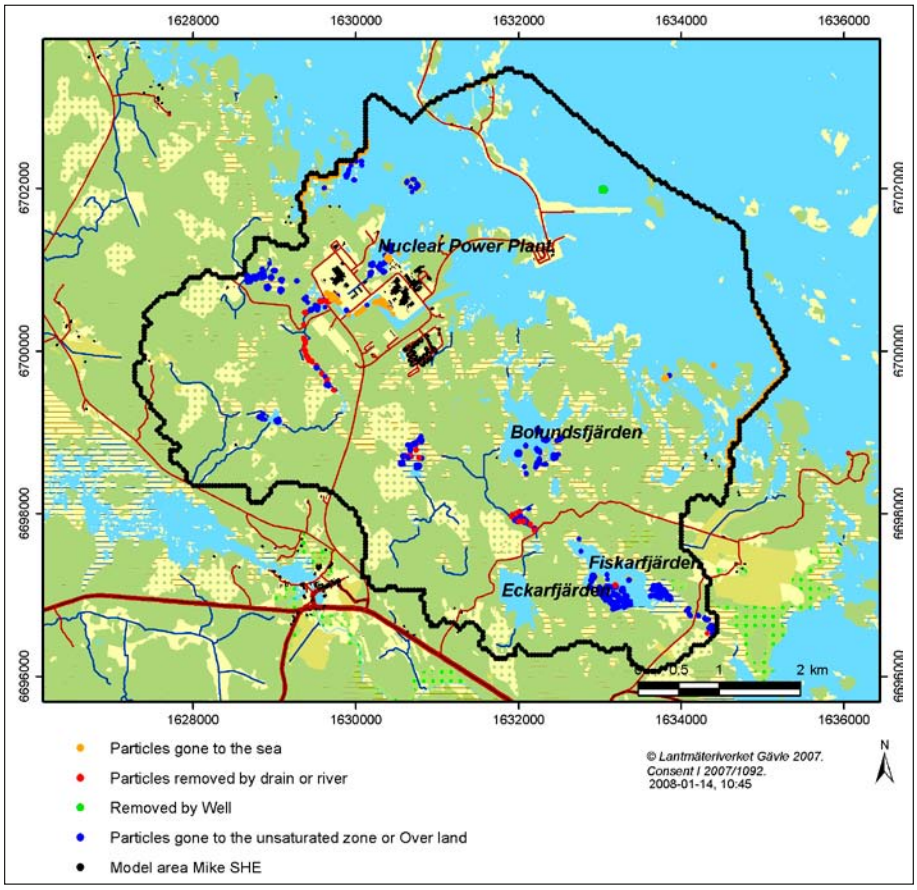

Figure 4-51. *Sinks for the particles in PT5_allover with the SFR-drainage /Bosson et al. 2008/.*

Figure 4-52 shows the accumulated particle count for each cell at 150, 130, 110 and 90 m.b.s.l. at the end of the simulation. The accumulated particle count is a way to present the density of the flow paths. Each time a particle passes a cell the accumulated particle count is increased, i.e. the higher the value for a particular cell in the model, the more particles have passed that specific cell. The particles are introduced at 140 m.b.s.l. Since one particle has been introduced to each cell, the minimum accumulated particle count at this level is one. The pink colour indicates that no particles have passed the cell.

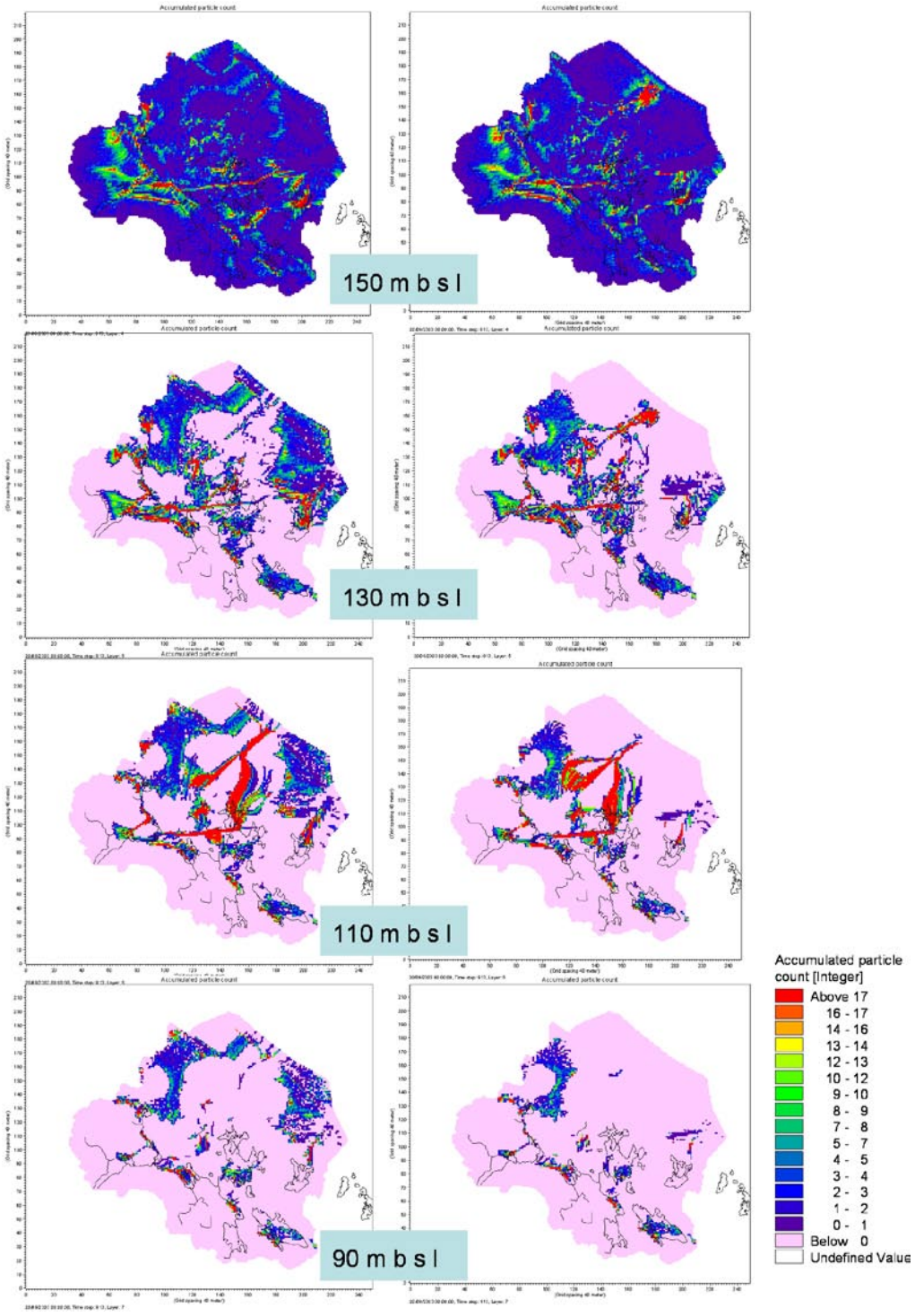

Figure 4-52. *Accumulated particle count at 150, 130, 110, and 90 m.b.s.l. The particles move towards the sheet joints in the layer at 110 m.b.s.l. The graphs to the left present the results from PT5_allover without the SFR-drainage, and the graphs to the right the results from the PT5_allover with the SFR-drainage /Bosson et al. 2008/.*

The flow paths concentrate to specific areas on their way towards the surface. At 110 m.b.s.l. the horizontal sheet joints have their deepest representation in the model. It can be seen that the particles concentrate to this layer, see the red areas in the figure. The same pattern is seen for both cases, without and with the SFR-pumping included. When pumping at SFR, particles released in the northeastern part of the model area, move towards SFR. The majority of the particles moves towards SFR at 110 m.b.s.l. Above this level only 40% of the cells that received a particle at 110 m.b.s.l. is hit by a particle.

In *PT5_repository*, 1,501 particles were released at 140 m.b.s.l. inside the area corresponding to the planned repository. After 300 years only 10% of the particles had left the model volume and all these particles had gone to the sea. When pumping at SFR, 18% of the particles had left the model volume through the pumping in SFR. The rest of the particles were still in the model. For both cases, without and with SFR-drainage, the major part of the particles moved toward the sea at 110 m.b.s.l. (Figure 4-53). The particles concentrated to this sheet-joint layer and the horizontal transport was dominating.

Above this level only a few cells were passed by a particle. When pumping at SFR, no particles reached higher than 70 m.b.s.l. Thus, there were no exit points at the surface after 300 years of simulation when pumping at SFR. When the SFR-pumping was not active, a few particles reached the sea. These exit points were located close to the shoreline.

Since many particles were still in the model volume after 300 years, an additional longer simulation was run for *PT5_repository*. The simulation was run for 5,000 years. The exit points at the surface after 5,000 years are shown in Figure 4-54. As a comparison the exit points after 300 years are also shown in the same figure. The transport times were long and even after 5,000 years 81% of the particles were still in the model volume.

No exit points were found in the on-land part of the model area. All the particles left the model volume at sea. 79 particles, 5% of the total number of introduced particles, were stuck in the marine sediments. Apart from this, no particles were left in the upper calculation layers. All the particles that were left in the model after 5,000 years were found in the deeper bedrock between layer 8 at 110 m.b.s.l and layer 14 at 600 m.b.s.l.

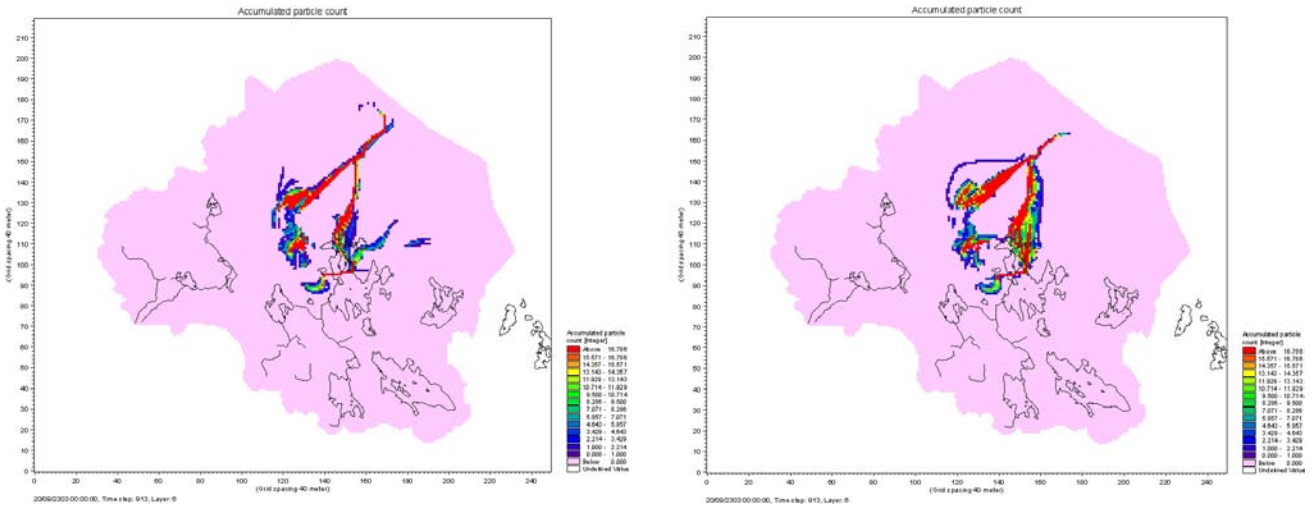

Figure 4-53. *Accumulated particle count at 110 m.b.s.l. for the case with particle release within the repository area only. The particles concentrate to the sheet joints layer at this level. The simulation without the SFR-pumping is shown to the left and the simulation with the SFR-pumping activated to the right /Bosson et al. 2008/.*

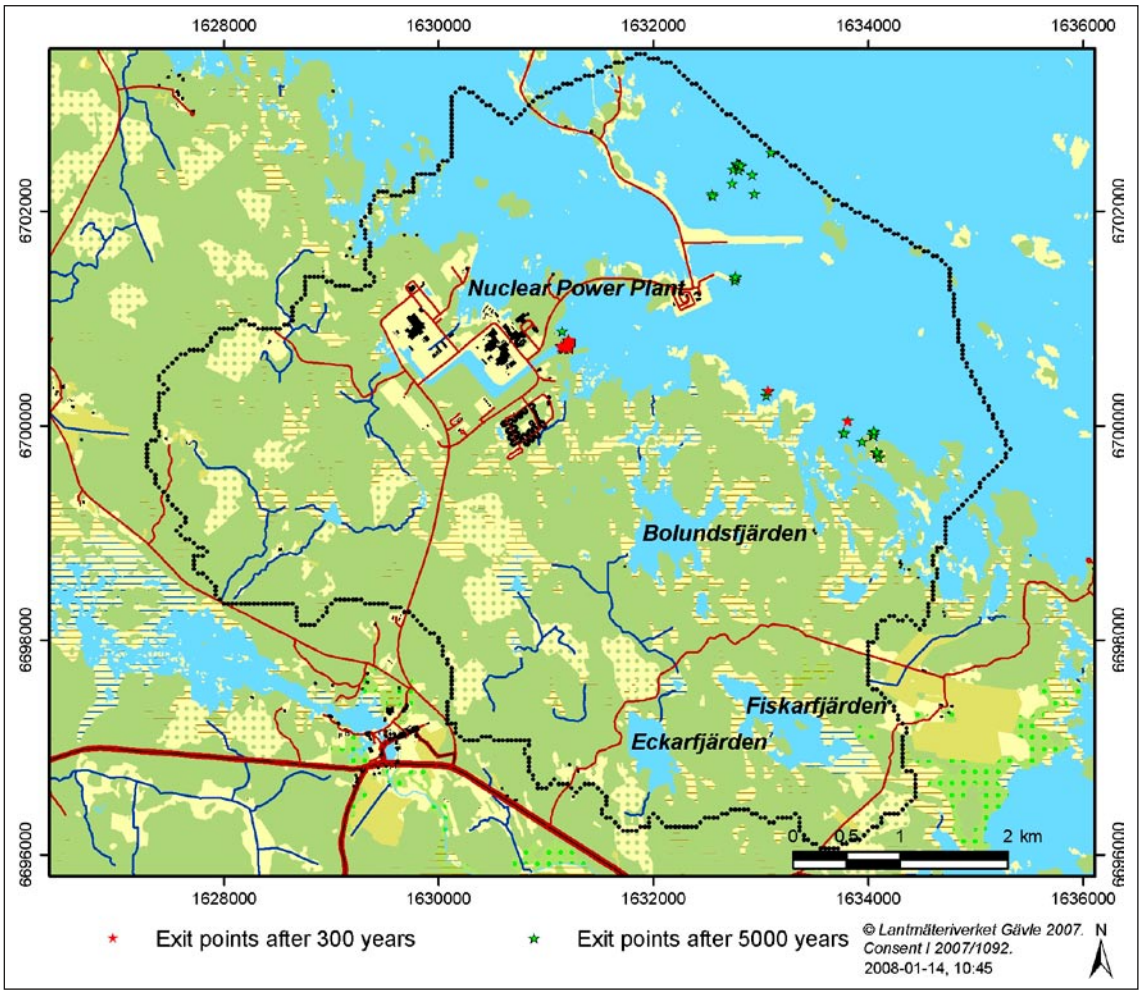

Figur 4-54. *Exit points at the surface after 5,000 years of simulation (without the SFR drainage). As a comparison the exit points after 300 years are also shown in the figure /Bosson et al. 2008/.*

5 Resulting site description

5.1 Summary of the site description

5.1.1 Physiographic setting

The Forsmark area is situated on the eastern coast of Sweden in the northeastern part of Uppsala county, c. 120 km north of Stockholm. The land area within the site investigation area is characterized by a low relief with a small-scale topography. The study area is almost entirely situated below 20 m.a.s.l. Forest is the dominating land cover. Only in the southeastern part of the area, at Storskäret, agriculture is an important landuse.

The main lakes, Lake Fiskarfjärden, Lake Bolundsfjärden, Lake Eckarfjärden and Lake Gällsboträsket have all sizes of less than one km^2 and are quite shallow. No major water courses flow through the central parts of the site investigation area. The brooks downstream Lake Gunnarsboträsket, Lake Eckarfjärden and Lake Gällsboträsket carry water most of the year, but can still be dry for long time periods during dry summers. Wetlands are frequent and cover more than 25% of some sub-catchments. Bogs are only found in the most elevated parts of the area. The peat in the wetlands can rest directly on till, or be underlain by gyttja and/or sand and clay above the till.

Till is the dominating Quaternary deposit, covering c. 75% of the terrestrial area. Bedrock outcrops are frequent, but constitute only c. 5% of the area. Wave-washed sand and gravel, clay, gyttja clay and peat cover 3–4% each. The only glaciofluvial deposit, the Börstilåsen esker, runs in a north-south direction along the coast. The Quaternary deposits are shallow, usually less than 5 m deep.The greatest depth to bedrock recorded in a drilling is 16 m southeast of Lake Fiskarfjärden.

Granitic rocks are dominating in the area. The bedrock hydrogeology reveals a significant hydraulic anisotropy within the tectonic lens, which covers the body of the candidate area. The upper c. 150 m of bedrock contains high-transmissive horizontal fractures/sheet joints. The horizontal fractures/sheet joints have transmissivities in the range c. $1\cdot10^{-6}$ –$1\cdot10^{-3}$ m^2/s (hydraulic conductivity c. $1\cdot10^{-6}$ –$1\cdot10^{-3}$ m/s). The bedrock in between the horizontal fractures/sheet joints, however, is considerably less conductive (hydraulic conductivity c. $1\cdot10^{-11}$ –$1\cdot10^{-8}$ m/s) except where it is intersected by transmissive steeply-dipping or gently-dipping deformation zones. Below the uppermost c. 150 m of bedrock the occurrence of high-transmissive horizontal fractures/sheet joints vanish and the conductive fracture frequency becomes very sparse and fairly low-transmissive (fracture transmissivity c. $1\cdot10^{-10}$ –$1\cdot10^{-7}$ m^2/s). In some of the 1,000 m deep cored boreholes there are almost no flowing fractures observed below c. 150 m depth.

5.1.2 Boundary conditions

External boundaries

Top boundary

The meteorological conditions constitute the top boundary of the hydrological and near-surface hydrogeological system. Water is added to the system by rainfall and snowmelt and abstracted by evapotranspiration. There is a relatively strong west-east gradient in precipitation in the region; the highest precipitation occurring some distance inland from the coast. The mean annual precipitation at Lövsta, approximately 15 km inland, is 690 mm, which can be compared with the corresponding value of 492 mm at the island of Örskär, c. 15 km northeast of Forsmark (corrected mean values for the period 1994–2006). From regional data the mean annual precipitation in the Forsmark site investigation area has been estimated to 559 mm for

the period 1961–1990. The precipitation during the site investigation has been quite close to the longterm average. For the 4-year period of June 2003–May 2007, the mean annual precipitation was 563 mm. The mean annual calculated potential evapotranspiration for the same period was 526 mm.

In the MIKE SHE modelling, a reduction of the calculated potential evapotranspiration by 15% was necessary to obtain a good agreement with the measured runoff. A comprehensive sensitivity analysis was performed, testing the parameters involved in the calculation of the actual evapotranspiration (root distribution, interception storage, leaf area index etc), within reasonable limits. However, the only possible way found to get a good matching between measured and simulated total runoff, was a reduction of the potential evapotranspiration. No definite conclusion can be drawn regarding to what extent the need for reduction of the potential evapotranspiration in the modelling was caused by an inability of the model to simulate the actual evapotranpriration processes. An alternative (or complementary) explanation could be that the calculated potential evapotranspiration used as input was overestimated.

Inland boundary

The close correlation between the topography of the ground surface and the groundwater level in the Quaternary deposits (QD) means that surface water and groundwater divides for the QD can be assumed to coincide. Regarding groundwater levels in the upper bedrock there is no strong coupling to the topography of the ground surface. This is most evident in the central part of the site investigation area, i.e. in the tectonic lens where the upper c. 150 m of the bedrock is known to have frequent horizontal and sub-horizonal highly transmissive fractures. However, westward increasing groundwater levels in the bedrock outside the tectonic lens indicate that the water divides of the flow systems involving the near-surface bedrock follow the surface water divide towards River Forsmarksån, i.e. the topography can be used for delineation of the inland boundary. No major fracture zones crossing the inland surface water divide against River Forsmarksån are known, with exception of the Eckarfjärden zone crossing south of Lake Eckarfjärden.

Sea boundary

From the conclusion that groundwater divides for the shallow groundwater systems limited to QD (till), where the major part of the water flow takes place, coincide with the surface water divides follows that such systems only may have lateral boundaries to the sea in the “rest” catchments adjacent to the sea and with no surface discharge in water courses. For the flow systems involving also the near-surface bedrock the situation is different due to the highly transmissive horizontal and sub-horizontal fracture zones extending below the sea. The vertical contact between these zones and the sea (direct via outcropping or indirectly via vertical fractures) will determine the boundary conditions of these systems. The superficial horizontal sheet joints have a tendency to follow the topography of the bedrock surface implying that direct hydraulic contact with the sea via outcropping is considered to be less common. The sea bottom is to a great extent covered by fine sediments (silt and clay) and till. However, areas with coarse sediments and also outcropping bedrock are frequent. The described features will determine the boundary conditions and the degree of hydraulic contact between the sea and the flow systems involving the near-surface bedrock.

During events of very high sea water levels, sea water flows into several of the lakes (Norra Bassängen, Puttan, Bolundsfjärden, Lillfjärden and Fiskarfjärden). During these events the sea obviously has an impact on both surface and groundwater flow systems in these lakes and their surroundings.

The conceptual hydrological and hydrogeological model, as implemented in the MIKE SHE model, resulted in a mean simulated annual outflow to the sea of 42 mm. The outflow of water from c. 150 m depth to the sea, traced in the particle tracking analyses performed in the MIKE SHE modelling, is manifested in a number of exit points at sea. However, according to the modelling, the residence times are quite long with only a few particles exiting within 5,000 years.

5.1.3 Infiltration and recharge

The infiltration capacity of the soils in the area exceeds the rainfall and snowmelt intensity with few exceptions. However, unsaturated (Hortonian) overland flow may appear over short distances, mainly on agricultural land covered with clayey till and on frozen ground where the soil water content was high during freezing. Also on outcropping bedrock, unsaturated overland flow may appear, but just over very short distances before the water reaches open fractures or the contact zone between bedrock and QD.

In the initial simulations with MIKE SHE, ponding and overland flow was generated, causing to sharp discharge peaks in brooks compared with the observations. This was not caused by an insufficient infiltration capacity, but merely by application of a too low hydraulic conductivity in the uppermost soil profile, see Section 5.1.4 below.

The shallow groundwater levels mean that there will be a strong interaction between evapotranspiration, soil moisture and groundwater. The groundwater levels in many monitoring wells in Quaternary deposits were within one metre below the ground all the year, and the groundwater level on average was less than 0.7 m below ground during 50% of the time. Also in what can be considered as typical recharge areas, the average groundwater level was not more than 1.2 m below ground. Only in locally elevated areas with relative steep slopes, considerably deeper groundwater levels can be assumed to exist. The annual variation in the groundwater level is mostly less than one metre in discharge areas, and 1.5 m in typical recharge areas. Diurnal fluctuations of the groundwater levels, driven by evapotranspiration cycles, were evident in the data from many of the groundwater monitoring wells in Quaternary deposits.

The very fast and strong responses of the groundwater level to rainfall also when the level is relatively deep below ground and the unsaturated zone deficit could be assumed to be relatively large, as in the summer/autumn of 2005 and 2006, indicate some kind of by-pass flow and/or a quite small specific yield. When the specific yields derived from the measurement were implemented in the Forsmark-HBV and MIKE SHE models, the responses in the groundwater levels and discharge were in most cases quite well captured. However, especially in the MIKE SHE modelling the responses after long dry periods were too slow and too small.

Direct recharge from precipitation is obviously the dominant source of groundwater recharge. However, the groundwater level measurements in the vicinity of Lake Bolundsfjärden and Lake Eckarfjärden show that the lakes may act as recharge sources to the till aquifers in the immediate vicinity of the lakes during summer. While the groundwater levels are well above the lake water levels during most of the year, they are considerably below the lake water levels during dry summer conditions. This is very clear close to the lake shores but also below the middle of the lakes the groundwater levels are slightly below the lake levels under such conditions (the difference is well outside the probable measurement error). The gradients from the lakes to the surrounding areas are created by direct and indirect groundwater abstraction caused by evapotranspiration. However, due to the low permeability of the bottom sediments, the resulting water fluxes can be assumed to be relatively small.

The observed phenomenon, with a drawdown of groundwater levels well below the lake water levels in the vicinity of the lakes caused by evapotranspiration, was well captured by the MIKE SHE model with the parameter settings from the conceptual model. The simulation of the recharge from Lake Eckarfjärden supported the assumption of small fluxes. During the dry summer of 2006, the simulated recharge from the lake was c. 10 mm.

The Baltic Sea can potentially also act as a source of groundwater recharge, especially during periods of high sea water levels. However, there is no correlation between the sea water level and the groundwater levels in QD-wells on land for most monitoring wells. Therefore, the influence of this recharge can be assumed to be restricted to areas below the sea and areas in the immediate vicinity of the coastline. Special conditions occur during events with extremely high sea water levels when relatively large low-lying areas at the shoreline and around some of the lakes are flooded and direct groundwater recharge from sea water may take place.

The prevailing conditions, with a strong interaction between evapotranspiration and the groundwater, imply that a clear definition of groundwater recharge is required. A commonly used definition is: “Process by which water is added from outside to the zone of saturation of an aquifer, either directly into a formation, or indirectly by way of another formation”. In the present situation, however, with very shallow groundwater, there is a large difference between gross and net recharge to the QD. The diurnal groundwater level fluctuations clearly illustrate the influence of evapotranspiration on the groundwater zone during dry periods. Of course, this influence is most accentuated in locations with very shallow groundwater, but it is also evident in some areas where the groundwater table is more than two metres below the ground surface. Therefore, when describing groundwater recharge and discharge there is a need to be quite specific and it is recommended to base the description on the downward och upward flow component across the soil water-groundwater zone interface or in the shallow groundwater zone. There is also a need for specifying if a certain time-period or average conditions are discussed

Studies of simulated water flow between the unsaturated and saturated zones by MIKE SHE in small areas at some wells, classified as situated either in typical discharge or recharge areas, showed a considerable upward transport in both types of areas during the dry summer of 2006. Furthermore, the analysis of the MIKE SHE simulations showed an upward flow between the uppermost two calculation layers of the saturated zone in extensive areas during dry conditions. The flow was induced by root water uptake and implied an expansion of discharge areas during dry conditions, if the existence of an upward flow component in the uppermost part of the groundwater zone was used as the definition of a discharge area.

5.1.4 Sub flow systems and discharge

Similar to the external boundaries of the model area, the internal surface water divides and the groundwater divides of the groundwater systems restricted to the QD are assumed to coincide. The strong correlation between the mean groundwater elevations observed in the till and ground surface elevation data means that the average vertical hydraulic flux at some point below the surface is less than the net infiltration into the saturated zone of the till. The decrease in hydraulic conductivity with depth and the anisotropy of the till, with $K_v < K_{h,}$ are plausible explanations, but a contribution from a contrast in vertical hydraulic conductivity between the till and the bedrock is also possible (the uppermost bedrock having a lower K_v). The small-scale topography and the hydraulic conductivity profile of the tills, dominating in the area, imply that many small catchments will be formed with local shallow groundwater flow systems in the QD, and that a dominating part of the groundwater will move along these shallow flow paths.

According to the conceptual model, the horizontal hydraulic conductivity of the till dominating the area decreases from more than 10^{-5} m/s in the uppermost part of the profile to c.10^{-6} and 10^{-7} m/s deeper down in the profile for coarse and fine-grained till, respectively. The specific yield decreases from 0.15–0.20 to 0.03–0.05. The permeability and storage characteristics of the till profile mean that very little water needs to be added to raise the groundwater table below a depth of approximately one metre. A groundwater recharge of 10 mm will give an increase in the groundwater level of c. 20 cm. During periods of abundant groundwater recharge the groundwater level, also in most recharge areas, reaches the shallow part of the QD-profile where the hydraulic conductivity is much higher and a significant lateral groundwater flow will take place. However, the transmissivity of this upper layer is so high that the groundwater level does not reach much closer to the ground surface than 0.5 m in typical recharge areas.

In the initial simulations with MIKE SHE, based on hydraulic properties of the Quaternary deposits from the conceptual model, ponding, overland flow, and too high groundwater levels were obtained. Furthermore, the low groundwater levels during dry conditions could not be simulated. The problem was mainly caused by the limitation of refinement in the vertical spatial resolution of the model in combination with the inability to simulate root water uptake in any layer but the topmost calculation layer. The problems met illustrated the importance of the vertical trend in the hydraulic properties in the uppermost part of the till for the dynamics in groundwater levels and the groundwater generated surface discharge.

The Forsmark-HBV modelling demonstrated the possibilities to simulate groundwater and surface water dynamics using the specific yields of the uppermost soil profile derived from site-specific measurements. In the MIKE SHE modelling the problems met were solved by introduction of a sub-surface drainage option simulating the measured high hydraulic conductivity of the uppermost soil layer and by using a 2.5 m deep upper calculation layer for the saturated zone. However, the sensitivity analyses also showed that introdution of an anisotropy where the horizontal hydraulic conductivity was increased by a factor of five and the vertical hydraulic conductivity was decreased by a factor of two considerably improved the agreement between measured and simulated groundwater levels. The introduction of the anisotropy is in good agreement with the site-specific measurements, but the simulations indicate at the scale of the modelling, a slightly higher hydraulic conductivity than the geometric mean of the measurements.

The local, small-scale recharge and discharge areas only involving groundwater flow systems restricted to QD will overlay the more large-scale flow systems associated with groundwater flow at greater depths. Interesting observations were made in groundwater level time series from nearby wells in till and bedrock within the tectonic lens, constituting the central part of the investigation area. Specifically, the groundwater levels in the till seem to be considerably higher than those in the bedrock in the central part of the site investigation area (within the tectonic lens). The differences between the levels in till and rock are generally much larger than between different sections in the bedrock boreholes sealed off by packers. In general, the groundwater levels in the bedrock in the central areas of the investigation area are still above the QD/rock interface, indicating that no unsaturated zone exists below the QD/rock interface. However, during dry summer conditions the QD-levels may fall below the groundwater levels in bedrock.

The groundwater levels in the till and the bedrock are well correlated. The natural groundwater level fluctuations are, however, smaller in the bedrock, but still to a great extent controlled by the annual precipitation and evapotranspiration cycles. The conditions prevailing within the northern part of the tectonic lens, with a lower groundwater level in bedrock than in QD, mean that the groundwater flow has a downward component at the sites studied and consequently an inflow from the till to the bedrock. The difference between the levels in till and bedrock indicates a limited hydraulic contact between QD and rock. This conclusion is supported by the observation that in general there is no discernable response in the groundwater levels in QD to disturbances (e.g. caused by pumping) of the groundwater levels in the bedrock.

A probable explanation for the low levels measured in the bedrock boreholes is that these intersect one/some of the highly conductive horizontal to sub-horizontal zones shown to exist in the shallow bedrock in the Forsmark area. The highly transmissive shallow bedrock acts a drain for water coming from above as well as from below. The available data indicate that flow systems involving the bedrock do not have discharge areas in the northern part of the tectonic lens but discharge into the sea. The only occasions when data from this area show a continuous upward flow gradient are during dry summers when the groundwater level in QD decrease below the levels in the bedrock.

Data gathered from monitoring wells in the till and bedrock below the middle of Lake Bolundsfjärden are of specific interest. The lake level and the groundwater level in till are considerably higher than the groundwater levels in the bedrock (HFM32). The levels are lowest in the two deepest sections. The difference between these two sections is small but after re-calculation to environmental head the second deepest section has the lowest head, i.e. the fractures in this section act as drains for water coming from above as well as from below. Interestingly, during a pumping test in bedrock in a well 500 m away, the responses were strongest in the two deepest well sections, but were also obvious in the upper two sections and also in the till well

Of the percussion-drilled boreholes around Lake Bolundsfjärden, the borehole in the middle of the lake (HFM32) has the lowest point water head. Only boreholes at the inlet of the cooling water canal (HFM38) and at SFR, have occasionally point water heads at the same low level or below. The groundwater level in HFM32 was below the sea level during the summer and autumn of 2006. Two possible, perhaps superposed, phenomena could explain this: (i) the

groundwater level in the bedrock is indirectly influenced by evapotranspiration extracting water from the groundwater zone in the QD inducing an upward flow from the bedrock, and/or (ii) the borehole is influenced by the pumping at SFR (c. 6 L/s). An influence from evapotranspiration requires that the groundwater level in the bedrock is above the QD/rock interface, which is the case in the low-lying areas surrounding Lake Bolundsfjärden, so that no unsaturated zone exists in the bedrock. The MIKE SHE simulations, with the field-based parameter setting, showed a clear upward flow gradient from the bedrock to the Quaternary deposits in the littoral zone of Lake Bolundsfjärden during the dry summer of 2006.

An influence from the pumping at SFR requires a good hydraulic contact all the way to SFR. From a pumping test in HFM33, immediately west of SFR, it is known that quick and strong responses were observed in e.g. HFM02 (c. 0.3 m) and HFM15 (c. 0.1 m) located c. 1.5 km from the pumping well. The pumping rate in HFM33 was approximately 3.8 L/s. Pumping tests in HFM14 have also shown quick and strong responses in other quite distant HFM-wells (c. 1 km away, such as HFM16 and HFM38), confirming the high transmissivity and low storativity of the upper bedrock.

The prevailing situation, with relatively low groundwater levels in the shallow bedrock within the northern parts of the tectonic lens, may partly be caused by the pumping at SFR. However, no definite conclusions on this issue can be drawn based on existing data.

Outside the tectonic lens, the groundwater level in the bedrock may be well above the groundwater levels in QD in nearby low-lying areas, implying that flow systems involving the bedrock may have local discharge areas in these parts of the site investigation area.

The lake water level-groundwater level relationship indicates that the lake sediments, the underlying till, and/or the uppermost bedrock have low vertical hydraulic conductivities. If the surface water-groundwater hydraulic contact had been good, the situation with groundwater level drawdown from evapotranspiration extending below the lakes, and the quick and extensive drawdowns from the pumping tests in percussion-drilled boreholes HFM14 and HFM33 in the rock below Lake Bolundfjärden and the sea, would not appear.

During the MIKE SHE modelling there was a general problem with too high simulated groundwater levels in the bedrock, whereas there was a good agreement between measured and simulated groundwater levels in the Quaternary deposits. Furthermore, with the original parameter settings the model was unable to simulate the drawdowns in the pumping tests in the percussion-drilled borehole HFM14; the pumping caused fast and extensive resposes in monitoring wells in bedrock more than one km from the borehole. To overcome these problems, several test simulations were conducted with different combinations of increased hydraulic conductivity of the bedrock, decreased vertical hydraulic conductivity of the bedrock and the Quaternary deposits, and a decreased specific storage of the bedrock compared with the data set obtained from the CONNECTFLOW-modelling.

The outcome of these tests was that the specific storage had to be lowered considerably from the values used initially (varying from $1 \cdot 10^{-7}$ to $1 \cdot 10^{-5}$ 1/m) to obtain a good match between measured and simulated responses in the pumping test. In the final calibrated model a value of $5 \cdot 10^{-8}$ 1/m was used. Furthermore, an increase of the horizontal hydraulic conductivity of the sheet joints, as implemented in the upper bedrock part of the model, by a factor 10 was found to be necessary together with a decrease of the vertical hydraulic conductivity of the upper 200 m of the bedrock by a factor 10 to obtain a good fit between measured and simulated pumping test responses. A further decrease of the vertical hydraulic conductivity of the Quaternary deposits turned out to have only a marginal effect on the groundwater levels.

However, the problem with the generally too high groundwater levels was only partly solved by the changes introduced. As a final test, the drainage pumping in the SFR-facility was introduced in a quite simplistic manner, i.e. as a well screened between c. 40 and 140 m depth. The introduction of this sink drastically improved the agreement between measured and simulated

groundwater levels in the bedrock, with the mean absolute error and mean error in the monitoring wells decreasing from 0.68 to 0.41 and –0.65 to –0.05 m, respectively (negative mean error indicates too high simulated level). Most wells showed errors of c. ± 0.2 m. Of the wells within the northern part of the tectonic lens, only HFM16 and HFM32 showed considerably larger errors with an overestimation and underestimation of c. one metre, respectively.

In discharge areas by definition no groundwater recharge takes place. However, not all discharge areas are saturated up to the ground surface, but water flows in the uppermost most permeable part of the soil profile. In unsaturated discharge areas, the soil water deficit is usually quite small and in these areas water levels respond quickly to rainfall and snowmelt and contribute to runoff generation. So-called saturated overland flow appears in discharge areas where the groundwater level reaches the ground surface. This type of discharge areas is quite common in the flat landscape of the site investigation area.

The brooks are considered as permanent discharge areas, although dry during parts of the year. The wetlands can either be in direct contact with the groundwater zone and constitute typical discharge areas or be separate hydrological systems with low-permeable bottom materials and have little hydraulic contact with the underlying aquifer. The flat terrain and the shallow groundwater within the area imply that the spatial extents of recharge and discharge areas may vary during the year. The flow systems around and below the lakes appear quite complex. The chemistry of the waters below the lakes indicates a very limited flow since relict water of marine origin is found.

Particle tracking simulations were performed using the final calibrated MIKE SHE model. Particles were released at 150 m below sea level; in one simulation case with particles all over the model area and in one simulation case only above the area of the planned repository. The first set of simulations was run for 300 years, both with and without the SFR-pumping included. For the case where particles were released all over the model area, the dominating sink without SFR-pumping is the combined overland compartment/unsaturated zone. It is not possible to separate these two sinks in the model. At the end of the simulation 65% of the particles were still in the model volume, i.e. it took less than 300 years for 35% of the particles to reach the ground surface or the sea from 150 m depth.

When including the pumping at SFR, 66% of the particles were still in the model volume after 300 years. SFR was the dominating sink with 15% of the particles leaving the model volume through this pumping, and only 5% of the particles moved to the sea, compared with 14% when the SFR-pumping was not active. In the model, the deepest layer with horizontal sheet joints is located at 110 m.b.s.l. The results show that the particles concentrate to this layer. The pattern is the same for both cases, with and without the SFR-pumping included. When pumping at SFR, the majority of the particles released in the northeastern part of the model area move towards SFR at 110 m.b.s.l. Above this level only 40% of the cells that received a particle at 110 m.b.s.l. is hit by a particle.

When particles were released at 140 m.b.s.l. only inside the area corresponding to the planned repository, only 10% of the particles had left the model volume after 300 years and all these particles had gone to the sea. When pumping at SFR, 18% of the particles had left the model volume through the pumping in SFR. The rest of the particles were still in the model. For both cases, the particles concentrated to the sheet joint layer at 110 m.b.s.l. and the horizontal transport was dominating. Above this level only a few cells were passed by a particle. When pumping at SFR, no particles reached higher than 70 m.b.s.l. Thus, there were no exit points at the surface after 300 years of simulation when pumping at SFR. When the SFR-pumping was not activated, a few particles reached the sea with exit points close to the shoreline.

Since many particles were still in the model volume after 300 years, an additional longer simulation was run for 5,000 years with particles only released above the planned repository. The transport times were long and even after 5,000 years 81% of the particles were still in the model volume. No exit points were found in the on-land part of the model area. All the particles

exited the model volume at sea. It was also found that 79 particles, 5% of the total number of introduced particles, were stuck in the marine sediments. Apart from them, no particles were left in the upper calculation layers. All the particles that were left in the model after 5,000 years were found in the deeper bedrock between layer 8 at 110 m.b.s.l and layer 14 at 600 m.b.s.l.

Although providing potentially important information guiding further analyses, the particle tracking results presented should be interpreted with great caution. The results heavily depend on the geometry and hydraulic properties of the hydrogeological structures of the bedrock which are implemented in the model in a quite simplistic way.

5.1.5 Water balance

A longterm overall water balance of the area may be estimated based on 30-year precipitation data from SMHI-stations surrounding the site investigation area and the shortterm site specific meterorological and hydrological monitoring data. If the full three-year period of April 15, 2004 until April 14, 2007 is considered, the corrected mean precipitation was 546 mm/year while the mean specific discharge of the largest catchment of 5.6 km^2 was 154 mm/year. From a comparison of groundwater and surface water levels at the start and end of the period it can be concluded that the these storages were a little smaller at the end of the period but only corresponding to a difference of c. 5 mm/year. The mean precipitation was 13 mm/year lower than the 30-year normal precipitation estimated by SMHI. Since approximately 2/3 of the precipitation goes to evapotranspiration, the precipitation deficit should correspond to a discharge deficit of approximately 5 mm/year. These estimates of storage changes and precipitation deficit indicate that the measured three-year mean discharge should be close to the longterm normal discharge. A rough estimate of the longterm overall water balance of the area is then: P (precipitation) = 560 mm/year, ET (actual evapotranspiration) = 400–410 mm/year, and R (runoff) = 150–160 mm/year.

The water balance in the MIKE SHE modelling was calculated for the four-year period Sep. 2003–Aug. 2007 for the on-land part of the model area (the sea excluded). The mean annual precipitation for this period was 533 mm and the mean annual actual evapotranspiration was 405 mm. The annual total interception was 122 mm/year, the transpiration from plants 169 mm/year, and the calculated runoff (discharge) was 144 mm/year.

The infiltration to the unsaturated zone was 351 mm/year, whereas the groundwater recharge from the unsaturated zone to the uppermost calculation layer of the saturated zone was 124 mm/year. The flow to the second calculation layer in QD, at 2.5 m depth, was c. 45 mm. There are many local recharge and discharge areas within this layer; 41 mm was transported back to the uppermost QD layer. Only c.11 mm was flowing down to the uppermost bedrock, calculation layer 3. The upward flow from the rock to the QD corresponded to some 8–9 mm, which means that the net downward flow was only 2–3 mm. When the SFR-pumping was active in the model, the downward flow in the upper bedrock was somewhat increased, but below 150 depth the influence of the pumping was insignificant. The simulated vertical flow at this depth was very small, 0.3 mm/year downward and 0.2 mm/year upward. These flows correspond well to the flows calculated in the CONNECTFLOW modelling at 150 m depth.

5.2 Summary of uncertainties

The comprehensive investigation and monitoring programme forms a strong basis for the developed conceptual and descriptive model of the hydrological and near-surface hydrological system of the site investigation area. However, there are some remaining uncertainties regarding the interaction of deep and near-surface groundwater, and surface water of importance for the understanding of the system:

- The groundwaters in till below Lake Eckarfjärden, Lake Gällsboträsket, Lake Fiskarfjärden and Lake Bolundsfjärden have high salinity. The hydrological and hydrochemical interpretations indicate that these waters are relict waters of mainly marine origin. From the perspective of the overall water balance, the water below the central parts of the lakes can be considered as stagnant. However, according to the hydrochemical interpretation, these waters also contain weak signatures of deep saline water /Tröjbom et al. 2007/. Rough chloride budget calculations for the Gällboträsket depression also raise the question of a possible upward flow of deep groundwater. No absolute conclusion can be drawn from the existing data analyses regarding the key question of whether there is a small ongoing upward flow of deep saline water. However, Lake Bolundsfjärden is an exception where the clear downward flow gradient from the till to the bedrock excludes the possibility of an active deep saline source.
- The available data indicate that there are no discharge areas for flow systems involving deep bedrock groundwater in the northern part of the tectonic lens, where the repository is planned to be located. However, it can not be excluded that such areas exist. Data indicate that the prevailing downward vertical flow gradients from the Quaternary deposits to the bedrock are highly dependent on the very transmissive horizontal and sub-horizontal fractures of the uppermost bedrock and that evapotranspiration induced flow may change these directions during dry conditions in some areas.
- Data as well as the simulations with MIKE SHE raise the question if the prevailing groundwater levels in the northern part of the tectonic lens are influenced by the pumping for the drainage of SFR (c. 6 L/s). Another possibly influencing sink is the pumping for drainage of the Forsmark nuclear plant reactor buildings 1 and 2 (c. 1–2 L/s). These sinks may influence the vertical flow gradients within some parts of the investigation area, and it is strongly recommended that additional investigations are performed to resolve this uncertainty.

References

Albrecht J, 2005. Study of Quaternary sediments in connection with investigations of bedrock lineaments. Forsmark site investigation**.** SKB P-05-138, Svensk Kärnbränslehantering AB.

Alexandersson H, 2003. Korrektion av nederbörd enligt enkel klimatologisk metodik. SMHI, Meteorologi, Nr 111. (In Swedish.)

Alm P, Gebrezghi M, Werner K, 2006. Supplementary hydraulic tests in Quaternary deposits. Forsmark site investigation**.** SKB P-06-224, Svensk Kärnbränslehantering AB.

Andersson A-C, Andersson O, Gustafson G, 1984. Brunnar. Undersökning – Dimensionering – Drift. BFR Report R42:1984. Byggforskningsrådet (BFR). (In Swedish.)

Andrejev O, Sokolov A, 1997. The data assimilation system for data analysis in the Baltic Sea. System Ecology Contributions No. 3.

Aquilonius K, Karlsson S, 2003. Snow depth, frost in ground and ice cover during the winter 2002/2003. Forsmark site investigation. SKB P-03-117, Svensk Kärnbränslehantering AB.

Berg C, Nilsson A-C, Borgiel M, 2006. Hydrochemical monitoring of near surface groundwaters. Results from sampling of five shallow soil monitoring wells, one BAT pipe and three private wells, July 2005–April 2006. Forsmark site investigation. SKB P-06-304, Svensk Kärnbränslehantering AB.

Bergman B, Palm H, Juhlin C, 2004. Estimate of bedrock topography using seismic tomography along reflection seismic profiles. Forsmark site investigation. SKB P-04-99, Svensk Kärnbränslehantering AB.

Bergström S, 1976. Development and application of a conceptual runoff model for Scandinavian catchments. SMHI RH07, Norrköping, Sweden.

Bergström S, Sandberg G, 1983. Simulation of groundwater response by conceptual models – Three case studies. Nordic Hydrology, vol. 14, pp. 71–84.

Beven K J, Kirby M J, 1979. A physically based variable contributing area model of basin hydrology. Hydrological Sciences Bulletin, vol. 24, pp. 43–69.

Beven K J, Binley A M, 1992. The future of distributed models: model calibration and uncertainty prediction, Hydrological Processes, vol. 6, pp. 279–298.

Beven K J, Freer J, 2001. Equifinality, data assimilation, and uncertainty estimation in mechanistic modelling of complex environmental systems using the GLUE methodology, J. of Hydrology, vol. 249, pp. 11–29.

Beven K J, 2006. A manifesto for the equifinality thesis, J. of Hydrology, vol. 320, pp.18–36.

Boresjö Bronge L, Wester K, 2003. Vegetation mapping with satellite data of the Forsmark, Tierp and Oskarshamn regions. SKB P-03-83, Svensk Kärnbränslehantering AB.

Bosson E, Berglund S, 2006. Near-surface hydrogeological model of Forsmark. Open repository and solute transport applications – Forsmark 1.2. SKB R-06-52, Svensk Kärnbränslehantering AB.

Bosson E, Gustafsson L-G, Sassner M, 2008. Numerical modelling of surface hydrology and near-surface hydrogeology at Forsmark. Site descriptive modelling, SDM-Site Forsmark. SKB R-08-09, Svensk Kärnbränslehantering AB.

Brunberg A-K, Blomqvist P, 1998. Vatten i Uppsala län. 1997. Beskrivning, utvärdering, åtgärdsförslag. Rapport nr 8/1998. Upplandsstiftelsen. (In Swedish.)

Brunberg A-K, Carlsson T, Blomqvist P, Brydsten L, Strömgren M, 2004. Identification of catchments, lake-related drainage parameters and lake habitats. SKB P-04-25, Svensk Kärnbränslehantering AB.

Brydsten L, 2004. A method for construction of digital elevation models for site investigation program in Forsmark and Simpevarp. SKB P-04-03, Svensk Kärnbränslehantering AB.

Brydsten L, Strömgren M, 2004. Digital elevation models for site investigation programme in Forsmark. Site description version 1.2. SKB R-04-70, Svensk Kärnbränslehantering AB.

Brydsten L, Strömgren M, 2005. Measurements of brook gradients and lake thresholds. SKB P-04-141, Svensk Kärnbränslehantering AB.

Brydsten L, 2006a. A model for landscape development in terms of shoreline displacement, sediment dynamics, lake formation, and lake choke-up processes. SKB TR-06-40, Svensk Kärnbränslehantering AB.

Brydsten L, 2006b. Modelling groundwater discharge areas using only digital elevation models as input data. SKB TR-06-39, Svensk Kärnbränslehantering AB.

Butler J J Jr, 1998. The design, performance and analysis of slug tests. Lewis Publisher, Boca Raton, Florida, U.S.A.

Carlsson T, Brunberg A-K, Brydsten L, Strömgren M, 2005. Characterisation of running waters, including vegetation, substrate and technical encroachments. SKB P-05-150, Svensk Kärnbränslehantering AB.

Chow Ven Te, 1959. Open channel hydraulics. McGraw Hill Book Co, New York, U.S.A.

Chyssanthakis P, Tunbridge L, 2005a. Borehole KFM06A. Determination of P-wave velocity, transverse borehole core. Forsmark site investigation. SKB P-05-04, Svensk Kärnbränslehantering AB.

Chyssanthakis P, Tunbridge L, 2005b. Borehole KFM07A. Determination of P-wave velocity transverse borehole core. Forsmark site investigation. SKB P-05-125, Svensk Kärnbränslehantering AB.

Chyssanthakis P, Tunbridge L, 2005c. Borehole: KFM08A. Determination of P-wave velocity, transverse borehole core. Forsmark site investigation. SKB P-05-216, Svensk Kärnbränslehantering AB.

Chyssanthakis P, Tunbridge L, 2006. Borehole KFM09A Determination of P-wave velocity, transverse borehole core. Forsmark site investigation. SKB P-06-24, Svensk Kärnbränslehantering AB.

DHI Software, 2007. MIKE SHE – User Manual. DHI Water & Environment, Hørsholm, Denmark.

DHI Software, 2008. MIKE SHE – User Manual. DHI Water & Environment, Hørsholm, Denmark.

Elhammer A, Sandkvist Å, 2004. Detailed marine geological mapping. Forsmark site investigation. SKB P-03-101, Svensk Kärnbränslehantering AB.

Engelen G B, Jones G P (eds.), 1986. Developments in the analysis of groundwater flow systems. IAHS Publ. no. 163.

Engqvist A, Omstedt A, 1992. Water exchange and density structure in a multi-basin estuary. Continental Shelf Research, 12, 1003–1026.

Engqvist A, Stenström P, 2004. Archipelago strait exchange processes – an overview. Deep Sea Research II, 51, 371–392.

Engqvist A, Andrejev O, 2008. Validation of coastal oceanographic models at Forsmark. Site descriptive modelling. SDM-Site Forsmark. SKB TR-08-01, Svensk Kärnbränslehantering AB.

Eriksson B, 1981. Den ”potentiella” evapotranspirationen i Sverige. SMHI RMK Nr 28. Sveriges Meteorologiska och Hydrologiska Institut (SMHI). (In Swedish.)

Follin S, Årebäck M, Jacks G, 1996. Förstudie Östhammar. Grundvattnets rörelse, kemi och långsiktiga förändringar. SKB Djupförvar, PR D-96-017, Svensk Kärnbränslehantering AB.

Follin S, Johansson P-O, Hartley L, Jackson P, Roberts D, Marsic N, 2007a. Hydrogeological conceptual model development and numerical modelling using CONNECTFLOW. Forsmark modelling stage 2.2. SKB R-07-49, Svensk Kärnbränslehantering AB.

Follin S, Johansson P-O, Levén J, Hartley L, Holton D, McCarthy R, Roberts D, 2007b. Updated strategy and test of new concepts for groundwater flow modelling in Forsmark in preparation of site descriptive modelling stage 2.2. SKB R-07-20, Svensk Kärnbränslehantering AB.

Follin S, Levén J, Hartley L, Jackson P, Joyce S, Roberts D, Swift B, 2007c. Hydrogeological characterisation and modelling of deformation zones and fracture domains, Forsmark modelling stage 2.2. SKB R-07-48, Svensk Kärnbränslehantering AB.

Follin S, Hartley L, Jackson P, Roberts D, Marsic N, 2008. Conceptual model development and numerical modelling using CONNECTFLOW, Forsmark modelling stage 2.3. SKB R-08-23, Svensk Kärnbränslehantering AB.

Forssberg O, Maersk Hansen L, Koyi S, Vestgård J, Öhman J, Petersson J, Albrecht J, Hedenström A, Gustafsson J, 2007. Detailed fracture and bedrock mapping, Quaternary investigations and GPR measurements at excavated outcrop AFM001264. Forsmark site investigation. SKB P-05-269, Svensk Kärnbränslehantering AB.

Fredriksson D, 2004. Peatland investigation Forsmark. Forsmark site investigation. SKB P-04-127, Svensk Kärnbränslehantering AB.

Freer J E, McMillan H, McDonnell J J, Beven K J, 2004. Constraining dynamic TOPMODEL responses for imprecise water table information using fuzzy rule based performance measures. J. of Hydrology, vol. 291, pp. 254–277.

Freeze R A, Cherry J A, 1979. Groundwater. Prentice-Hall Inc., Englewood Cliffs, New Jersey, U.S.A.

Gokall-Norman K, Ludvigson J-E, 2005. Hydraulic interference tests. Boreholes HFM16, HFM19 and KFM02A. Forsmark site investigation. SKB P-05-78, Svensk Kärnbränslehantering AB.

Gokall-Norman K, Ludvigson J-E, 2007a. Hydraulic interference test in borehole HFM14. Forsmark site investigation. SKB P-06-196, Svensk Kärnbränslehantering AB.

Gokall-Norman K, Ludvigson J-E, 2007b. Hydraulic interference test in borehole HFM14, summer of 2007. SKB P-07-228, Svensk Kärnbränslehantering AB.

Gokall-Norman K, Ludvigson J-E, 2008. Hydraulic interference test in borehole HFM33, autumn 2007. SKB P-07-229, Svensk Kärnbränslehantering AB.

Grip H, Rodhe A, 1985. Vattnets väg från regn till bäck. Forskningsrådens förlagsstjänst, 156 pp. (In Swedish.)

Gustafsson J, Gustafsson C, 2004. RAMAC and BIPS logging in borehole KFM03A and KFM03B. Forsmark site investigation. SKB P-04-41. Svensk Kärnbränslehantering AB.

Gustafsson L-G, Sassner M, Bosson E, 2008. Numerical modelling of solute transport at Forsmark with MIKE SHE. Site descriptive modelling, SDM-Site Forsmark. SKB R-08-106, Svensk Kärnbränslehantering AB.

Hedenström A, 2003. Investigation of marine and lacustrine sediments in lakes. Field data 2003. Forsmark site investigation. SKB P-03-24, Svensk Kärnbränslehantering AB.

Hedenström A, Sohlenius G, Albrecht J, 2004. Stratigraphical and analytical data from auger drillings and pits. Forsmark site investigation. SKB P-04-111, Svensk Kärnbränslehantering AB.

Hedenström A, 2004a. Investigation of marine and lacustrine sediments in lakes. Stratigraphical and analytical data. Forsmark site investigation. SKB P-04-86, Svensk Kärnbränslehantering AB.

Hedenström A, 2004b. Stratigraphical and analytical data of Quaternary deposits. Forsmark site investigation. SKB P-04-148, Svensk Kärnbränslehantering AB.

Hedenström A, Sohlenius G, 2008. Description of the regolith at Forsmark. Site descriptive modelling. SDM-Site Forsmark. SKB R-08-04, Svensk Kärnbränslehantering AB.

Hedenström A, Sohlenius G, Strömgren M, Brydsten L, Nyman H, 2008. Depth and stratigraphy of regolith at Forsmark. Site descriptive modelling. SDM-Site Forsmark. SKB R-08-07, Svensk Kärnbränslehantering AB.

Heneryd N, 2004. Snow depth, ground frost and ice cover during the winter 2003/2004. Forsmark site investigation. SKB P-04-137, Svensk Kärnbränslehantering AB.

Heneryd N, 2005. Snow depth, ground frost and ice cover during the winter 2004/2005. Forsmark site investigation. SKB P-05-134, Svensk Kärnbränslehantering AB.

Heneryd N, 2006. Snow depth, ground frost and ice cover during the winter 2005/2006. Forsmark site investigation. SKB P-06-97, Svensk Kärnbränslehantering AB.

Heneryd N, 2007. Snow depth, snow water content and ice cover during the winter 2006/2007. Forsmark site investigation. SKB P-07-81, Svensk Kärnbränslehantering AB.

Hock R, 2003. Temperature index melt modeling in mountain areas. J. of Hydrology, vol. 282, pp.104–115.

Isaksson H, Keisu M, 2005. Interpretation of airborne geophysics and integration with topography Stage 2 (2002–2004). An integration of bathymetry, topography, refraction seismics and airborne geophysics. Forsmark site investigation. SKB P-04-282, Svensk Kärnbränslehantering AB.

Jarsjö J, ShibuoY, Prieto C, Destouni G, 2005. GIS-based modelling of coupled groundwater – surface water hydrology in the Forsmark and Simpevarp areas. SKB R-05-67. Svensk Kärnbränslehantering AB.

Jarsjö J, Destouni G, Persson K, Prieto C, 2007. Solute transport in coupled inland-coastal water systems. General conceptualisation and application to Forsmark. SKB R-07-65, Svensk Kärnbränslehantering AB.

Johansson P-O, 1987a. Estimation of groundwater recharge in till with two different methods using groundwater level fluctuations. J. of Hydrology, vol. 90, pp. 183–198.

Johansson P-O, 1987b. Spring discharge and aquifer characteristics in a sandy till area in southeastern Sweden. Nordic Hydrology, vol. 18, pp. 203–218.

Johansson P-O, 2003. Drilling and sampling in soil. Installation of groundwater monitoring wells and surface water gauges. Forsmark site investigation. SKB P-03-64, Svensk Kärnbränslehantering AB.

Johansson P-O, 2004. Undisturbed pore water sampling and permeability measurements with BAT filter tips. Soil sampling for pore water analyses. Forsmark site investigation. SKB P-04-136, Svensk Kärnbränslehantering AB.

Johansson P-O, Werner K, Bosson E, Juston J, 2005. Description of climate, surface hydrology, and near-surface hydrogeology. Preliminary site description. Forsmark area – version 1.2. SKB R-05-06, Svensk Kärnbränslehantering AB.

Johansson P-O, 2005a. Installation of brook discharge gauging stations. Forsmark site investigation. SKB P-05-154, Svensk Kärnbränslehantering AB.

Johansson P-O, 2005b. Manual discharge measurements in brooks, April 2002–April 2005. Forsmark site investigation. SKB P-05-153, Svensk Kärnbränslehantering AB.

Johansson P-O, Juston J, 2007. Monitoring of brook levels, water electrical conductivities, temperatures and discharges from April 2004 until March 2007. Forsmark site investigation. SKB P-07-135, Svensk Kärnbränslehantering AB.

Johansson P-O, Öhman J, 2008. Presentation of meteorological, hydrological and hydrogeological monitoring data from Forsmark. Site descriptive modelling, SDM-Site Forsmark. SKB R-08-10, Svensk Kärnbränslehantering AB.

Juhlin C, Bergman B, 2004. Reflection seismics in the Forsmark area. Updated interpretation of Stage 1 (previous report R-02-43). Updated estimate of bedrock topography (previous report P-04-99). SKB P-04-158, Svensk Kärnbränslehantering AB.

Juston J, Johansson P-O, 2005. Analysis of meteorological data, surface water level data, and groundwater level data. Forsmark site investigation. SKB P-05-152, Svensk Kärnbränslehantering AB.

Juston J, Johansson P-O, Levén J, Tröjbom M, Follin S, 2007. Analysis of meteorological, hydrological and hydrogeological monitoring data. Forsmark – stage 2.1. SKB R-06-49, Svensk Kärnbränslehantering AB.

Kellner E, 2004. Wetlands – different types, their properties and functions. SKB TR-04-08, Svensk Kärnbränslehantering AB.

Kristensen K-J, Jensen S-E, 1975. A model for estimating actual evapotranspiration from potential evaporation. Nordic Hydrology, vol. 6, pp. 170–188.

Laaksoharju M, Smellie J, Tullborg E-L, Gimeno M, Hallbeck L, Molinero J, Waber N, 2008. Bedrock hydrogeochemistry Forsmark. Site descriptive modelling. SDM-Site Forsmark. SKB R-08-47, Svensk Kärnbränslehantering AB.

Larsson-McCann S, Karlsson A, Nord M, Sjögren J, Johansson L, Ivarsson M, Kindell S, 2002. Meteorological, hydrological and oceanographical information and data for the site investigation program in the communities of Östhammar and Tierp in the northern part of Uppland. SKB TR-02-02, Svensk Kärnbränslehantering AB.

Lind B, Lundin L, 1990. Saturated hydraulic conductivity of Scandinavian tills. Nordic Hydrology, vol. 21, pp. 107–118.

Lindborg T (ed.), 2005. Description of surface systems. Preliminary site description. Forsmark area – version 1.2. SKB R-05-03, Svensk Kärnbränslehantering AB.

Lindborg T (ed.), 2008. Surface system Forsmark. Site descriptive modelling. SDM-Site Forsmark. SKB R-08-11, Svensk Kärnbränslehantering AB.

Lindell S, Ambjörn C, Juhlin B, Larsson-McCann S, Lindqvist K, 2000. Available climatological and oceanographical data for site investigation program. SKB R-99-70, Svensk Kärnbränslehantering AB.

Lindström G, Johansson B, Persson M, Gardelin M, Bergström S, 1997. Development and test of the distributed HBV-96 hydrological model. J. of Hydrology, vol. 201, pp. 272–288.

Lokrantz H, Hedenström A, 2006. Description, sampling and analyses of Quaternary deposits in connection with groundwater monitoring wells, pumping wells and BAT filter tips. Forsmark site investigation. SKB P-06-92, Svensk Kärnbränslehantering AB.

Ludvigson J-E, 2002. Brunnsinventering i Forsmark. SKB R-02-17, Svensk Kärnbränslehantering AB. (In Swedish.)

Lundin L, Lode E, Stendahl J, Melkerud P-A, Björkvald L, Thorstensson A, 2004. Soils and site types in the Forsmark area. SKB R-04-08, Svensk Kärnbränslehantering AB.

Lundin L, Stendahl J, Lode E, 2005. Soils in two large trenches. Forsmark site investigation. SKB P-05-166, Svensk Kärnbränslehantering AB.

Lusczynski N J, 1961. Head and flow of groundwater of variable density. J. of Geophysical Research, vol. 66, no. 12, pp. 4247–4256.

Löfgren, A (ed.), 2008. The terrestrial ecosystems at Forsmark and Laxemar-Simpevarp. Site descriptive modelling. SDM-Site. SKB R-08-01, Svensk Kärnbränslehantering AB.

Marek R, 2004a. A co-ordinated interpretation of ground penetrating radar data from the Forsmark site. Forsmark site investigation. SKB P-04-156, Svensk Kärnbränslehantering AB.

Marek R, 2004b. Ground penetrating radar survey 2003. Forsmark site investigation. SKB P-04-78, Svensk Kärnbränslehantering AB.

Nash J E, Sutcliffe I V, 1970. River flow forecasting through conceptual models: Part 1 – A discussion of principles. J. of Hydrology, vol. 10, pp. 282–290.

Nilsson A-C, Karlsson S, Borgiel M, 2003. Sampling and analyses of surface waters. Results from sampling in the Forsmark area, March 2002 to March 2003. SKB P-03-27, Svensk Kärnbränslehantering AB.

Nilsson A-C, Borgiel M, 2004. Sampling and analyses of surface waters. Results from sampling in the Forsmark area, March 2003 to March 2004. SKB P-04-146, Svensk Kärnbränslehantering AB.

Nilsson A-C, Borgiel M, 2005a. Sampling and analyses of surface waters. Results from sampling in the Forsmark area, March 2004–June 2005. Forsmark site investigation. SKB P-05-274, Svensk Kärnbränslehantering AB.

Nilsson A-C, Borgiel M, 2005b. Sampling and analyses of near surface groundwaters. Results from sampling of shallow soil monitoring wells, BAT pipes, a natural spring and private wells, May 2003–April 2005. Forsmark site investigation. SKB P-05-171, Svensk Kärnbränslehantering AB.

Nilsson A-C, Borgiel M, 2007. Sampling and analyses of surface waters. Results from sampling in the Forsmark area, July 2005–June 2006. Forsmark site investigation. SKB P-07-95, Svensk Kärnbränslehantering AB.

Nissen J, 2004. Ground penetrating radar (GPR) and resistivity (CVES) surveys – interpretation of new and previous measurements. Forsmark site investigation. SKB P-04-105, Svensk Kärnbränslehantering AB.

Nyberg G, Wass E, Askling P, Johansson P-O, 2004. Hydro monitoring program. Report for June 2002–July 2004. Forsmark site investigation. SKB P-04-313, Svensk Kärnbränslehantering AB.

Nyberg G, Wass E, 2005. Hydro monitoring program. Report for August 2004–July 2005. Forsmark site investigation. SKB P-05-245, Svensk Kärnbränslehantering AB.

Nyberg G, Wass E, 2006. Hydro monitoring program. Report for August 2005–September 2006. Forsmark site investigation. SKB P-06-263, Svensk Kärnbränslehantering AB.

Nyberg G, Wass E, 2007. Hydro monitoring program. Report for October 2006–March 2007. Forsmark site investigation. SKB P-07-113, Svensk Kärnbränslehantering AB.

Petersson J, Skogsmo G, Vestgård J, Albrecht J, Hedenström A, Gustafsson J, 2007. Bedrock mapping and magnetic susceptibility measurements, Quaternary investigations and GPR measurements in trench AFM001265. Forsmark site investigation. SKB P-06-136, Svensk Kärnbränslehantering AB.

Post V, Kooi H, Simmons C, 2007. Using hydraulic head measurements in variable-density ground water flow analyses. Ground Water, vol. 45, no. 6, pp. 664–671.

Rhén I, Gustafson G, Wikberg P, 1997. Äspö HRL – Geoscientific evaluation 1997/5. Models based on site characterization 1986–1995. SKB TR-97-06, Svensk Kärnbränslehantering AB.

Rhén I, Follin S, Hermanson J, 2003. Hydrogeological site descriptive model – a strategy for its development during site investigations. SKB R-03-08, Svensk Kärnbränslehantering AB.

Seibert J, 2000. Multi-criteria calibration of a conceptual runoff model using a genetic algorithm. Hydrologic and Earth System Sciences 4(2), pp. 215–244.

SKB, 2000. Förstudie Östhammar. Slutrapport. ISBN-91-972810-4-2, Svensk Kärnbränslehantering AB. (In Swedish.)

SKB, 2001. Site investigations. Investigation methods and general execution programme. SKB TR-01-29, Svensk Kärnbränslehantering AB.

SKB, 2002. Forsmark – site descriptive model version 0. SKB R-02-32, Svensk Kärnbränslehantering AB

SKB, 2004. Preliminary site description. Forsmark area – version 1.1. SKB R-04-15, Svensk Kärnbränslehantering AB.

SKB, 2005a. Preliminary site description. Forsmark area – version 1.2. SKB R-05-18, Svensk Kärnbränslehantering AB.

SKB, 2005b. Programme for further investigations of geosphere and biosphere. Forsmark site investigation. SKB R-05-14, Svensk Kärnbränslehantering AB.

SKB, 2008. Site description of Forsmark at completion of the site investigation phase. SKB TR-08-05, Svensk Kärnbränslehantering AB.

SMHI, 1985. Svenskt vattenarkiv. Vattendragsregistret. Sveriges Meteorologiska och Hydrologiska Institut (SMHI). (In Swedish.)

Sohlenius G, Rudmark L, 2003. Mapping of unconsolidated Quaternary deposits. Stratigraphical and analytical data. Forsmark site investigation. SKB P-03-14, Svensk Kärnbränslehantering AB.

Sohlenius G, Rudmark L, Hedenström A, 2003. Mapping of unconsolidated Quaternary deposits. Field data 2002. Forsmark. SKB P-03-11, Svensk Kärnbränslehantering AB.

Sohlenius G, Hedenström, Rudmark L, 2004. Mapping of unconsolidated Quaternary deposits 2002–2003. Map description. Forsmark site investigation. SKB R-04-39, Svensk Kärnbränslehantering AB.

Strömgren M, Brydsten L, 2008. Digital elevation models for Forsmark. Site descriptive modelling. SDM-Site Forsmark. SKB R-08-62, Svensk Kärnbränslehantering AB.

Sundh M, Sohlenius G, Hedenström A, 2004. Stratigraphical investigation of till in machine cut trenches. Forsmark site investigation. SKB P-04-34, Svensk Kärnbränslehantering AB.

Toresson B, 2005. Seismic refraction survey 2004. Forsmark site investigation. SKB P-05-12, Svensk Kärnbränslehantering AB.

Toresson B, 2006. Seismic refraction survey 2005–2006. Forsmark site investigation. SKB P-06-138, Svensk Kärnbränslehantering AB.

Tröjbom M, Söderbäck B, 2006. Chemical characteristics of surface systems in the Forsmark area. Visualisation and statistical evaluation of data from shallow groundwater, precipitation, and regolith. SKB R-06-19, Svensk Kärnbränslehantering AB.

Tröjbom M, Söderbäck B, Johansson P-O, 2007. Hydrochemistry in surface water and shallow groundwater. Site descriptive modelling. SDM-Site Forsmark. SKB R-07-55, Svensk Kärnbränslehantering AB.

UNESCO, 1992. International Glossary of Hydrology. UNESCO, Paris.

Vikström M, 2005. Modelling of soil depth and lake sediments. An application of the GeoEditor at the Forsmark site. SKB R-05-07, Svensk Kärnbränslehantering AB.

Wern L, Jones J, 2006. Meteorological monitoring at Forsmark, June 2003 until July 2005. Forsmark site investigation. SKB P-05-221, Svensk Kärnbränslehantering AB.

Wern L, Jones J, 2007a. Meteorological monitoring at Forsmark, August 2005 until September 2006. Forsmark site investigation. SKB P-06-322, Svensk Kärnbränslehantering AB.

Wern L, Jones J, 2007b. Meteorological monitoring at Forsmark, October 2006 until June 2007. Forsmark site investigation. SKB P-07-175, Svensk Kärnbränslehantering AB.

Werner K, 2004. Supplementary slug tests in groundwater monitoring wells in soil. Forsmark site investigation. SKB P-04-140, Svensk Kärnbränslehantering AB.

Werner K, Johansson P-O, 2003. Slug tests in groundwater monitoring wells in soil. Forsmark site investigation. SKB P-03-65, Svensk Kärnbränslehantering AB.

Werner K, Lundholm L, 2004a. Pumping test in wells SFM0074. Forsmark site investigation. SKB P-04-142, Svensk Kärnbränslehantering AB.

Werner K, Lundholm L, 2004b. Supplementary drilling and soil sampling, installation of groundwater monitoring wells, a pumping well and surface water level gauges. Forsmark site investigation. SKB P-04-139, Svensk Kärnbränslehantering AB.

Werner K, Lundholm L, Johanssson P-O, 2004. Drilling and pumping test of wells at Börstilåsen. Forsmark site investigation. SKB P-04-138, Svensk Kärnbränslehantering AB.

Werner K, Bosson E, Berglund S, 2005a. Description of climate, surface hydrology, and near-surface hydrogeology. Simpevarp 1.2. SKB R-05-04, Svensk Kärnbränslehantering AB.

Werner K, Bosson E, Berglund S, 2005b. Description of climate, surface hydrology, and near-surface hydrogeology. Preliminary site description. Laxemar subarea – version 1.2. SKB R-05-61, Svensk Kärnbränslehantering AB.

Werner K, Lundholm L, Johansson P-O, 2006. Supplementary drilling and soil sampling, and installation of groundwater monitoring wells, pumping wells and BAT filter tips. Forsmark site investigation. SKB P-06-89, Svensk Kärnbränslehantering AB.

Werner K, Johansson P-O, Brydsten L, Bosson E, Berglund S, Tröjbom M, Nyman H, 2007. Recharge and discharge of near-surface groundwater in Forsmark. Comparison of classification methods. SKB R-07-08, Svensk Kärnbränslehantering AB.

Wijnbladh E, Aquilonius K, Floderus S, 2008. The marine ecosystems at Forsmark and Laxemar-Simpevarp. Site descriptive modelling. SDM-Site. SKB R-08-03, Svensk Kärnbränslehantering AB.

Appendix 1

PM by the Swedish Meterorological Institute (SMHI)

(originally in Swedish, translated by the author)

Monthly precipitation at Forsmark and Oskarshamn

Introduction

SKB has need for extension of the time series of monthly precipitation from the four SKB-stations Forsmark (Högmasten), Storskäret, Plittorp, and Äspö. SKB also needs return periods for different monthly sums of precipitation.

Methodology

To enable extension of the time series, correlation coefficients between the SKB-stations and the nearby SMHI-stations have been calculated, see Tables A-1a and A-1b. From Table A1-1a it can be seen that Äspö and Plittorp have the highest correlation with Kråkemåla followed by Oskarshamn. Forsmark and Storskäret have the highest correlation with Östhammar followed by Risinge and Films Kyrkby, respectively (Table A1-1b). Unfortunately, data were missing from numerous months at Films Kyrkby. Therefore, Risinge was seclected as the second station also for Storskäret.

Quotients of monthly precipitation between SKB- and SMHI-stations are presented in Tables A1-2a and A1-2b. The time series for the SKB-stations have been extended by multiplying the monthly precipitation from the selected SMHI-stations by the quotients in the tables. From this, continuous time series of monthly precipitation have been obtained for Plittorp and Äspö from January 1961 and for Forsmark and Storskäret from February 1962.

The extended time series of measured precipitation have been corrected to “true” precipitation by corrections for measurement losses, mainly wind losses. The corrections have been made according to the method of /Alexandersson 2003/, see Table A1-3.

Table A1-1a. Correlation coefficients of monthly precipitation for the Oskarshamn area.

	Plittorp	Äspö	Time period
Oskarshamn	0.79	0.86	Jan-61–Aug-05
Krokshult	0.77	0.85	Jan-68–Aug-05
Kråkemåla	0.94	0.97	Jun-90–Aug-05
Ölands norra udde	0.68	0.78	Jan-61–Aug-05

Table A1-1b. Correlation coefficients of monthly precipitation for the Forsmark area.

	Forsmark	Storskäret	Time period
Films kyrkby	0.60	0.84	Apr-63–Aug-05
Lövsta	0.63	0.77	Jan-68–Jul-05
Risinge	0.72	0.77	Feb-62–Aug-05
Östhammar	0.82	0.85	Nov-88–Aug-05

Table A1-2a. Quotients of monthly precipitation between SKB- and SMHI-stations at Oskarshamn.

	Plittorp	Äspö
Kråkemåla	1.07	0.90
Oskarshamn	1.03	0.86

Table A1-2b. Quotients of monthly precipitation between SKB- and SMHI-stations at Forsmark.

	Forsmark	Storskäret
Östhammar	0.93	0.90
Risinge	0.83	0.82

Table A1-3. Corrections for measurement losses at SKB's precipitations stations (%).

Station	Jan.	Feb.	Mar	Apr	May	Jun.	Jul.	Aug.	Sep.	Oct.	Nov.	Dec.
Forsmark	13	14	13	11	10	10	10	10	10	10	11	12
Storskäret	13	14	13	11	10	10	10	10	10	10	11	12
Äspö	21	21	19	16	14	14	14	14	14	16	17	20
Plittorp	12	13	12	10	10	9	9	10	10	10	10	12

Return periods

The montly precipitation values have been been analysed by extreme value analysis. An example of different fittings to data are shown in Figure A1-1.

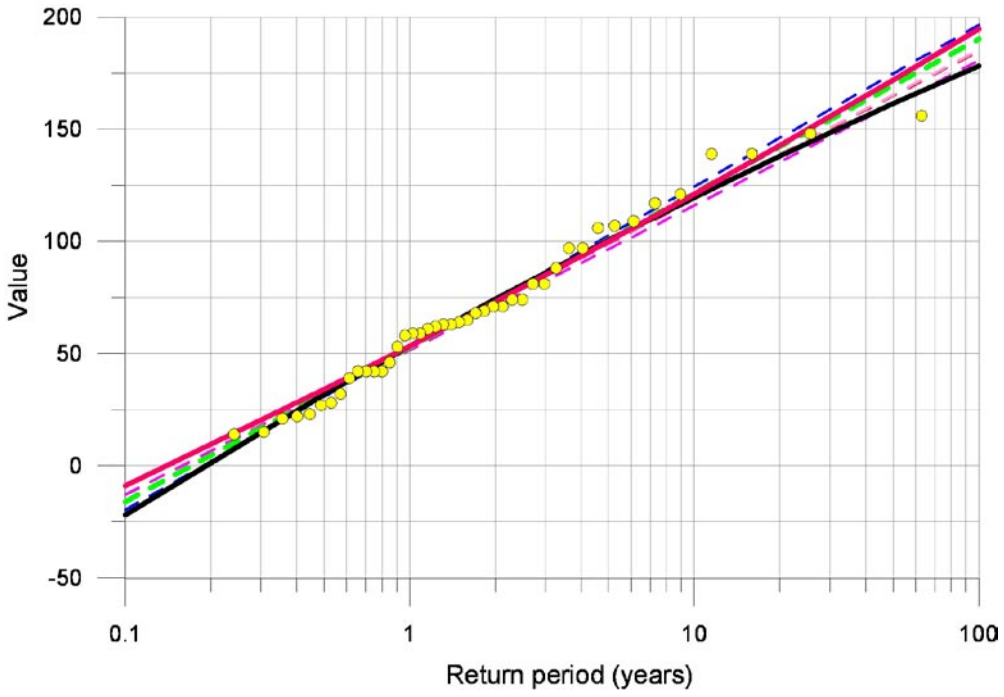

Figure A1-1. *An example of fitting to data in the extreme value analysis performed on the monthly precipitation data.*

Below the equations used for calculation of return periods of different monthly precipitation values are given. Theta, sigma, and my are given in Tables A1-4 to A1-11 below.

High precipitation values

f = exp(–(1-theta*(z-my)/sigma)**(1/theta))
R = exp(-log(-log(f)))

Low precipitation values

f = exp(–(1-theta*(-z-my)/sigma)**(1/theta))
R = exp(-log(-log(f)))

where z = monthly precipitation i mm, and R = return period in years.

Table A1-4. Forsmark. Variable values. High precipitation values.

Var.	Jan.	Feb.	Mar.	Apr.	May	Jun.	Jul.	Aug.	Sep.	Oct.	Nov.	Dec.	Year
Theta	0.151	0.151	0.151	0.151	–0.036	–0.036	–0.036	–0.036	–0.036	–0.036	0.151	0.151	0.140
Sigma	17.397	17.797	13.401	18.745	15.144	22.257	28.220	30.118	24.127	24.513	25.532	26.531	90.378
My	34.760	25.388	24.006	26.875	21.858	34.557	52.099	48.069	43.088	40.502	47.484	37.759	539.813

Table A1-5. Storskäret. Variable values. High precipitation values.

Var.	Jan.	Feb.	Mar.	Apr.	May	Jun.	Jul.	Aug.	Sep.	Oct.	Nov.	Dec.	Year
Theta	0.145	0.145	0.145	0.145	–0.030	–0.030	–0.030	–0.030	–0.030	–0.030	0.145	0.145	0.140
Sigma	16.949	17.311	12.837	18.002	14.946	21.656	26.234	29.095	22.673	23.717	24.193	25.613	88.872
My	33.720	24.321	22.744	25.829	21.374	33.502	50.607	46.255	42.992	38.893	45.715	37.052	516.639

Table A1-6. Äspö. Variable values. High precipitation values.

Var.	Jan.	Feb.	Mar.	Apr.	May	Jun.	Jul.	Aug.	Sep.	Oct.	Nov.	Dec.	Year
Theta	–0.007	–0.007	–0.007	–0.007	–0.017	–0.017	–0.017	–0.017	–0.017	–0.017	–0.007	–0.007	0.100
Sigma	24.059	16.062	14.518	18.741	15.618	24.363	30.462	22.732	25.370	27.708	21.787	26.233	97.034
My	31.723	27.825	22.083	28.746	29.488	37.042	48.058	43.501	42.160	34.292	42.412	38.629	536.998

Table A1-7. Plittorp Variable values. High precipitation values.

Var.	Jan.	Feb.	Mar.	Apr.	May	Jun.	Jul.	Aug.	Sep.	Oct.	Nov.	Dec.	Year
Theta	–0.003	–0.003	–0.003	–0.003	–0.013	–0.013	–0.013	–0.013	–0.013	–0.013	–0.003	–0.003	0.100
Sigma	27.069	18.590	16.520	21.350	18.123	28.110	34.550	26.575	29.481	31.564	24.275	29.437	108.826
My	35.515	30.967	24.773	32.625	34.005	42.594	54.967	50.212	48.834	38.831	47.649	43.256	610.420

Table A1-8. Forsmark. Variable values. Low precipitation values.

Var.	Jan.	Feb.	Mar.	Apr.	May	Jun.	Jul.	Aug.	Sep.	Oct.	Nov.	Dec.	Year
Theta	0.271	0.405	0.353	0.395	0.949	0.701	0.543	0.559	0.594	0.661	0.485	0.699	0.324
Sigma	18.725	20.377	15.019	21.384	21.837	32.001	39.446	42.268	34.118	35.065	30.050	32.631	100.704
My	–49.264	–39.005	–34.619	–41.309	–31.631	–52.389	–77.548	–74.918	–64.061	–60.771	–65.939	–53.861	–613.772

Table A1-9. Storskäret. Variable values. Low precipitation values.

Var.	Jan.	Feb.	Mar.	Apr.	May	Jun.	Jul.	Aug.	Sep.	Oct.	Nov.	Dec.	Year
Theta	0.254	0.500	0.386	0.408	0.917	0.676	0.536	0.567	0.614	0.679	0.499	0.687	0.326
Sigma	18.150	20.554	14.651	20.725	21.471	30.861	36.392	40.669	31.995	33.809	28.716	31.592	99.140
My	–48.097	–36.791	–32.767	–39.677	–31.206	–51.027	–74.159	–71.799	–62.237	–58.049	–63.155	–52.889	–589.256

Table A1-10. Äspö. Variable values. Low precipitation values.

Var.	Jan.	Feb.	Mar.	Apr.	May	Jun.	Jul.	Aug.	Sep.	Oct.	Nov.	Dec.	Year
Theta	0.726	0.658	0.494	0.695	0.500	0.501	0.505	0.250	0.713	0.850	0.538	0.633	0.365
Sigma	33.725	22.337	19.479	26.186	21.187	33.062	41.391	27.756	35.853	39.399	29.584	36.337	113.432
My	–49.799	–40.566	–35.066	–43.192	–43.599	–59.038	–75.478	–67.412	–61.724	–53.287	–61.312	–59.853	–618.497

Table A1-11. Plittorp. Variable values. Low precipitation values.

Var.	Jan.	Feb.	Mar.	Apr.	May	Jun.	Jul.	Aug.	Sep.	Oct.	Nov.	Dec.	Year
Theta	0.722	0.646	0.495	0.697	0.500	0.499	0.488	0.257	0.709	0.852	0.526	0.628	0.371
Sigma	37.788	25.707	22.086	29.727	24.493	37.974	46.526	32.445	41.490	44.711	32.735	40.590	127.548
My	–55.841	–45.798	–39.482	–48.986	–50.284	–67.870	–86.260	–77.910	–71.499	–60.292	–68.807	–67.062	–701.472

Results

The average montly precipitation for the years 1961–1990 have been calculated. This time period is seclected because it is a meteorological standard time period.

Table A1-12. Calculated average precipitation (P) och standard deviation (SD) in mm for the years 1961–1990.

	Jan	Feb	Mar	Apr	May	Jun	Jul	Aug	Sep	Oct	Nov	Dec	Year
Forsmark P	44	33	29	35	27	39	71	66	61	53	61	50	568
Forsmark SD	18	19	15	17	17	22	34	41	32	33	29	31	108
Storskäret P	42	32	28	34	26	38	69	64	59	51	59	49	549
Storskäret SD	17	19	15	17	17	21	33	40	31	32	28	30	104
Plittorp P	54	39	36	43	45	51	73	61	64	51	56	56	630
Plittorp SD	41	25	23	25	24	32	39	30	34	41	27	39	122
Äspö)	49	35	32	38	39	44	64	53	55	45	49	50	553
Äspö SD	37	22	20	22	21	28	34	26	29	36	24	35	108

By use of the extended corrected time series, precipitation values for different return periods have been calculated according to the extreme value analysis briefly described above, see Tables A1-13 and A1-14.

Table A1-13a. High precipitation values in mm for different return periods for Forsmark.

Return period	Jan	Feb	Mar	Apr	May	Jun	Jul	Aug	Sep	Oct	Nov	Dec	Year
5 years	61	51	44	54	46	71	100	99	84	81	83	73	675
10 years	70	60	51	64	57	88	121	122	102	99	97	87	722
20 years	78	68	57	72	69	105	143	145	120	118	108	99	766
50 years	87	78	64	83	84	128	172	176	145	144	122	114	817
100 years	94	85	69	89	97	146	195	200	165	163	132	123	851

Table A1-13b. High precipitation values in mm for different return periods for Storskäret.

Return period	Jan	Feb	Mar	Apr	May	Jun	Jul	Aug	Sep	Oct	Nov	Dec	Year
5 years	60	49	41	52	45	69	95	95	81	78	80	72	649
10 years	68	58	48	61	56	85	114	117	97	95	93	85	696
20 years	76	67	54	70	67	101	134	139	115	113	104	97	739
50 years	86	76	61	80	83	124	161	169	138	138	117	111	789
100 years	92	83	66	87	95	141	182	192	156	157	126	121	823

Table A1-13c. High precipitation values in mm for different return periods for Plittorp.

Return period	Jan	Feb	Mar	Apr	May	Jun	Jul	Aug	Sep	Oct	Nov	Dec	Year
5 years	78	61	52	67	63	90	113	98	96	88	88	91	778
10 years	97	74	64	82	76	110	138	117	117	111	105	111	840
20 years	116	87	75	96	89	130	162	136	138	133	122	132	898
50 years	141	104	91	116	106	157	196	161	166	164	144	159	968
100 years	160	117	102	131	120	177	221	181	188	187	161	180	1,017

Table A1-13d. High precipitation values in mm for different return periods for Äspö.

Return period	Jan	Feb	Mar	Apr	May	Jun	Jul	Aug	Sep	Oct	Nov	Dec	Year
5 years	70	54	46	59	55	78	99	85	83	78	78	81	686
10 years	87	65	57	72	66	96	121	101	101	98	94	99	742
20 years	104	76	67	85	77	113	143	117	120	118	109	118	793
50 years	126	91	80	103	92	137	173	140	144	145	130	143	856
100 years	144	103	91	116	104	155	196	156	163	165	145	161	900

Table A1-14a. Low precipitation values in mm for different return periods for Forsmark.

Return period	Jan	Feb	Mar	Apr	May	Jun	Jul	Aug	Sep	Oct	Nov	Dec	Year
5 years	25	15	16	16	14	22	35	30	29	26	32	22	488
10 years	17	9	11	9	11	16	26	20	21	19	24	17	450
20 years	11	4	7	4	10	12	19	14	16	15	19	13	421
50 years	4	0	3	0	9	10	14	8	12	12	13	10	390
100 years	0	0	1	0	9	9	11	5	10	10	11	9	373

Table A1-14b. Low precipitation values in mm for different return periods for Storskäret.

Return period	Jan	Feb	Mar	Apr	May	Jun	Jul	Aug	Sep	Oct	Nov	Dec	Year
5 years	24	15	15	15	13	21	35	29	30	25	31	22	465
10 years	16	10	10	9	11	15	26	20	23	19	24	16	429
20 years	10	6	7	4	9	11	20	13	18	15	19	13	400
50 years	3	2	3	0	8	9	15	8	15	12	14	10	370
100 years	0	1	1	0	8	7	12	5	13	10	11	9	353

Table A1-14c. Low precipitation values in mm for different return periods for Plittorp.

Return period	Jan	Feb	Mar	Apr	May	Jun	Jul	Aug	Sep	Oct	Nov	Dec	Year
5 years	20	20	15	20	21	26	34	35	32	21	33	26	547
10 years	13	15	9	15	15	16	22	22	24	15	25	18	504
20 years	10	12	5	12	10	9	13	10	20	12	19	12	471
50 years	7	9	1	9	6	3	5	0	17	10	15	8	438
100 years	5	8	0	8	4	0	1	0	15	9	12	6	420

Table A1-14d. Low precipitation values in mm for different return periods for Äspö.

Return period	Jan	Feb	Mar	Apr	May	Jun	Jul	Aug	Sep	Oct	Nov	Dec	Year
5 years	18	18	13	18	18	23	30	31	27	19	30	23	480
10 years	12	14	8	13	13	14	19	19	21	14	22	16	442
20 years	9	11	5	10	9	8	12	9	17	11	17	11	412
50 years	6	9	1	8	5	2	5	–2	15	9	13	7	382
100 years	5	8	0	7	3	0	2	–9	13	8	11	6	365

Appendix 2

Comparison of point water heads and environmental heads in percussion-drilled borehole sections

Measured groundwater levels, i.e. point water heads, have been registered in HFM-boreholes and SFM-boreholes. HFM-boreholes are equipped with packers, dividing the water column into sections. Groundwater densities have been measured in these sections.

The point water heads, densities and borehole geometry (depth, packer positions /secup and seclow/) have been used to calculate environmental water heads per section according to the method presented in Section 1.4.2 of the main report. When applicable, groundwater head values in corresponding SFM-borehole close to the HFM-borehole have been used in the calculation to obtain the direction of the vertical flow gradient all the way to the ground surface. For some HFM-boreholes, the calculations have been made with reference to two different SFM-wells. Other HFM-boreholes are not located close to any SFM-wells and the calculations have therefore been done internally for that borehole (calculating heads in lower sections with reference to measurements in the topmost section). According to the applied method, the vertical gradient in a borehole is calculated as head difference between two sections.

The tables below illustrate the vertical gradient components based on differences in point water heads (PWH) and environmental water heads (EWH) between borehole sections. They also present the mean compensation per section between the two head components (EWH-PWH).

Arrows and colours show gradients, where:

- Blue (↓) > 0.05 m difference, downward gradient.
- Yellow (↔) < 0.05 and > –0.05 m difference, no or small vertical gradient.
- Red (↑) < –0.05 m difference, upward gradient.

Examples can be found (i.e. in HFM15) where the average differences between section heads indicate the same direction of the gradient through all sections both for PWH and EWH. Other examples can be found (i.e.in HFM19) where the average differences between section heads indicae downward gradient for PWH, whereas the gradient varies for EWH.

The frequency of the three gradient classes above has been analysed. In the tables average conditions as well as the 0.02 and 0.98 percentiles are shown (2% correspond to a duration of approximately one week per year of the gradient).

HFM1 (Constant)

QD =SFM0003

Section	Min		Percentil 0.02		Ave		Percentil 0.98		Max		Section	Compensation EWH-PWH mean
QD	PWHQD	EWHQD	PWHQD	EWHQD	PWHQD	EWHQD	PWHQD	EWHQD	PWHQD	EWHQD	QD	
	-1.45 ↓	-1.44 ↓	-1.38 ↓	-1.37 ↓	-0.93 ↓	-0.92 ↓	-0.63 ↓	-0.62 ↓	-0.62 ↓	-0.61 ↓		
3	PWH3	EWH3	PWH3	EWH3	PWH3	EWH3	PWH3	EWH3	PWH3	EWH3	3	0.01
	-0.11 ↓	-0.1 ↓	-0.07 ↓	-0.06 ↓	-0.01 ↔	-0.01 ↔	0.04 ↔	0.05 ↔	0.08 ↑	0.08 ↑		
2	PWH2	EWH2	PWH2	EWH2	PWH2	EWH2	PWH2	EWH2	PWH2	EWH2	2	0.01
	-0.09 ↓	-0.06 ↓	-0.08 ↓	-0.06 ↓	-0.05 ↔	-0.03 ↔	-0.03 ↔	0 ↔	-0.02 ↔	0 ↔		
1	PWH1	EWH1	PWH1	EWH1	PWH1	EWH1	PWH1	EWH1	PWH1	EWH1	1	0.03

HFM2 (Constant)

QD =SFM0003

Section	Min		Percentil 0.02		Ave		Percentil 0.98		Max		Section	Compensation EWH-PWH mean
QD	PWHQD	EWHQD	PWHQD	EWHQD	PWHQD	EWHQD	PWHQD	EWHQD	PWHQD	EWHQD	QD	
	-4.33 ↓	-4.33 ↓	-2.19 ↓	-2.19 ↓	-0.93 ↓	-0.93 ↓	-0.19 ↓	-0.19 ↓	0.53 ↑	0.53 ↑		
3	PWH3	EWH3	PWH3	EWH3	PWH3	EWH3	PWH3	EWH3	PWH3	EWH3	3	0.00
	-0.53 ↓	-0.5 ↓	-0.1 ↓	-0.08 ↓	0.02 ↔	0.05 ↔	0.1 ↑	0.13 ↑	2.81 ↑	2.84 ↑		
2	PWH2	EWH2	PWH2	EWH2	PWH2	EWH2	PWH2	EWH2	PWH2	EWH2	2	0.03
	-0.15 ↓	-0.06 ↓	-0.08 ↓	0 ↔	0.02 ↔	0.11 ↑	0.08 ↑	0.17 ↑	0.2 ↑	0.28 ↑		
1	PWH1	EWH1	PWH1	EWH1	PWH1	EWH1	PWH1	EWH1	PWH1	EWH1	1	0.12

HFM2 (Constant)

QD =SFM0104

Section	Min		Percentil 0.02		Ave		Percentil 0.98		Max		Section	Compensation EWH-PWH mean
QD	PWHQD	EWHQD	PWHQD	EWHQD	PWHQD	EWHQD	PWHQD	EWHQD	PWHQD	EWHQD	QD	
	-2.33 ↓	-2.33 ↓	-2.25 ↓	-2.25 ↓	-0.83 ↓	-0.83 ↓	0.52 ↑	0.52 ↑	0.6 ↑	0.6 ↑		
3	PWH3	EWH3	PWH3	EWH3	PWH3	EWH3	PWH3	EWH3	PWH3	EWH3	3	0.00
	-0.53 ↓	-0.22 ↓	-0.1 ↓	-0.01 ↔	0.02 ↔	0.08 ↑	0.1 ↑	0.14 ↑	2.81 ↑	0.29 ↑		
2	PWH2	EWH2	PWH2	EWH2	PWH2	EWH2	PWH2	EWH2	PWH2	EWH2	2	0.03
	-0.15 ↓	0.05 ↑	-0.08 ↓	0.08 ↑	0.02 ↔	0.12 ↑	0.08 ↑	0.14 ↑	0.2 ↑	0.18 ↑		
1	PWH1	EWH1	PWH1	EWH1	PWH1	EWH1	PWH1	EWH1	PWH1	EWH1	1	0.11

HFM3 (Constant)

QD =SFM0003

Section	Min		Percentil 0.02		Ave		Percentil 0.98		Max		Section	Compensation EWH-PWH mean
QD	PWHQD	EWHQD	PWHQD	EWHQD	PWHQD	EWHQD	PWHQD	EWHQD	PWHQD	EWHQD	QD	
	-4 ↓	-4 ↓	-2.02 ↓	-2.02 ↓	-0.82 ↓	-0.82 ↓	-0.11 ↓	-0.11 ↓	0.55 ↑	0.55 ↑		
2	PWH2	EWH2	PWH2	EWH2	PWH2	EWH2	PWH2	EWH2	PWH2	EWH2	2	0.00
	-0.4 ↓	-0.4 ↓	-0.19 ↓	-0.19 ↓	-0.02 ↔	-0.02 ↔	0.04 ↔	0.04 ↔	0.58 ↑	0.58 ↑		
1	PWH1	EWH1	PWH1	EWH1	PWH1	EWH1	PWH1	EWH1	PWH1	EWH1	1	0.00

HFM3 (Constant)

QD =SFM0104

Section	Min		Percentil 0.02		Ave		Percentil 0.98		Max		Section	Compensation EWH-PWH mean
QD	PWHQD	EWHQD	PWHQD	EWHQD	PWHQD	EWHQD	PWHQD	EWHQD	PWHQD	EWHQD	QD	
	-2.11 ↓	-2.11 ↓	-2.03 ↓	-2.03 ↓	-0.69 ↓	-0.69 ↓	0.56 ↑	0.56 ↑	0.62 ↑	0.62 ↑		
2	PWH2	EWH2	PWH2	EWH2	PWH2	EWH2	PWH2	EWH2	PWH2	EWH2	2	0.00
	-0.4 ↓	-0.25 ↓	-0.19 ↓	-0.2 ↓	-0.02 ↔	-0.04 ↔	0.04 ↔	0.01 ↔	0.58 ↑	0.01 ↔		
1	PWH1	EWH1	PWH1	EWH1	PWH1	EWH1	PWH1	EWH1	PWH1	EWH1	1	0.00

HFM4 (Constant)

QD =SFM0004

Section	Min		Percentil 0.02		Ave		Percentil 0.98		Max		Section	Compensation EWH-PWH mean
QD	PWHQD	EWHQD	PWHQD	EWHQD	PWHQD	EWHQD	PWHQD	EWHQD	PWHQD	EWHQD	QD	
	-4.03 ↓	-4.03 ↓	-3.01 ↓	-3.01 ↓	-2.02 ↓	-2.02 ↓	-1.63 ↓	-1.63 ↓	-1.4 ↓	-1.4 ↓		
3	PWH3	EWH3	PWH3	EWH3	PWH3	EWH3	PWH3	EWH3	PWH3	EWH3	3	0.00
	-1.64 ↓	-1.64 ↓	-1.2 ↓	-1.2 ↓	-0.41 ↓	-0.41 ↓	-0.08 ↓	-0.08 ↓	0.14 ↑	0.14 ↑		
2	PWH2	EWH2	PWH2	EWH2	PWH2	EWH2	PWH2	EWH2	PWH2	EWH2	2	0.00
	-0.29 ↓	-0.29 ↓	-0.21 ↓	-0.21 ↓	0.06 ↑	0.06 ↑	0.8 ↑	0.8 ↑	1.47 ↑	1.47 ↑		
1	PWH1	EWH1	PWH1	EWH1	PWH1	EWH1	PWH1	EWH1	PWH1	EWH1	1	0.00

HFM8 (Constant)

Section	Min		Percentil 0.02		Ave		Percentil 0.98		Max		Section	Compensation EWH-PWH mean
2	PWH2	EWH2	PWH2	EWH2	PWH2	EWH2	PWH2	EWH2	PWH2	EWH2	2	
	-0.36 ↓	0.32 ↑	-0.35 ↓	0.33 ↑	-0.28 ↓	0.4 ↑	-0.21 ↓	0.47 ↑	-0.18 ↓	0.49 ↑		
1	PWH1	EWH1	PWH1	EWH1	PWH1	EWH1	PWH1	EWH1	PWH1	EWH1	1	0.68

HFM10 (Constant)

QD =SFM0057

Section	Min		Percentil 0.02		Ave		Percentil 0.98		Max		Section	Compensation EWH-PWH mean
QD	PWHQD	EWHQD	PWHQD	EWHQD	PWHQD	EWHQD	PWHQD	EWHQD	PWHQD	EWHQD	QD	
	-1.98 ↓	-1.98 ↓	-1.31 ↓	-1.31 ↓	-0.7 ↓	-0.7 ↓	-0.32 ↓	-0.32 ↓	-0.26 ↓	-0.26 ↓		
2	PWH2	EWH2	PWH2	EWH2	PWH2	EWH2	PWH2	EWH2	PWH2	EWH2	2	0.00
	-1.43 ↓	-0.93 ↓	-0.8 ↓	-0.28 ↓	-0.35 ↓	0.15 ↑	0.14 ↑	0.65 ↑	0.19 ↑	0.7 ↑		
1	PWH1	EWH1	PWH1	EWH1	PWH1	EWH1	PWH1	EWH1	PWH1	EWH1	1	0.51

HFM11 (Constant)

Section	Min		Percentil 0.02		Ave		Percentil 0.98		Max		Section	Compensation EWH-PWH mean
2	PWH2	EWH2	PWH2	EWH2	PWH2	EWH2	PWH2	EWH2	PWH2	EWH2	2	0.00
	-0.81 ↓	-0.81 ↓	-0.71 ↓	-0.71 ↓	-0.53 ↓	-0.53 ↓	-0.23 ↓	-0.23 ↓	-0.05 ↓	-0.05 ↓		
1	PWH1	EWH1	PWH1	EWH1	PWH1	EWH1	PWH1	EWH1	PWH1	EWH1	1	0.00

HFM12 (Constant)

Compensation EWH-PWH

Section	Min		Percentil 0.02		Ave		Percentil 0.98		Max		Section	mean
2	PWH2	EWH2	PWH2	EWH2	PWH2	EWH2	PWH2	EWH2	PWH2	EWH2	2	0.00
	-5.41 ↓	-5.37 ↓	-0.06 ↓	-0.03 ↔	0.05 ↑	0.09 ↑	0.25 ↑	0.29 ↑	1.38 ↑	1.42 ↑		
1	PWH1	EWH1	PWH1	EWH1	PWH1	EWH1	PWH1	EWH1	PWH1	EWH1	1	0.04

HFM13 (Constant)

Compensation EWH-PWH

Section	Min		Percentil 0.02		Ave		Percentil 0.98		Max		Section	mean
3	PWH3	EWH3	PWH3	EWH3	PWH3	EWH3	PWH3	EWH3	PWH3	EWH3	3	0.00
	-4.45 ↓	-4.45 ↓	-3.91 ↓	-3.91 ↓	-1.7 ↓	-1.7 ↓	-0.93 ↓	-0.93 ↓	-0.85 ↓	-0.85 ↓		
2	PWH2	EWH2	PWH2	EWH2	PWH2	EWH2	PWH2	EWH2	PWH2	EWH2	2	0.00
	-2.5 ↓	-1.7 ↓	-2.11 ↓	-1.32 ↓	-0.81 ↓	0.02 ↔	-0.49 ↓	0.33 ↑	-0.3 ↓	0.52 ↑		
1	PWH1	EWH1	PWH1	EWH1	PWH1	EWH1	PWH1	EWH1	PWH1	EWH1	1	0.83

HFM15 (Constant)

QD =SFM0058

Compensation EWH-PWH

Section	Min		Percentil 0.02		Ave		Percentil 0.98		Max		Section	mean
QD	PWHQD	EWHQD	PWHQD	EWHQD	PWHQD	EWHQD	PWHQD	EWHQD	PWHQD	EWHQD	QD	
	-9.17 ↓	-9.17 ↓	-3.2 ↓	-3.2 ↓	-0.91 ↓	-0.91 ↓	0.15 ↑	0.15 ↑	0.26 ↑	0.26 ↑		
2	PWH2	EWH2	PWH2	EWH2	PWH2	EWH2	PWH2	EWH2	PWH2	EWH2	2	0.00
	-0.57 ↓	-0.56 ↓	-0.37 ↓	-0.36 ↓	-0.07 ↓	-0.08 ↓	0.66 ↑	0.54 ↑	2.41 ↑	2.42 ↑		
1	PWH1	EWH1	PWH1	EWH1	PWH1	EWH1	PWH1	EWH1	PWH1	EWH1	1	0.01

HFM16 (Constant)

QD =SFM0021

Compensation EWH-PWH

Section	Min		Percentil 0.02		Ave		Percentil 0.98		Max		Section	mean
QD	PWHQD	EWHQD	PWHQD	EWHQD	PWHQD	EWHQD	PWHQD	EWHQD	PWHQD	EWHQD	QD	
	-1.34 ↓	-1.34 ↓	-0.91 ↓	-0.91 ↓	-0.33 ↓	-0.33 ↓	0.83 ↑	0.84 ↑	1.01 ↑	1.01 ↑		
3	PWH3	EWH3	PWH3	EWH3	PWH3	EWH3	PWH3	EWH3	PWH3	EWH3	3	0.00
	-0.05 ↔	-0.05 ↓	-0.03 ↔	-0.04 ↔	0 ↔	0 ↔	0.09 ↑	0.09 ↑	0.11 ↑	0.1 ↑		
2	PWH2	EWH2	PWH2	EWH2	PWH2	EWH2	PWH2	EWH2	PWH2	EWH2	2	0.00
	-0.05 ↔	-0.04 ↔	-0.05 ↔	-0.03 ↔	-0.01 ↔	0 ↔	0.01 ↔	0.02 ↔	0.01 ↔	0.02 ↔		
1	PWH1	EWH1	PWH1	EWH1	PWH1	EWH1	PWH1	EWH1	PWH1	EWH1	1	0.01

HFM16 (Constant)

QD =SFM0105

Compensation EWH-PWH

Section	Min		Percentil 0.02		Ave		Percentil 0.98		Max		Section	mean
QD	PWHQD	EWHQD	PWHQD	EWHQD	PWHQD	EWHQD	PWHQD	EWHQD	PWHQD	EWHQD	QD	
	-1.09 ↓	-1.09 ↓	-1.08 ↓	-1.09 ↓	-0.72 ↓	-0.72 ↓	-0.41 ↓	-0.42 ↓	-0.17 ↓	-0.17 ↓		
3	PWH3	EWH3	PWH3	EWH3	PWH3	EWH3	PWH3	EWH3	PWH3	EWH3	3	0.00
	-0.05 ↔	-0.04 ↔	-0.03 ↔	-0.04 ↔	0 ↔	-0.01 ↔	0.09 ↑	0.01 ↔	0.11 ↑	0.02 ↔		
2	PWH2	EWH2	PWH2	EWH2	PWH2	EWH2	PWH2	EWH2	PWH2	EWH2	2	-0.01
	-0.05 ↔	0 ↔	-0.05 ↔	0 ↔	-0.01 ↔	0.01 ↔	0.01 ↔	0.02 ↔	0.01 ↔	0.02 ↔		
1	PWH1	EWH1	PWH1	EWH1	PWH1	EWH1	PWH1	EWH1	PWH1	EWH1	1	0.01

HFM18 (Constant)

QD =SFM0106

Compensation EWH-PWH

Section	Min		Percentil 0.02		Ave		Percentil 0.98		Max		Section	mean
QD	PWHQD	EWHQD	PWHQD	EWHQD	PWHQD	EWHQD	PWHQD	EWHQD	PWHQD	EWHQD	QD	
	-3.07 ↓	-3.07 ↓	-3.05 ↓	-3.05 ↓	-2.33 ↓	-2.33 ↓	-1.16 ↓	-1.16 ↓	-1.06 ↓	-1.06 ↓		
3	PWH3	EWH3	PWH3	EWH3	PWH3	EWH3	PWH3	EWH3	PWH3	EWH3	3	0.00
	-1.32 ↓	-0.96 ↓	-0.99 ↓	-0.81 ↓	-0.17 ↓	-0.1 ↓	0.33 ↑	0.34 ↑	0.35 ↑	0.35 ↑		
2	PWH2	EWH2	PWH2	EWH2	PWH2	EWH2	PWH2	EWH2	PWH2	EWH2	2	0.00
	-0.07 ↓	-0.07 ↓	-0.07 ↓	-0.07 ↓	-0.03 ↔	-0.03 ↔	0 ↔	-0.01 ↔	0 ↔	0 ↔		
1	PWH1	EWH1	PWH1	EWH1	PWH1	EWH1	PWH1	EWH1	PWH1	EWH1	1	0.00

HFM19 (Constant)

QD =SFM0058

Compensation EWH-PWH

Section	Min		Percentil 0.02		Ave		Percentil 0.98		Max		Section	mean
QD	PWHQD	EWHQD	PWHQD	EWHQD	PWHQD	EWHQD	PWHQD	EWHQD	PWHQD	EWHQD	QD	
	-5.63 ↓	-5.63 ↓	-2.5 ↓	-2.5 ↓	-0.8 ↓	-0.8 ↓	0.26 ↑	0.26 ↑	0.44 ↑	0.44 ↑		
3	PWH3	EWH3	PWH3	EWH3	PWH3	EWH3	PWH3	EWH3	PWH3	EWH3	3	0.00
	-0.43 ↓	-0.15 ↓	-0.26 ↓	-0.01 ↔	-0.07 ↓	0.13 ↑	0.06 ↑	0.26 ↑	0.09 ↑	0.27 ↑		
2	PWH2	EWH2	PWH2	EWH2	PWH2	EWH2	PWH2	EWH2	PWH2	EWH2	2	0.21
	-0.78 ↓	-0.24 ↓	-0.64 ↓	-0.09 ↓	-0.51 ↓	-0.03 ↔	0.32 ↑	0.08 ↑	0.35 ↑	0.12 ↑		
1	PWH1	EWH1	PWH1	EWH1	PWH1	EWH1	PWH1	EWH1	PWH1	EWH1	1	0.76

HFM20 (Constant)

QD =SFM0107

Compensation EWH-PWH

Section	Min		Percentil 0.02		Ave		Percentil 0.98		Max		Section	mean
QD	PWHQD	EWHQD	PWHQD	EWHQD	PWHQD	EWHQD	PWHQD	EWHQD	PWHQD	EWHQD	QD	
	-0.57 ↓	-0.57 ↓	-0.51 ↓	-0.52 ↓	-0.19 ↓	-0.19 ↓	0.02 ↔	0.02 ↔	0.16 ↑	0.16 ↑		
4	PWH4	EWH4	PWH4	EWH4	PWH4	EWH4	PWH4	EWH4	PWH4	EWH4	4	0.00
	-0.98 ↓	-0.74 ↓	-0.66 ↓	-0.69 ↓	-0.22 ↓	-0.24 ↓	0.03 ↔	0.05 ↔	0.09 ↑	0.09 ↑		
3	PWH3	EWH3	PWH3	EWH3	PWH3	EWH3	PWH3	EWH3	PWH3	EWH3	3	0.00
	-0.46 ↓	-0.27 ↓	-0.24 ↓	-0.25 ↓	-0.05 ↔	-0.07 ↓	0.07 ↑	0.04 ↔	0.12 ↑	0.05 ↑		
2	PWH2	EWH2	PWH2	EWH2	PWH2	EWH2	PWH2	EWH2	PWH2	EWH2	2	-0.03
	-0.24 ↓	-0.04 ↔	-0.03 ↔	0.01 ↔	0.09 ↑	0.1 ↑	0.18 ↑	0.18 ↑	0.39 ↑	0.39 ↑		
1	PWH1	EWH1	PWH1	EWH1	PWH1	EWH1	PWH1	EWH1	PWH1	EWH1	1	-0.03

HFM27 (Constant)

QD =SFM0003

Section	Min		Percentil 0.02		Ave		Percentil 0.98		Max		Section	Compensation EWH-PWH mean
QD	PWHQD	EWHQD	PWHQD	EWHQD	PWHQD	EWHQD	PWHQD	EWHQD	PWHQD	EWHQD	QD	
	-1.29 ↓	-1.29 ↓	-1.21 ↓	-1.22 ↓	-0.71 ↓	-0.71 ↓	-0.31 ↓	-0.31 ↓	-0.28 ↓	-0.28 ↓		
4	PWH4	EWH4	PWH4	EWH4	PWH4	EWH4	PWH4	EWH4	PWH4	EWH4	4	0.00
	-0.09 ↓	-0.09 ↓	-0.08 ↓	-0.08 ↓	-0.03 ↔	-0.03 ↔	0.01 ↔	0.01 ↔	0.01 ↔	0.01 ↔		
3	PWH3	EWH3	PWH3	EWH3	PWH3	EWH3	PWH3	EWH3	PWH3	EWH3	3	0.00
	-0.13 ↓	-0.01 ↔	-0.12 ↓	0 ↔	-0.11 ↓	0.01 ↔	-0.1 ↓	0.02 ↔	-0.1 ↓	0.02 ↔		
2	PWH2	EWH2	PWH2	EWH2	PWH2	EWH2	PWH2	EWH2	PWH2	EWH2	2	0.12
	-0.55 ↓	-0.53 ↓	-0.07 ↓	-0.04 ↔	0.1 ↑	0.13 ↑	0.33 ↑	0.36 ↑	0.86 ↑	0.89 ↑		
1	PWH1	EWH1	PWH1	EWH1	PWH1	EWH1	PWH1	EWH1	PWH1	EWH1	1	0.14

HFM27 (Constant)

QD =SFM0104

Section	Min		Percentil 0.02		Ave		Percentil 0.98		Max		Section	Compensation EWH-PWH mean
QD	PWHQD	EWHQD	PWHQD	EWHQD	PWHQD	EWHQD	PWHQD	EWHQD	PWHQD	EWHQD	QD	
	-1.64 ↓	-1.64 ↓	-1.55 ↓	-1.55 ↓	-0.92 ↓	-0.92 ↓	-0.04 ↔	-0.04 ↔	-0.02 ↔	-0.02 ↔		
4	PWH4	EWH4	PWH4	EWH4	PWH4	EWH4	PWH4	EWH4	PWH4	EWH4	4	0.00
	-0.09 ↓	-0.09 ↓	-0.08 ↓	-0.08 ↓	-0.03 ↔	-0.03 ↔	0.01 ↔	0.01 ↔	0.01 ↔	0.01 ↔		
3	PWH3	EWH3	PWH3	EWH3	PWH3	EWH3	PWH3	EWH3	PWH3	EWH3	3	0.00
	-0.13 ↓	-0.01 ↔	-0.12 ↓	0 ↔	-0.11 ↓	0.01 ↔	-0.1 ↓	0.02 ↔	-0.1 ↓	0.02 ↔		
2	PWH2	EWH2	PWH2	EWH2	PWH2	EWH2	PWH2	EWH2	PWH2	EWH2	2	0.12
	-0.55 ↓	-0.53 ↓	-0.07 ↓	-0.07 ↓	0.1 ↑	0.13 ↑	0.33 ↑	0.39 ↑	0.86 ↑	0.89 ↑		
1	PWH1	EWH1	PWH1	EWH1	PWH1	EWH1	PWH1	EWH1	PWH1	EWH1	1	0.14

HFM32 (Constant)

QD =SFM0023

Section	Min		Percentil 0.02		Ave		Percentil 0.98		Max		Section	Compensation EWH-PWH mean
QD	PWHQD	EWHQD	PWHQD	EWHQD	PWHQD	EWHQD	PWHQD	EWHQD	PWHQD	EWHQD	QD	
	-0.6 ↓	-0.6 ↓	-0.36 ↓	-0.36 ↓	-0.25 ↓	-0.25 ↓	0.81 ↑	0.81 ↑	1.65 ↑	1.65 ↑		
4	PWH4	EWH4	PWH4	EWH4	PWH4	EWH4	PWH4	EWH4	PWH4	EWH4	4	0.00
	-0.05 ↓	-0.04 ↔	-0.05 ↔	-0.03 ↔	0.02 ↔	0.04 ↔	0.18 ↑	0.19 ↑	0.18 ↑	0.19 ↑		
3	PWH3	EWH3	PWH3	EWH3	PWH3	EWH3	PWH3	EWH3	PWH3	EWH3	3	0.01
	-2.12 ↓	-2.12 ↓	-1.58 ↓	-1.58 ↓	-0.27 ↓	-0.27 ↓	-0.1 ↓	-0.1 ↓	-0.07 ↓	-0.07 ↓		
2	PWH2	EWH2	PWH2	EWH2	PWH2	EWH2	PWH2	EWH2	PWH2	EWH2	2	0.01
	-0.14 ↓	-0.05 ↓	-0.09 ↓	0.02 ↔	0.02 ↔	0.12 ↑	0.18 ↑	0.27 ↑	0.19 ↑	0.27 ↑		
1	PWH1	EWH1	PWH1	EWH1	PWH1	EWH1	PWH1	EWH1	PWH1	EWH1	1	0.10

HFM32 (Constant)

QD =SFM0040

Section	Min		Percentil 0.02		Ave		Percentil 0.98		Max		Section	Compensation EWH-PWH mean
QD	PWHQD	EWHQD	PWHQD	EWHQD	PWHQD	EWHQD	PWHQD	EWHQD	PWHQD	EWHQD	QD	
	-0.58 ↓	-0.58 ↓	-0.43 ↓	-0.43 ↓	-0.33 ↓	-0.33 ↓	-0.26 ↓	-0.26 ↓	-0.24 ↓	-0.24 ↓		
4	PWH4	EWH4	PWH4	EWH4	PWH4	EWH4	PWH4	EWH4	PWH4	EWH4	4	0.00
	-0.05 ↓	-0.04 ↔	-0.05 ↔	-0.03 ↔	0.02 ↔	0.04 ↔	0.18 ↑	0.19 ↑	0.18 ↑	0.19 ↑		
3	PWH3	EWH3	PWH3	EWH3	PWH3	EWH3	PWH3	EWH3	PWH3	EWH3	3	0.01
	-2.12 ↓	-2.12 ↓	-1.58 ↓	-1.58 ↓	-0.27 ↓	-0.27 ↓	-0.1 ↓	-0.1 ↓	-0.07 ↓	-0.07 ↓		
2	PWH2	EWH2	PWH2	EWH2	PWH2	EWH2	PWH2	EWH2	PWH2	EWH2	2	0.01
	-0.14 ↓	-0.05 ↓	-0.09 ↓	-0.01 ↔	0.02 ↔	0.1 ↑	0.18 ↑	0.26 ↑	0.19 ↑	0.27 ↑		
1	PWH1	EWH1	PWH1	EWH1	PWH1	EWH1	PWH1	EWH1	PWH1	EWH1	1	0.10

HFM34 (Constant)

Section	Min		Percentil 0.02		Ave		Percentil 0.98		Max		Section	Compensation EWH-PWH mean
3	PWH3	EWH3	PWH3	EWH3	PWH3	EWH3	PWH3	EWH3	PWH3	EWH3	3	0.00
	-2.61 ↓	-2.6 ↓	-2.58 ↓	-2.58 ↓	-2.34 ↓	-2.34 ↓	-2.26 ↓	-2.26 ↓	-2.24 ↓	-2.24 ↓		
2	PWH2	EWH2	PWH2	EWH2	PWH2	EWH2	PWH2	EWH2	PWH2	EWH2	2	0.00
	Missing	Missing	Missing	Missing	Missing	Missing	Missing	Missing	Missing	Missing		
1	PWH1	EWH1	PWH1	EWH1	PWH1	EWH1	PWH1	EWH1	PWH1	EWH1	1	Missing

HFM35 (Constant)

Section	Min		Percentil 0.02		Ave		Percentil 0.98		Max		Section	Compensation EWH-PWH mean
4	PWH4	EWH4	PWH4	EWH4	PWH4	EWH4	PWH4	EWH4	PWH4	EWH4	4	0.00
	-5.36 ↓	-5.36 ↓	-5.29 ↓	-5.29 ↓	-5.22 ↓	-5.22 ↓	-5.14 ↓	-5.14 ↓	-5.11 ↓	-5.11 ↓		
3	PWH3	EWH3	PWH3	EWH3	PWH3	EWH3	PWH3	EWH3	PWH3	EWH3	3	0.00
	0.04 ↔	0.05 ↔	0.04 ↔	0.05 ↑	0.05 ↔	0.06 ↑	0.06 ↑	0.08 ↑	0.08 ↑	0.09 ↑		
2	PWH2	EWH2	PWH2	EWH2	PWH2	EWH2	PWH2	EWH2	PWH2	EWH2	2	0.01
	0.07 ↑	0.08 ↑	0.08 ↑	0.08 ↑	0.1 ↑	0.1 ↑	0.17 ↑	0.17 ↑	0.25 ↑	0.25 ↑		
1	PWH1	EWH1	PWH1	EWH1	PWH1	EWH1	PWH1	EWH1	PWH1	EWH1	1	0.01

To further illustrate the measured and calculated heads of the different sections, selected HFM-boreholes with differences between PWH and EWH greater than 0.1 m are presented below as graphs. Both the PWH and EWH per section are presented. For reference, the graphs are presented with the level of the sea and/or a nearby lake, and whenever appropriate with the groundwater level of a nearby SFM-well. For quick reference, the tables corresponding to the HFM-borehole (selected from the tables presented above) are presented below the graphs on the same page.

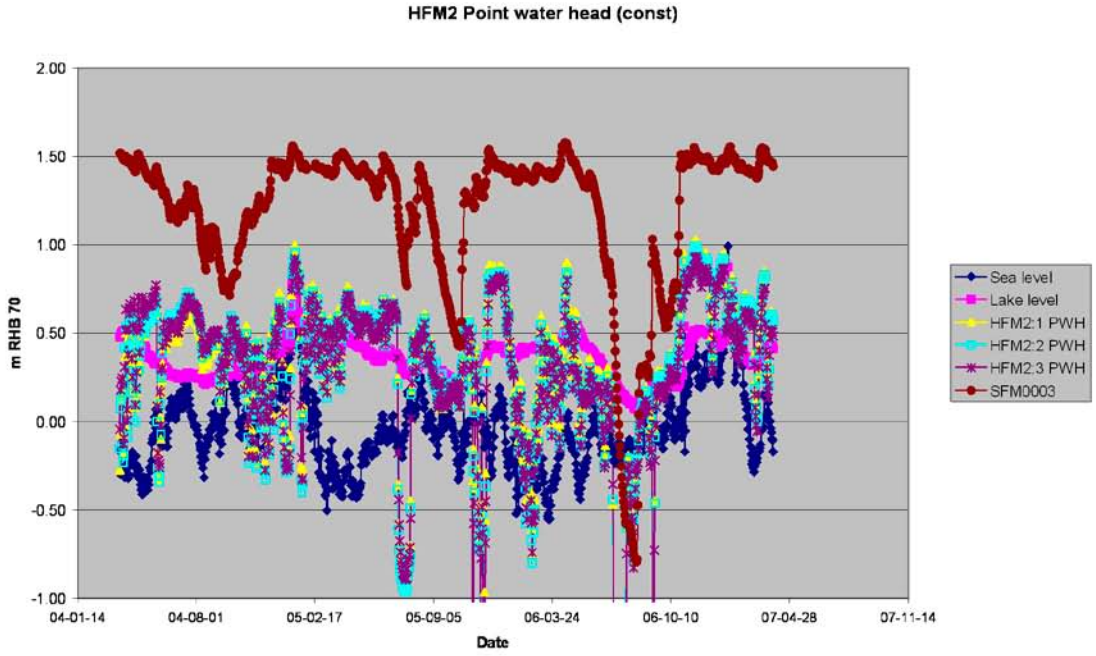

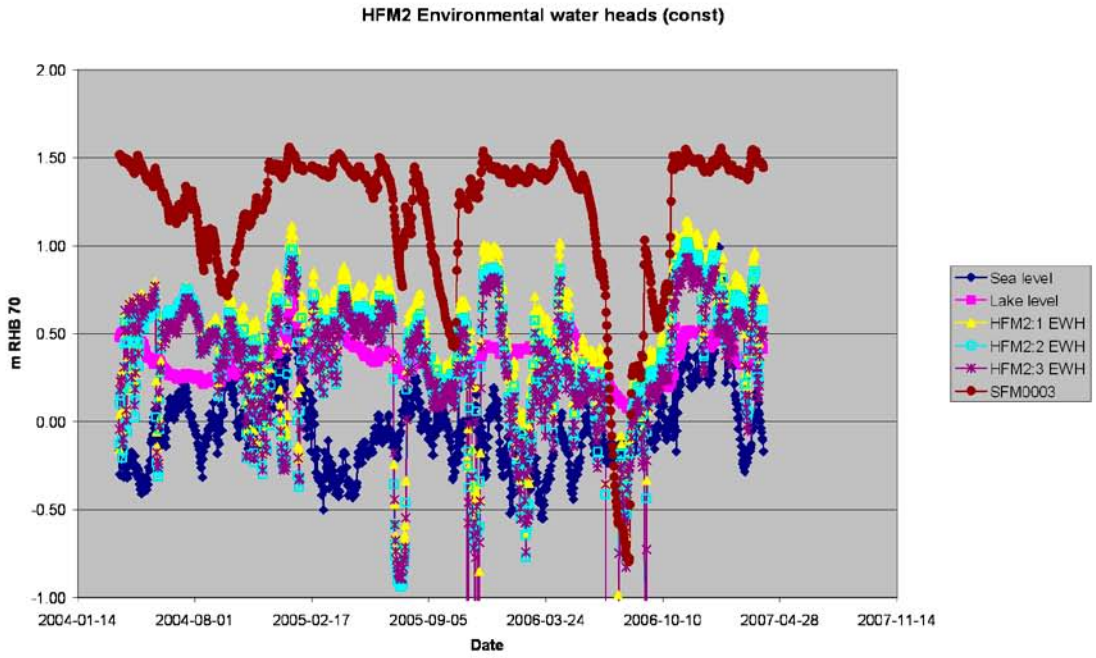

HFM2 (Constant) QD =SFM0003

Section	Min		Percentil 0.02		Ave		Percentil 0.98		Max		Section	Compensation EWH-PWH mean
QD	PWHQD	EWHQD	PWHQD	EWHQD	PWHQD	EWHQD	PWHQD	EWHQD	PWHQD	EWHQD	QD	
	-4.33 ↓	-4.33 ↓	-2.19 ↓	-2.19 ↓	-0.93 ↓	-0.93 ↓	-0.19 ↓	-0.19 ↓	0.53 ↑	0.53 ↑		
3	PWH3	EWH3	PWH3	EWH3	PWH3	EWH3	PWH3	EWH3	PWH3	EWH3	3	0.00
	-0.53 ↓	-0.5 ↓	-0.1 ↓	-0.08 ↓	0.02 ↔	0.05 ↔	0.1 ↑	0.13 ↑	2.81 ↑	2.84 ↑		
2	PWH2	EWH2	PWH2	EWH2	PWH2	EWH2	PWH2	EWH2	PWH2	EWH2	2	0.03
	-0.15 ↓	-0.06 ↓	-0.08 ↓	0 ↔	0.02 ↔	0.11 ↑	0.08 ↑	0.17 ↑	0.2 ↑	0.25 ↑		
1	PWH1	EWH1	PWH1	EWH1	PWH1	EWH1	PWH1	EWH1	PWH1	EWH1	1	0.12

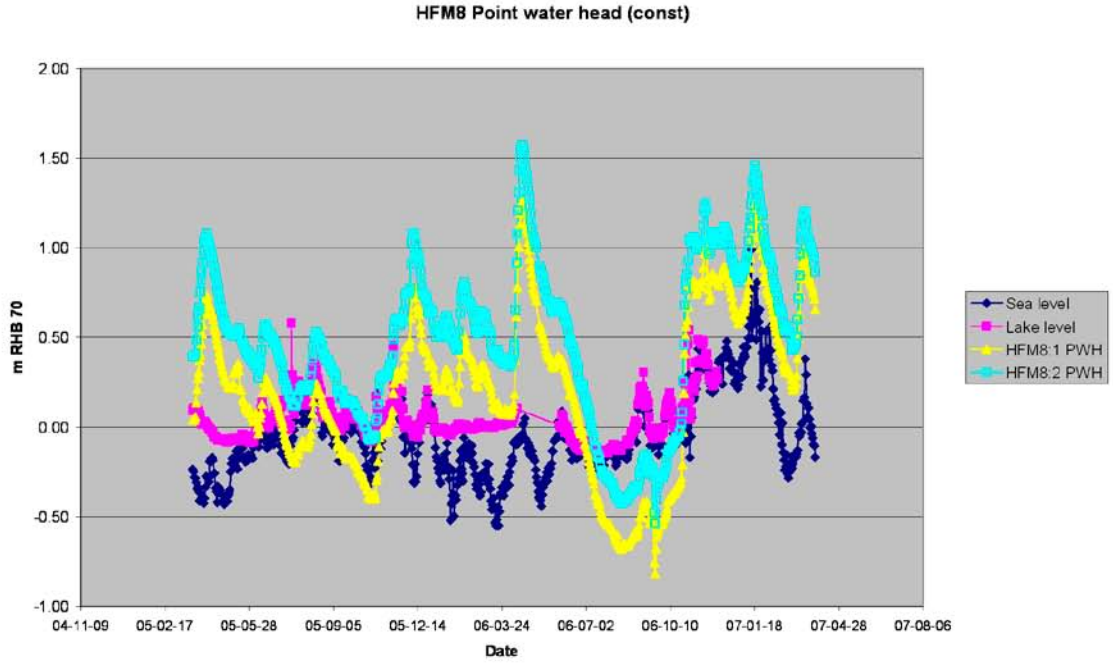

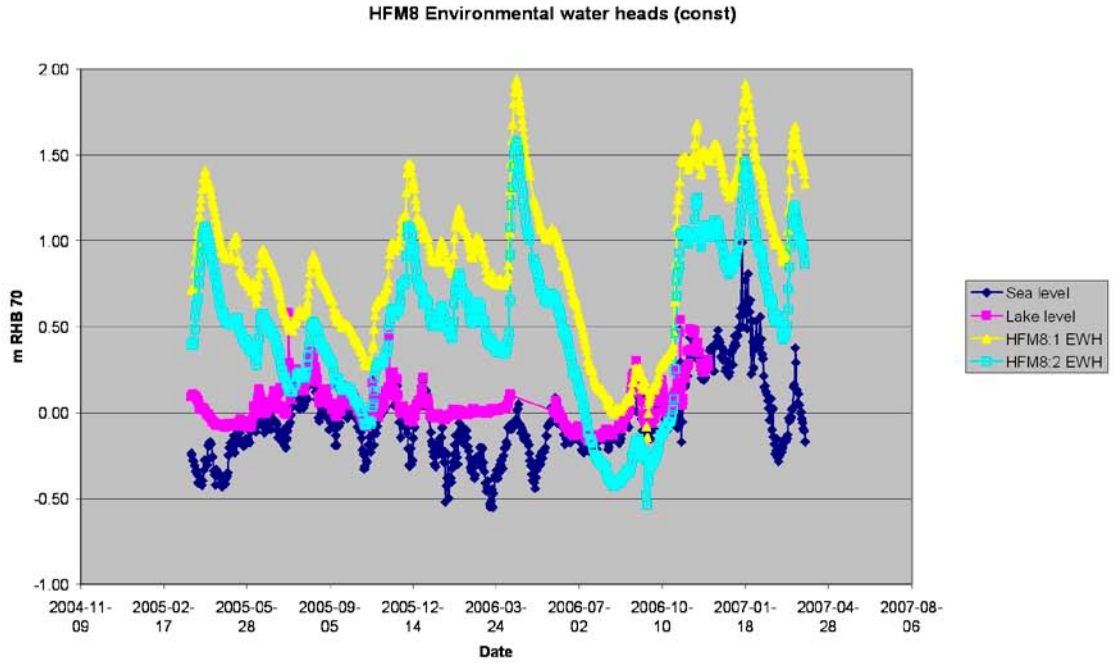

HFM8 (Constant)

Section	Min		Percentil 0.02		Ave		Percentil 0.98		Max		Section	Compensation EWH-PWH mean
2	PWH2	EWH2	PWH2	EWH2	PWH2	EWH2	PWH2	EWH2	PWH2	EWH2	2	
	-0.36	0.32	-0.35	0.33	-0.28	0.41	-0.21	0.47	-0.18	0.49		
1	PWH1	EWH1	PWH1	EWH1	PWH1	EWH1	PWH1	EWH1	PWH1	EWH1	1	0.68

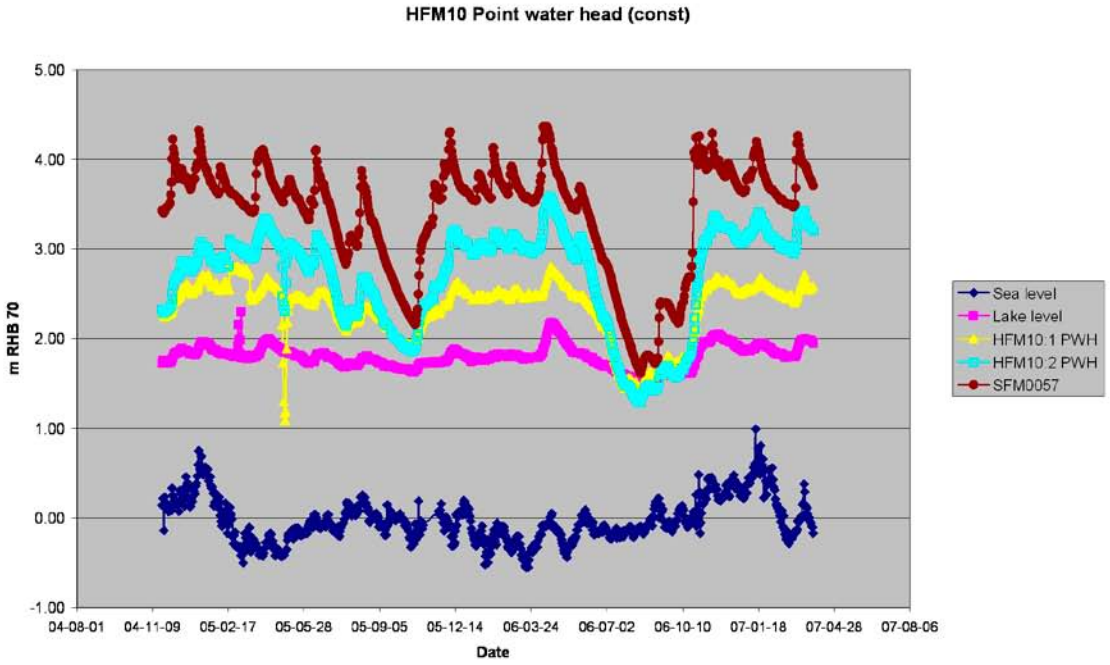

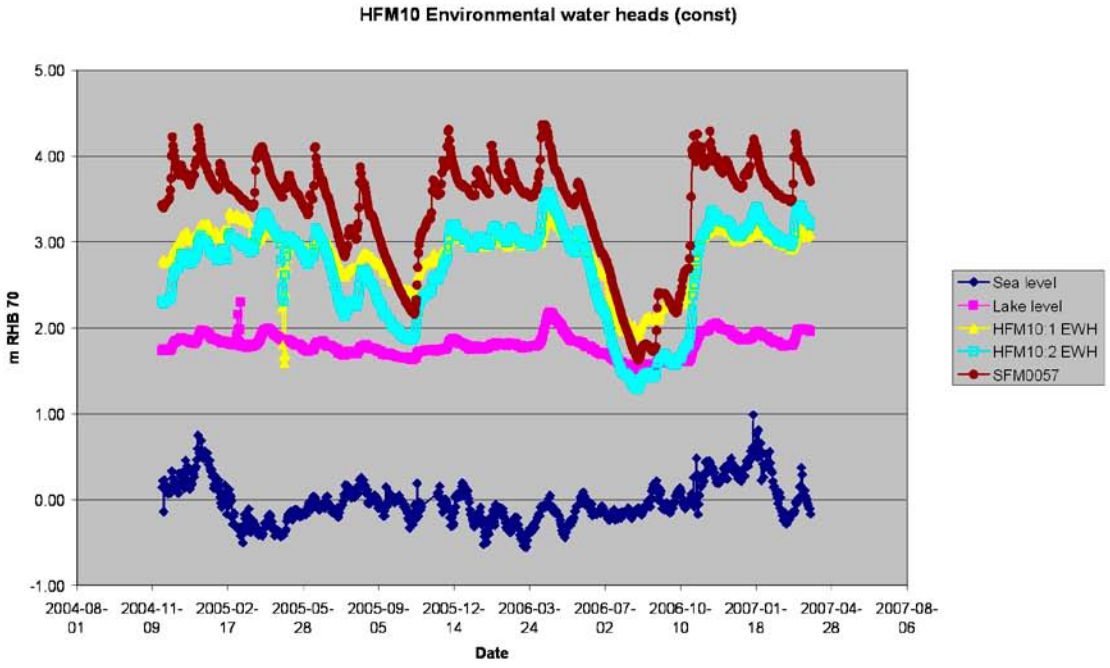

HFM10 (Constant) QD =SFM0057

Section	Min		Percentil 0.02		Ave		Percentil 0.98		Max		Section	Compensation EWH-PWH mean
QD	PWHQD	EWHQD	PWHQD	EWHQD	PWHQD	EWHQD	PWHQD	EWHQD	PWHQD	EWHQD	QD	
	-1.98 ↓	-1.98 ↓	-1.31 ↓	-1.31 ↓	-0.7 ↓	-0.7 ↓	-0.32 ↓	-0.32 ↓	-0.26 ↓	-0.26 ↓		
2	PWH2	EWH2	PWH2	EWH2	PWH2	EWH2	PWH2	EWH2	PWH2	EWH2	2	0.00
	-1.43 ↓	-0.93 ↓	-0.8 ↓	-0.29 ↓	-0.35 ↓	0.15 ↑	0.14 ↑	0.65 ↑	0.19 ↑	0.7 ↑		
1	PWH1	EWH1	PWH1	EWH1	PWH1	EWH1	PWH1	EWH1	PWH1	EWH1	1	0.51

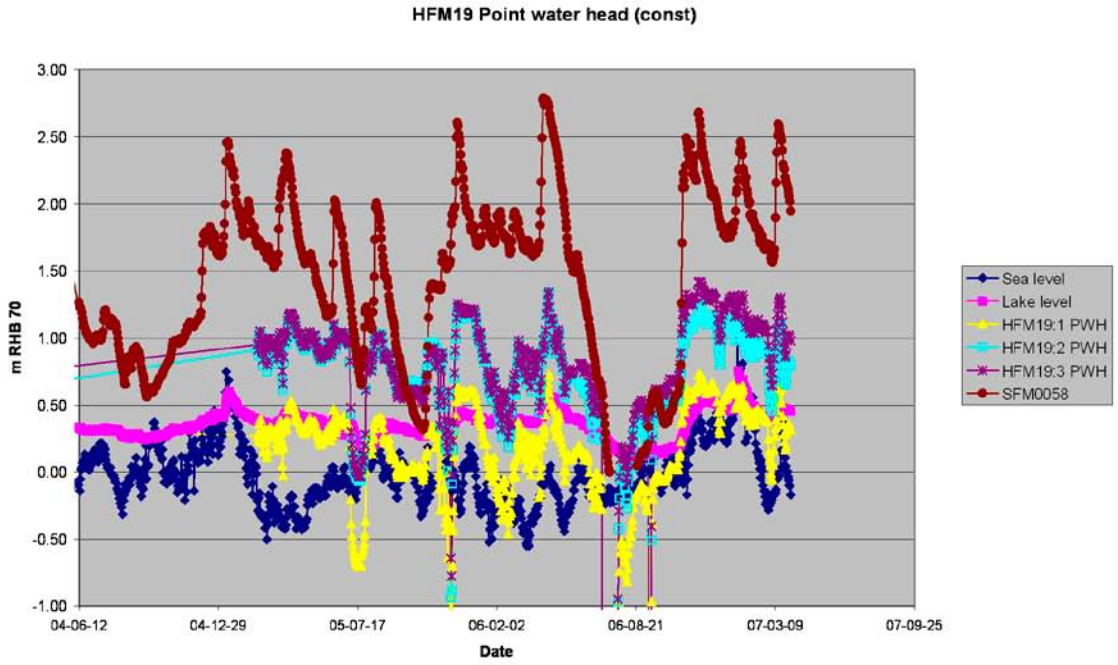

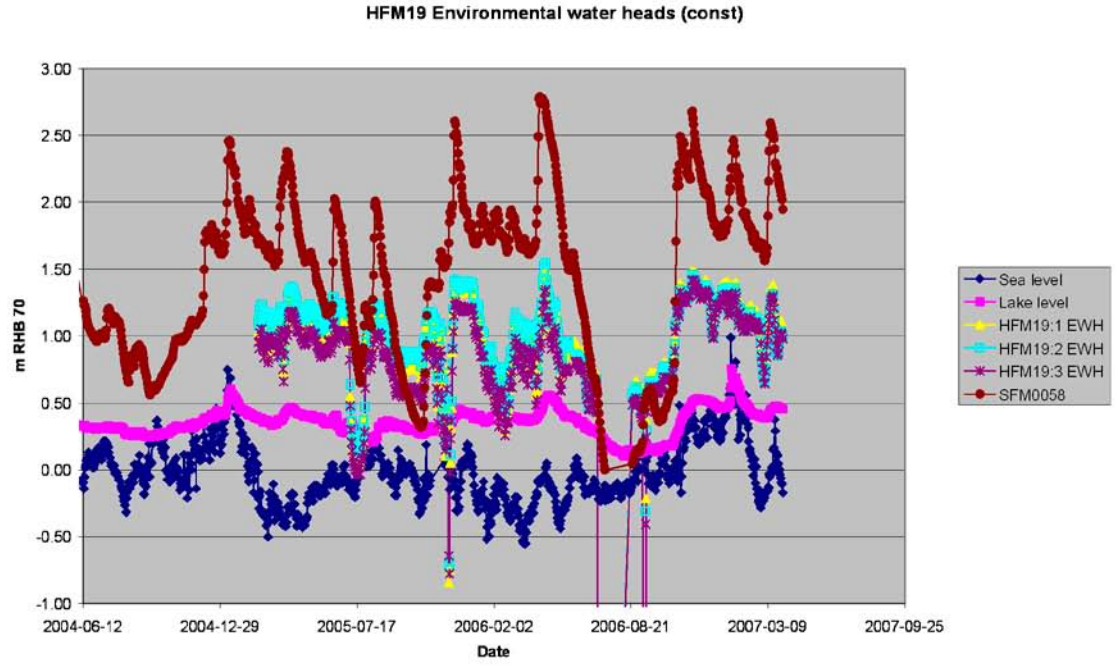

HFM19 (Constant) QD =SFM0058

Section	Min		Percentil 0.02		Ave		Percentil 0.98		Max		Section	Compensation EWH-PWH mean
QD	PWHQD	EWHQD	PWHQD	EWHQD	PWHQD	EWHQD	PWHQD	EWHQD	PWHQD	EWHQD	QD	
	-5.63 ↓	-5.63 ↓	-2.5 ↓	-2.5 ↓	-0.8 ↓	-0.8 ↓	0.25 ↑	0.25 ↑	0.44 ↑	0.44 ↑		
3	PWH3	EWH3	PWH3	EWH3	PWH3	EWH3	PWH3	EWH3	PWH3	EWH3	3	0.00
	-0.43 ↓	-0.15 ↓	-0.28 ↓	-0.01 ↔	-0.07 ↓	0.13 ↑	0.08 ↑	0.26 ↑	0.09 ↑	0.27 ↑		
2	PWH2	EWH2	PWH2	EWH2	PWH2	EWH2	PWH2	EWH2	PWH2	EWH2	2	0.21
	-0.78 ↓	-0.24 ↓	-0.64 ↓	-0.09 ↓	-0.51 ↓	-0.03 ↔	0.32 ↑	0.08 ↑	0.35 ↑	0.12 ↑		
1	PWH1	EWH1	PWH1	EWH1	PWH1	EWH1	PWH1	EWH1	PWH1	EWH1	1	0.76

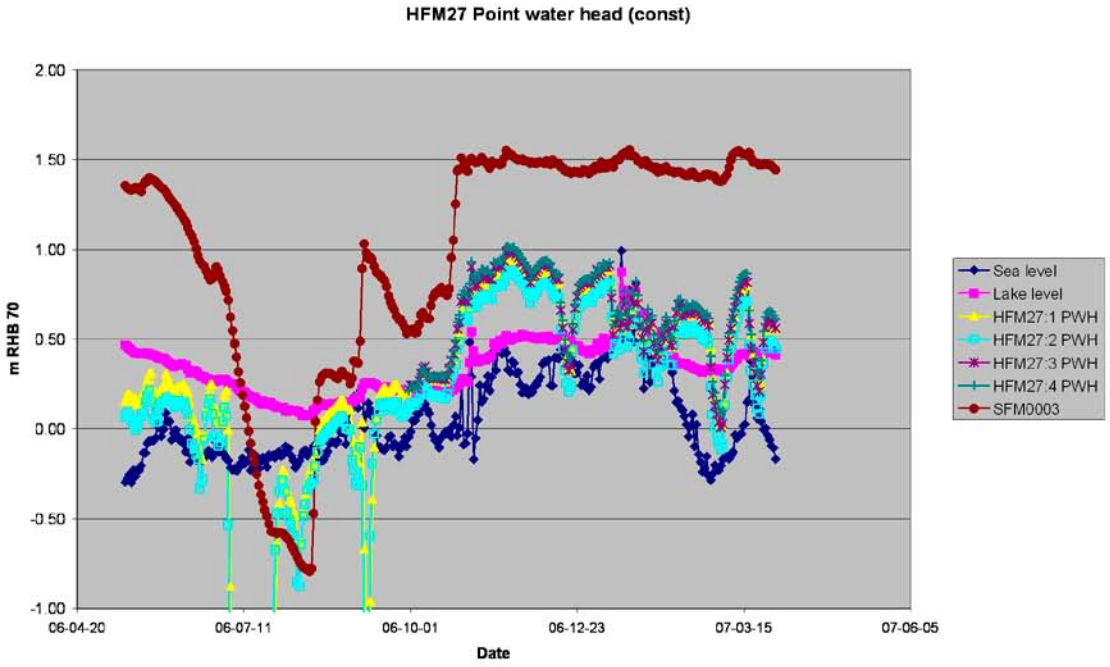

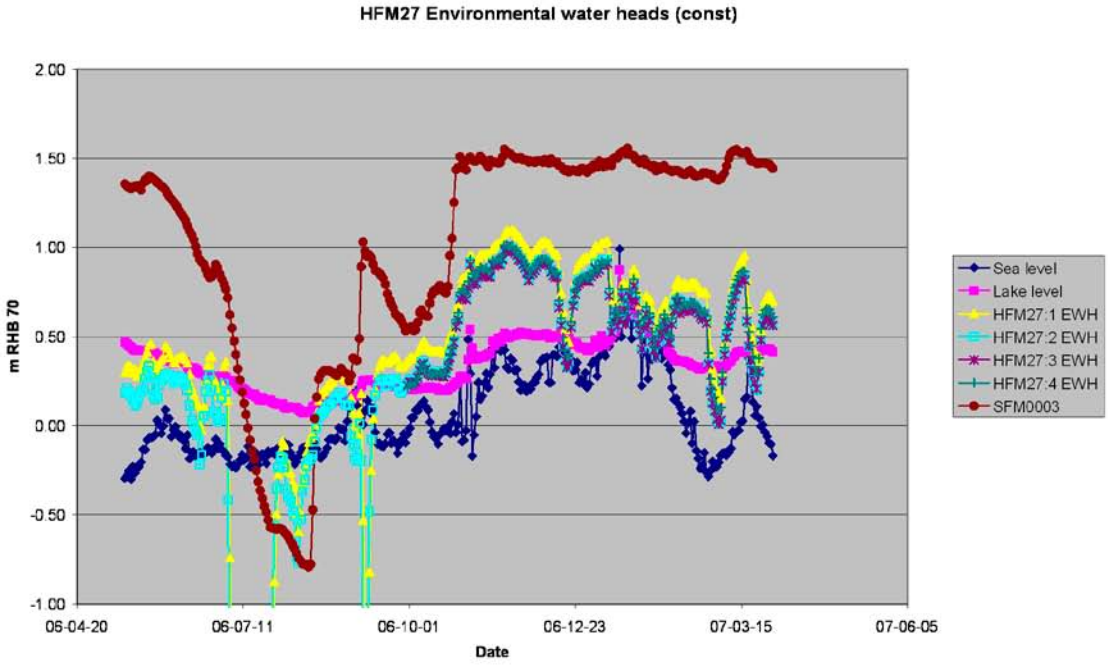

HFM27 (Constant) QD =SFM0003

Section	Min		Percentil 0.02		Ave		Percentil 0.98		Max		Section	Compensation EWH-PWH
QD	PWHQD	EWHQD	PWHQD	EWHQD	PWHQD	EWHQD	PWHQD	EWHQD	PWHQD	EWHQD	QD	mean
	-1.29 ↓	-1.29 ↓	-1.21 ↓	-1.22 ↓	-0.71 ↓	-0.71 ↓	-0.31 ↓	-0.31 ↓	-0.28 ↓	-0.28 ↓		
4	PWH4	EWH4	PWH4	EWH4	PWH4	EWH4	PWH4	EWH4	PWH4	EWH4	4	0.00
	-0.09 ↓	-0.09 ↓	-0.08 ↓	-0.08 ↓	-0.03 ↔	-0.03 ↔	0.01 ↔	0.01 ↔	0.01 ↔	0.01 ↔		
3	PWH3	EWH3	PWH3	EWH3	PWH3	EWH3	PWH3	EWH3	PWH3	EWH3	3	0.00
	-0.13 ↓	-0.01 ↔	-0.12 ↓	0 ↔	-0.11 ↓	0.01 ↔	-0.1 ↓	0.02 ↔	-0.1 ↓	0.02 ↔		
2	PWH2	EWH2	PWH2	EWH2	PWH2	EWH2	PWH2	EWH2	PWH2	EWH2	2	0.12
	-0.55 ↓	-0.53 ↓	-0.07 ↓	-0.04 ↔	0.1 ↓	0.13 ↓	0.32 ↓	0.36 ↓	0.56 ↓	0.59 ↓		
1	PWH1	EWH1	PWH1	EWH1	PWH1	EWH1	PWH1	EWH1	PWH1	EWH1	1	0.14

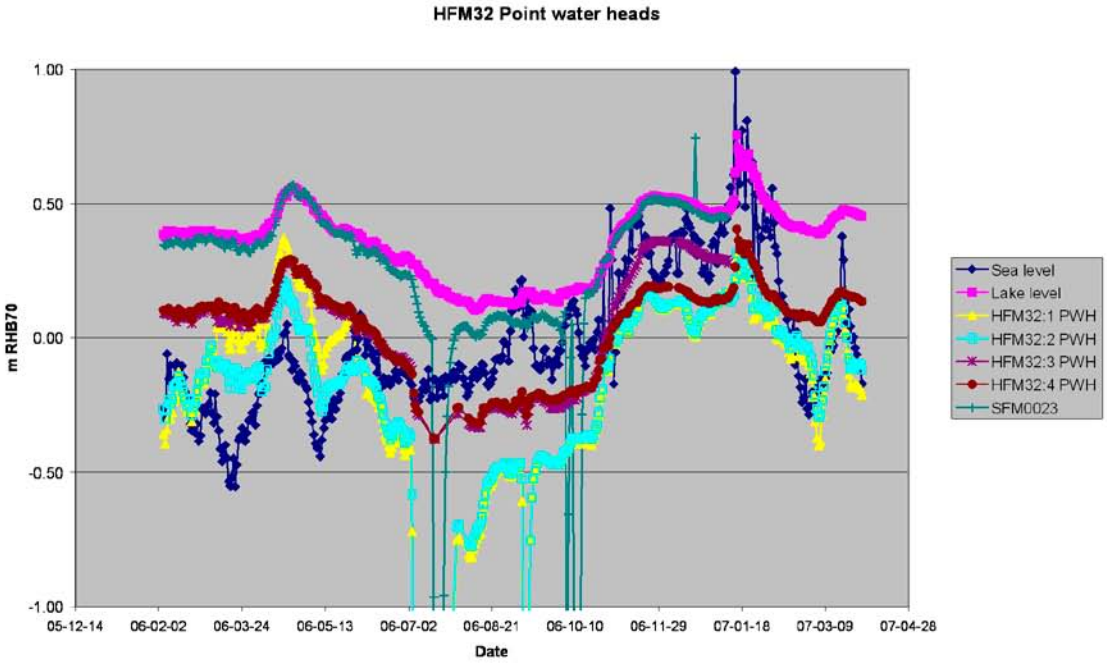

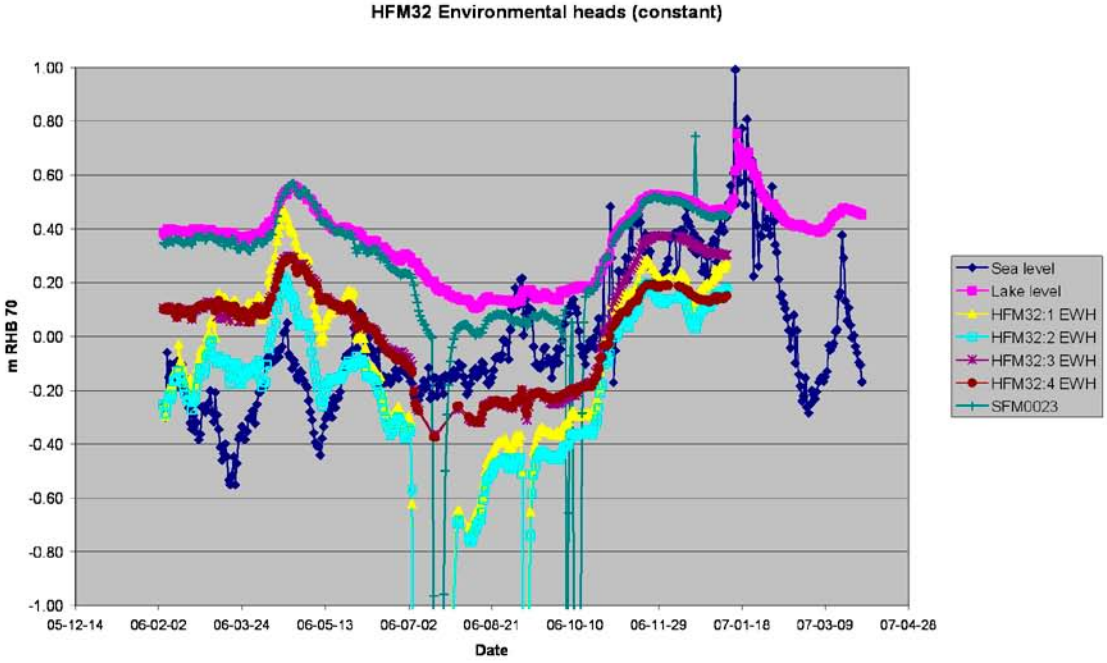

HFM32 (Constant) QD =SFM0023

Section	Min		Percentil 0.02		Ave		Percentil 0.98		Max		Section	Compensation EWH-PWH mean
QD	PWHQD	EWHQD	PWHQD	EWHQD	PWHQD	EWHQD	PWHQD	EWHQD	PWHQD	EWHQD	QD	
	-0.6 ↓	-0.6 ↓	-0.36 ↓	-0.36 ↓	-0.25 ↓	-0.25 ↓	0.81 ↑	0.81 ↑	1.65 ↑	1.65 ↑		
4	PWH4	EWH4	PWH4	EWH4	PWH4	EWH4	PWH4	EWH4	PWH4	EWH4	4	0.00
	-0.05 ↓	-0.04 ↔	-0.05 ↔	-0.03 ↔	0.02 ↔	0.04 ↔	0.18 ↑	0.19 ↑	0.18 ↑	0.19 ↑		
3	PWH3	EWH3	PWH3	EWH3	PWH3	EWH3	PWH3	EWH3	PWH3	EWH3	3	0.01
	-2.12 ↓	-2.12 ↓	-1.58 ↓	-1.58 ↓	-0.27 ↓	-0.27 ↓	-0.1 ↓	-0.1 ↓	-0.07 ↓	-0.07 ↓		
2	PWH2	EWH2	PWH2	EWH2	PWH2	EWH2	PWH2	EWH2	PWH2	EWH2	2	0.01
	-0.14 ↓	-0.05 ↓	-0.09 ↓	0.02 ↔	0.02 ↔	0.12 ↑	0.18 ↑	0.27 ↑	0.19 ↑	0.27 ↑		
1	PWH1	EWH1	PWH1	EWH1	PWH1	EWH1	PWH1	EWH1	PWH1	EWH1	1	0.10